Trinity College Dublin
Coláiste na Tríonóide, Baile Átha Cliath
The University of Dublin

Investigating the Signalling and Function of C5aR2

Thesis submitted to the University of Dublin

for the Degree of Doctor of Philosophy

by

Oliver Wright

2023

GSK

Stevenage, UK

School of Biochemistry and Immunology

Trinity Biomedical Sciences Institute

Trinity College Dublin

Dublin, Ireland

DECLARATION

I declare that this thesis has not been submitted as an exercise for a degree at this or any other university and it is entirely my own work, excluding the following:

- Figures 4.1, 4.41 and 4.42 were generated with technical support from Maxim Durand (GSK IRU)
- Section 4.8 and onwards made use of cells initially generated by Abbie Jayyaratnam (GSK IRU) and Darren Gormley (GSK IRU)
- Figures 5.11, 5.12, 5.13, 5.14 made use of cells generated by Lee Booty (GSK Immunology Network) and Anna Harris (GSK, University of Nottingham)
- Computational biology in support of Chapter 6 was contributed to by You Zhou (Cardiff University), Van Dien Nguyen (Cardiff University), and supported by Darren Gormley (GSK IRU) and Lee Booty (GSK Immunology Network).
- P32 and P59 were synthesised by Albert Isidro Llobet (GSK Chemical Biology)

I agree to deposit this thesis in the University's open access institutional repository or allow the Library to do so on my behalf, subject to Irish Copyright Legislation and Trinity College Library conditions of use and acknowledgement.

I consent to the examiner retaining a copy of the thesis beyond the examining period, should they so wish (EU GDPR May 2018).

Oliver Wright

ABSTRACT

Complement component 5a receptor 2 (C5aR2) is an enigmatic receptor for anaphylatoxin C5a. It was initially thought to be a decoy receptor, competitively binding to C5a to negatively regulate C5aR1 signalling. However, recent research has revealed various and conflicting examples of pro-inflammatory and anti-inflammatory effects of C5aR2. Most recently, studies on primary human monocyte-derived macrophages have demonstrated that C5aR2 negatively regulates C5aR1-driven ERK1/2 phosphorylation and suppresses PRR-induced cytokine secretion. However, the literature remains inconsistent, there are limited tools with which to study C5aR2, and the molecular mechanisms underlying the immunomodulatory function of C5aR2 remain largely unexplored.

This project aimed to investigate the function and signalling of C5aR2 in macrophages. Initial experiments aimed to validate the effect of C5aR2 agonists P32 and P59 on C5aR1-induced ERK1/2 phosphorylation. P32 and P59 lacked activity in these experiments, therefore novel monoclonal C5aR1 knockout (KO) and C5aR2 KO THP-1 cell lines were generated using CRISPR-Cas9. KO cell lines were characterised using PCR, DNA sequencing and flow cytometry. To investigate immunomodulatory functions of C5aR2, a panel of PRR ligands was used to stimulate WT, C5aR1 KO and C5aR2 KO THP-1 cells, and cytokine secretion was assessed using immunoassays. Use of agonists and antagonists of the cGAS-STING pathway demonstrated that STING-induced IFN-β secretion was significantly increased in C5aR2 KO THP-1 cells and primary human monocyte-derived macrophages. Western blotting demonstrated that expression of cGAS-STING pathway proteins was increased in C5aR2 KO THP-1 cells. Finally, RNAseq revealed that key antiviral signalling pathways were up-regulated in C5aR2 KO cells. Significantly regulated genes and pathways were identified, further characterising the antiviral phenotype of C5aR2 KO cells and providing direction for future work.

These results indicate that C5aR2 is a signalling receptor with unique immunomodulatory functions, and suggest that C5aR2 is a negative regulator of antiviral signalling in macrophages. By further characterising the molecular mechanisms underpinning the function of C5aR2, future work could explore its therapeutic potential in inflammatory and infectious disease.

ACKNOWLEDGEMENTS

I am grateful to GSK and Trinity College Dublin for supporting my project and giving me this opportunity, and have many people to thank for their help along the way.

I am extremely grateful to Eva and Kathy for their supervision. Eva – thanks for always providing encouragement exactly when I needed it. Kathy – thanks for your endless positivity (even in the face of the worst of the Western blots).

Thank you to Luke for his supervision and for helping me navigate the PhD process from afar, and thank you to Cáit and Fiona for your supreme problem-solving skills.

Thanks to the Immunology Research Unit and the Immunology Catalyst at GSK for your support and companionship. In particular, thank you to Maxim for swooping in with your flow cytometry support right when I needed it, thank you to Abbie and Anna for your genome editing support, thanks to Darren for helping me to think like a bioinformatician, and thanks to YoYo and Dien for your computational biology support.

Massive thanks to Lee Booty for your tireless support and for teaching me to think like a scientist.

Finally, thank you to Jenny for your patience, love and support, and for all of our trips out in London, rainy camping holidays and listening to me bang on about the North East every minute of every day. I couldn't have finished this without you.

ABBREVIATIONS

Abbreviation	Definition
AIM2	Absent in melanoma 2
AMP	Adenosine monophosphate
ANOVA	Analysis of variance
APC	Allophycocyanin
ASC	Apoptosis-associated Speck-like protein containing a Caspase recruitment domain
ATP	Adenosine triphosphate
BCA	Bicinchoninic acid
BLAST	Basic Local Alignment Search Tool
bp	Base pairs
BRET	Bioluminescence Resonance Energy Transfer
BSA	Bovine serum albumin
C	Complement
C3a	Complement component 3a
C3a-desArg	C3a desarginated
C3aR	C3a receptor
C5a	Complement component 5a
C5a-desArg	C5a desarginated
C5aR1	C5a receptor 1
C5aR2	C5a receptor 2
C5L2	C5aR-like 2 (C5aR2)
cAMP	Cyclic AMP
CD	Cluster of Differentiation
cGAMP	Cyclic guanosine monophosphate–adenosine monophosphate
cGAS	cGAMP synthase
coIP	Co-immunoprecipitation
CR	Complement Receptor
CRISPR	Clustered Regularly Interspaced Short Palindromic Repeat
crRNA	CRISPR RNA
DAMP	Damage-associated molecular pattern
DKO	Double knockout
DNA	Deoxyribonucleic acid
DPBS	Dulbecco's phosphate-buffered saline
ds	Double-stranded
E. coli	*Escherichia coli*
EC50	Half maximal effective concentration
EDTA	Ethylenediaminetetraacetic acid
ELISA	Enzyme-linked immunosorbent assay
ERK	Extracellular signal-regulated kinase
Fc	Fragment crystallisable
FC	Fold change
FBS	Foetal bovine serum
FDA	Food and Drug Administration
g	Gram
g	gravity

GDP	Guanine diphosphate
G-CSF	Granulocyte colony stimulating factor
GMP	Guanosine monophosphate
GO	Gene ontology
GPCR	G protein-coupled receptor
GPR77	GPCR 77 (C5aR2)
gRNA	Guide RNA
GSEA	Gene Set Enrichment Analysis
GTP	Guanine triphosphate
GWAS	Genome-wide association study
HEK	Human embryonic kidney
iC3b	Inactivated C3b
ICE	Inference of CRISPR edits
IFN	Interferon
Ig	Immunoglobulin
IKK	IκB Kinase
IL	Interleukin
IRAK	IL-1 receptor-associated kinase
IRF	Interferon regulatory factor
JAK	Janus kinase
JNK	c-Jun N-terminal Kinase
KEGG	Kyoto Encyclopaedia of Genes and Genomes
KO	Knockout
L	Litre
LPS	Lipopolysaccharide
M	Molar
mAb	Monoclonal antibody
MAC	Membrane attack complex
MACS	Magnetic-activated cell sorting
MAPK	Mitogen-activated protein kinase
MASP	Mannan-binding lectin serine protease
MAVS	Mitochondrial antiviral-signalling protein
MBL	Mannan-binding lectin
M-CSF	Macrophage colony-stimulating factor
MDA5	Melanoma differentiation-associated protein 5
MDM	Monocyte-derived macrophage
MFI	Median fluorescence intensity
mRNA	Messenger RNA
MSD	Meso Scale Discovery
mw	Molecular weight
MYD88	Myeloid differentiation primary response 88
NES	Normalised enrichment score
NF-κB	Nuclear factor-κB
NLR	NOD-like receptor
NLRP3	NLR family pyrin domain containing 3
NTC	Non-targeted control
OD	Optical density
p90RSK	p90 ribosomal s6 kinase

pAb	Polyclonal antibody
PAMP	Pathogen-associated molecular pattern
PANTHERdb	Protein Analysis Through Evolutionary Relationships database
PBMC	Peripheral blood mononuclear cell
PC	Principal Component
PCA	Principal Component Analysis
PCR	Polymerase Chain Reaction
pERK	phospho-ERK
PMA	Phorbol 12-myristate 13-acetate
PI3K	Phosphoinositide 3-kinase
PRR	Pattern Recognition Receptor
RBL	Rat basophil leukaemia
RIG-I	Retinoic acid inducible gene I
RIPA	Radioimmunoprecipitation assay
RLR	RIG-I-like receptor
RNA	Ribonucleic acid
RNAi	RNA interference
RNAseq	RNA sequencing
RNP	Ribonucleoprotein
RT	Room temperature
RT-qPCR	Quantitative reverse transcription PCR
SD	Standard deviation
sgRNA	Single gRNA
SNP	Single nucleotide polymorphism
ss	Single-stranded
STAT	Signal transducer and activator of transcription
STING	Stimulator of Interferon Genes
STRINGdb	Search Tool for the Retrieval of Interacting Genes/Proteins database
SW	SimpleWestern
TANK	TRAF family member-associated NF-κB activator
TBK1	TANK-binding kinase 1
tERK	Total ERK
TIR	Toll-interleukin-1 receptor
TLR	Toll-like receptor
TNF	Tumour necrosis factor
TRAF	TNF receptor-associated factor
tracrRNA	Trans-activating crRNA
TRIF	TIR-domain-containing adapter-inducing IFN-β
WT	Wild type

TABLE OF CONTENTS

CHAPTER 1 - INTRODUCTION 1

1. Introduction 2
1.1. The innate immune system 2
1.1.1. TLRs 3
1.1.2. Nucleic acid sensing and the cGAS-STING pathway 5
1.1.3. Inflammasomes 7
1.2. The complement system 9
1.2.1. Initiation 9
1.2.1.1. Classical Pathway 10
1.2.1.2. Lectin Pathway 11
1.2.1.3. Alternative Pathway 12
1.2.2. Complement effector fragments 13
1.2.2.1. Opsonins 13
1.2.2.2. Terminal pathway 14
1.2.2.3. Anaphylatoxins 15
1.3. Anaphylatoxin receptors 16
1.3.1. C3aR 17
1.3.2. C5aR1 19
1.3.2.1. Structure 19
1.3.2.2. Expression 20
1.3.2.3. Function 20
1.3.3. C5aR2 21
1.3.3.1. Structure 21
1.3.3.2. Expression 22
1.4. C5aR2 function 23
1.4.1. Ligands 23
1.4.2. GPCR function 23
1.4.3. Signal transduction by C5aR2 24
1.4.3.1. C5aR2 and β-arrestins 25
1.4.3.2. C5aR2 and MAP kinase signalling 26
1.4.3.3. C5a translocation by C5aR2 27
1.4.4. Pro- and anti-inflammatory cross-talk by C5aR2 28
1.4.4.1. Cross-talk between C5aR1 and C5aR2 28
1.4.4.1. Cross-talk between TLR4, C5aR1 and C5aR2 28
1.4.4.2. Cross-talk between the NLRP3 inflammasome, C5aR1 and C5aR2 29
1.4.4.3. Cross-talk between TLR4 and C5aR2 30
1.4.4.4. Cross-talk between PRRs and C5aR2 30
1.4.4.5. Summary of C5aR2 as an innate immune modulator 31
1.5. C5aR2 in disease 31
1.5.1. C5aR2 in models of disease 31
1.5.2. Therapeutic value of targeting C5aR2 33
1.6. Aims 35

CHAPTER 2 - MATERIALS AND METHODS 36

2. Materials and Methods 37
2.1. Materials 37
2.1.1. Reagents 37
2.1.2. Antibodies 40
2.1.3. Agonists and antagonists 41

2.1.4. Buffers 42
2.1.5. Guide RNA Sequences 43
2.1.6. Primer Sequences 43
2.1.7. Equipment 44
2.1.8. Software 45
2.2. Methods 46
2.2.1. Human cell culture 46
2.2.1.1. MDM culture 46
2.2.1.1.1. Isolation of peripheral blood mononuclear cells by density gradient centrifugation 46
2.2.1.1.2. Isolation of $CD14^+$ monocytes by MACS positive selection 46
2.2.1.1.3. Culture of monocyte-derived macrophages 47
2.2.1.2. THP-1 cell culture 47
2.2.1.2.1. Thawing and initial culture of THP-1 cells 47
2.2.1.2.2. Maintenance of THP-1 cell cultures 48
2.2.1.2.3. Differentiation of THP-1 cells using PMA 48
2.2.1.2.4. Cryopreservation of THP-1 cells 48
2.2.2. ERK1/2 phosphorylation experiments 49
2.2.2.1. Experimental Treatment Conditions 49
2.2.2.1.1. C5a Titration 49
2.2.2.1.2. PMX53 Titration 49
2.2.2.1.3. Anti-C5aR2 Titration 49
2.2.2.1.4. C5aR2 Agonist Titration 49
2.2.2.1.5. C5aR2 Agonist Time Course 50
2.2.2.2. Phospho-ERK 50
2.2.2.3. ELISA 50
2.2.3. Generation of polyclonal NTC, C5aR1 KO, C5aR2 KO and C5aR1/2 DKO THP-1 cells 50
2.2.3.1. RNP assembly 51
2.2.3.2. Electroporation and Cationic Lipid Transfection of RNP 52
2.2.3.3. Polyclonal KO THP-1 cell culture maintenance 52
2.2.4. Generation of AJ C5aR2 KO THP-1 cells using CRISPR-Cas9 53
2.2.5. Characterising KO cells by PCR and Sanger sequencing analysis 53
2.2.5.1. PCR 53
2.2.5.2. Nucleic Acid Electrophoresis 54
2.2.5.3. Sanger Sequencing by GENEWIZ 54
2.2.6. Generating monoclonal C5aR1 KO and C5aR2 KO cell lines by limiting dilution 55
2.2.7. Characterising monoclonal C5aR1 KO and C5aR2 KO cells by PCR and Sanger sequencing analysis 56
2.2.8. Assessing C5aR1 expression in WT and C5aR1 KO cells using confocal fluorescent microscopy 56
2.2.9. Assessing C5aR1 and C5aR2 expression using flow cytometry 57
2.2.10. Cytokine Secretion Experiments 58
2.2.10.1. Experimental Treatment Conditions 58
2.2.10.1.1. PRR Stimulation Experiment 58
2.2.10.1.2. cAIM$(PS)_2$ Difluor (Rp/Sp) Titration Experiment 58
2.2.10.1.3. cAIM$(PS)_2$ Difluor (Rp/Sp) Time Course Experiment 58
2.2.10.1.4. cGAS Ligand Experiment 58
2.2.10.1.5. STING and TBK1 Antagonist Experiment 59
2.2.10.2. Cytokine Detection Assays 59
2.2.10.3. Viability Assay 59
2.2.11. Peggy Sue Automated Western Blot 59
2.2.11.1. Experimental Treatment Conditions 60
2.2.11.2. Protein Detection by Peggy Sue 60

2.2.12. Generation of polyclonal C5aR2 KO primary human MDMs using CRISPR-Cas9 60
2.2.12.1. MDM culture and handling 60
2.2.12.2. CRISPR-Cas9 60
2.2.12.3. Characterising NTC and C5aR2 KO MDMs 61
2.2.13. Stimulation of C5aR2 KO MDMs with cAIM(PS)$_2$ Difluor (Rp/Sp) 61
2.2.13.1. Experimental Treatment Conditions 61
2.2.13.2. IFN-β ELISA 61
2.2.14. RNAseq 61
2.2.14.1. Sample Generation 61
2.2.14.2. Quality Control IFN-β ELISA 61
2.2.14.3. RNASeq 62
2.2.15. Data Analysis 62
2.2.15.1. Phospho-ERK ELISA Data 62
2.2.15.2. PCR and Sequencing Data 62
2.2.15.3. Microscopy Data 63
2.2.15.4. Flow Cytometry Data 63
2.2.15.5. Cytokine Secretion Data 63
2.2.15.6. Viability Data 63
2.2.15.7. Peggy Sue Data 63
2.2.15.8. RNAseq 64
2.2.15.9. Statistical Analysis 66

CHAPTER 3 - RESULTS 1 **67**

3. Assessing C5aR2 agonism by P32 and P59 using ERK1/2 phosphorylation assays **68**
3.1. Introduction 68
3.2. Results 70
3.2.1. C5a Titration 70
3.2.2. PMX53 Titration 72
3.2.3. Anti-C5aR2 Titration 74
3.2.4. C5aR2 Agonist Titration 76
3.2.5. C5aR2 Agonist Time Course 78
3.3. Discussion 81

CHAPTER 4 - RESULTS 2 **84**

4. Generating monoclonal C5aR1 KO and C5aR2 KO THP-1 cell lines using CRISPR-Cas9 **85**
4.1. Introduction 85
4.2. Results 87
4.2.1. Confirming expression of C5aR1 and C5aR2 in WT THP-1 cells 87
4.2.2. Generating C5aR1 KO, C5aR2 KO and C5aR1/2 DKO THP-1 cells 89
4.2.2.1. Selecting PCR Primers for C5aR1 and C5aR2 91
4.2.2.2. Confirming successful PCR amplification product generation 92
4.2.2.3. Confirmation of C5aR1 indel in polyclonal C5aR1 KO THP-1 cells 93
4.2.2.4. Confirmation of C5aR1 indel in polyclonal C5aR1/2 DKO THP-1 cells 97
4.2.2.5. Optimising PCR and sequencing for C5aR2 100
4.2.2.6. Lack of C5aR2 indel in C5aR2 KO or C5aR1/2 DKO cells 103
4.2.2.7. Selecting primers “AJ C5aR2 KO” PCR 107
4.2.2.8. Optimising PCR conditions to characterise “AJ C5aR2 KO” THP-1 cells 112
4.2.2.9. PCR for C5aR2 using primers designed to target longer amplicons 127
4.2.3. Generating monoclonal C5aR1 KO and C5aR2 KO THP-1 cells 132
4.2.3.1. Generation of monoclonal cell lines by limiting dilution 132

4.2.3.2. Identification of monoclonal C5aR1 KO THP-1 and C5aR2 KO cell lines by PCR and sequencing 133
4.2.3.3. Characterising C5aR1 KO and C5aR2 KO monoclonal THP-1 cell lines using fluorescent confocal microscopy and flow cytometry 146
4.3. Discussion 152
4.3.1. Study limitations 152
4.3.1.1. CRISPR-Cas9 protocol variations 153
4.3.1.2. Cell lines vs primary cells 153
4.3.1.3. C5aR1/2 DKO cell line 154
4.3.1.4. C5aR1 KO clone H9 154
4.3.1.5. NTC vs WT control for CRISPR-Cas9 154
4.3.2. Future work 155

CHAPTER 5 - RESULTS 3 **156**

5. Investigating PRR modulation by C5aR1 and C5aR2 **157**
5.1. Introduction 157
5.2. Results 158
5.2.1. PRR Panel Experiment 158
5.2.1.1. Optimising PRR ligand stimulation conditions 158
5.2.1.2. Assessing the cytokine secretion response of WT, C5aR1 KO and C5aR2 KO cells stimulated with a panel of PRR ligands 161
5.2.1.2.1. Regulation of IL-1β by C5aR1 KO and C5aR2 KO 163
5.2.1.2.2. Regulation of IL-6 by C5aR1 KO and C5aR2 KO 163
5.2.1.2.3. Regulation of IL-10 by C5aR1 KO and C5aR2 KO 164
5.2.1.2.4. Regulation of TNFα by C5aR1 KO and C5aR2 KO 164
5.2.1.2.5. Cytotoxicity of PRR ligands in C5aR1 KO and C5aR2 KO THP-1 cells 164
5.2.1.3. Identification of C5a-dependent effects of C5aR1 KO or C5aR2 KO on PRR pathway regulation 165
5.2.1.3.1. Regulation of IL-1β by C5a in C5aR1 KO and C5aR2 KO THP-1 cells 167
5.2.1.3.2. Regulation of IL-6 by C5a in C5aR1 KO and C5aR2 KO THP-1 cells... 167
5.2.1.3.3. Regulation of IL-10 by C5a in C5aR1 KO and C5aR2 KO cells 167
5.2.1.3.4. Regulation of TNFα by C5a in C5aR1 KO and C5aR2 KO cells 168
5.2.1.3.5. C5a-dependent cytotoxicity of PRR ligands in C5aR1 KO and C5aR2 KO THP-1 cells 169
5.2.2. Summary of PRR ligand panel 169
5.2.3. Regulation of STING-induced IFN-β secretion by C5aR1 and C5aR2 170
5.2.3.1. Optimising stimulation concentration of cAIM(PS)$_2$ Difluor (Rp/Sp) 172
5.2.3.2. Optimising incubation time for cAIM(PS)$_2$ Difluor (Rp/Sp) 175
5.2.3.3. Characterising the cGAS-STING pathway in C5aR1 KO and C5aR2 KO cells using cGAS agonist 178
5.2.3.4. Characterising the cGAS-STING pathway in C5aR1 KO and C5aR2 KO cells using inhibitors 179
5.2.3.5. Assessing the expression and phosphorylation of cGAS-STING pathway proteins by Peggy Sue 182
5.2.4. Assessing the effect of C5aR2 KO on STING agonism in primary human monocyte-derived macrophages 186
5.2.4.1. Generating C5aR2 KO primary human MDMs using CRISPR-Cas9 186
5.2.4.2. Confirmation of C5aR2 KO by PCR and Sequencing 186
5.2.4.3. STING agonism of C5aR2 KO primary human MDMS 193
5.3. Discussion 198
5.3.1. Summary 198
5.3.2. Study Limitations 199
5.3.2.1. cGAMP ELISA 199

5.3.2.2. Peggy Sue 200
5.3.2.3. Confirmation of C5aR2 KO in primary human MDMs 200
5.3.2.4. Reproducibility between multiple C5aR1 KO clones 201
5.3.3. Future work 201

CHAPTER 6 - RESULTS 4 **203**

6. Characterising the transcriptomic effect of C5aR2 KO on the response to STING agonism **204**
6.1. Introduction 204
6.2. Results 205
6.2.1. Sample Generation for RNAseq 205
6.2.2. Principal Component Analysis 210
6.2.3. Differential Gene Expression Analysis 232
6.2.4. Pathway Analyses 236
6.2.4.1. Pathway analysis approaches 236
6.2.4.1.1. Gene Set Enrichment Analysis 239
6.2.4.1.2. STRINGdb and PANTHERdb analyses 244
6.2.4.1.3. Manual curation of inflammatory pathways 255
6.3. Discussion 258
6.3.1. Summary 258
6.3.2. Study Limitations - C5aR1 KO Clone C3 259
6.3.3. Future Work 259

CHAPTER 7 - DISCUSSION **261**

7. Discussion **262**
7.1. Aims 262
7.2. Summary of findings 262
7.2.1. C5aR2 agonism using P32 and P59 failed to regulate C5aR1-induced ERK1/2 phosphorylation 263
7.2.2. Generation of novel C5aR2 KO THP-1 cells using CRISPR-Cas9 265
7.2.3. C5aR2 and the cGAS-STING pathway 266
7.2.4. Proposed mechanism of C5aR2-dependent regulation of cGAS-STING signalling 268
7.2.5. Confirmation of antiviral pathway regulation using RNAseq 269
7.3. Future Studies 270
7.3.1. C5aR2, IFN-β and the cGAS-STING pathway 271
7.3.2. RNAseq dataset 272
7.4. Therapeutic relevance of C5aR2 272

REFERENCES **275**

APPENDIX 1 - SUPPLEMENTARY DATA FOR CHAPTER 4 **290**

8. Appendix 1 – Supplementary Data for Chapter 4 **291**
8.1. C5aR1 Sequence for C5aR1 Primer Design 291
8.2. C5aR2 Sequence for C5aR2 Primer Design 295
8.3. C5aR2 Sequence for AJ C5aR2 Primer Design 300
8.4. C5aR1 Monoclone Sequencing Data 307
8.4.1. Forward primer 307
8.4.2. Reverse primer 309
8.5. C5aR2 Monoclone Sequencing Data 324

8.5.1. Forward primer 324
8.5.2. Reverse primer 327

APPENDIX 2 - SUPPLEMENTARY DATA FOR CHAPTER 5 355

9. Appendix 2 - Supplementary Data for Chapter 5 356
9.1. Antagonist Vehicle Control Data 356
9.2. Peggy Sue Raw Data 357

APPENDIX 3 - SUPPLEMENTARY DATA FOR CHAPTER 6 368

10. Appendix 3 – Supplementary Data for Chapter 369
10.1. Pathway analysis of Untreated C5aR1/2 KO vs WT cells 369
10.2. Gene lists for manually curated KEGG pathways 370
10.3. Additional Analysis from STRINGdb 372

LIST OF FIGURES

Figure	Title	Page
1.1.	TLRs, TLR ligands and downstream signalling targets.	4
1.2.	cGAS-STING pathway summary.	6
1.3.	Canonical NLRP3 activation.	7
1.4.	The complement system.	9
1.5.	Structure of C5aR1.	18
1.6.	Structure of C5aR2.	20
1.7.	Proposed molecular mechanisms of C5aR2 function.	23
3.1.	Titration of C5a on primary human MDMs	68
3.2.	Titration of C5aR1 KO inhibitor PMX53 on C5a-treated primary human MDMs.	70
3.3.	Titration of anti-C5aR2 mAb on C5a-treated primary human MDMs.	72
3.4.	Titration of C5aR2 agonists on C5a-treated primary human MDMs.	74
3.5.	Time course of C5aR2 agonists on C5a-treated primary human MDMs.	76
4.1.	C5aR1 and C5aR2 expression on THP-1 cells confirmed using flow cytometry.	84
4.2.	CRISPR-Cas9 Experimental Design.	86
4.3.	Confirmation of PCR amplification product generation in NTC and KO sequences by nucleic acid gel electrophoresis.	88
4.4.	C5aR1 KO sequence differs from NTC sequence.	89
4.5.	Identification of C5aR1 indels in C5aR1 KO THP-1 cells.	91
4.6.	Identification of C5aR1 indels in C5aR1/2 DKO THP-1 cells.	94
4.7.	C5aR2 PCR primer optimisation and selection using nucleic acid gel electrophoresis.	96
4.8.	Confirmation of C5aR2 PCR amplification product in C5aR1 KO, C5aR2 KO and C5aR1/2 DKO THP-1 cells using nucleic acid gel electrophoresis.	98
4.9.	ICE alignment confirms that no indels are present in C5aR2 KO THP-1 cells.	100
4.10.	ICE alignment confirms that no indels are present in C5aR1/2 DKO THP-1 cells.	101
4.11.	Selection of AJ C5aR2 PCR primers by nucleic acid gel electrophoresis of WT PCR amplification product.	103
4.12.	Selection of AJ C5aR2 PCR primers by nucleic acid gel electrophoresis of AJ C5aR2 KO PCR amplification product.	104
4.13.	AJ Forward Primers 1 and 4 generate sequences which align to C5aR2 gene.	106
4.14.	AJ Reverse Primers 1 and 4 generate sequence which align to C5aR2 gene.	107
4.15.	Optimising PCR conditions for AJ C5aR2 Primer Pairs 1 and 4 using a gradient of annealing temperatures.	109
4.16.	Sequence alignment from PCR amplification product generated at 59°C using WT lysate and AJ Forward Primers 1 and 4.	112
4.17.	Sequence alignment from PCR amplification product generated at 59°C using WT lysate and AJ Reverse Primers 1 and 4.	114
4.18.	Sequence alignment from PCR amplification product generated at 59°C using AJ C5aR2 KO lysate and AJ Forward Primer 4.	115

4.19. Sequence alignment from PCR amplification product generated at 59°C using AJ C5aR2 KO lysate and AJ Reverse Primer 4. 116
4.20. Band excision to isolate target amplicon. 117
4.21. Nucleic acid gel electrophoresis of PCR amplification products from new lysates using AJ Primer Pair 4. 119
4.22. Sequence alignment from PCR amplification product generated using second batch of AJ C5aR2 KO lysate and AJ Forward Primer 4. 120
4.23. Sequence alignment from PCR amplification product generated using second batch of AJ C5aR2 KO lysate and AJ Reverse Primer 4. 121
4.24. AJ Primer Pair 8L generated a single PCR amplification product with no visible off-target bands. 123
4.25. AJ Primer Pair 8L generated a single PCR amplification product with no visible off-target bands in AJ C5aR2 KO THP-1 lysates. 124
4.26. PCR amplification product generated using AJ Primer Pair 8L successfully aligned to C5aR2 gene sequence. 125
4.27. Confirmation of C5aR2 indels in AJ C5aR2 KO THP-1 cells. 127
4.28. Visualisation of PCR amplification product from C5aR1 KO Clone A1 using nucleic acid gel electrophoresis. 129
4.29. Confirmation of PCR amplification product from C5aR2 KO A1 using nucleic acid gel electrophoresis. 131
4.30. C5aR1 KO sequencing for monoclone B6. 134
4.31. C5aR1 KO sequencing for monoclone C3. 135
4.32. C5aR1 KO sequencing for monoclone F11. 136
4.33. C5aR1 KO sequencing for monoclone G8. 137
4.34. C5aR1 KO sequencing for monoclone H9. 138
4.35. C5aR2 KO sequencing for monoclone A6. 139
4.36. C5aR2 KO sequencing for monoclone C9. 140
4.37. C5aR2 KO sequencing for monoclone D3. 140
4.38. C5aR2 KO sequencing for monoclone F3. 141
4.39. C5aR2 KO sequencing for monoclone F7. 141
4.40. Fluorescent confocal microscopy for C5aR1 in WT and C5aR1 KO THP-1 cells. 142
4.41. Flow cytometry confirming C5aR1 KO. 144
4.42. Flow cytometry confirming C5aR2 KO. 145
4.43. Summary of flow cytometry data. 146
5.1. Titration of PRR ligands on WT THP-1 cells to identify optimum stimulation concentrations. 155
5.2. C5aR1 KO and C5aR2 KO significantly modulate PRR-induced cytokine secretion in response to PRR ligands. 158
5.3. Effects of C5a on PRR regulation in WT, C5aR1 KO and C5aR2 KO THP-1 cells. 162
5.4. C5aR2 KO significantly amplifies STING-induced IFNB secretion in THP-1 cells. 167
5.5. C5a has no significant effect on STING-induced IFN-β secretion in THP-1 cells. 167
5.6. Titration of STING agonist onto WT, C5aR1 KO and C5aR2 KO THP-1 cells. 169
5.7. Time course of STING agonist onto WT, C5aR1 KO and C5aR2 KO THP-1 cells. 172
5.8. C5aR2 KO increases cGAS agonist-induced IFN-β secretion. 174
5.9. cGAS-STING pathway antagonism inhibits the response to cAIM(PS)$_2$ Difluor (Rp/Sp) in WT, C5aR1 and C5aR2 KO cells. 176

5.10. Expression and phosphorylation of cGAS-STING pathway proteins is amplified in C5aR2 KO cells. 180
5.11. Confirmation of indels in C5aR2 PCR amplification product using nucleic acid gel electrophoresis. 183
5.12. C5aR2 KO sequencing for primary human MDMs. 188
5.13. C5aR2 KO increases cGAS-STING pathway-induced IFN-β secretion in primary human MDMs at day 10 post-CRISPR-Cas9 editing. 190
5.14. Excluding unresponsive donors reveals a significant increase of cGAS-STING pathway-induced IFN-β secretion in C5aR2 KO primary human MDMs. 192
6.1. IFN-β ELISA for QC of RNAseq samples. 203
6.2. Treatment conditions are primary drivers of variance within WT datasets. 208
6.3. Genotype is the primary driver of variance between untreated C5aR1/2 KO clones and WT cells. 210
6.4. C5a treatment is the primary driver of variance within clone datasets, excluding C5aR1 KO clone C3. 212
6.5. STING agonism is the primary driver of variance within clone datasets. 214
6.6. Genotype is the primary driver of variance between C5a-treated C5aR1/2 KO clones and WT cells. 216
6.7. Genotype is the primary driver of variance between STING agonist-treated C5aR1/2 KO clones and WT cells. 218
6.8. Genotype is the primary driver of variance between Untreated grouped C5aR2 KO cells and WT cells. 220
6.9. C5a treatment is not the primary driver of variance within grouped KO datasets. 222
6.10. STING agonism is the primary driver of variance within grouped KO datasets. 224
6.11. Genotype is the primary driver of variance between C5a-treated grouped C5aR1/2 KO cells and WT cells. 226
6.12. Experiment Day, followed by Genotype, is the primary driver of variance between STING agonist-treated grouped C5aR1/2 KO cells and WT cells. 228
6.13. C5a or STING agonist-dependent gene regulation in WT, C5aR1 KO or C5aR2 KO THP-1 cells 231
6.14. Genotype-dependent gene regulation in Untreated, C5a-treated or STING agonist-treated WT, C5aR1 KO and C5aR2 KO cells. 232
6.15. Analysis pipeline for Differentially Expressed Gene data. 235
6.16. Pathway analysis for C5a-treated C5aR1 KO cells vs C5a-treated WT cells. 237
6.17. Pathway analysis for C5a-treated C5aR2 KO cells vs C5a-treated WT cells. 238
6.18. Pathway analysis for STING agonist-treated C5aR1 KO cells vs STING agonist-treated WT cells. 239
6.19. Pathway analysis for STING agonist-treated C5aR2 KO cells vs STING agonist-treated WT cells. 240
6.20. Unique genotype-dependent treatment-dependent significantly regulated genes. 241
6.21. No significantly regulated pathways from unique significantly up-regulated genes in STING-agonised C5aR1 KO cells. 243
6.22. No significantly regulated pathways from unique significantly down-regulated genes in STING-agonised C5aR1 KO cells. 244

6.23. Significantly regulated pathways from unique significantly up-regulated genes in STING-agonised C5aR2 KO cells. 245
6.24. STRINGdb interactome reveals novel significantly up-regulated pathways clustered around IFN-β in STING-agonised C5aR2 KO cells. 246
6.25. No significantly regulated pathways from unique significantly down-regulated genes in STING-agonised C5aR2 KO cells. 247
6.26. PANTHERdb Pathway analysis reveals top regulated pathways in STING-agonised C5aR1 and C5aR2 KO cells. 251
6.27. Manual curation of significantly regulated KEGG pathways identifies key significantly regulated genes in STING agonist-treated C5aR2 KO cells vs WT cells. 254
S4.1. C5aR1 sgRNA target sequence and primer design. 287
S4.2. C5aR2 sgRNA target sequence and primer design. 292
S4.3. C5aR2 "AJ C5aR2 KO" sgRNA target sequence and primer design. 298
S4.4. C5aR1 monoclone sequencing data. 315
S4.5. C5aR2 monoclone sequencing data. 348
S5.1. Figure 5.9 including DMSO vehicle controls. 350
S5.2. Peggy Sue area data. 361
S6.1. Additional pathway analysis of untreated C5aR1/2 KO cells vs WT cells. 363
S6.2. Gene lists for manually curated KEGG pathways. 366
S6.3. Functional enrichments in STRINGdb analysis from GO, STRING, KEGG and Reactome pathways. 367
S6.2. Gene lists for manually curated KEGG pathways. 366
S6.3. Functional enrichments in STRINGdb analysis from GO, STRING, KEGG and Reactome pathways. 367

LIST OF TABLES

Table	Title	Page
1.1	Expression location and ligands of the human TLRs.	3
1.2	Roles of C5aR2 in disease models.	31
2.1	Reagents and consumables.	37
2.2	Antibodies.	38
2.3	Agonists and antagonists.	39
2.4	Buffers.	40
2.5	Guide RNA sequences.	41
2.6	Primer sequences.	42
2.7	Equipment.	42
2.8	Software.	43
3.1	Agonists and antagonists of C5aR1 and C5aR2.	65
4.1	Summary of C5aR1 forward and reverse primer sequencing data.	130
4.2	Summary of C5aR2 reverse primer sequencing data.	132
5.1	Summary of C5aR2 forward primer sequencing data from primary human MDMs.	189
6.1	Samples sent to GENEWIZ for RNAseq.	206
6.2	Summary of STRINGdb analysis	249

Chapter 1 - Introduction

1. Introduction

The complement system is a complex network of proteins which mediates various immunomodulatory effects across the immune system. The complement anaphylatoxins C3a, C5a, C3a-desArg and C5a-desArg are inflammatory mediators which bind to their receptors C3a Receptor (C3aR), C5a Receptor 1 (C5aR1) and C5a Receptor 2 (C5aR2). C3aR and C5aR1 have been comprehensively studied, however C5aR2 is poorly understood. C5aR2 is implicated in various diseases and mediates pro-inflammatory and anti-inflammatory roles, however its value as a potential therapeutic target is unknown. This project therefore aims to identify the underlying mechanisms of C5aR2 signalling and function, in order to better understand its contradictory roles in inflammation and disease.

1.1. The innate immune system

The innate immune system is the first line of defence for the host. It provides protection against pathogen invasion through barrier functions, detects infection and injury through recognition of conserved molecular motifs, eliminates pathogens and toxic debris through phagocytosis, and mobilises the adaptive immune response through antigen presentation and the cytokine system.

The innate immune system comprises a complex network of innate immune cells which act as sentinels, distinguishing self from non-self and responding to pathogens or damaged cells. The primary mechanism by which this is mediated is through a group of germline-encoded pattern recognition receptors (PRRs) which recognise pathogen-associated molecular patterns (PAMPs) and damage-associated molecular patterns (DAMPs). PAMPs are generic molecular markers which are highly conserved between pathogens, and DAMPs are generic molecular markers of cellular damage. Through recognition of highly conserved PAMPs and DAMPs, PRRs can initiate an inflammatory response quickly and effectively. Several families of PRRs work together to drive the

innate immune response, including the Toll-like receptor (TLR), the NOD-like receptor (NLR), and the RIG-I-like receptor (RLR) families, and the complement system. The TLRs, the cGAS-STING pathway, the NLRP3 inflammasome and the complement system are the most well-studied in the context of C5aR2, and will be introduced in further detail below.

1.1.1. TLRs

The TLRs are a group of PRRs which initiate the innate immune response to several conserved PAMPs and DAMPs (**Figure 1.1**). There are 10 TLRs, 6 of which are expressed on the plasma membrane (TLR1, 2, 4, 5, 6, and 10) and generally recognise microbial membrane components such as lipids or proteins, and 4 of which are expressed on intracellular vesicles (TLR3, 7, 8 and 9) and respond to microbial nucleic acids [1] (**Table 1.1**).

TLR	Expression	Ligand
1/2	Plasma Membrane	Triacyl lipopeptide e.g. Pam3CSK4
3	Intracellular	Double-stranded ribonucleic acid (dsRNA)
4	Plasma Membrane	Lipopolysaccharide (LPS)
5	Plasma Membrane	Flagellin
6	Plasma Membrane	Diacyl lipopeptide
7	Intracellular	Single-stranded ribonucleic acid (ssRNA)
8	Intracellular	ssRNA
9	Intracellular	Deoxyribonucleic acid (DNA)
10	Plasma Membrane	Unknown; anti-inflammatory [2]

Table 1.1. Expression location and ligands of the human TLRs.

Upon ligand binding, for example LPS binding to TLR4, the TLRs drive downstream nuclear factor-κB (NF-κB) activation. This results in the expression of pro-inflammatory genes, including pro-inflammatory cytokines Interleukin-6 (IL-6), Tumour Necrosis Factor α (TNFα) and anti-inflammatory cytokine IL-10 [1]. The TLRs thereby play a key role in mediating the innate immune response.

A.

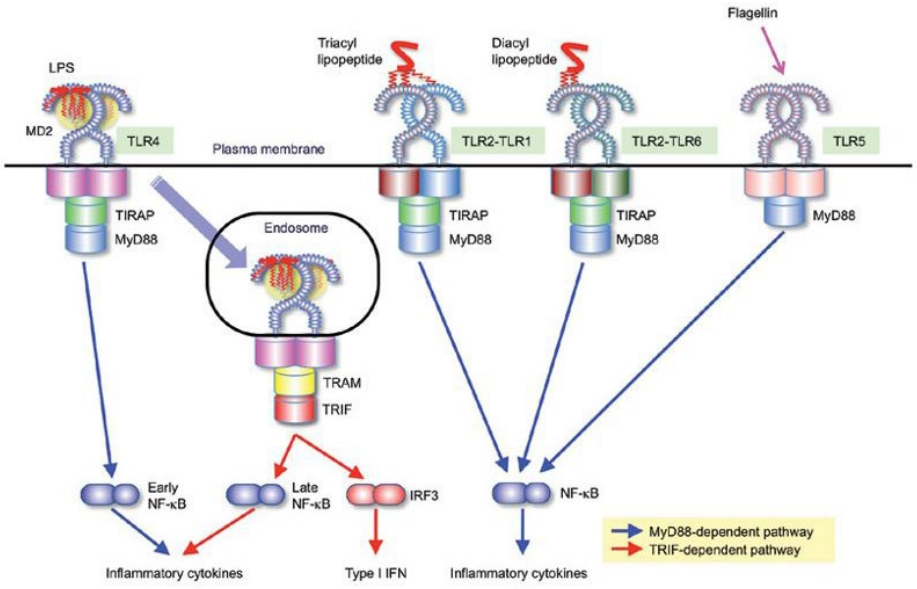

B.

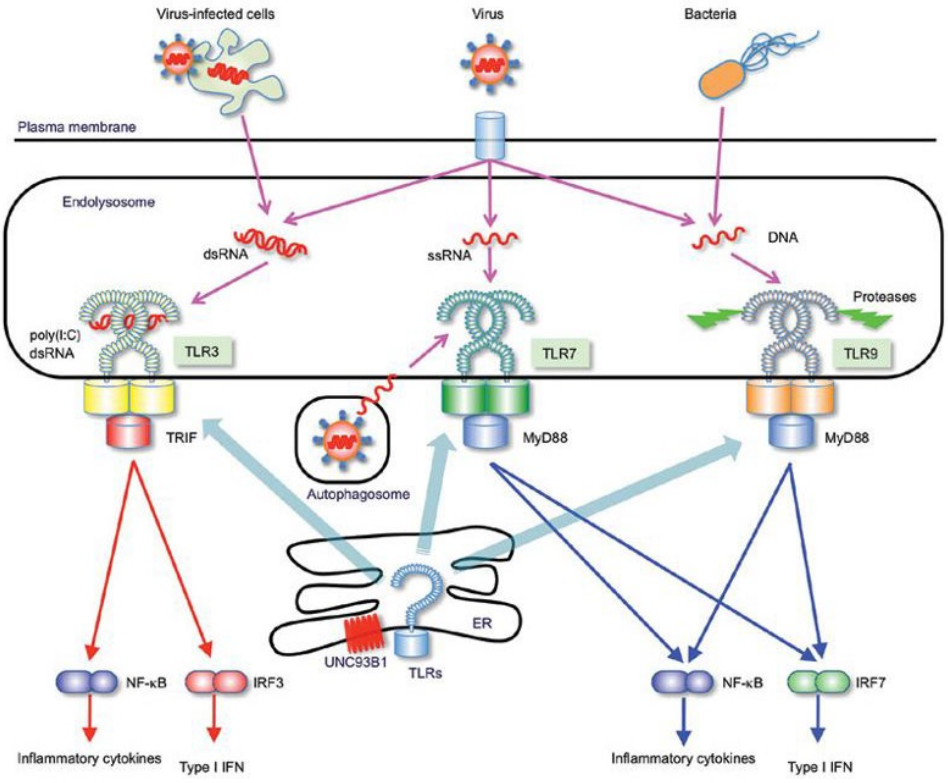

Figure 1.1. TLRs, TLR ligands and downstream signalling targets. A. surface-expressed and **B.** intracellular TLRs**.** Taken from Kawai and Akira, 2010 [1].

1.1.2. Nucleic acid sensing and the cGAS-STING pathway

Nucleic acid sensing is a critical immune function to protect against viral infection and for the surveillance of tumour-associated DAMPs. Various PRRs sense nucleic acid, including the TLR family members discussed above. TLR3, TLR7, TLR8 and TLR9 are all expressed in endosome membranes. TLR3 responds to dsRNA by signalling to NF-κB via Toll-interleukin-1 receptor-domain-containing adapter-inducing IFN-β (TRIF), resulting in pro-inflammatory cytokine release. It also signals to TANK-binding kinase 1 (TBK1) and interferon regulatory factor 3 (IRF3) to induce a Type I Interferon (IFN) response [3]. TLR7, TLR8 and TLR9 respond to nucleic acid by binding myeloid differentiation primary response 88 (MYD88) and signalling via IL-1 receptor-associated kinase 4 (IRAK4) and IRAK1/2 to NF-κB for a pro-inflammatory cytokine secretion response, and IRF7 for a Type I IFN response [1,3,4].

Alongside the TLRs, there are various nucleic acid sensors expressed in the cytosol, including absent in melanoma 2 (AIM2), retinoic acid inducible gene I (RIG-I), melanoma differentiation associated gene 5 (MDA5) and cyclic GMP-AMP synthase (cGAS). AIM2 is a DNA sensor which generates an inflammasome inducing Caspase-1 cleavage and IL-1β secretion [5]. RIG-I and MDA5 sense dsRNA, and signal via mitochondrial antiviral-signalling protein (MAVS) to IRF3/7 to generate a Type I Interferon response [6,7]. Of particular note is the DNA-sensing cGAS-Stimulator of Interferon genes (STING) pathway (**Figure 1.2**), which has links with the complement system [8].

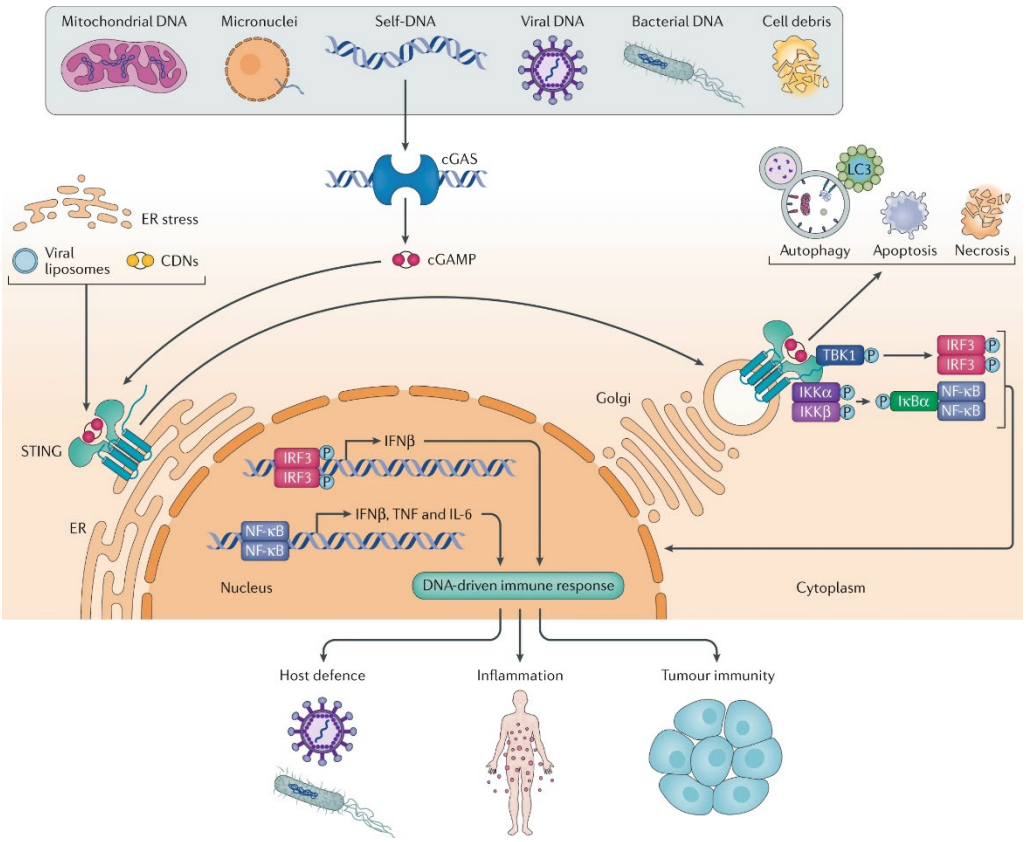

Figure 1.2. cGAS-STING pathway summary. Taken from Motwani, Pesiridis and Fitzgerald, 2019 [9].

cGAS is activated upon binding cytosolic dsDNA [10], and generates second messenger cyclic GMP-AMP (cGAMP) [11]. cGAMP activates STING [12], which dimerises [13] and translocates from the endoplasmic reticulum to the Golgi [14], recruiting TBK1 and IkB kinase (IKK) [12]. TBK1 phosphorylates IRF3, which dimerises and translocates to the nucleus to promote a Type I Interferon response, inducing the synthesis and secretion of IFN-α proteins and IFN-β [15]. IKK phosphorylates NF-κB inhibitor IκBα, which disassociates from NF-κB, allowing it to translocate to the nucleus and activate transcription of pro-inflammatory cytokine genes such as IL-1β, IL-6, and TNFα [16].

1.1.3. Inflammasomes

Inflammasomes are a group of large multiprotein complexes which function as cytosolic PRRs and innate immune sensors, assembling in response to recognition of a diverse range of PAMPs and DAMPs to generate an inflammatory response [17]. Inflammasomes consist of a sensor/scaffold protein, usually a member of the NLR family, adaptor protein Apoptosis-associated Speck-like protein containing a Caspase recruitment domain (ASC), and effector molecule caspase-1. Inflammasomes are activated by a broad range of stimuli, and are therefore important for responding to bacterial infection and cellular damage [18]. They are regulated by a 2-signal activation mechanism. Signal 1 is a priming step, where transcription and translation of inflammasome components such as NLRs and pro-IL-1β are up-regulated in order to prime the cell to quickly respond to a stimulus. Priming is classically mediated by TLR signalling through NF-κB, but various other stimuli can prime the inflammasome [19]. Signal 2 provides an activating stimulus to the inflammasome-primed cell, allowing rapid activation of the inflammasome, generation of mature IL-1β and IL-18, cleavage of Gasdermin D, and secretion of IL-1β and IL-18 via Gasdermin D pores. Different NLRs are sensitive to different stimuli, facilitating the recognition of various ligands by different inflammasomes, and specific responses to specific immunogens. For example, NLRP3 responds to a broad range of stimuli associated with membrane damage, such as cholesterol crystals, monosodium urate crystals, lysosomal rupture and cathepsin G release, nigericin, sublytic membrane attack complex (MAC), or other sources of K^+ or Ca^{2+} flux [18] (**Figure 1.3**). NLRP3 inflammasome activation is also mediated by adenosine triphosphate (ATP) through P2X7 [20], and non-canonically via intracellular LPS and caspase-4/5 [21].

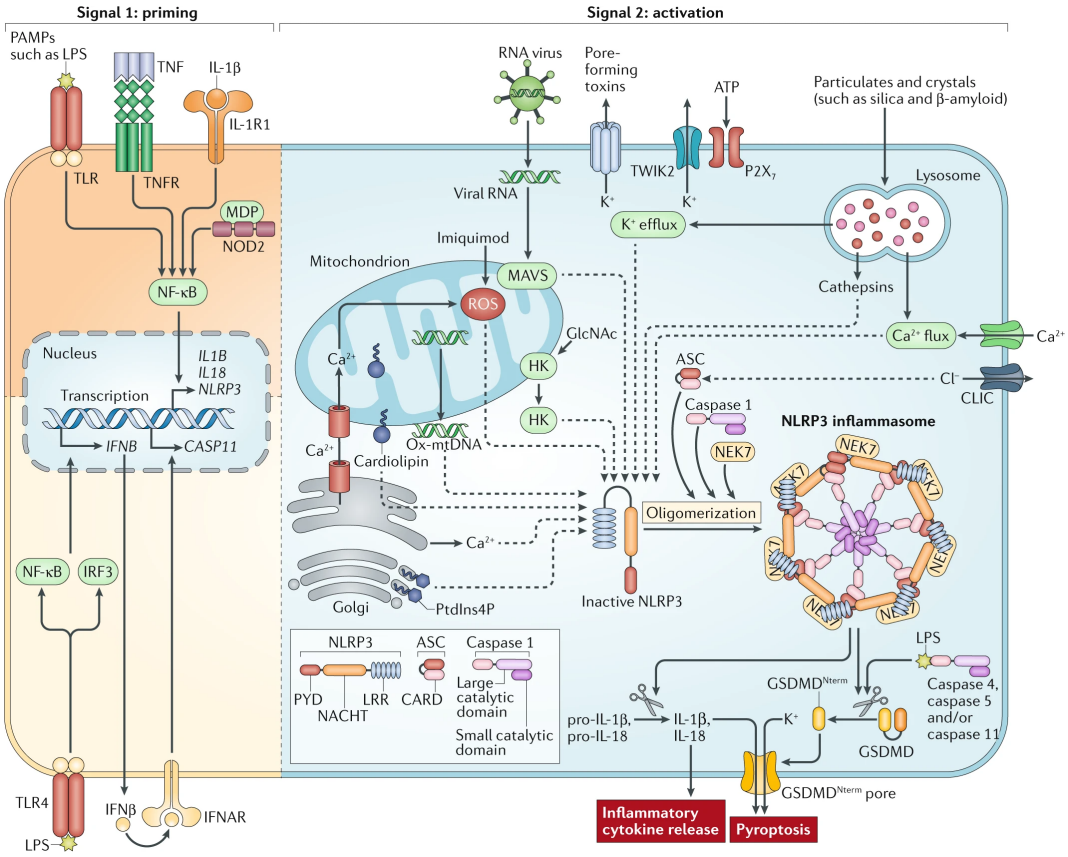

Figure 1.3. Canonical NLRP3 activation. Taken from Swanson, Deng and Ting, 2019 [22].

The inflammasomes are key regulators of inflammation and gatekeepers of IL-1β and IL-18, which are potent pro-inflammatory cytokines. Like the TLRs, the inflammasomes show a large degree of cross-talk between other PRR systems, including the complement system.

1.2. The complement system

The complement system is an innate immune surveillance system consisting of an extensive and complex network of fluid-phase, membrane-associated, and intracellular proteins. Complement proteins are activated via a tightly regulated proteolytic cascade, generating various effector protein fragments which act as PRRs, opsonins, pro-inflammatory mediators, and pore-forming toxins (**Figure 1.4**).

Initially, the complement system was believed to function primarily to opsonise pathogens and "complement" the adaptive immune response. However, it has become apparent that it plays a much broader role in inflammation. The complement system is evolutionarily ancient, and so much of the human immune system has evolved in the presence of complement. As such, it is tightly and extensively integrated into processes across the entire immune system. The complement system is capable of mounting and modulating sophisticated and complex immune responses, supported by a significant level of cross-talk and synergy between different families of innate immune system PRRs [23]. It is therefore of great interest due to its therapeutic potential across a wide range of inflammatory and autoimmune diseases. Through these widespread activities, the complement system acts as a key modulator of the innate and adaptive immune systems.

1.2.1. Initiation

Initiation of the complement cascade begins in one of three distinct pathways – Classical, Lectin or Alternative – each recognising different ligands, allowing the complement system to act as an extracellular PRR system with a broad range of specificity. All pathways converge on the generation of a C3 convertase.

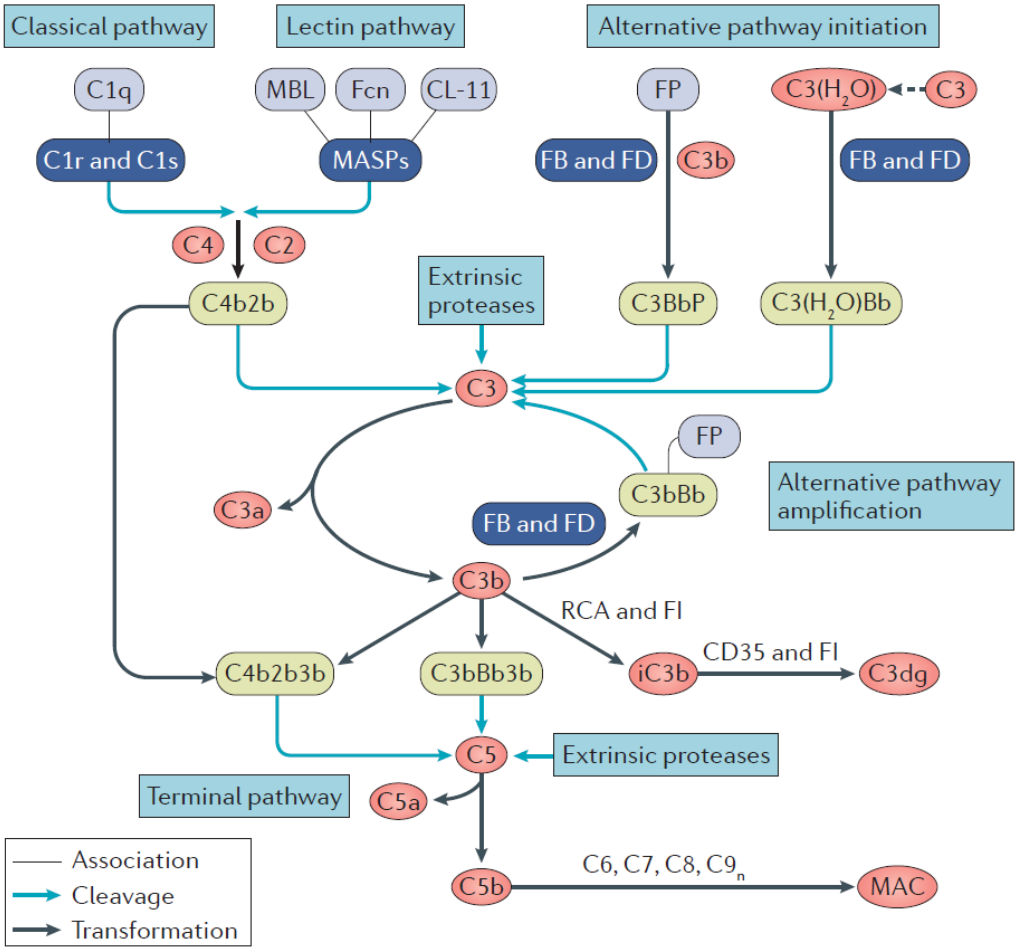

Figure 1.4. The complement system. Taken from Ricklin *et al.*, 2016 [23].

1.2.1.1. Classical Pathway

The Classical Pathway is initiated by the C1 complex, containing the PRR C1q, and a heterotetramer of proteases, $C1r_2C1s_2$, formed of two molecules of C1r and two molecules of C1s [24]. C1q primarily recognises immunoglobulin bound to target surfaces. This facilitates local complement activation at a target-bound antibody, amplifying the ongoing immune response. IgM pentamers and IgG hexamers offer multiple binding sites leading to high-avidity interactions, resulting in high levels of complement fixation by immunoglobulins [25]. C1q also recognises additional targets, including apoptotic cells and microbial PAMPs.

Upon binding to an activating surface, C1q undergoes significant conformational changes to facilitate autoactivation of the C1r molecules in the complex. Activated C1r

subsequently activates C1s, which possesses proteolytic activity. Following these conformational changes, the C1 complex gains affinity for C4, which binds to the complex and is cleaved into C4a and C4b fragments by C1s. The cleavage event exposes a reactive thioester bond in C4b, resulting in the covalent deposition of C4b onto the target surface in close proximity to the C1 complex. C4b has affinity for C2, facilitating the binding of C2 to C4b and its cleavage by the nearby C1s into C2a and C2b fragments. C2b remains bound to C4b to form the Classical Pathway C3 convertase C4b2b [24].

1.2.1.2. Lectin Pathway

The Lectin Pathway is initiated by mannose-binding lectin (MBL), ficolin-1, ficolin-2, ficolin-3 [24,26] and collectin-11 [27]. These molecules are structurally similar to C1q and also act as PRRs, recognising potential pathogens by binding to conserved bacterial carbohydrates. Each MBL or ficolin monomer contains a carbohydrate recognition domain which recognises monosaccharides such as mannose, fucose and N-acetylglucosamine. These are expressed in abundance on microbial cell surfaces but rarely at the termini of oligosaccharides on mammalian glycoproteins or glycolipids. MBL and ficolins form oligomers, resulting in multivalent interactions with microbial sugars.

MBL, ficolins and collectin-11 associate with MBL-associated serine protease (MASP) dimers composed of MASP-1 and MASP-2. MASPs are structurally and functionally similar to C1r and C1s, and are activated following PAMP binding. Similar to the Classical Pathway, MASPs cleave C4 into C4a and C4b. C4b covalently binds to the target surface and binds to C2, resulting in the cleavage of C2 by MASPs to generate C2a and C2b. C2b remains bound to C4b generating the C3 convertase C4b2b [24,26].

1.2.1.3. Alternative Pathway

The Alternative Pathway acts as a surveillance system through constitutive low-level activation in the blood in a process known as "tickover" [28]. Spontaneous hydrolysis of C3 generates C3(H_2O), which undergoes a conformational change allowing C3 to bind to Factor B, a plasma protein of the Alternative Pathway and constituent of the Alternative Pathway Convertase. Upon binding C3(H_2O), Factor B itself undergoes a conformational change which allows Factor D, a serum protease which specifically recognises Factor B, to cleave it. This generates the C3(H_2O)Bb Alternative Pathway C3 convertase. This complex is stabilised by Properdin (C3(H_2O)BbP), thereby allowing efficient cleavage of C3 to C3a and C3b. When the Alternative Pathway is activated against a nucleated host cell, complement regulatory proteins CD46, CD55 and CD59 will inhibit further activation of the complement system [29]. Plasma membrane-expressed CD35 and soluble, recruitable Factor H and C4BP also contribute to complement regulation. However, when activated against an invasive pathogen, tickover allows for rapid activation of the complement system against the target [28].

The Alternative Pathway may also have roles in pattern recognition. There is limited evidence that Properdin can function as a PRR, similar to C1q of the Classical Pathway or MBL of the Lectin Pathway, recognising PAMPs such as antigen from *Neisseria gonorrhoeae* or zymosan from fungi [30], and DAMPs such as antigen from necrotic cells [31]. This function allows the Alternative Pathway to be directly activated alongside its constant surveillance through tickover. However, this PRR function is highly controversial, and the function of properdin as a convertase complex stabiliser is more clearly established.

The role of the Alternative Pathway as an amplification loop is key to the function of the complement system. Factor B can bind to any C3b molecule, irrespective of the convertase which generated it (C4b2b, C3(H_2O)BbP or C3bBb), meaning that the

Alternative Pathway can amplify all three of the initiation pathways. Formation of the Alternative Pathway C3 convertase leads to the cleavage of additional C3 to generate C3a and C3b. C3b will be deposited locally, allowing Factor B to bind and be cleaved by Factor D, resulting in the generation of multiple C3 convertases and dense deposition of C3b on target surfaces. In certain contexts, the Alternative Pathway is responsible for 80-90% of C5a and MAC formation [32], demonstrating its importance as the central positive feedback amplification loop of the complement system.

1.2.2. Complement effector fragments

All initiation pathways converge on the formation of a C3 convertase, and the cleavage of C3, which is the most abundant protein of the complement system. The cleavage of C3 results directly and indirectly in a wide array of immunomodulatory effector functions, including generation of pro-inflammatory mediators, opsonisation of target surfaces, and initiation of the Terminal Pathway.

C3 is cleaved by C3 convertases into C3a and C3b fragments. C3b is incorporated into the C3 convertase to form a C5 convertase, which cleaves C5 into C5a and C5b. C3a and C5a are small pro-inflammatory mediators, whereas C3b and C5b are larger fragments which are deposited onto target surfaces in close proximity to the convertase, facilitating their function as opsonins [23].

1.2.2.1. Opsonins

Upon cleavage of C3, C3b is released and undergoes a conformational change which exposes a reactive thioester bond. This enables its covalent deposition onto an antigen surface. Following deposition, C3b undergoes sequential proteolytic cleavage by Factor I and cofactors Factor H and CR1 to generate C3b degradation products iC3b, C3dg and C3d. These degradation steps prevent C3b from any further convertase activity, however these molecules act as potent opsonins and are recognised by

complement receptors CR1, CR2, CR3, CR4 and CRIg, expressed by various immune cells [23].

iC3b is the inactivated form of C3b, generated through cleavage by Factor I mediated via cofactor activity of CR1, Factor H or CD46. iC3b is bound by CR1, CRIg and by CR2 with low affinity. Recognition of iC3b by CR1, CR3, CR4 or CRIg induces phagocytosis of the complement-opsonised targets by phagocytes, and CR1 is implicated in the clearance of immune complexes [23,33].

Further proteolytic cleavage generates C3dg and C3d fragments. These opsonins are high affinity ligands for CR2. Through binding C3d(g)-opsonised antigen, CR2 acts as a bridge between the innate and adaptive immune systems by acting as a modulator of B cell activation [34]. Complement-opsonised antigen is retained in germinal centres through tethering by follicular dendritic cells via CR2 binding. Furthermore, the threshold stimulus for B cell activation is dramatically reduced following concurrent ligation of the B cell receptor by its cognate antigen and stimulation of CR2 on the B cell with C3dg bound to the antigen.

1.2.2.2. Terminal pathway

Generation of C5b results in the initiation of the Terminal Pathway. All complement initiation pathways converge on the Terminal Pathway, which results in formation of the C5b-9 MAC and lysis of a complement-targeted cell [35,36].

Following cleavage of C5 and the release of C5a, C5b remains in association with the convertase and undergoes a conformational change to facilitate C6 binding. C5b is stabilised upon C6 binding, without which it remains unstable and undergoes rapid decay. Following binding to C5b, C6 also undergoes a conformational change which facilitates C7 binding, resulting in displacement of the C5b-7 complex from the convertase and association with the outer leaflet of the target membrane through a hydrophobic site on the C5b-7 complex. If not associated with a membrane, C8 in the

plasma rapidly binds free C5b-7 and inactivates it. If bound to a membrane, the C5b-7 complex can recruit C8, which further stabilises the complex and penetrates the target membrane, disrupting the inner leaflet. Finally, C9 is recruited into the complex. It binds, unfolds and inserts itself through the target membrane to penetrate the cell. Incorporation of additional C9 molecules leads to rapid generation of the C5b-9 MAC. A high concentration of MAC deposition leads to rapid osmotic lysis of the target cell [35].

The MAC is only indispensable for clearing infections by a small number of pathogens, including *Neisseria*, *Moraxella* and *Haemophilus* species [35]. Nucleated host cells employ several mechanisms to limit MAC formation and remove it from the plasma membrane, thus minimising inappropriate activation of complement against host cells and tissues [29]. Despite their protection from MAC-induced lysis by CD46, CD55 and CD59, sublytic concentrations of MAC mediate a wide range of effects on various cell types, including homeostatic functions such as regulation of the cell cycle, protein synthesis and apoptosis [37]. This also includes immune functions, such as pro-inflammatory cytokine release, degranulation, and platelet activation. Sublytic concentrations of MAC have been found to activate the NLRP3 inflammasome murine bone marrow-derived dendritic cells [38] and human lung epithelia via increase in intracellular Ca^{2+} concentration [39]. Sublytic MAC can also modulate immunometabolism in human monocyte-derived macrophages (MDMs) to influence inflammasome activation and IL-18 secretion [40].

1.2.2.3. Anaphylatoxins

The anaphylatoxins, C3a and C5a, are potent inflammatory mediators [41]. Both are small polypeptides; C3a consists of 77 amino acids, C5a consists of 74 amino acids, and they share 36% amino acid identity. They are cleaved from soluble C3 and C5 by cell surface-bound convertases at sites of complement activation, resulting in the local generation

of soluble anaphylatoxins which drive inflammation to the site of complement activation. The anaphylatoxins mediate a broad range of effects, primarily acting as powerful chemoattractants for immune cells, such as macrophages, neutrophils, B cells, T cells, basophils and mast cells. They also have broader roles in inflammation, including vasodilation, altering blood vessel permeability, smooth muscle contraction, basophil and mast cell degranulation, oxidative burst in myeloid cells, pro-inflammatory cytokine production in B cells, monocytes and neutrophils, and additional non-immune roles including tissue regeneration and fibrosis [41].

C3a and C5a are rapidly degraded by serum carboxypeptidases to C3a-desArg and C5a-desArg by proteolytic removal of the C-terminal arginine [42]. This process does not result in a conformational change in C3a-desArg, which retains the tertiary structure of C3a but loses affinity for its canonical receptor C3aR and no longer possesses pro-inflammatory properties [43]. C3a-desArg gains activity as a metabolic hormone, driving triglyceride synthesis [44] and glucose transport [45] in adipocytes. C5a des Arg undergoes a conformational change [46], resulting in a 100-fold reduction in binding affinity to its canonical receptor, C5aR1 despite retaining 5-10% of its chemotactic properties [47].

Anaphylatoxins may also be generated intracellularly by non-complement proteases including cathepsin L [48]. Intracellular C5a has been shown to interact with mitochondrial C5aR1 to drive sterile inflammation via the generation and processing of pro-IL-1β [49]. Whilst this proposal remains controversial and the differences between convertase-cleaved C5a and complosome-generated C5a remain largely undefined, the presence of intracellular C5a could have implications for intracellular anaphylatoxin receptors which bind to C5a, such as C5aR2.

1.3. Anaphylatoxin receptors

The anaphylatoxins and their desArg forms bind to the anaphylatoxin receptors C3aR, C5aR1 and C5aR2. There are three identified anaphylatoxin receptors. C3aR and C5aR1

are the canonical anaphylatoxin receptors, and are well-characterised modulators of the innate immune response [41]. The third anaphylatoxin receptor, C5aR2, also known as C5aR-Like 2 (C5L2) and GPR77, was discovered in 2000 by Ohno *et al.* [50] . Comparatively little research has been performed on C5aR2, and its function is controversial and poorly understood [51].

The anaphylatoxin receptors, C3aR, C5aR1 and C5aR2, form a family of three proteins which belong to the G protein-coupled receptor (GPCR) superfamily. Canonical GPCRs contain 7 transmembrane domains and associate with heterotrimeric G proteins, which consist of α, β, and γ subunits [52]. Upon ligand binding, a conformational change in the GPCR facilitates the exchange of guanine diphosphate (GDP) for guanine triphosphate (GTP) and the subsequent dissociation of the Gα subunit. Signal transduction is then mediated through stimulation or inhibition of second messenger cyclic adenosine monophosphate (cAMP) production, depending on the subtype of the Gα protein (Gαs or Gαi). Signalling is regulated by GPCR kinases, recruitment of β-arrestins and subsequent internalisation in clathrin-coated pits. β-arrestins also transduce signals to multiple downstream signalling pathways [53].

C3aR, C5aR1 and C5aR2 are all 7-transmembrane receptors and share sequence homology [54]. However, their ligand specificities and functions differ. C3aR and C5aR1 are functional GPCRs. C5aR2, however, is not a functional GPCR, and limited data have been published describing its activity. Recent evidence has suggested that C5aR2 has distinct and key roles in inflammation and disease, and this project will therefore investigate the molecular mechanisms underpinning C5aR2 function.

1.3.1. C3aR

C3aR is a 54 kDa GPCR consisting of 482 amino acids. It is expressed by a broad range of immune cells including neutrophils, basophils, eosinophils, mast cells, monocytes, macrophages, dendritic cells and microglia. It is also expressed by non-immune cells

such as astrocytes, endothelial cells, epithelial cells, smooth muscle and lung parenchyma [41]. C3aR has a large extracellular loop which facilitates ligand binding [55]. C3aR binds to C3a [56], but not to C3a-desArg or C5a. Upon C3a binding, C3aR transduces signals via G proteins leading to downstream signalling events including the influx of extracellular calcium ions, activation of protein kinase C by phospholipase C, activation of extracellular signal-regulated kinase 1/2 (ERK1/2) and activation of phosphoinositide 3-kinase (PI3K), and Akt, resulting in NF-κB activation, chemotactic effects and cytokine secretion in cells expressing C3aR [41,57].

1.3.2. C5aR1

1.3.2.1. Structure

C5aR1, also known as CD88, is a 42 kDa protein comprising 350 amino acids, which forms a 7-transmembrane GPCR (**Figure 1.5**).

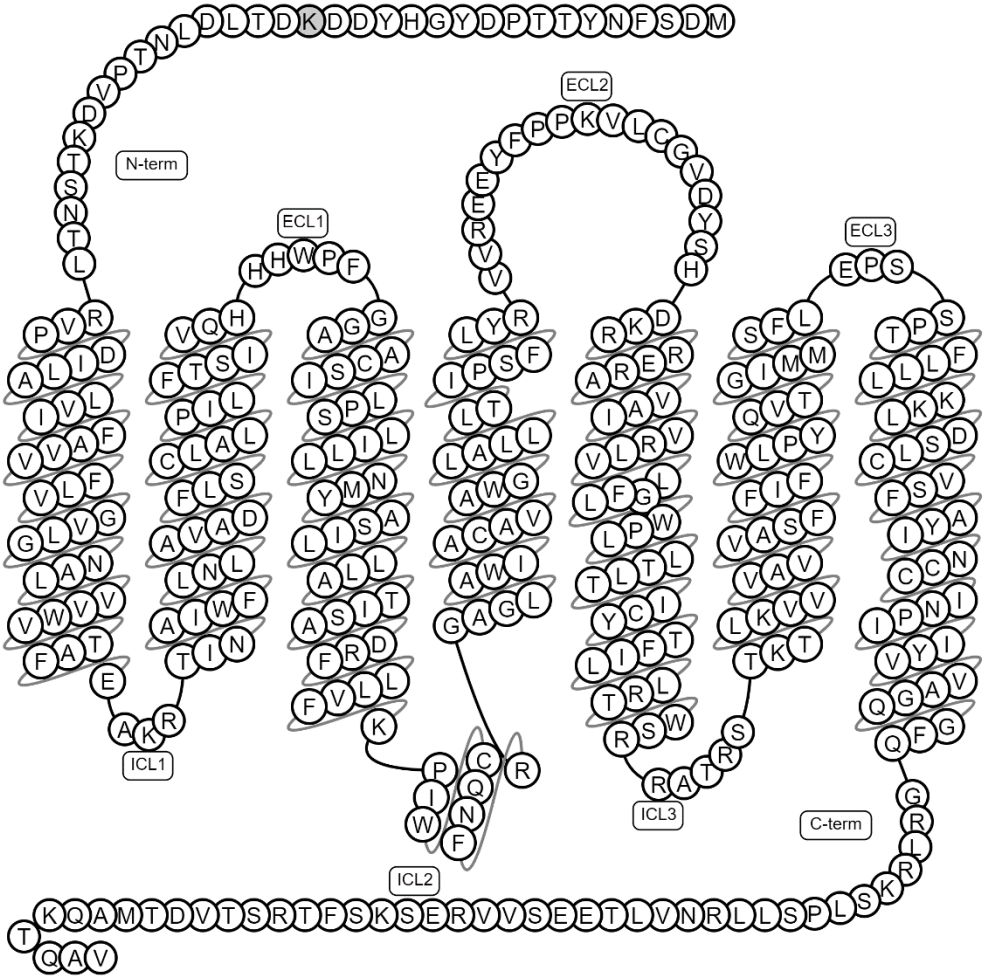

Figure 1.5. Structure of C5aR1. Amino acid structure of C5aR1 generated using GPCRdb [58]. N-Term = N-Terminus. C-Term = C-Terminus. ICL = Intracellular Loop. ECL = Extracellular Loop.

1.3.2.2. Expression

C5aR1 is expressed in various cell types, primarily by myeloid cells such as neutrophils, eosinophils, basophils, monocytes, macrophages, mast cells and dendritic cells, but also by lymphoid cells and microglia [41,59]. It is also expressed by non-immune cells, including astrocytes and neurons in the central nervous system, and cells of the kidney, spleen, heart and skin amongst others.

1.3.2.3. Function

C5aR1 binds to C5a [56] with a high affinity, binds to C5a-desArg with 100-fold lower affinity, and does not bind to C3a or C3a-desArg. C5aR1 is predominantly implicated in the modulation of pro-inflammatory cytokine secretion, and in the chemotaxis and degranulation of neutrophils [41].

Similarly to C3aR, ligand binding induces signal transduction via heterotrimeric G proteins, resulting in calcium ion fluxes, β-arrestin recruitment and downstream signalling. C5aR1 activates various downstream signalling pathways, including PI3K, protein kinase B, phospholipase C, and mitogen-activated protein (MAP) kinase [60]. C5aR1 signalling activates NF-κB [57] which drives pro-inflammatory cytokine secretion [61] and also recruits Wiskot-Aldrich Syndrome Protein, which regulates actin dynamics and therefore may influence C5aR1-induced chemotaxis [62] .

1.3.3. C5aR2

1.3.3.1. Structure

C5aR2 is a 37 kDa protein made up of 337 amino acids. It is also a 7-transmembrane receptor and shares high sequence similarity with C5aR1; 58% in transmembrane domains [63] and 38% overall [54].

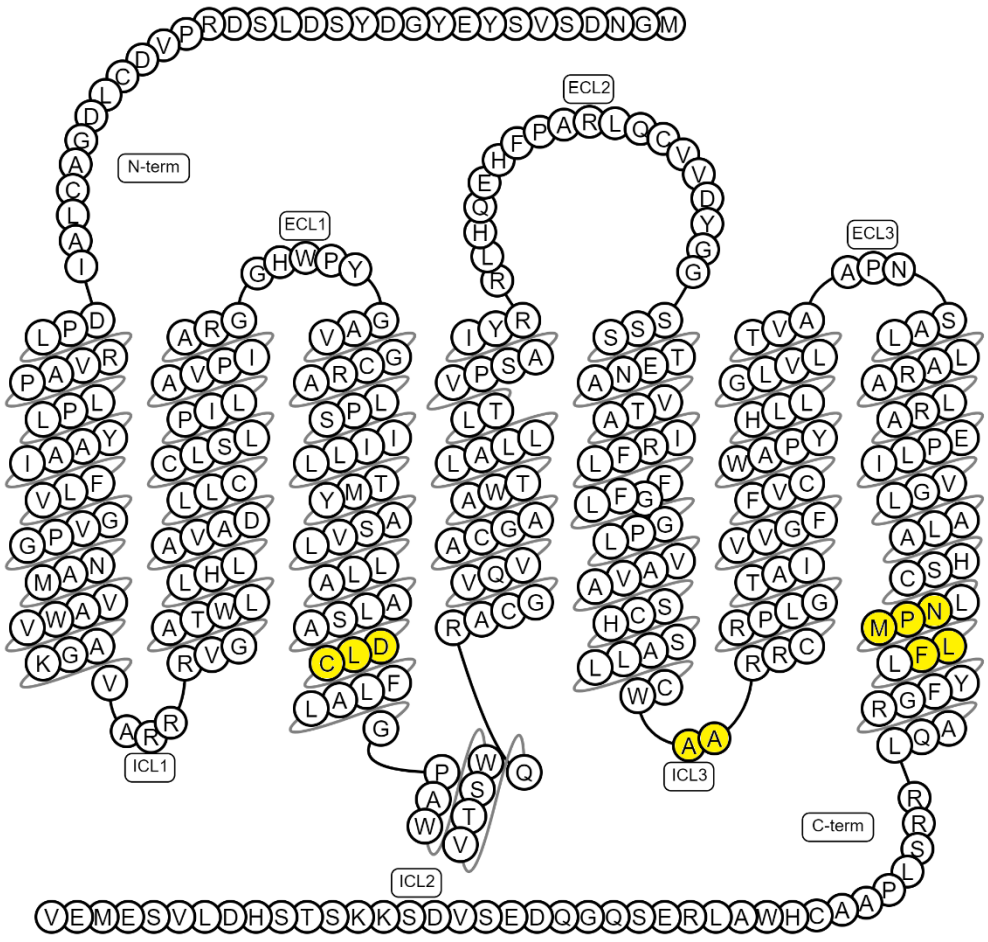

Figure 1.6. Structure of C5aR2. Amino acid structure of C5aR2 generated using GPCRdb [58]. N-Term = N-Terminus. C-Term = C-Terminus. ICL = Intracellular Loop. ECL = Extracellular Loop. Key structural differences for GPCR functionality marked in yellow.

C5aR2 has three key structural differences which prevent its canonical functionality as a GPCR [51] (**Figure 1.6**). GPCRs contain two highly conserved motifs: a Gα protein coupling motif DRY in the third transmembrane domain, and an internalisation and signal transduction sequence NPXXY in the seventh transmembrane domain. C5aR2

contains DLC instead of DRF, preventing Gα protein coupling, and NPXXF instead of NPXXY, disrupting internalisation and signal transduction. It also has a truncated third intracellular loop lacking serine and threonine residues which are important for G protein recognition in C5aR1. C5aR2 is therefore unable to couple to G proteins, and does not function as a GPCR [64, 65].

1.3.3.2. Expression

C5aR2 has a broad expression pattern. At a tissue level, C5aR2 is expressed predominantly in the blood and spleen [66]. In a study tracking fluorescently-tagged C5aR2 in murine cells, C5aR2 was found to be expressed in all myeloid cells and various additional cell types. It was highly expressed in neutrophils across all tissues, in eosinophils, dendritic cells and macrophages variably depending on tissue residence, in B cells but not naïve or activated T cells, and in tissue compartments including the brain, bone marrow and airways [67]. In this mouse study, C5aR2 was expressed in macrophages derived from bone marrow, peritoneal cavity, lamina propria of the small intestine, airways, lung tissue, visceral adipose tissue and brain. Expression was highest in peritoneal macrophages, and heterogeneous in other macrophage populations: 80-85% of lamina propria macrophages, airway macrophages and microglia expressed C5aR2, with a reduction to 60% in brain and pulmonary macrophages. In another study assessing messenger RNA (mRNA) in human cells and tissues by microarray, C5aR2 was found again to have a broad expression pattern, similar to C5aR1 but consistently at a lower level. It was expressed in various cells of the immune system, but most highly expressed on neutrophils and eosinophils [68].

The subcellular location of C5aR2 is a controversial issue in the literature. In some studies, C5aR2 is predominantly expressed intracellularly [68–70]. It has also been shown to be constitutively recycled from the plasma membrane, possibly leading to its intracellular expression [64]. However, other studies found that C5aR2 was expressed on

the plasma membrane, and upon ligation it was internalised into Rab 5/7/11^{+} endosomal vesicles before being returned to the plasma membrane [71]. These differences are likely to be cell-type and microenvironment-dependent. This is an area of great interest for future research given its controversy and potential impact for understanding the regulation of C5aR2.

1.4. C5aR2 function

1.4.1. Ligands

C5aR2 has more binding partners than the other anaphylatoxin receptor family members, as it binds to C5a, C5a-desArg, and C3a-desArg [72]. It binds to C5a and C5a-desArg with similar affinities; its affinity for C5a is similar to that of C5aR1, but its affinity for C5a-desArg is higher than C5aR1 [54]. Furthermore, C5aR2 binds to C5a and C5a-desArg by different mechanisms [73]. C5aR2 is also reported to be a receptor for C3a-desArg, which mediates changes in triglyceride synthesis and glucose transport in adipocytes [45]. However, this observation is controversial, and there is contrary evidence that C5aR2 does not bind C3a-desArg [72].

1.4.2. GPCR function

Due to the lack of key structural motifs required for G protein coupling [51], C5a stimulation of C5aR2 does not induce calcium ion mobilisation [64], phosphorylation by GPCR kinases or ligand-induced receptor internalisation [74]. This is not unprecedented in atypical GPCRs, for example D6R, which lacks the GPCR function of its canonical counterpart CCR2, similar to the relationship between C5aR2 and C5aR1 [75]. As C5aR2 lacks many of the functional features of GPCRs, it was initially proposed that C5aR2 functioned as a decoy receptor, negatively regulating C5aR1 signalling by acting as a sink for C5a by sequestering it in intracellular compartments [64]. However, more recent studies have demonstrated that C5aR2 is functionally active and able to transduce signals distinct from those driven by C5aR1.

1.4.3. Signal transduction by C5aR2

There is a growing body of evidence that C5aR2 can signal independently upon ligation by C5a, C5a-desArg or C3a-desArg. The *in vitro* evidence for signalling downstream of C5aR2 is focussed on the recruitment of β-arrestins and phosphorylation of ERK 1/2 (**Figure 1.7**).

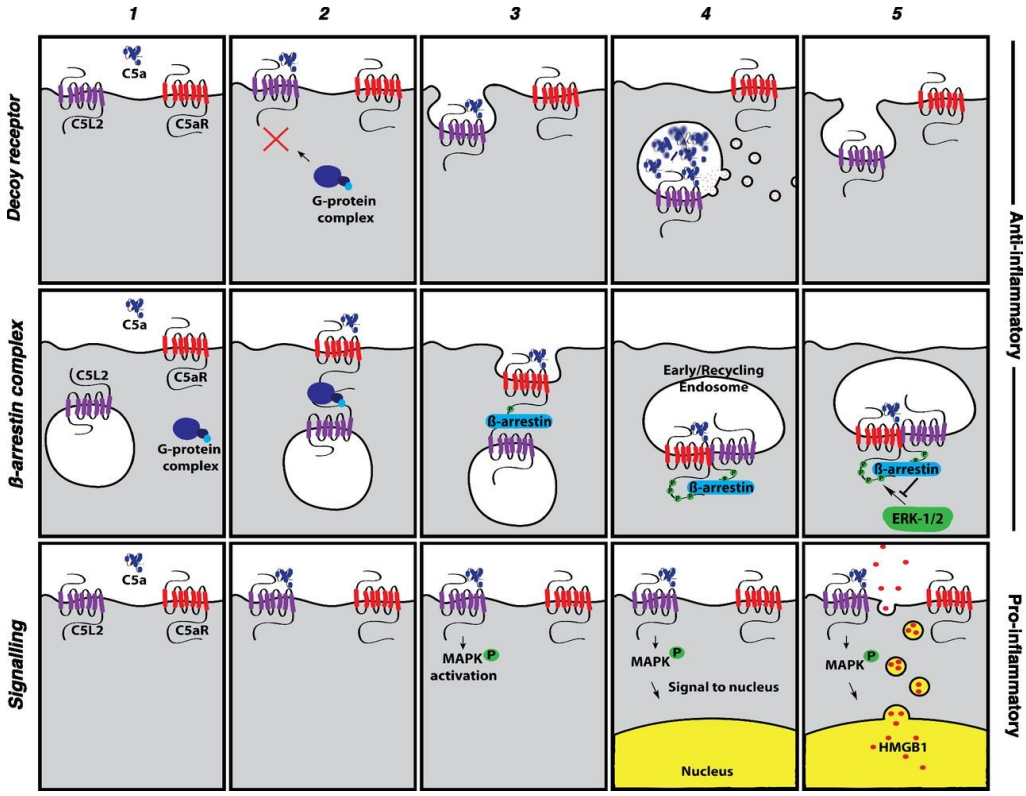

Figure 1.7. Proposed molecular mechanisms of C5aR2 function. Adapted from Li *et al.*, 2012 [69].

Top row: **C5aR2 is a decoy receptor. 1.** C5aR2 binds C5a, preventing C5aR1:C5a interaction. **2.** C5aR2 does not couple G proteins, so there is no signal transduction. **3.** C5aR2 internalises upon C5a binding. **4.** C5a is degraded in intracellular vesicles. **5.** C5aR2 is recycled to the plasma membrane.

Middle row: C5aR2 induces β-arrestin signalling. 1. C5aR2 is expressed intracellularly. **2.** C5aR1 binds C5a, recruiting a G protein heterotetramer and C5aR2 to the complex. G protein-coupled receptor kinases phosphorylate the C termini of C5aR1 and C5aR2. **3.** β-arrestin is recruited to the complex. **4.** The complex is internalised. **5.** β-arrestin prevents C5aR1 from inducing MAP kinase pathway signalling.

Bottom row: C5aR2 induces MAP kinase signalling. 1. C5aR2 is expressed on the plasma membrane. **2.** C5aR2 competitively binds C5a. **3.** C5aR2 induces MAP kinase pathway signalling. **4.** Through an unknown mechanism, C5aR2-induced MAP kinase pathway signals to the nucleus. **5.** Pro-inflammatory mediators are up-regulated.

1.4.3.1. C5aR2 and β-arrestins

C5aR2 is reported to interact with β-arrestins. Initial studies were performed on transfected human cell lines. β-arrestin recruitment to C5aR2 was first shown in HEK-293 cells (a human embryonic kidney cell line) expressing human C5aR2 and GFP-tagged β-arrestin, where 15 minutes incubation with 1 μM C5a or C5a-desArg caused the redistribution of β-arrestin [45]. This result was confirmed in a follow-up study in which C5a and C3a-desArg induced co-localisation of C5aR2 and β-arrestin in a time-dependent manner [71]. These observations were reproduced in another study using HEK293 cells which demonstrated β-arrestin 1/2 recruitment to C5aR2 using fluorescent microscopy and co-immunoprecipitations [75]. Another study using U2OS cells (a human bone osteosarcoma epithelial cell line) showed that stimulation of $C5aR2^{+}$ $C5aR1^{-}$ cells with C5a resulted in the redistribution of GFP-tagged β-arrestin into intracellular vesicles in a concentration-dependent manner [76]. Additional studies on primary human cells confirmed these observations. C5aR2 and β-arrestin were assessed using fluorescent microscopy, and co-localised upon C5a stimulation in human polymorphonuclear cells (PMNs) [68]. A similar effect was shown using a bioluminescence resonance energy transfer (BRET) assay, where C5aR2 recruited β-arrestin upon stimulation with C5a [72,77].

β-arrestins are key negative regulators of GPCRs including C5aR1. These data show that C5aR2 can independently recruit β-arrestins in response to ligand binding, and therefore suggest that C5aR2 may be able to negatively regulate C5aR1 signalling. If C5aR2 and C5aR1 can dimerise, active C5aR2-bound β-arrestin may be able to directly influence local ERK signalling initiated by complexed C5aR1. The C5aR1-dependent recruitment of C5aR2 to the cell surface may therefore be a negative regulatory mechanism for C5aR1 activity, inducing trafficking of C5aR2 from intracellular compartments to the activated C5aR1 molecule in the plasma membrane, leading to recruitment of β-arrestin to the same complex and the resultant down-regulation of

C5aR1-driven β-arrestin-sensitive G protein signalling. C5aR2 may also be responsible for initiating independent signalling downstream of β-arrestins [53], suggesting that C5aR2 may be a multi-functional receptor, acting as a decoy/sink for C5aR1, recruiting β-arrestin to C5aR1 to down-regulate its signalling, and driving its own independent signalling or regulatory functions. However, more work is required to test these hypotheses and elucidate the downstream effects.

1.4.3.2. C5aR2 and MAP kinase signalling

Alongside β-arrestins, C5aR2 is reported to activate MAP kinase signalling through phosphorylation of ERK1/2. Initial work on murine cells investigated signalling pathways in several cell types. One study examined the signalling downstream of C5aR2 in mice. It showed that both C3a and C5a induced ERK1/2 phosphorylation in neutrophils, that C3a induced AKT phosphorylation in neutrophils, that C5a induced c-Jun N-terminal Kinase (JNK) and p38 phosphorylation in neutrophils, and that C5a induced ERK1/2 and Akt phosphorylation in macrophages. C5aR2 KO reversed all of these effects [78], suggesting that C5aR2 is required for all of these downstream signalling events. Additionally, a murine model of acute experimental colitis demonstrated that C5aR2 was required for C5a-mediated ERK activation [79]. In direct contrast, another study using a rat basophilic leukaemia (RBL) cell line showed that C5aR2 did not induce ERK1/2 phosphorylation. RBLs were transfected with C5aR1 or C5aR2 plasmids, and stimulated with C5a and C5a-desArg. ERK1/2 phosphorylation was detected in $C5aR1^{+}$ cells, but neither ligand induced ERK1/2 phosphorylation in $C5aR2^{+}$ cells [77].

More recent work on human cells added to the observations on ERK1/2 phosphorylation. The same study that used transfected RBL cells assessed the effect of C5aR2 ligation on ERK1/2 in human MDMs. C5a and C5a-desArg induced ERK1/2 phosphorylation in a concentration-dependent manner, and antibody blockade of

C5aR2 increased it, suggesting that C5aR2 suppressed C5aR1-driven ERK1/2 phosphorylation in human MDMs [77]. A follow-up study by the same group using functionally selective C5aR2 agonists on human MDMs showed that C5a and C5a-desArg induced ERK1/2 phosphorylation. Stimulation of C5aR2 did not induce ERK1/2 phosphorylation, but did suppress C5a-induced ERK1/2 activation. This link was developed further in a study assessing the signalling downstream of C5aR2 using a phospho-protein array on lysates of HEK293 cells overexpressing C5aR2. C5aR2 was found to drive p90 ribosomal s6 kinase (p90RSK) phosphorylation [75], which is known to interact with the MAPK pathway [80]

Although these data are inconsistent, it must be noted that they were generated using various cell types from different species. The experiments performed on human MDMs by Croker *et al.* clearly demonstrate a C5a and C5a-desArg-dependent activation of ERK1/2, and a C5aR2-dependent suppression [72,77]. This work was performed in primary human cells, and the role of C5aR2 was validated using two separate approaches, and therefore it is convincing that C5aR2 has a role in regulation of C5aR1-induced ERK1/2 phosphorylation, possibly as a result of β-arrestin recruitment.

These studies implicate C5aR2 as a signalling receptor with roles potentially distinct from C5aR1. MAP kinase signalling occurs downstream of cytokine receptor ligation, and is thereby implicated in various chronic inflammatory diseases [81]. By regulating MAPK signalling via ERK1/2 phosphorylation, C5aR2 could therefore act as a regulator of a key driver of inflammation. As the mechanism is poorly understood, this a key area of interest for future research to elucidate the downstream mechanisms underpinning the function of C5aR2.

1.4.3.3. C5a translocation by C5aR2

A recent study has described a novel function for C5aR2 as a translocator of C5a across membrane barriers to direct neutrophil chemotaxis and induce neutrophilic

inflammation [82]. This implicates C5aR2 as a mediator of neutrophillic inflammation, which is a key early response in the innate immune response to infection or damage. However, there is no known mechanism, therefore mechanistic understanding of signalling driven by C5aR2 is critical to understand its function as a mediator of inflammation.

1.4.4. Pro- and anti-inflammatory cross-talk by C5aR2

Although the underlying signalling mechanisms are not yet well-characterised, C5aR2 has been shown to regulate pro-inflammatory signalling pathways initiated by other PRR systems.

1.4.4.1. Cross-talk between C5aR1 and C5aR2

Alongside its suggested role as a decoy receptor, C5aR2 actively regulates C5aR1 signalling by co-localisation, heteromer formation and recruitment of β-arrestin to C5aR1. Fluorescent microscopy experiments have shown that, upon stimulation by C5a, C5aR1 and C5aR2 co-localise in human PMNs [68] and MDMs [70]. Using murine cells, another study showed that C5aR2 was required for C5a-mediated internalisation of C5aR1 [79]. BRET assays were also used to demonstrate that C5a, but not C5a-desArg, induced heteromer formation between C5aR1 and C5aR2 [77,83]. These results suggest a role for C5aR2 in regulating C5aR1 activity. BRET assays were also used to demonstrate that upon formation of C5aR1 and C5aR2 heteromers, β-arrestin was recruited preferentially to C5aR2, leading to the reduction of C5aR1-dependent ERK1/2 phosphorylation in response to stimulation by C5a or selective peptide agonists [72,77]. C5aR2 is therefore able to negatively regulate C5aR1 signalling via an active recruitment of β-arrestin, rather than simply acting as a decoy receptor.

1.4.4.1. Cross-talk between TLR4, C5aR1 and C5aR2

Whilst the synergy and cross-talk between the complement system and the TLRs is well-established [84], the role of C5aR2 in this system is not as well understood. However, several studies have now suggested that C5aR2 may regulate the C5aR1-driven modulation of TLR4-induced pro-inflammatory cytokine secretion.

In mouse cells, LPS-induced IL-6 secretion was suppressed by C5a in macrophages but amplified by C5a in neutrophils. LPS-induced TNFα secretion was suppressed by C5a in both cell types. C5aR2 KO prevented the C5a-induced modulation in all cases [78]. Due to the differences in C5a-driven modulation of LPS-induced cytokine secretion between cell types, it is likely that the role of C5aR2 differs between cell types.

In human MDMs, co-stimulation with LPS and 1 nM C5a did not modulate granulocyte-colony stimulating factor (G-CSF) release, but concentrations of 100 nM and 200 nM induced C5aR1 and C5aR2 co-localisation and the subsequent amplification of G-CSF [77] demonstrating that C5aR2 is present during C5a-dependent regulation of G-CSF release. However, studies using C5a without additional genetic modulation cannot dissect the function of C5aR1 and C5aR2 as they share C5a as a common ligand.

1.4.4.2. Cross-talk between the NLRP3 inflammasome, C5aR1 and C5aR2

A similar effect to the modulation of TLR4-driven pro-inflammatory signalling has been shown on NLRP3 inflammasome activation. A study on NLRP3 inflammasome activation demonstrated that C5a suppressed LPS-induced pro-IL-1β mRNA, NLRP3 mRNA, and LPS + ATP-induced IL-1β protein production in mouse peritoneal macrophages, but amplified it in bone marrow cells [85]. C5aR1 KO led to an incomplete reduction in suppression of inflammasome activity in macrophages, suggesting that C5aR1 is not completely responsible for C5a:TLR4:NLRP3 cross-talk in macrophages. As C5aR2 is known to negatively regulate pro-inflammatory C5aR1 signalling, it may be responsible for this anti-inflammatory effect of C5a.

Limited literature is available directly linking C5aR2 and the inflammasomes. A model of sepsis in mice showed that NLRP3 and IL-1β mRNA was expressed in cardiomyocytes, but not in the absence of C5aR2, suggesting that C5aR2 can prime the NLRP3 inflammasome [86]. In mouse macrophages, C5aR2 deficiency restricted NLRP3 activation, and C5aR2 was found to drive NLRP3 activation by activating protein kinase R expression [87]. However, NLRP3 activation and C5aR2 have yet to be linked in human cells.

1.4.4.3. Cross-talk between TLR4 and C5aR2

A distinct functional role for C5aR2 in regulation of TLR4 signalling was established by Croker *et al.* (2016). In primary human MDMs, C5a suppressed LPS-induced IL-6 and TNFα secretion, and amplified IL-10 secretion. However, when stimulated with P32 or P59 (selective peptide agonists for C5aR2) there was no impact on LPS-induced TNFα or IL-10 secretion, but IL-6 secretion was suppressed in a concentration-dependent manner [72]. This shows that C5aR2 is responsible for the regulation of LPS-induced IL-6 secretion, that it is able to differentially regulate secretion of different cytokines, and that it has distinct roles from C5aR1.

1.4.4.4. Cross-talk between PRRs and C5aR2

A critical follow-up study using P32 and P59 demonstrated the role of C5aR2 as a modulator of a wide range of PRRs. C5aR2 agonism significantly reduced TLR4, TLR7, Mincle and STING-induced IL-6 secretion, and Dectin-2, Mincle and STING-induced TNF-α and IL-10 secretion in human MDMs [8]. This observation demonstrates that C5aR2 is a key negative regulator of PRR-induced cytokine secretion across a wide range of PRRs, highlighting its emerging role as a regulator of the immune response.

These observations are promising, but not without limitations. They have been generated in a single study with a single set of reagents, and have not yet been confirmed independently. There are also reported issues with P32 and P59 as C5aR2

ligands. They are partial agonists of C5aR2, cannot induce C5aR1-C5aR2 heterodimerisation (which is critical for the negative regulation of C5aR1 by C5aR2), and weakly bind to C5aR1, which may activate C5aR1 to regulate PRR signalling [8]. It is therefore critical that the regulation of TLR4, TLR7, Mincle, Dectin-2 and STING-induced NF-κB-dependent cytokine secretion by C5aR2 is confirmed in an independent study.

1.4.4.5. Summary of C5aR2 as an innate immune modulator

Taken together, these studies demonstrate that C5aR2 has a distinct and active role in the regulation of PRR-induced pro-inflammatory cytokine secretion. This is a key area of emerging interest as these PRRs are important initiators and mediators of the innate immune response. The function of C5aR2 as a modulator of PRR-induced cytokine secretion is being established, however there is no known or proposed mechanism for these effects.

1.5. C5aR2 in disease

1.5.1. C5aR2 in models of disease

In addition to *in vitro* studies, various and conflicting examples of C5aR2 mediating pro- and anti-inflammatory effects have been demonstrated *in vivo*, implicating C5aR2 as a potential therapeutic target [51,69] (**Table 1.2.**). Furthermore, the Cianflone lab have linked C3a-desArg and C5aR2 to lipid metabolism and obesity [88], meaning that C5aR2 could also play a role in the pathophysiology of chronic metabolic disorders.

However, these studies are inconsistent and contradictory [51]. Genome-wide association studies (GWAS) can be used to investigate whether genomic variants of a gene are associated with a disease or a specific trait. Genetic associations do not imply functionality and therefore do not replace *in vitro* and *in vivo* studies, but can be used to identify potential targets for research. Searching for C5aR2 in publicly available

GWAS databases shows that C5aR2 does not have any single nucleotide polymorphisms (SNPs) present in disease populations compared to healthy populations in published datasets [89]. Further *in silico* analysis of publicly available databases may highlight C5aR2 as a target, however there is currently no clear implication.

Table 1: C5aR2 KO on BALB/c background.

Source	Disease model	Properties of C5aR2
J. Köhl's laboratories, University of Lübeck, Germany	OVA- and HDM-induced experimental allergic asthma	Dual functions: anti-inflammation on mDCs, proinflammation on pulmonary cells
	TLR induction in vitro and in vivo	Dual functions: anti-inflammation—C5aR2 negatively modulates TLRs-C5aR1 on PBMCs and whole blood cells; proinflammation—C5aR2 promotes HMGB1 expression
	Peritoneal membrane fibrosis	No function
TL31 KO from Amgen, South San Francisco	DSS-induced acute colitis	Proinflammation
Lexicon Genetics, the Woodlands, Texas	OVA-sensitized, methacholine-induced asthma	Proinflammation
Dr. Craig Gerard, Harvard Medical School—C57BL/6 mice backcrossed to the BALB/c background	OX-induced experimental allergic contact dermatitis	Anti-inflammation
	LPS-induced acute lung injury	Anti-inflammation

Table 2: C5aR2 KO on C57BL/6 background.

Source	Disease model	Properties of C5aR2
B. Lu, Harvard Medical School, USA	IC-induced acute lung injury	Anti-inflammation
	Anti-mMPO-induced ANCA NCGN	Anti-inflammation
	CLP-induced sepsis and in vitro assays on leukocytes	Proinflammation and indispensable for HMGB-1 release
	CLP-induced sepsis	On CMs—proinflammation and causes cardiac dysfunction
	Acute pyelonephritis	Proinflammation
	Renal I/R injury	Proinflammation
	Experimental cerebral malaria	No function*
	S. aureus bloodstream infection	Anti-inflammation
	AKI induced by LPS, IC, or C5a	Proinflammation
Genotyping and breeding in University of Michigan according to the method of Dr. Craig Gerard	CLP-induced sepsis	Indispensable for G-CSF release by macrophages
	CLP-induced sepsis	On CMs—proinflammation: activation of the cardiac NLRP3 inflammasome
Professor A. Klos, Hannover Medical School, Germany	Wire-induced endothelial denudation of the carotid artery, diet-induced atherosclerosis	Proinflammation
The Jackson Laboratory	In vitro atherosclerosis model	On PBMCs and BMDMs—proinflammation
Lexicon Genetics, the Woodlands, Texas	Thioglycollate-induced peritonitis and air-pouch inflammation	Proinflammation
	LPS-induced septic shock	Anti-inflammation

Table 1.2. Roles of C5aR2 in disease models. Taken from Zhang, Garstka and Li, 2017.

Recent novel data described above has implicated C5aR2 as a regulator of the inflammatory response, however this has not yet led to a clear elucidation of the links between C5aR2 and disease. Rather than focussing on models of disease, it may be more fruitful to identify the fundamental signalling and function of C5aR2 by using a screening approach to associate it with known inflammatory pathways, after which the data can be considered in the context of diseases with C5aR2-associated pathogeneses. The mechanism underlying C5aR2 function must first be understood in order to direct further research into the potential role of C5aR2 as a therapeutic target.

1.5.2. Therapeutic value of targeting C5aR2

Complement has attracted recent attention as a potential therapeutic target [90]. However, targeting the complement cascade can be challenging due to the extremely high concentration of certain complement proteins in the plasma including C3, and due to the difficulty of targeting specific local events to interrupt conformational changes, for example during convertase formation. Instead, approaches to develop complement therapeutics tend to target protein-protein interactions, serine proteases to prevent proteolytic cleavage of complement proteins at sites of complement activation, siRNA to reduce expression of pathogenic complement proteins in target tissues, or GPCR antagonists to reduce anaphylatoxin receptor signalling at sites of inflammation. Eculizumab is an anti-C5 monoclonal antibody which inhibits the Terminal Pathway of complement, approved by the FDA for the treatment of paroxysmal nocturnal haemoglobinuria [91] and atypical haemolytic uremic syndrome [92]. Despite its efficacy in these diseases, it is one of the world's most expensive medicines, and only approved in rare diseases. Similarly, Ravulizumab is a recombinant monoclonal antibody which inhibits terminal complement pathway activation by targeting C5, which reduces haemolysis and thrombotic microangiopathy in atypical haemolytic uremic syndrome [93] and paroxysmal nocturnal haemoglobinuria [94]. Sutimlimab is a monoclonal antibody targeting C1s to inhibit activation of the Classical

Pathway and thereby reduce erythrocyte haemolysis [95]. Pegcetacoplan has a different mechanism of action, as it is a C3 inhibitor used to treat anaemia in patients with paroxysmal nocturnal haemoglobinuria after failure of a C5 inhibitor [96]. It is also used to treat geographic atrophy in the eyes of patients with age-related macular degeneration, which is a leading cause of blindness [97]. There are also various drugs in late-stage development, including Iptacopan, which is a Factor B inhibitor used to prevent convertase activity to restrict haemolysis in paroxysmal nocturnal haemoglobinuria [98], Crovalimab, which is an anti-C5 monoclonal antibody which recycles bound C5 antigen in endosomes to increase its target binding capacity and aims to treat of paroxysmal nocturnal haemoglobinuria [99], and Narsoplimab, a MASP-2 inhibitor used to reduce Lectin Pathway activation in adult haematopoietic stem cell Transplantation-associated thrombotic microangiopathy [100].

Despite the recent successes in complement-based therapeutics, there remains a great deal of potential for targeting the complement system in inflammatory and autoimmune disease [90]. Targeting the anaphylatoxin receptors may be a useful approach to impact the broad inflammatory functions of the complement system. Avacopan is a small molecular antagonist of C5aR1 which selectively blocks the effect of C5a [101]. It is licensed for use in anti-neutrophil cytoplasmic antibody-associated vasculitis in the USA, and in microscopic polyangiitis and granulomatosis with polyangiitis in Japan [102]. It is a first-in-class C5a receptor inhibitor, providing a novel approach to treat complement-mediated disease, and proof-of-concept for anaphylatoxin receptor inhibitors. Due to its emerging immunomodulatory functions and implication across a wide range of disease phenotypes, specific exploration of the signalling and function of C5aR2 will direct and develop its potential as a novel therapeutic target.

1.6. Aims

C5aR2 is an important receptor of the innate immune system as it has been demonstrated to signal independently and modulate PRR-induced cytokine secretion in macrophages. However, the literature is inconsistent, and the molecular mechanisms underpinning the function of C5aR2 remain largely unexplored. The tools with which to study C5aR2 are also limited and poorly validated.

This project therefore aims to validate existing tools and generate novel tools with which to study C5aR2, and use them to further characterise the inflammatory function of C5aR2 and investigate the key molecular mechanisms underpinning it. Understanding these mechanisms will facilitate exploration of the therapeutic potential of targeting C5aR2 in infectious and inflammatory diseases in the future.

The central hypothesis of this project is that C5aR2 regulates the PRR system in macrophages. To address this hypothesis, this project aims to:

- Validate the effect of selective peptide agonists P32 and P59 on ERK1/2 phosphorylation in MDMs [72], and assess additional endpoints using the validated stimulation conditions.
- Generate stable monoclonal C5aR1 and C5aR2 knockout (KO) THP-1 cell lines using CRISPR-Cas9 to use as a novel and reliable tool with which to study C5aR2.
- Validate C5aR2-dependent modulation of PRR-induced cytokine secretion [8] using the novel C5aR2 KO THP-1 cells, and investigate the underlying mechanisms using molecular biology approaches.
- Use RNAseq to identify key genes and pathways involved in the downstream signalling of C5aR2 following C5a stimulation, and in the context of PRR stimulation.

Chapter 2 - Materials and Methods

2. Materials and Methods

2.1. Materials

2.1.1. Reagents

Reagent	Supplier	Reference #
1.5 mL Microcentrifuge tube	Fisherbrand	05-408-129
12-230 kDa Separation Module for Peggy sue or Sally Sue Systems	ProteinSimple	SM-S001
15 mL Falcon tube	Corning	352097
50 mL Falcon tube	Corning	352070
50 mL Leucosep tube	Greiner Bio-one	227290
96-well V-bottom PCR Microplate	Eppendorf	10258984
Alt-R S.p. Cas9 Nuclease V3 Protein	IDT	1081059
Attune performance tracking beads	Invitrogen	449754
Bambanker	Lymphotec	14681
BSA Solution, 30% in PBS	Sigma Aldrich	A9676- 50ML
$CaCl_2$	Sigma	C3881-500g
Calibrator 1	MSD	C0060-2
CD14 microbeads, human	Miltenyi Biotech	130-050-201
Cell Staining Buffer	Biolegend	420201
Cellstar 96 well cell culture plate, sterile, flat bottom with lid	Greiner Bio-one	655180
Cellstar 96-well U-bottom microplate, clear, Cellstar TC with lid, sterile, single packed	Greiner Bio-one	650180
CellTiter-Glo Luminescent Cell Viability Assay	Promega	G7570
Costar 24-well Clear TC-Treated Multiwell Plate	Corning	3524
Costar 6-well Clear TC-treated Multiple Well Plate	Corning	3516
Custom primers Details below	IDT	-
Detachin	Gelantis	T100100
Diluent 3	MSD	R50AP-2
Diluent 43	MSD	R50AG-1
DPBS (-Ca^{2+}/-Mg^{2+})	Gibco	14190-094
EasySeal Plate Sealers	Greiner Bio-one	676001
EDTA, Ultrapure, 0.5M, pH 8.0	Invitrogen	03690
E-Gel 1 Kb Plus DNA Ladder	Invitrogen	10488090
E-Gel Agarose Gel with SYBR Safe DNA Gel Stain, 2%	Invitrogen	A42135
E-Gel EX Agarose Gel, 2%	Invitrogen	G401002

E-Gel Sample Loading Buffer, 1x	Invitrogen	10482055
ERK1/2 (pT202/Y204) + Total ERK1/2 SimpleStep ELISA Kit	Abcam	Ab176660
Falcon 25 cm^3 Rectangular Canted Neck Cell Culture Flask with Vented Cap	Corning	353108
Falcon 5 mL Round Bottom polystyrene test tube (Flow cytometry tube)	Corning	352052
Falcon 75cm^2 Rectangular Canted Neck Cell Culture Flask with Vented Cap	Corning	353136
FBS	Gibco	10500-064
Ficoll Paque Plus	GE Healthcare	17-1440-03
Fixation Buffer	Biolegend	420801
Formalin Solution, 10% Neutral Buffered	Sigma Aldrich	HT5012-60ML
Gene KO Kit V2 – C5aR1, C5aR2	Synthego	-
Gene KO Kit V2 – Non-targeting control GeCKO v2 Human CRISPR KO Pooled Library, Addgene #1000000048, #1000000049	Synthego	-
Halt Protease and Phosphatase Inhibitor Cocktail (100x)	Thermo Fisher Scientific	78440
Hoescht	Thermo Fisher Scientific	62249
Human IFN-β DuoSet ELISA	R&D Systems	DY814-05
Human TruStain FcX Fc Receptor Blocking Solution	Biolegend	422302
Intracellular Staining Permeabilisation Buffer	Biolegend	421002
L-glutamine Stock concentration 200 mM	Gibco	25030-024
Lipofectamine 2000 Transfection Reagent	Thermo Fisher Scientific	11668019
LS Column	Miltenyi Biotech	130-042-401
M-CSF	R&D Systems	216-MC/CF
$MgCl_2$	Sigma	M2670-500g
MQ-H_2O	GSK	-
Mr Frosty Freezing Container	Thermo Fisher Scientific	5100-0001
Nuclease-Free Duplex Buffer	IDT	11-01-03-01
Nuclease-Free Water	Invitrogen	AM9932
Nunc Lab-Tek II Chamber Slide Systems	Thermo Fisher Scientific	154534
Nunc MaxiSorp flat-bottom plate for ELISA	Invitrogen	44-2404-21
P3 Primary Cell 4D Nucleofector Kit S	Lonza	#V4XP-3032
Penicillin/Streptomycin 10,000 U/mL	Gibco	15140-122
Phusion High Fidelity PCR Master Mix	Thermo Fisher Scientific	
Pierce Rapid Gold BCA Protein Assay Kit	Thermo Fisher Scientific	A53225

Pierce RIPA Lysis and Extraction Buffer, 100 ml	Thermo Fisher Scientific	89900
PMA	Sigma Life Science	P1585-1MG
Proteinase K	Thermo Fisher Scientific	17916
PureLink Pro 96 Purification Kit	Thermo Fisher Scientific	K310096A
QIAquick Gel Extraction Kit	Qiagen	28704
QIAquick PCR Purification Kit	Qiagen	28104
QIAshredder	Qiagen	79656
Read Buffer T (4x)	MSD	R92TC-1
Reagent Diluent Concentrate 2 for ELISA	R&D Systems	DY995
RPMI 1640 Medium	Gibco	11875093
Saponin	Sigma Aldrich	S130-2
Stop Solution	MSD	R50A0-1
Stop solution 2N Sulphuric Acid for ELISA	R&D Systems	DY994
Substrate Reagent Pack for ELISA	R&D	DY999
TaqMan Assays C5aR2 Primer A-D	Thermo Fisher Scientific	4351372, Hs00218495_m1
THP-1 cells, WT GSK Biocat 140554	ATCC	TIB-202
Tris EDTA (pH 7.4)	Thermo Fisher Scientific	BP2477-500g
Triton X-100	Sigma Aldrich	X100-1L
U-Plex 5-Assay 96-well Sector Plate	MSD	N05230A-1
U-Plex Linker 1	MSD	E2226-3
U-Plex Linker 10	MSD	E2235-3
U-Plex Linker 3	MSD	E2228-3
U-Plex Linker 8	MSD	E2233-3
Vectashield antifade mounting medium for fluorescence	Vector laboratories	H-1000
Via2-Cassette	Chemometec	941-0024

Table 2.1. Reagents and consumables.

2.1.2. Antibodies

Reagent	Supplier	Reference #
Alexa Fluor 488 goat anti-mouse IgG (H+L)	Invitrogen	A11017
Anti-C5aR1 Purified anti-human CD88 (C5aR) antibody Mouse IgG2a, κ mAb, Clone S5/1 Stock concentration: 1 mg/mL	Biolegend	344302
Anti-C5aR1-APC Purified anti-human CD88 (C5aR) antibody, APC conjugate Mouse IgG2a, κ mAb, Clone S5/1 Stock concentration: 100 µg/mL	Biolegend	344310
Anti-C5aR2 anti-human C5aR2 antibody Mouse IgG2a, κ mAb, Clone 1D9-M12 Stock concentration: 400 µg/mL	Biolegend	342402
Anti-C5aR2-APC anti-human C5aR2 antibody, APC conjugate Mouse IgG2a, κ mAb, Clone 1D9-M12 Stock concentration: 400 µg/mL	Biolegend	342406
anti-IRF3 Rabbit mAb Clone EPR2418Y	Abcam	ab68481
Anti-Mouse Detection Module for Jess, Wes, Peggy Sue or Sally Sue	ProteinSimple	DM-002
Anti-phospho-IRF3 (Ser386) XP Rabbit mAb Clone E7J8G	Cell Signaling Technology	37829
Anti-phospho-STING (Ser366) Rabbit mAb Clone E9A9K	Cell Signaling Technology	50907
Anti-Rabbit Detection Module for Jess, Wes, Peggy Sue or Sally Sue	ProteinSimple	DM-001
Anti-STING Polyclonal antibody, Rabbit pAb	Thermo Fisher Scientific	PA5-23381
Anti-β-Actin mouse mAb AC-15	Abcam	Ab6276
Biotin Human IL-10 Capture Antibody	MSD	C21TZ-3
Biotin Human IL-1β Capture Antibody	MSD	C21TU-3
Biotin Human IL-6 Capture Antibody	MSD	C21TX-3
Biotin Human TNFα Capture Antibody	MSD	C21UC-3
Isotype control antibody (IgG2a, κ)	Biolegend	400202
Isotype control antibody-APC, 100 µg/mL	Biolegend	400222
Sulfo-Tag Human IL-10 Detection Antibody	MSD	D21TZ-3
Sulfo-Tag Human IL-1β Detection Antibody	MSD	D21TU-3
Sulfo-Tag Human IL-6 Detection Antibody	MSD	D21TX-3
Sulfo-Tag Human TNFα Detection Antibody	MSD	D21UC-3

Table 2.2. Antibodies.

2.1.3. Agonists and antagonists

Reagent	Supplier	Reference #
BX795 TBK1/IKKε inhibitor – InvitroFit, 5 mg	Invivogen	Tlrl-bx7
C5a	Complement Technologies	A144
cAIM(PS)$_2$ Difluor (Rp/Sp) cAIMP bisphosphorothioate and difluorinated STING agonist, 2 x 100 ug	Invivogen	Tlrl-nacairs-2
G3-YSD Y-form DNA, cGAS agonist, 200 µg	Invivogen	Tlrl-ydna
H-151 Synthetic Indole Derivative STING Inhibitor – InvitroFit, 10 mg	Invivogen	Inh-h151
LPS-EK Ultrapure Ultrapure lipopolysaccharide from *E. coli* K12 TLR4 agonist	Invivogen	Tlrl-peklps
P32 Ac-RHYPYWR-OH Mw = 1118.541 Stock concentration = 10 mg/mL = 8.9402 mM	GSK Albert Isidro Llobet	N67876-80-1
P59 Ac-LIRLWR-OH Mw = 897.555 Stock concentration = 10 mg/mL = 11.1414 mM	GSK Albert Isidro Llobet	N67876-80-2
Pam3CSK4 Synthetic triacylated lipopeptide; TLR2/TLR1 agonist, 1 mg	Invivogen	Tlrl-pms
PMX53	Tocris	5473
PMX53c	Tocris	5697

Table 2.3. Agonists and antagonists.

2.1.4. Buffers

Buffer	Components
Culture medium	RPMI 1640 Medium
	10% foetal bovine serum
	2 mM L-glutamine
	100 U/mL Penicillin-streptomycin
MACS buffer	DPBS
	0.5% BSA
	2 mM EDTA
CRISPR Lysis Buffer	1 mM $CaCl_2$
	3 mM $MgCl_2$,
	1% (v/v) Triton X-100
	10 mM Tris EDTA
	0.2 mg/mL Proteinase K (added fresh before lysis)
Staining Medium	DPBS
	0.02% BSA
Permeabilisation medium	Staining Medium
	0.02% Saponin
Peggy Sue Lysis Buffer	Pierce RIPA Lysis and Extraction Buffer
	1:100 Halt Protease and Phosphatase Inhibitor Cocktail

Table 2.4. Buffers.

2.1.5. Guide RNA Sequences

Guide RNA	Sequence
Non-targeted control (NTC)	GCACTACCAGAGCTAACTCA
C5aR1	ATCAGGGGTGGTATAATTGA
	TTTTATCCACAGGGGTGTTG
	CTGCAAAGATGACCAAGGCC
C5aR2	ATTCTGTCAGCTACGAGTAT
	GGCCATCGACCCGCTGCGCG
	GGGGGTGCCGGGCAATGCCA
AJ C5aR2 KO	CTGAACCGTAGACCACC

Table 2.5. Guide RNA sequences.

2.1.6. Primer Sequences

Desired amplicons spanned 250bp up-stream and 250bp down-stream from the centre of the guide RNA target sequence. Primers for this amplicon were designed using Primer-BLAST (NCBI).

C5aR1		
Primer Pair 1	Forward	GCAGGAGAGGAAGTCGGCTA
	Reverse	AGAAAAAGCCACACAGGGGA
Primer Pair 2	Forward	CGCCAAGTTGAGGAACCAGAT
	Reverse	AGCCCTCAGCATCCCCATTT
Primer Pair 5	Forward	GGGCCAGTGGTGATGCTGTA
	Reverse	CACACAGGGGAAAAGCCACAT
C5aR2		
Primer Pair 1	Forward	AAGCACTGGAGTCCTTATGACG
	Reverse	ACAAACAGCACAGCAAATCCG
Primer Pair 5	Forward	ATATTCCAGTTTGCAAGGTGCTG
	Reverse	AACAGCACAGCAAATCCGCC
Primer Pair 6	Forward	CACTGGAGTCCTTATGACGCAAT
	Reverse	CAGAGACAAACAGCACAGCAAA
New Primer 1	Forward	TGATGGACACCCTAGATCTCC
	Reverse	AGGATGATGGAGGGCAGC
New Primer 2	Forward	ACCCGGCCTAGAATTCCAAT
	Reverse	AGGATGGGCAGAGACAAACA
New Primer A	C5aR2, FAM-MGB-conjugated	
	Hs00218495_m1, P19022-012 G11	
New Primer B	C5aR2, FAM-MGB-conjugated	
	Hs00218495_m1, P190223-003 D01	
New Primer C	GPR77, FAM-MGB-conjugated	
	Hs00218495_m1, 1408956 B1	
New Primer D	C5aR2, FAM-MGB-conjugated	
	Hs00218495_m1, 1659181 C5	
AJ Original Primer Pair 1	Forward	CACTGTATGCCGCCATCTTC
	Reverse	TGTCACGGGAGGACACGA

AJ Original Primer Pair 2	Forward	GATTTGCTGTGCTGTTTGTCTC
	Reverse	GTGGGATGGTGGACGACC
AJ Primer Pair 1	Forward	GCTGTGCTGTTTGTCTCTGC
	Reverse	CATTCTCGGTGCTGGAGGAG
AJ Primer Pair 2	Forward	CCTGCTGACCATGTATGCCA
	Reverse	CCGTAGTCCACCACACACTG
AJ Primer Pair 3	Forward	CCTCCATCATCCTGCTGACC
	Reverse	AGAAACCGGATGGCAGTCAC
AJ Primer Pair 4	Forward	GCGGATTTGCTGTGCTGTTT
	Reverse	AAGAAACCGGATGGCAGTCA
AJ Primer Pair 5	Forward	CCCTCCATCATCCTGCTGAC
	Reverse	ATGGCAGTCACCGCATTCTC
AJ Long Primer Pair 1	Forward	AGCACTGGAGTCCTTATGACG
	Reverse	GAAACCGGATGGCAGTCACC
AJ Long Primer Pair 4	Forward	CACCACACCCGGCCTAGAAT
	Reverse	GGATGGCAGTCACCGCATT
AJ Long Primer Pair 5	Forward	AAGCACTGGAGTCCTTATGACG
	Reverse	AAGAAACCGGATGGCAGTCAC
AJ Long Primer Pair 8	Forward	CATGGAGTTTCCTCCTCTGAGT
	Reverse	GCCAAAAAGAAACCGGATGG
AJ Long Primer Pair 10	Forward	ATATTCCAGTTTGCAAGGTGCT
	Reverse	GCCCCAGGAAGCCAAAAAGAA

Table 2.6. Primer sequences.

2.1.7. Equipment

Equipment	**Manufacturer**
405 LS Microplate Washer	BioTek
Airyscan LSM880	Zeiss
Attune NxT Flow Cytometer	Thermo Fisher Scientific
Bioclass 2 Safety Cabinet	Contained Air Solutions
E-Gel iBASE	Invitrogen
E-Gel Imager System with Blue Light Base	Invitrogen
Heracell VIOS 160i CO_2 incubator	Thermo Scientific
Heraeus Multifuge 3L-R	Heraeus
MSD Sector Imager	MSD
Nanodrop 8000 Spectrophotometer	Thermo Fisher Scientific
NucleoCounter NC-200	Chemometec
Nucleofector 4D	Lonza
NxT Attune	Life Technologies
Peggy Sue	ProteinSimple
Pherastar FSX	BMG
SimpliAmp Thermal Cycler	Applied Biosystems
Titramax 1000 Plate Shaker	Heidolph
Veriti 96-well Thermal Cycler	Applied Biosystems

Table 2.7. Equipment.

2.1.8. Software

Software	Version	Supplier
Attune NxT Software	3.1	Life Technologies
BioEdit	7.2.5	Tom Hall [103]
Clustal Omega	-	EMBL-EBI [104]
Compass for SW	5.0.1	ProteinSimple
Excel v2202	2202	Microsoft
FlowJo	10.8.1	FlowJo, LLC
ICE Analysis	3.0	Synthego
ND-1000	3.8.1	Thermo Fisher Scientific
PANTHER	17.0	National Science Foundation [105]
Pherastar FSX	5.70	BMG Labtech
Primer-BLAST	-	NCBI
Prism v8.1.2.	8.1.2	Graphpad
R	4.0.3	R Project [106]
Spotfire	11.4.4	Tibco
STRING	-	STRING Consortium [107]
Zen	2.6	Zeiss

Table 2.8. Software.

2.2. Methods

2.2.1. Human cell culture

The human biological samples were sourced ethically and their research use was in accord with the terms of the informed consents under an IRB/EC approved protocol.

2.2.1.1. MDM culture

2.2.1.1.1. Isolation of peripheral blood mononuclear cells by density gradient centrifugation

Whole human blood treated with 1 U/mL heparin sodium anticoagulant was collected from healthy volunteers at the on-site Blood Donation Unit. 15 mL of Ficoll Paque Plus (GE Healthcare) was added to Leucosep tubes (Greiner Bio-One) and centrifuged for 1 minute at 520 x *g* to transfer the Ficoll Paque Plus below the frit. Blood was diluted 12 with Dulbecco's Phosphate-Buffered Saline (DPBS) (Gibco), and 25 mL diluted blood was transferred above the frit of each Leucosep tube. The tubes were centrifuged for 20 minutes at 520 x *g* with no brake to separate the blood components. The peripheral blood mononuclear cell (PBMC) layers were transferred into 50 mL Falcon tube (Corning), DPBS was added up to 50 mL and the tube was centrifuged for 5 minutes at 300 g. The supernatant was aspirated and discarded. The PBMCs were washed by re-suspending the pellet in 50 mL DPBS and centrifuging for 5 minutes at 300 x *g* to maximise the removal of Ficoll Paque Plus. The supernatant was aspirated and discarded, and the pellet was re-suspended in 50 mL DPBS. A 1 mL aliquot of this cell suspension was removed to assess cell number and viability using a Nucleocounter NC-200 (Chemometec).

2.2.1.1.2. Isolation of $CD14^+$ monocytes by MACS positive selection

The PBMCs were centrifuged at 300 x *g* for 5 minutes, the supernatant was aspirated and discarded, and the pellet was re-suspended in 20 µL human CD14 MicroBeads

(Miltenyi) and 80 µL Magnetic-Activated Cell Sorting (MACS) buffer per 1 x 10^7 cells. The PBMCs were incubated at 4°C for 15 minutes, then diluted with 20 mL MACS buffer and centrifuged at 300 x *g* for 5 minutes. The supernatant was aspirated and discarded, and the pellet was re-suspended in 500 µL MACS buffer. An LS column (Miltenyi) was placed inside a magnetic field and primed with 5 mL MACS buffer. The PBMCs were transferred to the column and rinsed with 3 x 3 mL MACS buffer. The flow-through was discarded, the LS column was removed from the magnetic field, and 5 mL MACS buffer was forced through, collecting the $CD14^+$ cells in a 50 mL Falcon tube. These cells were diluted using 45 mL DPBS, and a 1 mL aliquot of this cell suspension was removed to assess cell number and viability using a Nucleocounter NC-200.

2.2.1.1.3. Culture of monocyte-derived macrophages

The $CD14^+$ monocyte suspension was centrifuged at 300 x *g* for 5 minutes, the supernatant was aspirated and discarded, and the pellet was re-suspended using culture medium. M-CSF (R&D Systems) was added at 100 ng/mL, and the $CD14^+$ monocytes were transferred to 96-well flat-bottom cell culture plates (Greiner Bio-One) at 1 x 10^5 cells/well in 100 µL. The $CD14^+$ monocytes were differentiated into MDMs at 37 °C, 5% CO_2 in a humidified atmosphere in an incubator for 5 days before use in experiments.

2.2.1.2. THP-1 cell culture

2.2.1.2.1. Thawing and initial culture of THP-1 cells

Cryopreserved aliquots of 1 x 10^7 THP-1 cells were thawed in a 37°C water bath until a small pellet of frozen medium remained, then quickly transferred to 50 mL Falcon tube containing 20 mL pre-warmed culture medium. The vial was rinsed using to maximise recovery. The cells were centrifuged at 350 x *g* for 5 minutes, the supernatant was aspirated and discarded, and the pellet was re-suspended in 20 mL pre-warmed

culture medium. The cell suspension was transferred to a 25 cm^3 flask and incubated at 37°C, 5% CO_2 in a humidified atmosphere.

2.2.1.2.2. Maintenance of THP-1 cell cultures

THP-1 cells were maintained in culture between 0.2 x 10^6 cells/mL and 1 x 10^6 cells/mL. They were passaged twice weekly by removing 8 x 10^6 cells from culture, centrifuging at 350 x *g* for 5 minutes, discarding the supernatant and re-suspending at 0.2 x 10^6 cells/mL in 40 mL culture medium to generate a cell density of 0.2 x 10^6 cells/mL. Cells were used in experiments at passage 15 or below.

2.2.1.2.3. Differentiation of THP-1 cells using PMA

A 1 mL aliquot of the THP-1 cell culture was counted using a Nucleocounter NC-200. Cells to be used in experiments were removed from culture and transferred to a 50 mL conical tube and centrifuged at 350 x *g* for 5 minutes. Supernatants were aspirated and discarded, and cells were re-suspended in culture medium containing 20 nM PMA (Merck). Cells were differentiated at 37°C, 5% CO_2 in a humidified atmosphere for 24 hours, followed by a 24 hour rest in fresh culture medium lacking PMA. Adherent differentiated THP-1 cells were then used in experiments.

Cells were differentiated in 96-well flat-bottom cell culture plates at 100,000 cells/well in 100 µL, Lab-Tek II Chamber Slide Systems (Thermo Fisher Scientific) coated with 0.1% gelatin (STEMCELL Technologies) at 80,000 cells/chamber in 400 µL, 6-well cell culture plates at 2 x 10^6 cells/well in 2 ml, or 75 cm^3 cell culture flasks (Thermo Fisher Scientific) at 1 x 10^7 cells/flask in 20 ml.

2.2.1.2.4. Cryopreservation of THP-1 cells

THP-1 cells were cryopreserved at a low passage. 1 x 10^7 cells were removed from culture and transferred to a 15 mL conical tube. The cells were centrifuged at 350 x *g* for 5 minutes, the supernatant was aspirated and discarded, and the cell pellets were

re-suspended in 1 mL DPBS. The cell suspensions were transferred to 1 mL microcentrifuge tubes, and centrifuged at 350 x *g* for 5 minutes. The supernatant was aspirated and discarded, and the cell pellets were re-suspended in 1 mL Bambanker (Lymphotec). The microcentrifuge tubes were transferred to -80°C storage in a Mr Frosty (Thermo Fisher Scientific) for 24 hours, then transferred to liquid nitrogen storage for long-term storage.

2.2.2. ERK1/2 phosphorylation experiments

2.2.2.1. Experimental Treatment Conditions

2.2.2.1.1. C5a Titration

MDMs were incubated with 0-1000 ng/mL C5a (Complement Technologies) for 10 minutes. Incubation with 100 nM PMA for 10 minutes was used as a positive control.

2.2.2.1.2. PMX53 Titration

MDMs were incubated with 0-1000 nM C5aR1 antagonist PMX53 (Tocris) or inactive control peptide PMX53c (Tocris) for 30 minutes, followed by 50 ng/mL C5a for 10 minutes. Incubation with 100 nM PMA for 10 minutes was used as a positive control.

2.2.2.1.3. Anti-C5aR2 Titration

MDMs were incubated with 0-1000 nM anti-C5aR2 mAb (1D9-M12) (Biolegend) or isotype control antibody (IgG2a, κ) (Biolegend) for 30 minutes, followed by 50 ng/mL C5a for 10 minutes. Incubation with 100 nM PMA for 10 minutes was used as a positive control.

2.2.2.1.4. C5aR2 Agonist Titration

MDMs were incubated with 0-500 µM P32 (Ac-RHYPYWR-OH) or P59 (Ac-LIRLWR-OH) for 30 minutes, followed by 50 ng/mL C5a for 10 minutes. Assay controls were established by incubating MDMS with 0 or 1 µM PMX53 for 30 minutes, followed by

50 ng/mL C5a for 10 minutes. Incubation with 100 nM PMA for 10 minutes was used as a positive control.

2.2.2.1.5. C5aR2 Agonist Time Course

MDMs were incubated with 100 µM P32 or P59 for 0-4 hours, followed by 50 ng/mL C5a for 10 minutes. Assay controls were established by incubating MDMs with 0 or 1 µM PMX53 for 30 minutes, followed by 50 ng/mL C5a for 10 minutes. Incubation with 100 nM PMA for 10 minutes was used as a positive control.

2.2.2.2. Phospho-ERK

2.2.2.3. ELISA

ERK1/2 (pT202/Y204) + Total ERK1/2 SimpleStep ELISA Kits (Abcam) were used to generate THP-1 cell lysates and measure ERK1/2 phosphorylation. OD_{450} data were acquired using a Pherastar FSX (BMG).

2.2.3. Generation of polyclonal NTC, C5aR1 KO, C5aR2 KO and C5aR1/2 DKO THP-1 cells

CRISPR-Cas9 is a widely-used molecular biology tool for sequence specific RNA-guided genome editing. Synthetic single guide RNA (sgRNA) (comprised of CRISPR RNA (crRNA) complementary to the target DNA, and tracrRNA which forms a complex between crRNA and Cas9) is used to guide Cas9 nucleases to target DNA. Ribonucleoprotein (RNP) complexes comprised of sgRNA and Cas9 are transfected into electroporated target cells, wherein Cas9 cleaves DNA to introduce double-stranded breaks in order to disrupt expression of the target gene.

THP-1 cells were thawed from low passage cryopreserved stocks and cultured until sufficient cells were available to perform the CRISPR-Cas9 genome editing experiment.

2.2.3.1. RNP assembly

The following sgRNA was used:

- NTC sgRNA (GeCKO v2 Human CRISPR KO Pooled Library, Addgene #1000000048, #1000000049) [108]

  GCACTACCAGAGCTAACTCA

- C5aR1 Gene KO Kit V2 (Synthego)

  ATCAGGGGTGGTATAATTGA

  TTTTATCCACAGGGGTGTTG

  CTGCAAAGATGACCAAGGCC

- C5aR2 Gene KO Kit V2 (Synthego)

  ATTCTGTCAGCTACGAGTAT

  GGCCATCGACCCGCTGCGCG

  GGGGGTGCCGGGCAATGCCA

1.5 nmol NTC, C5aR1 or C5aR2 sgRNA was reconstituted at 100 µM with 15 µL Nuclease-Free Duplex Buffer (IDT). For each reaction, 100 µM sgRNA was diluted to 25 µM using Nuclease-Free Duplex Buffer (1 µL sgRNA + 3 µL Nuclease-Free Duplex Buffer per reaction). For NTC cells, 1 µL NTC sgRNA was combined with 3 µL Nuclease-Free Duplex Buffer. For C5aR1 KO cells, 1 µL C5aR1 sgRNA was combined with 3 µL Nuclease-Free Duplex Buffer. For C5aR2 KO cells, 1 µL C5aR2 sgRNA was combined with 3 µL Nuclease-Free Duplex Buffer. For C5aR1/2 DKO cells, 0.5 µL C5aR1 KO sgRNA mix and 0.5 µL C5aR2 sgRNA mix was combined with 3 µL Nuclease-Free Duplex Buffer.

1 µL Alt-R S.p. Cas9 Nuclease V3 Protein (IDT) was added to each mixture, and the mixtures were incubated at RT for 10 minutes to allow RNP to form.

2.2.3.2. Electroporation and Cationic Lipid Transfection of RNP

Electroporation and cationic lipid transfection were used to transfect THP-1 cells with RNP using P3 Primary Cell 4D Nucleofector Kit S (Lonza). 250,000 cells were suspended in 16.1 µL P3 Buffer (Lonza) per reaction, then mixed with 3.9 µL RNP (NTC, C5aR1, C5aR2, or C5aR1/2) and transferred into a Nucleocuvette Strip. Cells were electroporated using protocol DE148 on a Lonza 4D-Nucleofector.

2.2.3.3. Polyclonal KO THP-1 cell culture maintenance

Electroporated polyclonal NTC, C5aR1 KO, C5aR2 KO, C5aR1/2 DKO THP-1 cells were transferred into wells of a 24-well cell culture plate (Corning) containing 2 mL pre-warmed culture medium. The plate was incubated at 37°C, 5% CO_2 in a humidified atmosphere for 4 days.

50,000 cells were removed from each culture and transferred into a microcentrifuge tube. The tubes were centrifuged at 350 x *g* for 5 minutes, the supernatants were aspirated and discarded, and the cell pellets were re-suspended in 1 mL DPBS. The tubes were centrifuged at 350 x *g* for 5 minutes, the supernatant was aspirated and discarded, and the cell pellets were stored at -80°C for lysis and characterisation of bulk-edited populations by PCR and sequencing (**2.2.5**).

The cultures were then transferred to 10 mL pre-warmed culture medium in a 25 cm^2 cell culture flask (Thermo Fisher Scientific) and maintained in culture until confluent (1 x 10^6 cells/mL). The cultures were transferred to 40 mL pre-warmed culture medium in 75 cm^3 cell culture flasks. These cultures were established, then were maintained as in **2.2.1.2.3.** and cryopreserved as in **2.2.1.2.4.**

2.2.4. Generation of AJ C5aR2 KO THP-1 cells using CRISPR-Cas9

AJ C5aR2 KO cells were generated using the protocol described in **2.2.3.** with an alternative C5aR2 gRNA (CUGAACCGUAGACCACC) (Invitrogen) by Abbie Jayyaratnam (GSK) and Darren Gormley (GSK).

2.2.5. Characterising KO cells by PCR and Sanger sequencing analysis

2.2.5.1. PCR

Cell pellets from **2.2.3.3.** were lysed using 20 µL CRISPR Lysis Buffer + 0.2 mg/mL Proteinase K (Thermo Fisher Scientific), and lysates were transferred to a V-bottom 96-well PCR plate (Eppendorf). The lysates were incubated in a SimpliAmp Thermal Cycler (Applied Biosystems) at 65 °C for 15 minutes (to activate proteinase K to deactivate nucleases) then 95 °C for 10 minutes (to denature proteinase K).

A PCR mixture was prepared in a V-bottom 96-well PCR plate. 2 µL lysate was used unless otherwise stated, adjusting the volume of nuclease-free H_2O to generate a final reaction volume of 20 µL. The following reagents were combined per reaction:

- 10 µL Phusion High Fidelity PCR Master Mix (Thermo Fisher Scientific)
- 6 µL Nuclease-free H_2O
- 1 µL 10 µM forward primer
- 1 µL 10 µM reverse primer
- 2 µL lysate

PCR was performed using a SimpliAmp Thermal Cycler with the following protocol:

1. 98 °C 30s
2. 98 °C 10s
3. 65 °C 15s
4. 72 °C 15s (return to step 2, 35 cycles)
5. 72 °C 60s
6. 10 °C hold

Annealing temperature (Step 3.) was 65°C unless otherwise stated. A Veriti 96-well Thermal Cycler (Applied Biosystems) was used for temperature gradient PCR. Cycle number was 35 unless otherwise stated.

2.2.5.2. Nucleic Acid Electrophoresis

2 µL PCR amplification products were mixed with 8 µL E-Gel Sample Loading Buffer, 1x (Invitrogen), and loaded into an E-Gel Agarose Gel with SYBR Safe DNA Gel Stain, 2% (Invitrogen), or E-Gel EX Agarose gel, 2% (Invitrogen) alongside 10 µL E-Gel 1 Kb Plus DNA Ladder (Invitrogen). Electrophoresis was performed using an E-Gel iBASE (Invitrogen) for approximately 15 minutes, and gels were imaged using an E-Gel Imager System with Blue Light Base (Invitrogen).

2.2.5.3. Sanger Sequencing by GENEWIZ

PCR amplification products were purified using a QIAquick PCR Purification Kit (Qiagen). Concentration of purified PCR amplification products was measured using a Nanodrop 8000 Spectrophotometer (Thermo Fisher Scientific). Purified PCR amplification product was diluted to 2 ng/µL in 10 µL using nuclease free-water in wells of a 96-well U-bottom plate (Greiner Bio-One). 5 µL of 5 µM sequencing primer was added to diluted purified PCR amplification product.

The samples were sent to GENEWIZ (Azenta Life Sciences) for Sanger Sequencing. .ab1 files were returned and visualised using BioEdit [103]. Modal sequences were exported from BioEdit and aligned using Clustal Omega (EMBL-EBI) [104]. To align all sequences in a population, .ab1 files were uploaded to Inference of CRISPR Edit (ICE) (Synthego) [104].

2.2.6. Generating monoclonal C5aR1 KO and C5aR2 KO cell lines by limiting dilution

450 C5aR1 KO cells and 450 C5aR2 KO cells were removed from polyclonal cultures and each diluted with culture medium to a total volume of 45 mL, resulting in 1 cell/100 µL. 100 µL of cell suspension was added to wells of four 96-well flat-bottom cell culture plates for each cell line. The plates were incubated at 37°C, 5% CO_2 in a humidified atmosphere for approximately two weeks until monoclonal cultures had established. Successful cultures were transferred to a fresh 96-well plate and clone names were designated according to the Well ID.

Once confluent, the cells were re-suspended and 10 µL of each was transferred to wells of a U-bottom 96-well plate. Plates were centrifuged at 350 x *g* for 5 minutes, the supernatants were aspirated and discarded, and the cell pellets were re-suspended in 100 µL DPBS. The plates were centrifuged at 350 x *g* for 5 minutes, the supernatant was aspirated and discarded, and the cell pellets were stored at -80°C for lysis and characterisation of bulk-edited populations by PCR and sequencing (**2.2.7.**).

Following characterisation, selected C5aR1 KO (B6, C3, F11, G8, H9) and C5aR2 KO (A6, C9, D3, F3, F7) clone cultures were transferred to 2 mL pre-warmed culture medium in a 24-well cell culture plate, and incubated at 37°C, 5% CO_2 in a humidified atmosphere. Once confluent, the cultures were then transferred to 10 mL pre-warmed culture medium in a 25 cm^2 cell culture flask (Thermo Fisher Scientific) and maintained in culture until confluent (1 x 10^6 cells/mL). The cultures were transferred to 40 mL pre-warmed culture medium in 75 cm^3 cell culture flasks. These cultures were established, then were maintained as in **2.2.1.2.3.** and cryopreserved as in **2.2.1.2.4.**

2.2.7. Characterising monoclonal C5aR1 KO and C5aR2 KO cells by PCR and Sanger sequencing analysis

Cell pellets from **2.2.6.** were lysed, and analysed using PCR, nucleic acid electrophoresis, and Sanger Sequencing by GENEWIZ, as in **2.2.5.** PCR amplification products were purified using a PureLink Pro 96 PCR Purification Kit (Invitrogen).

The samples were sent to GENEWIZ for Sanger Sequencing. .ab1 files were returned, visualised using BioEdit, and analysed using Clustal Omega and ICE.

2.2.8. Assessing C5aR1 expression in WT and C5aR1 KO cells using confocal fluorescent microscopy

PMA-differentiated WT and C5aR1 KO THP-1 cells in Lab-Tek II Chamber Slide Systems were washed twice in DPBS, then 200 µL 10% formalin solution (Sigma Aldrich) was added to the chambers to fix the cells. The chamber slides were incubated at RT for 15 minutes, the formalin was discarded, and the cells were washed in staining medium. The chambers were then blocked by adding 400 µL staining medium and incubating at RT for 1 hour. Mouse anti-human C5aR1 monoclonal primary antibody (Clone S5/1) (Biolegend) was diluted 1:100 in permeabilisation medium, 200 µL was added to the chambers, and the chamber slides were sealed and incubated at RT overnight. The THP-1 cells were washed three times in staining medium. Alexa Fluor 488 donkey anti-mouse IgG (H+L) was diluted 1:100 in permeabilisation medium, then 200 µL was added to the chambers, and the chamber slides were incubated at RT for 1 hour in the dark. The THP-1 cells were washed 3 times in staining medium. 1 µg/mL Hoescht (Thermo Fisher Scientific) was added to the chambers, and the chamber slides were incubated at RT for 15 minutes in the dark. The THP-1 cells were washed 3 times in staining medium, and the chambers were removed from the slides. Vectashield antifade mounting medium (Vector Laboratories) and cover slips were added to the slide, and the slide was sealed. The slides were imaged using an Airyscan LSM880

(Zeiss) using Zen (Zeiss). Images were acquired using a 20x oil immersion lens in a 5x5 tile, and 405 nm and 488 nm lasers. 3 representative images were taken from each well.

2.2.9. Assessing C5aR1 and C5aR2 expression using flow cytometry

1 x 10^7 undifferentiated WT, C5aR1 KO (Clone B6, C3, F11, G8, H9) and C5aR2 KO (Clone A6, C9, D3, F3, F7) THP-1 cells were transferred to 50 mL conical tubes. PMA-differentiated WT, C5aR1 KO and C5aR2 KO THP-1 cells in 75 cm^3 flasks were detached using 10 mL TrypLE Express (Gibco), and transferred to 50 mL conical tubes containing 40 mL pre-warmed culture medium. Cells were centrifuged at 350 for 5 minutes, the supernatants were aspirated and discarded, and cell pellets were re-suspended in Cell Staining Buffer (Biolegend). This was repeated for a total of three washes.

Cells were re-suspended in Cell Staining Buffer and transferred to wells of a 96-well plate at 2.5 x 10^5 cells/well. The plate was centrifuged at 350 x *g* for 5 minutes, the supernatants were aspirated and discarded, and Fc receptors were blocked by incubating cells with 100 µL 1:20 Human TruStain FcX (Biolegend) at 4°C for 10 minutes.

Extracellular staining was performed using Anti-C5aR1-APC (Clone S5/1) (Biolegend), anti-C5aR2-APC (Clone 1D9-M12) (Biolegend) and APC-conjugated isotype control antibody (Mouse IgG2a, κ) (Biolegend). Antibodies were used at 0.625 µg/mL in a staining volume of 200 µL to stain 2.5 x 10^5 cells. Cells were incubated with staining antibodies at 4°C for 20 minutes.

Cells were washed three times as above. Cells were re-suspended in 100 µL Fixation Buffer (4% paraformaldehyde) (Biolegend) and fixed at 4°C for 20 minutes. Cells were washed three times, and permeabilised by incubating with 100 µL Intracellular Staining Permeabilisation Wash Buffer (containing Saponin) (Biolegend) at 4°C for 5 minutes. Cells were washed three times, then intracellular staining was performed by

incubating cells with anti-C5aR1-APC, anti-C5aR2-APC or isotype control antibody-APC diluted in Intracellular Staining Permeabilisation Wash Buffer at 4 °C for 20 minutes. Cells were washed three times, and then re-suspended in Cell Staining Buffer. Attune Performance Tracking Beads (Invitrogen) were used to perform cytometer setup, and flow cytometry was performed using an Attune NxT (Life Technologies).

2.2.10. Cytokine Secretion Experiments

2.2.10.1. Experimental Treatment Conditions

2.2.10.1.1. PRR Stimulation Experiment

PMA-differentiated WT, C5aR1 KO (clone C3) or C5aR2 KO (clone F7) THP-1 cells in 96-well plates were stimulated with 10 µg/mL TLR1/2 agonist synthetic triacylated lipopeptide Pam3CSK4 (Invivogen), 10 ng/mL TLR4 agonist Ultrapure LPS from *E. coli* K12 (Invivogen) or 5 µg/mL STING agonist cAIM(PS)$_2$ Difluor (Rp/Sp) (Invivogen) ± 50 ng/mL C5a for 24 hours.

2.2.10.1.2. cAIM(PS)$_2$ Difluor (Rp/Sp) Titration Experiment

PMA-differentiated WT, C5aR1 KO or C5aR2 KO THP-1 cells in 96-well plates were stimulated with 0-20 µg/mL STING agonist cAIM(PS)2 Difluor (Rp/Sp) for 6 hours.

2.2.10.1.3. cAIM(PS)$_2$ Difluor (Rp/Sp) Time Course Experiment

PMA-differentiated WT, C5aR1 KO or C5aR2 KO THP-1 cells in 96-well plates were stimulated with 5 µg/mL STING agonist cAIM(PS)$_2$ Difluor (Rp/Sp) for 0-24 hours.

2.2.10.1.4. cGAS Ligand Experiment

PMA-differentiated WT, C5aR1 KO or C5aR2 KO THP-1 cells in 96-well plates were stimulated with 1 µg/mL cGAS ligand Y-form DNA G3-YSD (Invivogen) by cationic lipid transfection with Lipofectamine 2000 (Thermo Fisher Scientific) for 6 hours.

2.2.10.1.5. STING and TBK1 Antagonist Experiment

PMA-differentiated WT, C5aR1 KO or C5aR2 KO THP-1 cells in 96-well plates were pre-incubated with 100 nM or 1 µM TBK1 antagonist BX795 (Invivogen) or STING antagonist H-151 (Invivogen) for 30 minutes, followed by 5 µg/mL STING agonist cAIM(PS)$_2$ Difluor (Rp/Sp) for 6 hours.

2.2.10.2. Cytokine Detection Assays

Supernatants were harvested. IL-1β, IL-6, IL-10 and TNFα were measured using U-Plex multiplex immunoassay (MSD) and an MSD Sector Imager (MSD). IFN-β was measured using a Human IFN-β DuoSet ELISA (R&D Systems).

2.2.10.3. Viability Assay

Following cytokine harvest, cell viability was quantified using Cell Titre-Glo Luminescent Cell Viability Assay (Promega). Data were acquired using a Pherastar FSX (BMG).

2.2.11. Peggy Sue Automated Western Blot

Simple Western assays (ProteinSimple) are capillary-based Western blot assays performed using a Peggy Sue (ProteinSimple) automated Western blot system. Samples were incubated with master mix containing internal standards and DTT and heated to 95°C. Stacking and separation matrices were loaded into capillaries, followed by sample. Proteins were separated by electrophoresis, immobilised in the capillary, followed by incubation with primary and secondary antibodies and chemiluminescent signal detection. Peggy Sue Simple Western assays increase throughput, reproducibility and sensitivity, and require smaller amounts of sample and antibody compared to traditional Western blot methods.

2.2.11.1. Experimental Treatment Conditions

PMA-differentiated WT and C5aR2 KO cells in 6-well plates were incubated with 5 µg/mL STING agonist cAIM(PS)$_2$ Difluor (Rp/Sp) for 6 hours. Lysates were generated using 100 µL Peggy Sue Lysis Buffer. Lysates were passed through a QIAshredder (Qiagen), and concentrations were quantified using a Pierce Rapid Gold BCA Protein Assay Kit (Thermo Fisher Scientific). OD_{562} values were measured using a Pherastar FSX.

2.2.11.2. Protein Detection by Peggy Sue

Expression of STING, phospho-STING (Ser366), IRF3, phospho-IRF3 (Ser386) and loading control β-actin was measured using a 12-230 kDa Separation Module (ProteinSimple) and anti-STING rabbit pAb (Thermo Fisher), anti-phospho-STING (Ser366) rabbit mAb (Clone E9A9K) (Cell Signaling Technology), anti-IRF3 recombinant rabbit mAb (Clone EPR2418Y) (Abcam), anti-phospho-IRF3 (Ser386) XP rabbit mAb (Clone E7J8G) (Cell Signaling Technology) and anti-β-actin mouse mAb (Clone AC-15) (Abcam). Data were acquired using a Peggy Sue Automated Western Blot System (ProteinSimple).

2.2.12. Generation of polyclonal C5aR2 KO primary human MDMs using CRISPR-Cas9

2.2.12.1. MDM culture and handling

Frozen stocks of CD14$^+$ monocytes from 5 independent donors were thawed and differentiated using M-CSF as in **2.2.1.1.3**.

2.2.12.2. CRISPR-Cas9

MDMs were detached using neat Detachin Cell Detachment Solution (Genlantis). RNP assembly (**2.2.3.1.**), electroporation and cationic lipid transfection (**2.2.3.2.**) were performed as in **2.2.3.**

100,000 cells/well of electroporated RNP-transfected MDMs were transferred to wells of duplicate 96-well flat-bottom cell culture plates. One plate was used for a cAIM(PS)$_2$ Difluor (Rp/Sp) stimulation experiment (**2.2.12.**) and the other was used to confirm the presence of indels in C5aR2 cells vs NTC cells (**2.2.12.3**).

2.2.12.3. Characterising NTC and C5aR2 KO MDMs

PCR, nucleic acid electrophoresis and Sanger sequencing (GENEWIZ) was performed as in **2.2.5.**

2.2.13. Stimulation of C5aR2 KO MDMs with cAIM(PS)$_2$ Difluor (Rp/Sp)

2.2.13.1. Experimental Treatment Conditions

NTC and C5aR2 KO MDMs were cultured for 3 days or 10 days to allow for protein turnover, then were stimulated with 5 µg/mL STING agonist cAIM(PS)$_2$ Difluor (Rp/Sp) for 6 hours.

2.2.13.2. IFN-β ELISA

Supernatants were harvested, and IFN-β was measured by ELISA as in **2.2.9.2.**

2.2.14. RNAseq

2.2.14.1. Sample Generation

PMA-differentiated WT, C5aR1 KO and C5aR2 KO cells in 75 cm^2 flasks were incubated with culture medium, 50 ng/mL C5a or 5 µg/mL STING agonist cAIM(PS)$_2$ Difluor (Rp/Sp) for 6 hours. 3 technical replicates of 3 clones of each KO cell line were generated. Samples were generated over two experiment days due to a QC issue with a subset of samples generated on Experiment Day 1.

2.2.14.2. Quality Control IFN-β ELISA

Supernatants were harvested and assessed for IFN-β using a Human IFN-β DuoSet ELISA.

2.2.14.3. RNASeq

Following supernatant harvest, cells were washed twice using DPBS followed by incubation with neat TrypLE Express (Gibco) at 37°C, 5% CO_2 in a humidified atmosphere for 15 minutes. Once visibly detached, cells were transferred into 50 mL conical tubes, centrifuged at 350 x *g* for 5 minutes, and cell pellets were cryopreserved at -80°C. RNAseq was performed by GENEWIZ, comprising total RNA isolation, library preparation with poly(A) selection and 150-bp paired-end sequencing using a HiSeq 2500 (Illumina).

2.2.15. Data Analysis

2.2.15.1. Phospho-ERK ELISA Data

OD_{450} values were used to interpolate % of Total ERK1/2 values from a standard curve, and values were normalised to the mean PMA response (100%). Mean ± SD pERK (% of tERK) and pERK (% normalised to PMA) were plotted. A non-linear regression was performed to fit a 4-parameter curve.

2.2.15.2. PCR and Sequencing Data

PCR and sequencing primers were designed using Primer-BLAST (NCBI) [109]. Modal sequences were transferred from .ab1 files using BioEdit and aligned to C5aR1 (NCBI: >NC_000019.10:47309861-47322066 Homo sapiens chromosome 19, GRCh38.p13 Primary Assembly) or C5aR2 (NCBI: >NC_000019.10:47331614-47347329 Homo sapiens chromosome 19, GRCh38.p13 Primary Assembly) gene sequences, primer sequences and guide sequences using Clustal Omega. Asterisk indicates conservation of base between sequences. Mixed populations of sequences in .ab1 files were aligned using ICE. Edited sequences were then aligned to WT or NTC sequences using ICE, generating Trace, Discordance and Indel plots. Trace plots displayed modal sequence alignment around the guide site. Discordance plots displayed a discordance score (0-

1) between edited and control sequences, highlighting alignment and inference of indel between the sequences. Indel plots displayed the size and prevalence of indels in the population of sequences in each sample and editing efficiency scores.

2.2.15.3. Microscopy Data

Data from .czi files were analysed and exported as .tif files using Zen (Zeiss).

2.2.15.4. Flow Cytometry Data

Data were analysed using FlowJo 10.8 (BD Life Sciences). Doublets were excluded, and cells of interest were gated. Expression of C5aR1 and C5aR2 was plotted in histograms, and MFI of isotype compared to C5aR1/2 was plotted for each cell type and clone.

2.2.15.5. Cytokine Secretion Data

For MSD data, pg/mL values were interpolated from a standard curve using Discovery Workbench (MSD) and mean ± SD were plotted using Prism (Graphpad).

For ELISA data, pg/mL values were interpolated from a standard curve using $OD_{450\text{-}570}$ values, and mean ± SD were plotted using Prism. For titrations and time course experiments, a nonlinear regression was used to fit a four parameter curve to the data.

2.2.15.6. Viability Data

Viability data were normalised using the untreated values as 100%. Mean ± SD were plotted using Prism. For titrations and time course experiments, a nonlinear regression was used to fit a four parameter curve to the data.

2.2.15.7. Peggy Sue Data

Peggy Sue data were analysed using Compass for SW (ProteinSimple). Data were represented as pseudo-blots, and area under the mw-chemiluminescence curves were normalised to the β-actin loading control using Excel. Mean ± SD were plotted using Prism.

2.2.15.8. RNAseq

Raw data in FASTQ format were received from GENEWIZ. Data analysis was performed by You Zhou (Cardiff University) and Van Dien Nguyen (Cardiff University).

Genes were initially filtered, retaining genes which were expressed in <50% of the samples. RNA expression normalisation was performed, and Principal Component Analysis (PCA) was performed on variance stabilising transformed data. Comparisons between treatment condition within genotype, and between genotype within treatment condition, to confirm the experimental conditions were driving variance between samples as expected.

Differential Gene Expression analysis was then performed by You Zhou (Cardiff University) and Van Dien Nguyen (Cardiff University) using DESeq2 [110]. Potential batch effect due to the two experiment days was removed by fitting the design as "-Batch + condition". Fold change values, log_2 fold change values, and p values were generated for each differentially expressed gene. p values were adjusted using then Benjamini-Hochberg method. Log_2 fold change was plotted against adjusted p value to generate volcano plots by Darren Gormley (GSK) using Spotfire (Tibco).

Three further analysis approaches were taken:

- pathway analysis using Gene Set Enrichment Analysis (GSEA) on global differentially expressed genes using the Kyoto Encyclopaedia of Genes and Genomes (KEGG) PATHWAY database
- STRINGdb network analysis and PANTHERdb pathway analysis on unique genotype-dependent treatment-dependent significantly regulated genes
- a biased assessment of key genes using manually curated gene lists from significantly regulated pathways in the GSEA

Pathway analysis was performed by You Zhou (Cardiff University) and Van Dien Nguyen (Cardiff University). Gene lists were ranked and fast gene set enrichment analysis (fgsea) [111] was performed. Analyses and visualisation were performed using R [106], with an adjusted p value of 0.05 as a significance cut-off. The KEGG PATHWAY database [112] was used to identify significantly regulated pathways. Significantly regulated pathways were ranked based on p value and adjusted p value. Normalised Enrichment Scores indicate the overall magnitude and direction of regulation of the KEGG pathway based on its contributory genes.

Differentially expressed genes from STING-agonist-treated C5aR1 KO and C5aR2 KO cells were investigated further. Unique genotype-dependent treatment-dependent significantly regulated genes were identified by applying a significance threshold ($p \leq 0.05$, $-1 > \log_2 FC > 1$), then filtering out common genotype-independent and treatment-independent significantly regulated genes. Network analysis was performed using STRINGdb [107], and pathway analysis using GO Biological Process gene sets was performed using PANTHERdb [105] by Lee Booty (GSK).

Individual significantly regulated genes of interest were then identified using a biased assessment of significantly regulated KEGG pathways from the GSEA. Significantly regulated KEGG pathways were manually triaged to filter out stimulation-specific genotype-independent pathways and pathways common to all conditions. Genotype-specific stimulation-independent pathways, genotype-independent stimulation-independent pathways and unique pathways for each condition were then manually curated to identify inflammatory pathways significantly regulated in C5aR2 KO cells. Gene lists in the pathways of interest were then marked in volcano plots of all differentially expressed genes in STING agonist-treated C5aR2 KO cells vs STING agonist-treated WT cells using Spotfire.

2.2.15.9. Statistical Analysis

Prism was used to plot all figures and perform all statistical analyses on data unless otherwise stated. Kolmogrov-Smirnov normality tests were performed, followed by one-way ANOVA or Kruskal-Wallis tests, or paired Student's t tests. ns: $p>0.05$; *: $p \leq 0.05$; **: $p \leq 0.01$; ***: $p \leq 0.001$; ****:$p \leq 0.0001$.

Chapter 3 - Results 1

Assessing C5aR2 agonism by P32 and P59 using ERK1/2 phosphorylation assays

3. Assessing C5aR2 agonism by P32 and P59 using ERK1/2 phosphorylation assays

3.1. Introduction

C5aR2 has been reported to function independently of C5aR1 [72], however the molecular mechanisms driving the function of C5aR2 are unexplored and poorly understood [51]. The literature identifies two targets directly downstream of C5aR2: C5aR1-dependent ERK phosphorylation [72] and β-arrestin recruitment [75]. β-arrestins are negative regulators of GPCR function, including C5aR1 [53], therefore C5aR2 may be able to regulate C5aR1 function by modulating β-arrestin [72,77]. ERK1/2 phosphorylation occurs downstream of cytokine receptor activation and mediates the inflammatory response [81], potentially implicating C5aR2 as an immunoregulatory receptor.

The tools available with which to study C5aR2 are poorly characterised [51], and a limited number of studies describe their use. This includes P32 (Ac-RHYPYWR-OH) and P59 (Ac-LIRLWR-OH), synthetic C5a-based agonists of C5aR2, which are reported to be C5aR2-selective [72], but have only been described by a single group. There is no known independent function of C5aR2 which can be used as an endpoint to confirm C5aR2 activity separately from C5aR1 activity. Targeted stimulation requires complex pharmacological modulation of both receptors using an array of C5aR1 and C5aR2 antagonists and agonists (**Table 3.1**).

Reagent	Function
C5a	C5aR1/2 ligand [56,72]
PMX53	small molecule antagonist of C5aR1 [113]
P32, P59	C5a-based peptide, putative agonists of C5aR2 [72]
Anti-C5aR2 mAb Clone 1D9-M12	Anti-C5aR2 antibody, blocks C5a binding site [114,115]

Table 3.1. Agonists and antagonists of C5aR1 and C5aR2.

To investigate downstream effects of C5aR2, reproducible stimulation conditions were required to enable specific agonism of C5aR2 independently of C5aR1. This series of experiments therefore aimed to establish a protocol for C5aR2 activation by C5aR2 agonists P32 and P59, using ERK1/2 phosphorylation as an endpoint. To achieve this:

- Primary human MDMs, selected due to their use in previously published experiments [72] and relevance to the innate immune response, will be stimulated with C5a to induce ERK1/2 phosphorylation.
- C5aR1-dependency will be assessed using PMX53, a small molecule antagonist of C5aR1.
- P32 and P59 will be used to activate C5aR2, confirming the suggested negative regulation of C5aR1-dependent C5a-driven ERK phosphorylation by the agonists.
- Anti-C5aR2 mAb (Clone 1D9-M12) will then be titrated to assess whether P32/P59-driven inhibition of C5aR1-driven ERK1/2 phosphorylation is C5aR2-dependent

If successfully established, the C5aR2 activation protocol could be translated to alternative experimental setups, enabling the continued investigation of the immunological function of C5aR2.

3.2. Results

3.2.1. C5a Titration

The first step was to identify the optimum stimulation concentration for C5a. Primary human MDMs were stimulated with 0-1000 ng/mL C5a, using 100 nM PMA as a positive control (**Figure 3.1**). The incubation time of 10 minutes was selected based on previously published data [72]. Cell lysates were assessed by ELISA for ERK1/2 phosphorylation as a percentage of total ERK1/2, interpolated from a standard curve.

A

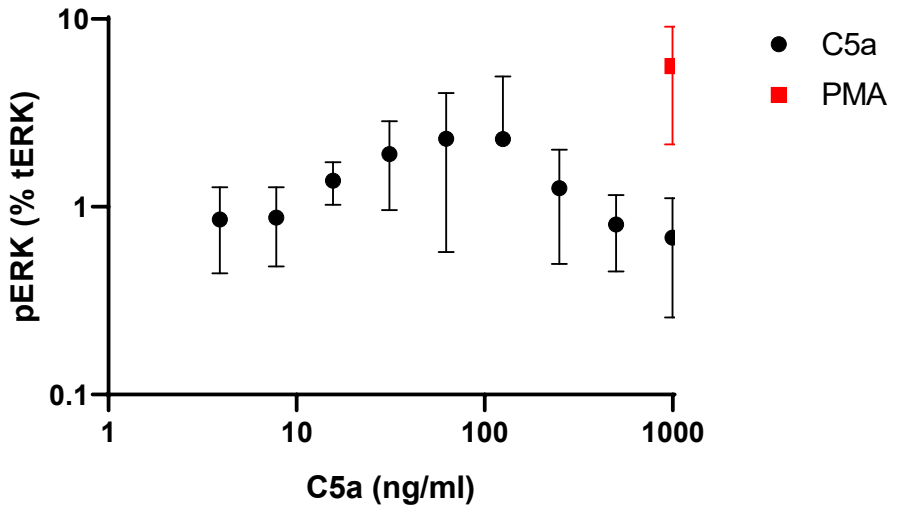

B

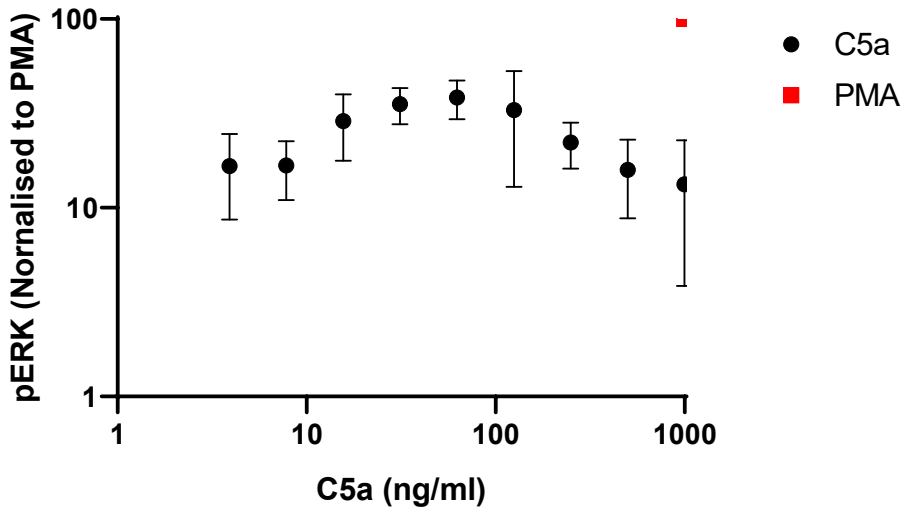

Figure 3.1. Titration of C5a on primary human MDMs. Primary human MDMs were incubated with 0-1000 ng/mL C5a for 10 minutes. 100 nM PMA was used as a positive control. Cells were lysed and assessed for phospho-ERK1/2 by ELISA. **A.** $OD_{450-570}$ values were interpolated with a standard curve and plotted as a % of total ERK1/2. **B.** The same values were normalised to the mean PMA response (100%). Mean ± SD were plotted, N=3 across 2 separate experiments.

When expressed as a percentage of total ERK1/2, high standard deviations indicate that the phospho-ERK1/2 values were variable (**Figure 3.1 A**), however normalisation to the PMA control reduced the impact of the biological variation between donors and revealed a concentration-dependent response to C5a (**Figure 3.1 B**). The phospho-ERK1/2 signal increased in a concentration-dependent manner to a maximum response at 62.5 ng/mL, which then reduced in a concentration-dependent manner up to 1000 ng/mL. Higher concentrations of C5a may have driven C5aR1 internalisation and subsequent down-regulation of signalling activity as a negative regulatory mechanism, however this is not clear from this dataset in isolation. 50 ng/mL C5a was therefore selected as an optimum concentration to stimulate primary human MDMs.

3.2.2. PMX53 Titration

To confirm that C5a-induced ERK1/2 phosphorylation is C5aR1-dependent, C5aR1 antagonist PMX53 was used to inhibit C5aR1 prior to C5a stimulation (**Figure 3.2**). Inactive control peptide PMX53c was used as a control for off-target effects of PMX53, and PMA was used as a positive control for ERK1/2 phosphorylation. Primary human MDMs were pre-incubated with 0-1000 nM PMX53 or inactive control peptide PMX53c for 30 minutes, followed by 50 ng/mL C5a or 100 nM PMA for 10 minutes. Cell lysates were assessed for phospho-ERK1/2 by ELISA.

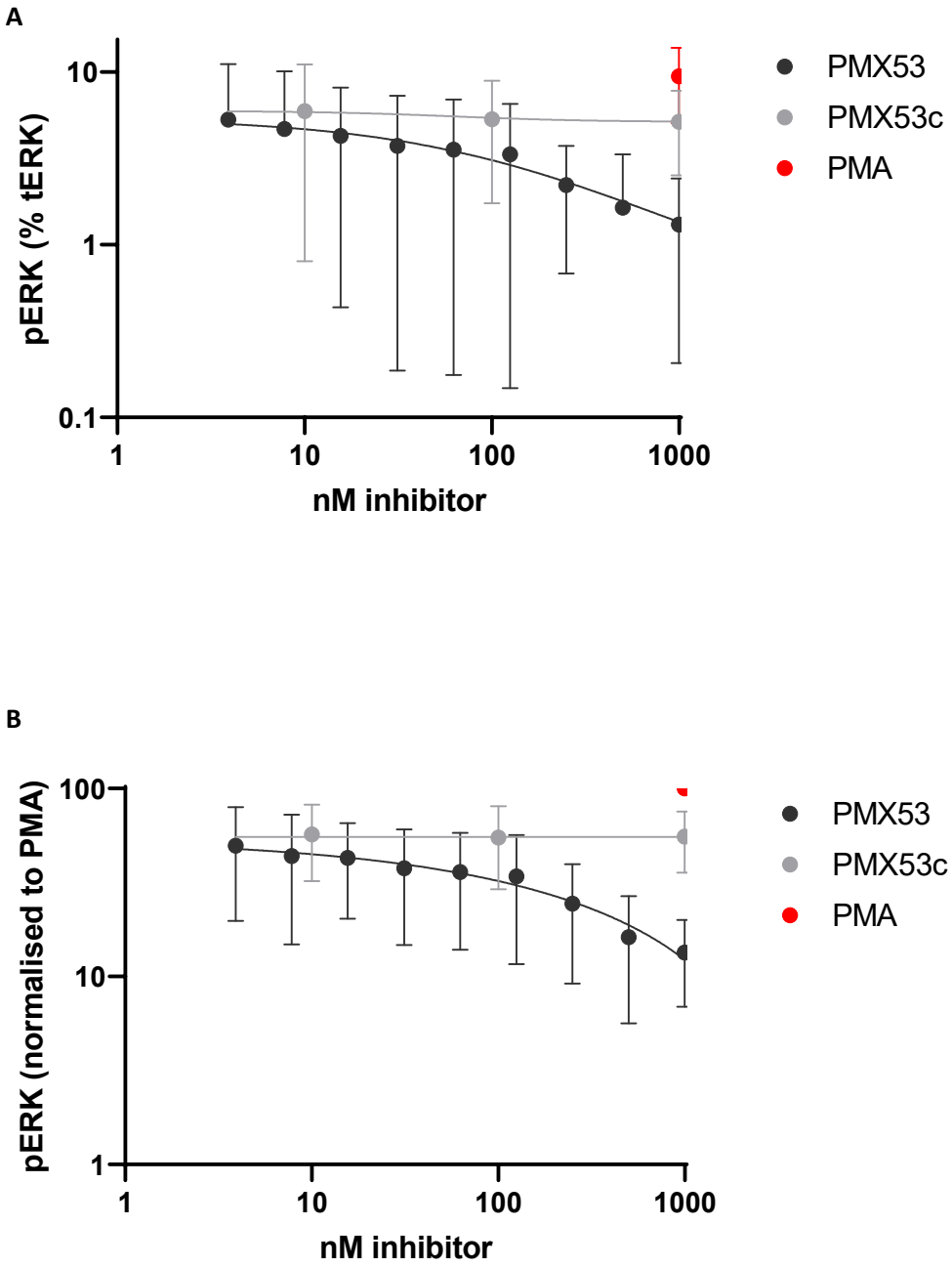

Figure 3.2. Titration of C5aR1 KO inhibitor PMX53 on C5a-treated primary human MDMs. Primary human MDMs were incubated with 0-1000 nM PMX53 or inactive control peptide PMX53c for 30 minutes, followed by 50 ng/mL C5a for 10 minutes. 100 nM PMA was used as a positive control. Cells were lysed and assessed for phospho-ERK1/2 by ELISA. **A.** $OD_{450-570}$ values were interpolated with a standard curve and plotted as a % of total ERK1/2. **B.** Values were normalised to the mean PMA response (100%). Mean ± SD were plotted, N=5 across 2 separate experiments.

As above, donor-donor variability generated high standard deviations at each concentration (**Figure 3.2 A**), however normalisation to the PMA control reduced the impact of biological variability between donors (**Figure 3.2 B**). C5a-induced ERK1/2 phosphorylation was inhibited in a concentration-dependent manner by PMX53. The majority of ERK phosphorylation was inhibited, however there was a low level of signal remaining at the maximum PMX53 concentration. This could have been due to noise in the assay, and the signal at approximately 10% may have represented the lowest detectable signal. Alternatively, the curve did not plateau, meaning that concentrations above the maximum 1000 nM may further inhibit C5aR1 activity. There is no effect of PMX53c at any concentration. A concentration of 1 µM PMX53 was selected for subsequent experiments.

3.2.3. Anti-C5aR2 Titration

To confirm that anti-C5aR2 mAb (Clone 1D9-M12) does not inhibit C5a-induced C5aR1-dependent ERK1/2 phosphorylation, primary human MDMs were stimulated with 0-1000 nM anti-C5aR2 or isotype control antibody (**Figure 3.3**). Cell lysates were assessed for phospho-ERK1/2 by ELISA.

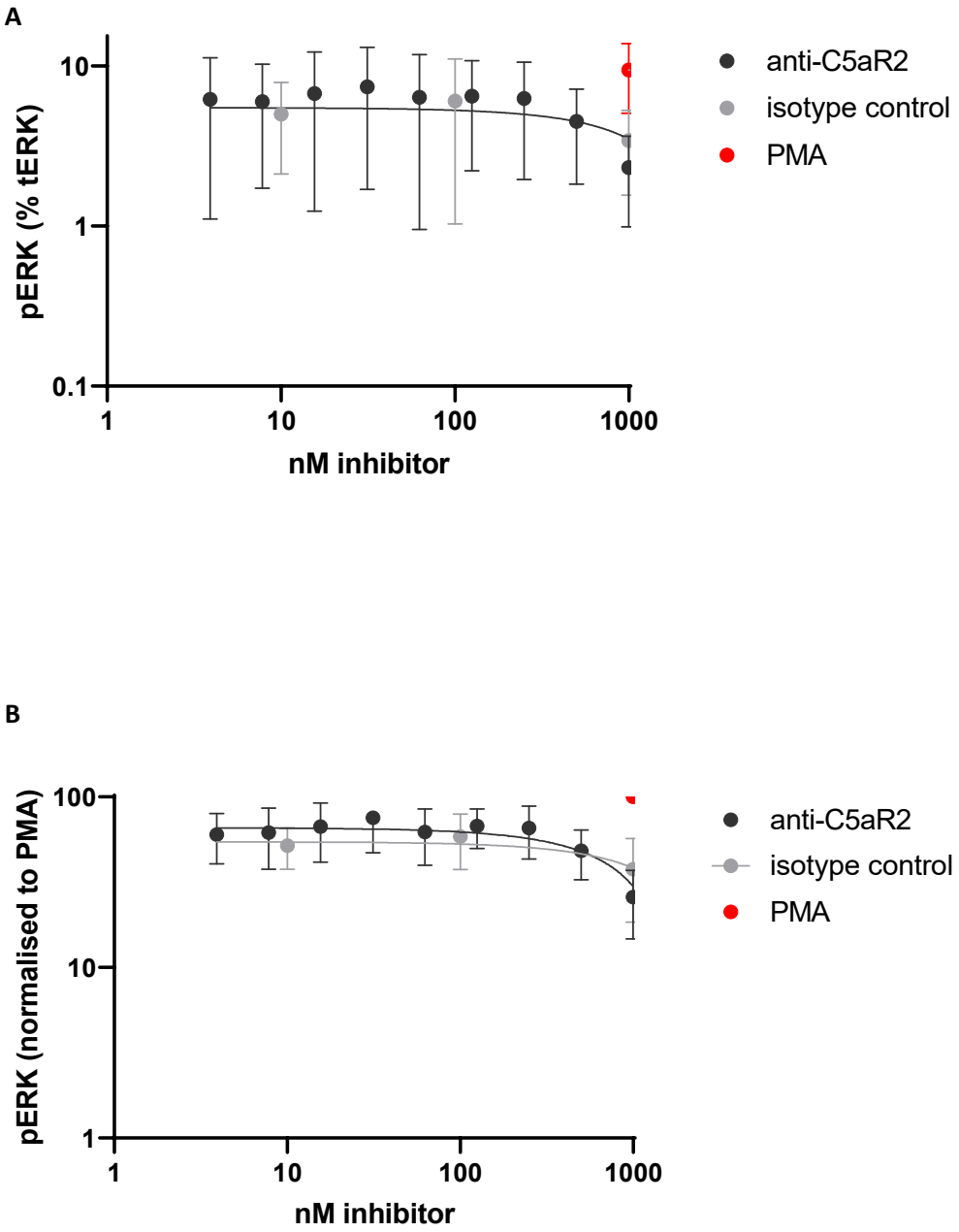

Figure 3.3. Titration of anti-C5aR2 mAb on C5a-treated primary human MDMs. Primary human MDMs were incubated with 0-1000 nM anti-C5aR2 (1D9-M12) or isotype control antibody (IgG2a, κ) for 30 minutes, followed by 50 ng/mL C5a for 10 minutes. 100 nM PMA was used as a positive control. Cells were lysed and assessed for phospho-ERK1/2 by ELISA. **A.** $OD_{450-570}$ values were interpolated with a standard curve and plotted as a % of total ERK1/2. **B.** Values were normalised to the mean PMA response (100%). Mean ± SD were plotted, N=5 across 2 separate experiments.

Biological variability between donors again generated high standard deviations, (**Figure 3.3 A**), however normalisation to the PMA control reduced the impact of this variability (**Figure 3.3 B**). There was no effect of anti-C5aR2 on ERK1/2 phosphorylation between 0-250 nM, as expected. There was a small isotype effect at 1000 nM, suggesting that the reduction in ERK1/2 phosphorylation at high concentrations of anti-C5aR2 was a non-specific isotype effect rather than a C5aR2-driven effect. Anti-C5aR2 was therefore not used at more than 250 nM in subsequent experiments.

3.2.4. C5aR2 Agonist Titration

As demonstrated above, an experimental setup was now established in which C5a stimulation generated a phospho-ERK1/2 signal, which was inhibited by C5aR1 antagonism. This protocol could now be used to assess the effects of putative C5aR2 agonists P32 and P59 on C5aR1-induced ERK1/2 phosphorylation, as they have been reported to negatively regulate this effect [72]. Primary human MDMs were pre-incubated with culture medium, 1 µM C5aR1 inhibitor PMX53, or 0-1000 nM C5aR2 agonists P32 or P59 for 30 minutes, followed by 50 ng/mL C5a or 100 nM PMA for 10 minutes (**Figure 3.4**). Cells were lysed, and phospho-ERK1/2 was measured by ELISA.

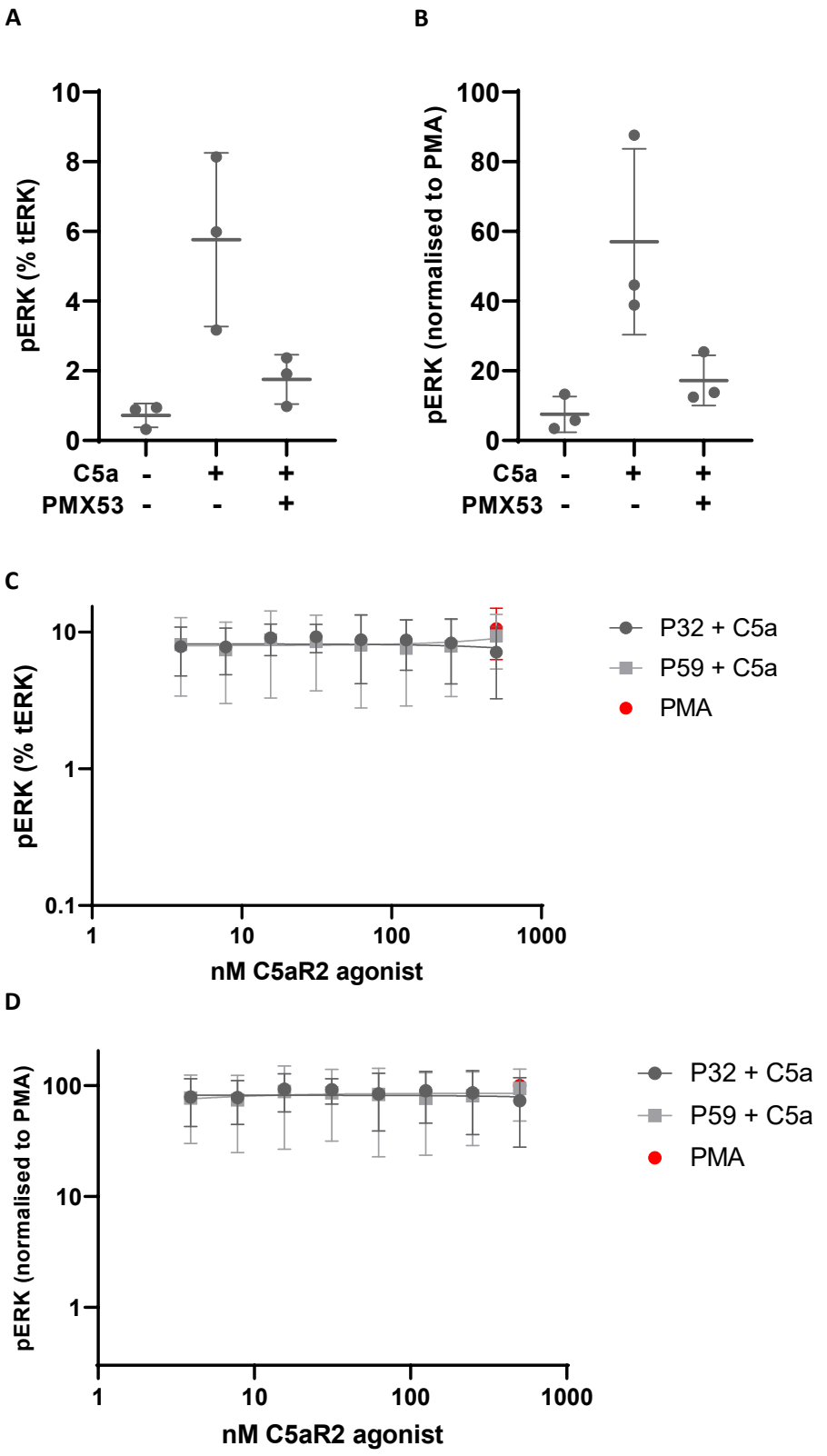

Figure 3.4. Titration of C5aR2 agonists on C5a-treated primary human MDMs. A. Primary human MDMs were incubated with 0 or 1 µM PMX53 for 30 minutes, followed by 50 ng/mL C5a for 10 minutes. **B.** Data were normalised to the mean PMA response (100%). **C.** Primary human macrophages were incubated with 0-500 µM P32 or P59 for 30 minutes followed by 50 ng/mL C5a for 10 minutes. 100 nM PMA was used as a positive control. $OD_{450-570}$ values were interpolated with a standard curve and plotted as a % of total ERK1/2. **D.** Data were normalised to the mean PMA response (100%). Mean ± SD were plotted, N=3 across 2 separate experiments.

Controls functioned as expected in this experiment, as C5a induced ERK1/2 phosphorylation, and inhibition by PMX53 demonstrated that this effect was C5aR1-dependent (**Figure 3.4 A**). When data were normalised to the PMA control, the effect was preserved (**Figure 3.4 B**). There was no effect of P32 or P59 on C5a-treated cells at any concentration (**Figure 3.4 C)**, and data normalised to the PMA control demonstrated the same result (**Figure 3.4 D)**.

3.2.5. C5aR2 Agonist Time Course

To confirm that the incubation time was sufficient to see an inhibitory effect, a range of incubation times for P32 and P59 were assessed (**Figure 3.5**). Primary human MDMs were pre-incubated with culture medium, 1 µM PMX53 for 30 minutes, or 100 µM P32 or P59 for 0-4 hours, followed by 50 ng/mL C5a or 100 nM PMA for 10 minutes. Lysates were assessed for ERK1/2 phosphorylation by ELISA.

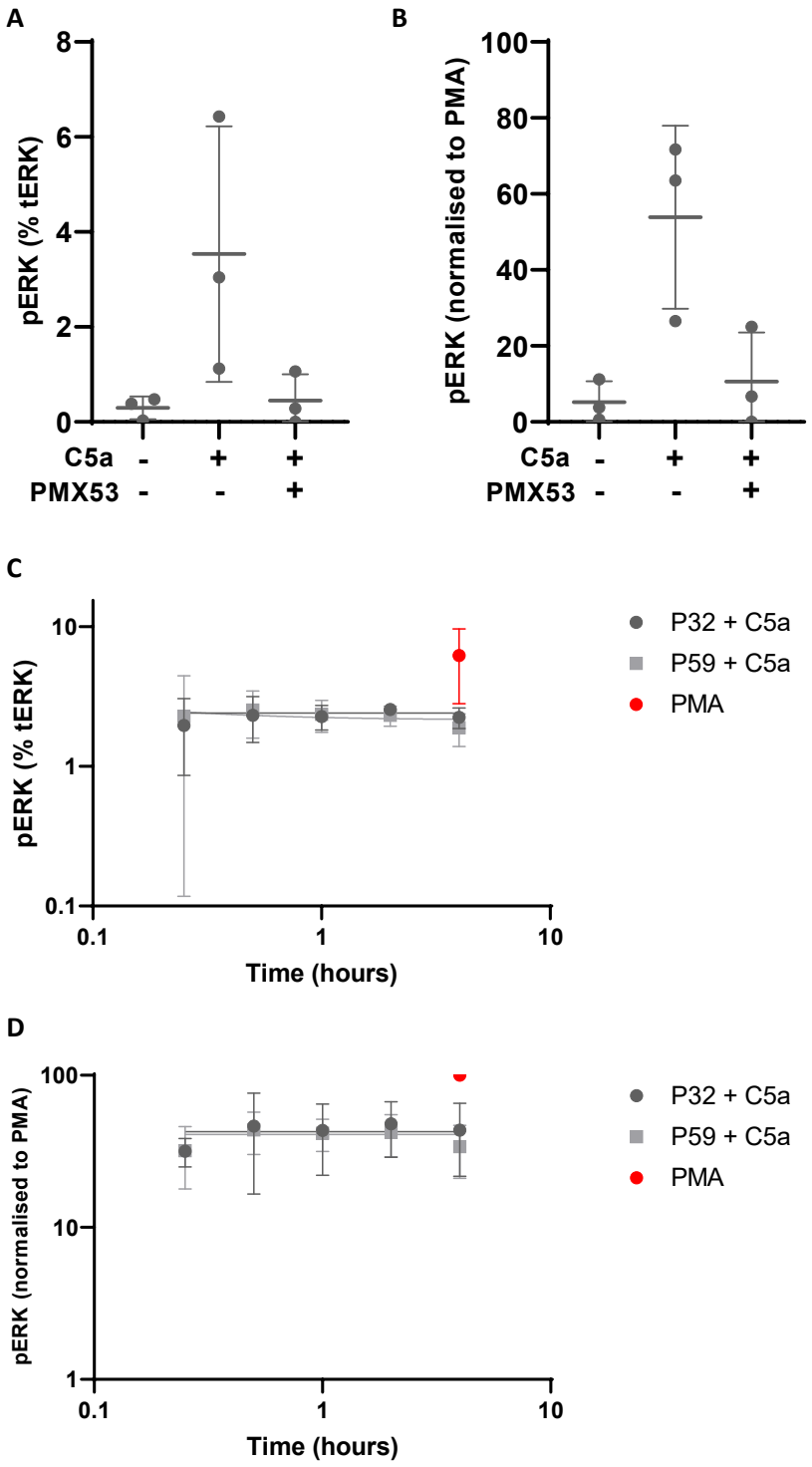

Figure 3.5. Time course of C5aR2 agonists on C5a-treated primary human MDMs. Primary human MDMs were incubated with 0 or 1 µM PMX53 for 30 minutes, followed by 50 ng/mL C5a or 100 nM PMA for 10 minutes. **A.** $OD_{450-570}$ values were interpolated with a standard curve and plotted as a % of total ERK1/2. **B.** Values were normalised to the mean PMA response (100%). **C.** Primary human MDMs were incubated with 100 µM P32 or 100 µM P59 for 0-4 hours, followed by 50 ng/mL C5a for 10 minutes. $OD_{450-570}$ values were interpolated with a standard curve and plotted as a % of total ERK1/2. **D.** Values were normalised to the mean PMA response (100%). Mean ± SD were plotted, N=3 across 2 separate experiments.

Controls functioned as expected in this experiment, as C5a induced ERK1/2 phosphorylation, and inhibition by PMX53 demonstrated that this effect was C5aR1-dependent (**Figure 3.5 A)**. Variation introduced by biological replicates was reduced by normalising within each donor to the PMA control (**Figure 3.5 B, D**). There was no effect of 100 μM P32 or P59 on C5a-treated cells at any incubation time (**Figure 3.5 C, D)**.

3.3. Discussion

This series of experiments aimed to establish an assay to demonstrate C5aR2 activity. There is no known direct downstream target of C5aR2, however it has been reported to negatively regulate C5aR1-induced ERK1/2 phosphorylation [72]. Stimulation of C5aR2 independently of C5aR1 is a challenge as its putative natural ligand C5a binds to both receptors, however P32 (Ac-RHYPYWR-OH) and P59 (Ac-LIRLWR-OH) have been reported to selectively agonise C5aR2 and down-regulate C5aR1-induced ERK1/2 phosphorylation [72].

This was not the case in this study. A C5aR1-dependent ERK1/2 phosphorylation assay was successfully established (**Figure 3.2,** reproduced in **Figure 3.4 A-B, 3.5 A-B**), however there was no detectable effect of P32 or P59 at any concentration (**Figure 3.4 C-D, Figure 3.5 C-D**). The reported effect of C5a was potent and rapid, with a 10 minute incubation sufficient to negatively regulate C5aR1-dependent ERK1/2 phosphorylation [72]. A range of incubation times between 15 minutes and 4 hours was tested with the same concentration of P32 and P59 used in the literature, however they did not function in this assay (**Figure 3.5**).

This discrepancy could have arisen through various mechanisms. Firstly, these peptides were synthesised in-house. Aliquots of the original P32 and P59 peptides may generate a different effect due to potential structural differences between the preparations. Cell culture may also have differed between these two studies: primary human monocyte-derived macrophages were used in each case, however primary cells can be extremely sensitive to culture conditions, and relatively small differences may have resulted in altered receptor expression levels between the two laboratories. Additionally, target accessibility may also pose a significant problem for this approach. C5aR2 is reportedly intracellular, possibly trafficking to the cell surface upon C5a stimulation, meaning that P32 and P59 may have not effectively reached intracellular

C5aR2 in these experiments. Confirmation of expression location by flow cytometry or fluorescent microscopy would confirm whether C5aR2 was accessible on the surface of these macrophages. If C5aR2 was intracellular in these cells, overexpression of P32 or P59 delivered via plasmid transfection may be able to activate intracellular C5aR2, however it would introduce an additional layer of variability between the experiments.

This project aimed to confirm C5aR2-dependent biological activity of P32 and P59, characterise them using titrations and time course experiments, then characterise anti-C5aR2 antibody 1D9-M12 as a negative regulator of C5aR2 activity. Establishing robust controls for C5aR2 activity would enable the study of C5aR2-dependent effects on alternative endpoints, for example the role of C5aR2 in PRR regulation, or broader multi-omic approaches to identify potential downstream signalling targets. This approach, however, will not be possible, as these putative C5aR2 ligands have not been effective in these assays.

There are few published studies characterising P32 and P59, meaning further hypothesis testing using them would be limited. The experimental setup was also complex, with a multi-faceted stimulations required to elicit an indirect effect of C5aR2 mediated via unknown intermediate proteins on C5aR1.

A simpler and more robust system was required to study C5aR2, which could be achieved by generating C5aR2 KO cell lines using CRISPR-Cas9. It would eliminate the need to rely on multiple stimulations with indirect endpoints, and facilitate the generation of robust and reproducible data investigating the function of C5aR2. Generation of C5aR2 KO cell lines would allow the proposed study to continue. The KO cells would be used to investigate the effect of C5aR2 KO on PRR-induced cytokine secretion and downstream immune function using hypothesis-driven functional experiments. They would also be used to perform an unbiased transcriptomics experiment to characterise the global effect of C5aR2 KO. These approaches aim to

yield data to confirm the reported functions of C5aR2, and generate an invaluable tool for the study of novel functions of C5aR2.

Chapter 4 - Results 2

Generating monoclonal C5aR1 KO and C5aR2 KO THP-1 cell lines using CRISPR-Cas9

4. Generating monoclonal C5aR1 KO and C5aR2 KO THP-1 cell lines using CRISPR-Cas9

4.1. Introduction

The study of C5aR2 currently relies on a limited number of tool molecules. The most successful studies of C5aR2 have relied on P32 and P59, selective peptide agonists of C5aR2 based on C5a. Potential roles for C5aR2 in the modulation of ERK1/2 phosphorylation [72] and PRR modulation [8] were identified. However, the data reported in **Chapter 3** was unsuccesssful in reproducing the effect of P32 and P59 on C5aR1-induced ERK1/2 phosphorylation. Due to the lack of availability of C5aR2 tools, a robust, reproducible and reliable tool system with which to study C5aR2 was required. This series of experiments aimed to use CRISPR-Cas9 to generate C5aR1 KO and C5aR2 KO cells with which to study C5aR2.

CRISPR-Cas9 is a commonly used gene editing tool, which can introduce highly targetted double-stranded breaks in DNA. Cas9 nucleases complexed with gRNA bind complementary genomic DNA, targeting Cas9-mediated DNA cleavage to specific genomic regions. This leads to genetic KO and subsequent loss of function [116]. CRISPR-Cas9 was therefore selected as a gene editing tool with which to generate C5aR1 KO and C5aR2 KO cells.

Previous work on C5aR2 has predominantly used primary human MDMs [8,72], including the data reported in **Chapter 3**. Primary cells are highly physiologically relevant, however they are less readily available and more sensitive to culture conditions than cell lines. Immortalised cell lines replicate in culture, acting as a constant source of genetically identical cells for use in experiments. THP-1 cells are a monocytic leukaemia cell line, which can be differentiated into adherent macrophage-like cells [117]. These cells were therefore selected due to their ease of culture and relevance as a model cell line for primary human MDMs.

This study aimed to use CRISPR-Cas9 to generate and characterise stable monoclonal C5aR1 KO, C5aR2 KO and C5aR1/2 double KO (DKO) THP-1 cells, which would function as reliable and reproducible tools with which to study C5aR2.

4.2. Results

4.2.1. Confirming expression of C5aR1 and C5aR2 in WT THP-1 cells

To confirm expression of the target proteins, undifferentiated and PMA-differentiated WT THP-1 cells were assessed for extracellular C5aR1 expression, extracellular C5aR2 expression and intracellular C5aR2 expression by flow cytometry (**Figure 4.1**). For extracellular staining, cells were fixed then stained with anti-C5aR1-APC, anti-C5aR2-APC or isotype control antibody-APC. For intracellular staining, cells were fixed and permeabilised, then stained with anti-C5aR2-APC or isotype control antibody-APC.

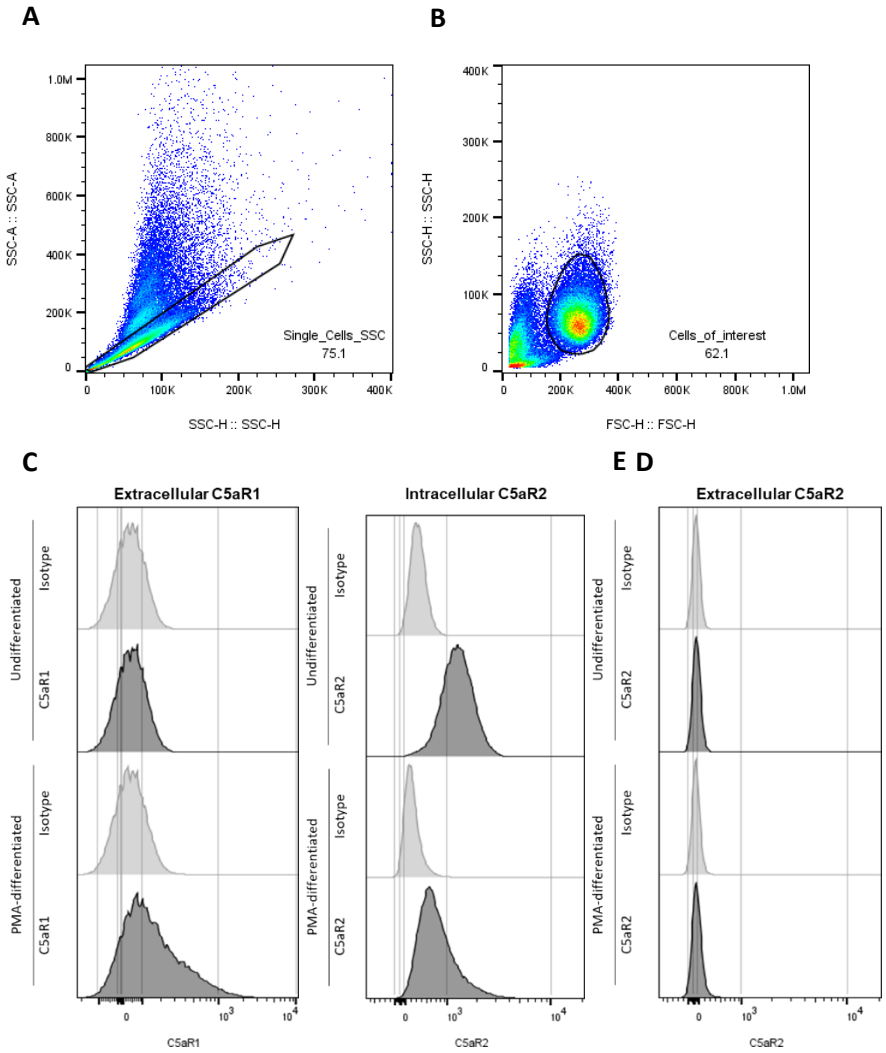

Figure 4.1. C5aR1 and C5aR2 expression on THP-1 cells confirmed using flow cytometry. Undifferentiated and PMA-differentiated WT THP-1 cells were fixed or fixed and permeabilised, stained using anti-C5aR1-APC, anti-C5aR2-APC and isotype control antibody-APC, then assessed by flow cytometry using an Attune NxT Acoustic Focusing Cytometer. Gating Strategy example shows that **A.** Doublets were excluded, and **B.** Cells of interest were gated. Expression of **C.** extracellular C5aR1**, D.** intracellular C5aR2 and **E.** extracellular C5aR2 was plotted using histograms.

Doublets were excluded (**Figure 4.1 A**) and cells of interest were gated (**Figure 4.1 B**). C5aR1 was expressed extracellularly in PMA-differentiated THP-1 cells, but not in undifferentiated cells (**Figure 4.1 C**). C5aR2 was expressed intracellularly in undifferentiated and PMA-differentiated THP-1 cells (**Figure 4.1 D**), but not extracellularly (**Figure 4.1 E**).

4.2.2. Generating C5aR1 KO, C5aR2 KO and C5aR1/2 DKO THP-1 cells

Once expression of the target protein had been confirmed, CRISPR-Cas9 was used to generate polylconal C5aR1 KO, C5aR2 KO and C5aR1/2 DKO cell lines (**Figure 4.2**). sgRNA for C5aR1, C5aR2 and NTC was purchased in Gene KO Kits V2 from Synthego, and PCR primers were designed using NCBI Primer Blast to target a 520 bp amplicon ranging 250bp upstream and downstream from the start and end of the central guide sequence (**Supplementary Figures 4.1, 4.2, 4.3**). THP-1 cells were electroporated using protocol DE148 on a Lonza 4D-Nucleofector, and RNP complexes containing C5aR1, C5aR2, C5aR1 + C5aR2 or NTC gRNA were delivered using cationic lipid transfection.

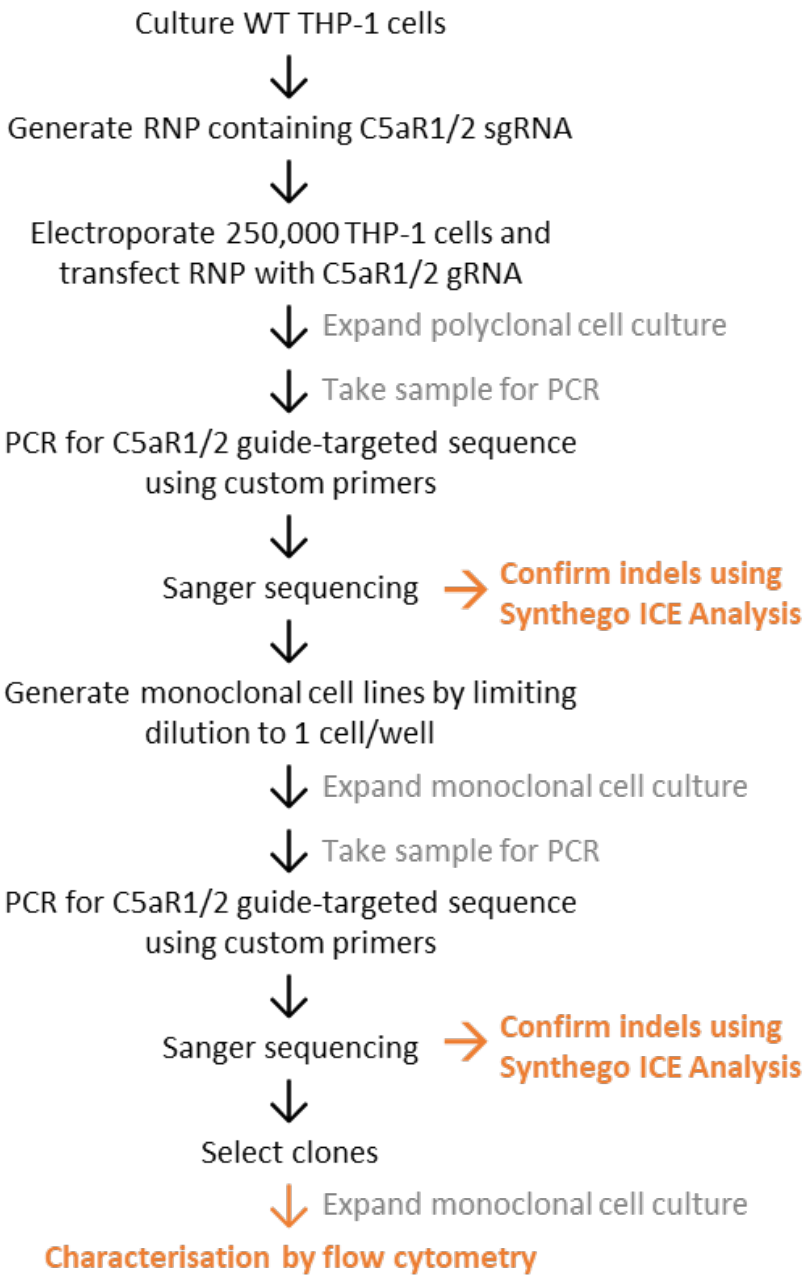

Figure 4.2. CRISPR-Cas9 Experimental Design. CRISPR-Cas9 was used to generate C5aR1 KO, C5aR2 KO and C5aR1/2 DKO monoclonal THP-1 cell lines. RNPs containing Cas9 and sgRNA were transfected into electroporated THP-1 cells. PCR and sequencing were used to confirm presence of indels in the polyclonal populations. Monoclonal cell lines were generated by limiting dilution. PCR and sequencing were used to confirm presence of indels in the monoclonal populations. Monoclones were selected, and loss of protein expression was confirmed by flow cytometry.

4.2.2.1. Selecting PCR Primers for C5aR1 and C5aR2

To select functioning primers, PCR was performed on WT THP-1 lysates using C5aR1 Primer Pair 1, 2 or 5 and C5aR2 Primer Pair 1, 5 or 6 (**Table 2.6**). PCR amplification products were separated using gel electrophoresis and visualised using an E-Gel. C5aR1 Primer Pair 5 and C5aR2 Primer Pair 5 were selected based on reactivity with WT lysate (data not shown).

4.2.2.2. Confirming successful PCR amplification product generation

PCR was then performed on lysate from NTC, C5aR1 KO, C5aR2 KO and C5aR1/2 DKO THP-1 cells using C5aR1 Primer Pair 5 and C5aR2 Primer Pair 5. PCR amplification products were separated by gel electrophoresis using an E-Gel, and visualised using an E-Gel Imager System (**Figure 4.3**). Bands were present in each lane, indicating successful PCR.

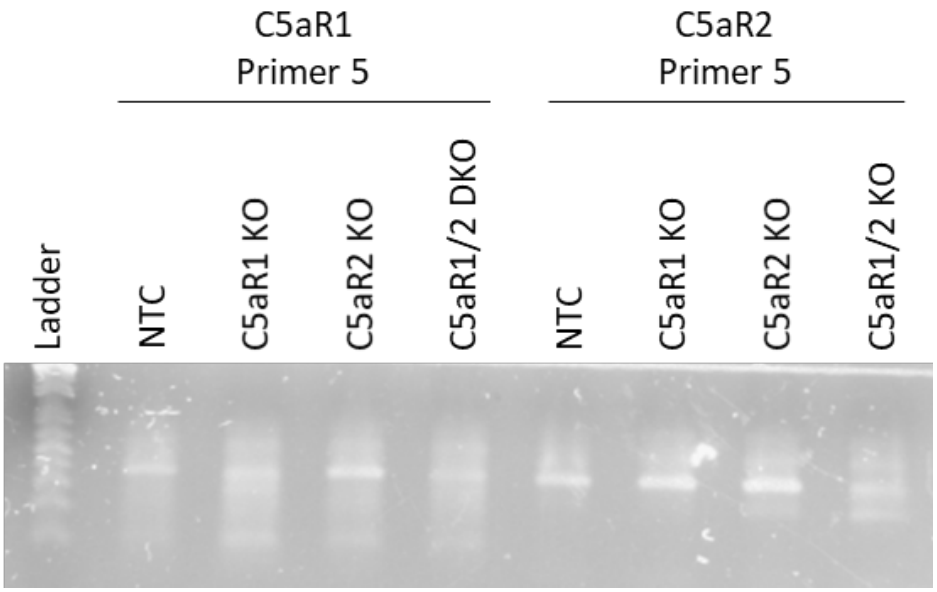

Figure 4.3. Confirmation of PCR amplification product generation in NTC and KO sequences by nucleic acid gel electrophoresis. Image of E-Gel containing PCR amplification product from NTC, C5aR1 KO, C5aR2 KO and C5aR1/2 DKO THP-1 lysate using C5aR1 Primer Pair 5 and C5aR2 Primer Pair 5.

4.2.2.3. Confirmation of C5aR1 indel in polyclonal C5aR1 KO THP-1 cells

These PCR amplification products were sent to GENEWIZ for Sanger sequencing. C5aR1 sequencing was successful, however PCR amplification products generated using C5aR2 primers were of insufficient quality to generate C5aR2 sequences.

To confirm on-target PCR and presence of indels, the modal C5aR1 forward primer sequences for NTC and C5aR1 KO were aligned using Clustal Omega (**Figure 4.4**).

```
           GCAGGANAGGAGTCGGCTACCGCCAAGTTGAGGAACCAGATGGCATTGATGGTCCGCTTG 60
C5aR1      --------------GGCTACCGCCAAGTTGAGGAACCAGATGGCATTGATGGTCCGCTTG 46
                         *********************************************

           GCCTCGAATGCCGTCACCCAGACCACCAGGGCATTGCCCAGCACTCCCACCAGGAAGACG 120
C5aR1      GCCTCGAATGCCGTCACCCAGACCACCAGGGCATTGCCCAGCACTCCCACCAGGAAGACG 106
           ************************************************************

           ACTGCAAAGATGACCAAGGCCAGGATGTCTGGAACACGCAGCGTGTTAGAAGTTTTATCC 180
C5aR1      ACTGCAAAGATGACCAAGTTGA---------------------------------------- 128
           *****************   *

           ACAGGGGTGTTGAGGTCCAGGGTATCCTTGTCATCATAGTGCCCATAATCAGGGGTGGTA 240
C5aR1      ------------------------------------------------------------ 128

           TAATTGAAGGAGTTCTAAGGGGAATCGGAGAGAGCAGAGAGGATGAGTCTGCAGACATGT 300
C5aR1      ------------------------------------------------------------ 128

           GCCCGGGTAGGGGGCATCCTGGCTCAGGCATGTGGCTTTTCCCCTGTGTG   350
C5aR1      ------------------------------------------------   128
```

Figure 4.4. C5aR1 KO sequence differs from NTC sequence. Clustal Omega alignment of the modal C5aR1 KO polyclone sequence (C5aR1) and modal NTC sequence (unlabelled). Asterisk indicates conservation of base between sequences.

Modal sequences were initially conserved, indicating that the desired amplicon had been generated by PCR. Alignment is lost after ACCAAG, followed by loss of sequence after AGTTGA in the C5aR1 KO, indicated by loss of asterisks under the sequences. This indicates successful editing and presence of indels within the polyclonal C5aR1 KO population.

To identify specific indels in the C5aR1 gene, sequences of PCR amplification products from the C5aR1 KO and NTC THP-1 cells were then aligned using Synthego ICE (**Figure 4.5**). The modal sequence from each population of sequences in the .ab1 files was exported from Bioedit and aligned using Clustal Omega, whereas Synthego ICE reports all indels present within the population of sequences in the .ab1 files.

A

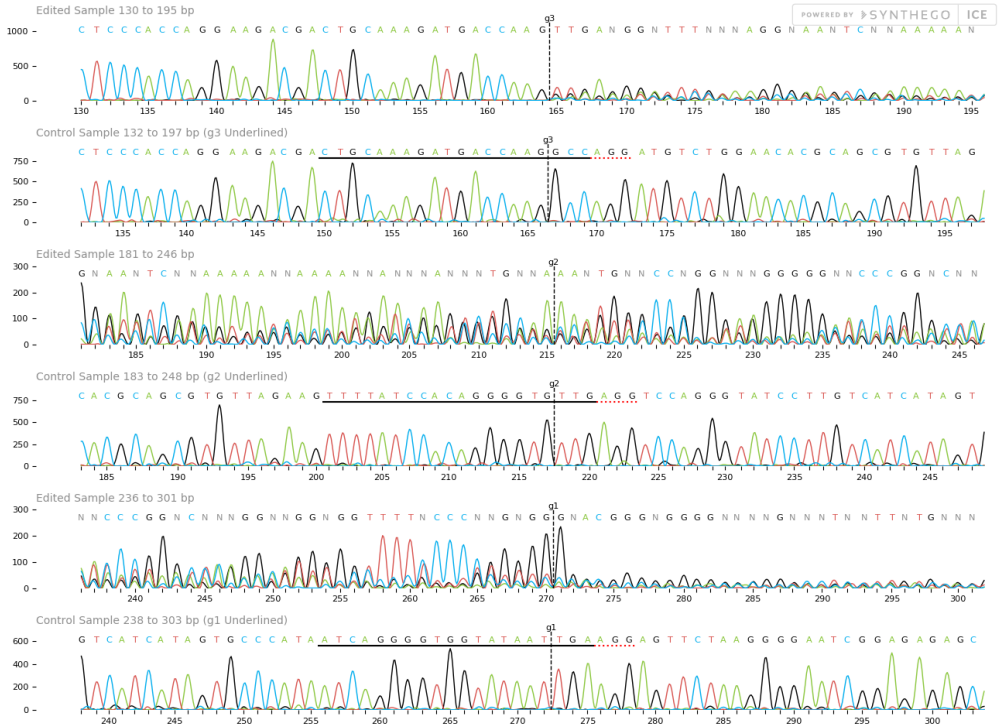

B **C**

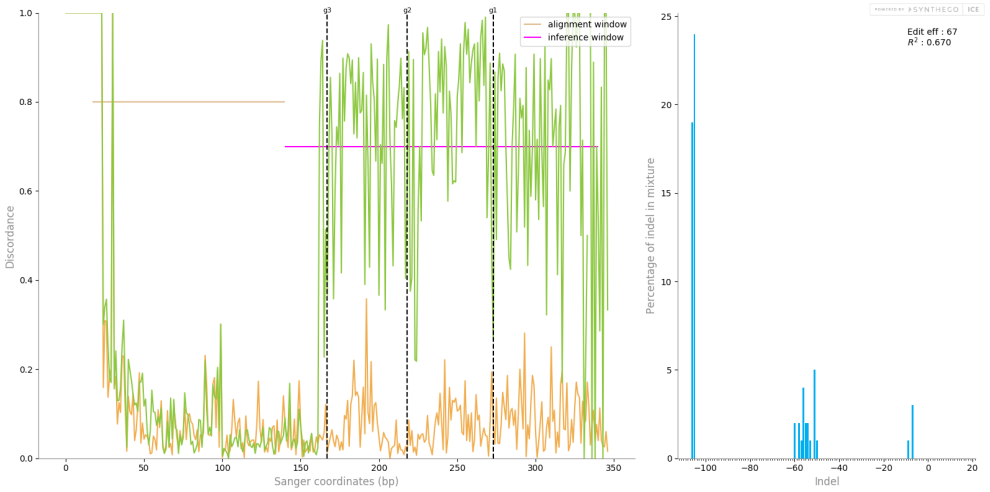

Figure 4.5. Identification of C5aR1 indels in C5aR1 KO THP-1 cells. Synthego ICE alignment of sequences from C5aR1-primed PCR amplification product from C5aR1 KO polyclonal THP-1 cells ("Edited") to sequences from C5aR1-primed PCR amplification product from NTC THP-1 cells ("Control"). **A.** Alignment shows sequence disruption in the edited C5aR1 KO population compared to NTC sequence following each guide target site (g1, g2, g3). **B.** Discordance between C5aR1 KO sequence and NTC sequence. Alignment window indicates conserved sequence between C5aR1 KO and NTC cells, and inference window indicates indels in C5aR1 KO sequence after guide sites (dotted lines). **C.** Size (bp) and percentage contribution of each detected indel in C5aR1 sequence vs. NTC sequence.

Sequence conservation between C5aR1 KO and NTC samples was lost after guide sites, indicating the presence of indels in the C5aR1 KO polyclonal population (**Figure 4.5 A**). Discordance is an algorithmically-generated measure of alignment between the edited sequence and the control sequence. There is a high level of discordance between the edited and control sequences after the guide sites (**Figure 4.5 B**), generated by a population of sequences comprised predominantly of 106 bp deletions (19%) and 105 bp deletions (24%) (**Figure 4.5 C**). These likely represent the same DNA sequences present in cells in the polyclonal C5aR1 KO population, and indicate that at least 45% of the population have a large 105-106 bp indel at a single position. Additional lower bp indels are also present at a lower incidence in the population.

Taken together, these results indicate that the C5aR1 KO cells had been successfully edited, and this polyclonal population contained cells with indels present in the C5aR1 gene. These cells could therefore be used to generate C5aR1 KO monoclonal cell lines by limiting dilution.

4.2.2.4. Confirmation of C5aR1 indel in polyclonal C5aR1/2 DKO THP-1 cells

To confirm the presence of indels in the C5aR1 gene of C5aR1/2 DKO cells, sequences of PCR amplification products from the C5aR1/2 DKO and NTC THP-1 cells were then aligned using Synthego ICE (**Figure 4.6**).

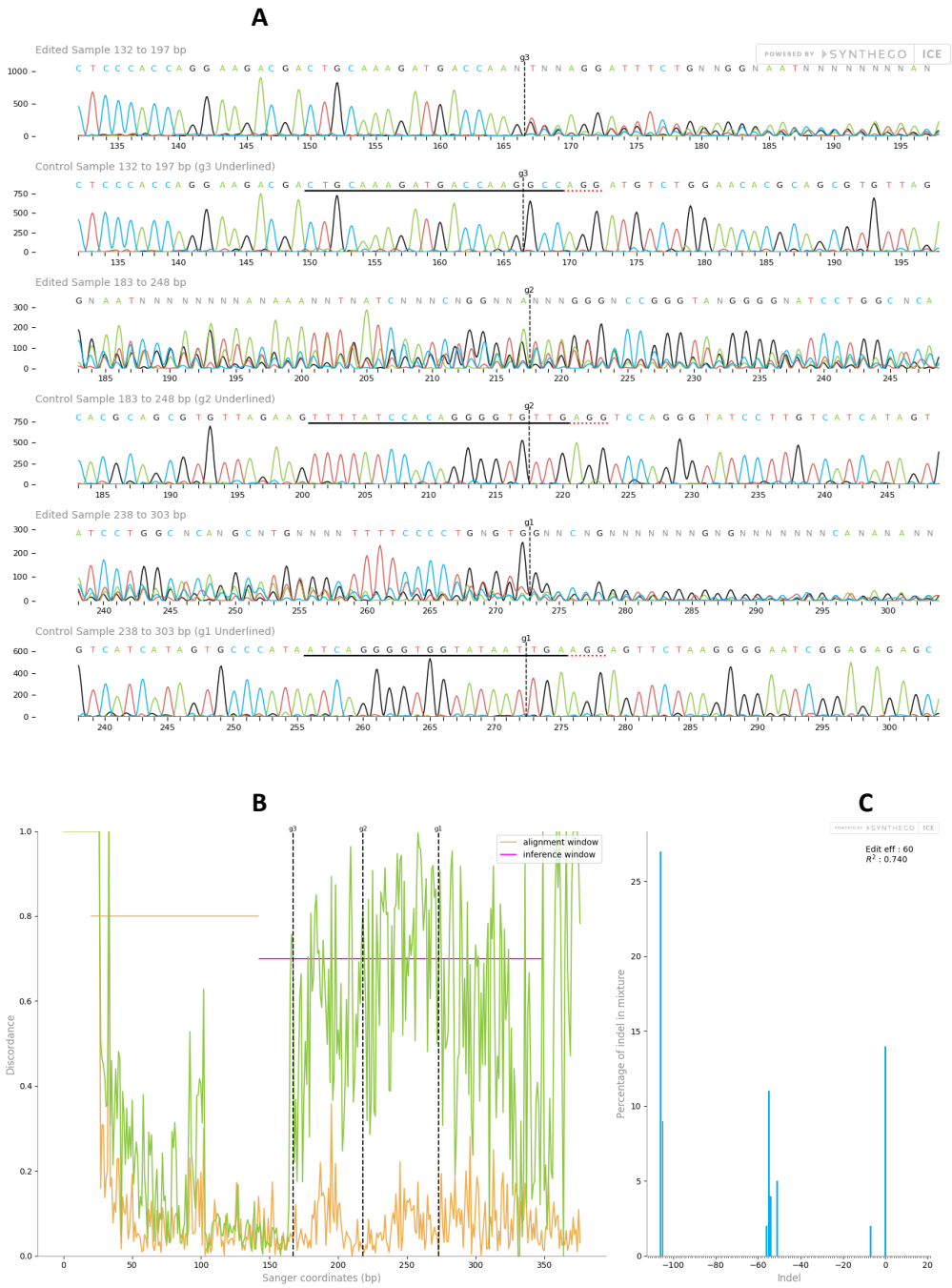

Figure 4.6. Identification of C5aR1 indels in C5aR1/2 DKO THP-1 cells. Synthego ICE alignment of sequences from C5aR1-primed PCR amplification product from C5aR1/2 DKO polyclonal THP-1 cells ("Edited") to sequences from C5aR1-primed PCR amplification product from NTC THP-1 cells ("Control"). **A.** Alignment shows sequence disruption in the edited C5aR1/2 DKO population compared to NTC sequence following each guide target site (g1, g2, g3). **B.** Discordance between C5aR1/2 DKO sequence and NTC sequence. **C.** Size (bp) and percentage contribution of each detected indel in C5aR1/2 DKO sequence vs. NTC sequence.

As with the C5aR1 KO THP-1 cells, sequences were initially conserved between C5aR1/2 DKO and NTC samples followed by loss of conservation after the guide sites, indicating the presence of indels in the target amplicon of the C5aR1 gene in the C5aR1/2 DKO polyclonal population (**Figure 4.6 A**). There is a high level of discordance between the edited and control sequences after the guide sites (**Figure 4.6 B**), generated by a population of sequences with indels of various sizes (**Figure 4.6 C**).

These results indicate that the C5aR1 had been successfully edited in the C5aR1/2 DKO cells. Sequencing and confirmation of indel in the C5aR2 gene is required before using these cells to generate monoclonal cell lines by limiting dilution.

4.2.2.5. Optimising PCR and sequencing for C5aR2

PCR amplification product from C5aR2 primer Primer Pair 5 failed to generate interpretable sequencing data. To generate higher quality PCR amplification products, the PCR protocol was optimised by performing PCR on the remaining NTC lysate using 2 different annealing temperatures (62°C and 65°C), and the 3 original C5aR2 primer pairs (1, 5 and 6) or 6 additional primers (New Primer 1, 2 and Primer A, B, C, D).

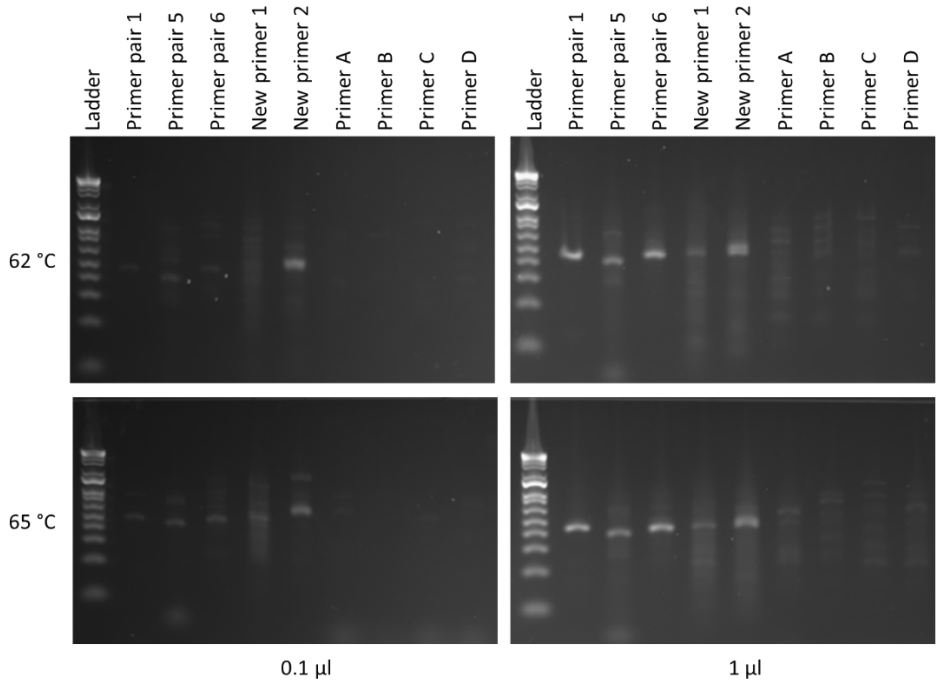

Figure 4.7. C5aR2 PCR primer optimisation and selection using nucleic acid gel electrophoresis. Image of E-Gel containing PCR amplification product from 0.1 or 1 µL NTC THP-1 lysate using original C5aR2 Primer Pairs 1, 5 and 6, New Primer 1, 2 and Primer A, B, C, D with annealing temperature 62°C or 65°C.

The PCR amplification products were separated by gel electrophoresis using an E-Gel and visualised using an E-Gel Imager System (**Figure 4.7**). New Primers 1 and 2 generated a PCR amplification product with a higher background signal than the original Primer Pairs 1, 5 and 6. Primers A, B, C and D failed to generate distinct bands. Primer Pairs 1 and 6 were the most successful, generating the brightest bands with the lowest background signal. Annealing temperature of 65°C using 1 µL lysate were the

best conditions for PCR, so these primers were used to confirm presence of PCR amplification product in the C5aR2 KO and C5aR1/2 DKO lysates.

PCR was performed on C5aR1 KO, C5aR2 KO and C5aR1/2 DKO lysates using Primer Pairs 1 and 6 at 65°C with 1 µL lysate. There was insufficient NTC lysate remaining, so C5aR1 KO lysate was used as an unedited control for the C5aR2 gene in this experiment. PCR amplification products were separated using gel electrophoresis and visualised using an E-Gel (**Figure 4.8**).

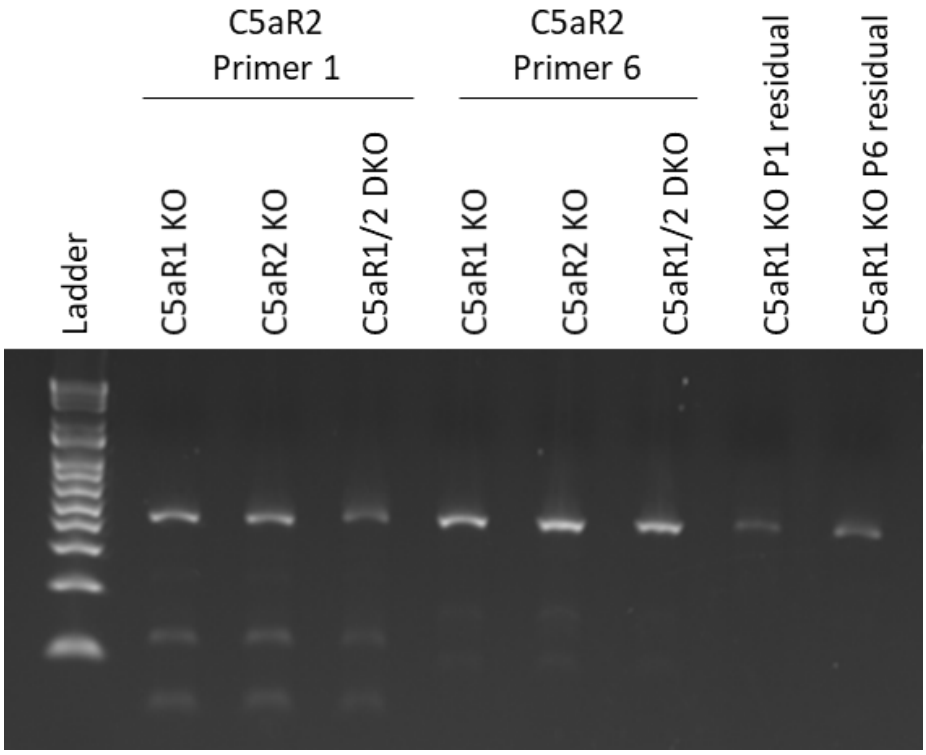

Figure 4.8. Confirmation of C5aR2 PCR amplification product in C5aR1 KO, C5aR2 KO and C5aR1/2 DKO THP-1 cells using nucleic acid gel electrophoresis. Image of E-Gel containing PCR amplification product from 1 µL C5aR1 KO, C5aR2 KO or C5aR1/2 DKO THP-1 lysate using C5aR2 Primer Pairs 1 and 6 with annealing temperature 62°C or 65°C. Lanes 7 and 8 contain remaining lysate from **Figure 4.7**, used as a positive control as they were known to be visible on an E-Gel.

Primers functioned as expected in all samples, generating bright individual bands. This indicated that target PCR amplicons had been amplified using the optimised PCR conditions. All samples were sent for Sanger sequencing using C5aR2 forward primer 1 as the sequencing primer.

4.2.2.6. Lack of C5aR2 indel in C5aR2 KO or C5aR1/2 DKO cells

To confirm the presence of indels in the C5aR2 gene, sequences of PCR amplification products from the C5aR2 KO (**Figure 4.9**) and C5aR1/2 DKO (**Figure 4.10**) THP-1 cells were aligned with sequences of PCR amplification products from C5aR1 KO THP-1 cells using Synthego ICE. PCR amplification product from the C5aR1 KO lysate was used as a control sequence as there was insufficient NTC lysate, which was possible as the C5aR2 amplicon was intact in these cells.

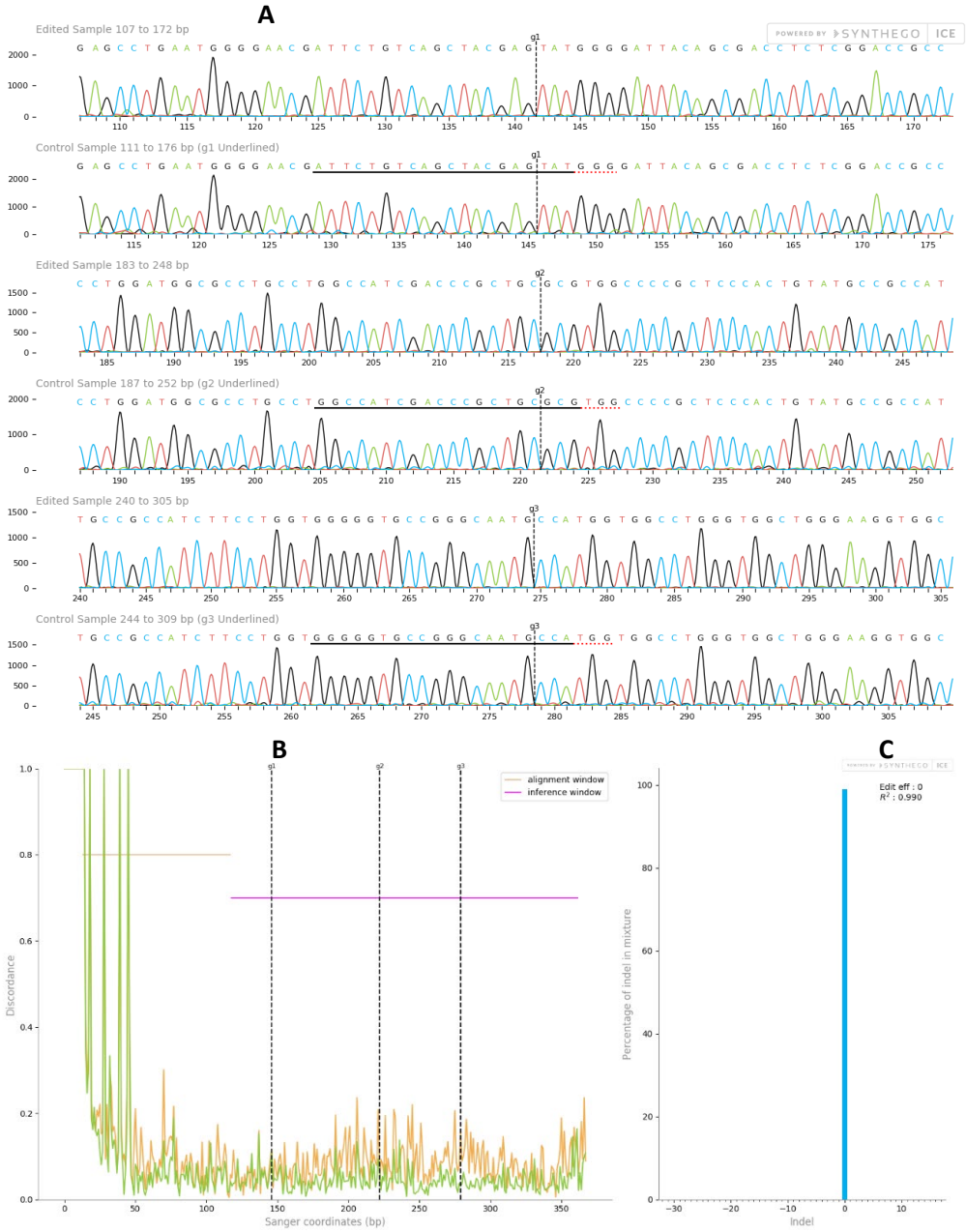

Figure 4.9. ICE alignment confirms that no indels are present in C5aR2 KO THP-1 cells. Synthego ICE alignment of sequences from C5aR2-primed PCR amplification product from C5aR2 KO polyclonal THP-1 cells ("Edited") to sequences from C5aR1-primed PCR amplification product from C5aR1 KO THP-1 cells ("Control"). **A.** Alignment shows no sequence disruption in the edited C5aR2 KO population compared to control sequence following each guide target site (g1, g2, g3). **B.** Discordance is low between C5aR2 KO sequence and control sequence. **C.** 100% of indels are 0bp, indicating no indels present in the Edited sequence.

A

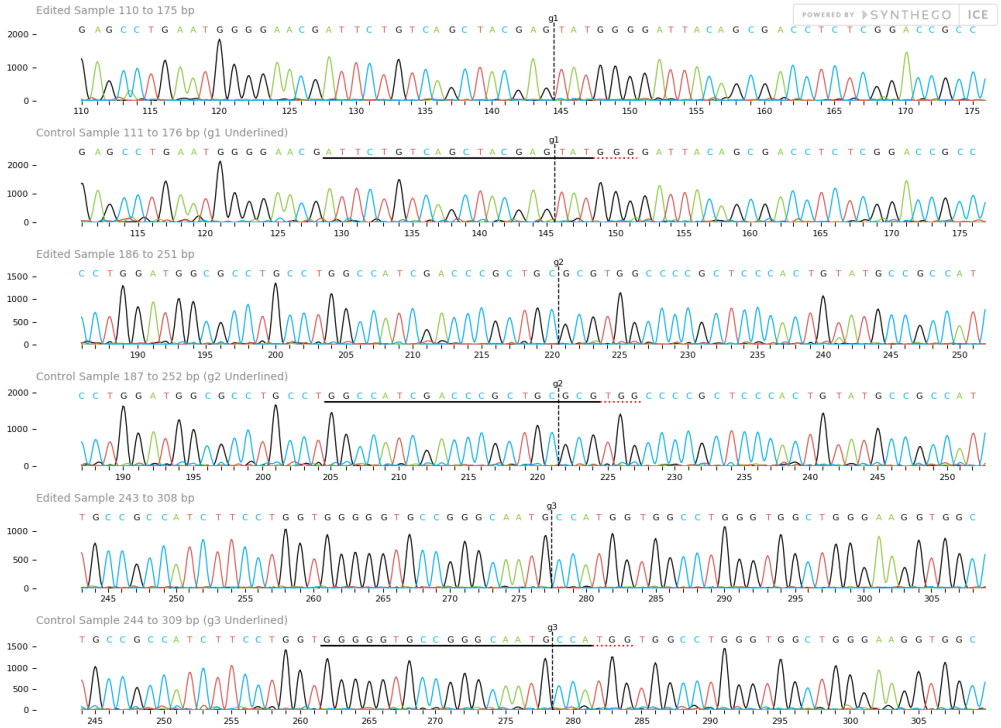

B **C**

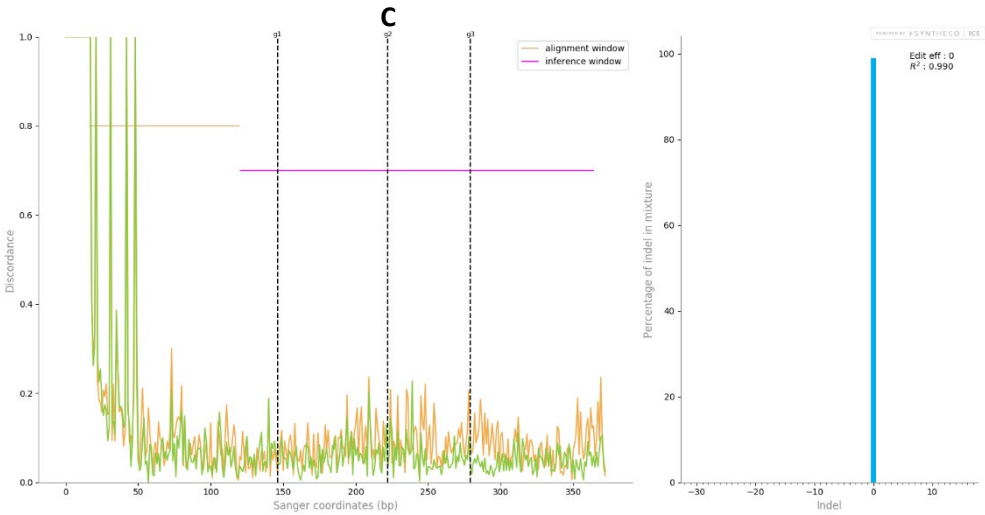

Figure 4.10. ICE alignment confirms that no indels are present in C5aR1/2 DKO THP-1 cells. Synthego ICE alignment of sequences from C5aR2-primed PCR amplification product from C5aR1/2 DKO polyclonal THP-1 cells ("Edited") to sequences from C5aR1-primed PCR amplification product from C5aR1 KO THP-1 cells ("Control"). **A.** Alignment shows no sequence disruption in the edited C5aR1/2 DKO population compared to control sequence following each guide target site (g1, g2, g3). **B.** Discordance is low between C5aR2 KO sequence and control sequence. **C.** 100% of indels are 0bp, indicating no indels present in the Edited sequence.

There was no evidence of indel in either polyclonal populations of cells. This indicates that the CRISPR-Cas9 edit of C5aR2 was not effective. The “C5aR2 KO” polyclonal THP-1 cells and “C5aR1/2 DKO” polyclonal THP-1 cells were therefore discarded from culture, as neither was a true C5aR2 KO. NTC THP-1 cells were also lost from culture due to COVID-19 pandemic-related laboratory access issues. WT cells were used in future experiments.

Loss of laboratory access during the COVID-19 pandemic also introduced significant time constraints to experimental work. Instead of generating new CRISPR-Cas9 KO cell lines with the same sgRNA, an aliquot of uncharacterised C5aR2 KO THP-1 cells (“AJ C5aR2 KO cells”) generated previously in the lab using an alternative gRNA by Abbie Jayyaratnam (GSK) and Darren Gormley (GSK) was retrieved from liquid nitrogen storage and cultured. These cells were characterised to confirm loss of protein expression, and used in subsequent experiments as C5aR2 KO cells.

4.2.2.7. Selecting primers "AJ C5aR2 KO" PCR

AJ C5aR2 KO cells were generated using an alternative gRNA (**Table 2.5**), therefore new PCR primers targeting the alternative gRNA site were required. PCR primers were designed using Primer Blast, and PCR using WT lysate was performed to identify the optimum primers. PCR was performed using 2 µL lysate, an annealing temperature of 65 °C, two primers designed previously by Abbie Jayyaratnam (GSK) and Darren Gormley (GSK) (AJ Original 1 and 2), and 5 newly-designed primers (AJ 1, 2, 3, 4 and 5). The PCR amplification products were separated by gel electrophoresis and visualised using an E-Gel (**Figure 4.11**).

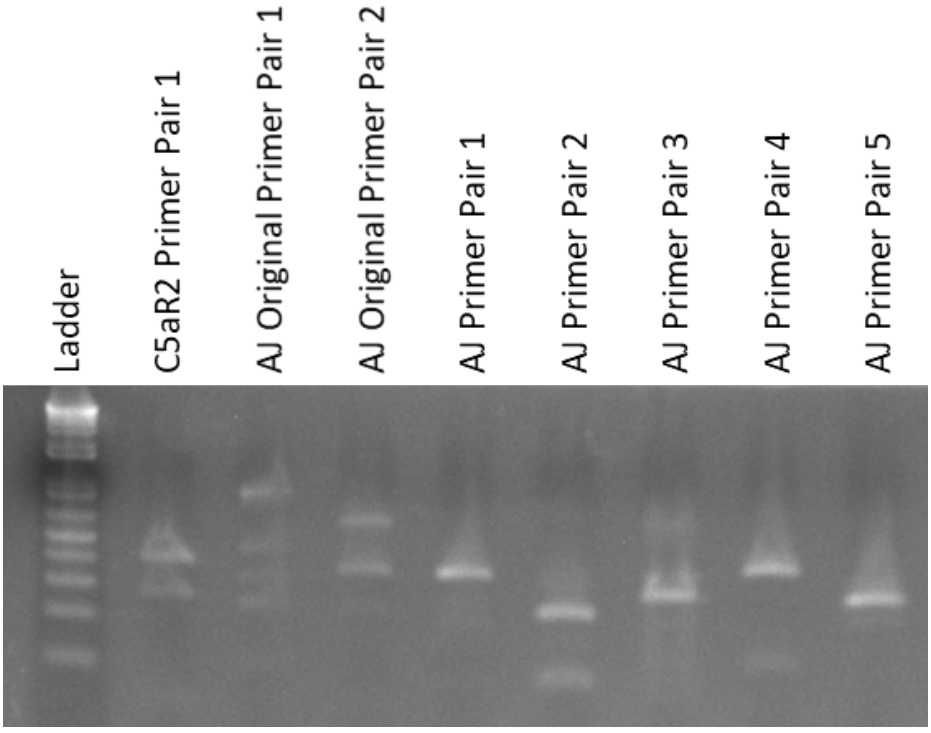

Figure 4.11. Selection of AJ C5aR2 PCR primers by nucleic acid gel electrophoresis of WT PCR amplification product. Image of E-Gel containing PCR amplification product from 2 µL WT THP-1 lysate with an annealing temperature of 65 °C using **2.** C5aR2 Primer Pair 1 as a positive control, **3-4** AJ Original Primer Pairs and **5-9** AJ Primer Pairs 1-5.

C5aR2 Primer Pair 1, from the PCR experiments in **Figures 4.7-4.10,** was used as a positive control to generate a PCR amplification product that could be visualised using

the E-gel. AJ Original Primer Pairs 1 and 2 performed poorly, generating multiple off-target bands. AJ Primer Pairs 1 and 4 generated a PCR amplification product that was visualised as a single, clear band in the E-gel at the expected bp length, with some lower bp signal generated by AJ Primer Pair 4. AJ Primer Pairs 2, 3 and 5 generated a lower bp amplicon, and AJ Primer Pair 3 generated a smeared signal.

The same primers were used to generate PCR amplification product using AJ C5aR2 KO THP-1 cell lysates The PCR amplification products were separated by gel electrophoresis and visualised using an E-Gel (**Figure 4.12**).

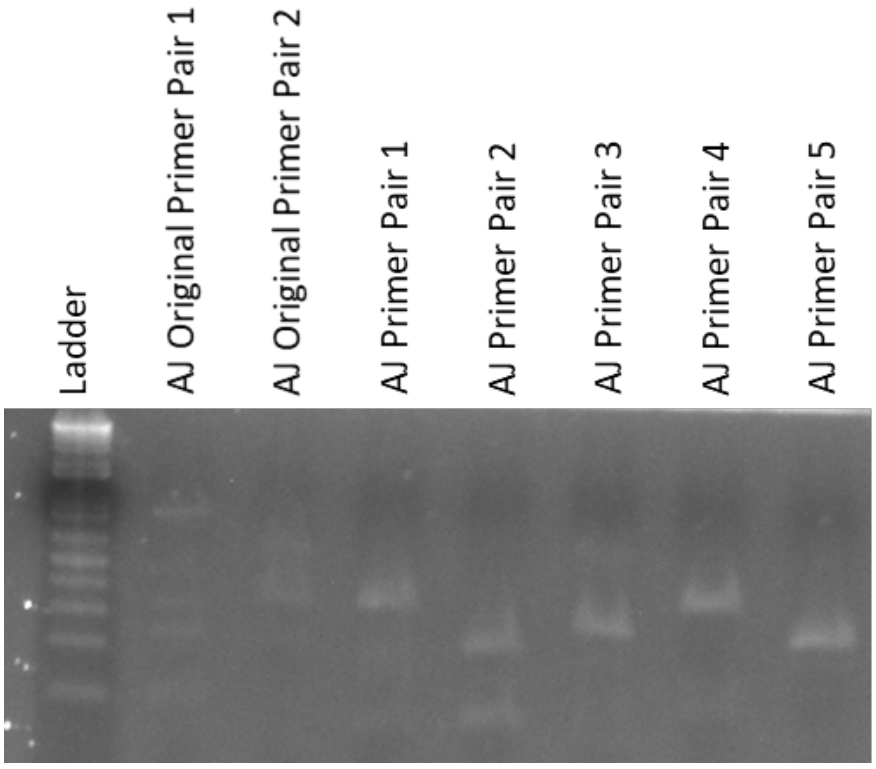

Figure 4.12. Selection of AJ C5aR2 PCR primers by nucleic acid gel electrophoresis of AJ C5aR2 KO PCR amplification product. Image of E-Gel containing PCR amplification product from 2 µL AJ C5aR2 THP-1 lysate with an annealing temperature of 65 °C using **2-3** AJ Original Primer Pairs and **4-8** AJ Primer Pairs 1-5.

In the AJ C5aR2 KO PCR amplification products, the visible bands in the E-gel formed a similar pattern to the WT PCR amplification product in **Figure 4.11**. AJ Original Primer Pairs 1 and 2 failed to generate clear bands, and AJ Primer Pair 2 generated an off-target band. AJ Primer Pairs 1, 3, 4 and 5 generated a single clear band.

As AJ C5aR2 Primer Pairs 1 and 4 generated the brightest on-target bands at the expected position with the fewest off-target bands, PCR amplification products from WT and AJ C5aR2 KO THP-1 cells generated using AJ Primer Pairs 1 and 4 were sent for Sanger sequencing. To confirm on-target PCR, sequences of PCR amplification product generated using AJ C5aR2 Primer Pairs 1 and 4 and WT THP-1 cell lysate were aligned with the primer sequences, guide RNA sequence and C5aR2 gene. Separate alignments of sequence generated using Forward Primers (**Figure 4.13**) and Reverse Primers (**Figure 4.14**) were performed using Clustal Omega.

```
WT4F        ------------------------------------------------------------  0
WT1F        ------------------------------------------------------------  0
Primer4F    GCGGATTTGCTGTGCTGTTT----------------------------------------  20
Primer1F    --------GCTGTGCTGTTTGTCTCTGC-------------------------------  20
C5aR2       GCGGATTTGCTGTGCTGTTTGTCTCTGCCCATCCTGGCAGTGCCCATTGCCCGTGGAGGC  9480
Guide       ------------------------------------------------------------  0

WT4F        ------------------------------------------------------------  0
WT1F        ----------------------CTGTCGGGCGCTGCCCTCCATCATCCTGCTGACCATG  37
Primer4F    ------------------------------------------------------------  20
Primer1F    ------------------------------------------------------------  20
C5aR2       CACTGGCCGTATGGTGCAGTGGGCTGTCGGGCGCTGCCCTCCATCATCCTGCTGACCATG  9540
Guide       ------------------------------------------------------------  0

WT4F        ------------CTGCTCCTGGCAGCTCTCAGTGCCGACCTCTGCTTCCTGGCTCTCGGG  48
WT1F        TATGCCAGCGTCCTGCTCCTGGCAGCTCTCANTGCCGACCTCTGCTTCCTGGCTCTCGGG  97
Primer4F    ------------------------------------------------------------  20
Primer1F    ------------------------------------------------------------  20
C5aR2       TATGCCAGCGTCCTGCTCCTGGCAGCTCTCAGTGCCGACCTCTGCTTCCTGGCTCTCGGG  9600
Guide       ------------------------------------------------------------  0

WT4F        CCTGCCTGGTGGTCTACGGTTCANCGGGCGTGCGGGGTGCAGGTGGCCTGTGGGGCAGCC  108
WT1F        CCTGCCTGGTGGTCTACGGTTCAGCGGGCGTGCGGGGTGCAGGTGGCCTGTGGGGCAGCC  157
Primer4F    ------------------------------------------------------------  20
Primer1F    ------------------------------------------------------------  20
C5aR2       CCTGCCTGGTGGTCTACGGTTCAGCGGGCGTGCGGGGTGCAGGTGGCCTGTGGGGCAGCC  9660
Guide       -------GGTGGTCTACGGTTCAG-----------------------------------  17

WT4F        TGGACACTGGCCTTGCTGCTCACCGTGCCCTCCGCCATCTACCGCCGGCTGCACCAGGAG  168
WT1F        TGGACACTGGCCTTGNTGCTCACCGTGCCCTCCGCCATCTACCGCCGGCTGCACCAGGAG  217
Primer4F    ------------------------------------------------------------  20
Primer1F    ------------------------------------------------------------  20
C5aR2       TGGACACTGGCCTTGCTGCTCACCGTGCCCTCCGCCATCTACCGCCGGCTGCACCAGGAG  9720
Guide       ------------------------------------------------------------  17

WT4F        CACTTCCCAGCCCGGCTGCAGTGTGTGGTGGACTACGGCGGCTCCTCCAGCACCGAGAAT  228
WT1F        CACTTCCCAGCCCGGCTGCAGTGTGTGGTGGACTACGGCGGCTCCTCCA-----------  266
Primer4F    ------------------------------------------------------------  20
Primer1F    ------------------------------------------------------------  20
C5aR2       CACTTCCCAGCCCGGCTGCAGTGTGTGGTGGACTACGGCGGCTCCTCCAGCACCGAGAAT  9780
Guide       ------------------------------------------------------------  17

WT4F        GCGGTGACTG--------------------------------------------------  238
WT1F        ------------------------------------------------------------  266
Primer4F    ------------------------------------------------------------  20
Primer1F    ------------------------------------------------------------  20
C5aR2       GCGGTGACTGCCATCCGGTTTCTTTTTGGCTTCCTGGGGCCCCTGGTGGCCGTGGCCAGC  9840
Guide       ------------------------------------------------------------  17
```

Figure 4.13. AJ Forward Primers 1 and 4 generate sequences which align to C5aR2 gene. Clustal Omega alignment of C5aR2 gene, primer sequences and AJ C5aR2 KO gRNA sequence with Forward primer-generated modal sequences of PCR amplification products generated using WT lysate and AJ C5aR2 Primer Pairs 1 and 4.

```
WT1R        ------------------------------------------------------------  0
Primer4R    ------------------------------------------------------------  0
Primer1R    ------------------------------------------------------------  0
C5aR2       GTGGCTGGGAAGGTGGCCCGCCGGAGGGTGGGTGCCACCTGGTTGCTCCACCTGGCCGTG  9420
Guide       ------------------------------------------------------------  0
WT4R        ------------------------------------------------------------  0

WT1R        ----------------TTTGTCTCTGCCCATCCTGGCAGTGCCCATTGCCCGTGGAGGC  43
Primer4R    ------------------------------------------------------------  0
Primer1R    ------------------------------------------------------------  0
C5aR2       GCGGATTTGCTGTGCTGTTTGTCTCTGCCCATCCTGGCAGTGCCCATTGCCCGTGGAGGC  9480
Guide       ------------------------------------------------------------  0
WT4R        ----------TGTGCTGTTTGTCTCTGCCCATCCTGGCAGTGCCCATTGCCCGTGGAGGC  50

WT1R        CACTGGCCGTATGGTGCAGTGGGCTGTCGGGCGCTGCCCTCCATCANCNNGNTGACCATG  103
Primer4R    ------------------------------------------------------------  0
Primer1R    ------------------------------------------------------------  0
C5aR2       CACTGGCCGTATGGTGCAGTGGGCTGTCGGGCGCTGCCCTCCATCATCCTGCTGACCATG  9540
Guide       ------------------------------------------------------------  0
WT4R        CACTGGCCGTATGGTGCAGTGGGCTGTCGGGCGCTGCCCTCCATCATCCTGCTGACCATG  110

WT1R        TATGCCAGCGTCCTGCTCCTGGCAGCTNTCAGTGCCGACCTCTGNNNCNTGGCTCTCGGG  163
Primer4R    ------------------------------------------------------------  0
Primer1R    ------------------------------------------------------------  0
C5aR2       TATGCCAGCGTCCTGCTCCTGGCAGCTCTCAGTGCCGACCTCTGCTTCCTGGCTCTCGGG  9600
Guide       ------------------------------------------------------------  0
WT4R        TATGCCAGCGTCCTGCTCCTGGCAGCTCTCAGTGCCGACCTCTGCTTCCTGGCTCTCGGG  170

WT1R        CCTGCCTGGTGGTNTACGGTTCAGCGGGCGTGCGGGGTGCAGGTGGCCTGTGGGGCAGCC  223
Primer4R    ------------------------------------------------------------  0
Primer1R    ------------------------------------------------------------  0
C5aR2       CCTGCCTGGTGGTCTACGGTTCAGCGGGCGTGCGGGGTGCAGGTGGCCTGTGGGGCAGCC  9660
Guide       -------GGTGGTCTACGGTTCAG------------------------------------  17
WT4R        CCTGCCTGGTGGTCTACGGTTCAGCGGGCGTGCGGGGTGCAGGTGGCCTGTGGGGCAGCC  230

WT1R        TGGACACTGGCCTTGNTGCTCACCGTGCCCTCCGCCATCTACC----------------  266
Primer4R    ------------------------------------------------------------  0
Primer1R    ------------------------------------------------------------  0
C5aR2       TGGACACTGGCCTTGCTGCTCACCGTGCCCTCCGCCATCTACCGCCGGCTGCACCAGGAG  9720
Guide       ------------------------------------------------------------  17
WT4R        TGGACACTGGCC--------------------------------------------------  242

WT1R        ------------------------------------------------------------  266
Primer4R    ------------------------------------------------------------  0
Primer1R    ----------------------------------------CTCCTCCAGCACCGAGAAT  19
C5aR2       CACTTCCCAGCCCGGCTGCAGTGTGTGGTGGACTACGGCGGCTCCTCCAGCACCGAGAAT  9780
Guide       ------------------------------------------------------------  17
WT4R        ------------------------------------------------------------  242

WT1R        ------------------------------------------------------------  266
Primer4R    ----TGACTGCCATCCGGTTTCTT-------------------------------------  20
Primer1R    G-----------------------------------------------------------  20
C5aR2       GCGGTGACTGCCATCCGGTTTCTTTTTGGCTTCCTGGGGCCCCTGGTGGCCGTGGCCAGC  9840
Guide       ------------------------------------------------------------  17
WT4R        ------------------------------------------------------------  242
```

Figure 4.14. AJ Reverse Primers 1 and 4 generate sequence which align to C5aR2 gene. Clustal Omega alignment of C5aR2 gene, primer sequences and AJ C5aR2 KO gRNA sequence with Reverse primer-generated modal sequences of PCR amplification products generated using WT lysate and AJ C5aR2 Primer Pairs 1 and 4.

The C5aR2 gene sequence aligns to sequences of PCR amplification products generated by all four primers and the gRNA sequence, indicating that these primers generate on-target amplicons.

However, these sequences failed to align when analysed using Synthego ICE. Synthego ICE requires very high quality sequencing data for successful alignment, and will not return data if a full alignment is not possible. Whilst the data are lower resolution in Clustal Omega analyses, this approach allows for basic comparisons to identify partial alignments where Synthego ICE fails. This is not sufficient to characterise individual indels, but it can be sufficient to indicate whether the amplicons are on or off-target. The lack of alignment in Synthego ICE is likely due to contaminating sequences not detected using Clustal Omega.

In contrast to the WT samples, sequencing of PCR amplification product generated using AJ C5aR2 KO THP-1 cell lysate failed. Taken together with the low quality WT sequence, these observations suggest that these primers are generating off-target PCR amplification products alongside amplifiying the target amplicon.

4.2.2.8. Optimising PCR conditions to characterise "AJ C5aR2 KO" THP-1 cells

PCR conditions were optimised to facilitate the generation of high quality sequencing data. PCR was performed on WT and AJ C5aR2 THP-1 cell lysates using AJ C5aR2 Primer Pairs 1 and 4 using a range of annealing temperatures from 55-65°C in 2°C increments. Short off-target PCR amplicons were suspected to be causing sequencing alignment issues, so this experiment aimed to rule out sub-optimal annealing temperature. PCR amplification products were separated by gel electrophoresis and visualised using an E-Gel (**Figure 4.15**).

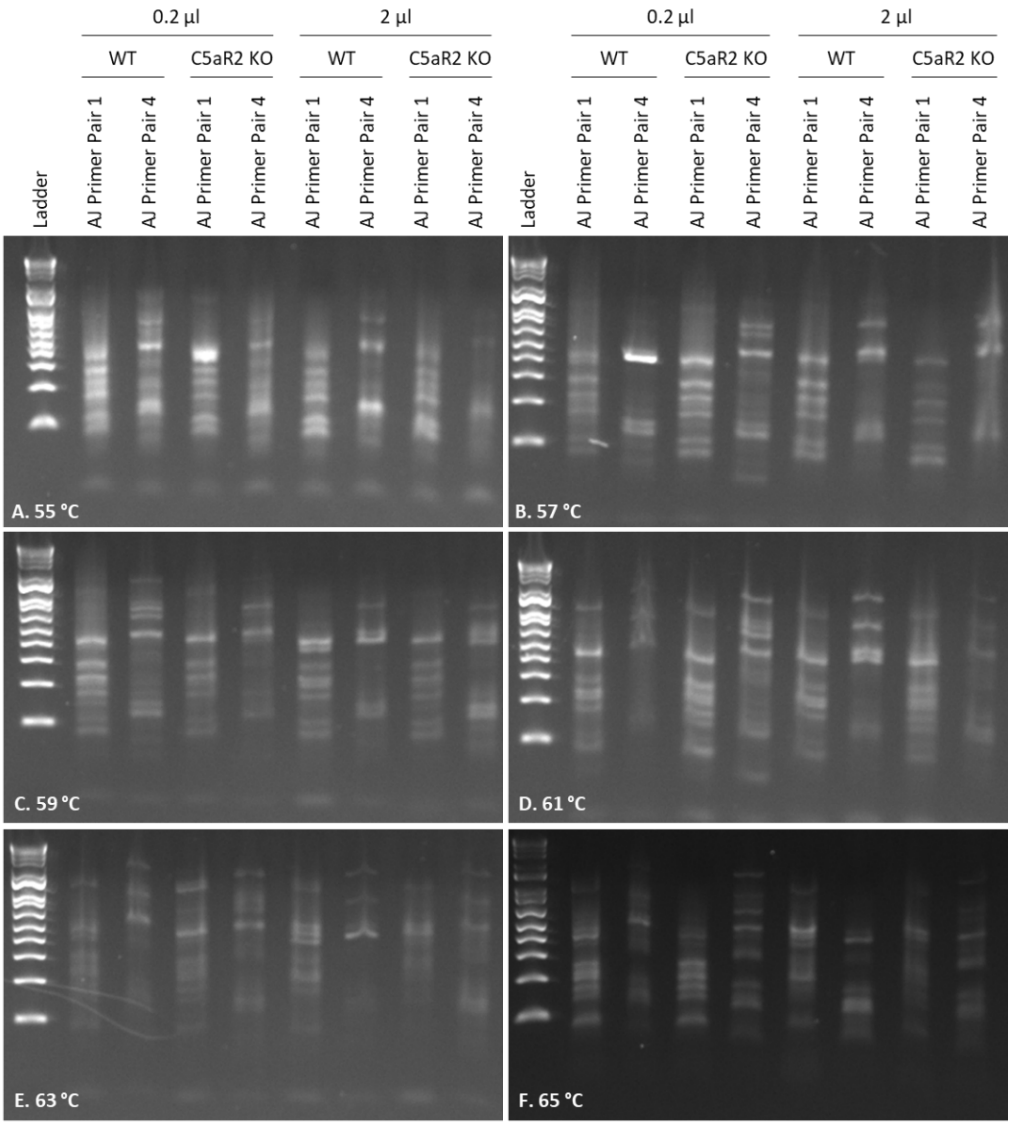

Figure 4.15. Optimising PCR conditions for AJ C5aR2 Primer Pairs 1 and 4 using a gradient of annealing temperatures. Images of E-Gels containing PCR amplification product from 0.2 µL or 2 µL WT or AJ C5aR2 KO THP-1 cell lysate with an annealing temperature of **A.** 55°C, **B.** 57°C, **C.** 59°C, **D.** 61°C, **E.** 63°C, **F.** 65°C.

There were off-target bands present across all lanes of all PCRs. An annealing temperature of 55-59 °C generated the brightest bands, whereas 61 °C, 63 °C and 65°C generated dimmer bands. Despite the off-target bands in these PCR amplification products, those generated with 0.2 µL lysate, AJ Primer Pair 1 and 4 with an annealing temperature of 55°C and 59°C were sent for Sanger sequencing.

Sequencing failed for the PCR amplification products generated at an annealing temperature of 55 °C, however there were sequences generated at 59 °C. Clustal Omega was used to align the C5aR2 gene, primer sequences and guide RNA sequence to PCR amplification products generated using WT lysate and forward primers (**Figure 4.16**), reverse primers (**Figure 4.17**) or AJ C5aR2 KO lysate and forward primers (**Figure 4.18**) or reverse primers (**Figure 4.19**) at 59 °C.

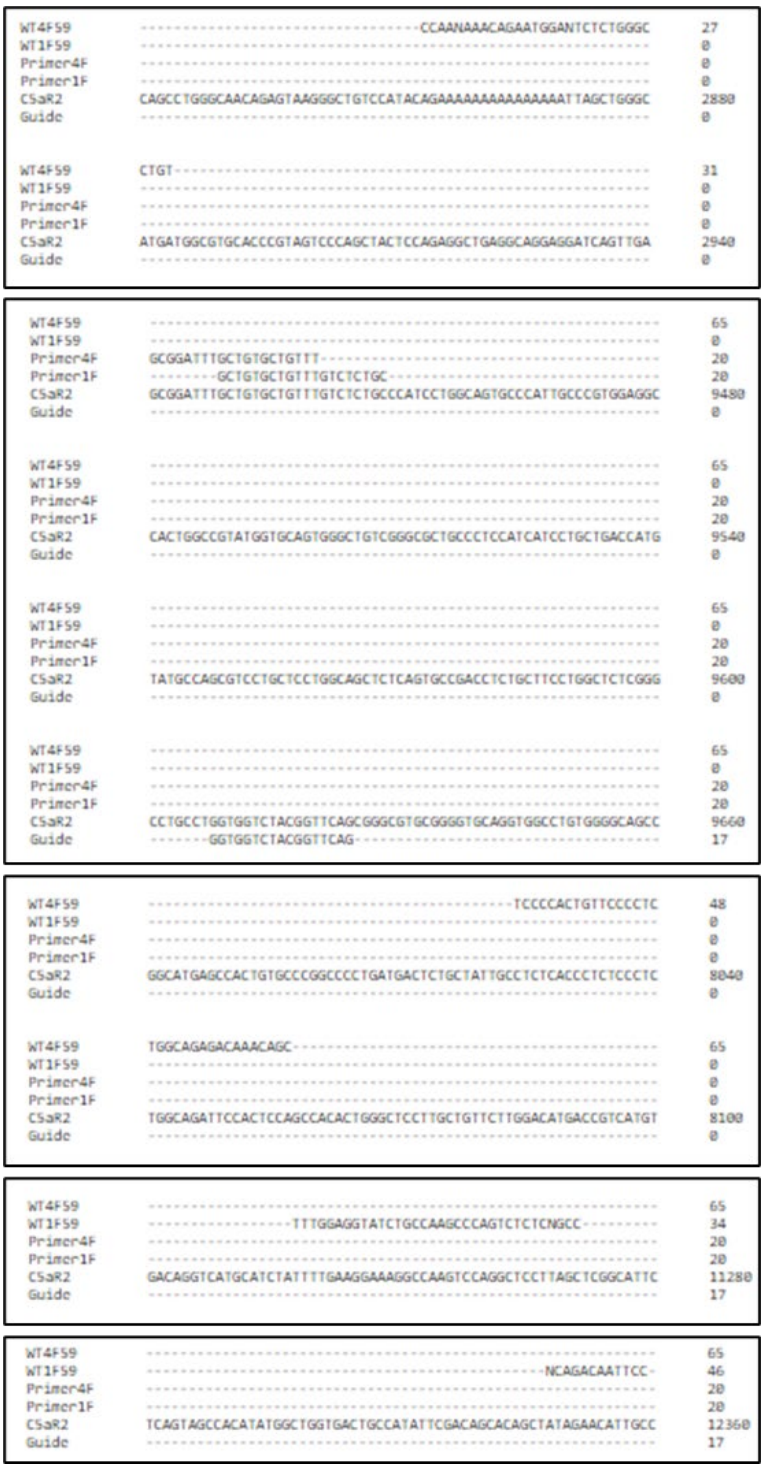
WT4F59 ----------CCAANAAACAGAATGGANTCTCTGGGC 27
WT1F59 ---------- 0
Primer4F ---------- 0
Primer1F ---------- 0
CSaR2 CAGCCTGGGCAACAGAGTAAGGGCTGTCCATACAGAAAAAAAAAAAAAAAATTAGCTGGGC 2880
Guide ---------- 0
WT4F59 CTGT---------- 31
WT1F59 ---------- 0
Primer4F ---------- 0
Primer1F ---------- 0
CSaR2 ATGATGGCGTGCACCCGTAGTCCCAGCTACTCCAGAGGCTGAGGCAGGAGGATCAGTTGA 2940
Guide ---------- 0
WT4F59 ---------- 65
WT1F59 ---------- 0
Primer4F GCGGATTTGCTGTGCTGTTT---------- 20
Primer1F --------GCTGTGCTGTTTGTCTCTGC---------- 20
CSaR2 GCGGATTTGCTGTGCTGTTTGTCTCTGCCCATCCTGGCAGTGCCCATTGCCCGTGGAGGC 9480
Guide ---------- 0
WT4F59 ---------- 65
WT1F59 ---------- 0
Primer4F ---------- 20
Primer1F ---------- 20
CSaR2 CACTGGCCGTATGGTGCAGTGGGCTGTCGGGCGCTGCCCTCCATCATCCTGCTGACCATG 9540
Guide ---------- 0
WT4F59 ---------- 65
WT1F59 ---------- 0
Primer4F ---------- 20
Primer1F ---------- 20
CSaR2 TATGCCAGCGTCCTGCTCCTGGCAGCTCTCAGTGCCGACCTCTGCTTCCTGGCTCTCGGG 9600
Guide ---------- 0
WT4F59 ---------- 65
WT1F59 ---------- 0
Primer4F ---------- 20
Primer1F ---------- 20
CSaR2 CCTGCCTGGTGGTCTACGGTTCAGCGGGCGTGCGGGGTGCAGGTGGCCTGTGGGGCAGCC 9660
Guide -------GGTGGTCTACGGTTCAG---------- 17
WT4F59 ----------TCCCCACTGTTCCCCTC 48
WT1F59 ---------- 0
Primer4F ---------- 0
Primer1F ---------- 0
CSaR2 GGCATGAGCCACTGTGCCCGGCCCCTGATGACTCTGCTATTGCCTCTCACCCTCTCCCTC 8040
Guide ---------- 0
WT4F59 TGGCAGAGACAAACAGC---------- 65
WT1F59 ---------- 0
Primer4F ---------- 0
Primer1F ---------- 0
CSaR2 TGGCAGATTCCACTCCAGCCACACTGGGCTCCTTGCTGTTCTTGGACATGACCGTCATGT 8100
Guide ---------- 0
WT4F59 ---------- 65
WT1F59 ----------TTTGGAGGTATCTGCCAAGCCCAGTCTCTCNGCC--------- 34
Primer4F ---------- 20
Primer1F ---------- 20
CSaR2 GACAGGTCATGCATCTATTTTGAAGGAAAGGCCAAGTCCAGGCTCCTTAGCTCGGCATTC 11280
Guide ---------- 17
WT4F59 ---------- 65
WT1F59 ----------NCAGACAATTCC- 46
Primer4F ---------- 20
Primer1F ---------- 20
CSaR2 TCAGTAGCCACATATGGCTGGTGACTGCCATATTCGACAGCACAGCTATAGAACATTGCC 12360
Guide ---------- 17

↓

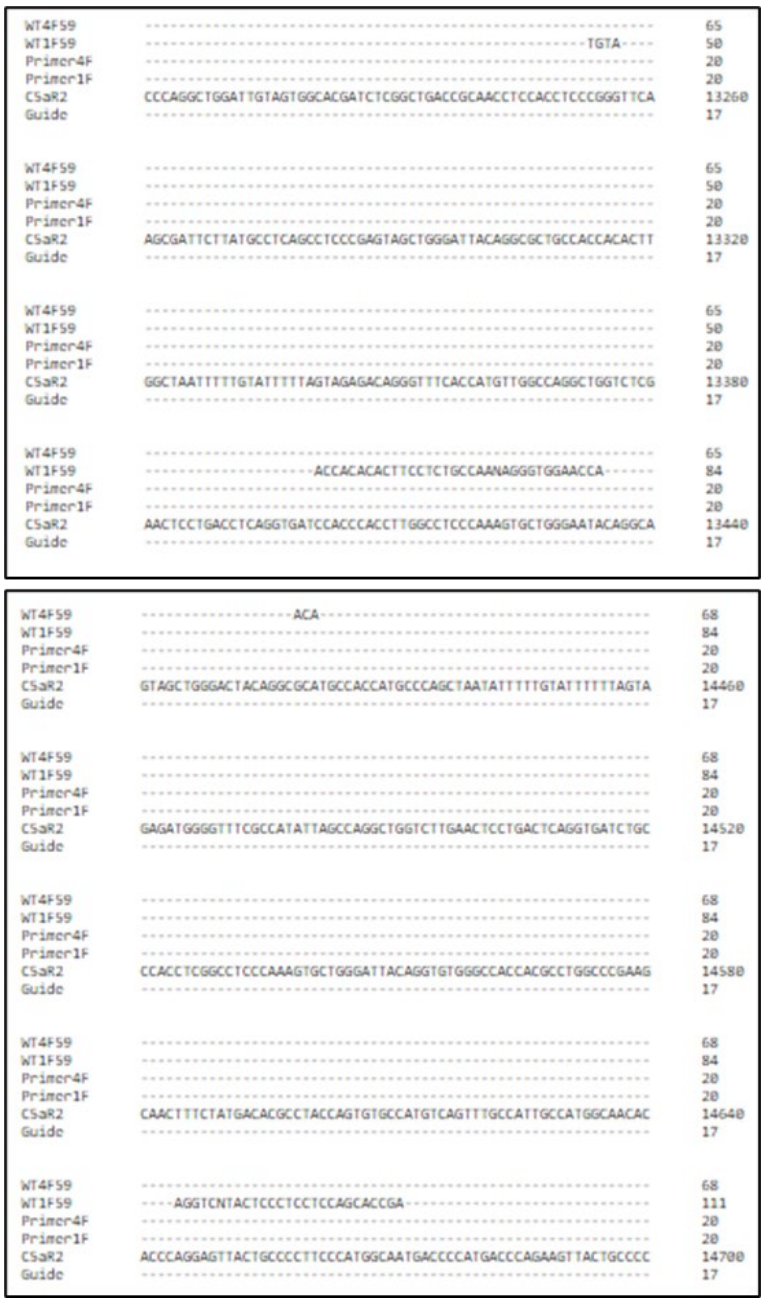

Figure 4.16. Sequence alignment from PCR amplification product generated at 59°C using WT lysate and AJ Forward Primers 1 and 4. Clustal Omega alignment of C5aR2 gene, primer sequences and AJ C5aR2 KO gRNA sequence with Forward primer-generated modal sequences of PCR amplification product generated using WT lysate and AJ C5aR2 Primer Pairs 1 and 4.

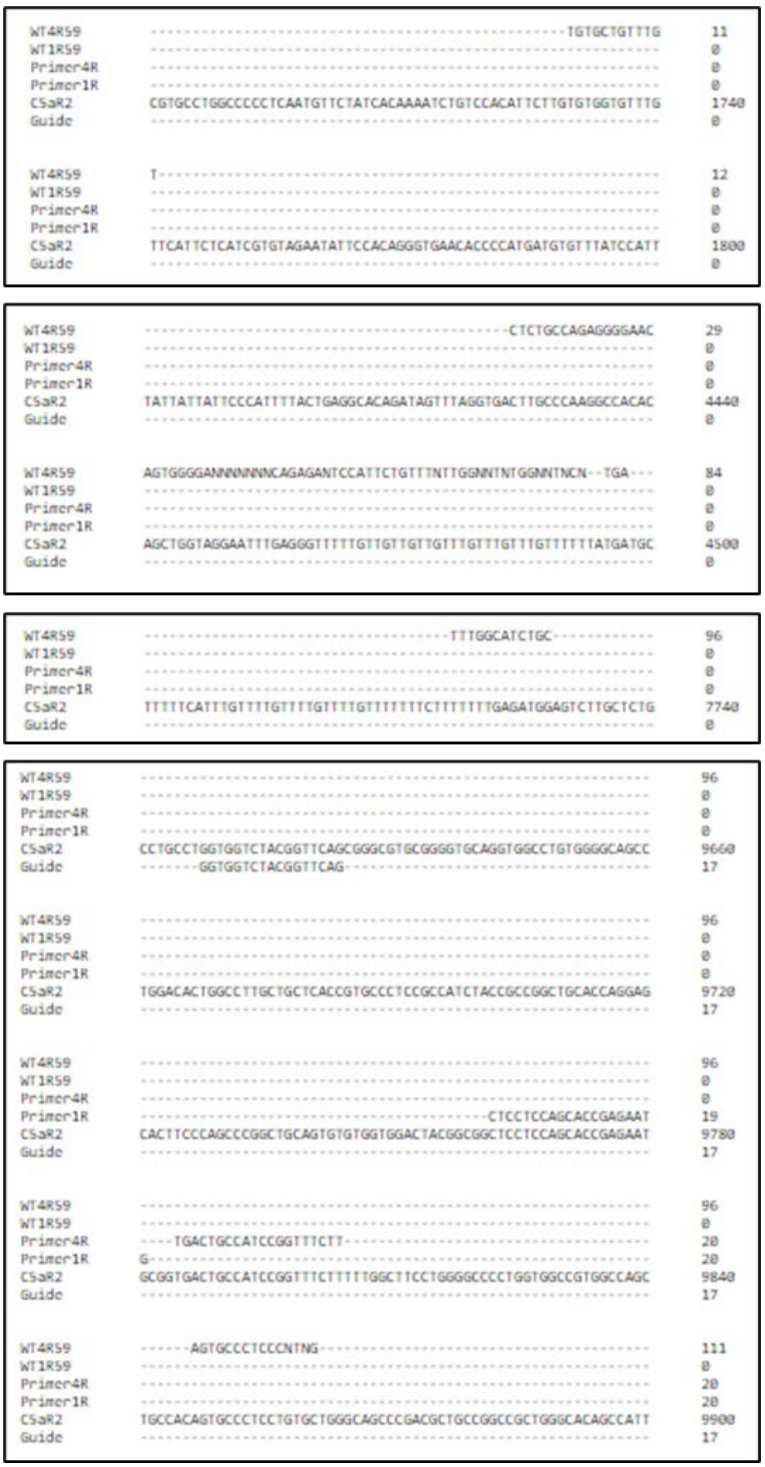
WT4R59 ----------TGTGCTGTTTG 11
WT1R59 ---------- 0
Primer4R ---------- 0
Primer1R ---------- 0
CSaR2 CGTGCCTGGCCCCCTCAATGTTCTATCACAAAATCTGTCCACATTCTTGTGTGGTGTTTG 1740
Guide ---------- 0
WT4R59 T---------- 12
WT1R59 ---------- 0
Primer4R ---------- 0
Primer1R ---------- 0
CSaR2 TTCATTCTCATCGTGTAGAATATTCCACAGGGTGAACACCCCATGATGTGTTTATCCATT 1800
Guide ---------- 0
WT4R59 ----------CTCTGCCAGAGGGGAAC 29
WT1R59 ---------- 0
Primer4R ---------- 0
Primer1R ---------- 0
CSaR2 TATTATTATTCCCATTTTACTGAGGCACAGATAGTTTAGGTGACTTGCCCAAGGCCACAC 4440
Guide ---------- 0
WT4R59 AGTGGGGANNNNNNNCAGAGANTCCATTCTGTTTNTTGGNNTNTGGNNTNCN--TGA--- 84
WT1R59 ---------- 0
Primer4R ---------- 0
Primer1R ---------- 0
CSaR2 AGCTGGTAGGAATTTGAGGGTTTTTGTTGTTGTTGTTTGTTTGTTTGTTTTTTATGATGC 4500
Guide ---------- 0
WT4R59 ----------TTTGGCATCTGC---------- 96
WT1R59 ---------- 0
Primer4R ---------- 0
Primer1R ---------- 0
CSaR2 TTTTTCATTTGTTTTGTTTTGTTTTGTTTTTTTCTTTTTTTGAGATGGAGTCTTGCTCTG 7740
Guide ---------- 0
WT4R59 ---------- 96
WT1R59 ---------- 0
Primer4R ---------- 0
Primer1R ---------- 0
CSaR2 CCTGCCTGGTGGTCTACGGTTCAGCGGGCGTGCGGGGTGCAGGTGGCCTGTGGGGCAGCC 9660
Guide -------GGTGGTCTACGGTTCAG---------- 17
WT4R59 ---------- 96
WT1R59 ---------- 0
Primer4R ---------- 0
Primer1R ---------- 0
CSaR2 TGGACACTGGCCTTGCTGCTCACCGTGCCCTCCGCCATCTACCGCCGGCTGCACCAGGAG 9720
Guide ---------- 17
WT4R59 ---------- 96
WT1R59 ---------- 0
Primer4R ---------- 0
Primer1R ----------CTCCTCCAGCACCGAGAAT 19
CSaR2 CACTTCCCAGCCCGGCTGCAGTGTGTGGTGGACTACGGCGGCTCCTCCAGCACCGAGAAT 9780
Guide ---------- 17
WT4R59 ---------- 96
WT1R59 ---------- 0
Primer4R ----TGACTGCCATCCGGTTTCTT---------- 20
Primer1R G---------- 20
CSaR2 GCGGTGACTGCCATCCGGTTTCTTTTTGGCTTCCTGGGGCCCCTGGTGGCCGTGGCCAGC 9840
Guide ---------- 17
WT4R59 ------AGTGCCCTCCCNTNG---------- 111
WT1R59 ---------- 0
Primer4R ---------- 20
Primer1R ---------- 20
CSaR2 TGCCACAGTGCCCTCCTGTGCTGGGCAGCCCGACGCTGCCGGCCGCTGGGCACAGCCATT 9900
Guide ---------- 17

↓

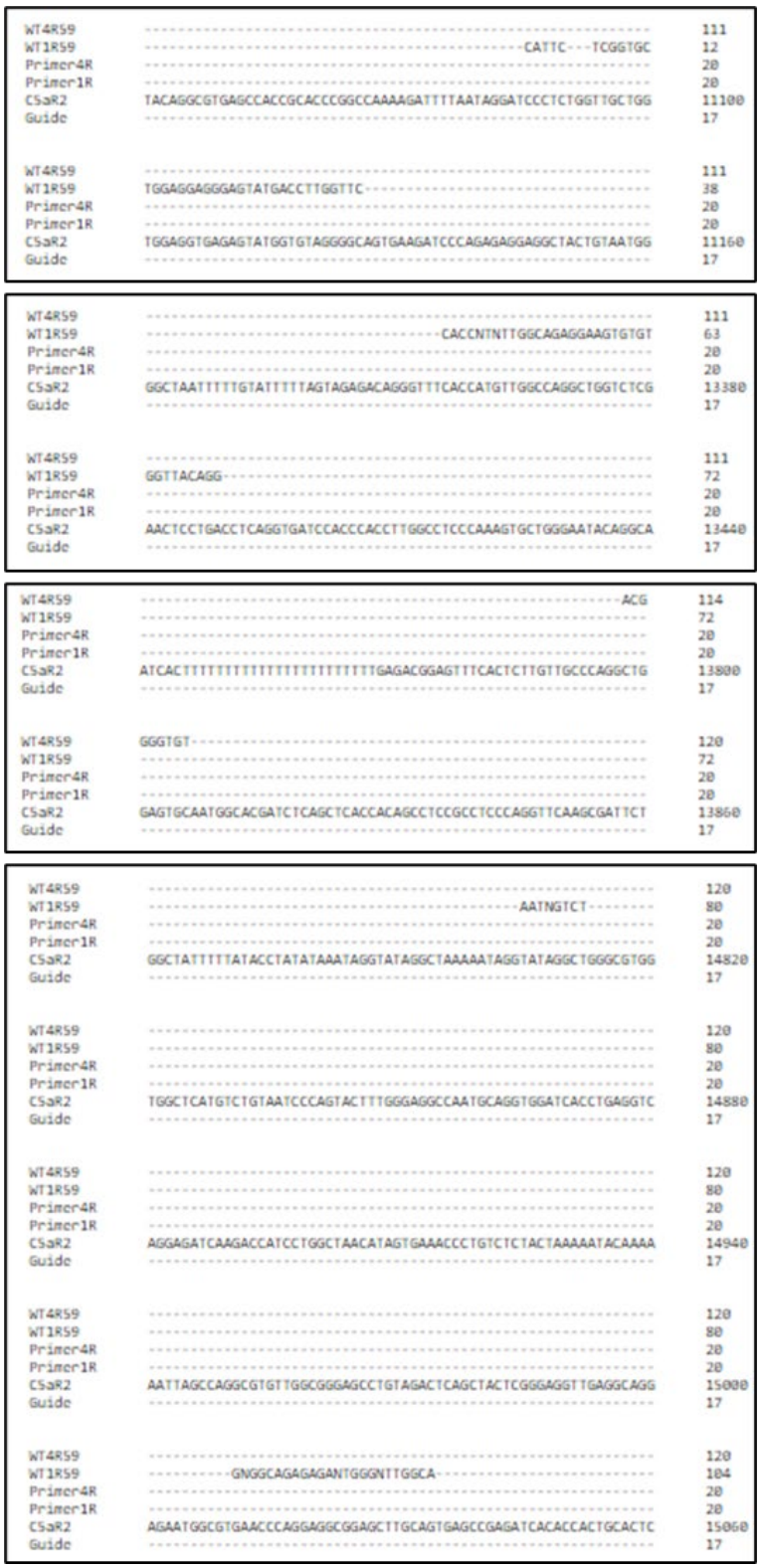

Figure 4.17. Sequence alignment from PCR amplification product generated at 59°C using WT lysate and AJ Reverse Primers 1 and 4. Clustal Omega alignment of C5aR2 gene, primer sequences and AJ C5aR2 KO gRNA sequence with Reverse primer-generated modal sequences of PCR amplification product generated using WT lysate and AJ C5aR2 Primer Pairs 1 and 4.

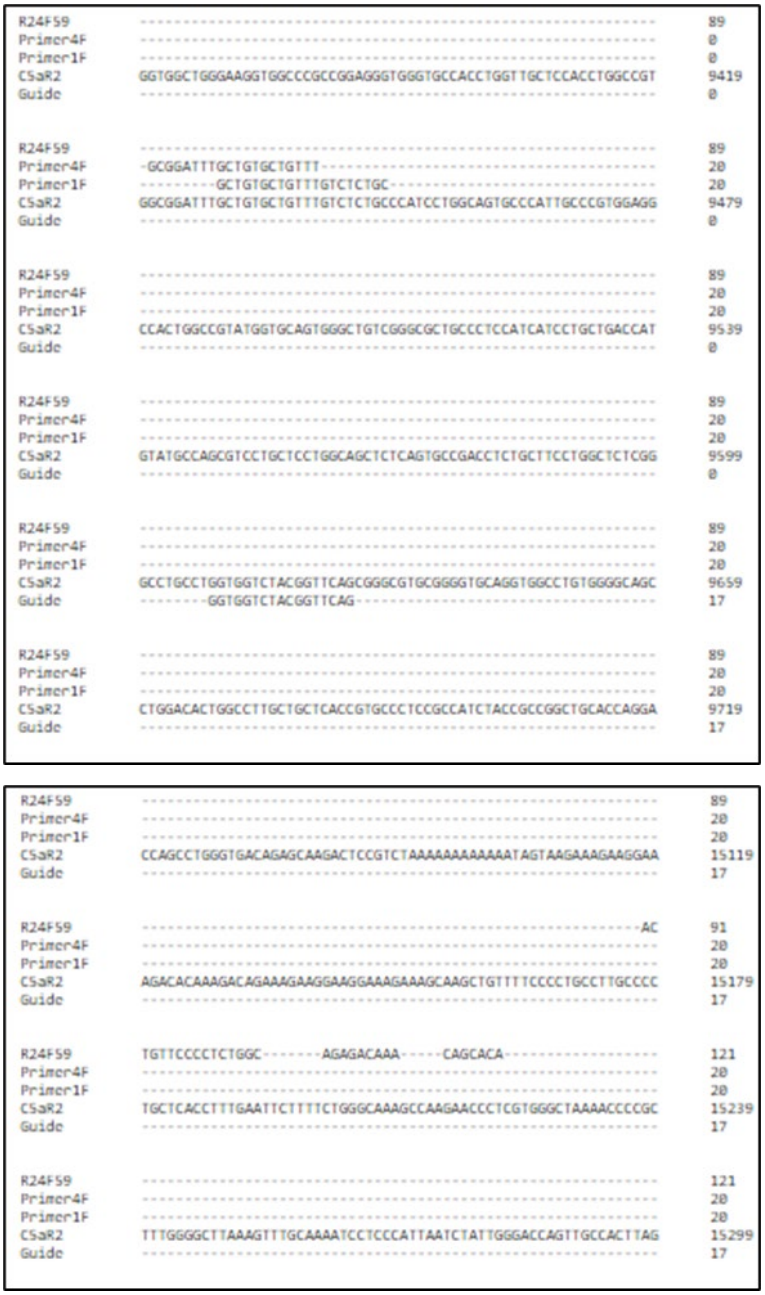

Figure 4.18. Sequence alignment from PCR amplification product generated at 59°C using AJ C5aR2 KO lysate and AJ Forward Primer 4. Clustal Omega alignment of C5aR2 gene, primer sequences and AJ C5aR2 KO gRNA sequence with Forward primer-generated modal sequences of PCR amplification product generated using AJ C5aR2 KO lysate and AJ C5aR2 Primer Pair 4.

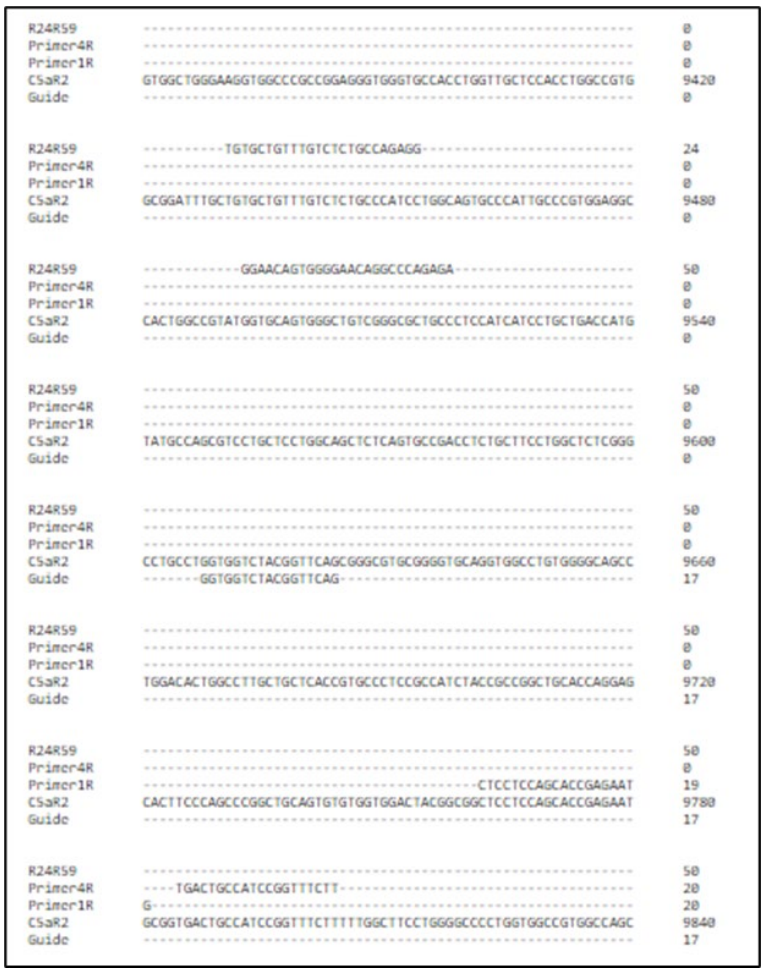

Figure 4.19. Sequence alignment from PCR amplification product generated at 59°C using AJ C5aR2 KO lysate and AJ Reverse Primer 4. Clustal Omega alignment of C5aR2 gene, primer sequences and AJ C5aR2 KO gRNA sequence with Reverse primer-generated modal sequences of PCR amplification product generated using AJ C5aR2 KO lysate and AJ C5aR2 Primer Pair 4.

Across all reactions, there are fragments of aligned sequences, but sequence alignment using Synthego ICE failed due to low-quality PCR amplification product. These sequencing data are therefore not interpretable.

A follow-up experiment was performed using AJ Primer Pair 4 and 2 µL of WT or AJ C5aR2 KO lysate and an annealing temperature of 57 °C. The PCR amplification product was separated using gel electrophoresis and was visualised using an E-gel Imager System (**Figure 4.20**).

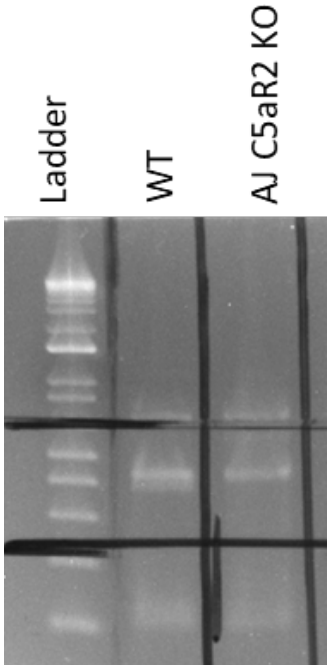

Figure 4.20. Band excision to isolate target amplicon. Image of E-Gel containing PCR amplification product from 2 µL WT or AJ C5aR2 KO THP-1 cell lysate with an annealing temperature of 57°C.

There were fewer off-target bands present in the gel than in the temperature gradient experiment (**Figure 4.15**), however there were off-target bands detected in the PCR amplification product. A Qiagen Gel Extraction Kit was therefore used to excise the bands at approximately 400 bp from the gel and isolate the PCR amplification product, which was then sent for Sanger sequencing. Sequencing of this extracted PCR amplification product was unsuccessful.

To ensure that lysate degradation was not to blame for the low-quality PCR amplification products, new lysates were generated using WT and AJ C5aR2 KO THP-1 cells, and new aliquots of all reagents were used to perform PCR with 0.2 µL or 2 µL of lysate and an annealing temperature of 59°C or 65°C. PCR amplification products were separated by gel electrophoresis and visualised using an E-Gel (**Figure 4.21**).

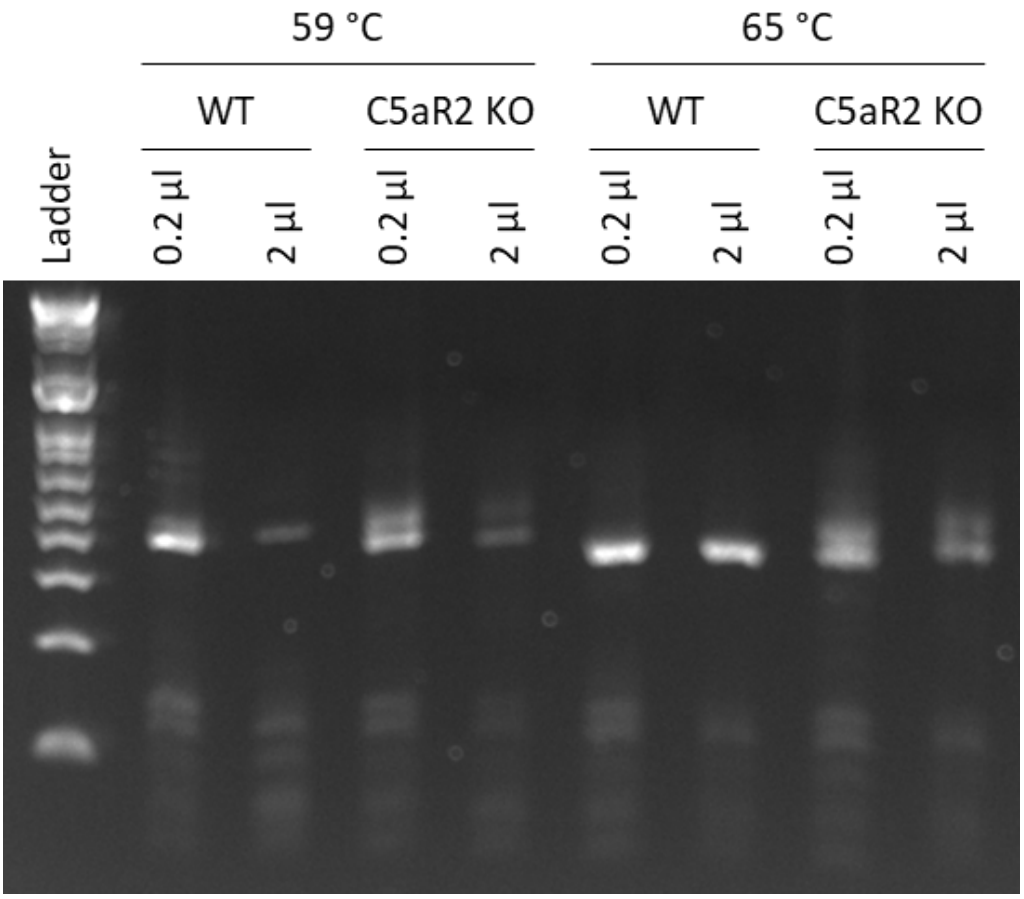

Figure 4.21. Nucleic acid gel electrophoresis of PCR amplification products from new lysates using AJ Primer Pair 4. Image of E-Gel containing PCR amplification product from 0.2 or 2 µL of WT or AJ C5aR2 KO THP-1 cell lysate with annealing temperatures of 59°C or 65°C.

The results were distinctly clearer than previous PCRs with this primer pair. Bright, clear bands were seen at approximately 400 bp, likely representing the target amplicon from the C5aR2 gene, although there were still short DNA fragments contaminating the lane and a smeared signal in some of the lanes, suggesting a low level of off-target PCR.

The WT lysates generated single bands at approximately 400 bp, whereas the AJ C5aR2 KO lysates generated double bands at approximately 400 bp. This suggests that two distinct amplicons are present in the AJ C5aR2 KO samples, but not in the WT samples, which is evidence of indels present in the target amplicon of the C5aR2 gene.

The PCR amplification products generated using 0.2 µL WT and AJ C5aR2 KO lysate and a 65°C annealing temperature were sent for Sanger Sequencing. Clustal Omega was used to align the C5aR2 gene, primer sequences and guide RNA sequence to PCR amplification products generated using WT lysate or AJ C5aR2 KO lysate and AJ C5aR2 Forward Primer 4 (**Figure 4.22**) or AJ C5aR2 Reverse Primer 4 (**Figure 4.23**).

```
WTF          ------------------------------------------------------------    0
R2F          ------------------------------------------------------------    0
Guide        ------------------------------------------------------------    0
C5aR2        GTGGCTGGGAAGGTGGCCCGCCGGAGGGTGGGTGCCACCTGGTTGCTCCACCTGGCCGTG    9420
Primer4F     ------------------------------------------------------------    0


WTF          ------------------------------------------------------------    0
R2F          ------------------------------------------------------------    0
Guide        ------------------------------------------------------------    0
C5aR2        GCGGATTTGCTGTGCTGTTTGTCTCTGCCCATCCTGGCAGTGCCCATTGCCCGTGGAGGC    9480
Primer4F     GCGGATTTGCTGTGCTGTTT----------------------------------------    20


WTF          ------------------------------------------------------------    0
R2F          ------------------------------------------------------------    0
Guide        ------------------------------------------------------------    0
C5aR2        CACTGGCCGTATGGTGCAGTGGGCTGTCGGGCGCTGCCCTCCATCATCCTGCTGACCATG    9540
Primer4F     ------------------------------------------------------------    20


WTF          ----GTTTCTTCCTGCTCCTGGCAGCTCTCANTGCCGACCTCTGCTTCCTGGCTCTCGGG    56
R2F          -------------TGCTCCTGGCAGCTCTCAGTGCCGACCTCTGCTTCCTGGCTCTCGGG    47
Guide        ------------------------------------------------------------    0
C5aR2        TATGCCAGCGTCCTGCTCCTGGCAGCTCTCAGTGCCGACCTCTGCTTCCTGGCTCTCGGG    9600
Primer4F     ------------------------------------------------------------    20


WTF          CCTGCCTGGTGGTCTACNGTTCANCGGGCGTGCGGGGTGCAGGTGGCCTGNGNNGCAGCC    116
R2F          CCTGCCTGGTGNTCTACGGTTCAGCGGGCGTGCGGGGTGCAGGTGGCCTGTGGGGCATCC    107
Guide        -----------GTCTACGGTTCAG-----------------------------------    13
C5aR2        CCTGCCTGGTGGTCTACGGTTCAGCGGGCGTGCGGGGTGCAGGTGGCCTGTGGGGCAGCC    9660
Primer4F     ------------------------------------------------------------    20


WTF          TGGANACTGGNCTTGCTGCTCANCNNGCCCTCCNCCATCNACCGCCGGCTGCNCCANGAN    176
R2F          TGNACACTGNCCTTGCTGCTCNCCNTGCCCTCCGCCATCTACCGCCGGCTGCACCAGGAG    167
Guide        ------------------------------------------------------------    13
C5aR2        TGGACACTGGCCTTGCTGCTCACCGTGCCCTCCGCCATCTACCGCCGGCTGCACCAGGAG    9720
Primer4F     ------------------------------------------------------------    20


WTF          CACTTCCCAGCCCGGCTGCANTGTGTGNNGGACTACGANNGCTCCTCCNGCACC------    230
R2F          CACTTCCCAGCCCGGCTGCNNTGTGTGGTGGACTACGGCGGCTCCTCCANCACCNANAAT    227
Guide        ------------------------------------------------------------    13
C5aR2        CACTTCCCAGCCCGGCTGCAGTGTGTGGTGGACTACGGCGGCTCCTCCAGCACCGAGAAT    9780
Primer4F     ------------------------------------------------------------    20


WTF          ------------------------------------------------------------    230
R2F          GCGGTGACTGCCNTCCGGTTTCTTAA---------------------------------    253
Guide        ------------------------------------------------------------    13
C5aR2        GCGGTGACTGCCATCCGGTTTCTTTTTGGCTTCCTGGGGCCCCTGGTGGCCGTGGCCAGC    9840
Primer4F     ------------------------------------------------------------    20
```

Figure 4.22. Sequence alignment from PCR amplification product generated using second batch of AJ C5aR2 KO lysate and AJ Forward Primer 4. Clustal Omega alignment of C5aR2 gene, primer sequences and AJ C5aR2 KO gRNA sequence with Forward primer-generated modal sequences of PCR amplification product generated using AJ C5aR2 KO lysate and AJ C5aR2 Primer Pair 4.

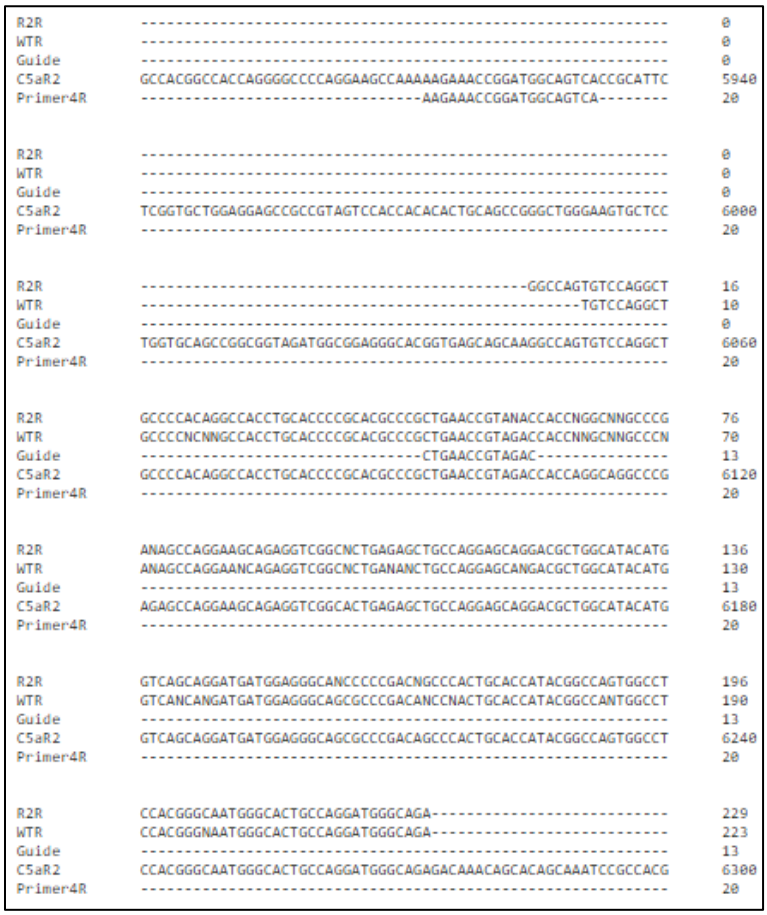

```
R2R         ------------------------------------------------------------    0
WTR         ------------------------------------------------------------    0
Guide       ------------------------------------------------------------    0
C5aR2       GCCACGGCCACCAGGGGCCCCAGGAAGCCAAAAAGAAACCGGATGGCAGTCACCGCATTC    5940
Primer4R    --------------------------------AAGAAACCGGATGGCAGTCA--------    20


R2R         ------------------------------------------------------------    0
WTR         ------------------------------------------------------------    0
Guide       ------------------------------------------------------------    0
C5aR2       TCGGTGCTGGAGGAGCCGCCGTAGTCCACCACACACTGCAGCCGGGCTGGGAAGTGCTCC    6000
Primer4R    ------------------------------------------------------------    20


R2R         ---------------------------------------------GGCCAGTGTCCAGGCT    16
WTR         ----------------------------------------------------TGTCCAGGCT    10
Guide       ------------------------------------------------------------    0
C5aR2       TGGTGCAGCCGGCGGTAGATGGCGGAGGGCACGGTGAGCAGCAAGGCCAGTGTCCAGGCT    6060
Primer4R    ------------------------------------------------------------    20


R2R         GCCCCACAGGCCACCTGCACCCCGCACGCCCGCTGAACCGTANACCACCNGGCNNGCCCG    76
WTR         GCCCCNCNNGCCACCTGCACCCCGCACGCCCGCTGAACCGTAGACCACCNNGCNNGCCCN    70
Guide       --------------------------------CTGAACCGTAGAC---------------    13
C5aR2       GCCCCACAGGCCACCTGCACCCCGCACGCCCGCTGAACCGTAGACCACCAGGCAGGCCCG    6120
Primer4R    ------------------------------------------------------------    20


R2R         ANAGCCAGGAAGCAGAGGTCGGCNCTGAGAGCTGCCAGGAGCAGGACGCTGGCATACATG    136
WTR         ANAGCCAGGAANCAGAGGTCGGCNCTGANANCTGCCAGGAGCANGACGCTGGCATACATG    130
Guide       ------------------------------------------------------------    13
C5aR2       AGAGCCAGGAAGCAGAGGTCGGCACTGAGAGCTGCCAGGAGCAGGACGCTGGCATACATG    6180
Primer4R    ------------------------------------------------------------    20


R2R         GTCAGCAGGATGATGGAGGGCANCCCCCGACNGCCCACTGCACCATACGGCCAGTGGCCT    196
WTR         GTCANCANGATGATGGAGGGCAGCGCCCGACANCCNACTGCACCATACGGCCANTGGCCT    190
Guide       ------------------------------------------------------------    13
C5aR2       GTCAGCAGGATGATGGAGGGCAGCGCCCGACAGCCCACTGCACCATACGGCCAGTGGCCT    6240
Primer4R    ------------------------------------------------------------    20


R2R         CCACGGGCAATGGGCACTGCCAGGATGGGCAGA--------------------------    229
WTR         CCACGGGNAATGGGCACTGCCAGGATGGGCAGA--------------------------    223
Guide       ------------------------------------------------------------    13
C5aR2       CCACGGGCAATGGGCACTGCCAGGATGGGCAGAGACAAACAGCACAGCAAATCCGCCACG    6300
Primer4R    ------------------------------------------------------------    20
```

Figure 4.23. Sequence alignment from PCR amplification product generated using second batch of AJ C5aR2 KO lysate and AJ Reverse Primer 4. Clustal Omega alignment of C5aR2 gene, primer sequences and AJ C5aR2 KO guide RNA sequence with Reverse primer-generated sequences of PCR amplification product generated using AJ C5aR2 KO lysate and AJ C5aR2 Primer Pair 4.

The PCR amplification product sequences aligned to the C5aR2 gene, suggesting sucessful amplification of the target amplicon in the C5aR2 gene. Alignment was less fragmented than in the original set of lysates (**Figure 4.16-4.19**), suggesting sample degradation may have been to blame for some of the poor quality PCR amplification products in previous experiments.

However, there is no clear difference between the two sequences generated by WT and AJ C5aR2 KO THP-1 cell lysates. Despite the second band visible in the E-gel, indicating two distinct sequences present, Clustal Omega was only able to display a single modal sequence exported from the .ab1 file using BioEdit. If the indels were only present across a small population of the sample, they may not be represented using

this alignment technique. Subsequent alignment using Synthgo ICE failed due to low quality sequencing results.

These cells likely have indels present in the target gene due to the double bands present in the AJ C5aR2 KO lanes in the E-Gel. These primers were effective as PCR primers as the target amplicon was successfully amplified. However, they were ineffective as sequencing primers, and generated low quality sequencing results that could not be further analysed. New primers for PCR and sequencing were required.

4.2.2.9. PCR for C5aR2 using primers designed to target longer amplicons

To generate higher quality sequences, new primers were designed to generate longer target amplicons. PCR was performed on 0.2 or 2 µL WT THP-1 lysate with an annealing temperature of 65°C using AJ Primer Pairs 1L, 4L, 5L, 8L, and 10L (**Table 2.6**). PCR amplification products were separated using gel electrophoresis and visualised using an E-gel (**Figure 4.24**).

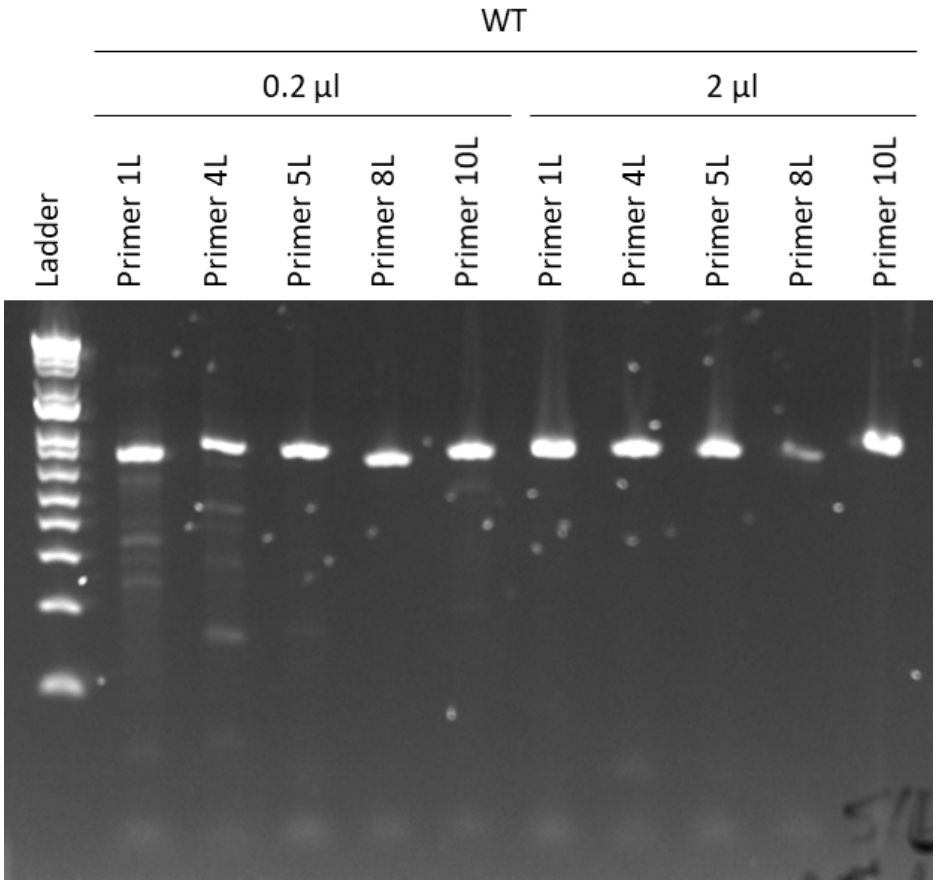

Figure 4.24. AJ Primer Pair 8L generated a single PCR amplification product with no visible off-target bands. Image of E-gel containing PCR amplification product from 0.2 or 2 µL of WT THP-1 cell lysate with an annealing temperature of 65°C and AJ C5aR2 Primer Pairs 1L, 4L, 5L, 8L and 10L.

Bright, single, clear bands were visible across all lanes, suggesting all primers had amplified the target amplicon successfully. AJ Primer Pair 8L had no additional off-target bands and very little background signal, so was used in a PCR on 0.1, 0.2, 1 or 2 µL AJ C5aR2 KO THP-1 cell lysates with an annealing temperature of 65 °C. PCR

amplification products were separated using gel electrophoresis and visualised using an E-Gel (**Figure 4.25**).

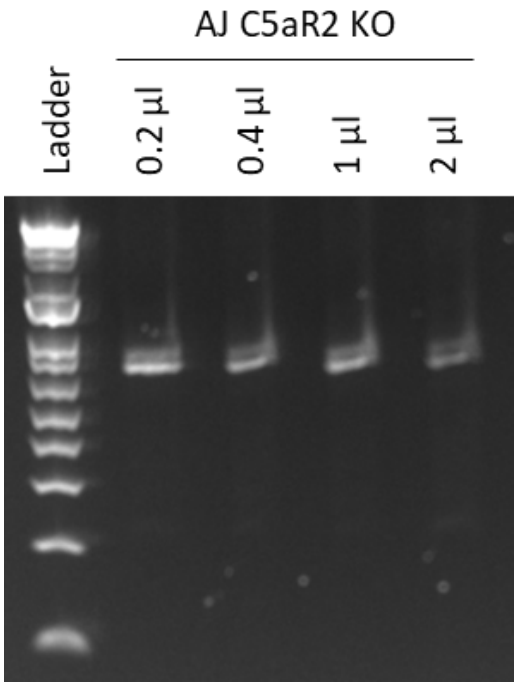

Figure 4.25. AJ Primer Pair 8L generated a single PCR amplification product with no visible off-target bands in AJ C5aR2 KO THP-1 lysates. Image of E-gel containing PCR amplification product from 0.1, 0.2, 1 or 2 µL of AJ C5aR2 KO THP-1 cell lysate with an annealing temperature of 65°C and AJ C5aR2 Primer Pair 8L.

In each lane there were double bands present at approximately 900 bp, with no off-target bands visible. The double band seen in the AJ C5aR2 KO sample was absent from the WT sample, suggesting that indels are present in the C5aR2 KO cell population. All four concentrations of lysate produced PCR amplification product effectively, so PCR amplification products generated using 0.2 µL and 2 µL WT and AJ C5aR2 KO lysate were sent for Sanger sequencing. Modal sequences were exported from BioEdit and aligned using Clustal Omega (**Figure 4.26**).

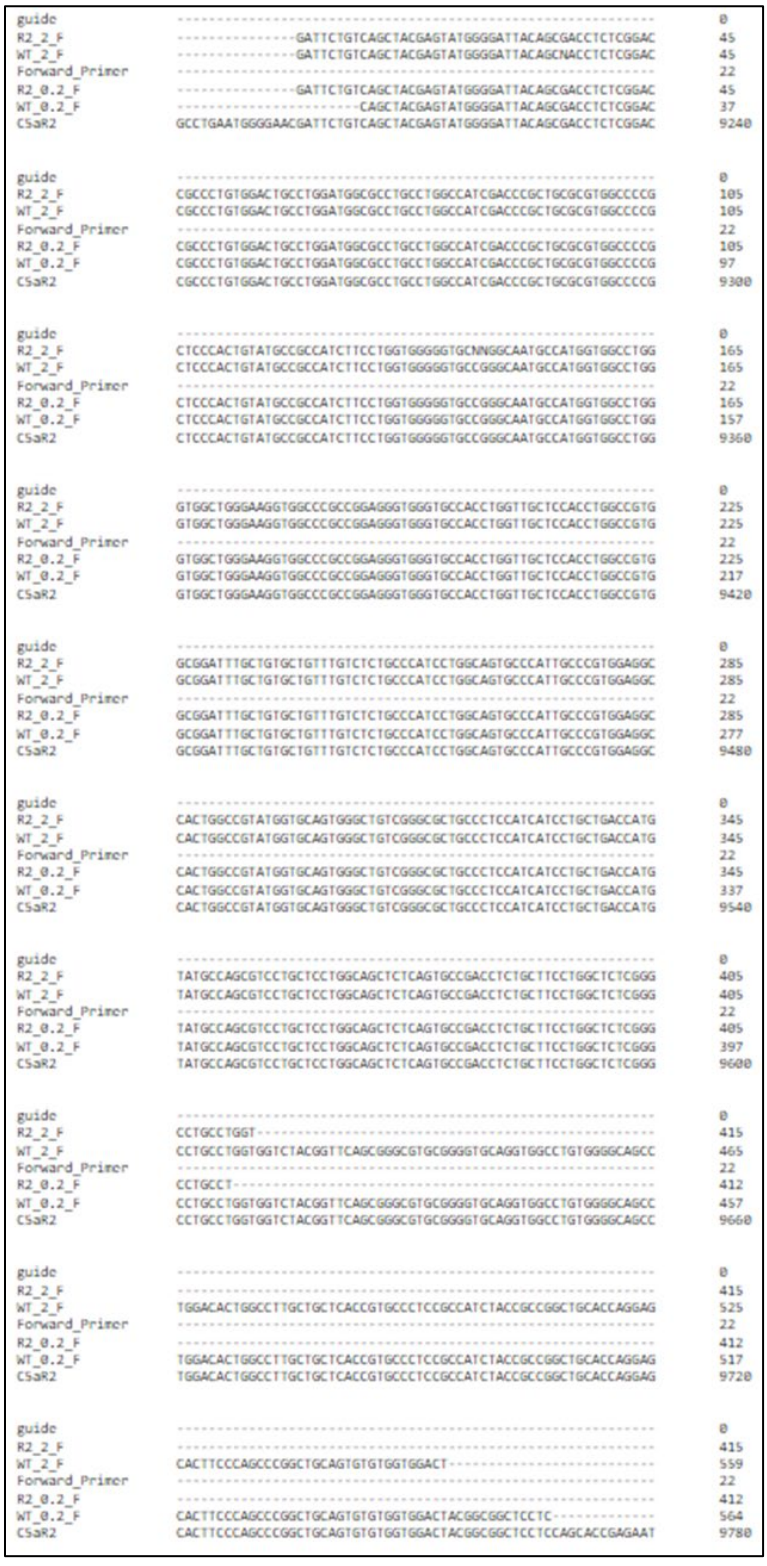

Figure 4.26. PCR amplification product generated using AJ Primer Pair 8L successfully aligned to C5aR2 gene sequence. Clustal Omega alignment of C5aR2 gene, forward primer sequence, and AJ C5aR2 KO gRNA sequence with Forward primer-generated modal sequences of PCR amplification product from WT and AJ C5aR2 KO lysate generated using AJ C5aR2 Primer Pair 8L.

AJ C5aR2 Primer Pair 8L generated PCR amplification products from WT and AJ C5aR2 KO THP-1 cells which was aligned with the C5aR2 gene. No indels were identified in the Clustal Omega alignment of modal sequences, however these PCR amplification products generated sequences of high enough quality to allow for alignment with Synthego ICE. Sequences of AJ C5aR2 KO PCR amplification products generated using 0.2 µL lysate were aligned with the WT sequence using Synthego ICE, and indels were identified in the KO cells (**Figure 4.27**).

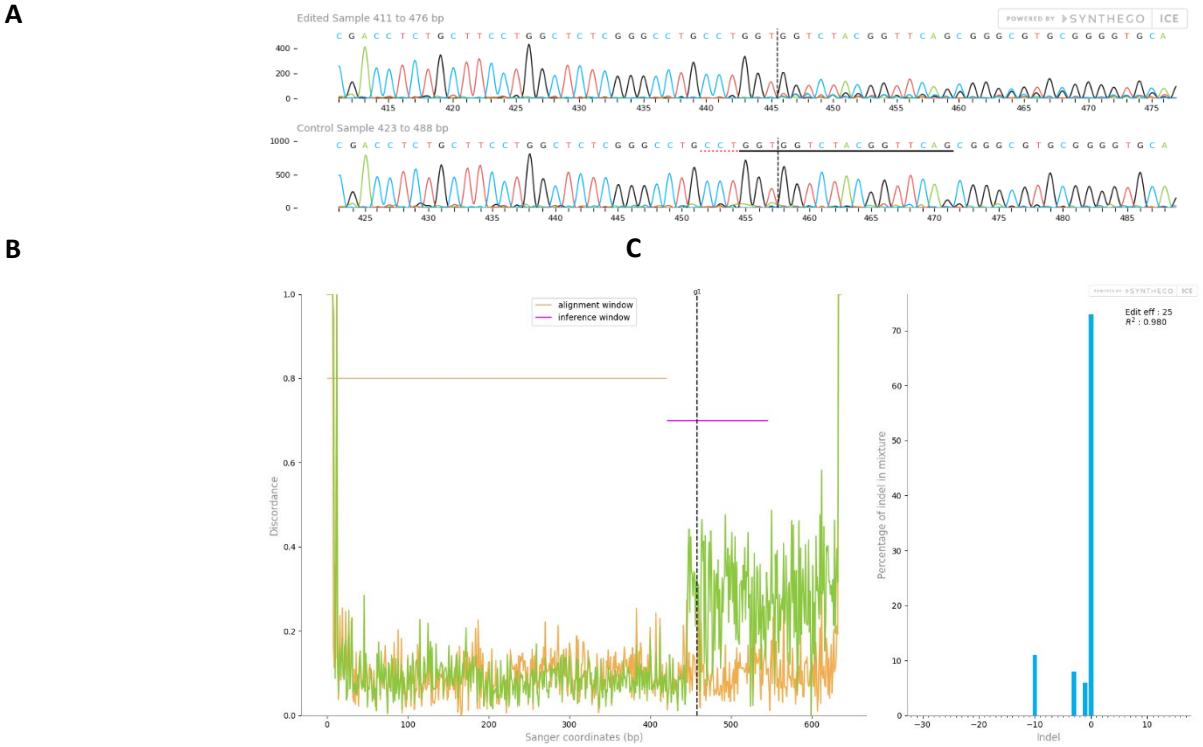

Figure 4.27. Confirmation of C5aR2 indels in AJ C5aR2 KO THP-1 cells. Synthego ICE alignment of sequences from AJ C5aR2 Primer Pair 8L-primed PCR amplification product from AJ C5aR2 KO polyclonal THP-1 cells ("Edited") to WT THP-1 cells ("Control"). **A.** Alignment shows no modal sequence disruption in the edited C5aR2 KO population compared to WT modal sequence following the guide target site (g1). However, **B.** discordance between AJ C5aR2 KO sequences and WT sequences reveals loss of conservation between sequences. Alignment window indicates conserved sequence between AJ C5aR2 KO and WT cells, and inference window indicates indels in C5aR2 KO sequence after guide site (dotted line). **C.** Size (bp) and percentage contribution of each detected indel in C5aR2 sequence vs. WT sequence.

As with the Clustal Omega alignment, no indels were identified by aligning the modal base at each position in the sequence (**Figure 4.27 A**). However, the discordance plot highlights a difference between WT and AJ C5aR2 KO sequences after the guide site (**Figure 4.27 B**). This discordance was generated by a small population of sequences in the PCR amplification product with indels of -1 (6%), -3 (8%) or -10 bp (11%) (**Figure 4.27 C**). WT sequence in the AJ C5aR2 KO sample generated 73% of the total sequences in the PCR amplification product.

These results indicate that the AJ C5aR2 KO cells had been successfully edited, and this population contained cells with indels in the C5aR2 gene. These cells, and the C5aR1 KO polyclonal cells, could now be used to generate monoclonal cell lines by limiting

dilution. From this point, “AJ C5aR2 KO” THP-1 cells will be referred to as C5aR2 KO cells.

4.2.3. Generating monoclonal C5aR1 KO and C5aR2 KO THP-1 cells

4.2.3.1. Generation of monoclonal cell lines by limiting dilution

Aliquots of cryopreserved, low passage, polyclonal C5aR1 KO and C5aR2 THP-1 cells were thawed and cultured. Once established in culture, the cells were diluted to 1 cell/100 µL, and each cultured in four 96-well plates. Once monoclonal cultures had established from single cells (indicated cells visibly clustering around the edges of the wells), the successfully established cultures were transferred to single 96-well plate. These cells were passaged, and the excess cells were transferred to a separate 96-well plate. The passaged cells were kept in culture, and a sample of the passaged cells were lysed for DNA extraction. PCR was performed on these monoclonal lysates to identify C5aR1 KO and C5aR2 KO monoclonal THP-1 cell lines.

4.2.3.2. Identification of monoclonal C5aR1 KO THP-1 and C5aR2 KO cell lines by PCR and sequencing

PCR was performed on WT and C5aR1 KO THP-1 lysates using C5aR1 Primer Pair 1. PCR was performed on WT and C5aR2 KO THP-1 lysates using AJ C5aR2 Primer Pair 8L. For each reaction, 2 µL lysate and an annealing temperature of 65 °C were used. The C5aR1 PCR amplification products from well A1 were separated using gel electrophoresis and visualised as a representative example using an E-gel (**Figure 4.28**).

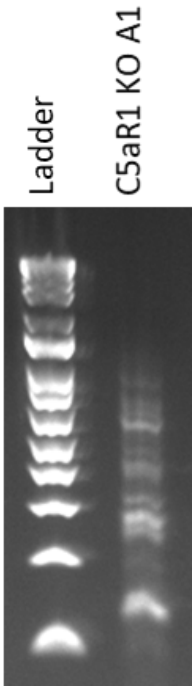

Figure 4.28. Visualisation of PCR amplification product from C5aR1 KO Clone A1 using nucleic acid gel electrophoresis. Images of E-Gel containing PCR amplification product from C5aR1 KO Clone A1, used to confirm successful PCR.

There was PCR amplification product present in the lane, suggesting succesful generation of PCR amplification products, however there were many lower mw bands present, suggesting off-target PCR and the likelihood of sequencing failure. Samples from all wells were sent for Sanger sequencing. As expected, the majority of the wells returned low quality sequences. Forward primer sequencing for D6 and H9 resulted in interpretable sequences, as did Reverse primer sequencing for A3, A4, A5, B5, B6, C3,

C4, E9, F7, F11, F12, G8, G12, H4 and H9 (**Table 4.1**). Trace, discordance and indel plots were generated for all clones (**Supplementary Figure 4.4**).

Well ID	Indel %	Model Fit
A3	100	0.42
A4	100	0.02
A5	100	0.02
B5	100	0.03
B6	100	0.58
C3	100	0.97
C4	100	0.02
D6	100	0.36
E9	100	0.34
F7	100	0.55
F11	100	0.74
F12	100	0.35
G8	100	0.55
G12	100	0.06
H4	100	0.54
H9 (f)	100	0.90
H9 (r)	100	0.52

Table 4.1. Summary of C5aR1 forward and reverse primer sequencing data. % contribution of indels to the population of sequences in each PCR amplification product, and a measure of model fit (range 0-1) was generated by Synthego ICE and summarised in this table for all C5aR1 KO sequences. (f) = forward primer or (r) = reverse primer used as sequencing primer.

The C5aR2 PCR amplification products from well A1 were separated using gel electrophoresis and visualised as a representative example using an E-gel (**Figure 4.29**).

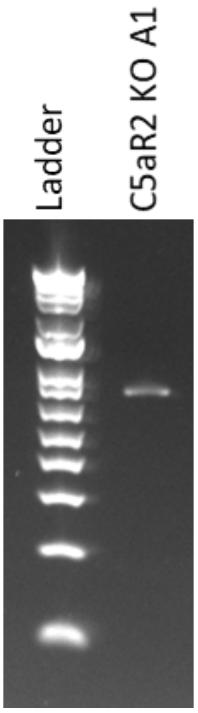

Figure 4.29. Confirmation of PCR amplification product from C5aR2 KO A1 using nucleic acid gel electrophoresis. Images of E-Gel containing PCR amplification product from C5aR2 KO A1, used to confirm successful PCR.

A single band was present in the lane with no off-target bands, indicating successful PCR. Samples from all wells were sent for Sanger sequencing.

Sequences were aligned using Synthego ICE. The forward primer sequencing returned 5 sequences that aligned with the WT sequence: A5, C3, C9, F6, and F10. The reverse primer performed well, generating sequences for the majority of wells (**Table 4.2**). Trace, discordance and indel plots were recorded for all clones (**Supplementary Figure 4.5**).

Well ID	Indel %	Model Fit
A1	0	0.89
A3	0	0.94
A4	0	0.93
A5	0	0.92
A6	93	0.93
A7	87	0.87
A8	0	0.99
A11	99	0.99
A12	0	0.94
B1	0	0.87
B2	42	0.89
B3	86	0.86
B4	0	0.99
B5	94	0.94
B6	14	0.2
B7	96	0.96
B9	91	0.91
B10	85	0.85
B11	0	0.96
C2	77	0.77
C3	64	0.64
C4	0	0.97
C5	85	0.85
C7	0	0.98
C8	30	0.3
C9	97	0.97
C10	83	0.83

Well ID	Indel %	Model Fit
C11	0	0.96
D2	0	0.81
D3	98	0.98
D4	81	0.81
D8	0	0.98
D9	55	0.55
D11	0	0.91
E2	0	0.82
E3	3	0.64
E4	12	0.96
E5	84	0.84
E6	0	0.81
E8	24	0.37
E10	0	0.78
E11	0	0.81
F2	52	0.54
F3	86	0.87
F4	0	0.87
F5	0	0.98
F6	0	0.98
F7	73	0.73
F9	5	0.05
F10	0	0.99
F11	0	0.9
G1	0	0.85
G2	0	0.8
G4	59	0.59
G6	43	0.43

Table 4.2. Summary of C5aR2 reverse primer sequencing data. % contribution of indels to the population of sequences in each PCR amplification product, and a measure of model fit (range 0-1) was generated by Synthego ICE and summarised in this table for all C5aR2 KO reverse primer sequences.

5 clones of C5aR1 KO cells and 5 clones of C5aR2 KO cells were selected based on the following indel characteristics:

- Cell lines with larger indels were prioritised, as small indels may have been more likely to cause silent mutations and large indels may have been more likely to cause large disruption to protein structure.
- Cell lines with multiple indels were deprioritised, as they may have originated from more than 1 cell, which could cause issues if the polyclonal culture changed in composition over time, potentially affecting the behaviour of the cells in experiments.
- Cell lines with -3 bp indels were deprioritised as frameshift mutations may result in truncations, potentially preserving expression, signal or function.
- Cell lines with an editing efficiency score of approximately 50% were deprioritised to reduce the risk of heterozygous mutation, which may preserve expression or function at a population level.

C5aR1 clones B6, C3, F11, G8, H9 were selected (**Figures 4.30-4.34**). C3 has a 106 bp deletion from the C5aR1 gene, and a 95% contribution to the sequence population, indicating that this is likely to be a monoclonal cell line. The remaining 5% is uninterpretable by the algorithm, likely due to a large sequence deletion preventing alignment. F11 has a 106 bp deletion and a 105 bp deletion contributing to 86% of the total sequence population. These is likely represent a single indel, with the second sequence caused by a misread base. B6, G8 and H9 have large indels at lower % contributions with some low bp noise. Despite these limitations, these clones were taken forward alongside clones C3 and F11, as a relatively low number of alternative clones were available due to low quality sequencing.

B6

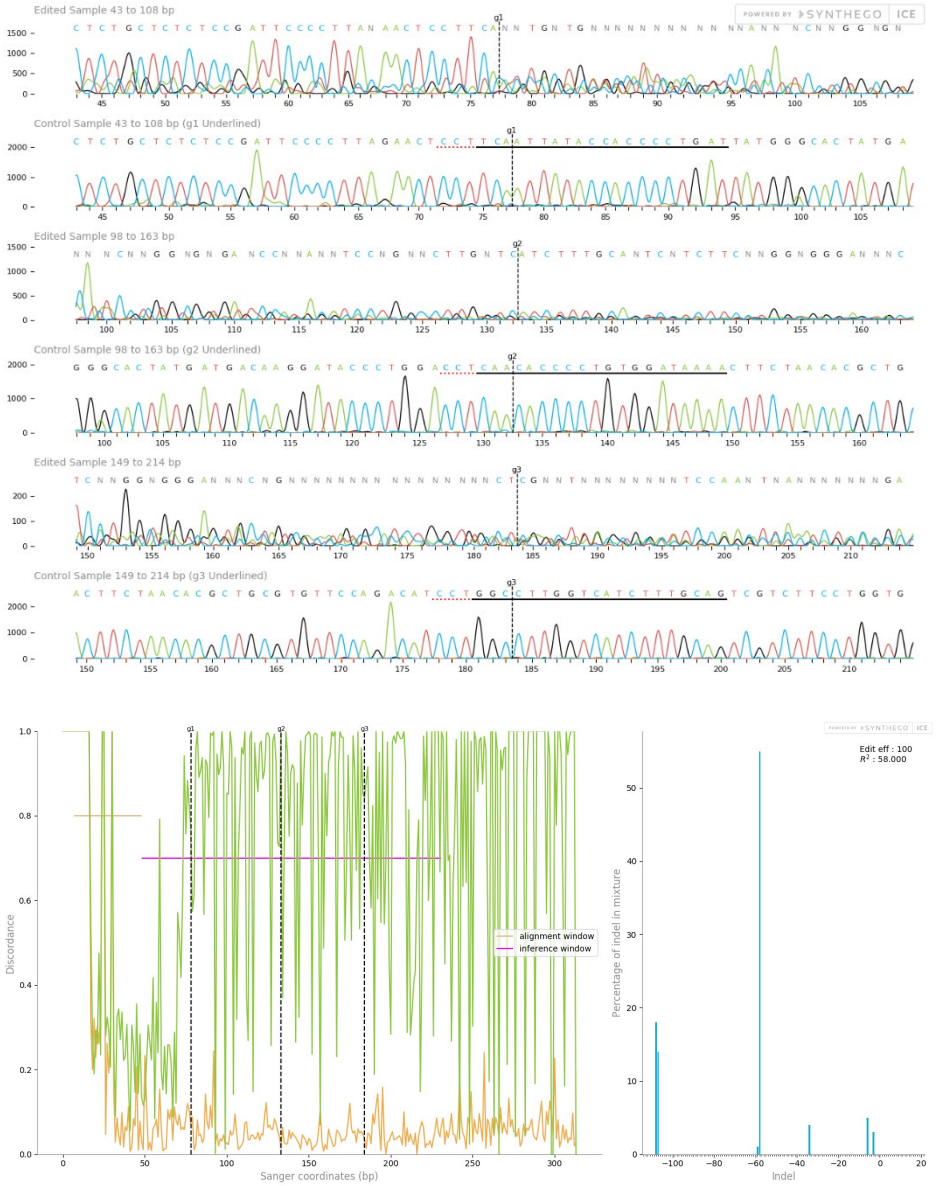

Figure 4.30. C5aR1 KO sequencing for monoclone B6. PCR amplification product generated using C5aR1 Primer Pair 1 was sent for sequencing with C5aR1 Reverse Primer 1, and sequences from C5aR1 KO monoclone B6 were aligned to the WT sequence using Synthego ICE.

C3

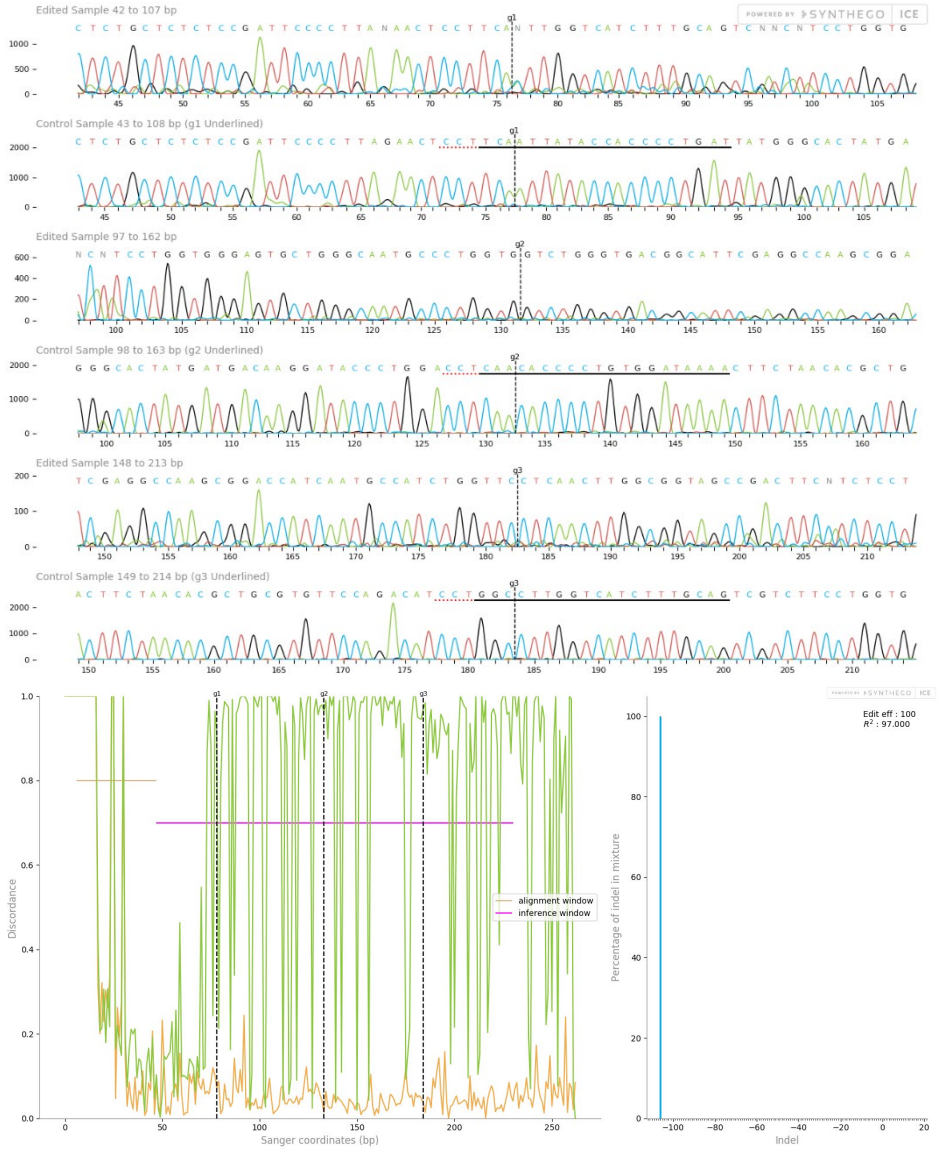

Figure 4.31. C5aR1 KO sequencing for monoclone C3. PCR amplification product generated using C5aR1 Primer Pair 1 was sent for sequencing with C5aR1 Reverse Primer 1, and sequences from C5aR1 KO monoclone C3 were aligned to the WT sequence using Synthego ICE.

F11

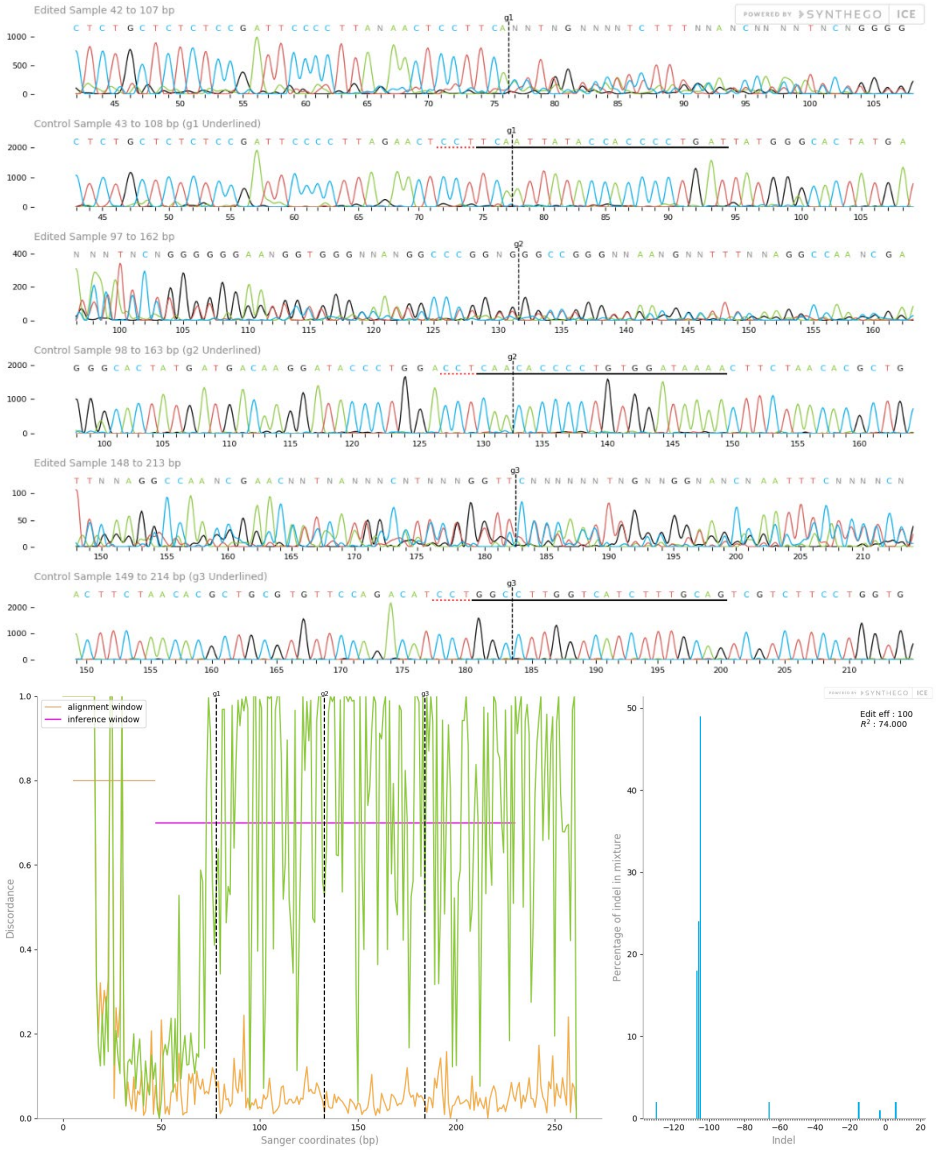

Figure 4.32. C5aR1 KO sequencing for monoclone F11. PCR amplification product generated using C5aR1 Primer Pair 1 was sent for sequencing with C5aR1 Reverse Primer 1, and sequences from C5aR1 KO monoclone F11 were aligned to the WT sequence using Synthego ICE.

G8

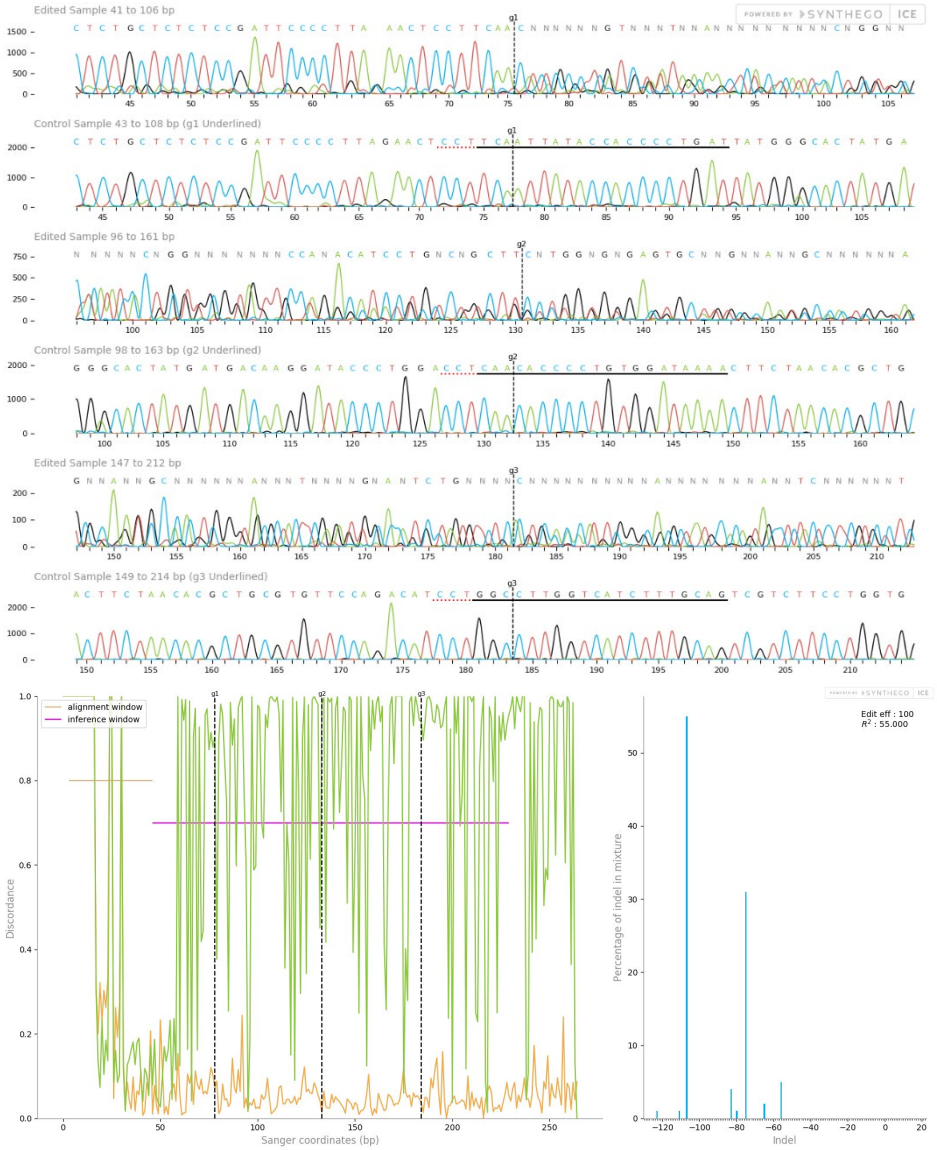

Figure 4.33. C5aR1 KO sequencing for monoclone G8. PCR amplification product generated using C5aR1 Primer Pair 1 was sent for sequencing with C5aR1 Reverse Primer 1, and sequences from C5aR1 KO monoclone G8 were aligned to the WT sequence using Synthego ICE.

H9

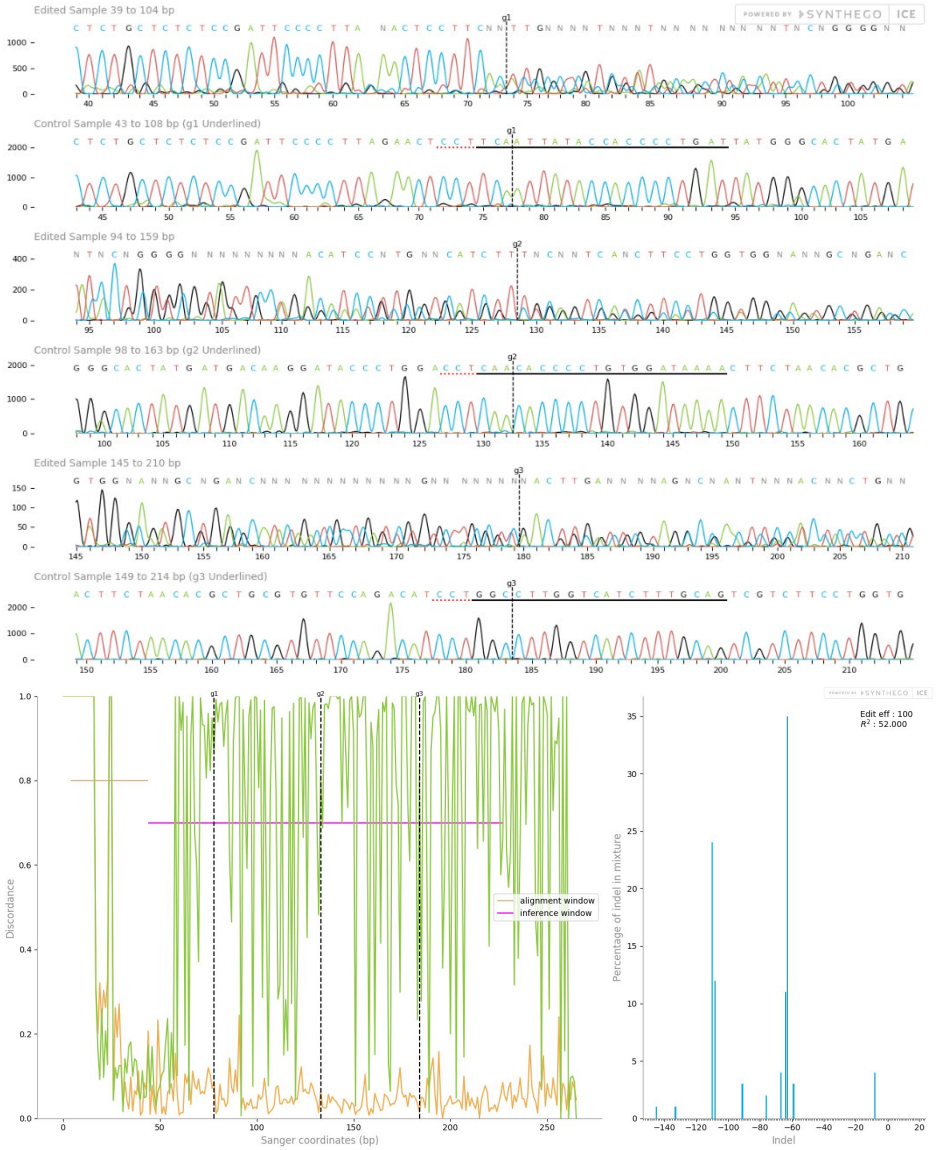

Figure 4.34. C5aR1 KO sequencing for monoclone H9. PCR amplification product generated using C5aR1 Primer Pair 1 was sent for sequencing with C5aR1 Reverse Primer 1, and sequences from C5aR1 KO monoclone H9 were aligned to the WT sequence using Synthego ICE.

C5aR2 clones A6, C9, D3, F3 and F7 were selected (**Figures 4.35-4.39**). C9 had a -16 bp deletion with a 97% contribution. D3 had a -10 deletion with a 98% contribution. F7 had a -8 bp deletion with a 73% contribution. Clones A6 and F3 were also taken forward. These clones had high % contribution indels (A6: -1 bp 70% and F3: -3 bp 84%) with additional indels present in the sequence. The remaining clones were rejected based on the presence of triplet indels, the presence of multiple different indels, and the presence of heterozygous indels.

A6

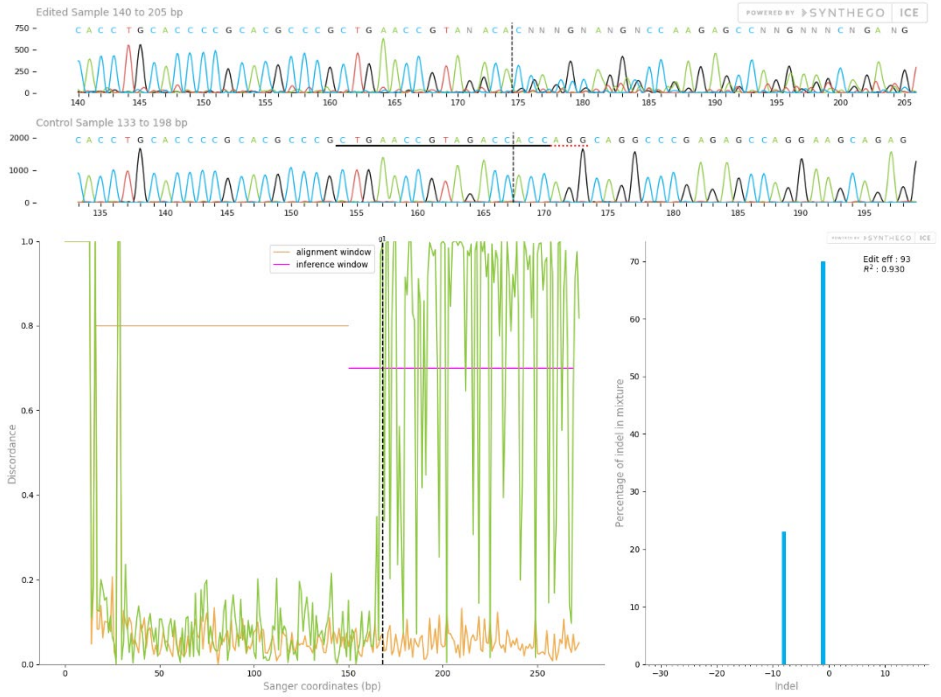

Figure 4.35. C5aR2 KO sequencing for monoclone A6. PCR amplification product generated using AJ C5aR2 Primer Pair 8L was sent for sequencing with AJ C5aR2 Reverse Primer 8L, and sequences from C5aR2 KO monoclone A6 were aligned to the WT sequence using Synthego ICE.

C9

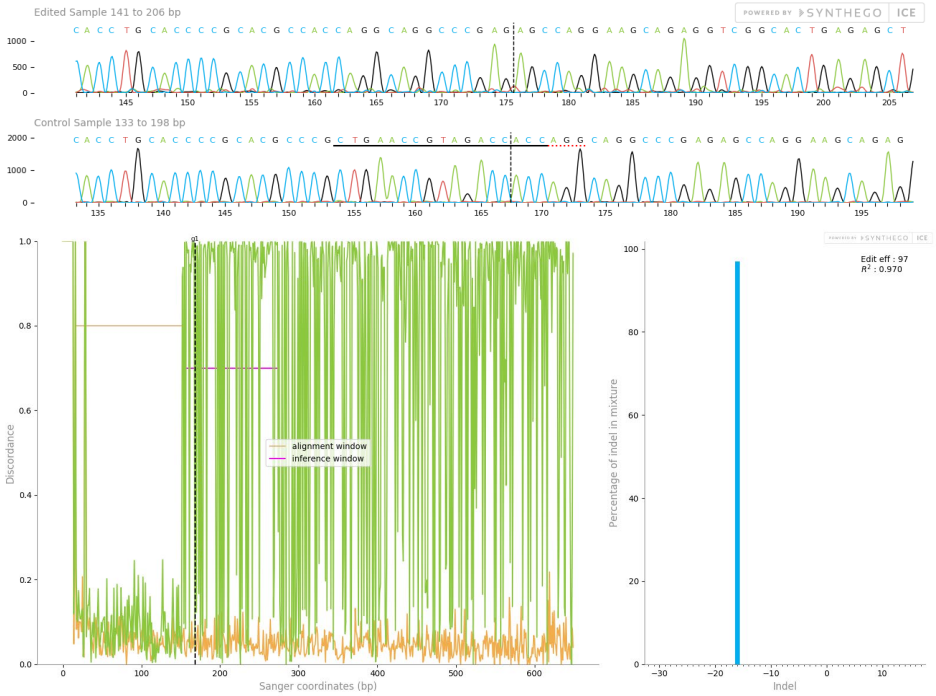

Figure 4.36. C5aR2 KO sequencing for monoclone C9. PCR amplification product generated using AJ C5aR2 Primer Pair 8L was sent for sequencing with AJ C5aR2 Reverse Primer 8L, and sequences from C5aR2 KO monoclone C9 were aligned to the WT sequence using Synthego ICE.

D3

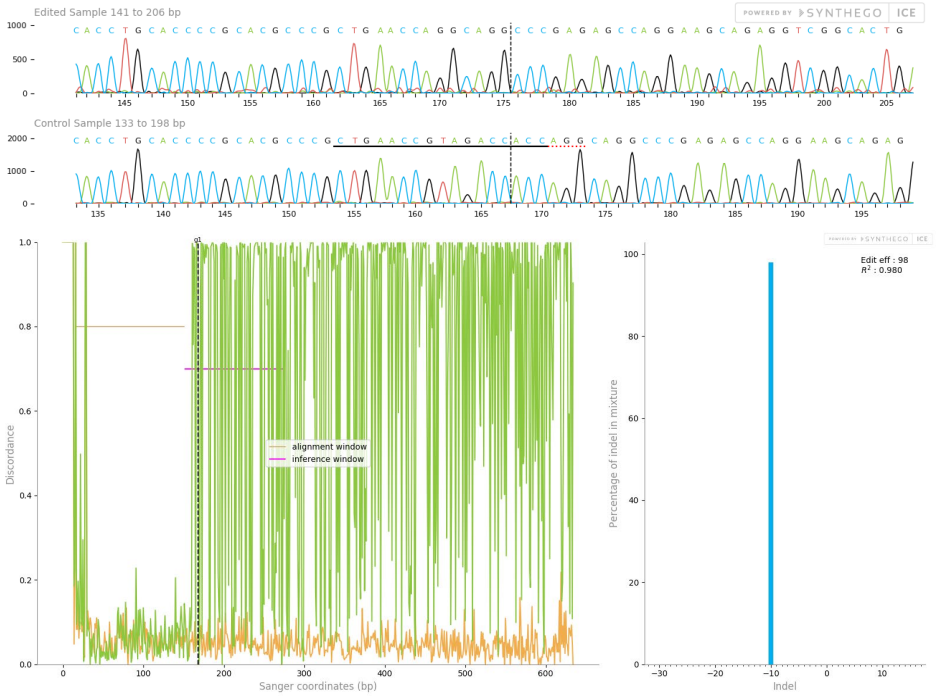

Figure 4.37. C5aR2 KO sequencing for monoclone D3. PCR amplification product generated using AJ C5aR2 Primer Pair 8L was sent for sequencing with AJ C5aR2 Reverse Primer 8L, and sequences from C5aR2 KO monoclone D3 were aligned to the WT sequence using Synthego ICE.

F3

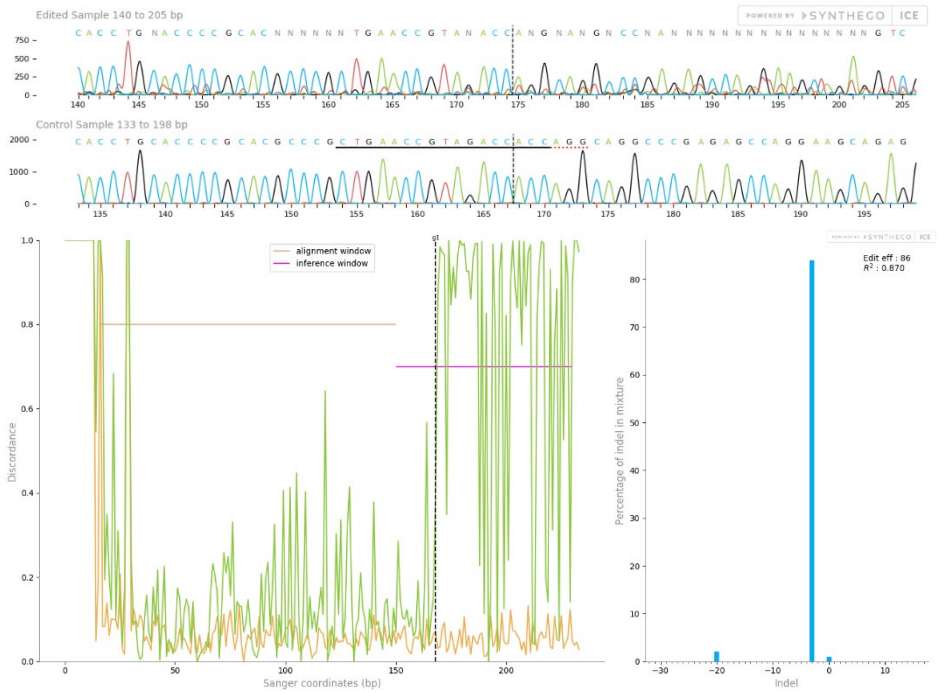

Figure 4.38. C5aR2 KO sequencing for monoclone F3. PCR amplification product generated using AJ C5aR2 Primer Pair 8L was sent for sequencing with AJ C5aR2 Reverse Primer 8L, and sequences from C5aR2 KO monoclone F3 were aligned to the WT sequence using Synthego ICE.

F7

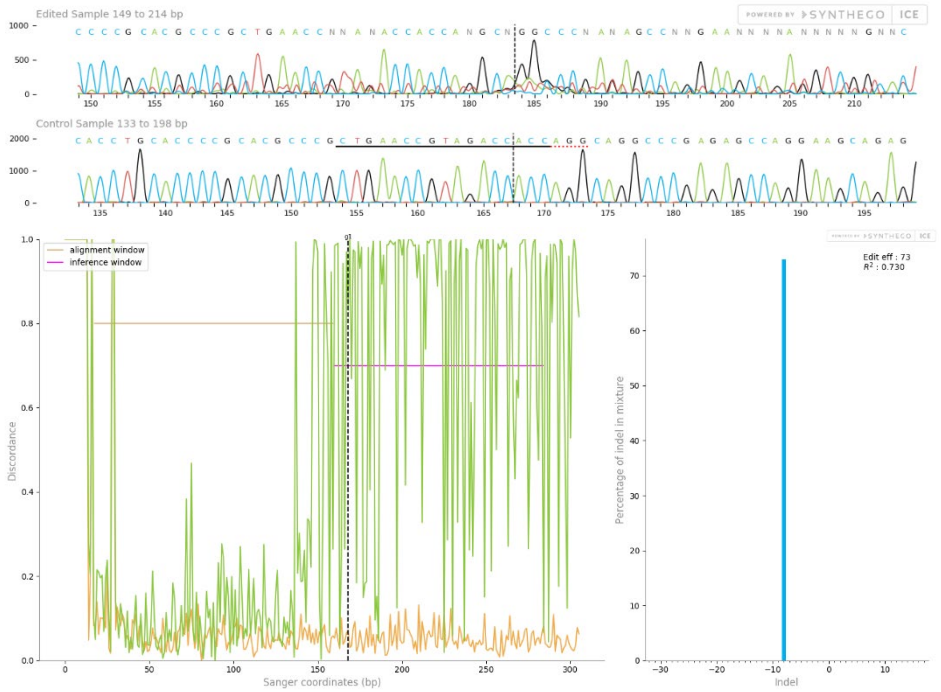

Figure 4.39. C5aR2 KO sequencing for monoclone F7. PCR amplification product generated using AJ C5aR2 Primer Pair 8L was sent for sequencing with AJ C5aR2 Reverse Primer 8L, and sequences from C5aR2 KO monoclone F7 were aligned to the WT sequence using Synthego ICE.

As the cultures expanded, these cells were transferred from the 96-well plates into 24-well plates, then 25 cm^3 flasks, then 75 cm^3 flasks, then cryopreserved for future use.

4.2.3.3. Characterising C5aR1 KO and C5aR2 KO monoclonal THP-1 cell lines using fluorescent confocal microscopy and flow cytometry

To confirm KO of C5aR1 and C5aR2, several protein detection techniques were employed to detect C5aR1 and C5aR2 protein expression in WT THP-1 cells.

Western blots for C5aR1 and C5aR2 failed to detect the protein in the WT lysate. This is likely due to epitope disruption during lysis (removing lipid membrane from around the transmembrane receptors and exposing hydrophobic residues, causing conformational change). Fluorescent confocal microscopy for C5aR1 demonstrated loss of protein expression in C5aR1 KO THP-1 cells clone C3 (**Figure 4.40**).

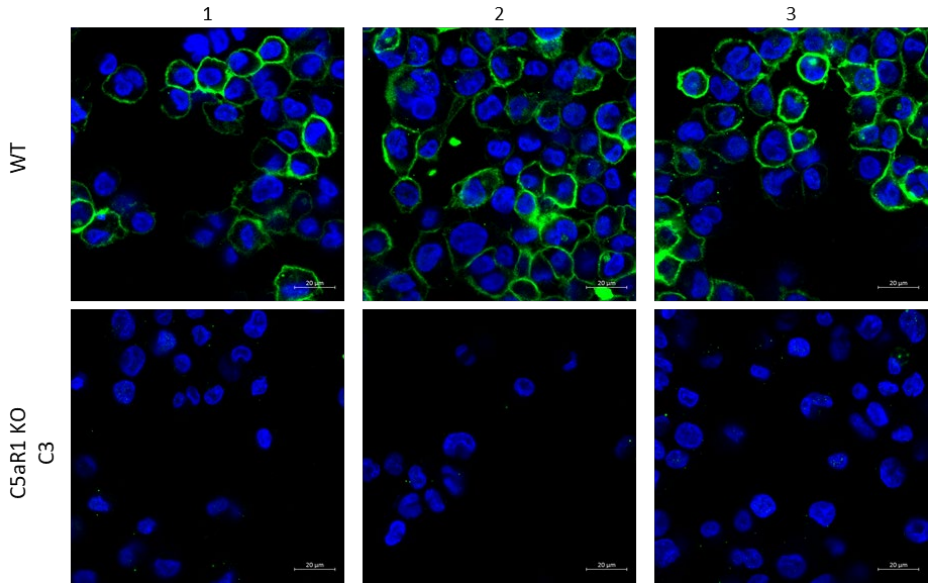

Figure 4.40. Fluorescent confocal microscopy for C5aR1 in WT and C5aR1 KO THP-1 cells. PMA-differentiated WT or C5aR1 KO clone C3 THP-1 cells were fixed, permeabilised and stained with an anti-C5aR1 mAb, secondary AF488-conjugated mAb (green) and Hoechst (blue).

C5aR1 is present at the plasma membrane of these cells, and the C5aR1 KO clone C3 has no C5aR1 signal, indicating loss of protein expression in the C5aR1 KO cells.

Microscopy for C5aR2 was not successful. It is unclear whether this is due to the lack of availability of highly specific antibodies or due to epitope disruption during fixation and permeabilisation.

Flow cytometry was used to detect extracellular C5aR1 (**Figure 4.41**) and intracellular C5aR2 (**Figure 4.42**) in WT and KO cell lines.

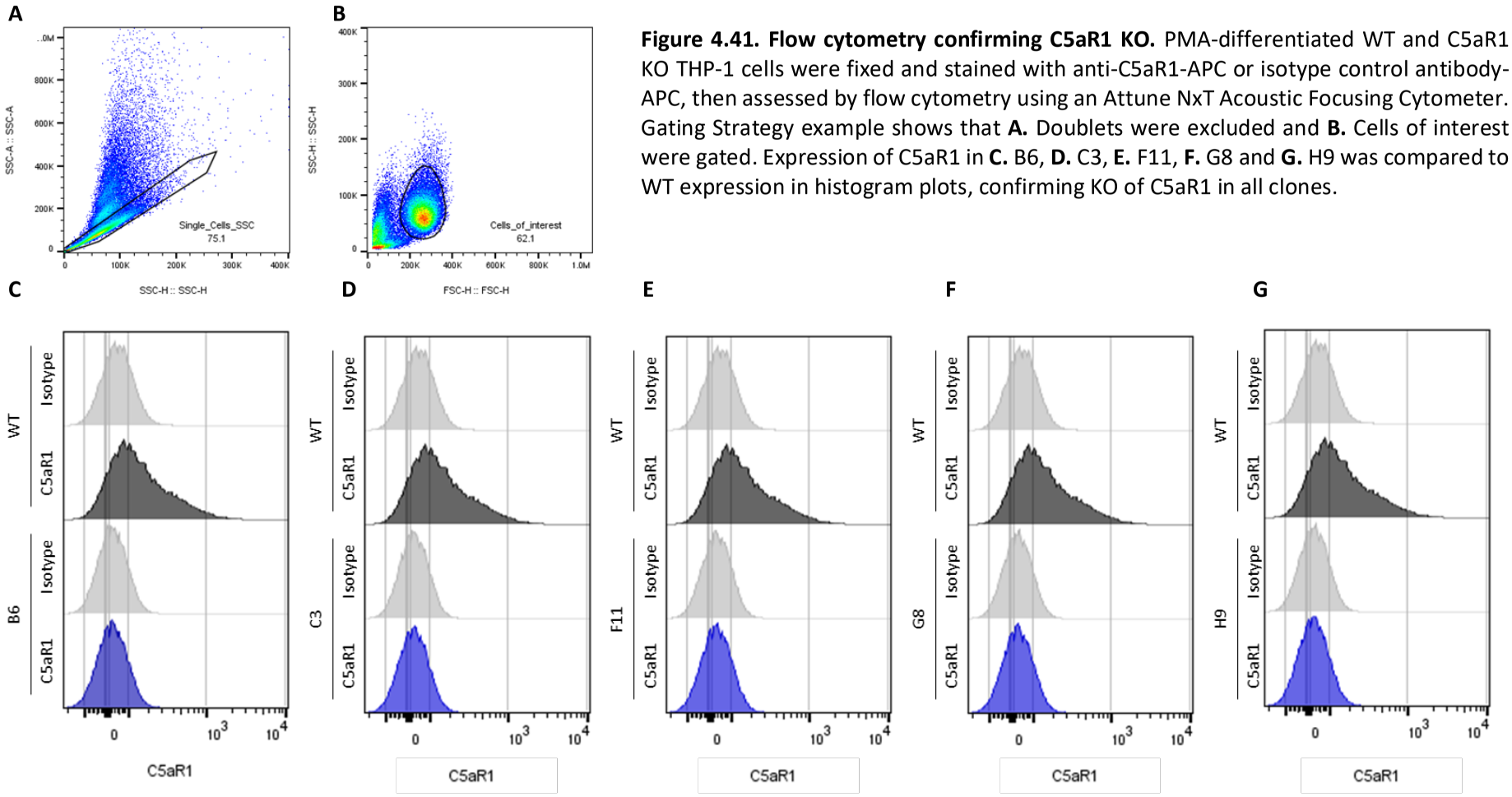

Figure 4.41. Flow cytometry confirming C5aR1 KO. PMA-differentiated WT and C5aR1 KO THP-1 cells were fixed and stained with anti-C5aR1-APC or isotype control antibody-APC, then assessed by flow cytometry using an Attune NxT Acoustic Focusing Cytometer. Gating Strategy example shows that **A.** Doublets were excluded and **B.** Cells of interest were gated. Expression of C5aR1 in **C.** B6, **D.** C3, **E.** F11, **F.** G8 and **G.** H9 was compared to WT expression in histogram plots, confirming KO of C5aR1 in all clones.

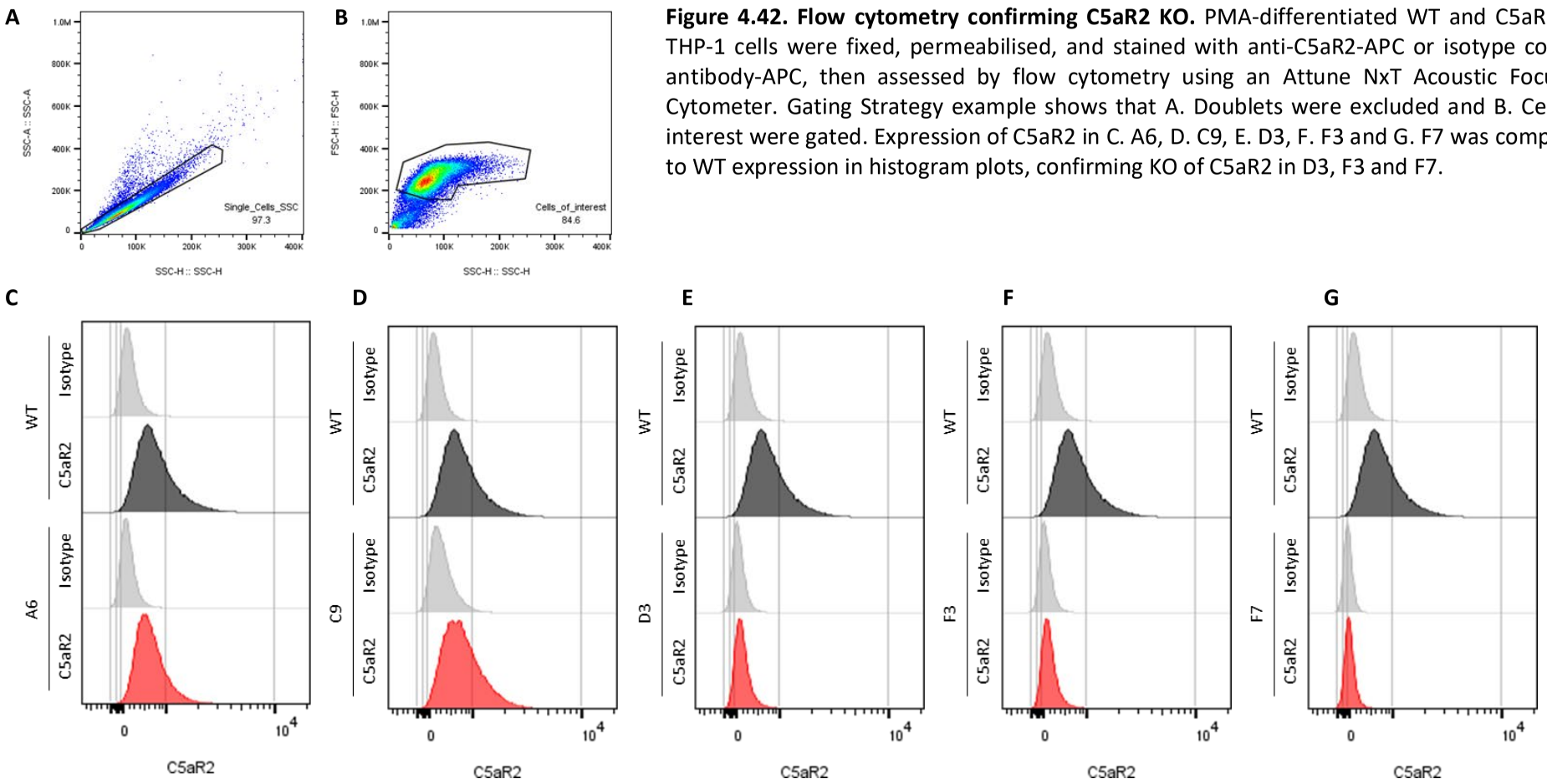

Figure 4.42. Flow cytometry confirming C5aR2 KO. PMA-differentiated WT and C5aR1 KO THP-1 cells were fixed, permeabilised, and stained with anti-C5aR2-APC or isotype control antibody-APC, then assessed by flow cytometry using an Attune NxT Acoustic Focusing Cytometer. Gating Strategy example shows that A. Doublets were excluded and B. Cells of interest were gated. Expression of C5aR2 in C. A6, D. C9, E. D3, F. F3 and G. F7 was compared to WT expression in histogram plots, confirming KO of C5aR2 in D3, F3 and F7.

C5aR1 was expressed in WT cells, indicated by an increase in MFI in the anti-C5aR1-stained cells compared to the isotype control. In the KO cell lines, there was no C5aR1 expression, and anti-C5aR1-stained cells had a signal indistinguishable from the isotype control signal. All five C5aR1 KO clones (B6, C3, F11, G8, H9) lacked expression of C5aR1 protein.

C5aR2 was expressed in WT cells, indicated by a distinct right-shift in the histogram generated by anti-C5aR2-stained cells in comparison to the isotype control. Clones A6 and C9 had signal comparable to the WT and much higher than the isotype control, suggesting that they retained C5aR2 expression. In contrast, clones D3, F3 and F7 were indistinguishable from the isotype control, therefore did not express C5aR2. Clones D3, F3 and F7 were C5aR2 KO cell lines and lacked expression of C5aR2 protein.

These results were summarised by plotting the MFI of the isotype control and the stained cells for C5aR1 KO cells (**Figure 4.43 A**) or C5aR2 KO cells (**Figure 4.43 B**).

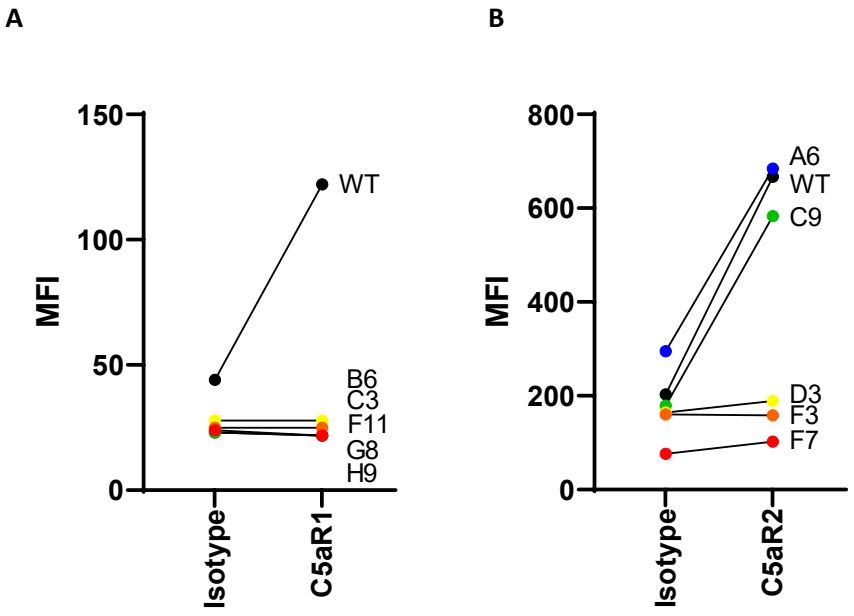

Figure 4.43. Summary of flow cytometry data. Median Fluorescence Intensity (MFI) from cells stained with isotype control antibody and anti-C5aR1 or anti-C5aR2 was plotted for WT and **A.** C5aR1 and **B.** C5aR2 KO clones.

WT cells have a high MFI when stained with anti-C5aR1 or anti-C5aR2 compared to the isotype control antibodies. All five C5aR1 KO clones separate from the WT, and do not have an increase in MFI compared to the isotype control antibody. C5aR2 KO clones D3, F3 and F7 separate from the WT and do not increase in MFI compared to the isotype control antibody, whereas A6 and C9 appear similar to the WT.

C5aR1 KO clones B6, C3, F11, G8 and H9 were confirmed to lack C5aR1 protein, and were used in future experiments. C5aR2 KO clones D3, F3 and F7 were confirmed to lack C5aR2 protein, and were used in future experiments. Clones A6 and C9 retained C5aR2 protein expression, so were removed from culture and not used in future experiments.

These results demonstrate that C5aR1 KO clones B6, C3, F11, G8 and H9 do not express C5aR1, and C5aR2 KO Clones D3, F3 and F7 do not express C5aR2. Monoclonal C5aR1 KO and C5aR2 KO THP-1 cell lines have been successfully generated.

4.3. Discussion

This series of experiments aimed to use CRISPR-Cas9 to generate C5aR1 KO and C5aR2 KO THP-1 cells. Previously, tools to study C5aR2 were poorly available, and data published using selective peptide agonists of C5aR2 [72] were not reproducible (**Chapter 3**). A simple and robust system with which to study C5aR2 was required.

CRISPR-Cas9 was used to generate C5aR1 KO and C5aR2 KO THP-1 cells, which were then characterised using DNA sequencing and protein detection. C5aR1 was not expressed in undifferentiated WT THP-1 cells, and was expressed extracellularly in PMA-differentiated WT THP-1 cells. C5aR2 was expressed intracellularly in undifferentiated and PMA-differentiated cells. The intracellular expression of C5aR2 has been reported previously albeit variably [68–70], however it appears clearly in this cell type. Despite the slight reduction in C5aR2 expression, PMA-differentiated THP-1 cells were selected as the model cell type to permit C5aR1 expression, which was absent in undifferentiated cells. Stable KO cells were generated rather than RNAi-mediated knockdown cells to eliminate variability between separate RNAi treatments, aiming to generate a highly characterised cell type which could be used across multiple different experiments for the duration of the project. These cells would not have to be generated for each experiment, unlike knockdown cells, eliminating a potential source of variability between experiments. The C5aR1 KO and C5aR2 KO THP-1 cell lines were successfully generated and characterised, ready for use in future experiments to investigate the function of C5aR2.

4.3.1. Study limitations

There were some limitations to note with this series of experiments. These include issues with cell culture, loss of the DKO cells, and CRISPR-Cas9 controls.

4.3.1.1. CRISPR-Cas9 protocol variations

There were differences between the CRISPR-Cas9 editing protocols employed between the C5aR1 KO and C5aR2 KO THP-1 cells. The C5aR1 KO cells used a triple guide approach, resulting in large indels and relatively high editing efficiencies. The C5aR2 KO cells, however, originated from a relatively small population of a polyclonal culture generated using a single guide CRISPR-Cas9 edit, resulting in a small indel. However, the initial low editing efficiency in the polyclonal population of C5aR2 KO cells was not conferred to the final monoclonal cell lines (which were all likely 100% KO originating fom a single cell), and indels in all of the selected KO clones conferred loss of protein expression.

4.3.1.2. Cell lines vs primary cells

Previous work was conducted in primary human MDMs [8,72] (**Chapter 3**). THP-1 cells were selected as a model of macrophages in this study, rather than primary human MDMs. THP-1 cells are an immortalised monocyte cell line, which can be differentiated into adherent macrophage-like cells [117]. There are phenotypic differences between primary macrophages and THP-1 cell lines, such as macrophage marker expression levels and immunocompetency [118], however THP-1 cells afford flexibility through their relative ease of culture, and eliminate the potential for donor-donor variability, which can reduce robustness of studies conducted using primary cells. Culture and handling of THP-1 cells is easier than primary cells, and cell lines are not limited in number due to their continuous replication in culture.

The THP-1 KO cell lines will be used to generate initial observations across a large number of experiments, and key observations will be reproduced using CRISPR-Cas9-edited primary human MDMs to ensure that the phenotype translates to primary cells.

4.3.1.3. C5aR1/2 DKO cell line

The C5aR1/2 DKO THP-1 cells lacked indels in the C5aR2 gene, so were discarded from culture as they were not true C5aR2 KOs. Due in part to time constraints, another attempt to generate a double KO was not deemed necessary for progressing the project, as the C5aR1 KO and C5aR2 KO cell lines were sufficient to investigate the function of C5aR2.

4.3.1.4. C5aR1 KO clone H9

Multiple aliquots of C5aR1 KO H9 failed to establish in culture after cryopreservation. This may have been due to a technical error in cryopreservation, but the clone was excluded from use in further experiments. Sufficient additional C5aR1 KO clones were available to continue the work.

4.3.1.5. NTC vs WT control for CRISPR-Cas9

The NTC cells were also lost due to contamination during extended culture throughout national COVID-19 lockdowns during Winter 2020-2021, and loss of access to the laboratory. WT cells were used as a replacement negative control throughout the remainder of the project. This is not optimal, as a NTC cells control for the effect of electroporation and transfection of Cas9 [116]. Acute inflammatory effects in the initial hours and days following electroporation, transfection and DNA damage and repair may generate high levels of background inflammation. Inflammation can also persist in cell cultures between passages, and epigenetic changes can accumulate in cell lines, all acting as potential sources of variability between experimental results. Due to time limitations, the pragmatic decision was taken to continue with WT cells. Whilst not optimal, these cells had to be used under the assumption that they were equivalent to NTC cells and would not generate a high level of variability. In order to ensure reproducibility, experimental observations would be reproduced using multiple clones, and confirmed in NTC primary cells in future work.

4.3.2. Future work

These novel C5aR1 KO and C5aR2 KO THP-1 cell lines were now robustly characterised and available to use to study the function of C5aR2. Previously, limited tools to study C5aR2 were available. This C5aR2 KO cell line is a robust novel tool which can now be used to interrogate the function of this receptor.

C5aR2 has been shown to modulate PRR-induced cytokine secretion. The next proposed experiment was therefore a stimulation using a panel of PRR ligands on WT, C5aR1 KO and C5aR2 KO cells, with immunoassays for a panel of NF-kB-dependent cytokines as a readout. This was to assess the effect of C5aR1 KO or C5aR2 KO on the response to PRR stimulation. If any hits were identified, the relationship between C5aR2 and the PRR of interest could be characterised using mechanistic experiments.

These cells also afforded the opportunity to carry out multi-omic approaches to investigate the signalling downstream of C5aR2. C5aR2 has no undisputed downstream targets and its function outside of PRR regulation is poorly studied. Transcriptomics, interactomics, proteomics and phosphoproteomics could be used to understand the effect of C5aR2 KO on the cells, the effect of C5a ligation of one of the two C5a receptors in isolation, the relationship between C5aR1 and C5aR2, and the effect that C5aR2 could be having on the regulation of the PRR system.

These proposed experiments, and future work to investigate C5aR2, are now possible without relying on complex experimental setups using indirect endpoints and poorly-characterised tools. These KO THP-1 cell lines have the potential to act as a key tools for the future study of C5aR1 and C5aR2.

Chapter 5 - Results 3

Investigating PRR modulation by C5aR1 and C5aR2

5. Investigating PRR modulation by C5aR1 and C5aR2

5.1. Introduction

Recent studies on C5aR2 have revealed that it is able to modulate PRR-induced cytokine secretion, greatly increasing its immunological relevance. Specifically, co-stimulation of C5aR2 and TLR4, TLR7, Mincle or STING significantly reduced IL-6 secretion, and co-stimulation of C5aR2 and Dectin-1, Mincle or STING significantly reduced TNF-α and IL-10 secretion in human MDMs [8]. This study relied on selective C5aR2 peptide agonists P32 and P59 [72]. However, they are partial C5aR2 agonists, partial C5aR1 agonists and do not induce C5aR1-C5aR2 heterodimerisation [8], highlighting a need to validate the observations. In **Chapter 3**, P32 and P59 failed to function in assays set up to measure C5aR1-induced phospho-ERK1/2, which has been reported to be susceptible to modulation by C5aR2 using the same agonists [72]. A reliable tool was required to study C5aR2. Stable monoclonal C5aR1 KO and C5aR2 KO THP-1 cell lines were therefore generated in **Chapter 4**. These cell lines are well-characterised, and eliminate the need for complex multi-stimulation experimental setups with indirect endpoints.

These KO cell lines could now be used to study the function of C5aR2. This series of experiments aimed to assess the ability of C5aR2 to regulate PRRs using the C5aR1 KO and C5aR2 KO THP-1 cell lines. Hits from an initial functional PRR screen would be investigated further using molecular biology approaches, in order to elucidate the underlying molecular mechanisms and characterise the biological function of C5aR2 in the context of inflammation.

5.2. Results

5.2.1. PRR Panel Experiment

C5aR2 has been shown to modulate PRR-induced cytokine secretion using selective peptide agonists P32 and P59 [8]. However, these molecules have not been independently validated, and did not function in the experiments reported in **Chapter 3**. This series of experiments aimed to investigate the ability of C5aR2 to modulate PRR activity in the context of genetic KO rather than pharmacological manipulation. To assess the role of C5aR1 and C5aR2 in the regulation of PRR signalling, a panel of PRR ligands (Pam3CSK4 for TLR1/2, LPS for TLR4, and cAIM(PS)$_2$ Difluor (Rp/Sp) for STING) was used to stimulate PMA-differentiated WT, C5aR1 KO and C5aR2 KO THP-1 cells.

5.2.1.1. Optimising PRR ligand stimulation conditions

The optimum concentration of each agonist was first determined by stimulating WT PMA-differentiated THP-1 cells with a range of concentrations of PRR ligands for 24 hours (**Figure 5.1**). Supernatants were assessed for IL-1β, IL-6, IL-10 and TNFα secretion by MSD U-plex, and lysates were assessed for viability using Cell Titre-Glo assays.

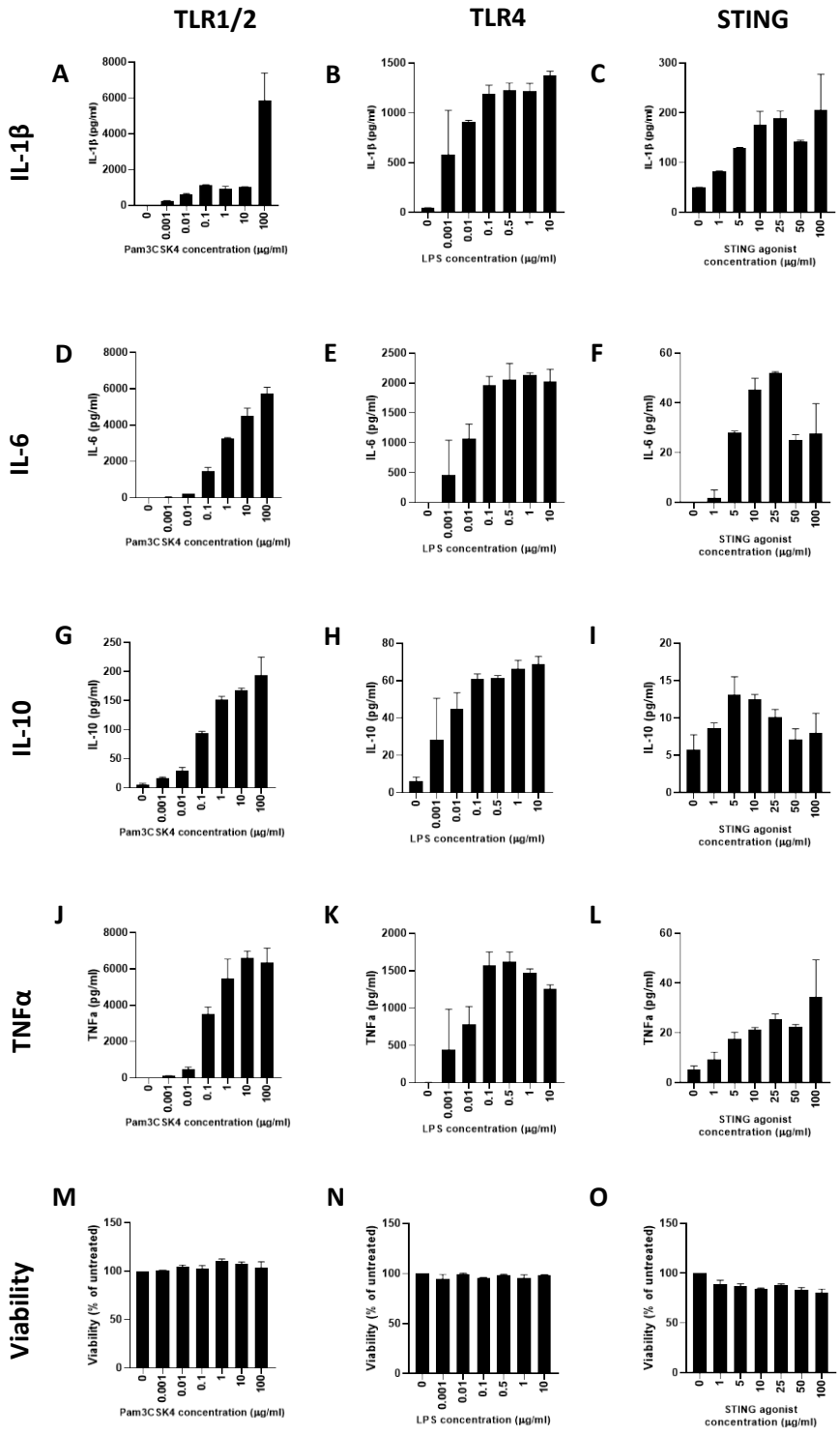

Figure 5.1. Titration of PRR ligands on WT THP-1 cells to identify optimum stimulation concentrations. WT THP-1 cells were stimulated with a range of concentrations of TLR1/2 agonist Pam3CSK4, TLR4 agonist LPS or STING agonist cAIM(PS)$_2$ Difluor (Rp/Sp) for 24 hours. Supernatants were harvested and assessed for **A-C** IL-1β, **D-F** IL-6, **G-I** IL-10 and **J-L** TNFα secretion by MSD. $OD_{450-570}$ values were interpolated with a standard curve and concentration (pg/mL) was calculated. **M-O** Lysates were assessed for viability by Cell Titre-Glo. Viability values were normalised to the untreated cells (100%). Mean ± SD. N=2 from 2 separate experiments.

TLR1/2 agonism generated ~1000 pg/mL of IL-1β secretion when stimulated with 1 ng/mL - 10 μg/mL Pam3CSK4, with a large increase in IL-1β secretion to ~6000 pg/mL at the maximum concentration of 100 μg/mL Pam3CSK4 (**Figure 5.1 A**). There was a concentration-dependent response to TLR1/2 agonism in IL-6 secretion up to ~6000 pg/mL (**Figure 5.1 D**), IL-10 secretion up to ~200 pg/mL (**Figure 5.1 G**), which both peaked at 100 μg/mL Pam3CSK4, and TNFα secretion (**Figure 5.1 J**), which peaked at ~6000 pg/mL using 10 μg/mL Pam3CSK4. There was no effect of TLR1/2 agonism on viability at any concentration (**Figure 5.1 M**). TLR1/2 agonist Pam3CSK4 elicited the maximum response across all cytokines at 10-100 μg/mL, so 10 μg/mL was used in future experiments.

TLR4 agonism generated similar levels of IL-1β secretion up to ~1000 pg/mL, with a concentration-dependent response plateauing at 100 ng/mL LPS (**Figure 5.1 B**). IL-6 secretion followed a similar pattern, with maximum secretion of ~2000 pg/mL occurring at 100 ng/mL LPS (**Figure 5.1 E**). IL-10 secretion (**Figure 5.1 H**) and TNFα secretion (**Figure 5.1K**) followed a similar pattern, peaking at ~60 pg/mL and ~1500 pg/mL, respectively. There was no effect of TLR4 agonism on viability at any concentration (**Figure 5.1 N**). TLR4 agonist LPS elicited the maximum response across all endpoints at 100 ng/mL, therefore 10 ng/mL was used in future experiments.

STING agonism induced a concentration-dependent response which peaks using 25 μg/mL cAIM(PS)$_2$ Difluor (Rp/Sp) for IL-1β secretion (**Figure 5.1 C**), IL-6 (**Figure 5.1 F**) and TNFα (**Figure 5.1 L**), and peaks at 5 μg/mL cAIM(PS)$_2$ Difluor (Rp/Sp) for IL-10 (**Figure 5.1 I**), followed by a reduction in cytokine concentration across all endpoints. STING-induced cytokines were secreted at a lower concentration across all conditions, with maximum responses of ~200 pg/mL IL-1β, ~50 pg/mL IL-6, ~15 pg/mL IL-10, and ~30 pg/mL TNFα. There was a slight concentration-dependent reduction in viability up to 100 μg/mL STING agonist (**Figure 5.1 O**). This could account for the variability in

cytokine secretion at 100 µg/mL cAIM(PS)$_2$ Difluor (Rp/Sp). The maximum cytokine secretion response was elicited at 25 µg/mL for IL-1β, IL-6 and TNFα, and at 5 µg/mL for IL-10, so 5 µg/mL cAIM(PS)$_2$ Difluor (Rp/Sp) was used for future experiments.

These concentrations were selected to elicit a sub-maximal or maximal response across the 4 cytokine endpoints, and to ensure that viability was not reduced by toxic concentrations of PRR ligands. The effect of C5aR1 and C5aR2 KO was then assessed by comparing the cytokine secretion response to the same panel of agonists in WT cells to that of the KO cells.

5.2.1.2. Assessing the cytokine secretion response of WT, C5aR1 KO and C5aR2 KO cells stimulated with a panel of PRR ligands

Having established the stimulation conditions using WT cells, KO THP-1 cells could now be stimulated to assess the effect of C5aR1 KO and C5aR2 KO. WT, C5aR1 KO and C5aR2 KO PMA-differentiated THP-1 cells were stimulated with 10 µg/mL Pam3CSK4, 10 ng/mL LPS or 5 µg/mL cAIM(PS)$_2$ Difluor (Rp/Sp) for 24 hours. Supernatants were assessed for IL-1β, IL-6, IL-10 and TNFα secretion by MSD, and lysates were assessed for viability using Cell Titre-Glo. Clones C3 (C5aR1 KO) and F7 (C5aR2 KO) were used as this was a preliminary study, and observations would be replicated in additional clones in future experiments.

These results are described in detail below, followed by a summary (**5.2.2.**).

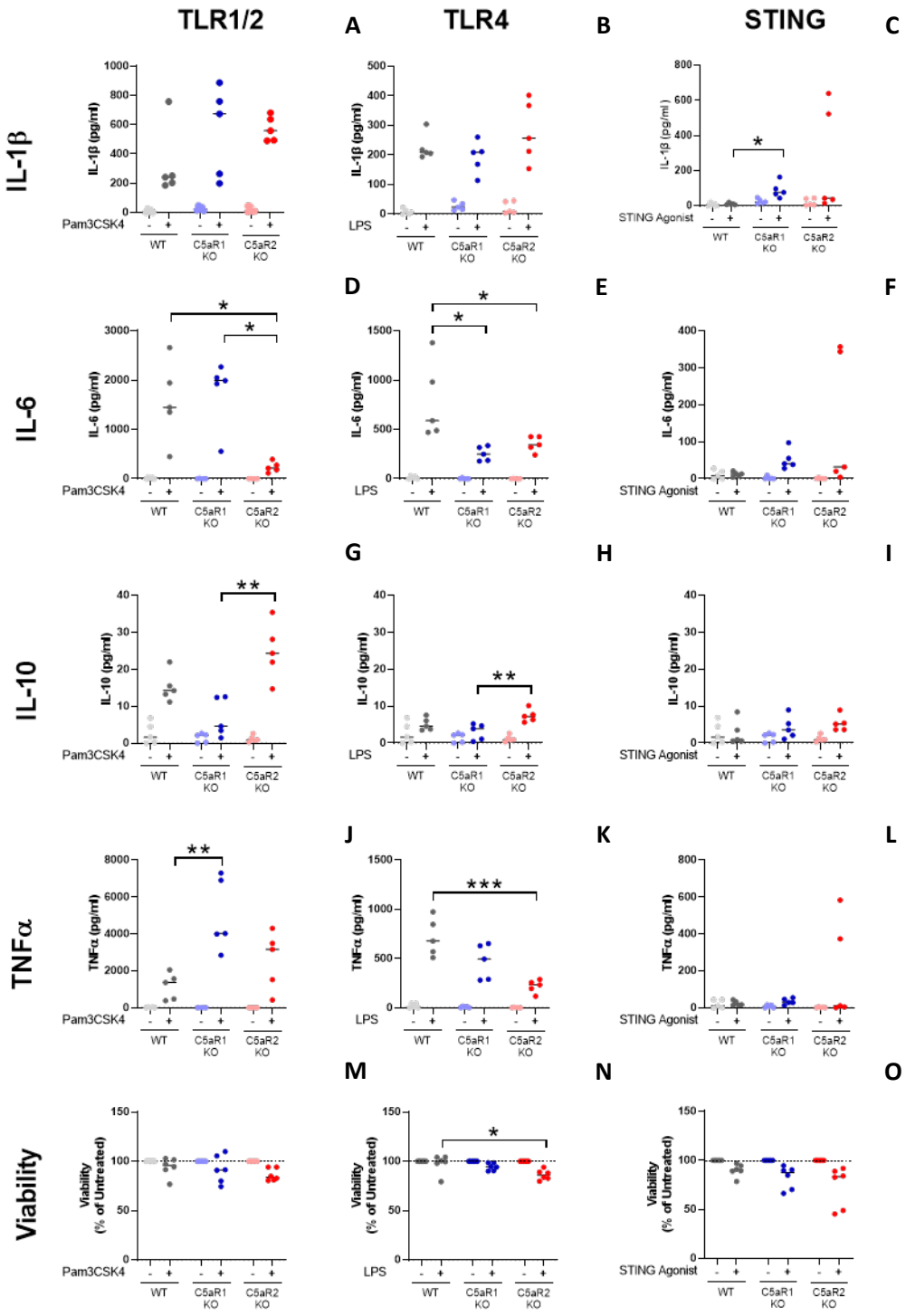

Figure 5.2 C5aR1 KO and C5aR2 KO significantly modulate PRR-induced cytokine secretion in response to PRR ligands. WT, C5aR1 KO Clone C3 and C5aR2 KO Clone F7 THP-1 cells were stimulated with 10 µg/mL TLR1/2 agonist Pam3CSK4, 10 ng/mL TLR4 agonist LPS or 5 µg/mL STING agonist cAIM(PS)$_2$ Difluor (Rp/Sp) for 24 hours. Supernatants were harvested and assessed for **A-C** IL-1β, **D-F** IL-6, **G-I** IL-10 and **J-L** TNFα secretion by MSD. $OD_{450-570}$ values were interpolated with a standard curve and concentration (pg/mL) was calculated. **M-O** Lysates were assessed for viability by Cell Titre-Glo. Viability values were normalised using the untreated cells as 100%. Mean ± SD were plotted with each point representing a single replicate; Kolmogrov-Smirnov normality tests and one-way ANOVA or Kruskal-Wallis tests were performed. ns: p>0.05; *: p ≤ 0.05; **: p≤0.01; ***: p≤0.001. N=5 from 3 separate experiments (cytokines), N=6 from 3 separate experiments (viability).

5.2.1.2.1. Regulation of IL-1β by C5aR1 KO and C5aR2 KO

TLR1/2 agonism induced ~200 pg/mL IL-1β (**Figure 5.2 A**). There was a slight increase induced by C5aR1 KO and C5aR2 KO, however responses were variable and there was no statistical significance.

TLR4 agonism elicited a similar level of IL-1β secretion, and there was no difference between C5aR1 KO or C5aR2 KO and WT (**Figure 5.2 B**).

STING agonism did not induce IL-1β secretion in WT cells (**Figure 5.2 C**). C5aR1 KO caused a significant increase in IL-1β secretion (Kruskal Wallis test; p=0.0175) to ~100 pg/mL. C5aR2 KO caused a large increase in IL-1β secretion in 2 replicates, but 3 did not respond. The mean was not significantly different to the WT, but was close to statistical significance (Kruskal Wallis test; p=0.0589), and the C5aR1 KO and C5aR2 KO values did not differ significantly.

5.2.1.2.2. Regulation of IL-6 by C5aR1 KO and C5aR2 KO

TLR1/2 agonism elicited a variable level of IL-6 secretion in WT cells, and C5aR1 KO had no significant effect on IL-6 secretion (**Figure 5.2 D**). The C5aR2 KO response was significantly lower than the WT (Kruskal Wallis test; p=0.0486) and the C5aR1 KO (Kruskal Wallis test; p=0.0112).

TLR4 agonism elicits lower levels of IL-6 secretion in WT cells compared to TLR1/2 agonism (**Figure 5.2 E**). C5aR1 KO causes a significant reduction in IL-6 secretion (one-way ANOVA; p=0.0118), as does C5aR2 KO (one-way ANOVA; p=0.0398).

STING agonism does not induce IL-6 secretion in WT cells (**Figure 5.2 F**). C5aR1 KO increases the response to STING agonism, but there is no statistical significance. C5aR2 KO increases the response in 2 replicates, similar to the IL-1β response, but not in the remaining 3. The standard deviation is therefore large and there is no statistical significance.

5.2.1.2.3. Regulation of IL-10 by C5aR1 KO and C5aR2 KO

IL-10 was secreted at extremely low concentrations across all stimulations and cell lines. TLR1/2 stimulation induced approximately 15 pg/mL IL-10 in WT cells (**Figure 5.2 G**). C5aR1 KO reduced this, and C5aR2 KO significantly increased IL-10 secretion to approximately 25 pg/mL (one-way ANOVA; p=0.0012). TLR4 agonism induced low levels (< 10 pg/mL) of IL-10 secretion in WT cells (**Figure 5.2 H**). C5aR1 KO had no effect, and C5aR2 KO slightly increased IL-10 secretion. This was statistically significant compared to the C5aR1 KO cells (one-way ANOVA; p=0.0098), which were not significantly different to WT cells. STING agonism induced extremely low levels of IL-10 secretion in WT, C5aR1 KO or C5aR2 KO cells (**Figure 5.2 I**).

5.2.1.2.4. Regulation of TNFα by C5aR1 KO and C5aR2 KO

TLR1/2 stimulation induced TNFα secretion in WT cells, which was significantly increased in C5aR1 KO cells (one-way ANOVA; p=0.0052) and variably increased in C5aR2 KO cells (ns) (**Figure 5.2 J**).

TLR4 agonism induced TNFα secretion in WT cells which was slightly suppressed in C5aR1 KO cells and significantly suppressed in C5aR2 KO cells (one-way ANOVA, p=0.0009) (**Figure 5.2 K**).

STING agonism induced a very low level of TNFα secretion in WT cells and C5aR1 KO cells, and C5aR2 KO amplified the TNFα response in 2 of the 5 replicates as seen with IL-1β and IL-6 (**Figure 5.2 L**).

5.2.1.2.5. Cytotoxicity of PRR ligands in C5aR1 KO and C5aR2 KO THP-1 cells

Stimulation with each of the three PRR ligands induced a variable reduction in viability over the 24 hour incubation.

TLR1/2 agonism had no significant effect on viability in WT, C5aR1 KO or C5aR2 KO cells (**Figure 5.2 M**). TLR4 agonism had no significant effect on viability in WT or C5aR1 KO cells, whereas C5aR2 KO had a slight but significant effect on viability compared to the WT cells (Kruskal Wallis test; p=0.0206) (**Figure 5.2 N**). STING agonism had no significant effect on viability in WT, C5aR1 or C5aR2 KO cells, however there was a reduction in viability in WT cells which was slightly amplified in C5aR1 KO cells and further amplified in C5aR2 KO cells in 2 of the 6 replicates (**Figure 5.2 O**).

5.2.1.3. Identification of C5a-dependent effects of C5aR1 KO or C5aR2 KO on PRR pathway regulation

C5a has been shown to regulate NF-κB-dependent cytokine secretion [72]. In order to identify C5a-dependent effects of C5aR1 KO and C5aR2 KO on PRR signalling, WT, C5aR1 KO and C5aR2 KO PMA-differentiated THP-1 cells were stimulated with 50 ng/mL C5a or co-stimulated with Pam3CSK4, LPS or $cAIM(PS)_2$ Difluor (Rp/Sp) and C5a for 24 hours. Supernatants were assessed for IL-1β, IL-6, IL-10 and TNFα secretion by MSD, and lysates were assessed for viability using Cell Titre-Glo. Clones C3 (C5aR1 KO) and F7 (C5aR2 KO) were used as this was a preliminary study. Data were plotted with data from **Figure 5.2**. Statistical tests focussed on the effect of PRR stimulation compared with C5a co-stimulation.

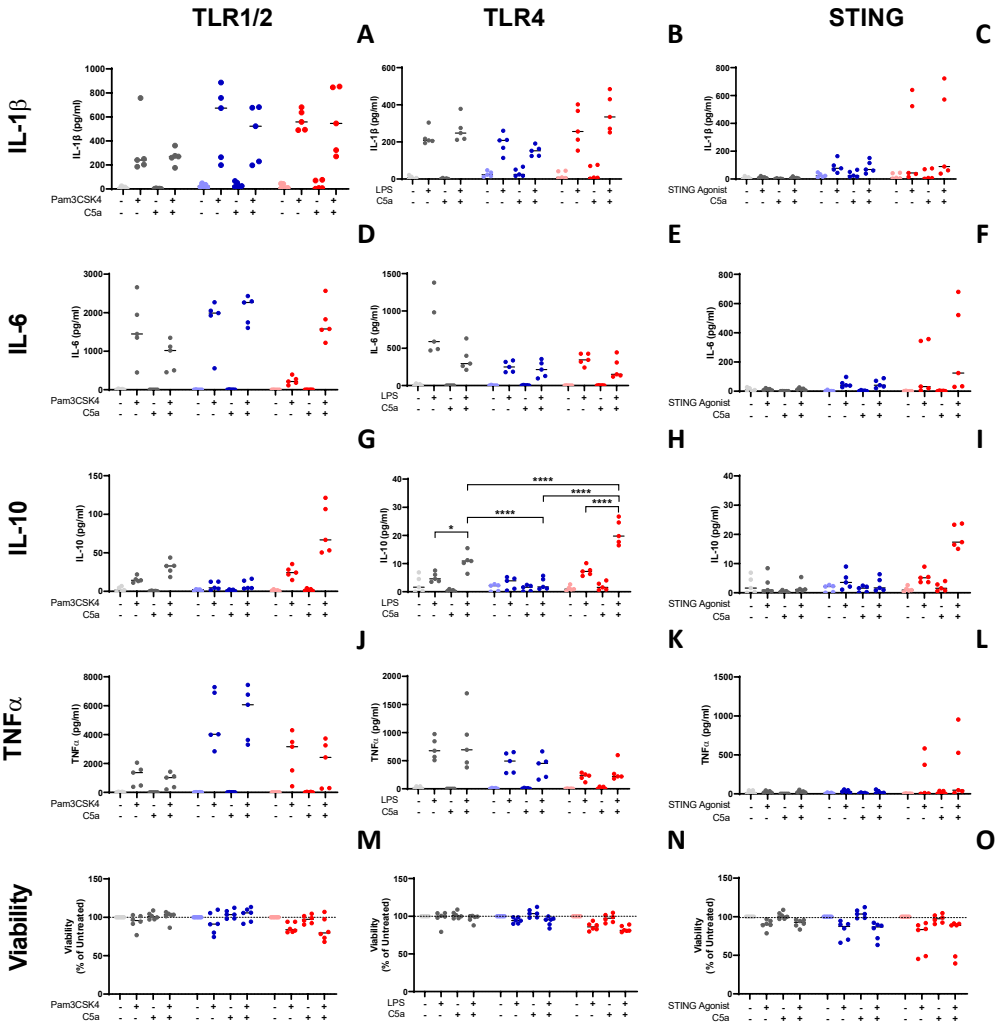

Figure 5.3. Effects of C5a on PRR regulation in WT, C5aR1 KO and C5aR2 KO THP-1 cells. WT, C5aR1 KO Clone C3 or C5aR2 KO Clone F7 THP-1 cells were stimulated with 10 µg/mL TLR1/2 agonist Pam3CSK4, 10 ng/mL TLR4 agonist LPS or 5 µg/mL STING agonist cAIM(PS)$_2$ Difluor (Rp/Sp) ± 50 ng/mL C5a for 24 hours. Supernatants were harvested and assessed for **A-C** IL-1β, **D-F** IL-6, **G-I** IL-10 and **J-L** TNFα secretion by MSD. $OD_{450-570}$ values were interpolated with a standard curve and concentration (pg/mL) was calculated. **M-O** Lysates were assessed for viability by Cell Titre-Glo. Viability values were normalised using the untreated cells as 100%. Mean ± SD were plotted with each point representing a single replicate; Kolmogrov-Smirnov normality tests and one-way ANOVA or Kruskal-Wallis tests were performed. ns: p>0.05; *: p ≤ 0.05; ****: p≤0.0001. N=5 from 3 separate experiments (cytokines), N=6 from 3 separate experiments (viability)

5.2.1.3.1. Regulation of IL-1β by C5a in C5aR1 KO and C5aR2 KO THP-1 cells

C5a has no effect on IL-1β secretion in WT, C5aR1 KO or C5aR2 KO cells in response to TLR1/2 agonism (**Figure 5.3 A**), TLR4 agonism (**Figure 5.3 B**) or STING agonism (**Figure 5.3 C**). This is notable as IL-1β is downstream of NF-κB activation along with IL-6 and IL-10, but is regulated by C5aR1- and C5aR2-independent mechanisms.

5.2.1.3.2. Regulation of IL-6 by C5a in C5aR1 KO and C5aR2 KO THP-1 cells

C5a has a more active role in IL-6 modulation, however none of these results were statistically significant.

In response to TLR1/2 agonism, C5a suppressed IL-6 secretion in WT cells (**Figure 5.3 D**). This effect was reduced in the C5aR1 KO cells, suggesting that the suppressive effect was C5aR1-dependent. In C5aR2 KO cells, TLR1/2-induced IL-6 secretion is suppressed as baseline, and is rescued or amplified by C5a co-stimulation, suggesting that C5aR2 regulates IL-6 secretion.

In response to TLR4 agonism, C5a down-regulates IL-6 secretion in WT cells (**Figure 5.3 E**). This effect is lost in the C5aR1 KO cells, and retained in the C5aR2 KO cells at a low level. However, secretion of IL-6 is generally suppressed by C5aR1/2 KO, meaning that the effect of C5a may be masked in the C5aR1 KO.

In response to STING agonism, there is no effect of C5a in the WT or C5aR1 KO cells (**Figure 5.3 F**). There may be an amplification in the C5aR2 KO cells, however this cannot be confirmed due to the variability of the data.

5.2.1.3.3. Regulation of IL-10 by C5a in C5aR1 KO and C5aR2 KO cells

C5a amplifies TLR1/2-dependent IL-10 secretion in WT cells (**Figure 5.3 G**). There is no effect in C5aR1 KO cells. C5a also amplifies TLR1/2-dependent IL-10 secretion in C5aR2 KO cells. The levels are higher in Pam3CSK4-stimulated cells and co-stimulated cells,

suggesting that the baseline response is increased rather than the response to C5a is increased.

The same pattern is seen with TLR4-dependent IL-10 secretion (**Figure 5.3 H**). Concentrations are lower than TLR1/2-dependent IL-10 secretion, but these results are statistically significant. C5a amplifies TLR4-dependent IL-10 secretion (one-way ANOVA; $p=0.0114$), which is lost in the C5aR1 KO (one-way ANOVA; $p<0.0001$). In the C5aR2 KO, C5a amplifies TLR4-dependent IL-10 secretion (one-way ANOVA; $p<0.0001$) to a level significantly higher than co-stimulated WT cells (one-way ANOVA; $p<0.0001$) or C5aR1 KO cells (one-way ANOVA; $p<0.0001$).

A different pattern is seen with STING-dependent IL-10 secretion (**Figure 5.3 I**). Very low levels of IL-10 are seen across the conditions. C5a has no effect on WT cells or C5aR1 KO cells, but C5aR2 KO cells have more STING-dependent IL-10 secretion which is amplified by C5a.

IL-10 secretion is suppressed in C5aR1 KO cells across all conditions. This is notable as it suggests that C5aR1 is required for IL-10 secretion downstream of these PRR pathways.

5.2.1.3.4. Regulation of TNFα by C5a in C5aR1 KO and C5aR2 KO cells

There is no effect of C5a on TNFα secretion downstream of TLR1/2 agonism (**Figure 5.3 J**), TLR4 agonism (**Figure 5.3 K**) or STING agonism (**Figure 5.3 L**). TNFα secretion occurs downstream of NF-κB activation along with IL-6 and IL-10, however it is not regulated by C5a-induced signalling.

5.2.1.3.5. C5a-dependent cytotoxicity of PRR ligands in C5aR1 KO and C5aR2 KO THP-1 cells

There is no effect of C5a on viability downstream of TLR1/2 agonism (**Figure 5.3 M**), TLR4 agonism (**Figure 5.3 N**) or STING agonism (**Figure 5.3 O**).

5.2.2. Summary of PRR ligand panel

There were several statistically significant C5aR1 and C5aR2-dependent modulations of the NF-κB-dependent cytokine response to PRR ligands in this dataset. Cytokine secretion downstream of the TLR1/2 pathway is differentially modulated: IL-6 is suppressed by C5aR2 KO, IL-10 is amplified by C5aR2 KO, and TNFα is amplified by C5aR1 KO or C5aR2 KO. The same is true for the TLR4 pathway. IL-6 is suppressed by C5aR1 KO and C5aR2 KO, IL-10 secretion is slightly amplified by C5aR2 KO, and TNFα secretion is suppressed by C5aR2 KO. Differential regulation of cytokines between cell lines confirms that C5aR1 and C5aR2 have independent roles.

The link between C5aR2 and STING has been observed previously [8], however is less clear in this dataset. It appears that in 2 of the 5 replicates, IL-1β, IL-6 and TNFα secretion are positively regulated in the C5aR2 KO cells compared to the WT cells. These are not necessarily the ideal endpoints to assess for the cGAS-STING pathway. cGAS-STING signals via NF-κB to induce expression of these cytokines, but the pathway signals more strongly via TBK1 and IRF3, resulting in IFN-β secretion. The primary function of the cGAS-STING pathway is an anti-viral sensor, and so the IFN-β secretion response is a more appropriate endpoint to assess for this pathway.

5.2.3. Regulation of STING-induced IFN-β secretion by C5aR1 and C5aR2

To assess the role of C5aR2 for regulating STING-induced IFN-β secretion, the same supernatants were assessed for IFN-β by ELISA.

STING agonism induces IFN-β secretion in WT THP-1 cells (mean = 457.26 pg/mL) (**Figure 5.4**). This is significantly increased in C5aR1 KO cells (mean = 2445.85 pg/mL, one-way ANOVA; $p<0.0001$), and further amplified in C5aR2 KO cells (mean = 8705.22 pg/mL, one-way ANOVA; $p<0.0001$). There is no effect of C5a on IFN-β secretion in WT, C5aR1 KO or C5aR2 KO THP-1 cells (Kruskal Wallis tests; ns) (**Figure 5.5**).

Despite variability in the NF-κB-dependent cytokine ELISAs (**Figure 5.2**), the IFN-β ELISAs revealed a clear and significant link between C5aR2 and the cGAS-STING pathway.

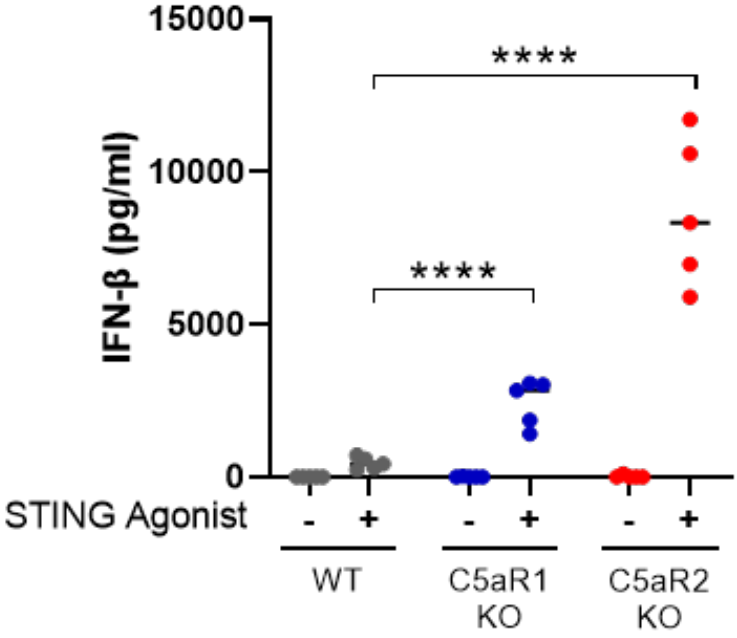

Figure 5.4. C5aR2 KO significantly amplifies STING-induced IFNB secretion in THP-1 cells. Supernatants from WT, C5aR1 KO Clone C3 or C5aR2 KO Clone F7 THP-1 cells stimulated with 5 µg/mL STING agonist cAIM(PS)$_2$ Difluor (Rp/Sp) for 24 hours were assessed for IFN-β by ELISA. $OD_{450-570}$ values were interpolated with a standard curve and concentration (pg/mL) was calculated. Mean ± SD were plotted with each point representing a single replicate; Kolmogrov-Smirnov normality tests and one-way ANOVA tests were performed. ns: p>0.05; ****: p≤0.0001. N=5 from 3 separate experiments.

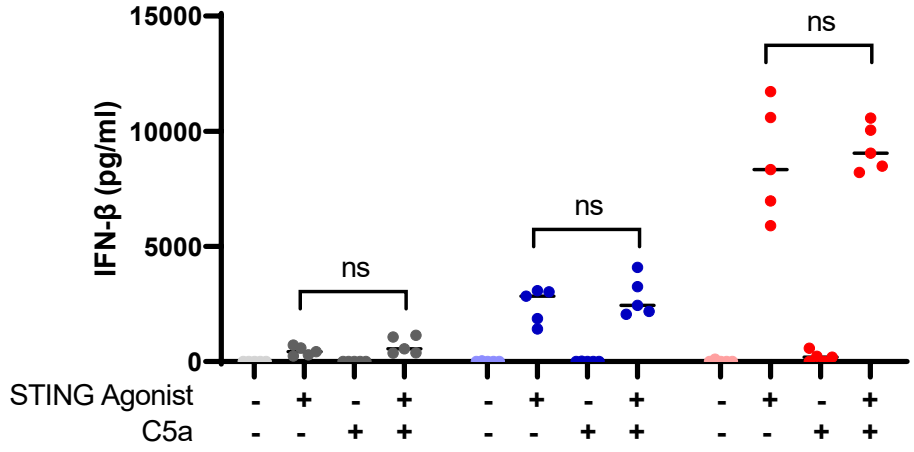

Figure 5.5. C5a has no significant effect on STING-induced IFN-β secretion in THP-1 cells. Supernatants from WT, C5aR1 KO Clone C3 or C5aR2 KO Clone F7 THP-1 cells stimulated with 5 µg/mL STING agonist cAIM(PS)$_2$ Difluor (Rp/Sp) ± 50 ng/mL C5a for 24 hours were assessed for IFN-β by ELISA. $OD_{450-570}$ values were interpolated with a standard curve and concentration (pg/mL) was calculated. Mean ± SD were plotted; Kolmogrov-Smirnov normality tests and Kruskal-Wallis tests were performed. ns: p>0.05. N=5 from 3 separate experiments.

5.2.3.1. Optimising stimulation concentration of cAIM(PS)$_2$ Difluor (Rp/Sp)

The STING stimulation conditions were optimised to gain an understanding of the kinetics of each cell line and limit any cytotoxic effects.

Multiple clones of C5aR1 KO (blue) and C5aR2 KO (red) THP-1 cells were used in this and all future experiments. This increased the robustness of the study as any KO-dependent effects would be present in 3 separate cell lines with distinct indels in the C5aR1 or C5aR2 genes, reducing the likelihood of false positives driven by clone-specific effects. C5aR1 KO clones B6 (circle), C3 (square), F11 (triangle) and G8 (diamond) were used, along with C5aR2 KO clones D3 (circle), F3 (square) and F7 (triangle). C5aR1 KO clone H9 failed to recover from cryopreservation across multiple aliquots so was not used in future work.

The concentration of STING agonist cAIM(PS)$_2$ Difluor (Rp/Sp) was optimised by performing a titration experiment. The incubation time was reduced from 24 hours to 6 hours to reduce the likelihood of cytotoxicity, and incubation time was optimised in the following experiment.

PMA-differentiated WT, C5aR1 KO and C5aR2 KO cells were stimulated with a 0-20 µg/mL cAIM(PS)$_2$ Difluor (Rp/Sp) for 6 hours. Supernatants were assessed for IFN-β by ELISA, and lysates were assessed for viability using Cell Titre-Glo. Non-linear regression analyses were performed to generate concentration-response curves (**Figure 5.6**).

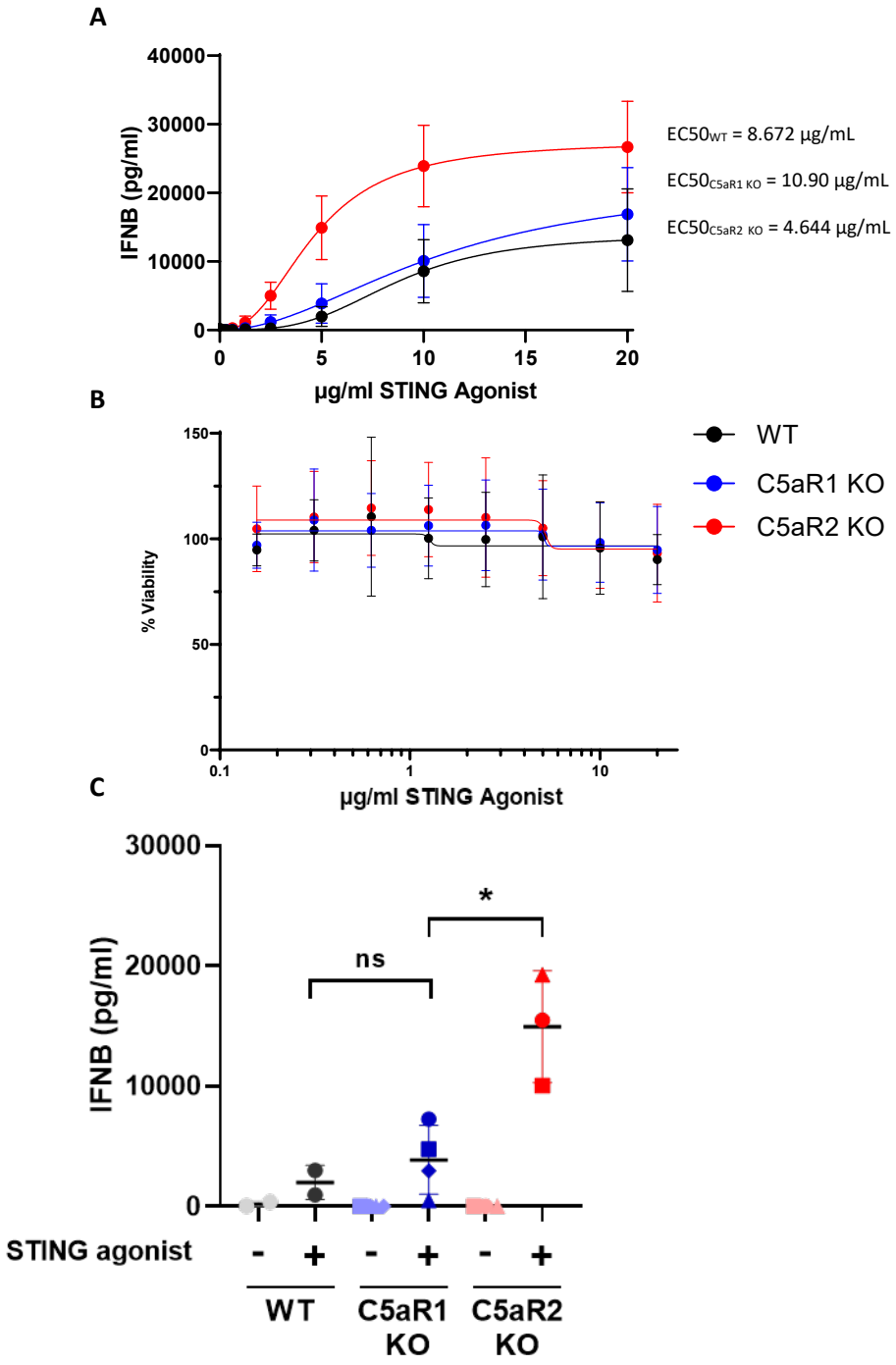

Figure 5.6. Titration of STING agonist onto WT, C5aR1 KO and C5aR2 KO THP-1 cells. WT, C5aR1 KO and C5aR2 KO THP-1 cells were stimulated with 0-20 µg/mL STING agonist cAIM(PS)$_2$ Difluor (Rp/Sp) for 6 hours. **A.** Supernatants were harvested and assessed for IFN-β by ELISA. $OD_{450-570}$ values were interpolated with a standard curve and concentration (pg/mL) was calculated. Mean ± SD were plotted, a nonlinear regression was used to fit a concentration-response curve, and EC50 values were calculated. **B.** Lysates were assessed for viability using Cell Titre-Glo. Viability values were normalised using the untreated cells as 100%. Mean ± SD were plotted, and a nonlinear regression was used to fit a concentration-response curve. **C.** Mean ± SD values generated using 5 µg/mL STING agonist were plotted; Kolmogrov-Smirnov normality tests and a Kruskal-Wallis tests was performed. *: $p<0.05$. N=2 WT replicates, N=4 C5aR1 KO (blue) clones (B6 - circle, C3 - square, F11 - triangle, G8 - diamond) and N=3 C5aR2 KO (red) clones (D3 - circle, F3 - square, F7 - triangle).

There were concentration-dependent IFN-β secretion responses to STING agonism in WT, C5aR1 KO and C5aR2 KO cells: the higher the STING agonist concentration, the higher the concentration of secreted IFN-β (**Figure 5.6 A**). The EC50 in WT cells was 8.672 μg/mL (R^2 = 0.8231) and the mean maximum concentration of IFN-β was 13109.3 pg/mL. The C5aR1 KO response was very similar, with an EC50 of 10.90 μg/mL (R^2 = 0.8196). The response in the C5aR2 KO cells is much higher. The EC50 is the lower value of 4.644 μg/mL (R^2 = 0.9309), indicating that more IFN-β is secreted in response to STING agonism than in the WT or C5aR1 KO THP-1 cells. The curve is left-shifted and has a higher plateau, with a mean maximum value of 26666.7 pg/mL.

The effect of STING agonism on cell viability is negligible between 0 and 5 μg/mL, however there is a reduction in viability at 10 and 20 μg/mL (**Figure 5.6 B**).

The concentration for STING agonism in future experiments was therefore set at 5 μg/mL. This is approximately the EC50 in C5aR2 KO cells, leaving a window in the concentration-response curve for inhibitory and excitatory effects to be observed. This STING agonist concentration generated a lower response in WT (1987 pg/mL) and C5aR1 KO (10068.4 pg/mL) cells, however this was still a strong response with an appropriate window available to detect lower and higher concentrations of IFN-β secretion in future experiments. The data generated with 5 μg/mL STING agonist were summarised (**Figure 5.6 C**), and generated a pattern similar to **Figure 5.4**. STING agonism induced IFN-β secretion in WT cells, which was non-significantly amplified in C5aR1 KO cells, and significantly (compared to C5aR1 KO) amplified in C5aR2 KO cells (Kruskal Wallis test; p=0.0228). The amplification of STING-induced IFN-β secretion in C5aR2 KO cells was reproducible between clones. Future experiments would use this concentration of cAIM$(PS)_2$ Difluor (Rp/Sp) .

5.2.3.2. Optimising incubation time for cAIM(PS)$_2$ Difluor (Rp/Sp)

Following titration of cAIM(PS)$_2$ Difluor (Rp/Sp) and selection of an optimum ligand concentration, the incubation time was optimised. This experiment aimed to identify an incubation time for 5 μg/mL STING agonist which induced a sub-maximal response (allowing for an assay window to detect higher and lower responses induced by other conditions in future experiments), and had a limited cytotoxic effect.

To identify the optimum incubation time, PMA-differentiated WT, C5aR1 KO and C5aR2 KO THP-1 cells were stimulated with 5 μg/mL cAIM(PS)$_2$ Difluor (Rp/Sp) for 0-24 hours. Supernatants were assessed for IFN-β by ELISA, and lysates were assessed for viability using Cell Titre-Glo. Non-linear regression analyses were performed to generate time-response curves (**Figure 5.7**).

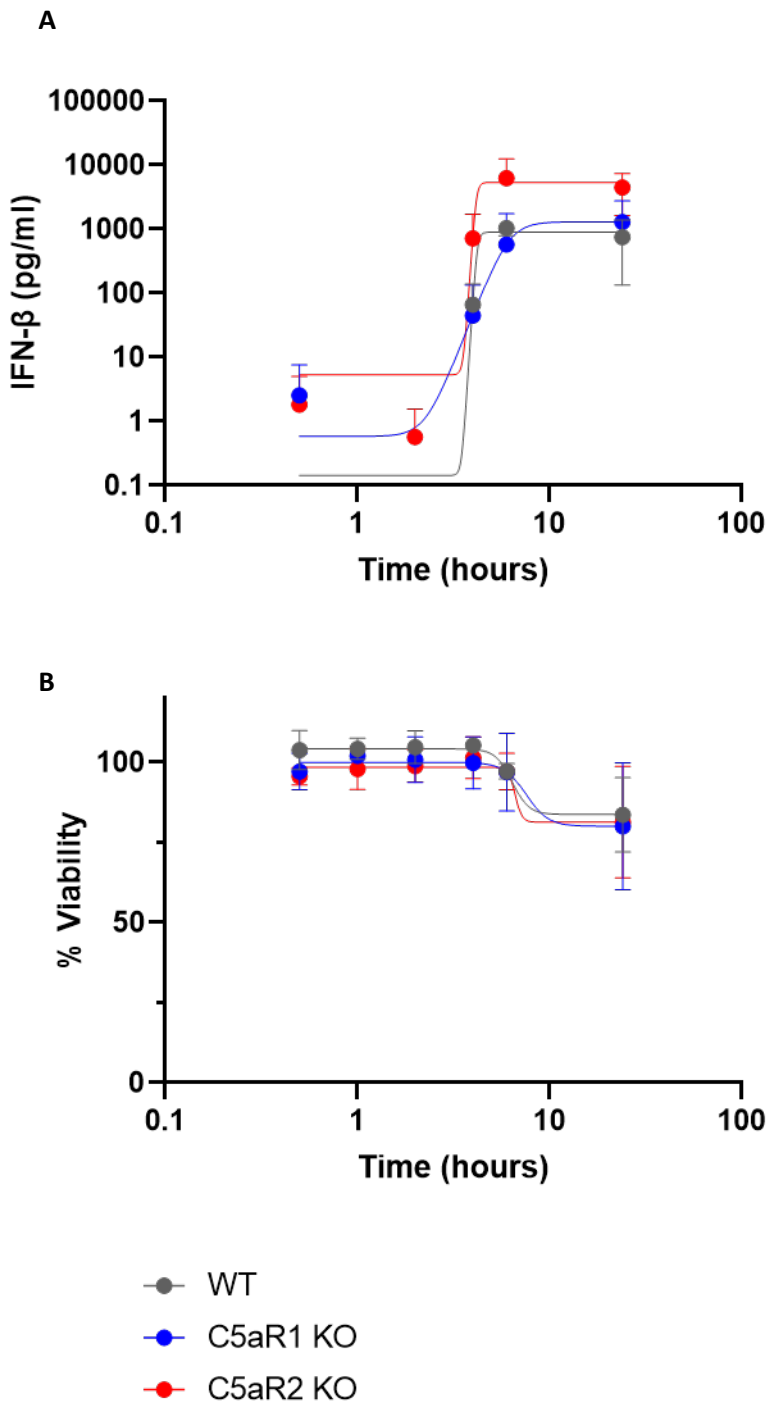

Figure 5.7. Time course of STING agonist onto WT, C5aR1 KO and C5aR2 KO THP-1 cells. WT, C5aR1 KO and C5aR2 KO THP-1 cells were stimulated with 5 µg/mL STING agonist cAIM(PS)$_2$ Difluor (Rp/Sp) for 0-24 hours. **A.** Supernatants were harvested and assessed for IFN-β by ELISA. $OD_{450-570}$ values were interpolated with a standard curve and concentration (pg/mL) was calculated. Mean ± SD were plotted, and a nonlinear regression was used to fit a time-response curve. **B.** Lysates were assessed for viability using Cell Titre-Glo. Viability values were normalised using the untreated cells as 100%. Mean ± SD were plotted, and a nonlinear regression was used to fit a time-response curve. N=3 WT replicates, N=4 C5aR1 KO (blue) clones (B6 - circle, C3 - square, F11 - triangle, G8 - diamond) and N=3 C5aR2 KO (red) clones (D3 - circle, F3 - square, F7 - triangle).

For WT, C5aR1 KO and C5aR2 KO cells, maximum IFN-β secretion occurs between 4 hours and 6 hours (**Figure 5.7 A**). Despite variability in the data and the resultant poor curve fit, there is a clear distinction between C5aR2 KO cells and WT cells. At 4, 6 and 24 hours, C5aR2 KO cells secreted more IFN-β in response to STING agonism than the WT or C5aR1 KO cells. The difference between C5aR2 KO cells and WT cells is at a maximum after 6 hours, after which all responses plateau at 24 hours. Viability was unaffected by STING agonism between 0 and 6 hours, however there was a distinct reduction in viability after 24 hours for WT, C5aR1 KO and C5aR2 KO cells (**Figure 5.7 B**). The distinction between C5aR2 KO cells and WT cells at 6 hours was robust, therefore an incubation time of 6 hours was selected for subsequent experiments.

5.2.3.3. Characterising the cGAS-STING pathway in C5aR1 KO and C5aR2 KO cells using cGAS agonist

Following optimisation of the stimulation conditions for STING agonist cAIM(PS)$_2$ Difluor (Rp/Sp), an alternative agonist of the cGAS-STING pathway, G3-YSD, was used to stimulate cells to further confirm the link between C5aR2 and the cGAS-STING pathway. G3-YSD is a Y-form DNA analogue for dsDNA which agonises cGAS. 1 µg/mL G3-YSD was transfected into WT, C5aR1 KO and C5aR2 KO cells using Lipofectamine 2000, and incubated for 6 hours. Supernatants were assessed for IFN-β by ELISA (**Figure 5.8**).

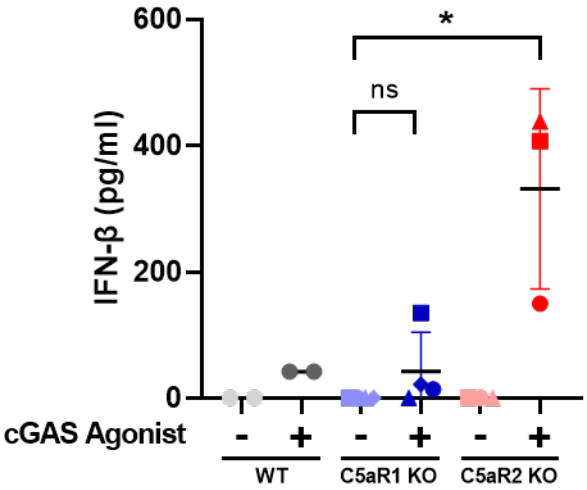

Figure 5.8. C5aR2 KO increases cGAS agonist-induced IFN-β secretion. WT, C5aR1 KO and C5aR2 KO THP-1 cells were stimulated with 1 µg/mL cGAS agonist G3-YSD by cationic lipid transfection for 6 hours. Supernatants were harvested and assessed for IFN-β by ELISA. $OD_{450-570}$ values were interpolated with a standard curve and concentration (pg/mL) was calculated. Mean ± SD were plotted; Kolmogrov-Smirnov normality tests and a Kruskal-Wallis tests was performed. ns: $p>0.05$; *: $p\leq0.05$. N=2 WT replicates, N=4 C5aR1 KO (blue) clones (B6 - circle, C3 – square, F11 - triangle, G8 - diamond) and N=3 C5aR2 KO (red) clones (D3 - circle, F3 - square, F7 - triangle).

G3-YSD transfection causes IFN-β secretion response in WT cells and C5aR1 KO cells, and a significantly higher IFN-β secretion response in C5aR2 KO cells (compared to C5aR1 KO untreated due to insufficient replicates in WT; Kruskal Wallis test; p=0.0292) (**Figure 5.8**). This agonist relies upon cGAS-driven cGAMP production to drive a more

physiological STING response, hence the lower magnitude of response compared to direct agonism of STING. This pattern is conserved with cAIM(PS)$_2$ Difluor (Rp/Sp) stimulation (**Figure 5.4, 5.5, 5.6**) and confirms that IFN-β production via modulation of the cGAS-STING pathway is C5aR2 KO-dependent.

5.2.3.4. Characterising the cGAS-STING pathway in C5aR1 KO and C5aR2 KO cells using inhibitors

To further implicate C5aR2 with the cGAS-STING pathway, BX795 and H-151 were used to inhibit TBK1 and STING, respectively. This experiment aimed to confirm that the C5aR2-dependent amplification of STING-induced IFN-β secretion was dependent on cGAS-STING pathway proteins TBK1 and STING.

PMA-differentiated WT, C5aR1 KO and C5aR2 KO THP-1 cells were pre-incubated with 100 nM or 1 μM BX795 or H-151 for 30 minutes, followed by 5 μg/mL cAIM(PS)$_2$ Difluor (Rp/Sp) for 6 hours. Supernatants were assessed for IFN-β by ELISA (**Figure 5.9**). Vehicle controls were included and had no effect on IFN-β secretion (**Supplementary Figure 5.1**).

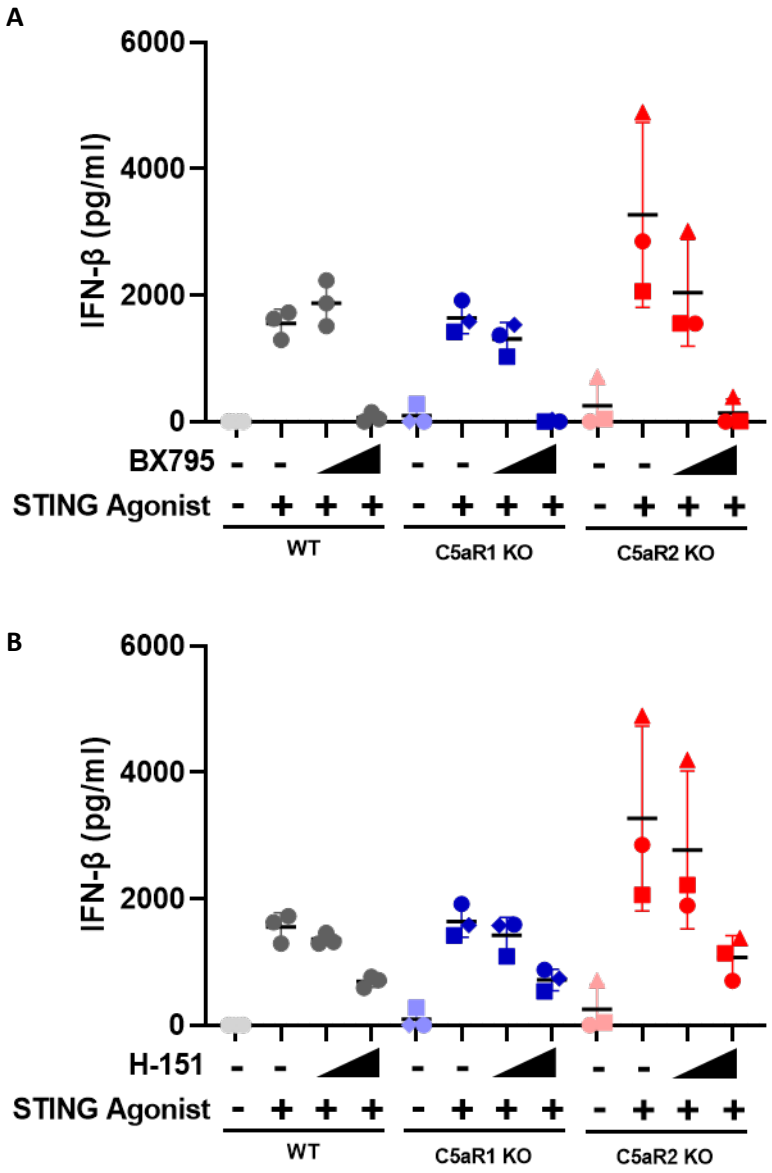

Figure 5.9. cGAS-STING pathway antagonism inhibits the response to cAIM(PS)$_2$ Difluor (Rp/Sp) in WT, C5aR1 and C5aR2 KO cells. WT, C5aR1 and C5aR2 KO cells were incubated with 100 nM or 1 µM **A.** TBK1 antagonist BX795 or **B.** STING antagonist H-151 for 30 minutes, followed by stimulation with 5 µg/mL STING agonist cAIM(PS)$_2$ Difluor (Rp/Sp) for 6 hours. Supernatants were harvested and assessed for IFN-β by ELISA. $OD_{450-570}$ values were interpolated with a standard curve and concentration (pg/mL) was calculated. Mean ± SD were plotted. N=3 WT replicates, N=4 C5aR1 KO (blue) clones (B6 - circle, C3 – square, F11 - triangle, G8 - diamond) and N=3 C5aR2 KO (red) clones (D3 - circle, F3 - square, F7 - triangle).

IFN-β secretion was suppressed by TBK1 antagonism and STING antagonism in WT, C5aR1 KO and C5aR2 KO cells (**Figure 5.9**). In WT cells, STING agonism induces IFN-β secretion, which is inhibited by BX795 in a concentration-dependent manner (**Figure 5.9 A**). This confirms the IFN-β secreted in response to cAIM(PS)$_2$ Difluor (Rp/Sp) is dependent on TBK1. This pattern is matched in C5aR1 KO cells. C5aR2 KO cells secrete more IFN-β than WT cells, which is also inhibited by BX795 in a concentration-dependent manner. This confirms that the amplified IFN-β response in the C5aR2 KO cells is also dependent on TBK1.

H-151 generates a similar response to BX795 (**Figure 5.9 B**). WT cells secrete IFN-β in response to STING agonism, which is inhibited in a concentration-dependent manner by H-151. This pattern is matched in the C5aR1 KO cells. C5aR2 KO cells secrete higher levels of IFN-β than WT cells, which is inhibited by H-151 in a concentration-dependent manner. This confirms that the IFN-β amplification in C5aR2 KO cells is dependent on STING.

The magnitude of IFN-β secretion in the C5aR2 KO relative to the WT is lower than in previous experiments, however the patterns observed are reproducible and C5aR2 KO still secretes more IFN-β in response to STING agonism when compared to WT cells.

Together, these data confirm that the effect of C5aR2 KO on IFN-β secretion in response to cAIM(PS)$_2$ Difluor (Rp/Sp) is dependent on STING and TBK1, further indicating that the cGAS-STING pathway-induced IFN-β secretion is regulated by C5aR2. To further elucidate the molecular mechanism of C5aR2-dependent IFN-β regulation, expression and phosphorylation of cGAS-STING pathway proteins STING and IRF3 was investigated.

5.2.3.5. Assessing the expression and phosphorylation of cGAS-STING pathway proteins by Peggy Sue

To identify potential interactors of C5aR2, this experiment aimed to assess whether expression and phosphorylation of key cGAS-STING pathway proteins IRF3 and STING was affected in the C5aR2 KO cells compared to the WT cells. PMA-differentiated WT, C5aR1 KO and C5aR2 KO cells were stimulated with cAIM$(PS)_2$ Difluor (Rp/Sp) for 6 hours, lysates were generated, and automated Western blotting system Peggy Sue was used to assess for IRF3 and STING expression and phosphorylation, using β-actin as a loading control (**Figure 5.10**).

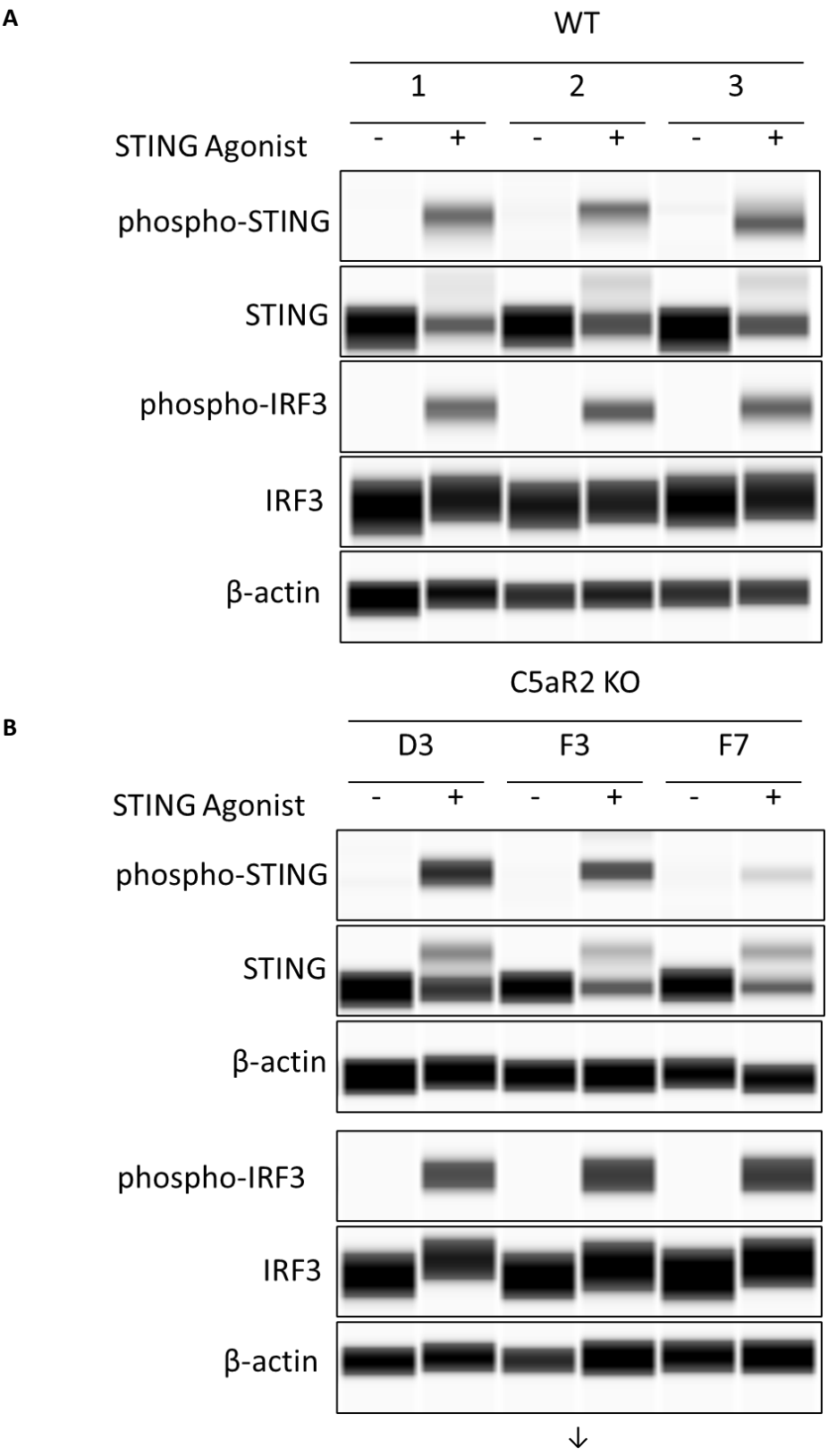
A
WT
1
2
3
STING Agonist
-
+
-
+
-
+
phospho-STING
STING
phospho-IRF3
IRF3
β-actin
C5aR2 KO
B
D3
F3
F7
STING Agonist
-
+
-
+
-
+
phospho-STING
STING
β-actin
phospho-IRF3
IRF3
β-actin

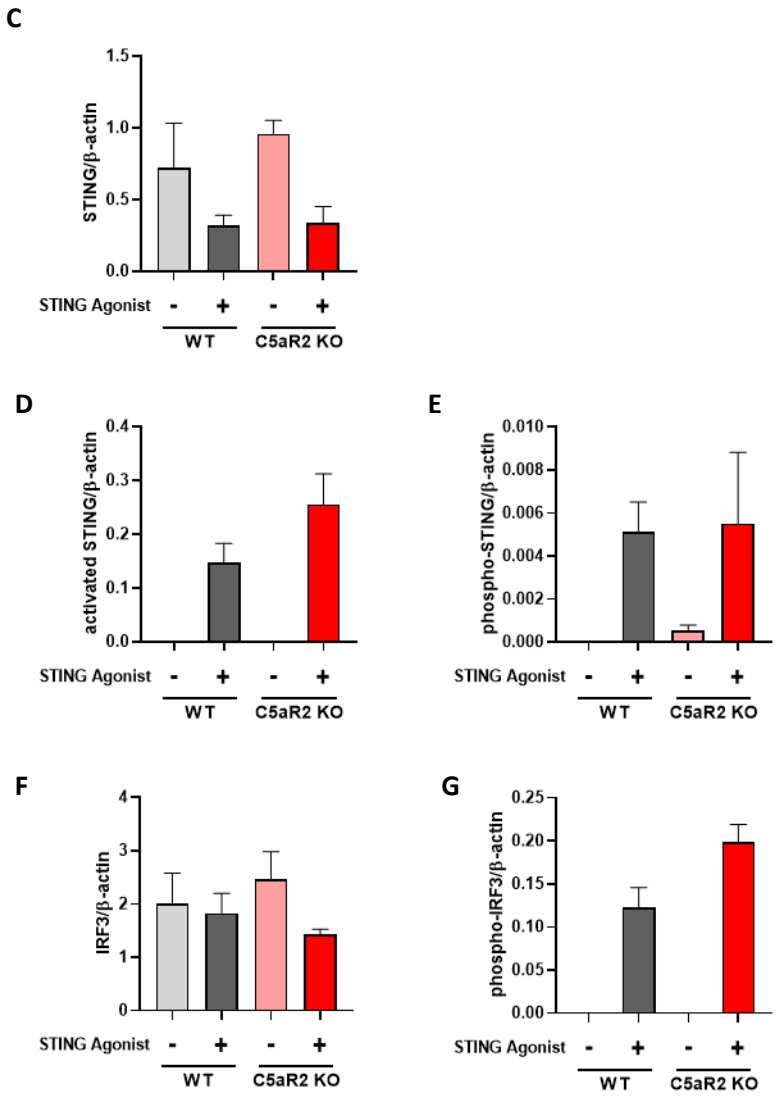

Figure 5.10. Expression and phosphorylation of cGAS-STING pathway proteins is amplified in C5aR2 KO cells. PMA-differentiated WT or C5aR2 KO cells were incubated with 5 µg/mL STING agonist cAIM(PS)$_2$ Difluor (Rp/Sp) for 6 hours. Lysates were generated and assessed using automated Western blotting system Peggy Sue for expression of STING and IRF3, and phosphorylation of STING (Ser386) and IRF3 (Ser366), with β-actin as a loading control. **A.** WT and **B.** C5aR2 KO data were represented as pseudo-blots. Area under the curve for **C.** STING, **D.** activated STING**, E.** phosphorylated STING**, F.** IRF3 and **G.** phosphorylated IRF3 was normalised to area under the loading control curve for WT (grey) and C5aR2 KO (red) and the mean ± SD were plotted; Kolmogrov-Smirnov normality tests and a Kruskal-Wallis tests were performed. ns: p>0.05. N=3.

In the C5aR2 KO clones, the expression and phosphorylation of STING and IRF3 is comparable to WT cells (**Figure 5.10 B**). STING is expressed highly in untreated cells, then reduced in treated cells, giving rise to an activated STING signal at a higher mw. STING phosphorylation is not present in unstimulated samples and is detected in stimulated samples. IRF3 expression is stable between conditions, and phospho-IRF3 signal is higher in agonised samples.

These data were quantified (**Figure 5.10 C-G**) by plotting the area under the curve generated by the chemiluminescent signal measured in the capillary, equivalent to densitometry in traditional Western blotting (**Supplementary Figure 5.2**).

There is a slight increase in mean total STING expression in C5aR2 KO cells compared to WT cells (**Figure 5.10 C**). There is also a higher mean level of activated STING in C5aR2 KO cells compared to WT cells (**Figure 5.10 D**). The mean phospho-STING signal is more variable due to the lower signal from clone F7 (**Figure 5.10 E**). Mean total IRF3 expression is also slightly higher in the C5aR2 KO cells, and more depleted upon stimulation (**Figure 5.10 F**), alongside a higher mean phospho-IRF3 signal in the C5aR2 KO compared to the WT cells (**Figure 5.10 G**).

This result suggests an up-regulation of cGAS-STING pathway proteins in the C5aR2 KO cells compared to the WT, suggesting that C5aR2 negatively regulates expression of these proteins in the WT. It is not clear whether there is more phosphorylation in the C5aR2 KO cells, or a larger pool of total protein leading to a similar proportion of phosphorylation following agonism. This is a semi-quantitative approach and there is no statistical significance, but the trends indicate an increase in expression. This suggests that C5aR2 may have a key role in regulating the expression and activation of the cGAS-STING pathway proteins, which could lead to an increased IFN-β response.

5.2.4. Assessing the effect of C5aR2 KO on STING agonism in primary human monocyte-derived macrophages

To confirm this result, a similar study was performed using primary human macrophages to increase physiological relevance and robustness of the observations made thus far. To test the hypothesis that C5aR2 regulates STING-induced IFN-β secretion in primary cells, CRISPR-Cas9 was used to generate C5aR2 KO and NTC MDMs. Cells were cultured, differentiated, electroporated and transfected by Lee Booty (GSK) and Anna Harris (GSK, University of Nottingham). These cells were then stimulated with 5 µg/mL cAIM(PS)$_2$ Difluor (Rp/Sp) for 6 hours, supernatants were harvested, and IFN-β was measured by ELISA.

5.2.4.1. Generating C5aR2 KO primary human MDMs using CRISPR-Cas9

Monocytes from 5 independent donors were thawed from frozen stocks and cultured for 6 days using 100 ng/mL M-CSF to differentiate them into monocyte-derived macrophages.

RNPs were assembled using sgRNA purchased from Synthego (**Table 2.5**). RNP complexes containing C5aR2 or NTC gRNA were delivered to MDMs via electroporation. Electroporated and transfected cells were transferred to 96-well flat-bottom cell culture plates and cultured for 3 or 10 days to ensure complete protein turnover.

5.2.4.2. Confirmation of C5aR2 KO by PCR and Sequencing

To confirm the presence of indels in the C5aR2 gene in the MDMs, PCR using C5aR2 Primer Pair 1 (**Table 2.6**) was performed. The amplification products were separated using gel electrophoresis and visualised using an E-gel (**Figure 5.11**).

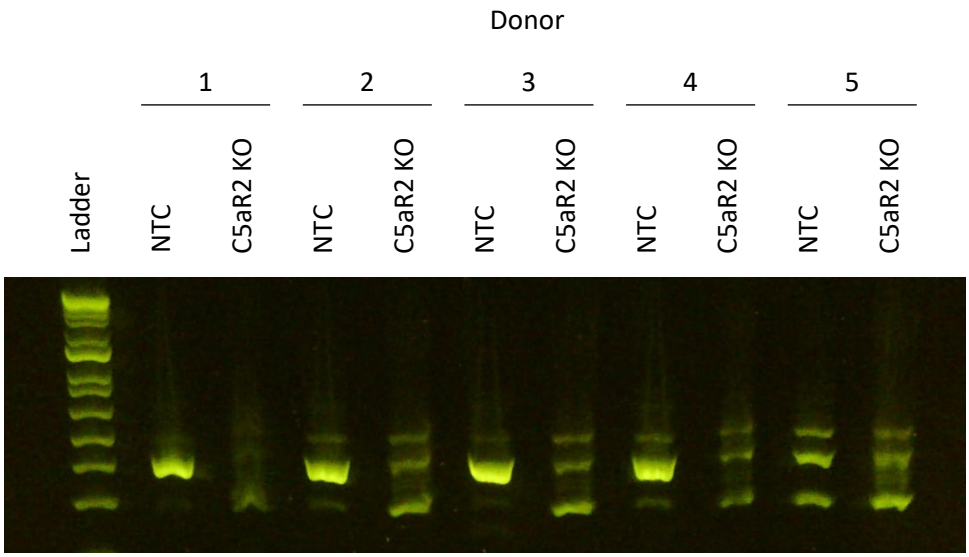

Figure 5.11. Confirmation of indels in C5aR2 PCR amplification product using nucleic acid gel electrophoresis. Image of E-gel containing PCR amplification product from NTC or C5aR2 KO MDM lysate using C5aR2 Primer Pair 1. Bands in all lanes confirm successful PCR, and loss of clear band in C5aR2 KO lanes confirm presence of indel in edited cells. N=5.

Bands were present in each lane, indicating successful PCR for each sample. There were clear bands in the NTC lysates, suggesting the presence of the target C5aR2 amplicon without disruption at the guide sites. This is less visible in Donor 5, however the middle band is the brightest, in line with the other 4 donors. The PCR amplification products from C5aR2 KO lysates had a wider range of sizes, suggesting that indels were present in the target amplicon and KOs had been generated successfully.

To confirm this, the PCR amplification products were then purified and sent for Sanger sequencing using C5aR2 Forward Primer 1 as the sequencing primer. Sequences were aligned using Synthego ICE (**Figure 5.12**).

A. Donor 1

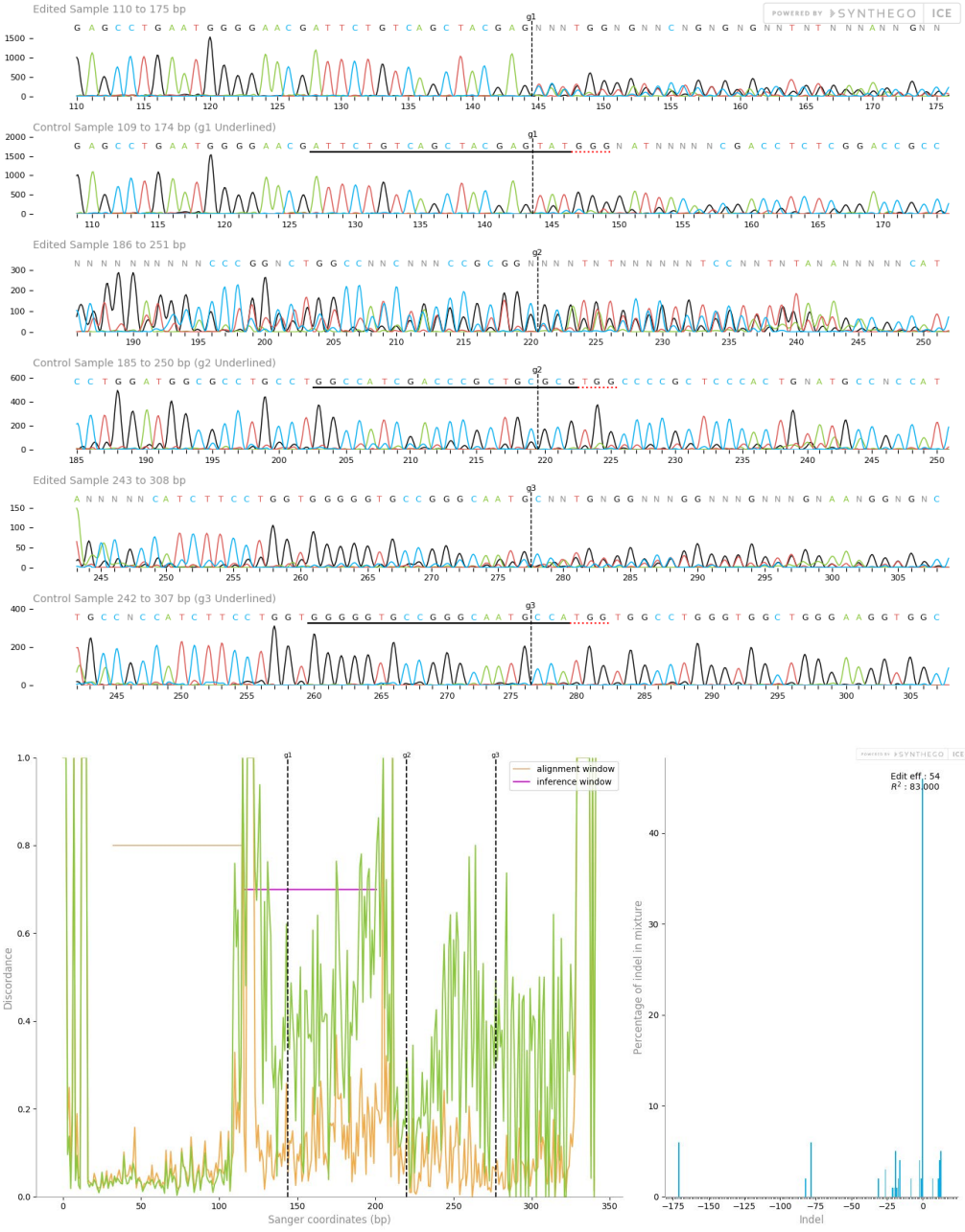
Edited Sample 110 to 175 bp
Control Sample 109 to 174 bp (g1 Underlined)
Edited Sample 186 to 251 bp
Control Sample 185 to 250 bp (g2 Underlined)
Edited Sample 243 to 308 bp
Control Sample 242 to 307 bp (g3 Underlined)
alignment window
inference window
Discordance
Sanger coordinates (bp)
Edit eff.: 54
R^2 : 83.000
Percentage of indel in mixture
Indel

B. Donor 2

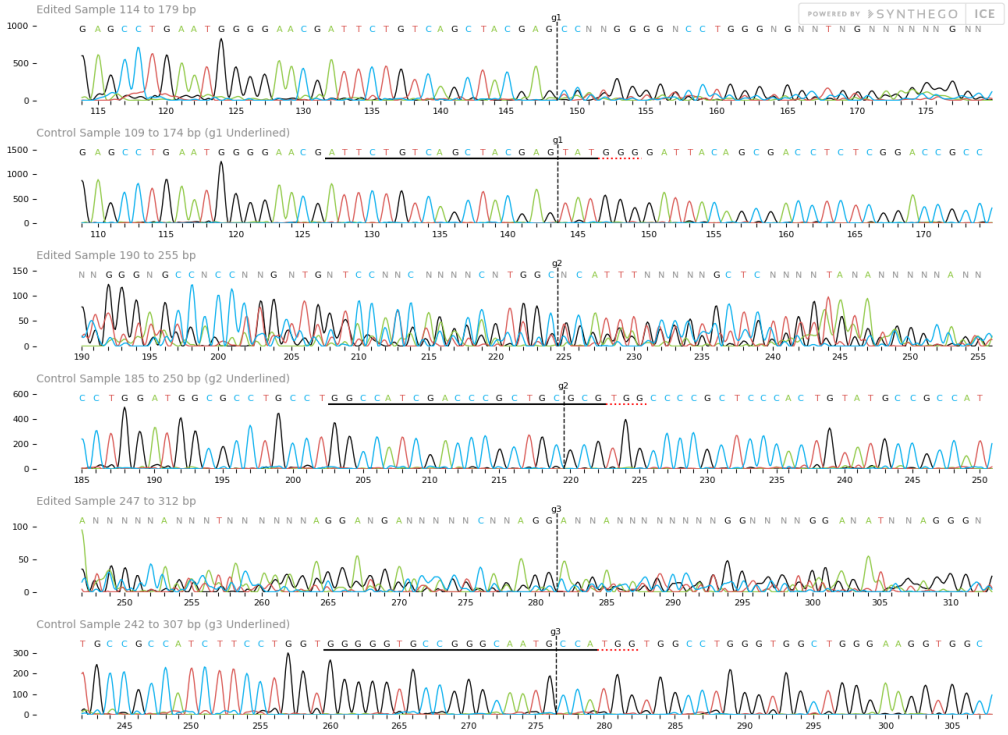
Edited Sample 114 to 179 bp
Control Sample 109 to 174 bp (g1 Underlined)
Edited Sample 190 to 255 bp
Control Sample 185 to 250 bp (g2 Underlined)
Edited Sample 247 to 312 bp
Control Sample 242 to 307 bp (g3 Underlined)

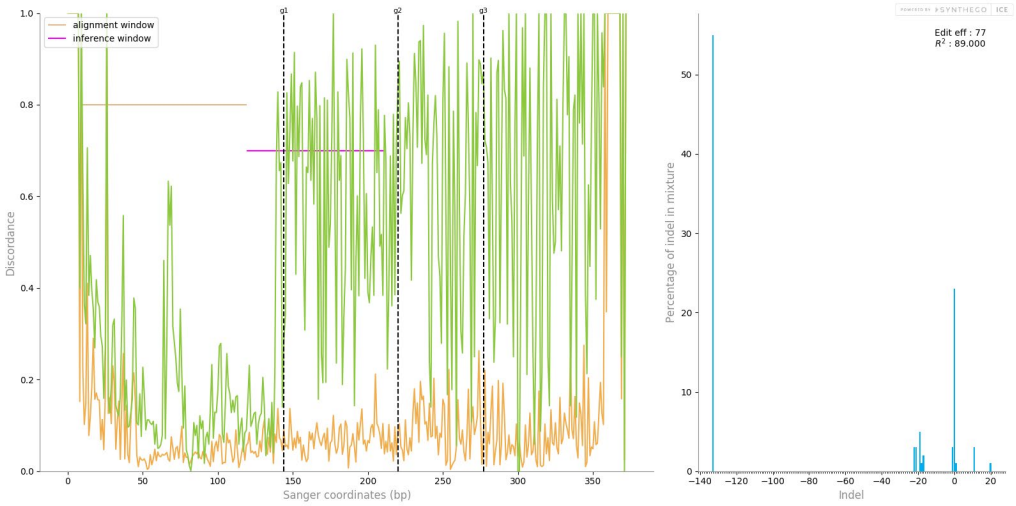
alignment window
inference window
Discordance
Sanger coordinates (bp)
Edit eff : 77
R^2 : 89.000
Percentage of indel in mixture
Indel

C. Donor 3

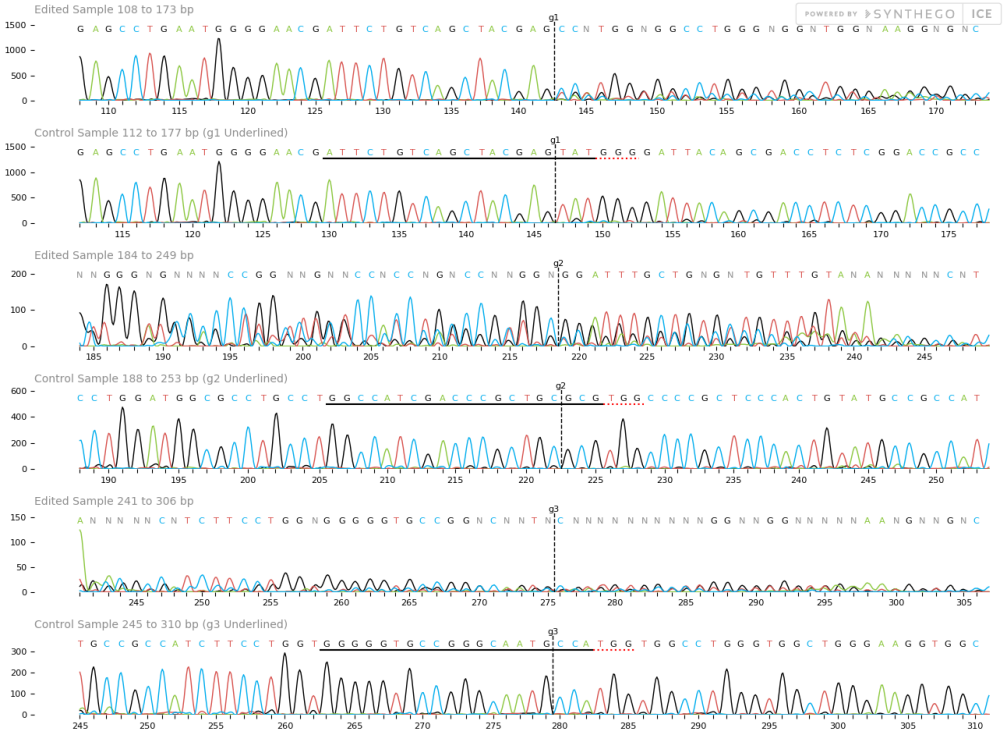
Edited Sample 108 to 173 bp
Control Sample 112 to 177 bp (g1 Underlined)
Edited Sample 184 to 249 bp
Control Sample 188 to 253 bp (g2 Underlined)
Edited Sample 241 to 306 bp
Control Sample 245 to 310 bp (g3 Underlined)

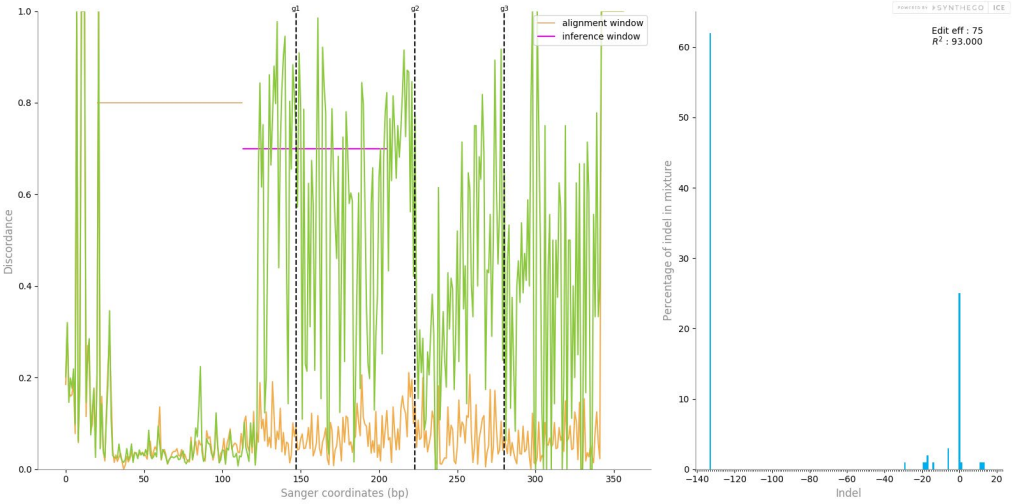
alignment window
inference window
Discordance
Sanger coordinates (bp)
Edit eff : 75
R^2 : 93.000
Percentage of indel in mixture
Indel

D. Donor 4

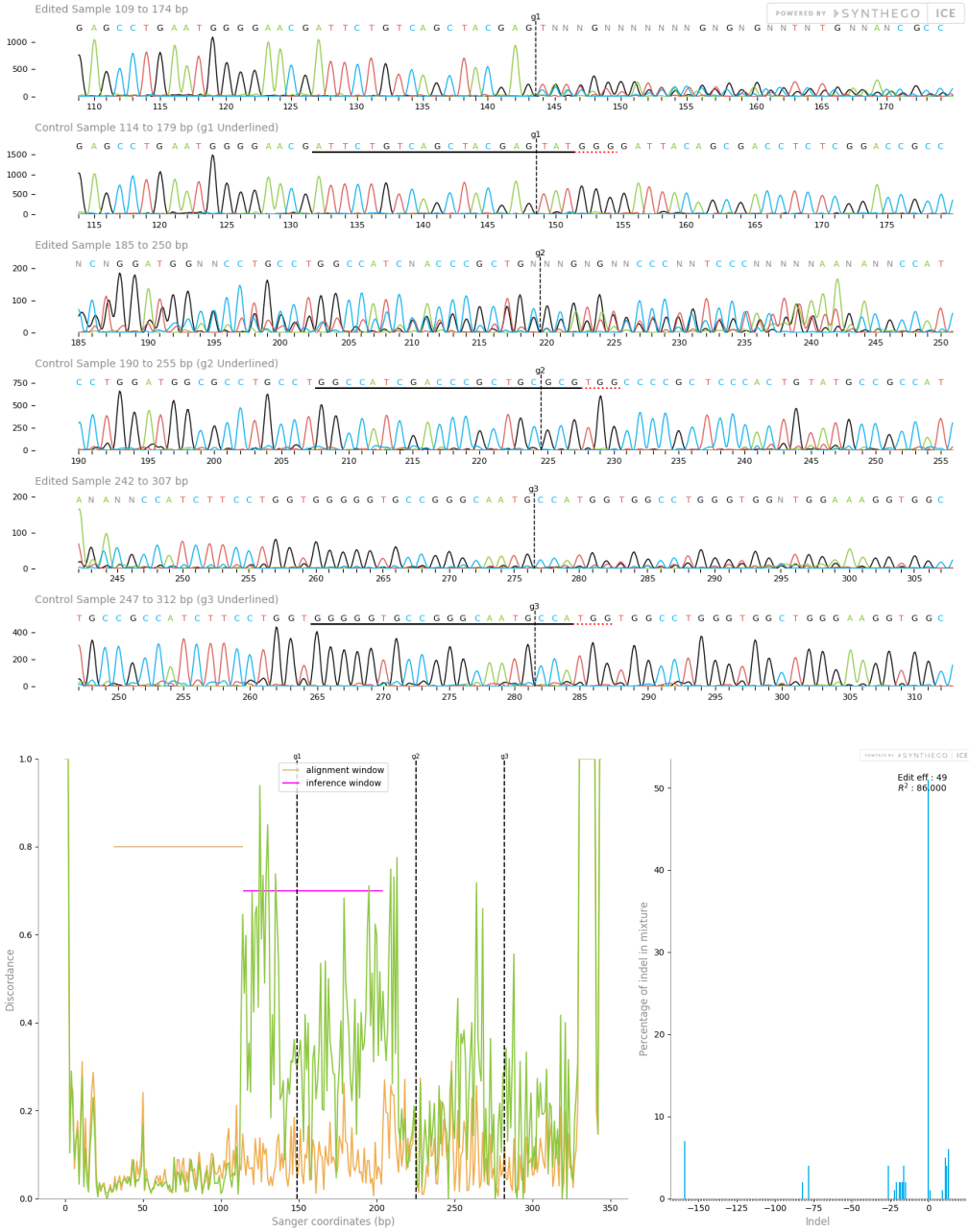
Edited Sample 109 to 174 bp
Control Sample 114 to 179 bp (g1 Underlined)
Edited Sample 185 to 250 bp
Control Sample 190 to 255 bp (g2 Underlined)
Edited Sample 242 to 307 bp
Control Sample 247 to 312 bp (g3 Underlined)
alignment window
inference window
Discordance
Sanger coordinates (bp)
Edit eff : 49
Percentage of indel in mixture
Indel

E. Donor 5

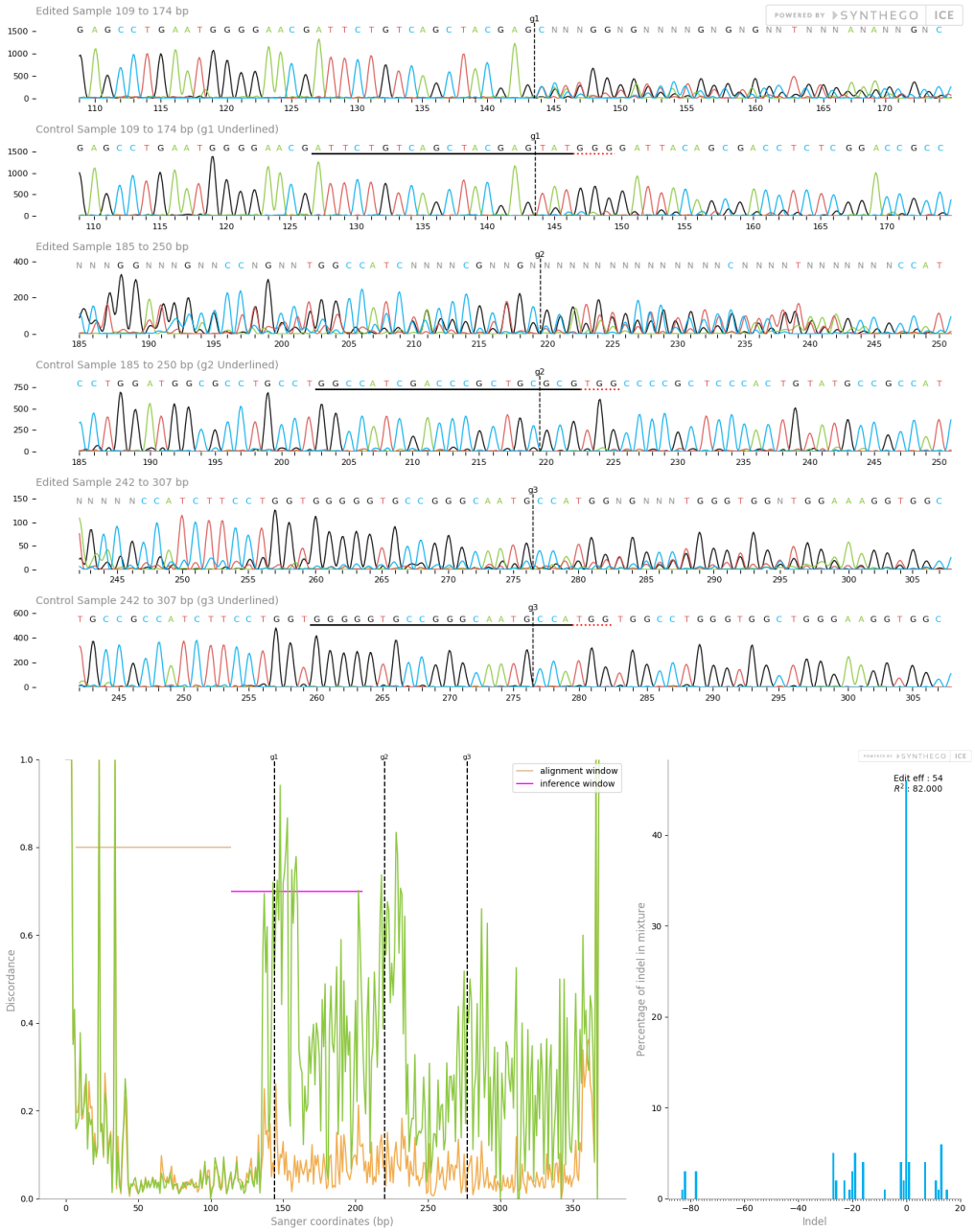

Figure 5.12. C5aR2 KO sequencing for primary human MDMs. PCR amplification products from **A.** Donor 1, **B.** Donor 2, **C.** Donor 3, **D.** Donor 4, and **E.** Donor 5 were sent for sequencing with C5aR2 Forward Primer 1, and C5aR2 KO sequences were aligned to the NTC sequence using Synthego ICE.

There were indels present in C5aR2 sequences from each donor, as demonstrated by the loss of sequence following the guide sites in the Trace plots, the misalignment between NTC sequence (orange) and C5aR2 KO sequence (green) in the Discordance plots, and the presence of indels of various sizes with various % contributions in the Indel plots. These were polyclonal populations of C5aR2 KO primary human MDMs, summarised in **Table 5.1**.

Donor	Indel %	Model Fit
1	54	83
2	77	89
3	75	93
4	49	86
5	54	82

Table 5.1. Summary of C5aR2 forward primer sequencing data from primary human MDMs. % contribution of indels to the population of sequences in each PCR amplification product, and a measure of model fit (range 0-1) was generated by Synthego ICE and summarised in this table for all C5aR2 KO sequences generated using primary human MDMs.

Monoclone generation was not possible as the cells were terminally differentiated. Degradation of existing C5aR2 was expected after 3 days [119], so the cells were cultured for 3 or 10 days following electroporation and RNP transfection to allow for protein turnover. An incubation period of 3 days was selected to minimise the risk of senescence and of loss of viability in culture, and a period of 10 days was selected to ensure complete protein turnover in case it had not been achieved at Day 3. These cells were then used in STING agonism experiments.

5.2.4.3. STING agonism of C5aR2 KO primary human MDMS

This experiment aimed to agonise STING in NTC or C5aR2 KO MDMs and assess levels of IFN-β secretion. After 3 or 10 days post CRISPR-Cas9 editing, NTC or C5aR2 KO

primary human MDMs were stimulated with 5 µg/mL cAIM(PS)$_2$ Difluor (Rp/Sp) for 6 hours, and supernatants were assessed for IFN-β by ELISA.

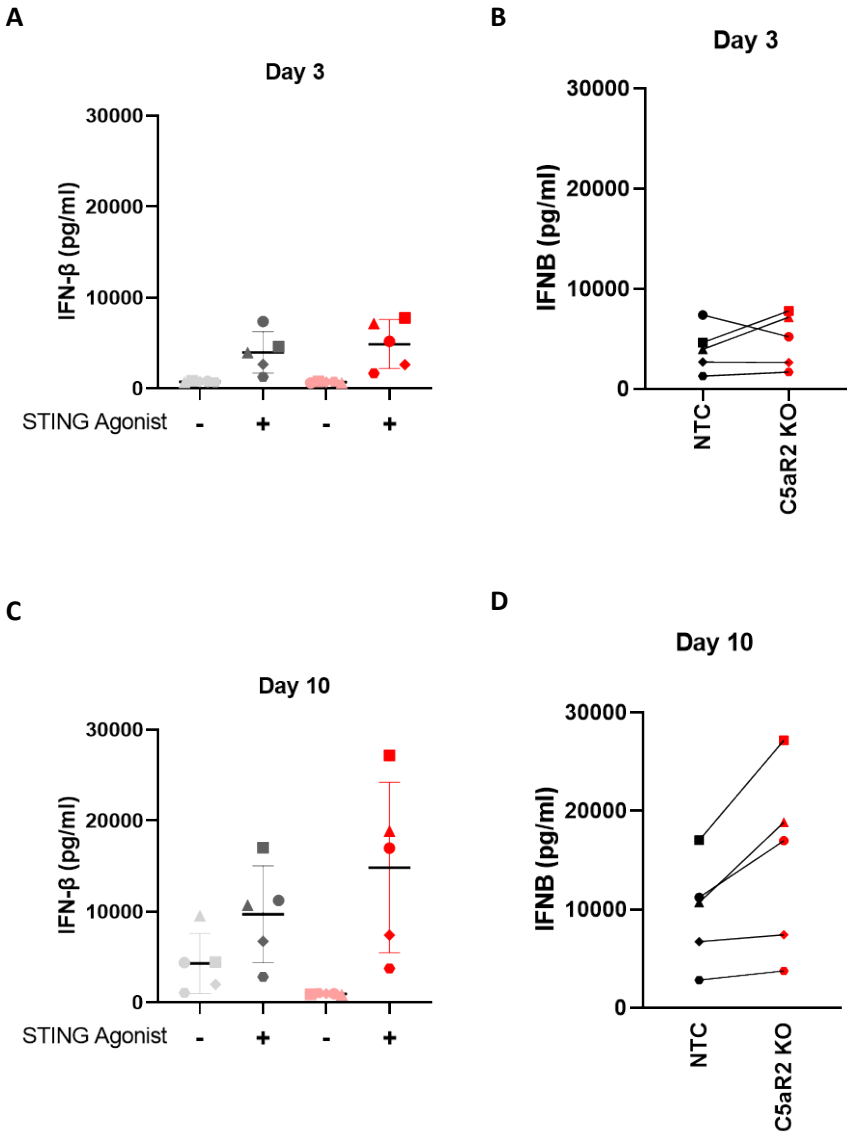

Figure 5.13. C5aR2 KO increases cGAS-STING pathway-induced IFN-β secretion in primary human MDMs at day 10 post-CRISPR-Cas9 editing. NTC (grey) and C5aR2 KO (red) primary human M-CSF-differentiated monocyte-derived macrophages were cultured for **A-B.** 3 days or **C-D** 10 days to allow for protein turnover, and then were stimulated with 5 µg/mL STING agonist cAIM(PS)$_2$ Difluor (Rp/Sp) for 6 hours. Supernatants were assessed for IFN-β by ELISA. $OD_{450-570}$ values were interpolated with a standard curve and concentration (pg/mL) was calculated. **A, C.** Mean ± SD were plotted, and **B, D.** data from individual donors was represented as a before-after plot. Paired Student's t test, ns: p>0.05. N=5: Donor 1 (circle), Donor 2 (square), Donor 3 (triangle), Donor 4 (diamond), and Donor 5 (hexagon).

STING agonism induced IFN-β secretion in WT cells and C5aR2 KO cells (**Figure 5.13**). After 3 days, there was no significant increase in IFN-β secretion in C5aR2 KO cells (**Figure 5.13 A**). IFN-β secreted by Donors 2 (square) and 3 (triangle) increased slightly, but decreased in Donor 1 (circle) (**Figure 5.13 B**). Donors 4 and 5 failed to respond to agonism.

After ten days, there was an increase in IFN-β secretion in C5aR2 KO cells compared to NTC (**Figure 5.13 C**). There was a much higher level of IFN-β secretion in responding donors (1, 2, 3) compared to Day 3. IFN-β secreted by Donors 2 and 3 increased as in Day 3, and also increased in Donor 1 (**Figure 5.13 D**). Donors 4 and 5 failed to respond to treatment, despite the higher background level of IFN-β.

There was a strong trend towards a C5aR2 KO-dependent amplification of IFN-β secretion, however the difference was not statistically significant compared to NTC cells. The data were therefore analysed further to test whether statistical significance could be achieved by excluding the donors which did not respond to STING agonism in the NTC population (**Figure 5.14**).

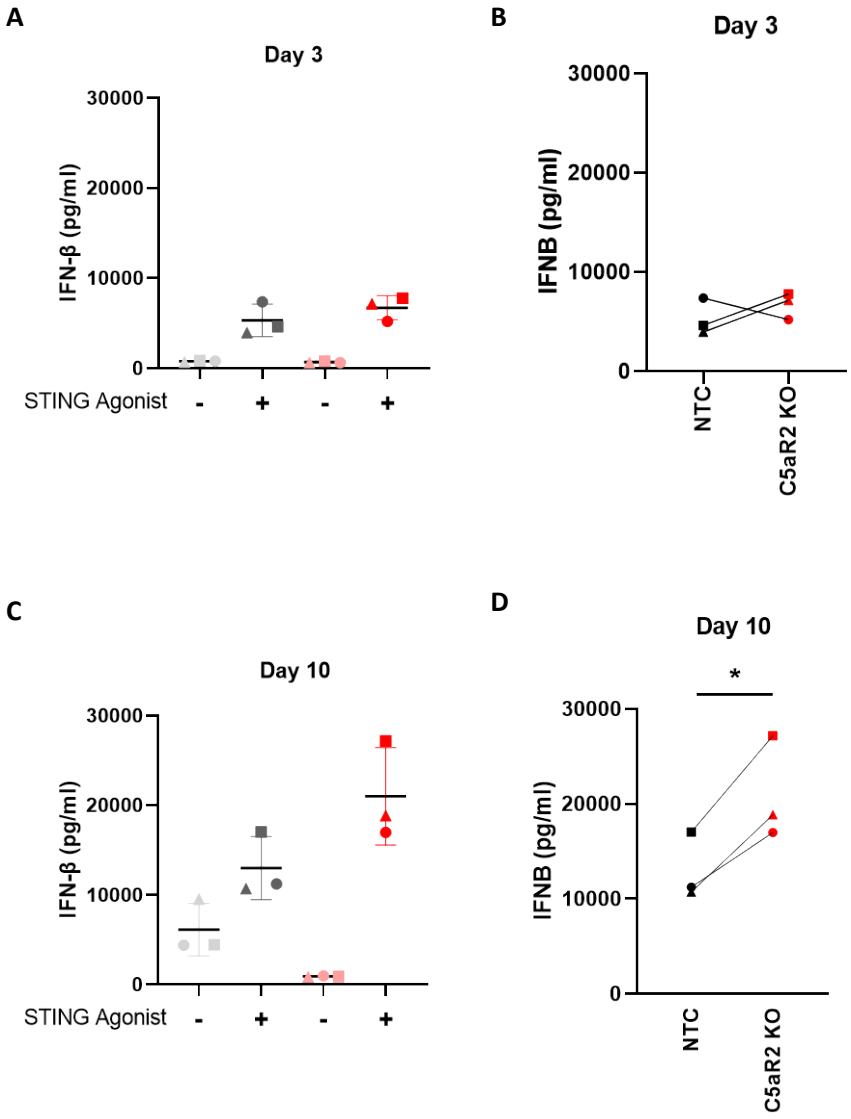

Figure 5.14. Excluding unresponsive donors reveals a significant increase of cGAS-STING pathway-induced IFN-β secretion in C5aR2 KO primary human MDMs. NTC (grey) and C5aR2 KO (red) primary human M-CSF-differentiated monocyte-derived macrophages were cultured for **A-B.** 3 days or **C-D** 10 days to allow for protein turnover, and then were stimulated with 5 µg/mL STING agonist cAIM(PS)$_2$ Difluor (Rp/Sp) for 6 hours. Supernatants were assessed for IFN-β by ELISA. $OD_{450-570}$ values were interpolated with a standard curve and concentration (pg/mL) was calculated. Non-responding donors were excluded from analysis. **A, C.** Mean ± SD were plotted, and **B, D.** data from individual donors was represented as a before-after plot. Paired Student's t test, ns: $p>0.05$, *: $p\leq0.05$. N=3: Donor 1 (circle), Donor 2 (square), Donor 3 (triangle).

The pattern in the results was conserved following analysis of the data from the responding donors. After 3 days, cAIM(PS)$_2$ Difluor (Rp/Sp) induces IFN-β secretion in WT cells, and the response of C5aR2 KO cells is not significantly different (paired Student's t test; ns) (**Figure 5.14 A**). There is a trend towards a C5aR2-dependent increase in data from Donors 2 and 3, but Donor 1 trends downwards following C5aR2 KO (**Figure 5.14 B**). After 10 days, and assumed turnover of all residual C5aR2 protein, there is a clear amplification of IFN-β secretion in C5aR2 KO cells compared to NTC cells (**Figure 5.14 C**). C5aR2 KO primary human MDMs secrete significantly more IFN-β in response to cAIM(PS)$_2$ Difluor (Rp/Sp) stimulation compared to NTC cells (paired Student's t test, p=0.0243) (**Figure 5.14 D**). C5aR2 KO in primary human MDMs causes a significant increase in STING-induced IFN-β secretion, confirming observations made using THP-1 cells in a more physiologically relevant cell type.

5.3. Discussion

5.3.1. Summary

This series of experiments aimed to use the novel C5aR1 KO and C5aR2 KO THP-1 cell lines to investigate the effect of C5aR2 KO on PRR-induced cytokine secretion. A panel of PRR ligands was used to assess the modulation of PRR-induced cytokine secretion by C5aR2 KO. The cGAS-STING pathway was then investigated, characterising the novel link between C5aR2 and STING.

The PRR ligand panel experiment identified a wide range of C5a-independent (**Figure 5.2**) and C5a-dependent (**Figure 5.3**) effects of C5aR1 KO and C5aR2 KO on NF-κB-dependent cytokine secretion. C5a-dependent modulation of cytokine secretion mediated by C5aR1 has been previously observed [72], however the C5a-independent effects suggest that regulation may also occur at baseline through a constitutive mechanism independently of exogenous ligand, or via an unknown ligand which is separate from canonical anaphylatoxin receptor activation by C5a. C5a may also be generated intracellularly via the complosome [48,49] to drive tonic anaphylatoxin receptor activation in the absence of extracellular C5a. This could be assessed by repeating this experiment with a C5 knockdown to assess whether the putative C5a-independent effect is reversed by preventing the formation of intracellular C5a.

Various potential C5aR2-dependent effects warrant further investigation, including the suppression of TLR1/2/4-induced IL-6 secretion and the suppression of TLR4-induced TNFα secretion, however the project focussed predominantly on the up-regulation of STING-dependent IL-6 secretion in C5aR2 KO THP-1 cells. This had been observed in a previously published study, where P32 and P59 significantly suppressed STING-induced IL-6 secretion [8]. Subsequent experiments revealed the key observation of this study, which was the link between C5aR2 and the cGAS-STING pathway (**Figure 5.4-5.14**). IFN-β secretion was significantly up-regulated in the C5aR2 KO cells. This was

the most robust and most significant result generated in the PRR panel experiment and was consistently reproducible across subsequent experiments.

C5aR2 KO significantly up-regulated cGAS/STING-induced IFN-β secretion in THP-1 cells, and use of antagonists of STING and TBK1 demonstrated that this is a STING-dependent and TBK1-dependent effect. Kinetics of the IFN-β response to STING agonism revealed that the baseline IFN-β secretion is not increased by C5aR2 KO, but the response to cGAS/STING agonism is. This suggests that rather than a systemic increase in the inflammatory response as baseline, the C5aR2 KO cells may be primed to respond to cGAS-STING agonism more than the WT cells upon stimulation. Assessing expression and phosphorylation of STING and IRF3 revealed an increased expression of these key cGAS-STING pathway proteins at baseline in the C5aR2 KO cells. Taken together, this could suggest that C5aR2 KO results in cells that are primed to respond to cGAS-STING pathway activation by a higher level of expression of the proteins in the pathway.

Finally, this result was replicated using primary human MDMs. The NTC condition included in the primary human MDM study confirms that the IFN-β phenotype is not an off-target effect of CRISPR-Cas9 editing, indicating that the result generated using THP-1 cells is also valid. The reproducibility of the cell line phenotype in primary human MDMs also increases the physiological relevance of these results. These data reproduce and develop previously unconfirmed observations from the literature and characterise the link between C5aR2, IFN-β and the cGAS-STING signalling pathway.

5.3.2. Study Limitations

5.3.2.1. cGAMP ELISA

To complement the agonist/antagonist experiments, a study investigating cGAMP levels in WT and C5aR2 KO cells was performed. WT, C5aR1 KO and C5aR2 KO THP-1 cells were stimulated with cGAS agonist G3-YSD, and cGAMP expression in lysates was

measured by ELISA. cGAS agonism was predicted to stimulate cGAMP synthesis, as it is the second messenger responsible for cGAS-induced STING activation [11]. If C5aR2 KO cells had altered levels of cGAMP synthesis, it would indicate a potential regulatory interaction between C5aR2 or its unknown downstream signalling targets and the cGAS-STING pathway. However, the cGAMP ELISA was prohibitively insensitive, meaning that all measured cGAMP concentrations were below or near the lower limit of detection and were highly sensitive to noise in the assay. The data could not be interpreted and so were not included. A future experiment using highly concentrated lysates may be able to address this issue and test the hypothesis, however time constraints and promising data describing C5aR2 KO-dependent changes in STING and TBK1 expression generated by Peggy Sue led to de-prioritisation of this hypothesis.

5.3.2.2. Peggy Sue

NF-κB, phospho-NF-κB, TBK1 and phospho-TBK1 were assessed as additional endpoints during the Peggy Sue experiment. Various commercially available antibodies were tested in a screen on WT THP-1 lysate at various concentrations with various lysis buffers, but no robust detection of pNF-κB or pTBK1 was achieved. Capillary Western blotting using the Peggy Sue is an extremely powerful tool for protein detection, and it would be well-suited for further optimisation of these endpoints or confirmation of hits from future multi-omics experiments. However, following the detection of increased expression of STING and IRF3 in C5aR2 KO cells, due to the availability of wider-reaching experimental approaches such as RNAseq, and due to time constraints, additional work using this approach was deprioritised.

5.3.2.3. Confirmation of C5aR2 KO in primary human MDMs

A limited number of cells was available for the primary human MDM experiment. Confirmation of loss of C5aR2 expression by flow cytometry was likely to be impossible due to the challenge of detaching macrophages from culture plates without negatively

impacting cell viability. C5aR2 detection by Western blot was not achieved, either due to loss of epitope from disruption of tertiary structure during lysis and membrane loss, or lack of functioning primary antibodies. However, the sequencing data confirmed the presence of indels in the target site of C5aR2, and the amplification of IFN-β in C5aR2 KO cells after 10 days matches the phenotype of the C5aR2 KO THP-1 cells. Confirming C5aR2 KO in these cells by Western blot or flow cytometry would be a useful control, however is not required to draw the conclusion that the effects observed in primary MDMs were due to C5aR2 KO.

5.3.2.4. Reproducibility between multiple C5aR1 KO clones

In the initial PRR panel experiment, C5aR1 KO clone C3 was used in isolation. This initial study showed a significant C5aR1-dependent amplification of STING-induced IFN-β. Later studies were made more robust through the introduction of additional KO clones. As a result, the C5aR2 KO observation became more robust, whereas C5aR1 KO did not regulate IFN-β secretion downstream of cGAS-STING agonism. The initial C5aR1 KO clone C3 was a high responder across many experiments, however the use of multiple clones allowed the mean values to reflect a more accurate phenotype where C5aR1 KO did not significantly up-regulate the response to STING agonism. Off-target CRISPR-Cas9 effects, or effects of inflammation or epigenetic changes in cell line cultures active for long periods of time can contribute to outlying effects in experiments, as seen in C3 in the response to STING agonism. Observations made in C5aR2 KO cells were robust and reproducible, and there were no similar clone-dependent effects.

5.3.3. Future work

The mechanism of this regulation is unknown and has not been studied previously. β-arrestin 2 has been shown to interact with the cGAS-STING pathway [120] and with C5aR2 [75], suggesting a potential regulatory mechanism. C5aR2 may also signal via an unknown

intermediate protein to the cGAS-STING pathway, interact with upstream regulators of the cGAS-STING pathway to modulate protein expression, or alternatively interact directly with cGAS-STING pathway proteins to disrupt their function. As this modulatory interaction has not been explored previously, the use of multi-omic approaches would be appropriate to investigate the mechanism driving the C5aR2 KO effect on cGAS/STING-induced IFN-β secretion. Experiments utilising transcriptomics, proteomics, phosphoproteomics and interactomics were proposed to generate a broad understanding of the phenotype and inflammatory status of these cells in the context of STING agonism, and to search for potential upstream regulators of cGAS-STING pathway protein expression. Protein detection of C5aR2 was extremely challenging due to lack of availability of highly-specific antibodies able to detect C5aR2 in lysates. RNAseq was therefore selected to generate a dataset describing C5aR1/2 KO cells at baseline compared to WT cells, and assess the effect of C5a agonism or STING agonism on the cells.

Chapter 6 - Results 4

Characterising the transcriptomic effect of C5aR2 KO on the response to STING agonism

6. Characterising the transcriptomic effect of C5aR2 KO on the response to STING agonism

6.1. Introduction

The C5aR2 KO cells (**Chapter 4**) were used successfully to identify novel links between C5aR2 and the cGAS-STING pathway (**Chapter 5**). cGAS/STING-induced IFN-β secretion was significantly higher in C5aR2 KO cells, and expression of cGAS-STING proteins STING and IRF3 was increased in C5aR2 KO THP-1 cells compared to WT THP-1 cells. The mechanism of this modulation may involve C5aR2-dependent negative regulation of upstream proteins, which is lost in the C5aR2 KO.

A multi-omic approach was proposed to investigate potential mechanisms of C5aR2-dependent PRR regulation. Detection of C5aR2 protein was not achieved using Western blotting, therefore proteomics and interactomics were not investigated further. RNAseq was selected as an approach to assess the global transcriptome of the THP-1 cells in the presence or absence of C5aR2. The primary aim of this experiment was to generate a dataset describing the transcriptome of the cells in the context of STING agonism to identify significantly regulated transcripts which could account for the regulation of pro-inflammatory pathways such as the cGAS-STING pathway.

The fundamental signalling underlying the function of C5aR2 has never been studied in detail, therefore this experiment also aimed to describe the response to C5a in WT cells and contrast it to the response in C5aR2 KO cells to identify novel downstream targets of C5aR2. This could provide novel fundamental mechanistic information for C5aR2 signalling, which will contribute heavily to the understanding of its role as an immune receptor. C5aR2 has a range of implications in models of disease [121], and the cGAS-STING pathway is currently being targeted in various clinical trials [9]. Investigating the molecular mechanism of the regulation of STING-induced IFN-β by C5aR2 may therefore lead to the generation of clinically relevant data.

6.2. Results

6.2.1. Sample Generation for RNAseq

RNAseq was used to assess the global transcriptome of Untreated, C5a-treated or STING agonist-treated C5aR1/2 KO THP-1 cells vs WT THP-1 cells. This experiment primarily aimed to investigate the molecular mechanism of controlling the up-regulation of cGAS-STING pathway protein expression and IFN-β secretion in C5aR2 KO cells, and secondarily to investigate the effect of C5aR2 KO at baseline in untreated cells, and to elucidate novel functions of C5aR2 when ligated with its putative natural ligand C5a. This approach aimed to address the following hypotheses:

- C5aR1 KO and C5aR2 KO change the transcriptome of THP-1 cells at baseline
- C5aR1 KO and C5aR2 KO change the transcriptomic response of THP-1 cells to C5a
- C5aR1 KO and C5aR2 KO change the transcriptomic response of THP-1 cells to STING agonist cAIM(PS)$_2$ Difluor (Rp/Sp)

Investigating these comparisons in an unbiased manner at a global transcriptome level aimed to identify relevant differentially expressed genes, which may be useful for elucidating the mechanism for C5aR2 KO-dependent IFN-β amplification.

To generate samples for the RNAseq experiment, PMA-differentiated WT, C5aR1 and C5aR2 KO THP-1 cells were stimulated with culture medium, 50 ng/mL C5a or 5 µg/mL STING agonist cAIM(PS)$_2$ Difluor (Rp/Sp) for 6 hours. Supernatants were harvested and assessed for IFN-β by ELISA to confirm that the cells had behaved in line with previous experiments (**Figure 6.1**), where STING-induced IFN-β secretion was amplified in C5aR2 KO cells, as established in **Chapter 5**.

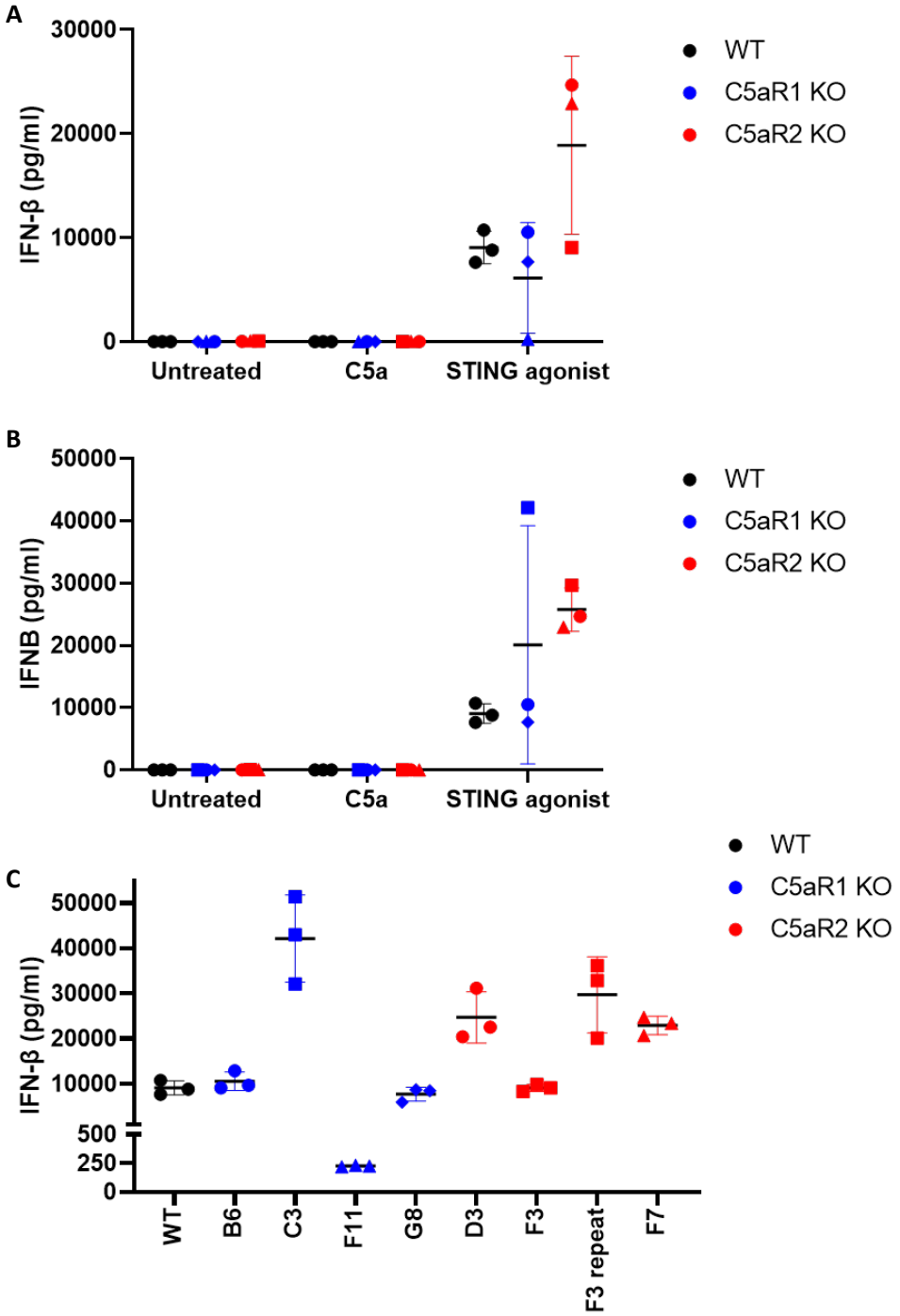

Figure 6.1. IFN-β ELISA for QC of RNAseq samples. PMA-differentiated WT, C5aR1 KO (clone B6 (circle), C3 (square), F11 (triangle), G8 (diamond)) and C5aR2 KO (clone D3 (circle), F3 (square), F7 (triangle)) THP-1 cells were incubated for 6 hours with culture medium, 50 ng/mL C5a or 5 µg/mL STING agonist cAIM(PS)$_2$ Difluor (Rp/Sp). Supernatants were harvested and assessed for IFN-β by ELISA. $OD_{450-570}$ values were interpolated with a standard curve and concentration (pg/mL) was calculated. Mean ± SD were plotted; N=3 WT replicates, N=4 C5aR1 KO clones (B6, C3, F11, G8) and N=3 C5aR2 KO clones (D3, F3, F7). **A.** C5aR1 KO clones B6, F11 and G8 were used on Experiment Day 1. **B.** C5aR1 KO clone C3 and C5aR2 KO clone F3 "repeat" were used on Experiment Day 2, and data were plotted with data from Experiment Day 1 excluding F11 and F3. **C.** Data from STING agonist-treated cells of each clone from both Experiment Days were plotted together.

In the initial experiment from Experiment Day 1 (**Figure 6.1 A**), the mean data reflected the previous results from **Chapter 5**. No IFN-β was secreted by Untreated or C5a-treated cells, whereas STING agonist-treated cells secreted IFN-β. WT and C5aR1 KO cell responses were comparable, and the response in C5aR2 KO cells was amplified. However, the clones were not behaving consistently within KO groups. C5aR1 KO clone F11 (blue triangle) did not respond to treatment, and C5aR2 KO clone F3 (red square) secreted less IFN-β than the other two C5aR2 KO clones. This particular culture of C5aR1 KO F11 THP-1 cells was discarded from culture and replaced with a fresh aliquot as it failed to respond in additional experiments performed during the same period.

Samples of responding cells were required for RNAseq. A repeat experiment was therefore performed using replacement C5aR1 KO clone C3 and a direct repeat of C5aR2 KO clone F3. The data generated on Experiment Day 2 using C5aR1 KO clone C3 (blue square) and C5aR2 KO clone F3 (red square) were plotted alongside data from Experiment Day 1, excluding the non-responding F11 data and the low-responding F3 data (**Figure 6.1 B**). The C5aR2 KO clones were now behaving consistently, and the response of clone F3 was no longer a concern. C5aR1 KO clone C3 did respond to treatment, improving on the result from clone F11, however it secreted a higher concentration of IFN-β than the other C5aR1 KO clones B6 and G8.

The data from both Experiment Days were plotted together (**Figure 6.1 C**), demonstrating that C3 generated a much higher level of IFN-β than the other two responsive C5aR1 KO clones B6 and G8 and the C5aR2 KO cells. This was not optimal, but was not unprecedented, as C3 had previously responded highly to STING agonism (C3 was used in isolation in **Figure 5.4** compared to all 4 C5aR1 KO clones in **Figure 5.6**). This result indicates that this cell line has a clone-specific phenotype which affects the relevant endpoint for this study. However, a third experiment day with a fresh aliquot of F11 would also introduce more variability, therefore, despite the high response of C5aR1 KO clone C3, the cells were included with the samples sent for RNAseq.

Following supernatant harvest, cells were lifted from culture using neat TrypLE, centrifuged and frozen as pellets. The following samples were sent to GENEWIZ for RNAseq (**Table 6.1**):

Sample #	Day	Treatment Time (hours)	Cell Line	Clone	Treatment	Treatment Replicate
1	1	0	WT	WT	Untreated	1
2	1	0	WT	WT	Untreated	2
3	1	0	WT	WT	Untreated	3
4	1	6	WT	WT	Untreated	1
5	1	6	WT	WT	Untreated	2
6	1	6	WT	WT	Untreated	3
7	1	6	C5aR1 KO	B6	Untreated	1
8	1	6	C5aR1 KO	B6	Untreated	2
9	1	6	C5aR1 KO	B6	Untreated	3
10	2	6	C5aR1 KO	C3	Untreated	1
11	2	6	C5aR1 KO	C3	Untreated	2
12	2	6	C5aR1 KO	C3	Untreated	3
13	1	6	C5aR1 KO	G8	Untreated	1
14	1	6	C5aR1 KO	G8	Untreated	2
15	1	6	C5aR1 KO	G8	Untreated	3
16	1	6	C5aR2 KO	D3	Untreated	1
17	1	6	C5aR2 KO	D3	Untreated	2
18	1	6	C5aR2 KO	D3	Untreated	3
19	2	6	C5aR2 KO	F3	Untreated	1
20	2	6	C5aR2 KO	F3	Untreated	2
21	2	6	C5aR2 KO	F3	Untreated	3
22	1	6	C5aR2 KO	F7	Untreated	1
23	1	6	C5aR2 KO	F7	Untreated	2
24	1	6	C5aR2 KO	F7	Untreated	3
25	1	6	WT	WT	C5a	1
26	1	6	WT	WT	C5a	2
27	1	6	WT	WT	C5a	3
28	1	6	C5aR1 KO	B6	C5a	1
29	1	6	C5aR1 KO	B6	C5a	2
30	1	6	C5aR1 KO	B6	C5a	3
31	2	6	C5aR1 KO	C3	C5a	1
32	2	6	C5aR1 KO	C3	C5a	2
33	2	6	C5aR1 KO	C3	C5a	3
34	1	6	C5aR1 KO	G8	C5a	1
35	1	6	C5aR1 KO	G8	C5a	2
36	1	6	C5aR1 KO	G8	C5a	3
37	1	6	C5aR2 KO	D3	C5a	1
38	1	6	C5aR2 KO	D3	C5a	2
39	1	6	C5aR2 KO	D3	C5a	3
40	2	6	C5aR2 KO	F3	C5a	1
41	2	6	C5aR2 KO	F3	C5a	2
42	2	6	C5aR2 KO	F3	C5a	3
43	1	6	C5aR2 KO	F7	C5a	1
44	1	6	C5aR2 KO	F7	C5a	2

↓

45	1	6	C5aR2 KO	F7	C5a	3
46	1	6	WT	WT	STING	1
47	1	6	WT	WT	STING	2
48	1	6	WT	WT	STING	3
49	1	6	C5aR1 KO	B6	STING	1
50	1	6	C5aR1 KO	B6	STING	2
51	1	6	C5aR1 KO	B6	STING	3
52	2	6	C5aR1 KO	C3	STING	1
53	2	6	C5aR1 KO	C3	STING	2
54	2	6	C5aR1 KO	C3	STING	3
55	1	6	C5aR1 KO	G8	STING	1
56	1	6	C5aR1 KO	G8	STING	2
57	1	6	C5aR1 KO	G8	STING	3
58	1	6	C5aR2 KO	D3	STING	1
59	1	6	C5aR2 KO	D3	STING	2
60	1	6	C5aR2 KO	D3	STING	3
61	2	6	C5aR2 KO	F3	STING	1
62	2	6	C5aR2 KO	F3	STING	2
63	2	6	C5aR2 KO	F3	STING	3
64	1	6	C5aR2 KO	F7	STING	1
65	1	6	C5aR2 KO	F7	STING	2
66	1	6	C5aR2 KO	F7	STING	3

Table 6.1. Samples sent to GENEWIZ for RNAseq. N=3 technical replicates of each condition, N=3 clones of C5aR1/2 KO cells, N=3 WT replicates. Variables = Cell Line (WT, C5aR1 KO, C5aR2 KO), Clone (B6, C3, G8, D3, F3, F7), Treatment (Untreated, C5a, STING agonist), Experiment Day (1, 2). Treatment time (0 or 6 hours) was included as a control for Untreated cells.

6.2.2. Principal Component Analysis

Following RNAseq, quality control analysis was performed by GENEWIZ (data not shown), and preliminary data analysis was performed by You Zhou (Cardiff University) and Van Dien Nguyen (Cardiff University). Transcripts per million normalised expression data were generated for each sample, and PCA was performed to confirm that treatment condition and genotype were driving variance between sample datasets as expected. PCA plots were generated for each C5aR1 KO and C5aR2 KO clone vs WT, and again for grouped C5aR1 KO or C5aR2 KO clones vs WT, to investigate whether clonal effects were conserved with KO effects.

PCA was first performed on data generated using WT cells to confirm that treatment condition drove variance between untreated and treated datasets (**Figure 6.2**). WT 0h Untreated and WT 6h Untreated cells formed separate clusters (**Figure 6.2 A**), indicating that there were differences between the transcriptomes of cells incubated for 6 hours and cells incubated for 0 hours. This indicates that there are transcriptomic changes driven by the length of culture over the experiment incubation time, which can be accounted for in future analysis if required.

Stimulation with C5a (**Figure 6.2 B**) or STING agonist cAIM(PS)$_2$ Difluor (Rp/Sp) (**Figure 6.2 C**) also contributed the most variance between the transcriptome of treated cells and untreated cells, as demonstrated by the clustering of the treated cells and clustering of untreated cells distally along the PC1 axis. These data indicate that the cells were responding to the stimulation conditions.

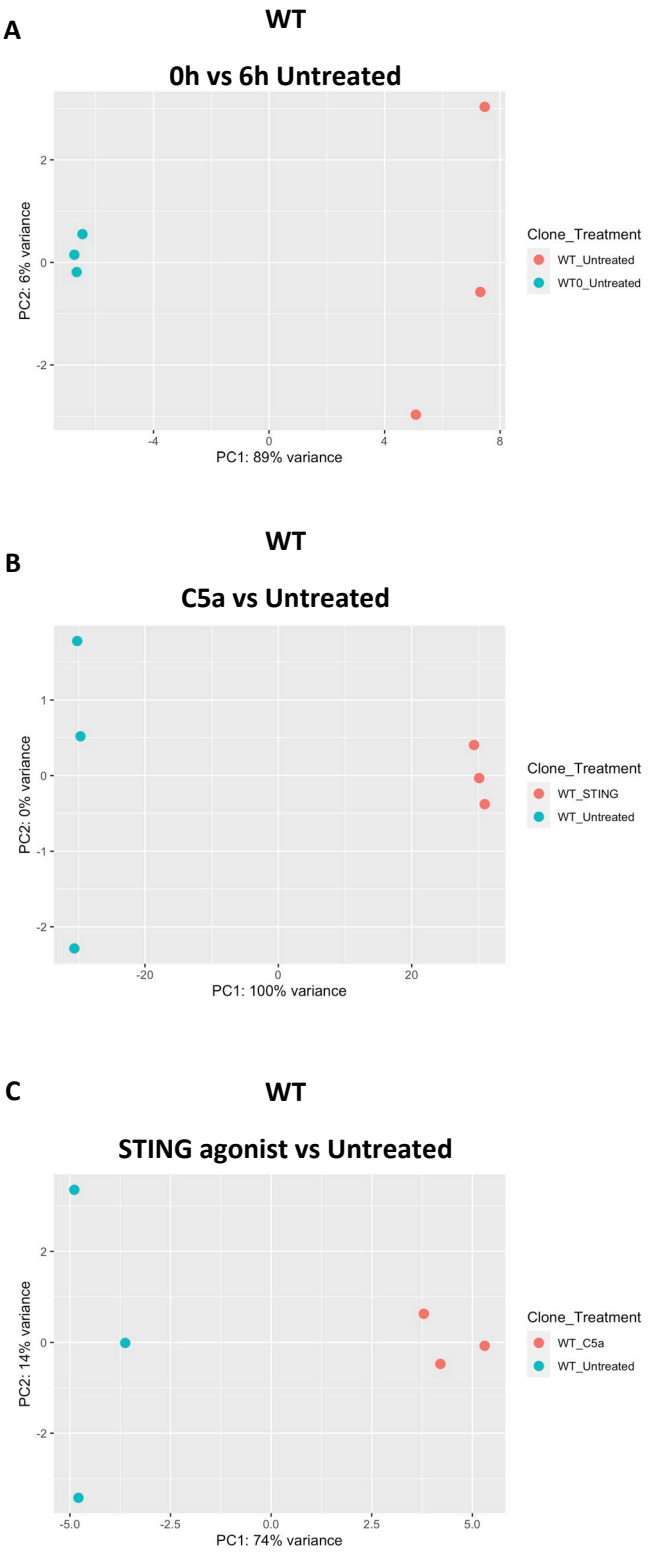

Figure 6.2. Treatment conditions are primary drivers of variance within WT datasets. PMA-differentiated WT THP-1 cells were incubated for 6 hours with culture medium, 50 ng/mL C5a or 5 µg/mL STING agonist cAIM(PS)$_2$ Difluor (Rp/Sp). RNAseq was performed, followed by principal component analysis on normalised expression data. Principal component scores (% variance) were plotted for **A.** Untreated WT cells at 0 hours vs 6 hours incubation times, **B.** C5a-treated vs Untreated WT cells and **C.** STING agonist-treated cells vs Untreated WT cells.

The next set of PCA plots compared untreated C5aR1/2 KO cells to untreated WT cells (**Figure 6.3**). Each C5aR1 KO clone (B6, C3, G8) and C5aR2 KO clone (D3, F3, F7) was compared to WT cells. This approach assesses whether baseline C5aR1 KO or C5aR2 KO drives transcriptomic change compared to WT cells in each of the C5aR1 KO and C5aR2 KO clones.

In C5aR1 KO clone B6, genotype is the primary driver of variance compared to WT cells at baseline (**Figure 6.3 A**). This is not the case with C5aR1 KO clone C3, as one of the three replicates is an outlier from the other two, and the unknown outlier effect is driving 94% of the variance between C3 and WT cells (**Figure 6.3 B**). However, the other two replicates are clustered, and the WT replicates are clustered away from all 3 of the C3 replicates, indicating that there is still a large degree of the variance between the datasets driven by genotype. C5aR1 KO clone G8 is separated from WT, similar to B6, indicating that genotype is the primary driver of variance compared to WT cells (**Figure 6.2 C**). This result, excluding one replicate of C3, suggests that C5aR1 KO influences the baseline transcriptome of THP-1 cells.

The data generated using C5aR2 KO cells are more consistent. C5aR2 KO clone D3 (**Figure 6.3 D**), F3 (**Figure 6.3 E**) and F7 (**Figure 6.3 F**) are distally clustered from WT replicates along the PC1 axis. PC1 generates 96%, 98% and 97%, respectively, of the variance between C5aR2 KO clone and WT datasets. This indicates that C5aR2 KO influences the baseline transcriptome of THP-1 cells.

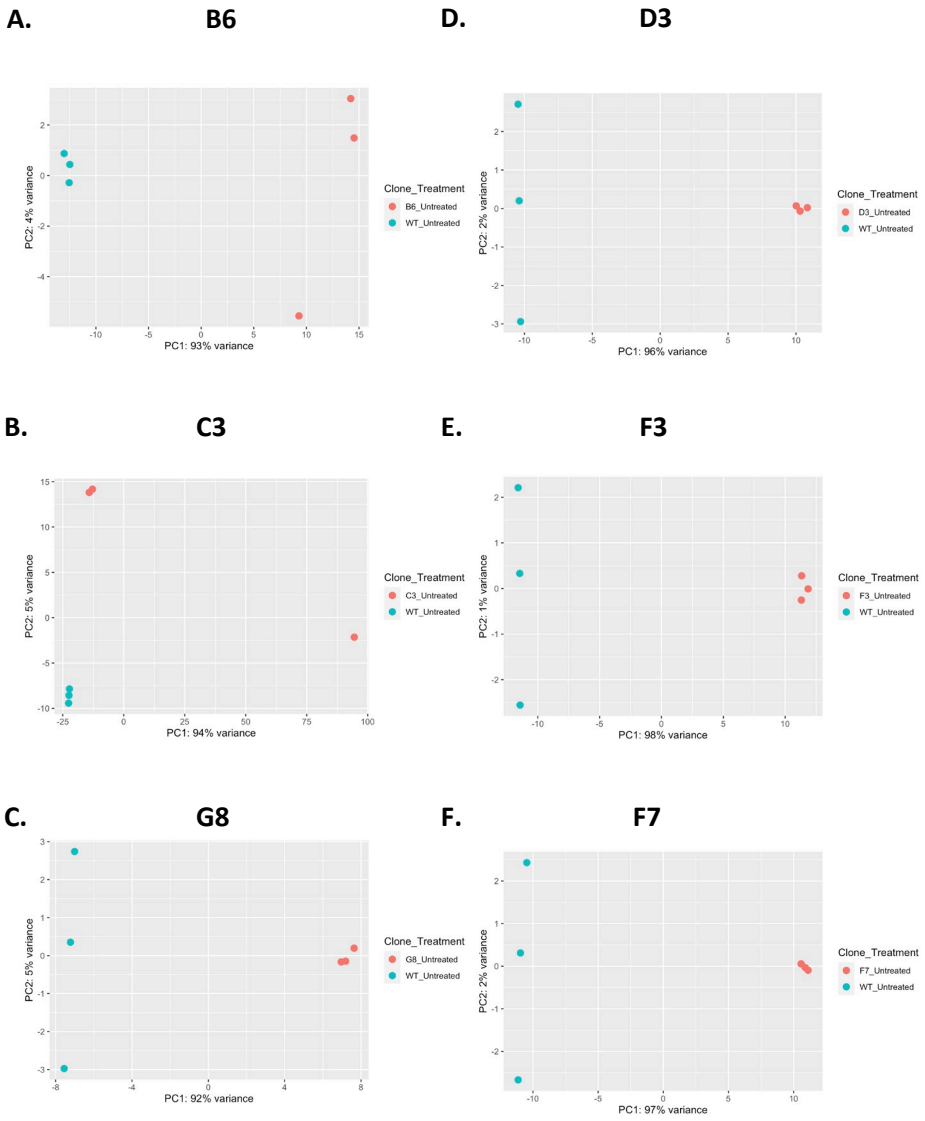

Figure 6.3. Genotype is the primary driver of variance between untreated C5aR1/2 KO clones and WT cells. PMA-differentiated WT, C5aR1 KO and C5aR2 KO THP-1 cells were incubated for 6 hours with culture medium. RNAseq was performed, followed by principal component analysis on normalised expression data. Principal component scores (% variance) were plotted for Untreated C5aR1 KO cells vs Untreated WT cells for clones **A.** B6, **B.** C3 and **C.** G8, and Untreated C5aR2 KO cells vs Untreated WT cells for clones **D.** D3, **E.** F3 and **F.** F7.

The effect of C5a treatment on C5aR1/2 KO cells was then assessed (**Figure 6.4**). In C5aR1 KO clone B6, C5a treatment generates the majority of the variance between treated and untreated datasets (**Figure 6.4 A**). This is not the case with clone C3 due to one outlier replicate, as seen in **Figure 6.3 B**, however the C5a-treated replicates are well-clustered and distinct from untreated cells (**Figure 6.4 B**). Clone G8 is more consistent, and C5a treatment drives the majority of variance between treated and untreated datasets (**Figure 6.4 C**).

C5aR2 KO clones are again more consistent. C5a-treated C5aR2 KO clones D3 (**Figure 6.4 D**), F3 (**Figure 6.4 E**) and F7 (**Figure 6.4 F**) form a cluster separate from untreated replicates. For each, PC1 generates 97% (D3), 81% (F3) and 95% (F7) variance between treated and untreated transcriptome data, indicating that C5a drives the majority of variance between treated and untreated datasets. Furthermore, C5a has an effect on cells in the individual absence of C5aR1 or C5aR2, demonstrating that C5a elicits a response via engagement of multiple receptors.

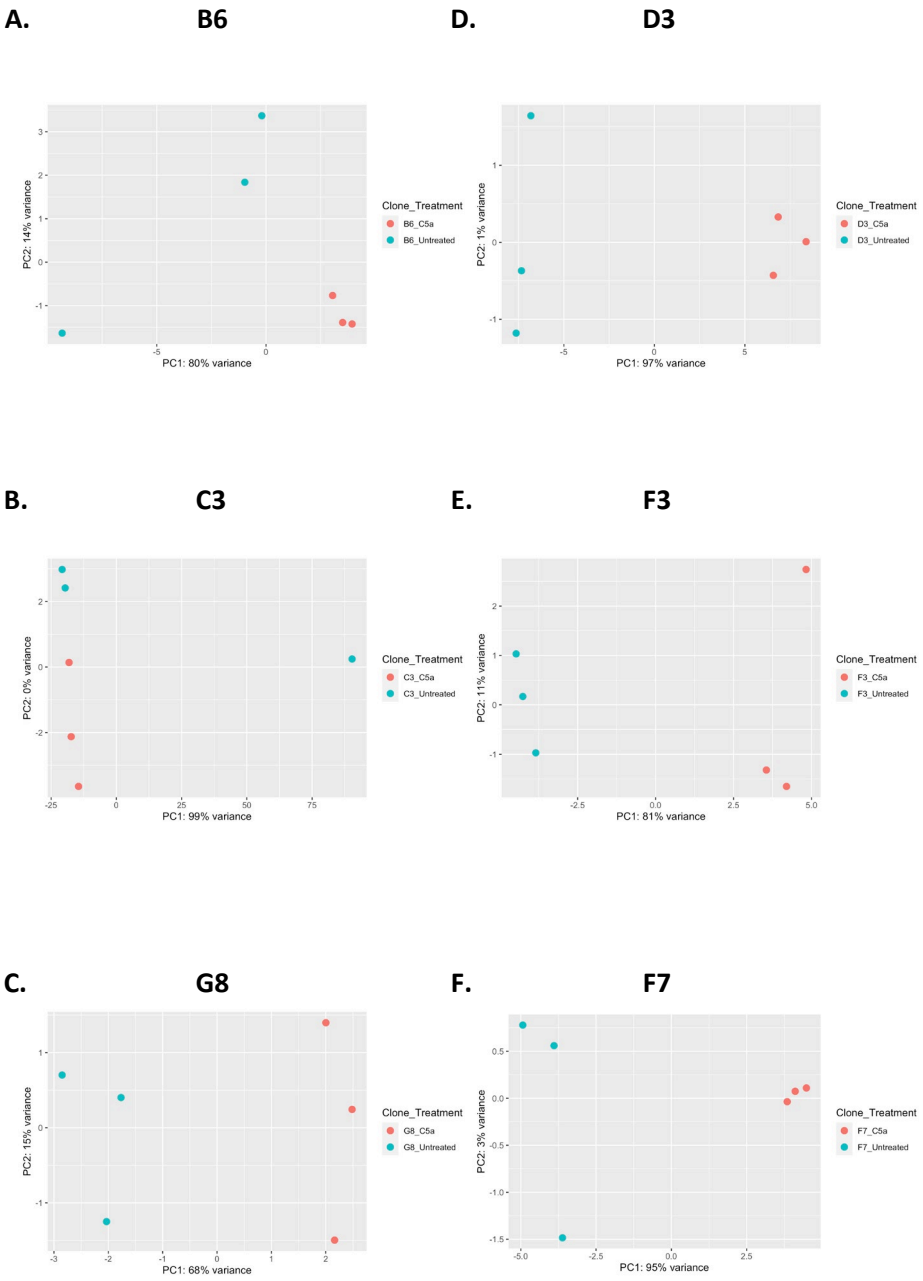

Figure 6.4. C5a treatment is the primary driver of variance within clone datasets, excluding C5aR1 KO clone C3. PMA-differentiated C5aR1 KO and C5aR2 KO THP-1 cells were incubated with culture medium or 50 ng/mL C5a for 6 hours. RNAseq was performed, followed by principal component analysis on normalised expression data. Principal component scores (% variance) were plotted for C5a-treated C5aR1 KO cells vs Untreated C5aR1 KO cells for clones **A.** B6, **B.** C3 and **C.** G8, and C5a-treated C5aR2 KO cells vs Untreated C5aR2 KO cells for clones **D.** D3, **E.** F3 and **F.** F7.

STING agonist treatment was assessed next, comparing the transcriptome data of untreated C5aR1/2 KO cells to treated cells (**Figure 6.5**). In C5aR1 KO clones B6 (**Figure 6.5 A**), C3 (**Figure 6.5 B**) and G8 (**Figure 6.5 C**), and C5aR2 KO clones D3 (**Figure 6.5 D**), F3 (**Figure 6.5 E**) and F7 (**Figure 6.5 F**), STING agonism generates the majority of variance between treated and untreated datasets. PC1 generates approximately 100% of the variance between treated and untreated datasets for all 3 C5aR2 KO clones. C5aR1 KO clones also respond to STING agonism, with 99% of variance between treated and untreated B6 cells, 71% of variance between treated and untreated C3 cells, and approximately 100% of variance between treated and untreated G8 cells generated by PC1 for each comparison. The outlying C3 untreated replicate still varies from the other 2 replicates, however this is not the strongest source of variance between treated and untreated datasets for this comparison, suggesting that the STING response is high and overcomes the variability induced by the outlying replicate. These data suggest that across all clones of both KO cell lines, STING agonism drives the majority of the differences between treated and untreated cells.

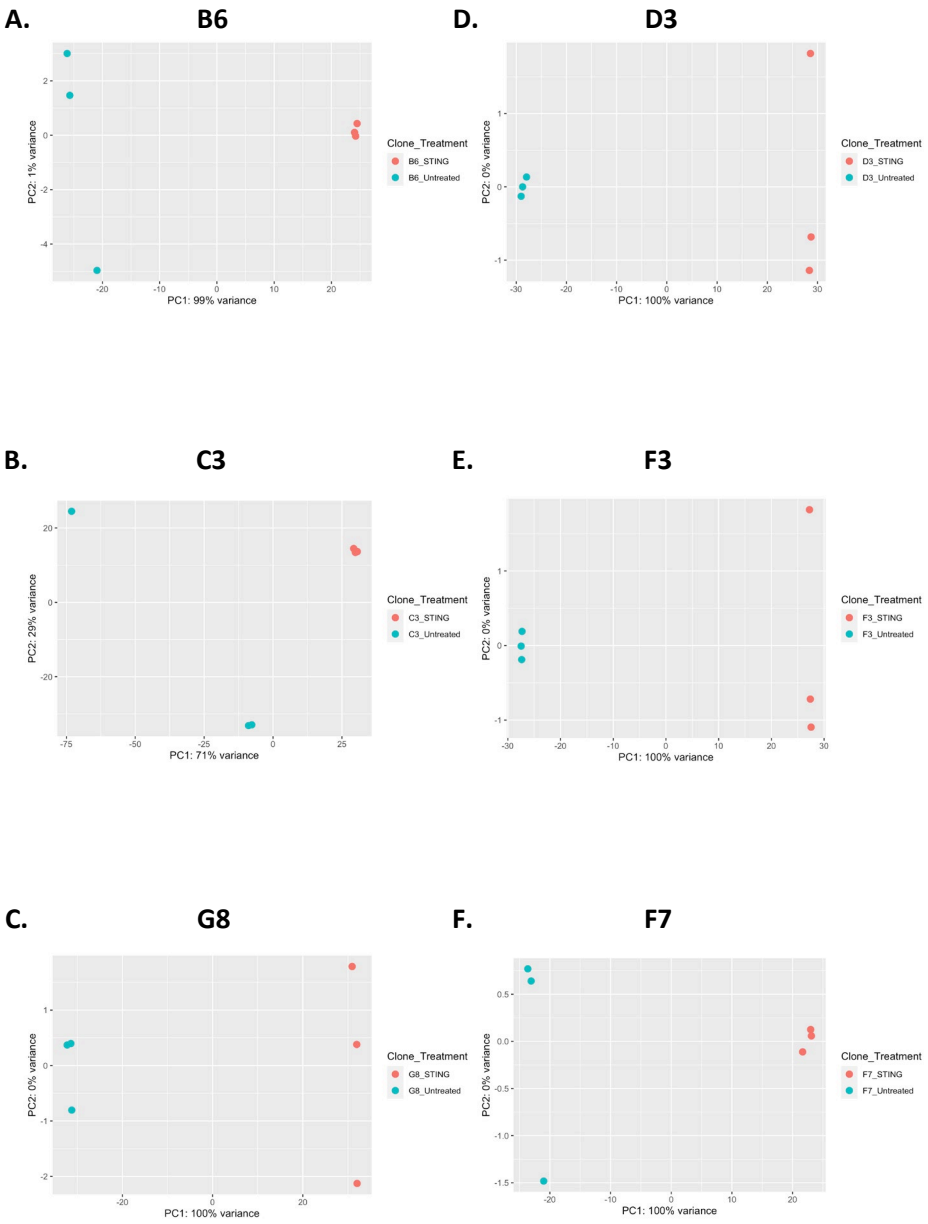

Figure 6.5. STING agonism is the primary driver of variance within clone datasets. PMA-differentiated C5aR1 KO and C5aR2 KO THP-1 cells were incubated with culture medium or 5 µg/mL STING agonist cAIM(PS)$_2$ Difluor (Rp/Sp) for 6 hours. RNAseq was performed, followed by principal component analysis on normalised expression data. Principal component scores (% variance) were plotted for STING agonist-treated C5aR1 KO cells vs Untreated C5aR1 KO cells for clones **A.** B6, **B.** C3 and **C.** G8, and STING agonist-treated C5aR2 KO cells vs Untreated C5aR2 KO cells for clones **D.** D3, **E.** F3 and **F.** F7.

Having established that both C5a and STING agonist treatment were driving differences between untreated and treated WT, C5aR1 KO and C5aR2 KO cells, the next set of PCA plots assessed the variance between treated KO cells and treated WT cells, to establish whether genotype (C5aR1 KO or C5aR2 KO vs WT) was generating transcriptomic variance in the context of C5a or STING agonist treatment.

The effect of C5aR1 KO and C5aR2 KO on C5a-treated THP-1 cells was assessed by PCA (**Figure 6.6**). For each clone of each KO cell line, genotype was the primary driver of variance between datasets. In clones B6 (**Figure 6.6 A**), C3 (**Figure 6.6 B**) and G8 (**Figure 6.6 C**), C5a-treated C5aR1 KO cells were clustered separately from C5a-treated WT cells. This was also true for C5aR2 KO cells; C5a-treated clones D3 (**Figure 6.6 D**), F3 (**Figure 6.6 E**) and F7 (**Figure 6.6 F**) were clustered separately from C5a-treated WT replicates. All KO clone vs WT comparisons had 97-99% variance driven by PC1. These data indicate that C5a induces different transcriptomic responses dependent on the genotype.

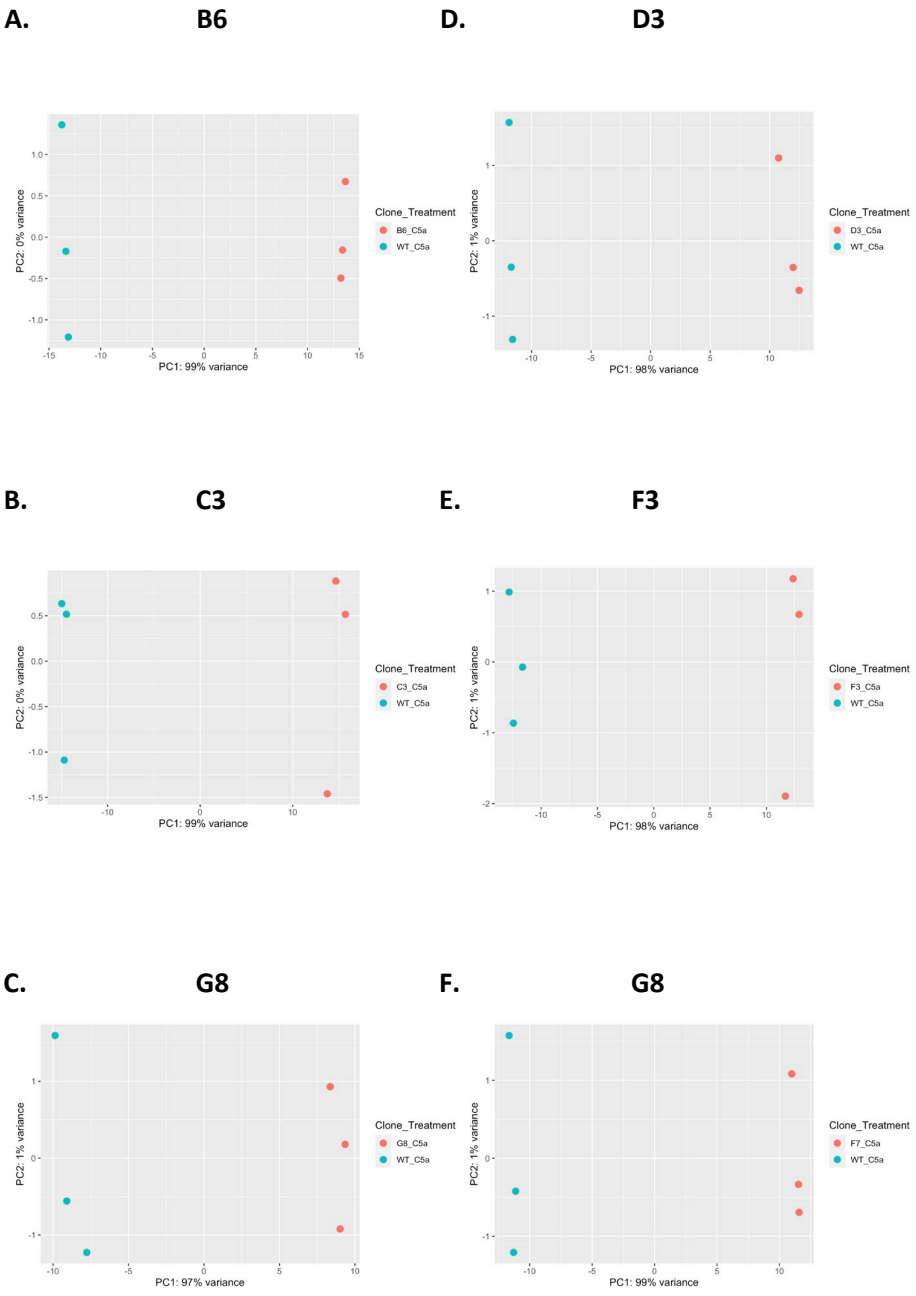

Figure 6.6. Genotype is the primary driver of variance between C5a-treated C5aR1/2 KO clones and WT cells. PMA-differentiated WT, C5aR1 KO and C5aR2 KO THP-1 cells were incubated with 50 ng/mL C5a for 6 hours. RNAseq was performed, followed by principal component analysis on normalised expression data. Principal component scores (% variance) were plotted for C5a-treated C5aR1 KO cells vs C5a-treated WT cells for clones **A.** B6, **B.** C3 and **C.** G8, and C5a-treated C5aR2 KO cells vs C5a-treated WT cells for clones **D.** D3, **E.** F3 and **F.** F7.

The same approach was taken to compare STING agonist-treated C5aR1/2 KO cells to STING agonist-treated WT cells (**Figure 6.7**). For each KO clone, genotype was the primary driver of variance when compared to the WT dataset. In clones B6 (**Figure 6.7 A**), C3 (**Figure 6.7 B**) and G8 (**Figure 6.7 C**), STING agonist-treated C5aR1 KO cells were clustered separately from STING agonist-treated WT cells. In clones D3 (**Figure 6.7 D**), F3 (**Figure 6.7 E**) and F7 (**Figure 6.7 F**), STING agonist-treated C5aR2 KO cells were clustered separately from STING agonist-treated WT cells. All KO clone vs WT comparisons had 96-99% variance generated by PC1. These data confirm that C5aR1 KO and C5aR2 KO cells have transcriptomic profiles that differ from WT cells when stimulated with STING agonist cAIM(PS)$_2$ Difluor (Rp/Sp).

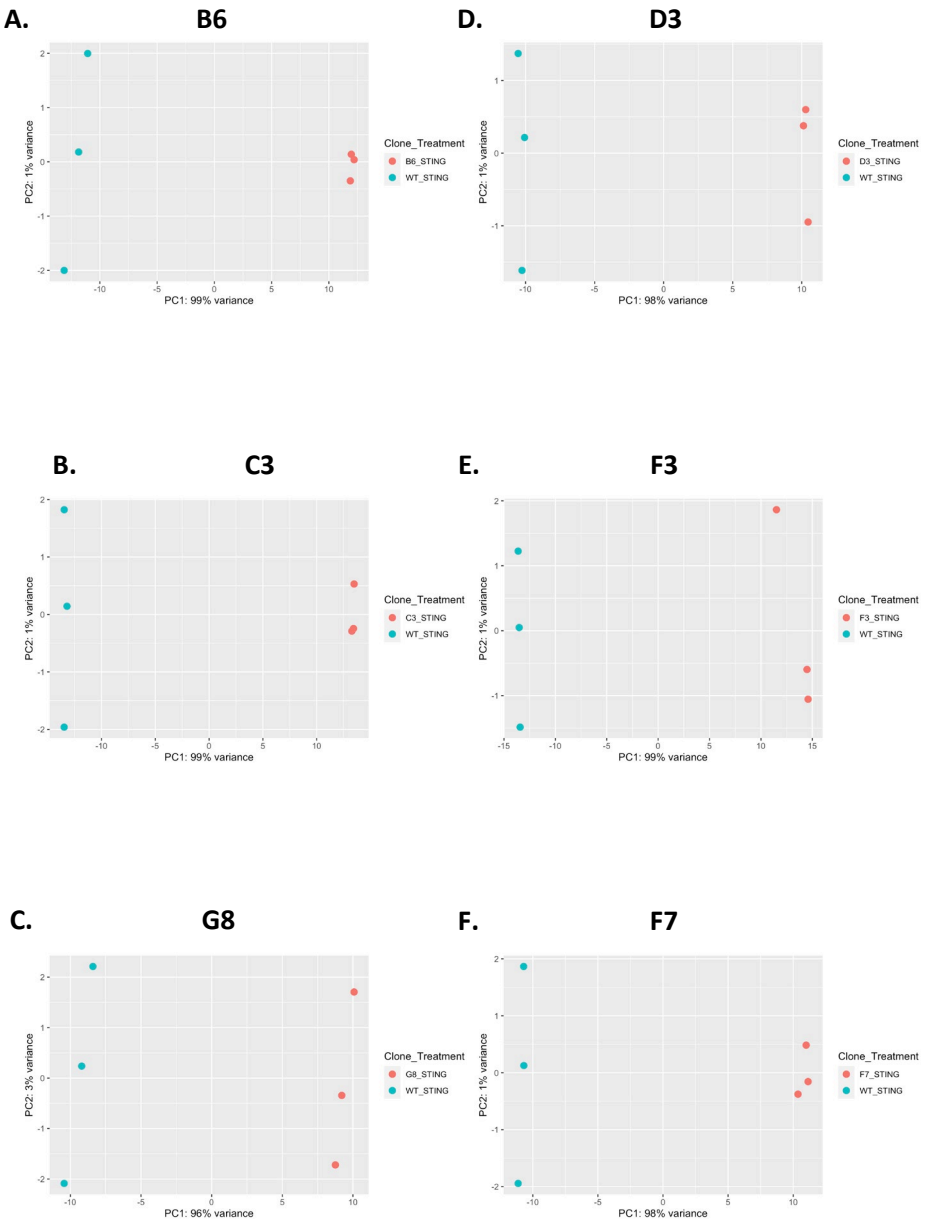

Figure 6.7. Genotype is the primary driver of variance between STING agonist-treated C5aR1/2 KO clones and WT cells. PMA-differentiated WT, C5aR1 KO and C5aR2 KO THP-1 cells were incubated with 5 µg/mL STING agonist cAIM(PS)$_2$ Difluor (Rp/Sp) for 6 hours. RNAseq was performed, followed by principal component analysis on normalised expression data. Principal component scores (% variance) were plotted for STING agonist-treated C5aR1 KO cells vs C5a-treated WT cells for clones **A.** B6, **B.** C3 and **C.** G8, and STING agonist-treated C5aR2 KO cells vs C5a-treated WT cells for clones **D.** D3, **E.** F3 and **F.** F7.

The above analyses demonstrated variance between individual clones and WT cells, or between treatment conditions within datasets from individual clones. For the majority of comparisons, variance was being driven by the intended experimental condition (genotype or treatment). In contrast, the following set of PCA plots were generated using grouped C5aR1 KO and C5aR2 KO datasets, rather than individual clones. This aimed to test whether the variance in C5aR1/2 KO comparisons was conserved with variance in clonal comparisons, informing the decision to compare individual clones or KO groups in subsequent analyses.

First, untreated C5aR1/2 KO cells were compared to untreated WT cells using a PCA (**Figure 6.8**). C5aR1 KO data do not cluster together, however they do not cluster with the WT data (**Figure 6.8 A**). This indicates variance within the C5aR1 KO dataset, but also variance between C5aR1 KO and WT datasets. C5aR1 KO data are clustered in 3 separate groups, suggesting that inter-clone variance is driving the majority of variance between these datasets.

C5aR2 KO data are clustered compared to WT data (**Figure 6.8 B**). There is variance within the C5aR2 KO datasets, and it appears that one of the clones varies from the other two clones. However, WT and C5aR2 KO differ despite the clonal variation within the KO group. These data indicate that C5aR1 KO and C5aR2 KO drive transcriptomic changes at baseline compared to WT cells.

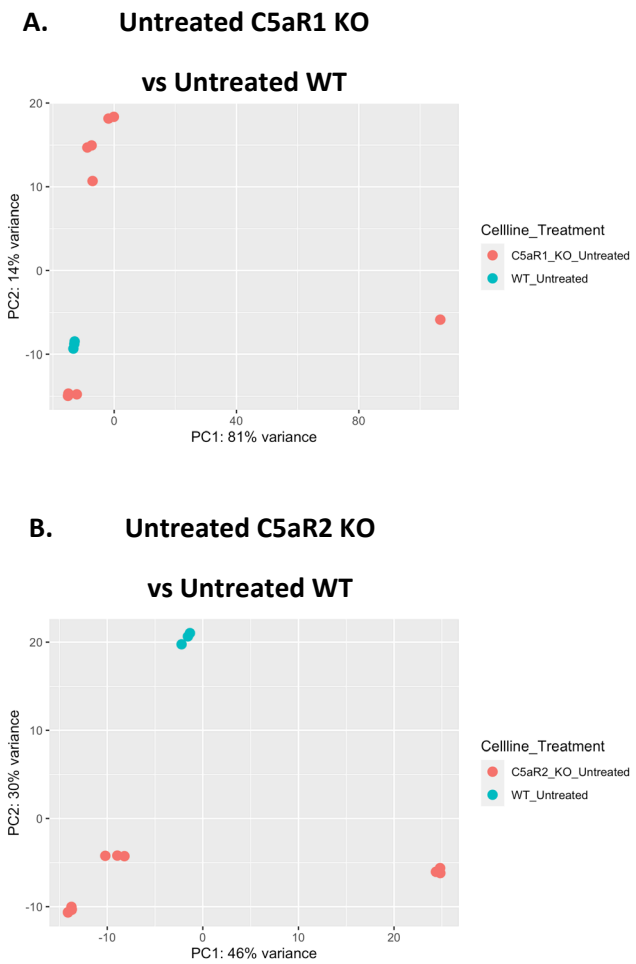

Figure 6.8. Genotype is the primary driver of variance between Untreated grouped C5aR2 KO cells and WT cells. PMA-differentiated WT, C5aR1 KO and C5aR2 KO THP-1 cells were incubated for 6 hours with culture medium. RNAseq was performed, followed by principal component analysis on normalised expression data. Clones B6, C3 and G8 were grouped into C5aR1 KO, and Clones D3, F3 and F7 were grouped into C5aR2 KO. Principal component scores (% variance) were plotted for **A.** untreated C5aR1 KO cells or **B.** untreated C5aR2 KO cells vs WT cells.

The effect of C5a treatment was then assessed in the same way. C5a-treated C5aR1/2 KO datasets were compared to Untreated C5aR1/2 KO datasets using PCA (**Figure 6.9**).

C5a treatment is not the primary driver of variance for C5aR1 KO cells (**Figure 6.9 A**). There are 3 main clusters, each containing clustered untreated and C5a-treated datasets, with a single outlying replicate. These are likely representative of the 3 clones. This is in contrast with data from individual clones (**Figure 6.4 A-C**), where C5a treatment is the primary driver of variance. The effects of C5a on individual C5aR1 KO clones are not conserved when the clones are grouped, suggesting that variance between clones is more significant than the effect of genotype on the response to C5a.

The C5aR2 KO data are similar, as C5a treatment does not drive the majority of variance between untreated and treated C5aR2 KO cells (**Figure 6.9 B**). There are 3 clusters, likely representing 3 clones, each containing untreated and treated datasets. There is a slight distinction between untreated and treated sub-clusters within each main cluster, representing the clear variance previously demonstrated between untreated and C5a-treated C5aR2 KO clones (**Figure 6.4 D-F**), however the data indicate that C5a treatment does not affect the transcriptome of C5aR2 KO cells as much as the baseline differences between individual C5aR2 KO clones.

These data indicate that C5a has a relatively small effect on the transcriptome of these cells. This does not suggest that there is no effect, however the differences between clonal replicates make this comparison less powerful for investigating the effect of C5a.

A. C5a-treated C5aR1 KO vs Untreated C5aR1 KO

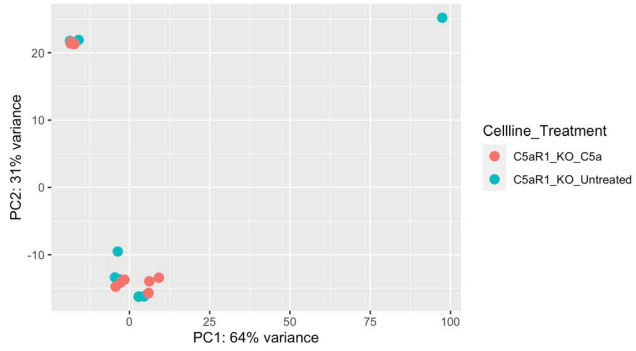

B. C5a-treated C5aR2 KO vs Untreated C5aR2 KO

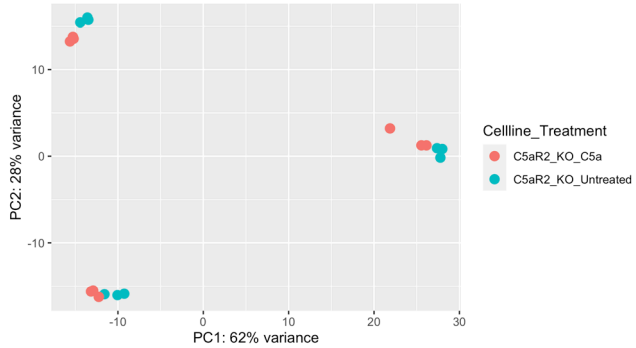

Figure 6.9. C5a treatment is not the primary driver of variance within grouped KO datasets. PMA-differentiated C5aR1 KO and C5aR2 KO THP-1 cells were incubated with culture medium or 50 ng/mL C5a for 6 hours. RNAseq was performed, followed by principal component analysis on normalised expression data. Clones B6, C3 and G8 were grouped into C5aR1 KO, and Clones D3, F3 and F7 were grouped into C5aR2 KO. Principal component scores (% variance) were plotted for C5a-treated vs untreated **A.** C5aR1 KO or **B.** C5aR2 KO cells.

The same approach was taken to investigate the effect of STING agonism on C5aR1/2 KO cells (**Figure 6.10**). The covariant "Experiment Day" was included in this analysis model as it was a major contributor of variance in this comparison.

STING agonism is the main driver of variance between treated and untreated C5aR1 KO cells (**Figure 6.10 A**). There is some variance between clonal replicates in each condition, but the treated and untreated datasets are clearly separated. PC1 contributes 75% of the variance between untreated and treated datasets, and the data are clustered distributed primarily along the PC1 axis.

STING agonism also drives variance between treated and untreated C5aR2 KO cells (**Figure 6.10 B**). The treated and untreated C5aR2 KO cells are clearly separated along the PC1 axis, and PC1 contributes 88% of the variance between the datasets. Experiment Day 2 is clustered at the top of the PC2 axis and Experiment Day 1 is clustered at the bottom, indicating that Experiment Day contributes significant variance to this dataset. However, this does not mask the effect of STING agonism on the C5aR2 KO cells.

These data, in contrast to the PCAs on C5a-treated vs untreated C5aR1/2 KO cells, demonstrate a clear effect of STING agonism on C5aR1/2 KO cells, conserved with the effect of STING agonism in individual clones.

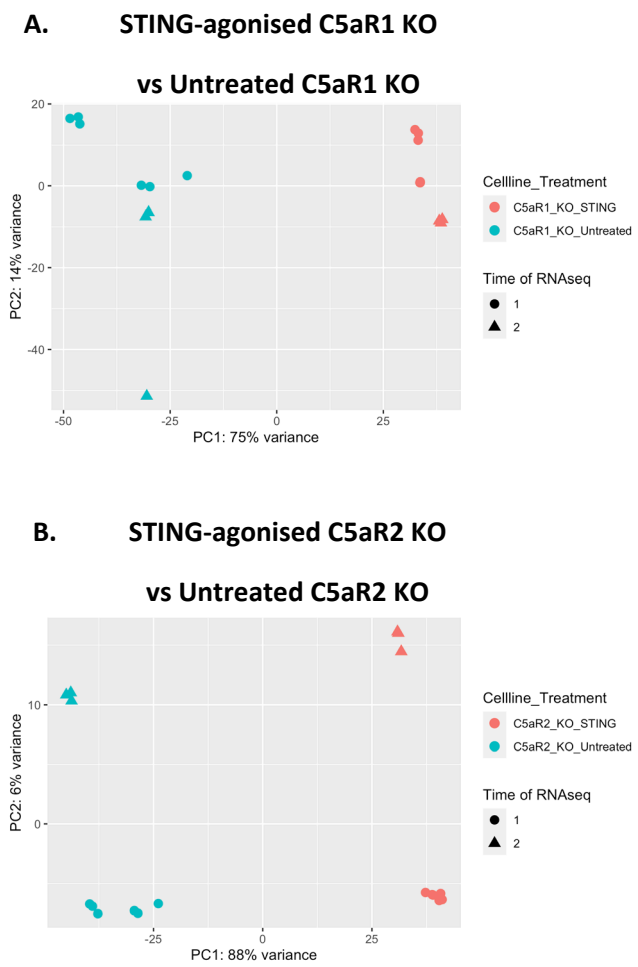

Figure 6.10. STING agonism is the primary driver of variance within grouped KO datasets. PMA-differentiated C5aR1 KO and C5aR2 KO THP-1 cells were incubated with culture medium or 5 µg/mL STING agonist cAIM(PS)$_2$ Difluor (Rp/Sp) for 6 hours. RNAseq was performed, followed by principal component analysis on normalised expression data. Clones B6, C3 and G8 were grouped into C5aR1 KO, and Clones D3, F3 and F7 were grouped into C5aR2 KO. Principal component scores (% variance) were plotted for STING agonist-treated vs Untreated **A.** C5aR1 KO or **B.** C5aR2 KO cells. Experiment Day 1 (Circle) and Day 2 (Triangle) were plotted.

The effect of genotype on treated cells was assessed next. C5a-treated grouped C5aR1/2 KO cells were compared to WT cells by PCA (**Figure 6.11**).

Despite the minimal variance driven by C5a treatment compared to untreated C5aR1/2 cells (**Figure 6.9**), there were clear differences between C5a-treated C5aR1 KO (**Figure 6.11 A**) and C5aR2 KO (**Figure 6.11 B**) cells vs C5a-treated WT cells. For C5a-treated C5aR1 KO and C5aR2 KO cells, genotype is a major driver of variance compared to C5a-treated WT cells. Both KO groups have genotype-independent variance within the group, but are clustered along the PC2 axis compared to WT replicates. These data indicate that C5a treatment generates different transcriptomic signatures dependent on the genotype of the THP-1 cells, suggesting that the removal of C5aR1 or C5aR2 causes marked changes in the phenotype of the cells in response to their natural ligand C5a.

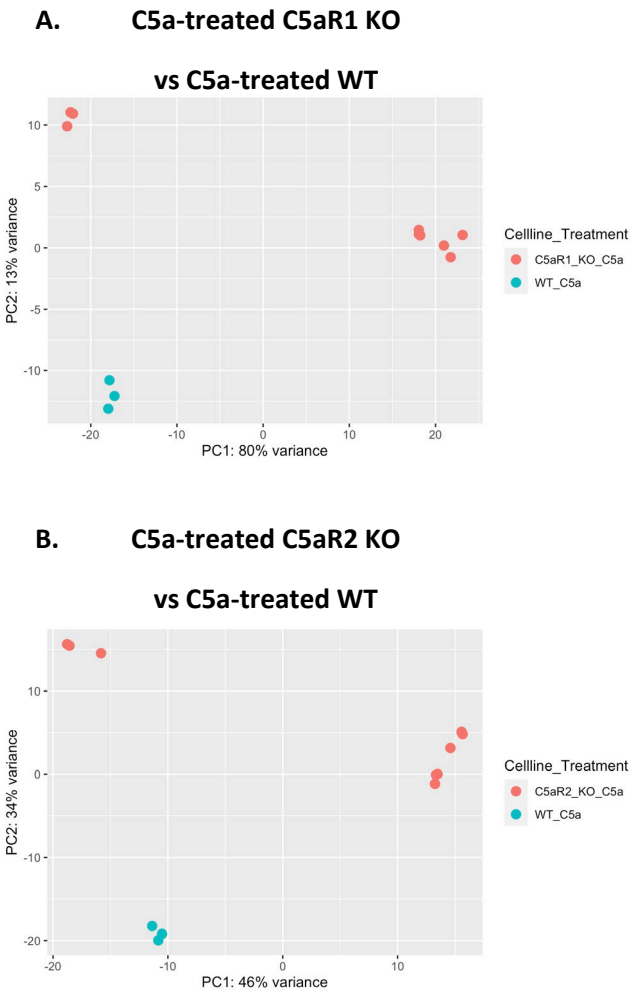

Figure 6.11. Genotype is the primary driver of variance between C5a-treated grouped C5aR1/2 KO cells and WT cells. PMA-differentiated WT, C5aR1 KO and C5aR2 KO THP-1 cells were incubated with 50 ng/mL C5a for 6 hours. RNAseq was performed, followed by principal component analysis on normalised expression data. Clones B6, C3 and G8 were grouped into C5aR1 KO, and Clones D3, F3 and F7 were grouped into C5aR2 KO. Principal component scores (% variance) were plotted for C5a-treated **A.** C5aR1 KO or **B.** C5aR2 KO cells vs C5a-treated WT cells.

A final comparison of STING-agonised C5aR1/2 KO cells and WT cells was performed using PCA (**Figure 6.12**). The effect of covariant "Experiment Day" was also visualised in this PCA plot, as it drove variance between these datasets.

C5aR1 KO clones were separated from WT replicates, indicating that genotype drives variance between STING-agonised C5aR1 KO cells and STING-agonised WT cells (**Figure 6.12 A**). Grouping C5aR1 clones generated a more complex comparison in comparison to the PCA on individual clones (**Figure 6.7 A-C**). In this PCA plot, the C5aR2 KO data did not form a single cluster, indicating that there are differences between clonal replicates which contribute to variance between the datasets. The overall effect, however, is that genotype drives variance between STING-agonised C5aR1 KO and WT cells.

There was a similar result for C5aR2 KO cells, which were separated from the WT data, indicating that genotype drives variance between STING-agonised C5aR2 KO cells and WT cells (**Figure 6.12 B**). The Experiment Day 2 data separated from the Experiment Day 1 data in the C5aR2 KO cells, suggesting that Experiment Day is a source of variance within the C5aR2 KO data. This result demonstrates that C5aR1/2 KO genotype affects the transcriptomic response of THP-1 cells to STING agonism.

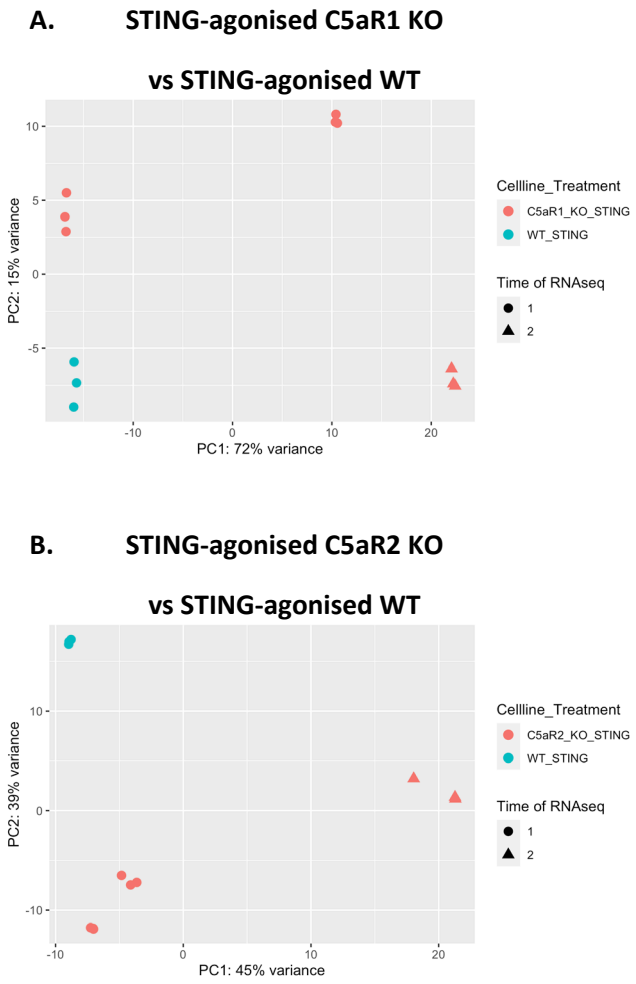

Figure 6.12. Experiment Day, followed by Genotype, is the primary driver of variance between STING agonist-treated grouped C5aR1/2 KO cells and WT cells. PMA-differentiated WT, C5aR1 KO and C5aR2 KO THP-1 cells were incubated with 5 µg/mL STING agonist cAIM(PS)$_2$ Difluor (Rp/Sp) for 6 hours. RNAseq was performed, followed by principal component analysis on normalised expression data. Clones B6, C3 and G8 were grouped into C5aR1 KO, and Clones D3, F3 and F7 were grouped into C5aR2 KO. Principal component scores (% variance) were plotted for STING agonist-treated **A.** C5aR1 KO or **B.** C5aR2 KO cells vs STING agonist-treated WT cells. Experiment Day 1 (Circle) and Day 2 (Triangle) were plotted.

6.2.3. Differential Gene Expression Analysis

Having used PCA to confirm that genotype drives variance in the transcriptomic signatures of C5aR1/2 KO cells compared to WT in untreated, C5a-treated and STING agonist-treated cells, differential gene expression data were generated. Volcano plots were generated to visualise significantly expressed genes by Darren Gormley (GSK).

C5a- or STING agonist-treated cells were compared to untreated cells (**Figure 6.13**). C5a treatment drove changes in gene expression in WT cells compared to untreated cells, establishing the baseline response to the stimulation. In C5aR1 KO clones B6, C3 and G8, fewer genes were significantly regulated compared to the WT, whereas C5aR2 KO clones D3, F3 and F7 appeared to have more significantly regulated genes compared to untreated cells. This pattern is reflected in the C5aR1 KO and C5aR2 KO group comparisons, where C5aR1 KO cells have no C5a-dependent significantly regulated genes, and C5aR2 KO have a small number of C5a-dependent significantly regulated genes. This suggests that C5aR1 is required for the response to C5a, or that C5aR2 negatively regulates the response to C5a; the two effects may be working in tandem as they both bind C5a.

STING agonism induces a large number of significantly regulated genes in treated WT cells compared to untreated WT cells. STING agonism in C5aR1 KO clones B6 and C3 also drives a large number of significantly regulated genes, whereas the effect of clone C3 is diminished. C5aR2 KO clones also have a high number of STING-induced significantly regulated genes. The patterns are reflected in the grouped C5aR1 KO and C5aR2 KO comparisons, where the effect of C5aR1 KO cells affects fewer genes, likely due to the diminished response of C3.

These data show that there is a strong response to C5aR1/2 and STING agonism, which changes between WT, C5aR1 KO and C5aR2 KO cells.

Differentially expressed genes in treated C5aR1 KO or C5aR2 KO cells were then compared to treated WT cells using volcano plots (Darren Gormley, GSK) (**Figure 6.14**). There were large numbers of significantly differentially expressed genes across all comparisons. In the grouped comparisons, fewer differentially expressed genes were significantly different in C5aR1/2 KO data compared to WT data. The significantly regulated genes present here represent the differentially expressed genes which are common to all clones within a KO group, and therefore comprise the most reproducible results between clones.

The volcano plots reveal significantly regulated genes across all conditions. These results identify genes which are differentially expressed under the same conditions that drove the amplification of IFN-β in C5aR2 KO cells compared to WT cells (**Chapter 5**). This warrants further investigation, as some of these genes may be linked to the mechanism underlying this effect.

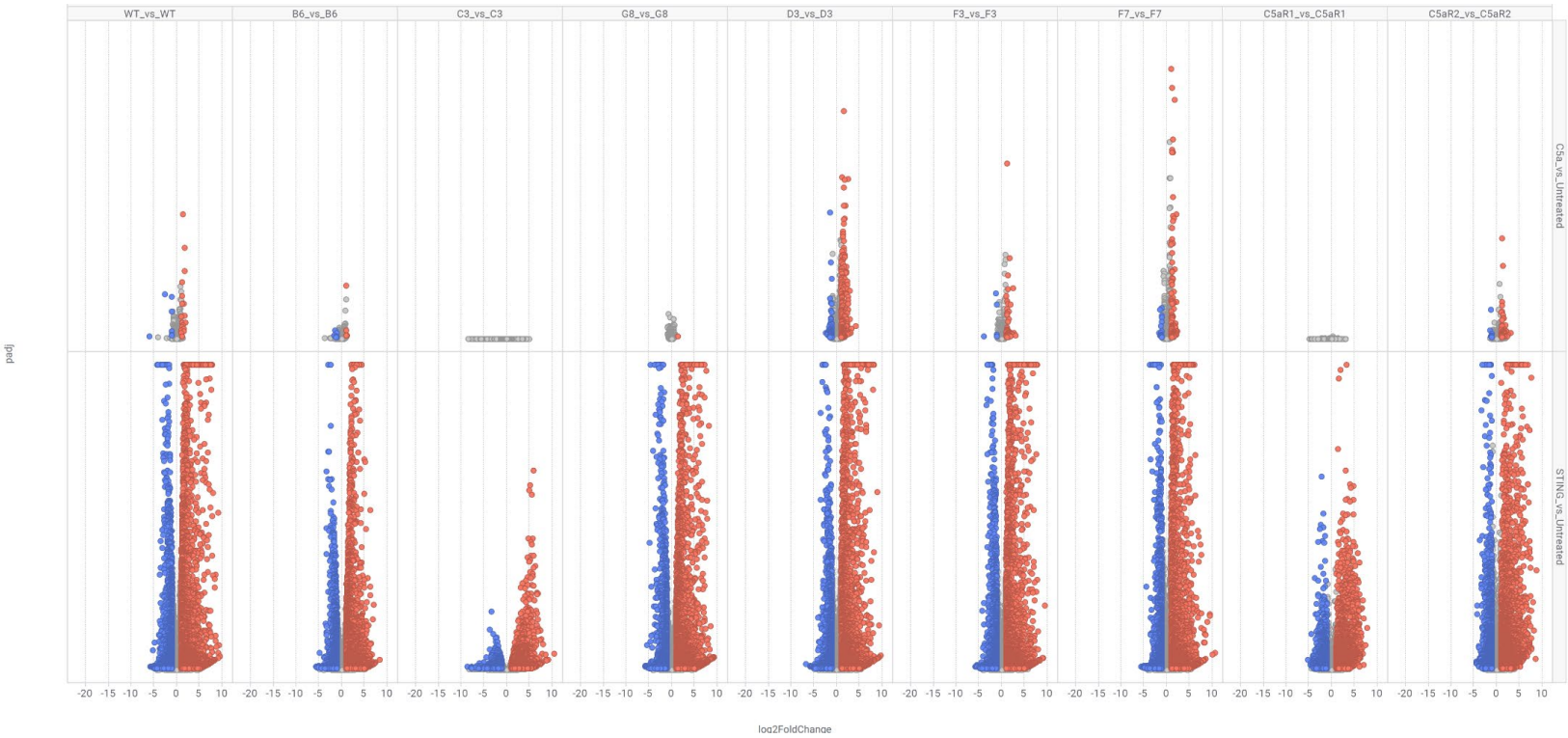

Figure 6.13. C5a or STING agonist-dependent gene regulation in WT, C5aR1 KO or C5aR2 KO THP-1 cells. PMA-differentiated WT, C5aR1 KO and C5aR2 KO THP-1 cells were incubated with culture medium, 50 ng/mL C5a or 5 µg/mL STING agonist cAIM(PS)$_2$ Difluor (Rp/Sp) for 6 hours. RNAseq was performed, followed by differential gene expression analysis. Normalised expression data were used to generate p value, adjusted p value and log$_2$ fold change for C5a or STING agonist-treated cells vs Untreated cells in WT, C5aR1 KO (clone B6, C3, G8, or grouped) or C5aR2 KO (clone D3, F3, F7 or grouped) THP-1 cells. Volcano plots were generated by plotting adjusted p value against log2FC for each comparison. Significantly regulated genes (p≥0.05) were marked in grey. Significantly regulated genes (p≤0.05) with a log2FC≥1 (FC≤2) were marked in red for up-regulated genes and blue for down-regulated genes. N=3 technical replicates for each clone. N=3 clones per KO group. Volcano plots generated by Darren Gormley (GSK).

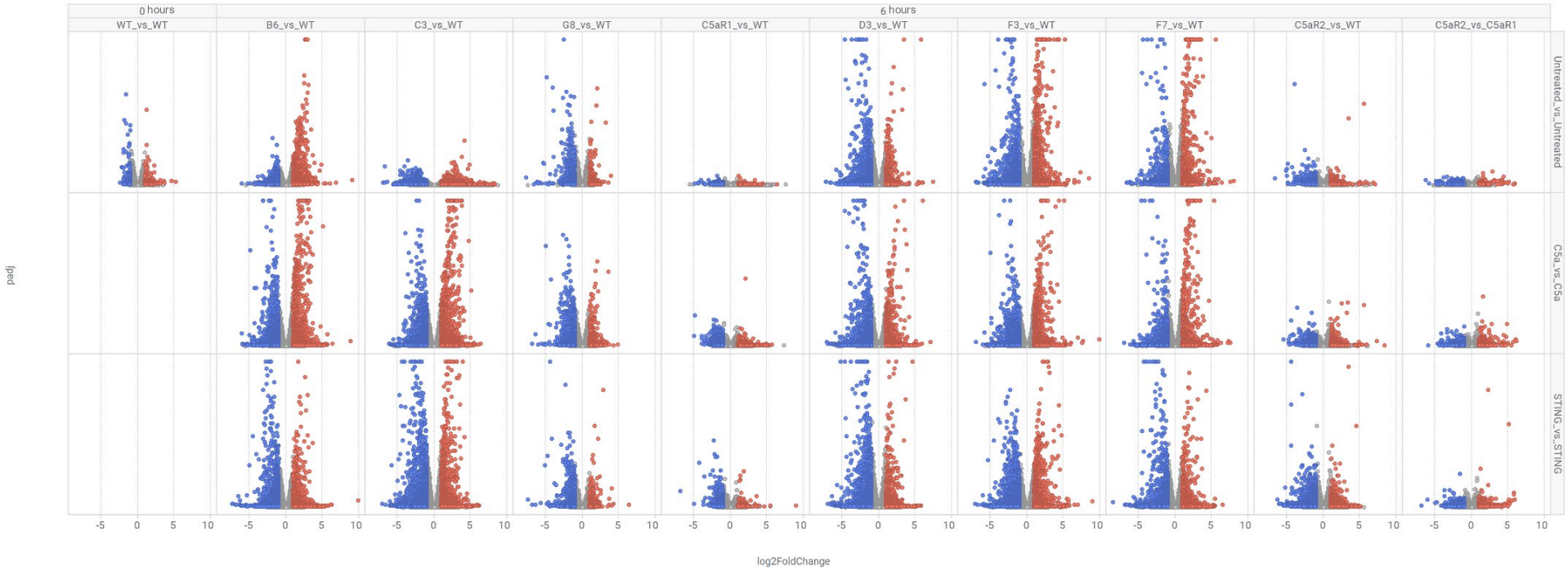

Figure 6.14. Genotype-dependent gene regulation in Untreated, C5a-treated or STING agonist-treated WT, C5aR1 KO and C5aR2 KO cells. PMA-differentiated WT, C5aR1 KO and C5aR2 KO THP-1 cells were incubated with culture medium, 50 ng/mL C5a or 5 µg/mL STING agonist cAIM(PS)$_2$ Difluor (Rp/Sp) for 6 hours. RNAseq was performed, followed by differential gene expression analysis. Normalised expression data were used to generate p value, adjusted p value and log$_2$ fold change for C5aR1 KO (clone B6, C3, G8, or grouped) or C5aR2 KO (clone D3, F3, F7 or grouped) vs WT cells in Untreated, C5a or STING agonist treatment groups. Volcano plots were generated by plotting adjusted p value against log2FC for each comparison. Significantly regulated genes (p≥0.05) were marked in grey. Significantly regulated genes (p≤0.05) with a log2FC≥1 (FC≤2) were marked in red for up-regulated genes and blue for down-regulated genes. N=3 technical replicates for each clone. N=3 clones per KO group. Volcano plots generated by Darren Gormley (GSK).

6.2.4. Pathway Analyses

Further analysis is required to elucidate pathways and individual genes that are regulated by C5aR2 KO. Rather than a large number of pathway analyses on individual KO clone vs WT comparisons which would require further analysis to identify common pathways, the KO group data comparisons were analysed. When assessed by PCA, grouping the KO clones introduced more variability, however the effects of genotype on agonised cells were conserved between grouped and clone comparisons. The variance between C5a- or STING agonist-stimulated C5aR1/2 KO cells and WT cells was primarily generated by genotype-dependent effects.

6.2.4.1. Pathway analysis approaches

To identify potential novel effects of C5a on C5aR2, and to investigate potential mechanisms for the up-regulation of cGAS/STING-induced IFN-β secretion in C5aR2 KO cells, pathway analysis was performed on C5a-stimulated grouped C5aR1 KO cells vs C5a-stimulated WT cells, STING agonist-stimulated grouped C5aR1 KO cells vs STING agonist-stimulated WT cells, C5a-stimulated grouped C5aR2 KO cells vs C5a-stimulated WT cells, and STING agonist-stimulated grouped C5aR2 KO cells vs STING agonist-stimulated WT cells. Three independent methods were employed to analyse the data (**Figure 6.15**).

The first was GSEA of differentially expressed genes to identify significantly regulated KEGG pathways, conducted by You Zhou and Van Dien Nguyen (Cardiff University) (**Figure 6.15 A**). This approach analysed all differentially expressed genes visualised in the volcano plots and reported the most significantly regulated pathways for the selected comparisons. No genes were excluded from this analysis, which may allow effects common across all groups, such as residual effects of CRISPR-Cas9, to skew the results.

To address this limitation, a second complementary approach was taken to perform an unbiased comparative analysis using STRINGdb and PANTHERdb by Lee Booty (GSK) (**Figure 6.15 B**). Unique, genotype-dependent, treatment-dependent significantly regulated genes were identified. Thresholds were applied to the data ($p \leq 0.05$, $\log_2 FC < \pm 1$, and significantly regulated genes that were common across genotypes or treatments were excluded. These unique significantly differentially expressed genes were analysed using STRINGdb to identify an interactome from published interactions, and analysed further using PANTHERdb to generate a pathway analysis using the GO Biological Process gene lists. This approach aimed to reduce the impact of agonism-generic responses, potential C5aR1-C5aR2 cross-talk and CRISPR-Cas9 effects on the cells in order to identify more physiologically relevant significantly differentially expressed genes, however any pathways shared between C5a and STING responses will not be detected.

The third approach was a biased assessment of the significantly regulated pathways identified in the first approach, identifying pathways relevant to inflammation and immunity. The gene lists from KEGG were highlighted in volcano plots of all differentially regulated genes to indicate their significance and magnitude. This approach aimed to focus on curated pathways with known relevance to IFN-β, the cGAS-STING pathway and the immune response, in order to investigate genes that were most likely involved in the IFN-β amplification phenotype in C5aR2 KO cells. This method may omit novel pathways, but aimed to contextualise the effect of C5aR2 KO on IFN-β within well-characterised inflammatory pathways.

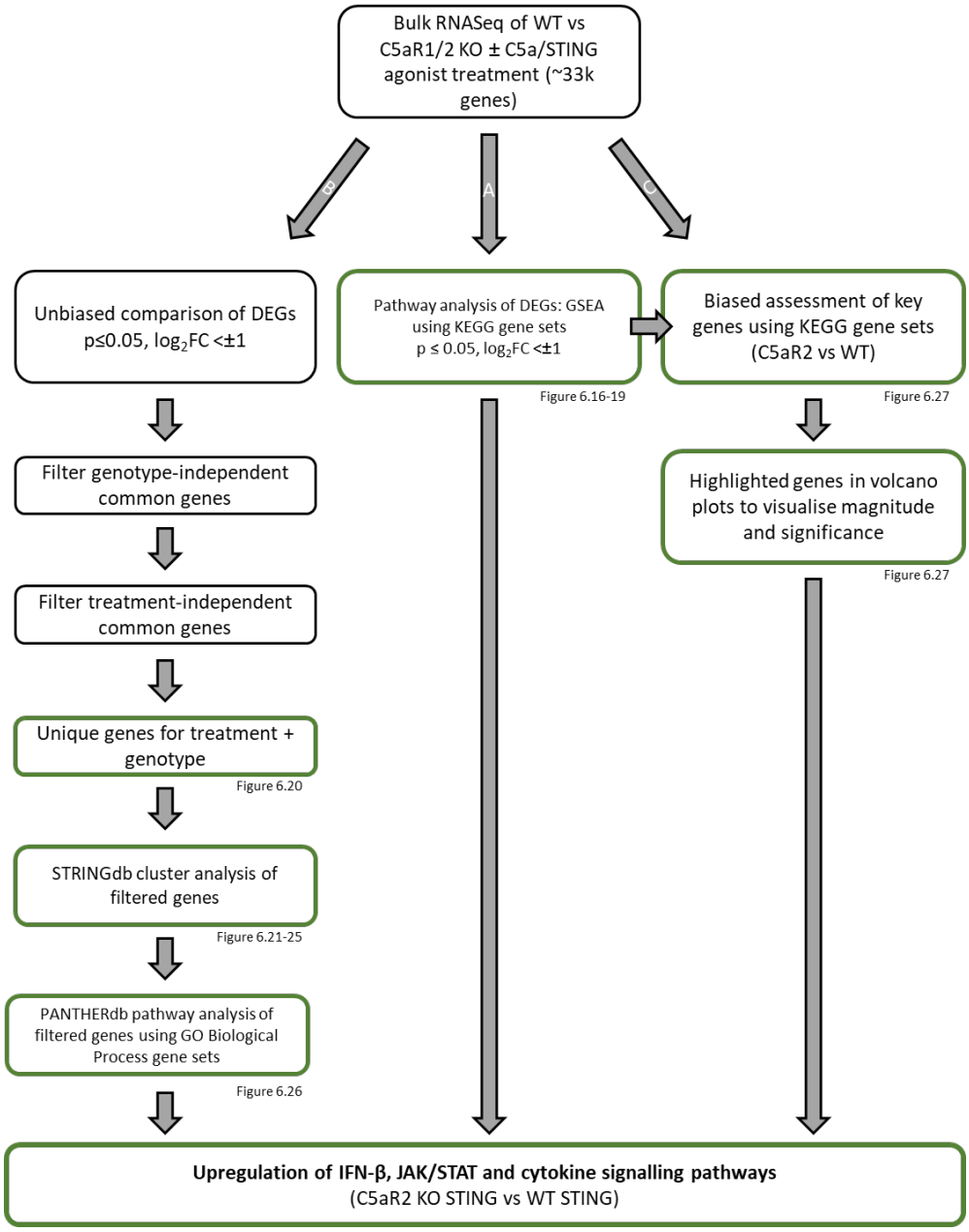

Figure 6.15. Analysis pipeline for Differentially Expressed Gene data. Three approaches were taken to analyse and interpret the Differentially Expressed Gene data from the RNAseq experiment. **A.** GSEA was performed by Van Dien Nguyen and You Zhou (Cardiff University), revealing significantly regulated KEGG gene sets. **B.** Unique, genotype-dependent, treatment-dependent significantly regulated genes ($p \leq 0.05$, $\log_2FC < \pm 1$) were identified by Lee Booty (GSK). Cluster analysis was performed using STRINGdb, and pathway analysis using GO Biological Process gene sets was performed using PANTHERdb. **C.** Significantly regulated KEGG gene sets from **A.** were manually triaged, selecting for unique pathways for each condition, genotype-specific stimulation-independent pathways, or genotype-independent stimulation-independent pathways, filtering out stimulation-specific genotype-independent pathways or pathways common to all conditions. Significantly regulated pathways from C5aR2 KO vs WT cells (C5a or STING agonist-treated) related to inflammation were manually curated. Gene lists were generated using selected C5aR2-dependent KEGG gene sets, and individual genes were marked in Volcano plots for STING agonist-treated C5aR2 KO cells vs STING agonist-treated WT cells. Green boxes indicate results with Figure reference.

6.2.4.1.1. Gene Set Enrichment Analysis

The first approach was GSEA on all differentially expressed genes to identify significantly regulated KEGG pathways. GSEA revealed significantly differentially regulated pathways for each comparison. In the C5a-treated C5aR1 KO pathway analyses, there is a wide variety of significantly regulated inflammatory pathways and cell signalling pathways compared to WT cells, including B cell receptor signalling, Type II diabetes mellitus, oxidative phosphorylation and others (**Figure 6.16**). This demonstrates that C5a-induced function of C5aR1 is important in the immune response. In the STING agonist-treated C5aR1 KO pathway analysis, there is a similar range of key cell signalling pathways which are modulated by C5aR1 KO compared to WT cells, including calcium signalling, natural killer cell signalling, NLR signalling, p53, TLR signalling and others (**Figure 6.18**). Further analysis of both is required to identify key genes involved in the response to each ligand.

In the C5aR2 KO pathway analyses, a theme of antiviral signalling emerged. C5a-treated C5aR2 KO cells have significantly up-regulated Cytosolic DNA Sensing, RIG-I-Like Receptor Signalling, JAK/STAT signalling, NOD-Like Receptor signalling pathways compared to WT cells (**Figure 6.17**), and STING agonist-treated C5aR2 KO cells have significantly up-regulated JAK/STAT signalling and Cytosolic DNA Sensing pathways compared to WT cells (**Figure 6.19**). This regulation occurs independently of stimulation, and occurs at baseline (**Supplementary Figure 6.1**)**,** indicating that antiviral signalling is up-regulated in C5aR2 KO cells, and not dependent on STING agonism. Cytosolic DNA sensing is up-regulated at baseline and following STING agonism, whereas JAK/STAT signalling is not altered at baseline and is up-regulated following STING agonism. Across all conditions, there are significantly regulated DNA replication and repair pathways, which may be indicative of CRISPR-Cas9-dependent effects that are generic across all KO cells. These must be disregarded to prevent them from skewing the pathway analysis data.

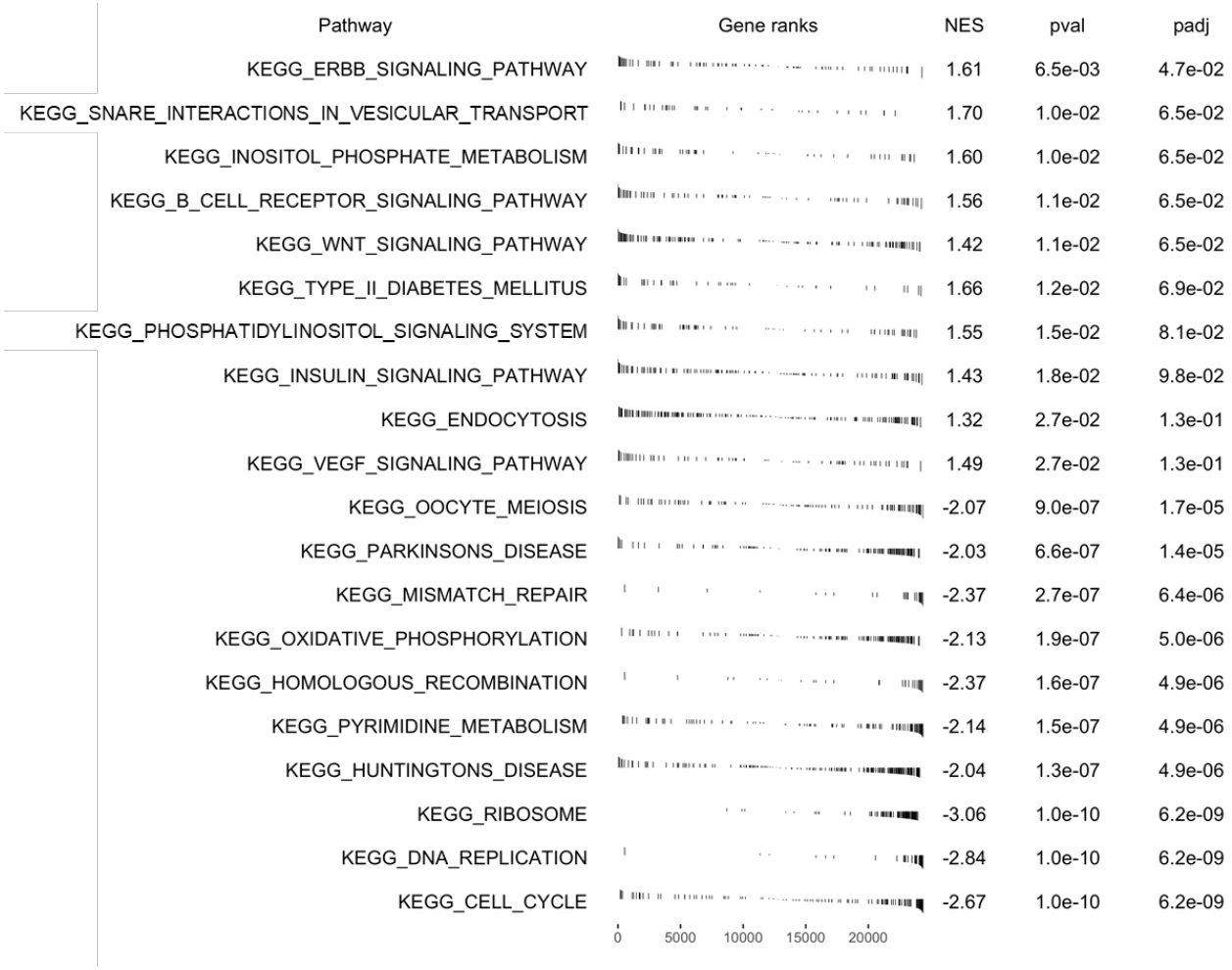

Figure 6.16. Pathway analysis for C5a-treated C5aR1 KO cells vs C5a-treated WT cells. GSEA was performed by Van Dien Nguyen and You Zhou (Cardiff University), revealing the most significantly regulated KEGG gene sets ($p \leq 0.05$) for C5a-treated C5aR1 KO cells vs C5a-treated WT cells. Genes in each pathway were ranked according to their directional regulation within the gene set, indicated by NES. p values and adjusted p values are reported.

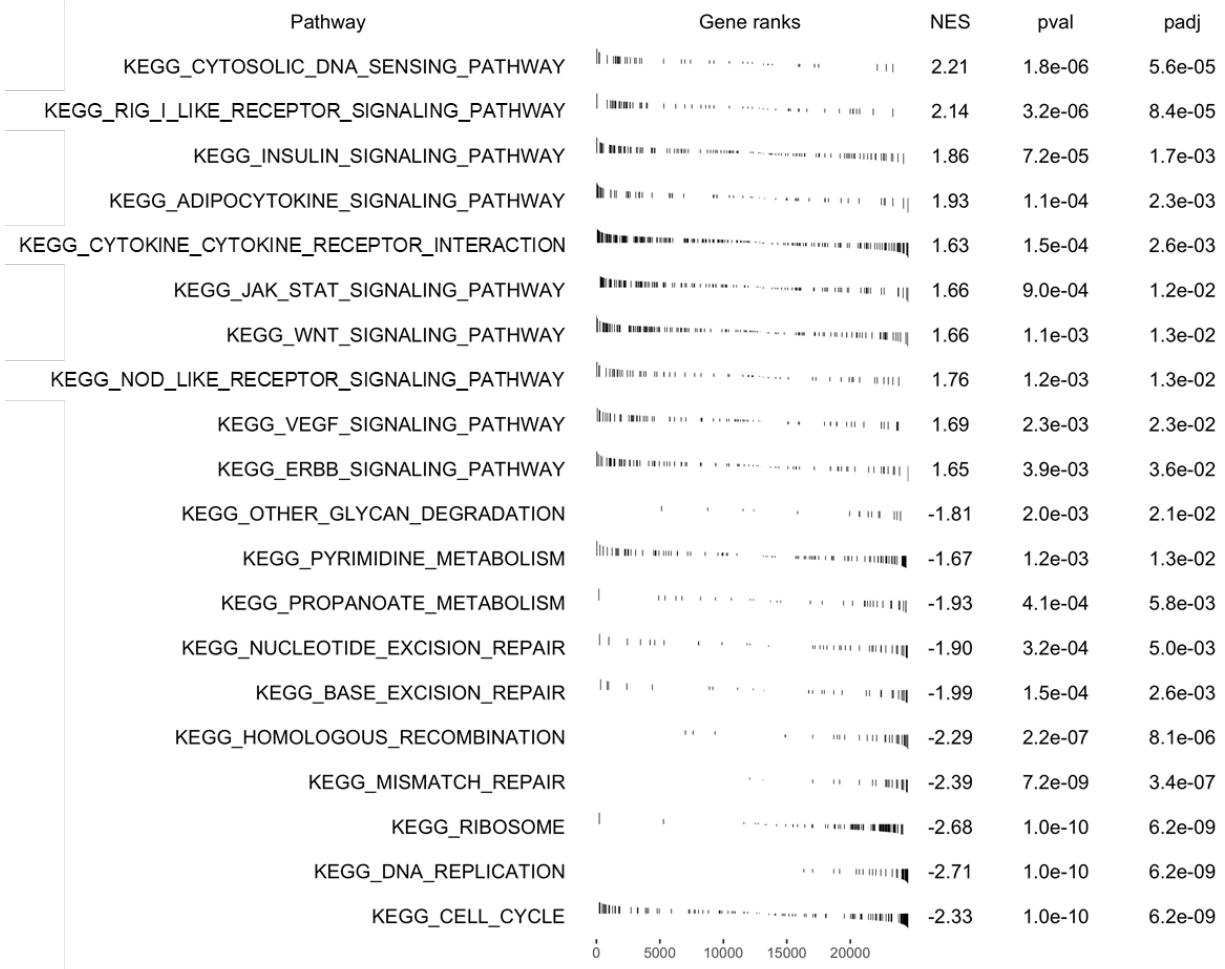

Figure 6.17. Pathway analysis for C5a-treated C5aR2 KO cells vs C5a-treated WT cells. GSEA was performed by Van Dien Nguyen and You Zhou (Cardiff University), revealing the most significantly regulated KEGG gene sets (p≤0.05) for C5a-treated C5aR2 KO cells vs C5a-treated WT cells. Genes in each pathway were ranked according to their directional regulation within the gene set, indicated by NES. p values and adjusted p values are reported.

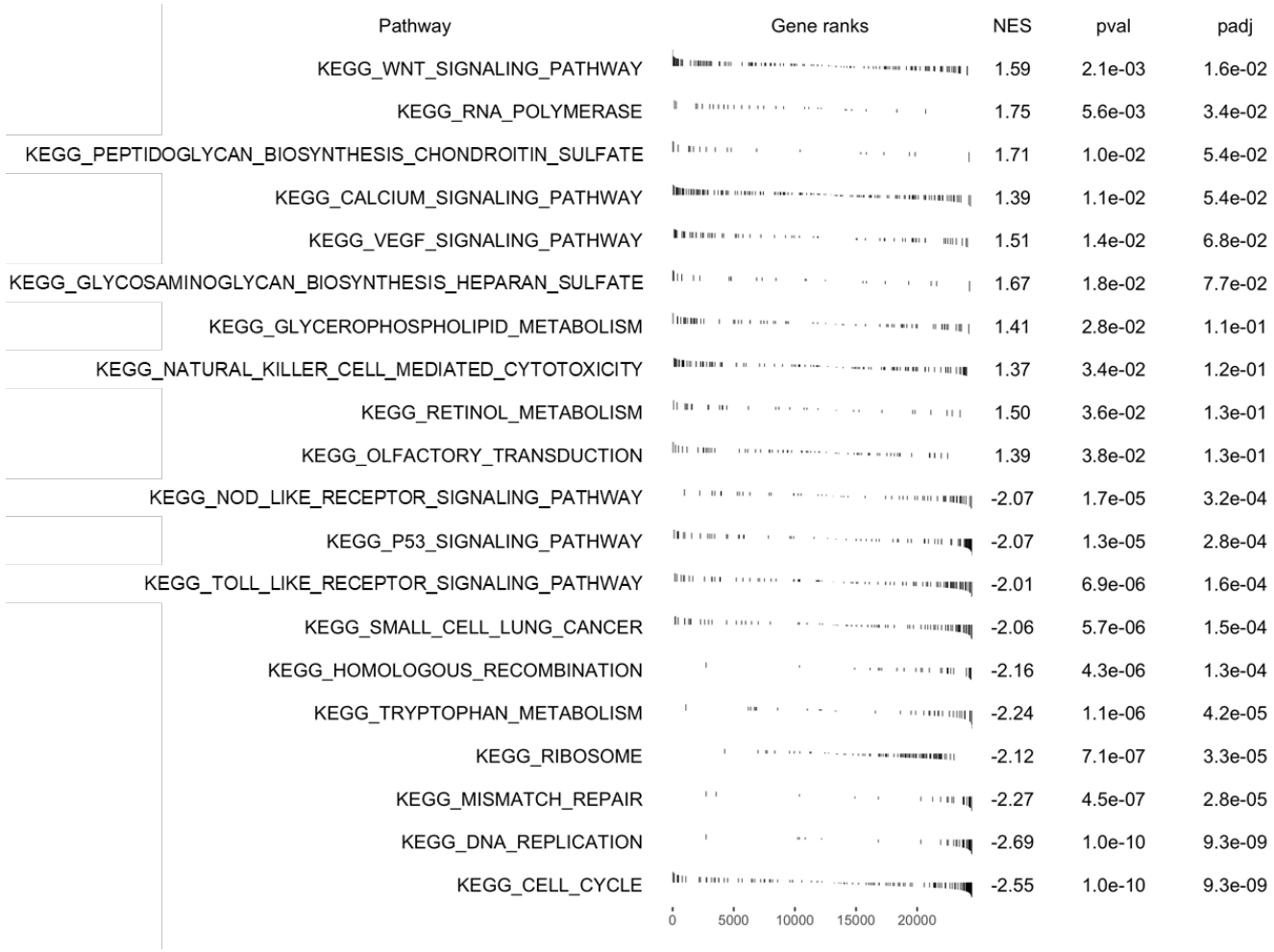

Figure 6.18. Pathway analysis for STING agonist-treated C5aR1 KO cells vs STING agonist-treated WT cells. GSEA was performed by Van Dien Nguyen and You Zhou (Cardiff University), revealing the most significantly regulated KEGG gene sets ($p \leq 0.05$) for STING agonist-treated C5aR1 KO cells vs STING agonist-treated WT cells. Genes in each pathway were ranked according to their directional regulation within the gene set, indicated by NES. p values and adjusted p values are reported.

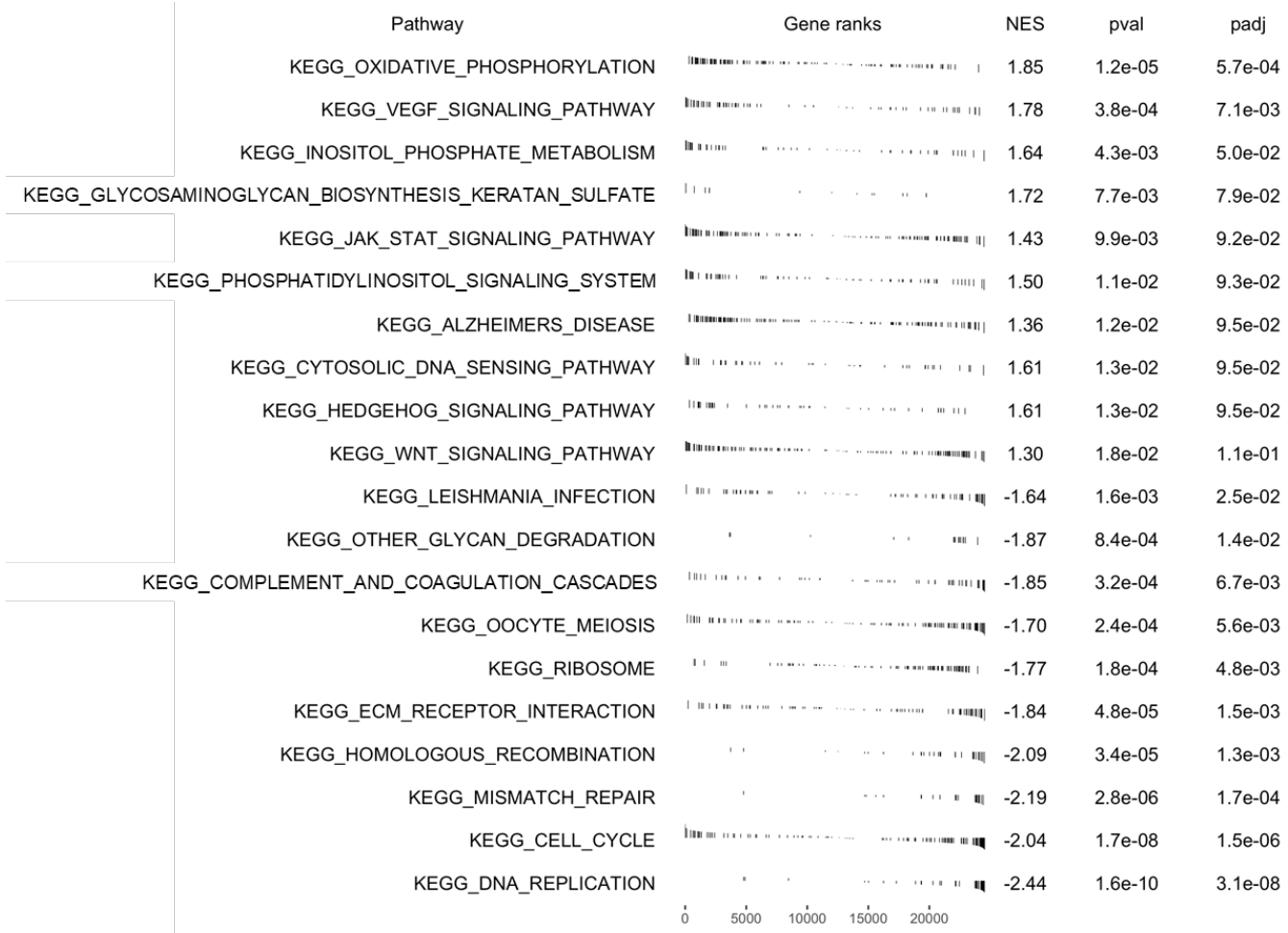

Figure 6.19. Pathway analysis for STING agonist-treated C5aR2 KO cells vs STING agonist-treated WT cells. GSEA was performed by Van Dien Nguyen and You Zhou (Cardiff University), revealing the most significantly regulated KEGG gene sets ($p \leq 0.05$) for STING agonist-treated C5aR2 KO cells vs STING agonist-treated WT cells. Genes in each pathway were ranked according to their directional regulation within the gene set, indicated by NES. p values and adjusted p values are reported.

6.2.4.1.2. STRINGdb and PANTHERdb analyses

The second approach aimed to filter out genes common to a treatment condition or common to a genotype, to reduce the impact of the baseline response to agonism or the baseline effect of CRISPR-Cas9 on the pathway analysis. To investigate the significant differentially expressed genes in more detail, unique genotype-dependent, treatment-dependent significantly regulated genes were identified (**Figure 6.20**). Genes which were regulated in both C5aR1 KO and C5aR2 KO cells compared to WT cells in each treatment condition were filtered out first, leaving genotype-dependent regulated genes. Genes which were regulated in response to 2 or more treatment conditions within a cell type (C5aR1 KO or C5aR2 KO compared to WT cells) were filtered out next, leaving treatment-dependent regulated genes.

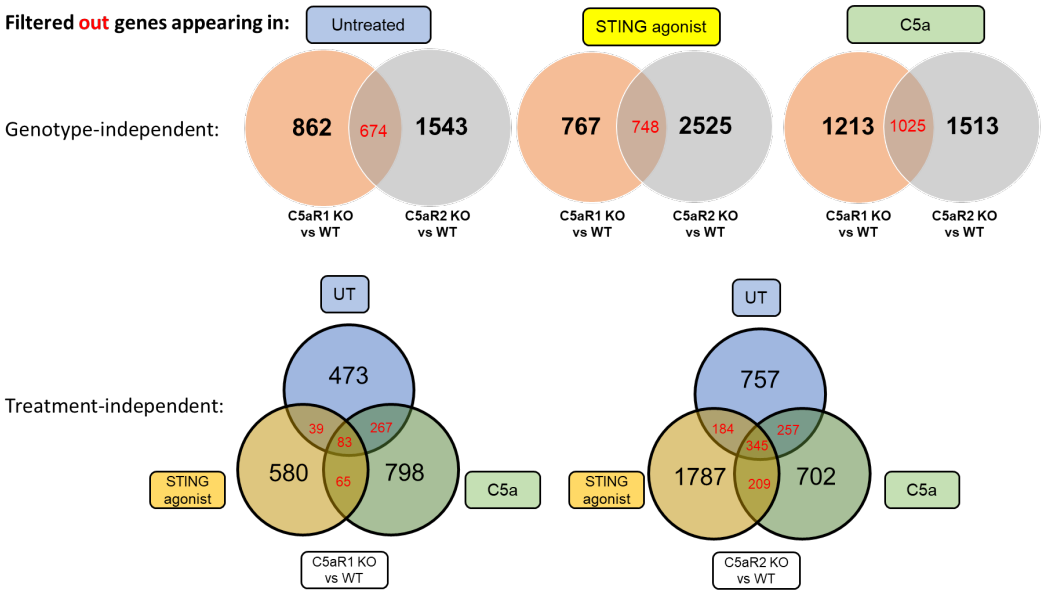

Figure 6.20. Unique genotype-dependent, treatment-dependent significantly regulated genes. Significance and fold change thresholds were applied to the list of differentially regulated genes ($p \leq 0.05$, $\log_2 FC < \pm 1$). Significantly regulated genes in C5aR1 KO cells and C5aR2 KO cells across all treatments were filtered out, followed by significantly regulated genes present in untreated, C5a-treated and STING agonist-treated C5aR1 KO or C5aR2 KO cells, generating a list of unique significantly regulated genes for each KO cell line. This triage was performed by Lee Booty (GSK).

These unique genotype-dependent, treatment-dependent, significantly regulated gene lists were used to further analyse the response to STING agonism in C5aR1/2 KO cells. There were more unique genes regulated by STING agonism in C5aR2 KO cells (1787) compared to C5aR1 KO cells (702), indicating that there was a C5aR2 KO-dependent effect on the response to STING activation (**Figure 6.20**). STRINGdb and PANTHERdb were then used to generate network and pathway analyses to investigate potential mechanisms driving the enhanced IFN-β signature in C5aR2 KO cells.

Lists of unique genotype-dependent, treatment-dependent, significantly regulated genes from STING-agonised C5aR1 KO cells and C5aR2 KO cells were used to generate an *in silico* network of published interactors using STRINGdb (**Figure 6.21-6.24**). Data were annotated with KEGG pathways to align with previous data (**Figures 6.16-6.19**), and significantly regulated KEGG pathways (false discovery rate ≤ 0.01) were indicated. Enrichments of pathways from alternative databases were also performed (**Supplementary Figure 6.3**).

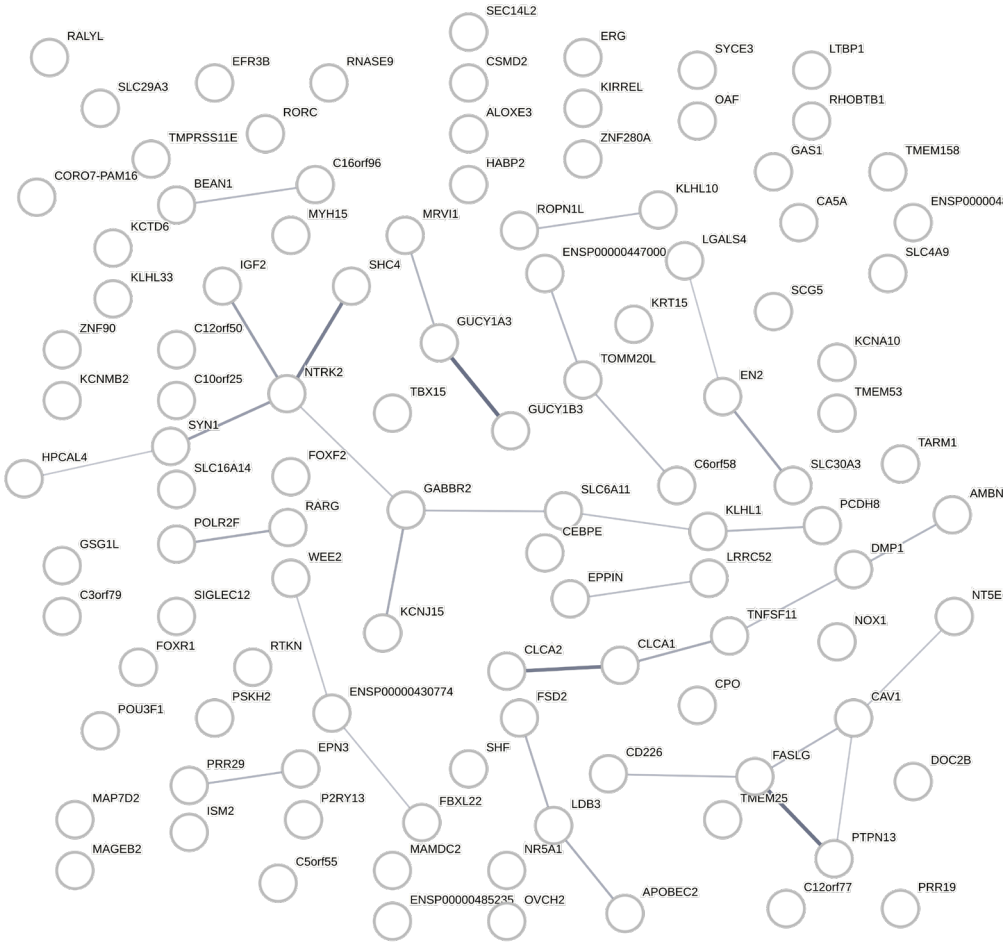

Figure 6.21. No significantly regulated pathways from unique significantly up-regulated genes in STING-agonised C5aR1 KO cells. STRINGdb was used to generate an interactome by Lee Booty (GSK). Unique genotype-dependent, treatment-dependent, significantly up-regulated genes from STING-agonised C5aR1 KO cells compared to STING-agonised WT cells were clustered. There were no KEGG pathways with false discovery rate ≤ 0.01.

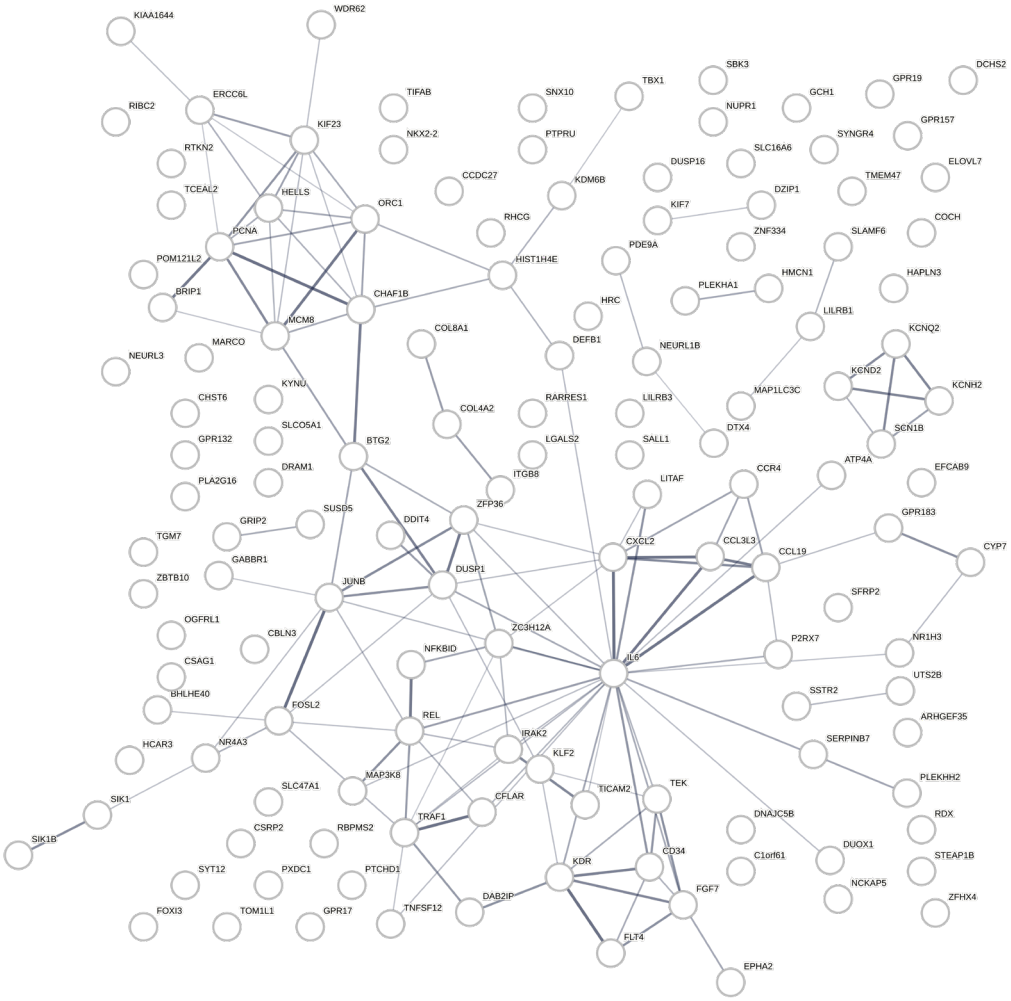

Figure 6.22. No significantly regulated pathways from unique significantly down-regulated genes in STING-agonised C5aR1 KO cells. STRINGdb was used to generate an interactome by Lee Booty (GSK). Unique genotype-dependent, treatment-dependent, significantly down-regulated genes from STING-agonised C5aR1 KO cells compared to STING-agonised WT cells were clustered. There were no KEGG pathways with false discovery rate ≤ 0.01.

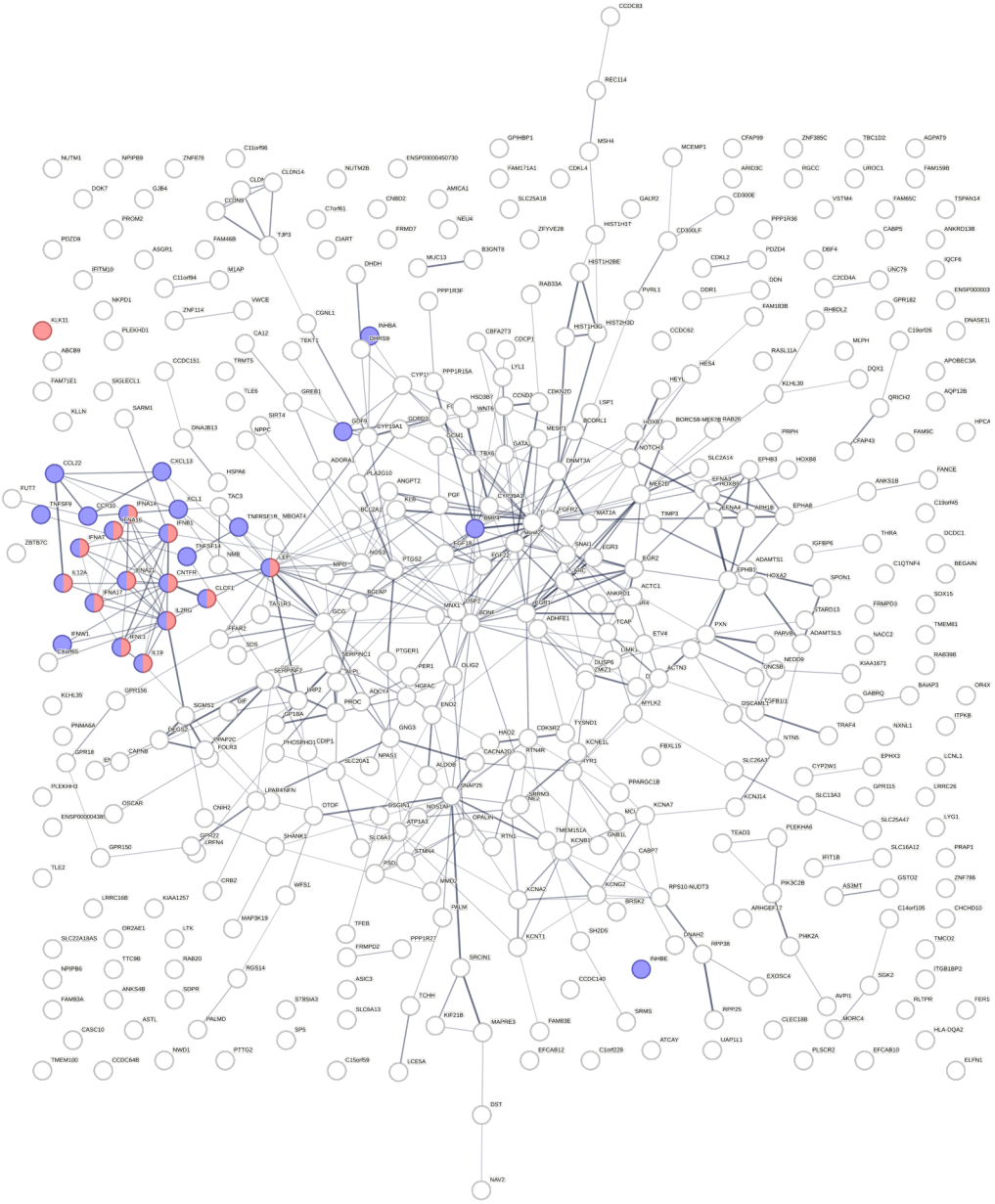

Figure 6.23. Significantly regulated pathways from unique significantly up-regulated genes in STING-agonised C5aR2 KO cells. STRINGdb was used to generate an interactome by Lee Booty (GSK). Unique genotype-dependent, treatment-dependent, significantly up-regulated genes from STING-agonised C5aR2 KO cells compared to STING-agonised WT cells were clustered. KEGG pathways with false discovery rate ≤ 0.01 were marked in red (Cytokine-cytokine receptor interaction) or blue (JAK/STAT signalling pathway).

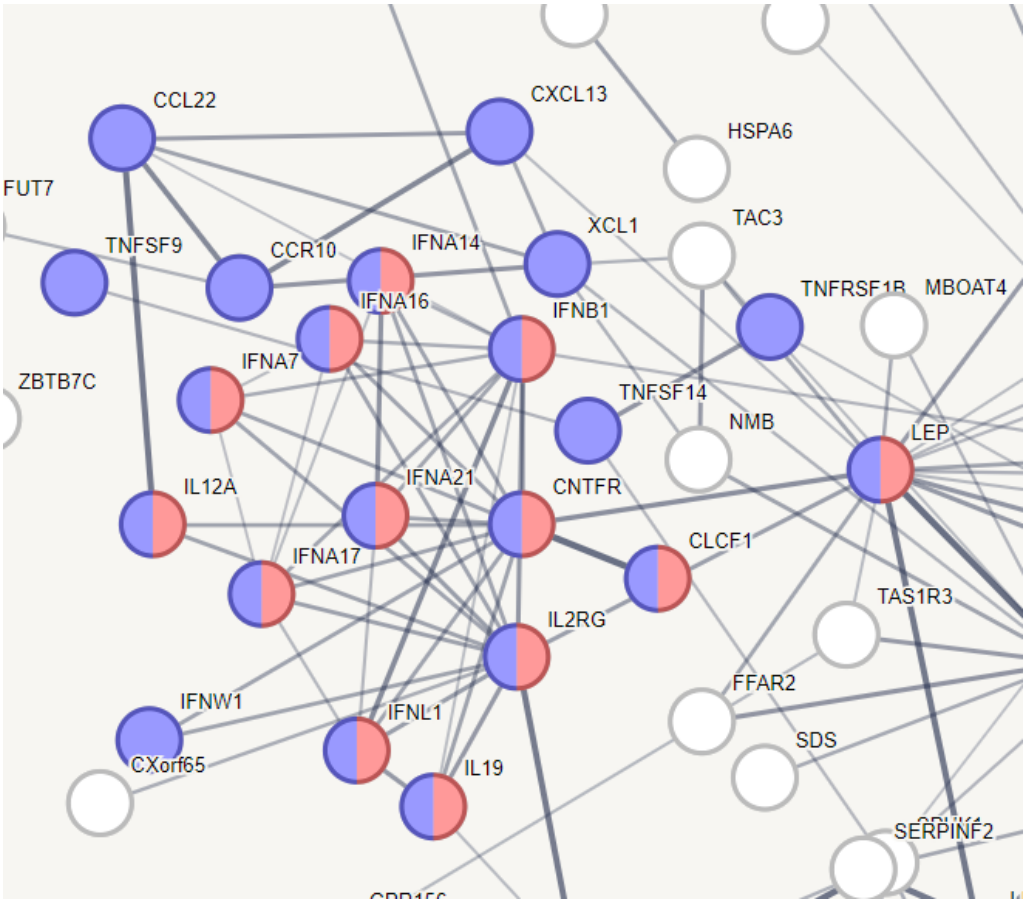

Figure 6.24. STRINGdb interactome reveals novel significantly up-regulated pathways clustered around IFN-β in STING-agonised C5aR2 KO cells. STRINGdb was used to generate an interactome by Lee Booty (GSK). Unique genotype-dependent, treatment-dependent, significantly up-regulated genes from STING-agonised C5aR2 KO cells compared to STING-agonised WT cells were clustered. KEGG pathways with false discovery rate ≤ 0.01 were marked in red (Cytokine-cytokine receptor interaction) or blue (JAK/STAT signalling pathway). The cluster-rich region from **Figure 6.23** was cropped to highlight individual genes.

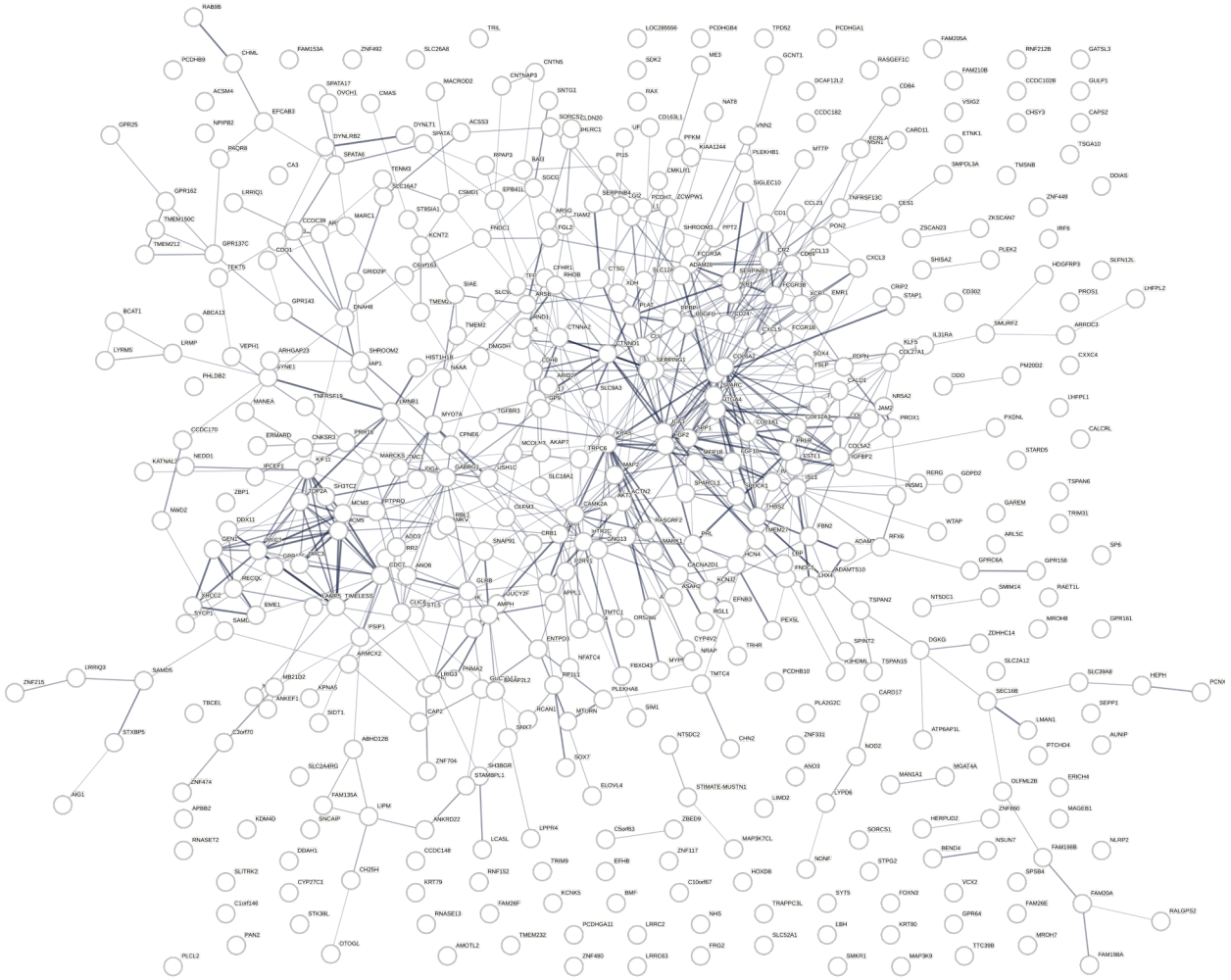

Figure 6.25. No significantly regulated pathways from unique significantly down-regulated genes in STING-agonised C5aR2 KO cells. STRINGdb was used to generate an interactome by Lee Booty (GSK). Unique genotype-dependent, treatment-dependent, significantly down-regulated genes from STING-agonised C5aR2 KO cells compared to STING-agonised WT cells were clustered. There were no KEGG pathways with false discovery rate ≤ 0.01.

In the C5aR1 KO analysis, weak clusters were generated, and there were no significantly up-regulated (**Figure 6.21**) or down-regulated (**Figure 6.22**) KEGG pathways. In the C5aR2 KO analysis, however, there was a stronger clustering of up-regulated (**Figure 6.23**) and down-regulated (**Figure 6.25**) genes. There were significantly up-regulated KEGG pathways (**Figure 6.24**) centred on IFN-β, which reflect the results of *in vitro* work in **Chapter 5**, where C5aR2 KO significantly up-regulated cGAS/STING-induced IFN-β secretion. Antiviral signalling pathways were also significantly up-regulated in the C5aR2 KO vs WT GSEA pathway analyses (**Figure 6.17, 6.19**). The significantly up-regulated genes in the cluster are members of the JAK/STAT signalling pathway KEGG gene list and the Cytokine-cytokine receptor interaction KEGG gene list (**Figure 6.24, Supplementary Figure 6.3**).

This analysis revealed a list of unique genotype-dependent, treatment-dependent, significantly up-regulated genes from significantly up-regulated KEGG pathways (**Table 6.2**). These genes are of interest as potential interactors of C5aR2 which lead to up-regulation of the cGAS-STING pathway proteins and the IFN-β response in C5aR2 KO cells.

KEGG Pathway	Gene Symbol
Cytokine-cytokine receptor	CCL22
	CCR10
	CLCF1
	CNTFR
	CXCL13
	IFNA14
	IFNA16
	IFNA17
	IFNA21
	IFNA7
	IFNB1
	IFNL1
	IFNW1
	IL12A
	IL19
	IL2RG
	LEP
	TNFRSF1B
	TNFSF9
	TNFSF14
	XLC1
JAK/STAT signalling pathway	CLCF1
	CNTFR
	IFNA14
	IFNA16
	IFNA17
	IFNA21
	IFNA7
	IFNB1
	IFNL1
	IL12A
	IL19
	IL2RG
	LEP

Table 6.2. Summary of STRINGdb analysis. Unique genotype-dependent, treatment-dependent, significantly up-regulated genes from significantly up-regulated KEGG pathways in **Figure 6.24.**

Lists of unique genotype-dependent, treatment-dependent, significantly regulated genes from STING-agonised C5aR1 KO cells and C5aR2 KO cells were then subjected to pathway analysis using PANTHERdb and GO Biological Processes gene sets (**Figure 6.26**). This analysis revealed that several immune cell signalling and metabolic pathways were up-regulated in C5aR1 KO and C5aR2 KO cells in response to STING agonism. In the C5aR2 KO cells, there was a series of significantly up-regulated pathways, which were highly relevant to the *in vitro* cGAS-STING pathway and IFN-β results from **Chapter 5**, and conserved with the results of the pathway analysis on untriaged differentially expressed genes in **Figure 6.19.** Response to virus, cellular response to virus, cellular response to Type I interferon and Type I interferon signalling pathways were significantly up-regulated in STING-agonised C5aR2 KO cells vs WT cells, which is in direct concordance with the observed up-regulation of STING-induced IFN-β secretion in C5aR2 KO cells. Genes in these pathways are potential interactors of C5aR2, which could drive the effect in the C5aR2 KO cells, and warrant further investigation.

Regulation of peptidyl-serine phosphorylation of STAT protein is represented in the GSEA results, where STING-agonised C5aR2 KO cells have significantly up-regulated JAK-STAT signalling pathways (**Figure 6.19)**. JAK/STAT signalling pathway is also significantly up-regulated in the STRINGdb cluster analysis (**Figure 6.24**). This result suggests that JAK-STAT signalling is likely related to the function of C5aR2 in the context of STING agonism.

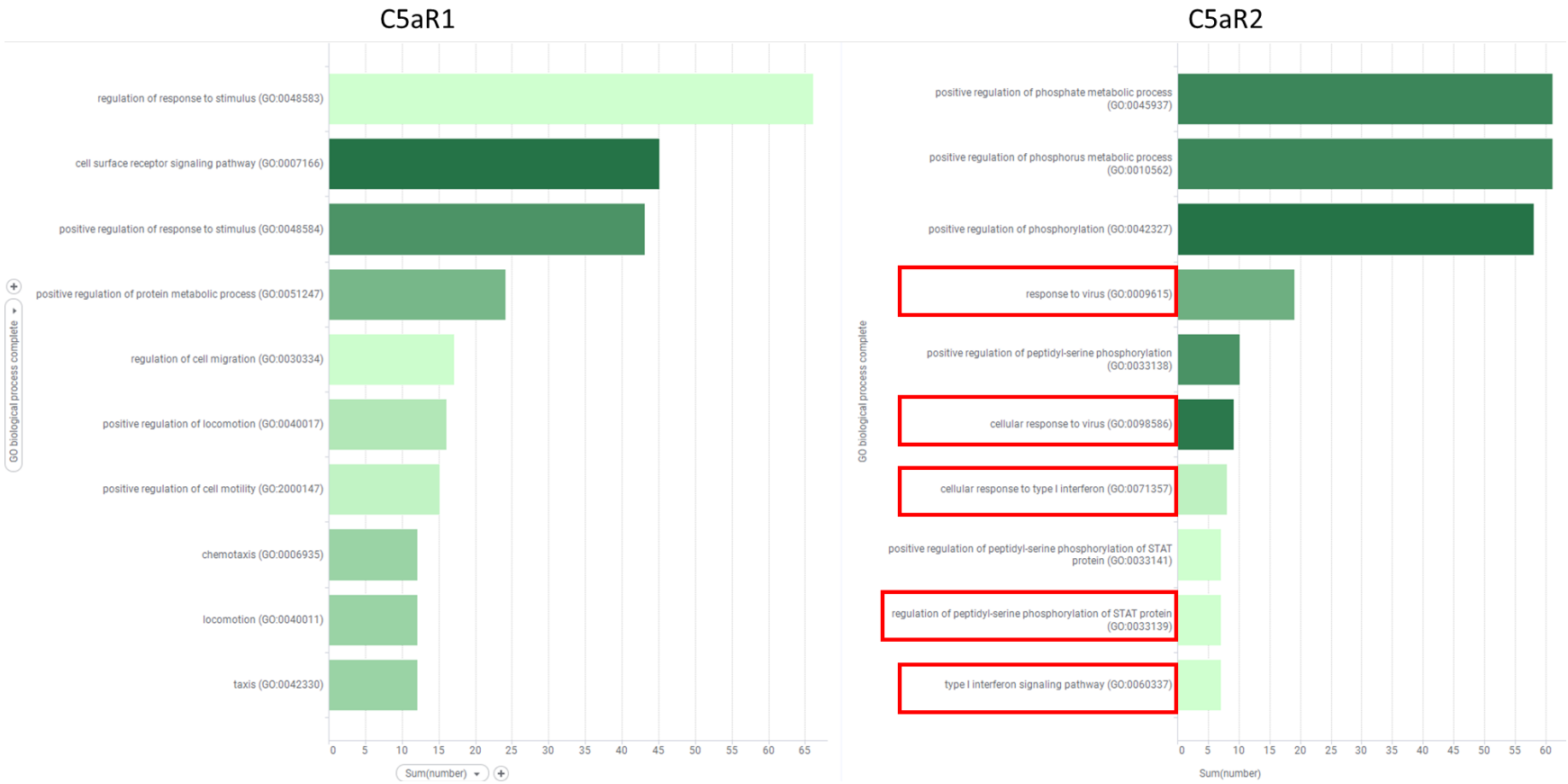

Figure 6.26. PANTHERdb Pathway analysis reveals top regulated pathways in STING-agonised C5aR1 and C5aR2 KO cells. PANTHERdb was used to generate a pathway analysis using GO Biological Process gene lists by Lee Booty (GSK). Unique genotype-dependent, treatment-dependent, significantly up- or down-regulated genes from STING-agonised C5aR1 KO cells or C5aR2 KO cells compared to STING-agonised WT cells were analysed. Top 10 significantly up-regulated pathways were reported and antiviral pathways in C5aR2 KO cells were marked in red.

6.2.4.1.3. Manual curation of inflammatory pathways

To complement the KEGG analysis above, the third approach involved the manual curation of significantly regulated pathways from the GSEA (**Figure 6.27**). The curated pathway list was C5aR2-dependent but treatment-independent. The pathway list was biased towards inflammatory pathways, but not biased for treatment as there may be relevant genes which are shared between responses to C5a and STING agonism.

Significantly regulated KEGG pathways (**Figure 6.16-19**) were colour-coded according to their presence in unique conditions, genotype-specific conditions, stimulation-specific and genotype-independent conditions, genotype-independent and stimulation-independent conditions (potentially unique in 2 separate conditions), or in all conditions (**Figure 6.27 A**). These pathways were filtered to remove pathways that were common across all conditions (red) or a treatment-dependent effect (yellow) (**Figure 6.27 B**). The pathway list was then manually curated, selecting for C5aR2 KO-dependent effects that were related to inflammatory pathways (**Figure 6.27 C**). This curation aimed to select pathways which were likely to be significantly regulated based on the previous cGAS-STING pathway and IFN-β secretion data, in order to search for C5aR2-dependent genes which could account for the up-regulation of the response to STING agonism in C5aR2 KO cells. The gene lists were thereby reduced to a manageable number of genes in highly relevant pathways, and were then highlighted in volcano plots of normalised expression data summarising global differentially expressed genes (**Figure 6.27 D**). This result identifies genes in the curated pathways were significantly regulated in STING-agonised C5aR2 KO cells compared to STING-agonised WT cells.

All three approaches converged on a similar set of results, wherein key inflammatory pathways were identified for the C5aR2-dependent regulation of antiviral signalling.

A.

	C5aR1 KO		C5aR2 KO	
	C5a	STING	C5a	STING
Up	ERBB signaling	WNT signaling	Cytosolic DNA sensing	Oxidative phosphorylation
	SNARE interactions	RNA polymerase	RLR signaling	VEGF signaling*
	Inositol phosphate metabolism	Glycosaminoglycan biosynthesis chondroitin sulfate	Insulin signaling	Inositol phosphate metabolism
	BCR signaling	Glycerophospholipid metabolism	Adipocytokine signaling	Glycosaminoglycan biosynthesis keratan sulfate
	WNT signaling	NK cell cytotoxicity	Cytokine cytokine receptor interaction	JAK STAT signaling
	Type 2 diabetes	Retinol metabolism	JAK STAT signaling	Alzheimers
	Phosphatidylinositol signaling	Olfactory transduction	WNT signaling	Cytosolic DNA sensing
	Insulin signaling		NLR signaling	Hedgehog signaling
	Endocytosis		VEGF signaling	WNT signaling
	VEGF signaling		ERBB signaling	
Down	Cell cycle	Cell cycle	Cell cycle	DNA replication
	DNA replication	DNA replication	DNA replication	Cell cycle
	Ribosome	Mismatch repair	Ribosome	Mismatch repair
	Huntingtons	Ribosome	Mismatch repair	Homologous recombination
	Pyrimidine metabolism	Tryptophan metabolism	Homologous recombination	ECM receptor interaction
	Homologous recombination	Homologous recombination	Base excision repair	Ribosome
	Oxidative phosphorylation	Small cell lung cancer	Nucleotide excision repair	Oocyte meiosis
	Mismatch repair	TLR signaling	Propanoate metabolism	Complement and coagulation cascades
	Parkinsons	P53 signaling	Pyrimidine metabolism	Glycan degradation
	Oocyte meiosis	NLR signaling	Glycan degradation	Leishmania infection

Unique
Genotype specific, stimulation independent
Stimulation specific, genotype independent
Common to all
Genotype independent, stimulation independent

B.

	C5aR1 KO vs WT		C5aR2 KO vs WT	
	C5a	STING agonist	C5a	STING agonist
Up-regulated	SNARE interactions	RNA polymerase	RLR signaling	Glycosaminoglycan biosynthesis keratan sulfate
	BCR signaling	Glycosaminoglycan biosynthesis chondroitin sulfate	Adipocytokine signaling	Alzheimers
	Type 2 diabetes	glycerophospholipid metabolism	Cytokine cytokine receptor interaction	Hedgehog signaling
	Phosphatidylinositol signaling	NK cell cytotoxicity	Cytosolic DNA sensing	JAK STAT signaling
	Endocytosis	Retinol metabolism	JAK STAT signaling	Cytosolic DNA sensing
	Inositol phosphate metabolism	Olfactory transduction	NLR signaling	Oxidative phosphorylation
				Inositol phosphate metabolism
Down-regulated	Huntingtons	Tryptophan metabolism	Base excision repair	ECM receptor interaction
	Parkinsons	Small cell lung cancer	Nucleotide excision repair	Complement and coagulation cascades
	Oxidative phosphorylation	TLR signaling	Propanoate metabolism	Leishmania infection
	Oocyte meiosis	P53 signaling	Glycan degradation	Glycan degradation
		NLR signaling		Oocyte meiosis

↓

C.

C5aR2 KO-dependent inflammatory pathways	
	Pathway of interest
Up-regulated	RLR signaling
	adipocytokine signaling
	Cytokine cytokine receptor interaction
	Cytosolic DNA sensing
	JAK STAT signaling
	NLR signaling
Down-regulated	Complement and coagulation cascades
	ECM receptor interaction
	Leishmania infection

D.

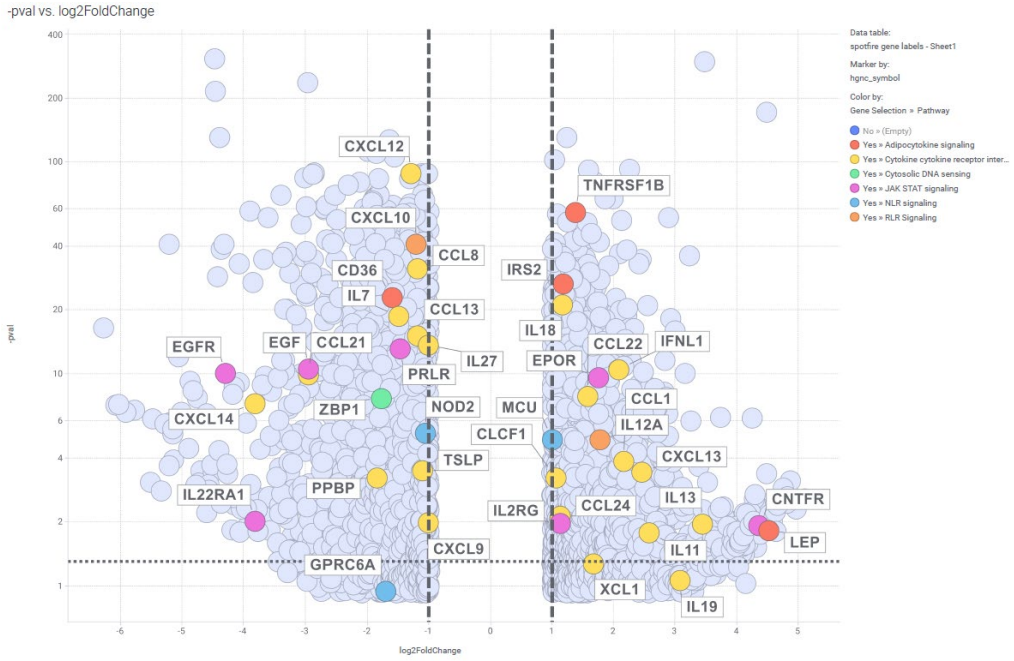

Figure 6.27. Manual curation of significantly regulated KEGG pathways identifies key significantly regulated genes in STING agonist-treated C5aR2 KO cells vs WT cells. A. Significantly regulated pathways from GSEA were colour-coded according to their commonality between conditions. **Green** pathways are unique to that comparison. **Blue** pathways are significantly regulated in C5aR1 KO or C5aR2 KO vs WT, independent of treatment. **Yellow** pathways are significantly regulated in C5a-treated C5aR1 KO and C5aR2 KO cells vs WT, independent of genotype. **Red** pathways are significantly regulated in all comparisons. **Orange** pathways are genotype-independent and treatment-independent but appear in more than one comparison. **B.** **Red** and **Yellow** pathways were filtered out. **C.** Remaining pathways were manually curated to identify C5aR2 KO-dependent inflammatory pathways. **D.** Genes from the selected pathways (**Supplementary Figure 6.2**) were highlighted in a Volcano plot.

6.3. Discussion

6.3.1. Summary

This RNAseq experiment primarily aimed to investigate the mechanism of C5aR2-dependent regulation of the cGAS-STING pathway. The link between C5aR2 and STING was first identified using selective peptide agonists [8], and was confirmed and characterised in **Chapter 5**. This study also aimed to generate a dataset which could be used to characterise the fundamental signalling function of C5aR2. C5aR2 negatively regulates C5aR1-induced ERK1/2 phosphorylation [72], and there has been a single and limited phospho-proteomic study performed [75], however no comprehensive mechanism for C5aR2 function has been reported previously.

The key findings of this study confirmed the enhanced antiviral phenotype of C5aR2 KO THP-1 cells. Three separate analysis approaches converged on the up-regulation of key antiviral signalling pathways in the C5aR2 KO cells. GSEA revealed up-regulation of JAK/STAT, cytosolic DNA sensing and RLR signalling pathways in C5aR2 KO cells. C5aR2 KO cells had up-regulated nucleic acid sensing pathways at baseline (**Supplementary Figure 6.1**) and following STING agonism (**Figure 6.19**) compared to WT cells. This suggests that the absence of C5aR2 primes these cells to respond to exogenous nucleic acid, indicating that C5aR2 negatively regulates immune sensing of nucleic acid at baseline in WT cells. Following STING activation, subsequent IFN release and IFN receptor activation, JAK/STAT signalling is also increased in C5aR2 KO cells. It is not clear whether the increased priming of nucleic acid sensing pathways drives a stronger JAK/STAT response, or whether JAK/STAT signalling was independently up-regulated, but future work could explore the relationship between C5aR2 and both sensing and responses to nucleic acids.

This observation was confirmed using additional pathway analyses. Following data filtering to reduce the potential impact of cell line-specific effects and CRISPR-Cas9

effects, unbiased STRINGdb clustering revealed STING agonist-dependent up-regulation of JAK/STAT signalling pathways, cytokine-cytokine receptor interaction pathways, and Type I interferon proteins in C5aR2 KO cells. Unbiased PANTHERdb pathway analysis demonstrated an up-regulation of viral response, Type I IFN signalling and STAT phosphorylation pathways. Additionally, the biased STING-agonised C5aR2 KO vs WT KO comparison revealed a list of regulated genes in inflammatory and antiviral pathways. All analyses strongly reported a regulation of antiviral signalling. This experiment thereby yielded lists of specific genes and signalling pathways to focus on in future investigations.

6.3.2. Study Limitations - C5aR1 KO Clone C3

A caveat to this study was the behaviour of C5aR1 KO clone C3. C3 responded highly to STING agonism in the IFN-β ELISA, and was an outlier in the PCA on individual clones. Future work should focus on alternative C5aR1 KO clones B6, F11 and G8 rather than C3 where possible. However, differential gene expression and pathway analyses focussed on differentially regulated genes and pathways that were present across all clones in a KO group, reducing the impact of clone-specific effects. RNAseq pathway analyses were consistent between approaches, and the C5aR2 KO results were not impacted by this clone.

6.3.3. Future Work

A significant level of additional analysis could be performed on this dataset. The response to STING agonism in C5aR2 KO cells has been investigated using pathway analysis, however there are significantly regulated genes in C5a-stimulated C5aR2 KO cells vs WT cells. This suggests that C5aR2 has unique C5a-dependent function which could be better understood using data from this experiment. It is surprising that C5a had an effect on C5aR1 KO cells compared to WT. C5aR1 KO cells lack an extracellular receptor for C5a, as C5aR2 is intracellular at baseline. Passive uptake of C5a may have

led to intracellular receptor engagement, and may have driven C5aR2 to the cell surface, which could be confirmed using flow cytometry. The differential gene expression in C5aR1 KO THP-1 cells compared to WT may also be driven an unknown alternative receptor for C5a. This could be further explored using a C5aR1/2 double knockout, as there should be no differential response to C5a if there are no other receptors. Future work to characterise the specific responses detected in these cells may therefore reveal previously unexplored functions for C5a.

Additional analysis to characterise regulated pathways and identify key genes will be helpful to further investigate fundamental function and underlying signalling pathways of C5aR2. This approach could be further complemented using selective peptide agonists P32 and P59. Despite their inactivity in **Chapter 3**, the effect of C5aR2 KO on the cGAS-STING pathway described here and in **Chapter 5** confirms previously published observations generated using these agonists [8]. A confirmatory study using C5aR2 agonists may reveal the opposite effect to C5aR2 KO, and thereby aid in distinguishing constitutive functions of C5aR2 from ligand-dependent functions.

The results of this study confirm the C5aR2 KO antiviral phenotype reported in **Chapter 5**, where C5aR2 KO cells displayed an enhanced response to the cGAS-STING pathway, likely driven by enhanced expression of key cGAS-STING pathway proteins. The RNAseq results further develop this observation, highlighting a general up-regulation of the anti-viral response in C5aR2 KO cells, and identifying various key pathways and genes which could contribute mechanistically.C5aR2 is a negative regulator of the antiviral response in macrophages, and future work to assess its effect in physiologically relevant models of viral infection is required to confirm its physiological function and establish its potential as a therapeutic target.

Chapter 7 - Discussion

7. Discussion

7.1. Aims

This project aimed to investigate the function of C5aR2, which is historically a poorly-understood non-canonical anaphylatoxin receptor of the complement system [51]. Published studies have demonstrated its ability to modulate PRR-induced cytokine secretion [8], however the majority of the literature remains contradictory or controversial, and the tools available to study C5aR2 were poorly available.

This project aimed to study the role of C5aR2 in the context of innate immunity. Specifically, this project aimed to:

- Validate the effect of selective peptide agonists P32 and P59 on ERK1/2 phosphorylation in MDMs [72], and assess additional endpoints using the validated stimulation conditions.
- Generate stable monoclonal C5aR1 and C5aR2 KO THP-1 cell lines using CRISPR-Cas9 to use as a novel and reliable tool with which to study C5aR2.
- Validate C5aR2-dependent modulation of PRR-induced cytokine secretion [8] using the novel C5aR2 KO THP-1 cells, and investigate the underlying mechanisms using molecular biology approaches.
- Use RNAseq to identify key genes and pathways involved in the downstream signalling of C5aR2 following C5a stimulation, and in the context of PRR stimulation.

7.2. Summary of findings

A phospho-ERK1/2 assay was established using C5a and PMX53, however putative selective C5aR2 agonists P32 and P59 were not effective in these experiments. C5aR1 KO and C5aR2 KO THP-1 cells were therefore generated using CRISPR-Cas9, and characterised using DNA sequencing and flow cytometry. The study on PRR

modulation characterised a novel link between C5aR2 and cGAS/STING-induced IFN-β secretion. The follow-up RNAseq experiment demonstrated that IFN and antiviral pathways were significantly regulated in response to STING agonism in C5aR2 KO cells compared to WT cells, identifying potential mechanisms for C5aR2-mediated antiviral pathway regulation. These results implicate C5aR2 as a negative regulator of antiviral signalling in macrophages.

7.2.1. C5aR2 agonism using P32 and P59 failed to regulate C5aR1-induced ERK1/2 phosphorylation

C5aR2 has previously been reported to modulate C5aR1-induced ERK1/2 phosphorylation [72], however there is no proposed molecular mechanism. ERK1/2 phosphorylation was therefore selected as a C5aR2-dependent endpoint for this study. This project aimed to establish stimulation conditions for C5aR2, then expand on the literature by using them to assess the effect of C5aR2 on previously unstudied endpoints.

A robust experimental setup for C5aR1-induced ERK1/2 phosphorylation was successfully established in **Chapter 3**. The aim was to use this as an endpoint for C5aR2 activity, however, putative C5aR2 agonists P32 and P59 had no biological activity in this experimental setup. If they had functioned as previously demonstrated [72], the project aimed to titrate P32 and P59 against C5a-stimulated cells to identify effective concentrations for inhibiting C5aR1-induced ERK phosphorylation. The effective concentrations of P32 and P59 could then be used to activate C5aR2 independently, and alternative endpoints could be assessed to investigate its function, for example co-stimulating C5aR2 and PRRs to assess the effect of C5aR2 on pro-inflammatory cytokine secretion.

This approach would have allowed for functional studies of C5aR2 to be performed by using optimised stimulation conditions across a range of models of inflammation,

addressing the role of C5aR2 in each. However, the failure of P32 and P59 in this assay means that work was not possible without an alternative approach to manipulate C5aR2.

There are some potential explanations for the inactivity of P32 and P59 in these experiments. Firstly, C5aR2 may have been expressed intracellularly in these cells, meaning it may not have been accessible to the ligand. The subcellular location of C5aR2 is contested in the literature, and is likely cell type and context-dependent. C5aR2 was expressed intracellularly in THP-1 cells, as demonstrated in **Chapter 4** using flow cytometry. This subcellular location may have contributed to the lack of activity, as C5a, P32 and P59 may not have been able to engage their binding sites if C5aR2 was sequestered in the cytosol. This may also have affected published experiments in which C5aR2 is stimulated using extracellular C5a, P32 or P59 in the medium. P32 or P59, delivered extracellularly in the cell culture medium, has demonstrated biological activity [72]. However, it is unknown where C5aR2 was expressed in these cells, and whether it had trafficked to the plasma membrane due to co-stimulation with C5a [70] or PRR ligands. More work is required to understand the expression location of C5aR2, and the physiological source of its ligand. C5aR2 may require co-localisation with C5aR1 at the cell surface to make the C5a binding site accessible [70], or it may be activated by intracellular C5a [48] or non-canonical ligands to exert its function independently of C5aR1.

Secondly, the agonists were synthesised in-house by GSK chemists based on the published amino acid sequences. They may not have been synthesised in precisely the same manner as those used in previously published studies [72], leading to functional differences. A repeat of these experiments with aliquots of the original ligands may yield different results, matching those previously published.

Future work using phospho-ERK as an endpoint is possible, as the phospho-ERK assay was well-controlled and robust. Future experiments could include revisiting the assay using the C5aR1/2 KO cells. These experiments could initially confirm loss of ERK phosphorylation in the C5aR1 KO, and later assess the effect of C5aR2 KO on ERK phosphorylation, or the effect of C5aR2 ligation in the C5aR1 KO cells on ERK phosphorylation. However, the ligands are not commercially available, therefore a novel tool was required to continue the study of C5aR2 in this project. The generation of C5aR2 KO cells was the clear next step for the project, to provide a novel, robust and reliable tool with which to study C5aR2.

7.2.2. Generation of novel C5aR2 KO THP-1 cells using CRISPR-Cas9

The next series of experiments aimed to generate a novel C5aR2 KO cell line which could be used to study the effect of C5aR2 in subsequent experiments. CRISPR-Cas9 was used to generate C5aR1 KO and C5aR2 KO THP-1 cell lines, which were validated using DNA sequencing and flow cytometry, confirming loss of C5aR1/2 sequence and protein expression. Multiple studies have used C5aR2 KO mice to show pro- and anti-inflammatory effects of C5aR2 on disease models [51], however human C5aR2 KO cells have not been generated previously.

The C5aR2 KO cells are more physiologically relevant than mouse studies as they were generated with a human cell line, allowing for human-specific understanding at a cellular and molecular level which is not possible with *in vivo or ex vivo* experiments on mice. The KO cells also decreased the technical challenge of studying C5aR2, as they are immortalised and generate a limitless supply of cells, and can be cryopreserved for use in future experiments. These cells are also more reliable than experiments using the peptide agonists P32 and P59, as replicating published results was unsuccessful in this study. The C5aR2 KO cells have been well-characterised by sequencing and flow

cytometry, and their function has been assessed across multiple endpoints and confirmed in primary human cells.

There are caveats to this dataset, as discussed in **Chapter 4**. A main deviation from the project plan set out in **Chapter 3** was the switch from primary human MDMs to the THP-1 cell line. Although they provide a stable source of KO cells, the cell lines require PMA differentiation to assess macrophage-like properties, which reduces physiological relevance. This was accounted for in the project plan: initial observations were to be generated quickly using the KO THP-1 cell lines, relying on their reproducibility to generate consistent results between experients. This would be followed by a confirmatory study using primary cells to ensure that the observations made were physiologically relevant, addressing concerns around cell line-dependent effects and reproducibility.

This approach has yielded tool cell lines which can be used to study the phenotype of cells which lack C5aR2, from which the role of C5aR2 in WT cells can be inferred**.** Outside the short scope of this PhD project, these cells represent a novel tool for studying the signalling and function of C5aR2. Tools to study C5aR2 have historically been unreliable and poorly available [121]. These cell lines could allow for clear and simple experiments to be performed, eliminating the need for complex multi-reagent experiments to be optimised, as in **Chapter 3**. These cells provide the opportunity to elucidate the interplay between the complement system and the immune response, which is an area of current interest and novelty in the Immunology community.

7.2.3. C5aR2 and the cGAS-STING pathway

Once the C5aR2 KO THP-1 cells had been generated and validated, they were used to identify novel functions of C5aR2. This study aimed to address the effect of C5aR2 KO in THP-1 cells on the response to PRR stimulation. Assessing IFN-β secretion in the PRR panel experiment led to the key finding of this project, which was the strong link

between C5aR2 and the cGAS-STING pathway. cGAS/STING-induced IFN-β secretion was significantly increased in C5aR2 KO THP-1 cells. Expression of key proteins of the cGAS-STING pathway were up-regulated at baseline, suggesting that the IFN-β phenotype could be driven by a constitutive negative regulation of cGAS-STING pathway protein expression by C5aR2 in WT cells, which is lost in C5aR2 KO cells. This expands on previously published observations, as the link between cGAS-STING and C5aR2 has never been thoroughly characterised or explored mechanistically. The C5aR2 KO-dependent amplification of STING-induced IFN-β secretion was conserved between THP-1 cells and primary human macrophages. This confirmatory study allowed for two key observations:

Firstly, the NTC control included in the primary human MDM study confirms that the IFN-β phenotype in the THP-1 cell lines is not an off-target effect of CRISPR-Cas9 editing. This was uncontrolled in the THP-1 study due to the loss of the NTC cell line culture. However there was no observed off-target effect of CRISPR-Cas9 editing on STING-induced IFN-β secretion as the NTC primary cells differed from the C5aR2 KO cells, meaning observations made in the cell lines were valid.

Secondly, the reproducibility of the cell line phenotype in primary human MDMs increases the physiological relevance of these results. The link between C5aR2 and cGAS-STING signalling in this study is a robust observation generated using two models of human macrophages, one of which originated from primary human donors. It is also supported in the literature in the study using P32 and P59 selective peptide agonists of C5aR2 [8]. This study revealed a key role for C5aR2 as a modulator of the antiviral response in human macrophages, which suggests that it may be a useful therapeutic target in chronic infection or DNA-driven inflammation in autoimmune conditions [9].

7.2.4. Proposed mechanism of C5aR2-dependent regulation of cGAS-STING signalling

C5aR2 KO amplifies IFN-β secretion in response to cGAS agonism and STING agonism, and the antagonist data show that TBK1 and STING are indispensable for the response to cAIM(PS)$_2$ Difluor (Rp/Sp), demonstrating that is a specific response to agonism of the cGAS-STING pathway.

The Peggy Sue data indicate that STING and IRF3 expression is increased in C5aR2 KO cells, which suggests an upstream regulation of the expression of these proteins. There may be a regulator of the transcription and translation of the cGAS-STING pathway proteins which is downstream of C5aR2. The response is amplified in C5aR2 KO cells, which suggests that C5aR2 negatively regulates this pathway in WT cells. This is aligned to the proposed roles of C5aR2 in the literature as a negative regulator of the immune response [121].

The effect of C5aR2 KO is C5a-independent, so the role of C5aR2 may be exerted through scaffold or adaptor function, independently from the canonical complement system. C5aR2 may interact directly with cGAS-STING pathway proteins to disrupt signalling and restrict the immune response to nucleic acid, for example by disrupting dimerization of STING or its translocation from the endoplasmic reticulum to the golgi. C5aR2 may also be activated by a non-canonical C5a generated by the complosome, which is an intracellular complement system driven by intracellular proteases [48]. C5aR2 is expressed intracellularly (**Figure 4.1**), therefore it may exert an unidentified intracellular function driven constitutively by intracellular C5a. This could be assessed by combining the C5aR2 KO with a C5 siRNA knockdown or CRISPR-Cas9 knockout, removing all C5 from the cell to remove the potential source of intracellular C5a. If the effect on IFN-β is reverted to WT levels, it would suggest that the effect of C5aR2 is dependent on endogenous C5a. There may also be unobserved C5a-dependent roles, as extracellular delivery of C5a may not have resulted in target engagement of intracellular C5aR2. Tonic intracellular activation of C5aR2 may be able to drive its

regulatory roles, but C5a ligation of extracellular C5aR2 driven to the cell surface by the inflammatory microenvironment may result in previously unobserved effects. More work on intracellular C5aR2 activation is required to understand the function of intracellular complement and C5aR2.

Additional work to identify the mechanism driving the enhanced antiviral response in C5aR2 KO cells is also required. Data from this study demonstrate that cGAS-STING proteins are overexpressed in C5aR2 KO cells, suggesting that C5aR2 negatively regulates expression of these proteins in WT cells. This observation led to the proposal of -omics experiments to search for potentially relevant pathways, proteins or genes which were also regulated in C5aR2 KO cells, and could therefore be regulated by C5aR2.

7.2.5. Confirmation of antiviral pathway regulation using RNAseq

Following the identification of C5aR2 as a modulator of the antiviral response, a range of -omics experiments was proposed to search for potential mechanisms for the C5aR2-mediated regulation of antiviral pathways. Given that C5aR2 protein detection had proved challenging due to lack of validated detection reagents, RNAseq was selected. This approach would confirm the effects reported in **Chapter 5**, and allow for a deeper investigation into gene expression in C5aR2 KO cells, which would identify potential contributors to the mechanism of C5aR2 function.

The RNAseq experiment yielded an expansive dataset reporting the effect of C5aR1 KO or C5aR2 KO on THP-1 cells at baseline, in response to C5a and in response to STING agonism, compared to WT cells. The dataset generated using the STING agonist-treated cells was analysed specifically to confirm the antiviral phenotype of C5aR2 KO cells described in **Chapter 5**, and to further identify key genes and pathways that are regulated in C5aR2 KO cells, which may be contributing to the antiviral phenotype. C5aR2 KO cells had an amplified Type I Interferon response, including IFN-β as

previously observed, but also including IFN-α 7, 14, 16, 17, 21, IFN-ω and other relevant pro-inflammatory cytokines. A wide array of significantly regulated genes and pathways was identified, which will be used to generate hypotheses for future investigation into the role of C5aR2 for regulation of the cGAS-STING pathway and antiviral signalling.

C5aR2 KO cells have not been used to generate an RNAseq dataset previously, therefore this is a novel approach to characterise the function of C5aR2. This approach was successful as it described a novel role for C5aR2 as antiviral modulator. The complement system is a key modulator of the innate immune response, and therefore is potentially implicated in infection and inflammation. Therapeutic modulation of C5aR2 may therefore be able to influence the immune response to viruses or DNA-based DAMPs to improve outcomes for patients with chronic infections or inflammatory conditions.

A significant amount of additional analysis is still possible with this dataset. In particular, investigating the specific effect of C5a on the C5aR2 KO cells may reveal the fundamental function of C5aR2 upon binding its putative cognate ligand, C5a. C5aR2 has potent but poorly-understood effects on critical inflammatory pathways, such as the cGAS-STING pathway, and so further study could reveal its potential as a therapeutic target.

7.3. Future Studies

This project has characterised a novel link between C5aR2 and the cGAS-STING pathway. Many observations generated in this project warrant further investigation to understand the function of this protein more thoroughly.

7.3.1. C5aR2, IFN-β and the cGAS-STING pathway

Initially, more work needs to be done to confirm the specificity of the effect of C5aR2 KO on IFN-β. There is a key experiment required to conclude the cGAS-STING pathway work in **Chapter 5**. An experiment using an alternative STING-independent stimulator of IFN-β secretion, for example IRF7 downstream of RIG-I activation by dsRNA [6], would confirm whether C5aR2 KO amplifies all IFN-β responses, or just those downstream of cGAS-STING regulation.

There are additional experiments which could be performed to further investigate the link between C5aR2 and STING. Given the trend towards increased STING and IRF3 expression (**Figure 5.10**), confirmatory flow cytometry experiments could be used to assess STING and IRF3 alongside additional cGAS-STING pathway proteins including cGAS, cGAMP, TBK1, IFN-α proteins and IFN-β, or members of alternative nucleic acid sensing pathways such as RIG-I, MDA5 and MAVS. This approach would reveal which antiviral pathway proteins are regulated by C5aR2, and allow for a more accurate semi-quantified comparison between WT and C5aR2 KO cells. Expression of these genes could also be assessed using RT-qPCR to assess whether C5aR2-induced regulation occurs at the transcription or translation level. Furthermore, increased protein expression does not necessarily confer increased function, so a competitive kinetics experiment could be used to assess whether more STING agonist is required to increase WT IFN-β concentrations to C5aR2 KO levels, which would suggest a direct expression-function relationship, as opposed to a more complex regulation upstream or downstream of the cGAS-STING pathway.

Having confirmed increased expression and function of cGAS-STING pathway proteins in C5aR2 KO cells, a mechanistic study would be required. Further analysis of the RNAseq dataset will direct this search, as it contains a range of potential interactors driving the C5aR2 KO phenotype. To complement this approach, an interactome

analysis would be critical to identify binding partners of C5aR2, to determine which proteins it targets and how it might be disrupting cGAS-STING signalling or suppressing the JAK/STAT response to IFN.

7.3.2. RNAseq dataset

Extensive further analysis on the RNAseq dataset could be performed. The effects of C5aR2 KO compared to WT at baseline have not been explored in specific detail, nor has the effect of C5a on C5aR2 KO cells compared to WT. These comparisons could yield an understanding of the baseline function of C5aR2 in macrophages, and also an understanding of the effects of C5a-induced C5aR2-mediated signalling on the transcriptome of macrophages. These comparisons, along with the pathways and genes identified in the STING-agonised cells, can then be contextualised with published data, followed by hit confirmation in independent replicate experiments using RT-qPCR and protein detection. If confirmed by RT-qPCR, mechanisms for C5aR2-mediated regulation via hit proteins could be hypothesised, and their functions explored.

Hits could be confirmed by using pharmacological inhibitors, RNAi, CRISPR-Cas9 or targeted mutagenesis to disrupt functionality and investigate whether IFN-β secretion is modulated in C5aR2 KO cells. If the phenotype is affected, a co-immunoprecipitation experiment on the target or C5aR2 could be performed to determine whether the proteins of interest interact with C5aR2. This could be confirmed using fluorescent microscopy, and further examined using interactomic approaches. Once the functions and interactions of C5aR2 are characterised, a complete mechanism for C5aR2-mediated regulation of antiviral signalling may be achieved.

7.4. Therapeutic relevance of C5aR2

The identification of C5aR2 as a regulator of the antiviral response in macrophages has potential therapeutic implications. C5aR2 could be a relevant target for acute viral

infection, e.g. SARS-CoV-2 or influenza, or for chronic viral infection, e.g. Hepatitis B or C. It could also be relevant for the response to DAMPs comprising cytoplasmic DNA in autoimmune conditions or cancer [9]. Experiments using live viral infections could be employed to assess the effect of C5aR2 KO on survival, viral clearance or antiviral cytokine secretion. If effective, C5aR2 could be further implicated as a key antiviral modulator. This could be translated to mouse infection models, using C5aR2 KO mice to assess the effect of C5aR2 on viral infection at an organism level. If C5aR2 negatively regulates the antiviral response, it could potentially be therapeutically modulated to increase or decrease its regulation of key antiviral pathways, to influence the severity of the pathological immune response.

The complement field is rapidly evolving. Diverse immunoregulatory effects have been identified [90], implicating various members of the complement system as therapeutic targets. There have been clinical trials of a wide array of complement therapeutics [90], as reviewed in **Chapter 1**, including Eculizumab and Avacopan. Eculizumab is a humanised monoclonal antibody which binds to C5, approved for treatment of patients with paroxysmal nocturnal haemoglobinuria [122], atypical haemolytic uremic syndrome [123], myasthenia gravis [124] and neuromyelitis optica [125]. Avacopan is a small molecule inhibitor of C5aR1, recently licensed for use in anti-neutrophil cytoplasmic autoantibody-associated vasculitis [102]. Avacopan is particularly relevant to C5aR2 as it is a proof-of-concept for drugs targeting anaphylatoxin receptors. Therapeutics which target C5aR2 may provide an immunomodulatory tool against infectious and inflammatory disease. The modulation of nucleic acid sensing and the IFN response by C5aR2 KO suggests that the sensing and response to viral and tumour nucleic acids could be impacted by a therapeutic targeting C5aR2.

C5aR2 could be therapeutically modulated through agonism or antagonism, depending on the indication. For example, C5aR2 agonism may be useful to suppress a pathogenic antiviral immune response which is driving tissue damage. Alternatively,

C5aR2 antagonism may de-repress an immune response to a virus, allowing more effective restriction and clearance.

C5aR2 would likely be difficult to target using a monoclonal antibody, as its intracellular expression may sequester it from extracellular immunoglobulin. Instead, a small molecule allosteric inhibitor or siRNA-based gene therapy may be appropriate, allowing the inhibition of intracellular protein or the prevention of its expression transiently during an infection, or for the duration of cancer treatment to promote immune clearance. Infectious disease and cancer often involve complex immune evasion strategies, and it is therefore likely that a single approach would be insufficient. C5aR2 therapeutics would likely be most beneficial as part of a combination therapy, assisting in the de-repression of the antiviral or antitumour immune response to drive up IFN-driven inflammation in a targeted manner alongside other strategies to complement the approach.

Whilst C5aR2 is still poorly understood, it is an emerging regulator of innate immunity, and this project has described a novel role for it as a key modulator of DNA sensing and the antiviral response. Future efforts by researchers using the C5aR2 KO cells, the RNAseq dataset and additional antiviral endpoints should continue to elucidate the role of C5aR2 in the innate immune response, characterise its role in the antiviral response, and assess it as a target for future therapeutic development.

References

References were formatted in the style of Nature using Mendeley.

1. Kawai, T. & Akira, S. The role of pattern-recognition receptors in innate immunity: Update on toll-like receptors. *Nature Immunology* vol. 11 373–384 at https://doi.org/10.1038/ni.1863 (2010).

2. Govindaraj, R. G., Manavalan, B., Lee, G. & Choi, S. Molecular modeling-based evaluation of hTLR10 and identification of potential ligands in toll-like receptor signaling. *PLoS One* **5**, 1–13 (2010).

3. Akira S, Uematsu S & Takeuchi O. Pathogen recognition and innate immunity. *Cell* **124**, 783–801 (2006).

4. Hornung, V. *et al.* Sequence-specific potent induction of IFN-α by short interfering RNA in plasmacytoid dendritic cells through TLR7. *Nat. Med.* **11**, 263–270 (2005).

5. Kumari, P., Russo, A. J., Shivcharan, S. & Rathinam, V. A. AIM2 in health and disease: Inflammasome and beyond. *Immunol. Rev.* **297**, 83–95 (2020).

6. Rehwinkel, J. & Gack, M. U. RIG-I-like receptors: their regulation and roles in RNA sensing. *Nat. Rev. Immunol.* **20**, 537–551 (2020).

7. Dias Junior, A. G., Sampaio, N. G. & Rehwinkel, J. A Balancing Act: MDA5 in Antiviral Immunity and Autoinflammation. *Trends Microbiol.* **27**, 75–85 (2019).

8. Li, X. X., Clark, R. J. & Woodruff, T. M. C5aR2 Activation Broadly Modulates the Signaling and Function of Primary Human Macrophages. *J. Immunol.* **205**, 1102–1112 (2020).

9. Motwani, M., Pesiridis, S. & Fitzgerald, K. A. DNA sensing by the cGAS–STING pathway in health and disease. *Nat. Rev. Genet.* **20**, 657–674 (2019).

10. Civril, F. *et al.* Structural mechanism of cytosolic DNA sensing by cGAS. *Nature*

498, 332–337 (2013).

11. Kato, K., Omura, H., Ishitani, R. & Nureki, O. Cyclic GMP-AMP as an endogenous second messenger in innate immune signaling by cytosolic DNA. *Annu. Rev. Biochem.* **86**, 541–566 (2017).

12. Ishikawa, H., Ma, Z. & Barber, G. N. STING regulates intracellular DNA-mediated, type i interferon-dependent innate immunity. *Nature* **461**, 788–792 (2009).

13. Shang, G. *et al.* Crystal structures of STING protein reveal basis for recognition of cyclic di-GMP. *Nat. Struct. Mol. Biol.* **19**, 725–727 (2012).

14. Dobbs, N. *et al.* STING activation by translocation from the ER is associated with infection and autoinflammatory disease. *Cell Host Microbe* **18**, 157–168 (2015).

15. Agalioti, T. *et al.* Ordered recruitment of chromatin modifying and general transcription factors to the IFN-β promoter. *Cell* **103**, 667–678 (2000).

16. Liu, T., Zhang, L., Joo, D. & Sun, S. C. NF-κB signaling in inflammation. *Signal Transduct. Target. Ther.* **2**, (2017).

17. Guo, H., Callaway, J. B. & Ting, J. P.-Y. Inflammasomes: Mechanism of action, role in disease, and therapeutics. *Nature Medicine* vol. 21 677–687 at https://doi.org/10.1038/nm.3893 (2015).

18. Bryant, C. & Fitzgerald, K. A. Molecular mechanisms involved in inflammasome activation. *Trends in Cell Biology* vol. 19 455–464 at https://doi.org/10.1016/j.tcb.2009.06.002 (2009).

19. Patel, M. N. *et al.* Inflammasome Priming in Sterile Inflammatory Disease. *Trends in Molecular Medicine* vol. 23 165–180 at

https://doi.org/10.1016/j.molmed.2016.12.007 (2017).

20. Karmakar, M., Katsnelson, M. A., Dubyak, G. R. & Pearlman, E. Neutrophil P2X7 receptors mediate NLRP3 inflammasome-dependent IL-1β secretion in response to ATP. *Nat. Commun.* **7**, 10555 (2016).

21. Broz, P. & Monack, D. M. Noncanonical Inflammasomes: Caspase-11 Activation and Effector Mechanisms. *PLoS Pathog.* **9**, e1003144 (2013).

22. Swanson, K. V., Deng, M. & Ting, J. P. Y. The NLRP3 inflammasome: molecular activation and regulation to therapeutics. *Nat. Rev. Immunol.* **19**, 477–489 (2019).

23. Ricklin, D., Reis, E. S. & Lambris, J. D. Complement in disease: a defence system turning offensive. *Nat. Rev. Nephrol.* **12**, 383–401 (2016).

24. Wallis, R., Mitchell, D. A., Schmid, R., Schwaeble, W. J. & Keeble, A. H. Paths reunited: Initiation of the classical and lectin pathways of complement activation. *Immunobiology* **215**, 1–11 (2010).

25. Diebolder, C. A. *et al.* Complement is activated by IgG hexamers assembled at the cell surface. *Science (80-.).* **343**, 1260–1263 (2014).

26. Wallis, R. Interactions between mannose-binding lectin and MASPs during complement activation by the lectin pathway. *Immunobiology* **212**, 289–99 (2007).

27. Ma, Y. J., Skjoedt, M. O. & Garred, P. Collectin-11/MASP complex formation triggers activation of the lectin complement pathway - The fifth lectin pathway initiation complex. *J. Innate Immun.* **5**, 242–250 (2013).

28. Nilsson, B. & Nilsson Ekdahl, K. The tick-over theory revisited: Is C3 a contact-activated protein? *Immunobiology* **217**, 1106–1110 (2012).

29. Morgan, B. P. Complement membrane attack on nucleated cells: resistance, recovery and non-lethal effects. *Biochem. J.* **264**, 1–14 (1989).

30. Spitzer, D., Mitchell, L. M., Atkinson, J. P. & Hourcade, D. E. Properdin Can Initiate Complement Activation by Binding Specific Target Surfaces and Providing a Platform for De Novo Convertase Assembly. *J. Immunol.* **179**, 2600–2608 (2007).

31. Kemper, C., Mitchell, L. M., Zhang, L. & Hourcade, D. E. The complement protein properdin binds apoptotic T cells and promotes complement activation and phagocytosis. *Proc. Natl. Acad. Sci. U. S. A.* **105**, 9023–8 (2008).

32. Harboe, M., Ulvund, G., Vien, L., Fung, M. & Mollnes, T. E. The quantitative role of alternative pathway amplification in classical pathway induced terminal complement activation. *Clin. Exp. Immunol.* **138**, 439–446 (2004).

33. Helmy, K. Y. *et al.* CRIg: A Macrophage Complement Receptor Required for Phagocytosis of Circulating Pathogens. *Cell* **124**, 915–927 (2006).

34. Carroll, M. C. & Isenman, D. E. Regulation of humoral immunity by complement. *Immunity* **37**, 199–207 (2012).

35. Morgan, B. P., Boyd, C. & Bubeck, D. Molecular cell biology of complement membrane attack. *Semin. Cell Dev. Biol.* **72**, 124–132 (2017).

36. Tegla, C. A. *et al.* Membrane attack by complement: the assembly and biology of terminal complement complexes. *Immunol. Res.* **51**, 45–60 (2011).

37. Morgan, B. P. The membrane attack complex as an inflammatory trigger. *Immunobiology* vol. 221 747–751 at https://doi.org/10.1016/j.imbio.2015.04.006 (2016).

38. Laudisi, F. *et al.* Cutting Edge: The NLRP3 Inflammasome Links Complement-

Mediated Inflammation and IL-1 Release. *J. Immunol.* **191**, 1006–1010 (2013).

39. Triantafilou, K., Hughes, T. R., Triantafilou, M. & Morgan, B. P. The complement membrane attack complex triggers intracellular Ca2+ fluxes leading to NLRP3 inflammasome activation. *J. Cell Sci.* **126**, 2903–2913 (2013).

40. Jimenez-Duran, G. *et al.* Complement membrane attack complex is an immunometabolic regulator of NLRP3 activation and IL-18 secretion in human macrophages. *Front. Immunol.* **13**, (2022).

41. Klos, A. *et al.* The role of the anaphylatoxins in health and disease. *Molecular Immunology* vol. 46 2753–2766 at https://doi.org/10.1016/j.molimm.2009.04.027 (2009).

42. Bokisch, V. A. & Müller-Eberhard, H. J. Anaphylatoxin inactivator of human plasma: its isolation and characterization as a carboxypeptidase. *J. Clin. Invest.* **49**, 2427–2436 (1970).

43. Bajic, G., Yatime, L., Klos, A. & Andersen, G. R. Human C3a and C3a desArg anaphylatoxins have conserved structures, in contrast to C5a and C5a desArg. *Protein Sci.* **22**, 204–212 (2013).

44. Cianflone, K. M. *et al.* Purification and characterization of acylation stimulating protein. *J. Biol. Chem.* **264**, 426–430 (1989).

45. Kalant, D. *et al.* C5L2 is a functional receptor for acylation-stimulating protein. *J. Biol. Chem.* **280**, 23936–23944 (2005).

46. Cook, W. J., Galakatos, N., Boyar, W. C., Walter, R. L. & Ealick, S. E. Structure of human desArg-C5a. *Acta Crystallogr. Sect. D Biol. Crystallogr.* **66**, 190–197 (2010).

47. Marder, S., Chenoweth, D., Goldstein, I. & Perez, D. Chemotactic responses of

human peripheral blood monocytes to the complement-derived peptides C5a and C5a des Arg. *J. Immunol.* **134**, 3325–3331 (1985).

48. Arbore, G., Kemper, C. & Kolev, M. Intracellular complement − the complosome − in immune cell regulation. *Molecular Immunology* vol. 89 2–9 at https://doi.org/10.1016/j.molimm.2017.05.012 (2017).

49. Niyonzima, N. *et al.* Mitochondrial C5aR1 activity in macrophages controls IL-1β production underlying sterile inflammation. *Sci. Immunol.* **6**, (2021).

50. Ohno, M. *et al.* A putative chemoattractant receptor, C5L2, is expressed in granulocyte and immature dendritic cells, but not in mature dendritic cells. *Mol. Immunol.* **37**, 407–412 (2000).

51. Zhang, T., Garstka, M. A. & Li, K. The Controversial C5a Receptor C5aR2: Its Role in Health and Disease. *Journal of Immunology Research* vol. 2017 1–16 at https://doi.org/10.1155/2017/8193932 (2017).

52. Rosenbaum, D. M., Rasmussen, S. G. F. & Kobilka, B. K. The structure and function of G-protein-coupled receptors. *Nature* vol. 459 356–363 at https://doi.org/10.1038/nature08144 (2009).

53. Rajagopal, S., Rajagopal, K. & Lefkowitz, R. J. Teaching old receptors new tricks: Biasing seven-transmembrane receptors. *Nature Reviews Drug Discovery* vol. 9 373–386 at https://doi.org/10.1038/nrd3024 (2010).

54. Cain, S. A. & Monk, P. N. The orphan receptor C5L2 has high affinity binding sites for complement fragments C5a and C5a des-Arg74. *J. Biol. Chem.* **277**, 7165–7169 (2002).

55. Ames, R. S. *et al.* Molecular cloning and characterization of the human anaphylatoxin C3a receptor. *J. Biol. Chem.* **271**, 20231–20234 (1996).

56. Wilken, H.-C., Rogge, S., Götze, O., Werfel, T. & Zwirner, J. Specific detection by flow cytometry of histidine-tagged ligands bound to their receptors using a tag-specific monoclonal antibody. *J. Immunol. Methods* **226**, 139–145 (1999).

57. Pan, Z. K. Anaphylatoxins C5a and C3a induce nuclear factor κB activation in human peripheral blood monocytes. *Biochim. Biophys. Acta - Gene Struct. Expr.* **1443**, 90–98 (1998).

58. Kooistra, A. J., Munk, C., Hauser, A. S. & Gloriam, D. E. An online GPCR structure analysis platform. *Nat. Struct. Mol. Biol.* **28**, 875–878 (2021).

59. Monk, P. N., Scola, A.-M., Madala, P. & Fairlie, D. P. Function, structure and therapeutic potential of complement C5a receptors. *Br. J. Pharmacol.* **152**, 429–448 (2007).

60. Sarma, J. V. & Ward, P. A. New developments in C5a receptor signaling. *Cell Health Cytoskelet.* **4**, 73–82 (2012).

61. Guo, R.-F., Riedemann, N. C. & Ward, P. A. Role of C5a-C5aR Interaction in Sepsis. *Shock* **21**, 1–7 (2004).

62. Tardif, M., Brouchon, L., Rabiet, M.-J. & Boulay, F. Direct binding of a fragment of the Wiskott-Aldrich syndrome protein to the C-terminal end of the anaphylatoxin C5a receptor. *Biochem. J.* **372**, 453–463 (2003).

63. Lee, D. K. *et al.* Identification of four novel human G protein-coupled receptors expressed in the brain. *Mol. Brain Res.* **86**, 13–22 (2001).

64. Scola, A. M., Johswich, K. O., Morgan, B. P., Klos, A. & Monk, P. N. The human complement fragment receptor, C5L2, is a recycling decoy receptor. *Mol. Immunol.* **46**, 1149–1162 (2009).

65. Wisniewski, S., Dragan, P., Makal, A. & Latek, D. Helix 8 in chemotactic

receptors of the complement system. *PLoS Comput. Biol.* **18**, (2022).

66. Zhu, Y. *et al.* An Integrated Analysis of C5AR2 Related to Malignant Properties and Immune Infiltration of Breast Cancer. *Front. Oncol.* **11**, (2021).

67. Karsten, C. M. *et al.* Monitoring C5aR2 Expression Using a Floxed tdTomato-C5aR2 Knock-In Mouse. *J. Immunol.* **199**, 3234–3248 (2017).

68. Bamberg, C. E. *et al.* The C5a receptor (C5aR) C5L2 is a modulator of C5aR-mediated signal transduction. *J. Biol. Chem.* **285**, 7633–7644 (2010).

69. Li, R., Coulthard, L. G., Wu, M. C. L., Taylor, S. M. & Woodruff, T. M. C5L2: a controversial receptor of complement anaphylatoxin, C5a. *FASEB J.* **27**, 855–864 (2013).

70. Croker, D. E., Halai, R., Fairlie, D. P. & Cooper, M. A. C5a, but not C5a-des Arg, induces upregulation of heteromer formation between complement C5a receptors C5aR and C5L2. *Immunol. Cell Biol.* **91**, 625–633 (2013).

71. Cui, W., Simaan, M., Laporte, S., Lodge, R. & Cianflone, K. C5a- and ASP-mediated C5L2 activation, endocytosis and recycling are lost in S323I-C5L2 mutation. *Mol. Immunol.* **46**, 3086–3098 (2009).

72. Croker, D. E. *et al.* Discovery of functionally selective C5aR2 ligands: Novel modulators of C5a signalling. *Immunol. Cell Biol.* **94**, 787–795 (2016).

73. Scola, A. M. *et al.* The role of the N-terminal domain of the complement fragment receptor C5L2 in ligand binding. *J. Biol. Chem.* **282**, 3664–3671 (2007).

74. Okinaga, S. *et al.* C5L2, a nonsignaling C5A binding protein. *Biochemistry* **42**, 9406–9415 (2003).

75. Pandey, S. *et al.* Intrinsic bias at non-canonical, β-arrestin-coupled seven

transmembrane receptors. *Mol. Cell* **81**, 4605-4621.e11 (2021).

76. Van Lith, L. H. C., Oosterom, J., Van Elsas, A. & Zaman, G. J. R. C5a-Stimulated Recruitment of ß-Arrestin2 to the Nonsignaling 7-Transmembrane Decoy Receptor C5L2. *J. Biomol. Screen.* **14**, 1067–1075 (2009).

77. Croker, D. E. *et al.* C5a2 can modulate ERK1/2 signaling in macrophages via heteromer formation with C5a1 and β-arrestin recruitment. *Immunol. Cell Biol.* **92**, 631–639 (2014).

78. Chen, N. J. *et al.* C5L2 is critical for the biological activities of the anaphylatoxins C5a and C3a. *Nature* **446**, 203–207 (2007).

79. Hsu, W. C., Yang, F. C., Lin, C. H., Hsieh, S. L. & Chen, N. J. C5L2 is required for C5a-triggered receptor internalization and ERK signaling. *Cell. Signal.* **26**, 1409–1419 (2014).

80. Frödin, M. & Gammeltoft, S. Role and regulation of 90 kDa ribosomal S6 kinase (RSK) in signal transduction. *Mol. Cell. Endocrinol.* **151**, 65–77 (1999).

81. Lu, N. & Malemud, C. J. Extracellular signal-regulated kinase: A regulator of cell growth, inflammation, chondrocyte and bone cell receptor-mediated gene expression. *Int. J. Mol. Sci.* **20**, (2019).

82. Miyabe, Y., Miyabe, C., Mani, V., Mempel, T. R. & Luster, A. D. Atypical complement receptor C5aR2 transports C5a to initiate neutrophil adhesion and inflammation. *Sci. Immunol.* **4**, (2019).

83. Poursharifi, P. *et al.* C5L2 and C5aR interaction in adipocytes and macrophages: Insights into adipoimmunology. *Cell. Signal.* **25**, 910–918 (2013).

84. Hajishengallis, G. & Lambris, J. D. More than complementing Tolls:

complement–Toll-like receptor synergy and crosstalk in innate immunity and inflammation. *Immunological Reviews* vol. 274 233–244 at https://doi.org/10.1111/imr.12467 (2016).

85. Haggadone, M. D., Grailer, J. J., Fattahi, F., Zetoune, F. S. & Ward, P. A. Bidirectional Crosstalk between C5a Receptors and the NLRP3 Inflammasome in Macrophages and Monocytes. *Mediators Inflamm.* **2016**, 1–11 (2016).

86. Kalbitz, M. *et al.* Complement-induced activation of the cardiac NLRP3 inflammasome in sepsis. *FASEB J.* **30**, 3997–4006 (2016).

87. Yu, S. *et al.* The complement receptor C5aR2 promotes protein kinase R expression and contributes to NLRP3 inflammasome activation and HMGB1 release from macrophages. *J. Biol. Chem.* jbc.RA118.006508 (2019) doi:10.1074/jbc.RA118.006508.

88. Fisette, A. & Cianflone, K. The ASP and C5L2 pathway: Another bridge between inflammation and metabolic homeostasis. *Clinical Lipidology* vol. 5 367–377 at https://doi.org/10.2217/clp.10.21 (2010).

89. Buniello, A. *et al.* The NHGRI-EBI GWAS Catalog of published genome-wide association studies, targeted arrays and summary statistics 2019. *Nucleic Acids Res.* **47**, D1005–D1012 (2019).

90. Morgan, B. P. & Harris, C. L. Complement, a target for therapy in inflammatory and degenerative diseases. *Nature Reviews Drug Discovery* vol. 14 857–877 at https://doi.org/10.1038/nrd4657 (2015).

91. Hillmen, P. *et al.* Long-term safety and efficacy of sustained eculizumab treatment in patients with paroxysmal nocturnal haemoglobinuria. *Br. J. Haematol.* **162**, 62–73 (2013).

92. Legendre, C. M. *et al.* Terminal complement inhibitor eculizumab in atypical

hemolytic-uremic syndrome. *N. Engl. J. Med.* **368**, 2169–81 (2013).

93. Syed, Y. Y. Ravulizumab: A Review in Atypical Haemolytic Uraemic Syndrome. *Drugs* **81**, 587–594 (2021).

94. Lee, J. W. & Kulasekararaj, A. G. Ravulizumab for the treatment of paroxysmal nocturnal hemoglobinuria. *Expert Opin. Biol. Ther.* **20**, 227–237 (2020).

95. Röth, A. *et al.* Sutimlimab in patients with cold agglutinin disease: results of the randomized placebo-controlled phase 3 CADENZA trial. *Blood* **140**, 980–991 (2022).

96. Gerber, G. F. & Brodsky, R. A. Pegcetacoplan for paroxysmal nocturnal hemoglobinuria. *Blood* **139**, 3361–3365 (2022).

97. Liao, D. S., Metapally, R. & Joshi, P. Pegcetacoplan treatment for geographic atrophy due to age-related macular degeneration: a plain language summary of the FILLY study. *Immunotherapy* **14**, 995–1006 (2022).

98. Jang, J. H. *et al.* Iptacopan monotherapy in patients with paroxysmal nocturnal hemoglobinuria: a 2-cohort open-label proof-of-concept study. *Blood Adv.* **6**, 4450–4460 (2022).

99. Röth, A. *et al.* The complement C5 inhibitor crovalimab in paroxysmal nocturnal hemoglobinuria. *Blood* **135**, 912–920 (2020).

100. Khaled, S. K. *et al.* Narsoplimab, a Mannan-Binding Lectin-Associated Serine Protease-2 Inhibitor, for the Treatment of Adult Hematopoietic Stem-Cell Transplantation-Associated Thrombotic Microangiopathy. *J. Clin. Oncol.* **3**, (2022).

101. Osman, M., Cohen Tervaert, J. W. & Pagnoux, C. Avacopan for the treatment of ANCA-associated vasculitis. *Expert Rev. Clin. Immunol.* **17**, 717–726 (2021).

102. Lee, A. Avacopan: First Approval. *Drugs* **82**, 79–85 (2022).

103. Hall, T. A. BIOEDIT: a user-friendly biological sequence alignment editor and analysis program for Windows 95/98/ NT. *Nucleic Acids Symp. Ser.* **41**, 95–98 (1999).

104. Madeira, F. *et al.* Search and sequence analysis tools services from EMBL-EBI in 2022. *Nucleic Acids Res.* **50**, W276–W279 (2022).

105. Thomas, P. D. *et al.* PANTHER: Making genome-scale phylogenetics accessible to all. *Protein Sci.* **31**, 8–22 (2022).

106. R-project, C. D. T. A Language and Environment for Statistical Computing. *R Found. Stat. Comput.* **2**, https://www.R–project.org (2020).

107. Szklarczyk, D. *et al.* The STRING database in 2021: Customizable protein-protein networks, and functional characterization of user-uploaded gene/measurement sets. *Nucleic Acids Res.* **49**, D605–D612 (2021).

108. Sanjana, N. E., Shalem, O. & Zhang, F. Improved vectors and genome-wide libraries for CRISPR screening. *Nat. Methods* **11**, 783–784 (2014).

109. Madden, T. L. *et al.* Primer-BLAST: a tool to design target-specific primers for polymerase chain reaction. *BMC Bioinformatics* **13**, 134 (2012).

110. Love, M. I., Anders, S. & Huber, W. Moderated estimation of fold change and dispersion for RNA-seq data with DESeq2. *Genome Biol.* **11**, R106 (2010).

111. Korotkevich, G. & Sukhov, V. Fast gene set enrichment analysis. 1–29 (2016).

112. Kanehisa, M., Furumichi, M., Sato, Y., Kawashima, M. & Ishiguro-Watanabe, M. KEGG for taxonomy-based analysis of pathways and genomes. *Nucleic Acids Res.* (2022) doi:10.1093/nar/gkac963.

113. Tamamis, P. *et al.* Insights into the mechanism of C5aR inhibition by PMX53

via implicit solvent molecular dynamics simulations and docking. *BMC Biophys.* **7**, (2014).

114. Raby, A.-C. *et al.* TLR activation enhances C5a-induced pro-inflammatory responses by negatively modulating the second C5a receptor, C5L2. doi:10.1002/eji.201041350.

115. Fonseca, M. I., McGuire, S. O., Counts, S. E. & Tenner, A. J. Complement activation fragment C5a receptors, CD88 and C5L2, are associated with neurofibrillary pathology. *J. Neuroinflammation* **10**, (2013).

116. Adli, M. The CRISPR tool kit for genome editing and beyond. *Nat. Commun.* **9**, (2018).

117. Tsuchiya, S. *et al.* Establishment and characterization of a human acute monocytic leukemia cell line (THP-1). *Int. J. Cancer* **26**, 171–176 (1980).

118. Chanput, W., Mes, J. J. & Wichers, H. J. THP-1 cell line: An in vitro cell model for immune modulation approach. *Int. Immunopharmacol.* **23**, 37–45 (2014).

119. Karlsson, M. *et al.* A single–cell type transcriptomics map of human tissues. *Sci. Adv.* **7**, (2021).

120. Zhang, Y. *et al.* β-arrestin 2 as an activator of cGAS-STING signaling and target of viral immune evasion. *Nat. Commun.* **11**, (2020).

121. Li, X. X., Lee, J. D., Kemper, C. & Woodruff, T. M. The Complement Receptor C5aR2: A Powerful Modulator of Innate and Adaptive Immunity. *J. Immunol.* **202**, 3339–3348 (2019).

122. Dmytrijuk, A. *et al.* FDA Report: Eculizumab (Soliris®) for the Treatment of Patients with Paroxysmal Nocturnal Hemoglobinuria. *Oncologist* **13**, 993–1000 (2008).

123. Wijnsma, K. L., Duineveld, C., Wetzels, J. F. M. & van de Kar, N. C. A. J. Eculizumab in atypical hemolytic uremic syndrome: strategies toward restrictive use. *Pediatr. Nephrol.* **34**, 2261–2277 (2019).

124. Dhillon, S. Eculizumab: A Review in Generalized Myasthenia Gravis. *Drugs* **78**, 367–376 (2018).

125. Chatterton, S., Parratt, J. D. E. & Ng, K. Eculizumab for acute relapse of neuromyelitis optica spectrum disorder: Case report. *Front. Neurol.* **13**, (2022).

Appendix 1 - Supplementary Data for

Chapter 4

8. Appendix 1 – Supplementary Data for Chapter 4

8.1. C5aR1 Sequence for C5aR1 Primer Design

>NC_000019.10:47309861-47322066 Homo sapiens chromosome 19, GRCh38.p13 Primary Assembly

TTTCAATATTCATTTTTATTTTCCTCATTAAAGTCATGTATACTTTTTTTTTAAGCTCAAAACAG
GTTACATACTATATGATTCCATTGAATAACATTCTTGAAATGACAACATTATAGAAATGGAGA
GTGGATTCCTGGTTGCCAGGGGTTAGGGACACGGCTGGGGTGTGGGGGTGGAGGGAAGT
GGGCATCCTGGGGATCCCTGTGGTGATGAGAATGTCCTGTATCTTCACTGTATCAATGTCAA
TATCCTGGTTATGAGACTACATTGTAGTTTTGCAAGATGTTGCCATTGGGGGAGGCTGGGTG
AAGGGTACACAAGATCCCTCTGTATCATTACTTACAATTGTGTTGAGTTTGCAATGATCTCAA
AATAGAAAGCATAATTTAAAAACAAAGTACAAACAAAACTGCAGGTTTTTTAGGTGTTTTTG
TTTTTGTTTTTGCTTTGCTTTTGAGACAGAGCCTCCCTCGGTCACCCAGGCTAGAGTGCAGTG
GTGCGATCATGGCTCACCACAACCTCCACCTCCAAGTTCGAGCAATTCTCCCACCTCAGCCTC
CCAAGTAGCTGGGATTACAGGCACCCACTACCATGCCCAGTTAATTTTTTGTATTTTTAGTAC
AGACGGGGTTTCACCATGCTGGCCAGCCTGGTCTGGAACTCTTGACCTCAGGTGATCCACCC
ACCTTAGCCTCCCAAAGTTCTGGGATTACAGGCGTGAGCCACTGCTCTCAGCCTAATTTTCTT
TTTTAAATTAACTCACTTACAAGAGCTTAGATAACTCCATGGACTTCTGTTTTGTCCCAAAGA
ACTTTTGAGATTCCAGTTACATATTTTCCAACTTGCCATAAAATAAATACATTTTTTTTAAGCG
AGAATCTTTCTACTTGTCTGTATTCTGAGTTCCCTGTTCACACCTATTGCCATATGGAAATATC
CCAGATACACGGGTTTCTGTTTGTTTTTCAAAAGCCTGGGATGGAAAGATGGTGTGTGTGGG
GGGGGTGGGGGGTGGGAGGGTGCTCCCTAGAAGGAAGTGTTCACCTTGCAAATGAGGAA
GGATGAGAAGAGTCCCGCTGGAAAAGGAGGGACAAGTCTGGGAAAGACAGGCAACATGG
AGGAGAGTTAGTTAGCTAAGGTAACACCATCCCACGAAAAGTGAAGTGAAAACAAGAGGG
AGAATGGCCGGGAAGGAAGGGGACATCGGGCCACAGTGGCCCATGAGGCTGTCGCCTACA
CTGCCTGGGTCTTCTGGGCCATAGTGTCCACTGTGGAGCGCGTGAATGACTTGCTCTCCCTA
ACCACGGACTCTTCAGTCAACACGTTCCGGAGGAGGCTGGGGAGGGATTTCCGCAGTCGGC
CCTGGAAGCCCTGGCCGGCCACCACGTAGATGATGGGGTTGATGCAGCAGTTGATGTAGGC
AAAGGAGACACACAGGGAGTCCAGCTTCTTCAGCAGCAGGAAGGTGGGTGACGATGGCTC
CAGGAAGGACATCATTATCCCCGTCACCTGGTAGGGCAACCAGAAGATAAAGAAACTGGCC
ACCACTGCCACCACCACCTTGAGTGTCTTGGTGGACCGCGTGGCCCTGCGGCTCCACGTCCG
GAGCAGGATGAAAGTGTAACAAATCGTGAGCGTGAGTAGAGGCCACAGGAAGCCCAGGAC
CAGCCGGACGATGGCCACGGCTCGCTCCCGCCGTTTGTCGTGGCTGTAGTCCACGCCACACA
ACACCTTTGGTGGAAAGTACTCCTCCCGGACCACCCGGTACAGGAAGGAGGGTATGGTCAG
CAGCAGGGCTAAACCCCAAGCCACGGCACAGGCGATCCAGGCCAAGCCAGCCCCTCGGAA
GTTCTGGCACCAGATGGGTTTAAACACCAGCAGAAAGCGGTCGGCGCTGATGGTGGCCAG
GAGCAGGATGCTGGCGTACATGTTGAGCAGGATGAGGGAGGGC*AGGATGCTGCAGGCGG*
CCCCGCCAAAGGGCCAGTGGTGATGCTGTACAATGGACGTGAACAAGATGGGCAGCGCCAG
GCAGGAGAGGAAGTCGGCTACCGCCAAGTTGAGGAACCAGATGGCATTGATGGTCCGCTTG
*GCCTCGAATGCCGTCACCCAGACCACCAGGGCATTGCCCAGCACTCCCACCAGGAAGACGA***C**
TGCAAAGATGACCAAGGCC*AGGATGTCTGGAACACGCAGCGTGTTAGAAG***TTTTATCCACA**
GGGGTGTTG*AGGTCCAGGGTATCCTTGTCATCATAGTGCCCATA***ATCAGGGGTGGTATAAT**
TGA*AGGAGTCCTAAGGGGAATCGGAGAGAGCAGAGAGGATGAGTCTGCAGACATGTGCCC*
GGGTAGGGGGCATCCTGGCTCAGGCATGTGGCTTTTCCCCTGTGTGGCTTTTTCTCACTAGG
AAATGGGGATGCTGAGGGCTGAGAGTCAACTAGGGTGTCACACCACTTATTAAAATATTGA
*GGCAGATGCCGTAGC*TCACGCCTGTCATCCCAGCACTTTGGGAGGCCGAGGCGGGCGGACT
GCTTGAGCCCAGGAGTTTGAGAATAGCCTGGGCAACATGGCAAAACCCCGTCTCTACTGAA
AATACAAAAATTAGCCAGGCGTGGTTGCACTTGCCTGTAGTCCCAGCTACTCCGGAGGCTGA
GGTAGGAGGATCACCTGACCCCAGGAGGCAGAGGTTAGAGTGAGCCGAGATCATACCATT
GCACTCCAGCTTAGGTGACAGAGTGAGACCCTGTCTCAAAAAAAAAAAAAAAAAAAAATG
AAATGATTCCATGCTAGTTGGACCCCTTGCCAGTCTGCCACCTCTCCCCTCAGTCCCATCCTG
CGAAGCCCCTGGGCTTCCCCACGATCCAGCAGCCTAACGTCAAAGTCTAGCCCTACTGGCCG

GGCACGGTGGCTCACACCTGTAATCCAGCACTTTGGGAGGCCGAGGTGGGTGGATCACGA
GGTCAGGAGTTGAAGATCAGCCTGACCAATGTAGTGAAACCCCGCCTCTACTAAAAATACAA
AAATTAGCCAGGCGTGGTAGTGGGCGCCTGTAATCCCAGCTACTTGGGAGGCTGAGGCAGA
AGACTTGCTTGAACCCAGGAGGCAGAGGTTGCAGTGAGCCGAAACAGCCCCATTGCACTCC
AGCCTGGGTAACAGAGTGAGACTCCATCTAAAAAAAAAAAAAAAAAAAAAAATAGAACAAA
AAGGTCCTGATCACTTCTTCCCAGACAGAGCTGAAGGAAGCTGTCATGCACCCAAGAAAGA
AAGGCTGCAGTCCATGGCAGCTGGACTGGAGAAAGCCTTGTAGGTGAAATCTGTGTCCAGA
GGCACCAGACACTGCAGTAAAGCACCCATCAGGGCACTGAGTGATCACCCGAAAGCAGCCA
GTACTTACTGAGCACCTACTATGCATGCGGCATGGAATTTGCTCTTTCCATCCTGACCACAAC
CTACAAGGAGGTTCTGTTAATATGCCCATTTCAGGCCAGGTGTGGTGGTGCACACCTATAAC
CCAAGCACTTTGGGAAGCCAAGGTGGGCAGATCACCTGAGGTCAGGGGTTCGAGACCAGC
CTGGCCAACATGGTGAAACCCCGTCTCTACTAAAAATACAAAAATTAGCCAGGCGTGGTGGC
GGGCACCTGTAATCCCAGCTACTCGGGAGGCTGAGGCAGGAGAATCACTTGAACCTGGGA
GGTGGAAGTTGCAATGAGCTGAGATAGCGACACTGCACTCCAGCCTGGGCGACAGAGTGA
GACTCCACCTCAAAAAAAAAAAAGAAAGAAAAAAAAATGCCCATTTCGCTGATGAAGAAGC
ACGAGGCACCAGAAGGTGAAGTAGGCTGTTCCAGGTCACTCAGAGAGGATGTGAACCCATA
CGGGCTGGAATGCAAACCAGACAGGCTGCCCCTGACCATTTCCAAGAGGTGAGTTTTGTGA
CCTATGGAGCTAGCCCAGTCCTGAAGGCCACTTTGACACCAACCCAGAGAAAAGGGGACAG
CAAGAAATAGAAATCATTCTGGAAATACTGAGAGCTGTATTTGCAGCTCTAAATATTTGAAT
TTGCAGATGGAGTTTTGTACATTTTTTTTTTTTTTTTGAGATGGAGTCTCACTCTGTCGCCACG
CTGGACTGCAGTGGCACGATCTCGGGTCACTGCAACCTCTGCCTCCCAGGTTCAAGCGATTC
TCCTGCCTCAGCCTCCTGAGTAGCTGGGACTAAAGGCACCTGCCACCACACCCTGCTAATTTT
TGTATTTTTAGTAGAGACAGGGTTCCACCATGTTGGTCAGGCTGGTCTCGAACTCCTGACCTC
GTGATCTGCCTGCCTTGGCCTCCCAAAATGCTGGGATTACAGGCATGAGCCACCACACCCGG
CCTGGTTTTTCTACCTTTAAAACACTCACCTCAAAGATTAAATAAGATGAAAAATGCCTAAGC
ACCTAGCACAGCGCCTGACACAGAGAAGAGGACAAGAAGTGGCAGCCATTGGTATTATTAT
TTGTCAGTTATTGAAGAGCTCAGATCCACATCCCTGAACCACTATATATATATATATATTTTTT
TTTTTTTGAGACTGAGTCTCACTCTGTCACCCAGGCTGTAGCTCAGGGGTGTGATCTTGGCTC
ACTGCAGCCTTGACTTCTCAGGCTCAAGTGATCCTCTTGCCTCAGCCTCCCAAGCAGCTGGG
ACTACAGGTGCATACTACTGTGCCCAGCTAATTTTTAATGTTTTTTTAAAGAGGAGGGTCTCA
CTGTATTGCCCAGGCTGGTCTCGAACTCCTGGGTTCAAGCAATCCTCCGGCCTTGGTCTCCCA
AAGTGCTGGGATTACAGGCATGAACCACCACGCCCAGCCCCGTTTTATATTTTTTTTTTTTTT
TTTTTTTGAGACGGGGTCTTGATCTGTCACCCAGGCTTATGTGCAGTGGTGCAATCATGGAT
CACTGTCACCCCAGCCCCTCTGGCTCAAGCAATCCTCCTGCCTCAGCCTCTTGAGTAGCTAGG
ACTACAATTGTGCACCACCACACCCAGCTAATTTTTGTATTTTTTTTCTTTTTTTTTTTTGGTAG
AGATGGGTCTCGCTTTGTTGCACAGGCTGGTCTCAAACTCCTAACTTCAAGCAACCCTCCTGC
CTTGAACTCCCAAAGTGCTGAGATTACAGATGTAAGCCACCATGCCTGGATAGTTTTGTTTTT
TTTTTTCTAGTTCCCTTACATTGCACCTGCCCAAGGTTAGCCAGGCTATGGGCAGTGGGCATT
TACTGGTGGAATCATATCCATGAGTAAATTATTGAAAGATAAGATGTCAGTATCTGCTAATG
AGTGAATGAAAAAGGTGGGGTTTAGCCACGTGGTGGAATATTACTCAGCTATGAAAAGGAA
GTGCTGACACATGCTGCAATGTGGATGAATCTTGAAAACATGATGCTAAGTGAAAGAAGCC
AGTCACAAAAGGCCATTAAAAATACAAAAATTAGCCAGAGTGTTGGCGCGCACCTGTAATCC
CAGCTACTCCAGAGACTGAGGCAGGAGAATCACTTGAACCTGGGAGGCGGAGGTTGCAGT
AAGCTGAGATCATGCCAATGCACTCCAGCCTTGACTGAGCAAGACTCTGTCTCAAAAAAAAA
AAAAGGTGATAGAAAGATGGATGGATATAAATAAACGGATGGATAGATAACGAATGGGTG
AATGAGTGGATGCATGGATGATGGACAGATAGATGACTGATGGACAGACAATGGATACAT
GGAGATATGATTGAGAGATAGATGATAGATAGATAGATGATAGATACATAGATAATGGGCT
GGGCATGGTGGCTCATGCCTGTAATCACTTGAGGCCAGAAGATCAAGACCAGCCTGGCCAA
CATAGTGAAACCCCATCTCCACTAAAAGTACAAAAAAATTAGCTGGGCCCAGTGGTGTGTGC
CTGTAGTCCCAGCTACTTGGGAGGCTGAGGCAGGAGAATCGCTTGAACCTGGGAGGTGGA
GGTTGCAGTGAGTCAAGATTGCGCCACTGCCCTCCAGCCTGGGCAACAGAACAAGACTCTG
TCTAAAAAAAAAAAATAGCTAGATAACGGATGGATGGATGGATGGATGGATGAATC
GATGGACAGATGGATGGATGGATGGATGGATAATGGAGAGACAGATACAGTAAATTTGGA
GAGTCTAGGTAAAATGTATATGTATATGAGCCTGTTCCATTCTTGTCATTTTTCCGTAAGTTT

GAAAATATTTCCAAATAGAAGGTTAACATTTTTAAAAATATTTTCACTGGTAAACAGCCCCTG
CCCTCAGCCACCCACTTCTTCTATTGCCCGCTCCCAGCACCCTAAGTTCCTGTTTCCTACTCTG
GGACACCCCCACTCCAGGTCGCCATGTTCATGTCACTAAAGAGTTAATGCTAGGTGCAGCAG
GAGGCCCTAGACCCTGCCCAGGGGACCTCTGCACTTTAGCACATTGTTAAATATTTTGAATG
TTCCCTTTGGCTGTGACGCATGAAGGTAAATTTTGCCTCTGCTGGTTTCGCAAGCTCCCAGCA
ATCCTTGACTGCAGAATGACTCAGACCCTCGTAAGGGGAGCCTCCCCACCCTCTGCTCTGAC
ATCGCCTTGTCACTCCCTCATCAGCTGACAAAGCTCCGTTCCTGCCATGAGCTCACTCAGTCC
TTTCCTCTGGTTGACTTCAGAAAGGCAGAAAAAATACGCTGATTCCAACGTCCTGTGGTTTCC
GGGATCTTCAGACGCAAACGGCTTGCAAAGTTTGCCACTGCAGCACCTCTCCAAAGACTGGA
AATAACTGACATGTCCAGCAAGAGGGGACTGGCTAAATTAATGATGGTACATCCAGGCAAC
AGAATACTACACAGCTATCAAAAAGAATGGAAAAGTTGGCCAGGTGCAGTGGCTCATGCCT
GTAATCCTAGCACTTTGGGAGGCTGAAGCAGGGGGATTGCTTGAGCCCAGGAGTTCAAGAT
CAGCCTGGGTAACCTAGCAAGACCCTATCCCTACAAAAAGGAAAAAAACAGACAAAAAGAA
TGTTTATATAATGATGTGGAAAGACCTCCAAGATCTAGGGTGAGGCCAGGCGTGGTGGCTC
ACGCCTGTAATCCCAGCACTTTGGGAGGCCAAGGAAGGTGGATCACTTGAAGTCAGGAGTT
CAAGCCCAGACTGGCCAACATAGTGAAACCCCGTCTCTACTAAAAATACAAAAATTAGCTGG
GTGTGATGGCAGGCACCTGTAATTCCAGCTACTCAGTAGACTGAGGCAGGAAAAACACTTG
AACCCAGGAGGTGGAGGTTGTAGTGAGCCGAGATCGTGCCACTGCACTCCAGCCTGGGCAA
CATAGCGAGACTCCATCTCTAAAAAATAAAATAGGCTGGACACGGTGGTTCACGCCTGTAAT
TCCAGCAATTTGGGAGGCCCAGGCGGGTGGATCACCTGAGGTCAGCAGTTCAAGACCAGCC
TGACCAACATGGTGAAACCCTGTCTCTACTAAAAATACAAAAATTAGCCAGGAGTGGTGGC
GTGCGCCTGTAATCCCAGCTATCTGGGAGGCTGAGGCAGAAGAATCACTGGAACCCGGGA
GGTGGAGGCTACAGTGAGCCGAGATCGCTTCACTATACTCCAGCCTGGGCAACAAGAGCAA
AACTCCATCTCAAAAATAAAATAAATAAAGTAAAATAAAATAAAATAGTGAAAAATAAACGT
AGGTAGCTGCATTGTGGCACGTGGCCCACATATTGGGCAGTGCAGGTCCAGGGCCACTCTG
GGGGTTCTAATTGCCCGGCACTATTCCATGTGCTTCCCAGGTGTTGGCTTAGTAATTTCCTAA
TCACAGTGCATATCTATGTGACAATAGCACAAAGGGCAGGGTACTATTATTCTTCCTAAATTC
ACATGCTCATTAGAGGAACAACCCTTGTCTGTTGCATGGAGAAAGGGGCAGAGAGCAGAAG
CTGGGAGGAAACGGAGATTGGAACTGTCCAGGTGACGTGAGGCATGACGGTGGCTTAGAC
AAGGGTGCTGGCCGCAAGATGTGAACGATCGGATGAGAACAGGGTGAAGGAGAAGGCGC
AGTACCTACAAGAACAGCCATAATCATTGCCAGGCTGTCCTGAGCCTTTCTCGTGTATTATCT
CATTGAACCCACAAAGCAACCCTAGGAGACTTACTTGTTGCAACAGCAACACTCATTTTCCAG
AAGAGAAAAATGAGGCTACAGAGAAATGAACAGACCTCTCCAAGTCTTCTCGGTTAGCAAG
AACAGAGACAGGAGAGAAACTCCTGAGAGCTGAGCCCCAGAGCCCTCTCTCTCTTTTTTTTT
TTTATGAGACGGAATCTCGCTCTGTCCCCAGGCTGGAGTGCAGTGGCGCGATCTCAGCTCAC
TGCAAGCTCCGCCTCCTGGATTCACACCATTTGCTAGCCTCAGCCTCCCGAGTAGCTGGGACT
ACAGGTGCCCGCCACCATGCCTGGCTAATTTTATTTTTAGTAGAGACAGGGTTTCACCGTGTT
AGCCAGGATAGTCTTGATCTCCTGACCTCGTGATCCACCCACCTCAGCCTCCCAAAGTGCTG
GGATTACAGGCATGAGCCACCGCGCCCAGCCCAGAGCCCTCTGTTTGAGTGGCTACCAGGC
AGGCCTAAAGTGCATTGGGAGTGGGGGGGCATGCATTCTAGGCAGAAAGGAGAGAGGAA
GGGCAGGTGGTGCACAGCAGAAACGAAAGGTCAGCATGGCTGGCAGGCGGCCAAGATAG
GACTGGAAGGTCTGCAGATGCTGAGTTAAAGAATGTGGCTGGACGCCAGGCGCGGTGGCT
CACGCCTATAATCCCAGCACTTTGGGAGGCTGAGGCGGGTGGATCACGAGGTCAGGAGTTC
GAGACCAGCCTGGCCAACATGGTGAAATCCCGTCTCTACTAAAATAAAATACAAAAATTAGC
CGTGTGTGGTGGCACGCACCTGTGATACCAGCTACTTGGGAGGCCGAGGCAGGAGAATCAC
CAGAATCCAGGAGGCAGAGGTGCAGTGAGCCAAGACTGCACCACTGCCCTCCAGGCTGGG
TGACAGAGCGAGACTCTGTCTCAAAACAAAACAAAACAGACCAAATATTAGAAGCAAACTA
AATTTCCATTGAAGGGGATGAAACCTCCTACTAGCATATTACTCAGCTGATAAAAGAAAGAA
AGAAGCACCAGGCTGGGCAACATAGCAAGACCCCACCTCTACAAAAAATTTTAAATCTAGCT
GGGTGTGGTGGCATGCACCTGTAGTCCCACCTACTCAGGAGGCTGAGGTGGAAGACCTCAG
TAGACCCTGTCTAGAAAAAAGAAAAAAAGGAGGAGGAGGAGGAGGCAACTCCCTTGAACT
ACACGGGAATGAAGTACCTTCCTCAAGGTTAAGGGGAAATTAATGAATGCCTAATACAACG
CCTGGTATGCAGTAAGCACTCAATAAATGCTAGTTAATAATACTATATGTTATTCATTTAAAA
AAGCCAGATGTAGAGTACTGTACAAAACATACTGCCATTTATAAGGCTGGGAAAGGATAGA

AATGTCACCCACATTGAGCGCCAACTGTATACCAGGCACTGCTACAAGAACTTTTCATGCATT
CACTCAGTCAATTCTCTCAACTAGCCTATGATGTAGATTCTAGTATTATCTTCACCTTAAAGAT
AAGGAGAAGGAGGCTGGGTGCGATGGCTCACGCCTGTAATCCCAGCACTTTGGGAGGCCA
AGGCGGGAAGATTGCTTGGGGCCAGGAGTTCAAGACCAGCCTGGCCAACACGGTGAAACC
CCGTCTCTACTAAAAATACAAAAATTAGCCAGGCATGGTGGCAGGCACCTGTAGTCCCAGCT
ACCTGGGAGGCTGAGGCAGGAGAATCACTTGAACCCAGGAGGTGGAGGTTACAGTGAGCT
GAGATCACACCACTGCACTCTAGCCTGGGCAACAGAGCAAGACACTGTCTCAAAAAACAAA
AAGATAAGGAGACAGAAGCACGGAGAGGACAGATCTCCGCAACTATTTCATAGTAGAGAC
AGAAGCTGAGCTCGGTTTTGGGGTTCCCCGCATCACACTAGTCCTTACTTTGTTCCCTAAGCA
TCTGTGCTCTCAGGCATCTGTAAACTGTTTCTGGAAGGATCCACCACAAACTGGCATCCCATG
GTTGCCCCAGGTAGGGTAGGAGGCAATGAAAAGGAGTCAGAGGGCCAGGTAGGGTGGCT
CATACCTGTAATCCCAGCACTTTGGGAGACCAATGTGGGTGGATCACGTGAGGTCAGGAGT
TCAAGACCAGCCTGGCCAACATGGTGAAACTCCGTCTCTACTAAAAAGACAAAAAATTAGCC
AGGCGTGGTGGCGCATGCCTGTAATCCCACCTAGTCGGGAGGCTGAGGCAGGAGAATTGCT
TGAAGCCGCGAGGCAGAGGTTGTGGTGAGCCAAGATCGTGCCATTGCACTCCAGCCTGGGC
GACAAGAGTGAAACTCTGTCTCAAAATAAAAGGAAAGAAAAGGAGTCAGAGGCTCTGGGG
TAGGCAGGGAGAATGAGTTTTTTTTTTCTATGTTTGTTTTTTGAGATGGCCCTGTTGCCAGG
CTGGAGTGCAGTAGAGCAATCTCGGCTCACTGCAACCTCTGCCTCATGGGTTCAAGCGATTG
TCGTGCCTCAGCCTCTCAAGTGCTGGGACTACAGGCGCCCGCTTATATGCCCAGCTAATTTTT
GTAGTTTTGGTAGAGACGGAGTTTCACCATGTTGGCCAGGATGGTCTCAATCTCCTGACCTT
GTGATCCGCCCGCCTCAGTCTCCCAAAGTGCTGGGATTACACGCATGAGCCACCGCGCCTGG
CCGAGAATGAGTTTTTACCAAGTATCATTTGGTACTTTGGAAAATGTTTTGGAAAGAAAAAA
AAAAAGAAGAAGAAGAATCAGAGAGTCCCGTTTGCCCAAGTCGGATCTCAAGGGTGGAAT
GCAGGAATGAAGCAACATCAGACCCCTCCCTGGTCCATCCAAACCATCTTCCGTTTCCTCTTT
GACACAGATGAAGCAAGGCAATGCCTGTGTTACAGCAGGTGCTGAATCGCAGCTCTGCTGG
CTCAGTGCCCAGGCCTCCAGACGCAGGGATGACAGGGACCCTCATTTAGCCTGGGGTGCAT
TCCTTCTGACACTCACAGAATCCATGGCATAACCTGCTTCTGCCACCAACCATGGAGGGTCCC
CATCCATCTCTGCTCCTGCCTGGGCCTCAGTTTCCCCATCTCTGTCATGCAGAACATCTCAAAC
GACCAGGCATAATGGCCTCATGCCAGTAATCCCAGAGCTTTGGGAGACCAAGGTGGGAGG
ATGGCTTGAGGCCAGGAATTTGAGACCAGCCCTGACAACATAGCAAGAACCCATCTCTACAA
GAATAAAAATTTTAAAAATTAGCCGGACATAGTGGTGCATGCCTGTGGTCCCAGATACTCAG
GAGGCTAAAGAGGGAGGATCACTTGAGCCCAAGAGTTCAAGACTGCAGTGAGCTATGATG
GTGCCACTGCACTCCAGCCTGGGCAACAGTGCAAGACCCCAAGTCGAAAAAGAAAAGAACA
TCTATCTGCAAGAGCATCTGAGTAACTTGACCATTCCTCCAAACTGGTTCTTTCCAGCCTCCC
AACATTTTCTCTGCCATTCCCACTGCCTGGAAGGCCTGTTCTAGATTTCTTCACTTGTGGAATT
CTTTAAATAAAAAAAAAAATACAGACAGGGTCTCACTATGTTGGCCAGGCTGGTCTTGAACT
CCTGGCCTCAAGCAATCCTCCCGCCTTGGCACAATCCCCAATGTGCTGGGATCACAGGTGTG
ACCCACTGCGCTCGGCTGCTTGTGGAATTCTTAGTCACCTTACTAGACCCAACTCAAGGGTCC
CCTCCCCTGGGGAATCTTCTCGGGCCCCAGCCCCACGAGGTTGCTGTTGCTCCCACAATCTTG
ACAATCTTATTCCCATGGCCACATCCCAGCCCTGGAGTGTGAGAGCCTGGGATGCAGGAGA
GAGGGAAGGTGGGAGGTGGAAGACAGGGAGAGAGAAGGAAAGGGAGAGACAGACAGA
GTTGACGGCGAGAGTTGGGGAGAGAGAAGGACCCACTGGAGCAAAGATGGGAGGGACCC
AGGACAAAGTTTCCTGCTCCCATTCCCCTTCGAGACTCACCATGTTCTGGTCTCCTGGGCTCC
CCGAGGATCGAAGGT

C5aR1 Primer Pair 1

Forward Primer: GCAGGAGAGGAAGTCGGCTA

Reverse Primer: AGAAAAAGCCACACAGGGGA

C5aR1 Primer Pair 2:

Forward Primer: CGCCAAGTTGAGGAACCAGAT

Reverse Primer: AGCCCTCAGCATCCCCATTT

C5aR1 Primer Pair 5:

Forward Primer: GGGCCAGTGGTGATGCTGTA

Reverse Primer: CACACAGGGGAAAAGCCACAT

Supplementary Figure 4.1. C5aR1 sgRNA target sequence and primer design. Black: C5aR1 gene sequence, *Green:* Target Amplicon, **Red**: gRNA target sequence.

8.2. C5aR2 Sequence for C5aR2 Primer Design

>NC_000019.10:47331614-47347329 Homo sapiens chromosome 19, GRCh38.p13 Primary Assembly

GCAAGACTCCATCTCTAAAAAAAGTAAAGCATCGCTATGGCCAACAACATCTTCCCATTCTAC
AGATGGAAAATTGAGGCCCAAGAAAGGAGTTGTTTGTGCTTTTTCTACCACTGAGGCGTTG
GGCCCTGCGCTCAGCTGCTGTGGTCTTTTTGTGGAGAATGTGACCCCAGGCTGTCTTCCTCA
GAGCCGAGGAGGAGGGAGGGATGTTTGTCTGTCCTGAGGCTGCAGAAGGGAGGGGTTGA
ACACAGTTAGAGGCCTGGAGGTGGCTGGGGGCAGCTGGCATGTTGTGGGCAAACAGAATC
CAGGCCAAGACCTCTAAGGCGTTAAAGAGCAAACCGCATGCAGGTCTGGCTTCCAGGAAGG
TGGGACTTCGAGACTAGGGTTGGGGACTTGGGATCAGCCCTCCACCCAACCGAGCCCTCTCC
TGCCCTGCCAGCCACCCCGTAATTTTGGGTTCTGTGAGTCACGGGAAGAAGACAGGACAAA
CACACCCTGAGAGCGAGACAAGGCCACTCCTATTTTGTACTGCTTATAAAGATTCACTGGGA
CTGGTGAGGTGGCAGTGCTCAGCAGCATCCGACAGGAGCCCTGGCAAACAGGACGGATTTC
CAGGACTCTACCAGCTGCCAGACACGGCAGGGAGAGACCCCAGACCTCCTGGGTCCTGGCT
GTGGGCCCGGATTGGGCTCCCAAGTGGCGTTTGACTCACGTGGGGACACTCTTGGAAGAGA
CGGTAAGGATGGAGGCTACAAGGGCGGGAAGGAGGGAGAGAGAGATTGCATGATCTTGG
CTTCTCGGAATCATTACTTTCAGAATCTGGGAAGCAGAACTAGAGTTTGAGAAGTGCAGTCT
TATTACAGCCACACTGGAACGCACGTCACAGTCCTGGGCTCTTGAATTAACTTGGGCAGCCC
AGCAGCAAAGCTCTTGTCAAAGGATCTAAGCATTTTTTTTCTTTCTCTTTTTGGAGACAGGTTT
TCATTCTTGTTGCCCAGGCTGGAGTGCAATGGTGCCATCTTGGCTCACCGCAACCTCCACCTC
CCAGGTTCAAGGGATTCTCTTGTCTCAGCTGGGATTACAAGCGCATGCCACCATGCCTGGCT
AATTTTGTATTTTTAGTAGAGATGGGGTTTCTCCATGTTGGTCAGGCTGGTCTCGAACTCCCG
ACCTCAGGTGATCTGTCCGCCTTGGCCTCCCAAAGTGCTGGGATTACAGGCGTGAGCCACTG
TGCCCTGCCCAAATGGTTTTTCACACACAGATGTATGGGAAACAGCCTCTCTCAAACCTGCA
GGAATTCCTGCAGCTTTCGGCAGATCCACCAAACTGTAGCATGTGTAGCAAGCAAGCCCTTT
AACTCAGCGATTCCAATTCTTTTCTCTTTCTTTCCTTTTCTCTCTTTCTTTCTTTTGACAGGGTCT
CACTCTGTCTCCCAGGCTGGAGTGCAGTGGTGCGATCTTGGCTCACTGCAACCTCCGCCTCC
CAGGTTCAAGTGATTCTCCTGCCCCAGCCTGCTGAGTAGCTGGGATTACAGGTGCACGCCAC
CACACCTAGCTAATTTTTGTATTTTTAGTAGAGATGGGGTTTCACCATGTTGGCCAGGCTGGT
CTCCAACTTTTGACCTCAGGTGATCCACCTACCTTGGCCTCCCAAAGTGCTGGGATTACAGGC
GTGAATCACCGTGCCTGGCCCCCTCAATGTTCTATCACAAAATCTGTCCACATTCTTGTGTGG

TGTTTGTTCATTCTCATCGTGTAGAATATTCCACAGGGTGAACACCCCATGATGTGTTTATCC
ATTCTGCTGTGGGTGGCTATTTGGACGGTTTCTCATCTTGGGCTGCTGTGAACATTCTGGCAC
ATGTATTCTGGTGAGCATATGTGTTCTTTTGCGGAAAGGAGGCTGATTGCTGGGTCGTGAG
GGAGGAATCCTAGAAGATGGATGTTCAGGAATAAAGAATGTTCAGACTCCTTTTTTTTTTTTT
TTTTTTTGAGATGGAGTCTTGCTCAGGCTGGAGTGCAGTGGTGCGATCTCGGCTCACTGCAA
CCTCCGCCTCCTGGGTTCACGCCATTCTCCTGCCTCAGCCTCCTGAGTAGCTGGGACTACAGG
CGCCCGCCACCGCGCCCAGCTAATTTTTTGTATTTTTTAGTAGAGATGGGGTTTCACCATGTT
AGCCAGGATGGTCTCGATCTCCTGACCTCGTGATCCACCTGCCTGGGCCTCCCAAAGTGCCG
GGGATTACAGGTGTGAGCCACTGCGCCCGGCCAGCCTTCTTTGATTCTGCTCCAGGGTTTTC
CAGAGCAGAGAACCCAGCAAGACTGGATGCACAGACAGGCGTGCACCAAGAGGCACATGT
GAGGGTGCTTGCAATCACAACAAAAGAAACCTAAGTGACCACTTAGTCTCTCTGTGCCTCAG
TTTACTCTTTTATCCTTTCACTTACCAAATATCGACCATGCCTGTGCTGTGTGCCAGGTTCTGT
CCCAGATGCCAGGGACACAGCGGCACCCGAGGCTGGAAGGAGCTGATGTTGTGGGATATG
AGGATGATAATATTGACCTCAAGGGTTTGTGTTGAGGGTTATATCTTGTAGGTCATAGGTGC
TCAATAAAAGCCATCTATTATTTTAATTATTATGAAATAATAAGAAGGGTACCTATGATTTAA
AAGCTAGATATAAGTACAGACGCTCTTTGACTTACAATGGGGTCCCATCTCTATCAACCCATC
GTAAGGCTGGGCACAGTGGCTCACGCCTGTAATGGCAGCACTTTTGGGAGGCTGAGGTGG
GAGGATTTCTTGAGCCCAGGAGTTTGAGATCAGCCTGGGCAACAGAGTAAGGGCTGTCCAT
ACAGAAAAAAAAAAAAAAAATTAGCTGGGCATGATGGCGTGCACCCGTAGTCCCAGCTACTC
CAGAGGCTGAGGCAGGAGGATCAGTTGAGCCTAGGAGGTAGAGGCTGTGGTGAGCCGAG
GTTGAACCACTGAACTCAGCTTGGGTGACTGAACAAGACGAAAACACAAAACAAAAGCCCC
CAACATTTTCAACATAAGTTGAAAATATTGTAAATCAAATTGGATTTAATACACCTAGCTTAC
TGAACATCATAGCCTACTTTTTTTTTTTGAGACAGGGTCTCACTCTGTTGTCCAGGCTGGAGT
GCAGTGGCGCGATCTTGGCTCACTGCAGCCTTGACCTCACGGGCGTAGCCTACCTCAAATGT
GTTCAGAACATTTACATTACCCAACAGCAAGACAAAATCATCTAAGCCAAATCCAATTTTTTT
TTTTTTGAGATGGAGTCTCACTCTGTCACCCATGCTGGAGTGCAGTGGTGTGATCTCAGCTG
ACTGCAACCTCCACCTCCCAGCTTCAAGGGATTCTCCTGCCTCGGCCTTCTGAGTAGCTGAGA
TTACAGGCACTCGCCCCCACGCCCAGCTAATTTTTTTTTTTTTTTTAAATCTTTAGCAGAGATGA
GATTTTATCATGTTGGCCAGGCTGGTCTCAAACTCCTGACCTCAAGTGATCCGTCTGCCTAGG
ACTCCCAAAGCGTTGGGATTACAGGTGTGAGCTTCTGCACCTGGCCCTGTTTCTCATTATTCT
CCTTACCATTGTTATTGAATGGCCTTTAGTTAATAAGCACCACTTGGGCAGACAGTGGACTGT
TTTTGATGCTTTGAGGACGAATGGGGTTGATATCTGTACAGATAGACAGGAAAACAGATAT
CGGGCACGTTAAGTGGAAAAGATGAAGAAATGGAACAACGTATGTTGAAAGCTCCCATTTC
TGGTTAAGACGTTACAAAGGAAATGCCATCTACGATACCATTGCTTTGGGCTTACAGCTGGG
CAAATTATATGCACAGAAAGTTTCCTGGATTGGGCTGGGCATGTTGACTCACGCCTGTAATC
CCAGCACTTTGGGAGGCCGAGGTGGGCGGATCATGAGGTCAGGAGATTGAGACCATCCTG
GCTAACACGGTGAAACCCTGTCTCTACTAAAAATACAAAAAATTAGCCGGAAGTGGTAGCG
GGCGCCTGTAGTCCCAGCTACTCGGGAGACTGAGGCAGGAGAATCATGCGAACCCGGGAG
GTGGAGCTTGCAGTGAGCCGAGATCGCACCACTGCACTCCAGCCTGGGCGACAGAGTGATA
CTCCGTCTCAAAAAAAAAAAAAAAAAAAAAAAAAAAAAAAAAGAAAGTTTTCGTTTTCTGGATT
GTAATCAACAAGGGCCAGGAAGGGTGGAGTCTTTGCGGGGTGAGAGGATGCGTGTGGACA
GTGATAACAGCAGCTAGCCTACGTATGACACCCACTGAAAACCAGCGCTATACACTCAGCTC
TACCCTTCTAACTTGTTGAATTCTTACAACACCCCCTAAGGCAGGAATATTATTATTCCCATTT
TACTGAGGCACAGATAGTTTAGGTGACTTGCCCAAGGCCACACAGCTGGTAGGAATTTGAG
GGTTTTTGTTGTTGTTGTTTGTTTGTTTGTTTTTTATGATGCAGTCTCGCTGTTGTCGCCCAGG
CTGGAGTGCAGTGGCATGATCTTGGCTCACTGCAACCTCTGCCTCCCGGGTTCCAGCGATTC
TCTTGCCTCAGTCTCCCGAGTAGCTGGAATTACAGGAGCCCACAACCATGCCTGGCTGATTTT
TGTATTTTTAGTAGAGACCAGGTTTCACCATGTTGCTCAGGCTGGTCTTGAACTCCTGGCCTC
AAGTGATCCGCCCACCTCGGCCTCCCAAAGTGCTGGGATTACAGGTGTGAGCCACTGTGCCC
GGCTAGGGGGGGTTCAGTTTTTAAATGCTGTACTCTTTCTTTCTTTCTTTCCTTCCTTCCTTCCT
TCCTTCCTTCCTTCCTTCCTTCCTTCCTTCCTTCCTTCCTTTCTTTCTTTCTTTCTTTTTCTTT
CTTTCTTGGGACAGGGTCTCACTCTGTTGCTCAGGCTGGAGTGCAGTGGCGCGATCATGGCT
AACTGCAGCCTCAAACTCCTGGGCTCATGTGATCTTCCACCCCAGTCTTAGAAAAGGTTGGG
ATTGCAGGCACGAACCACTATGCCTGGCTAATTTTTAAATTTTTTGTAGAGACAGAGGGTCT

CACTGTGTTGCCTAGGCTGGTCTTGAACTCTTGGCCTCAAGCGATCCTTCCTCCTCAACTCAG
CCTCCCAATGTACTGGGATTACAGGTGTGAGCCACTGCACCTGGCTAAATTCTGCACACCTTT
TACTCTAGGGATAAAAATAATACGAAAGTGGAATGCCAGACTCCGAATACACACACCAAGT
GGCCTGGACTCTTCACTGCTACCTGGCATGGGGGAGGGGAGTGCCCCAACTTCCTCTCTGTC
CTTCCTGTTGCCTCAACACCAGCTGGAGTGCTGAGCAGTGCCAGCCAACCCATAATAGTCAG
CAGAGAGCCTCAGGGCCAGGTCACTCTGACATTGTGGGGGTGGGGGGGTGGGGACTCCTG
CCTGGGTCCTGTGCTACCCACAGCTTTGTCTACCGGAGCCTGTGTGCCACGTGCTGGACAAA
TCTTAACTCCTCAAGGACTCCCAAAACCAGAGGTAGGTTCACCTCAATGACTCTTGTTTCCCC
GATGAGGAAATAGGCACAGCCAGCTGCAACTGACACCCACAGTCATGGAGGCCGGGGCTG
CTCAGGACCACTTGCTGTGCTGCCTGCCAGCTCTCCAGAGCCCAAGATTTGGAGATGGTAAT
ATTCTAGGGCATGGGGTTCTGCAGCGGGGACTAACACACTTTGAAATTTACCTACTTAGGGC
TGGGCGCGGTGGCTCATGCCTGCAATCCCAGCACTTTGGGAGGCTGAGGTGGGCGGATCAC
AAGGTCAGGAGTTCGAGACCAGCCTGGCCAATATGATGAAACCCCGTATCTACTAAAAATAC
ACAAATTAGTTGGGCATGGTGGCGGGTGCCTGTAGTCCCAGCTACTCAGGAGGCTGAGGCG
GGAGAATTGCTTGAACCCTGGAGGCGGAGGTTGCAGTGAGCCGAGATTGCGTCACTGCACT
CCAGCCTGGATGACAGAGCGAGACTCTGTCTCAAAAAAAAAAATTTTACCTACTTAGCTGAG
TGATCTTAGGTAAATTACTTAACTTCTCTGTGCCTTATCTGTAGAATAAATATAACAATAGTG
TCAAATTCAGACAGTTATTATAAGGTTTCAGTGAGGTCAGGCACGGTGGCTCATGCCTGTAA
TCCTAGCACTTTGGGAGGCCGTGGCAGGCAGACCACTTGAGGTCAGGAATTCCAAACCAGC
CTGACCAACATGGTGAAACCCCGTCTCTACTAAAAATACAAAAAATTAGCCCCGGGCATGGT
GGTGCACGCCTGTAATCCCAGCTACTCGGGAGGCTTGTGGCAGGAGTAATGCTTGAACCCA
GGAAGCAGAGGTTGCAGTGAGCCAAAATAGCGCCACTGCACTCCAGCCTGGGTAGCAGAG
TGAGACTCCGTCTCAAAAAAAAAAATAAATAAAATAAAATAAAACAAGGTTTCAGTGATACA
GTGTTTAAAGCTGCGTGGTGGCCACTGCCTGTAGTCCCAGCTACTCAGGGGGCAGAGGTGG
GAGGATCACTTGAGCACAGAGTTTGAGGCTGCAGTGAGCCGTGATTGCACCACTGCACTCC
AGCGTTGGCAAGATGGCGAGACCCTGTCTCTAAAAAAAATATATATATATAAATTTGCCAGG
TGTGGTGGTGCACACCTGTAGTCCCACGTACTCAGGAGGCTGAGGTGGGAGGACCACTTGA
GCCCAGGAGTTCGAGGCTGCAGTGAGCCAAGATAGTGCCATTGCATTCCAGCCTGAGTGAC
AGAGCAATATCTGTCCCTAAAAAAAAAAAAAAAGTTGACACAAAACACAAAATGTTCAAGA
AACAGTGGCTTCCAATAATAATAATTTTATTATTATTATTGTCAGGCACAGTGGCAATCA
TGCCTGTAATCCCAGCAGTTTGAGAGGCTGAGACAAGGCAGGTTGCTTAAGCCCCAGAATT
CAAGACCAGCATGGGCAACATGGTGAAACCAGATGACCTCCAAAATAATAATAATAATAAT
AATAATAATAATAATTAATCAGGCATGATGGTGTGCACCTGTAGTCCTAGCTACTTGGGAGG
GTGAGGTGGAGGGTTGCTTGAGCCCAGGAGATGGAGGCTGCAGTGAGCTGGGAAAGTGCC
GCTGCAGTCCAGTCTGGGCTACAGAGCCAGACCCTGTCTCAAAAAATAGTAATAATATAGTA
ATAATATTATTGTGGCCCGACATGGTGGCTCACGCCTGTAATCCCAGCACTTTGGGAGGCTG
AGGCAGGTGGATCACCTGAGGTCAGGAGTTCGACACCAGCCTGGCTAACATGGTGAAACCC
CATCTCTACTAAAAATACAAAAATTAGCCAGGTGTGGTGGCATGTACCTGTAATCTCAGCTA
CTTGGGAGGCTGAGGCAGGAGAATTGCTTGAACCCAGGAGGCGGAGGTTGCAGTGAGCCG
AGATCATGCCACCACACTCCAGCCTGGGCAACAGAGCAAAACTCTGTCTCAAAAAAAATAAA
TTATTGCTATGATAGATTATGTCGCTTCCTTGCTCAGCACCCTCCTATAGCACCTGTCTCATTT
GGAATAAATGATGATGTCCTTGCGTTGCCCACGTGGCCCTACATGCCGTGGCCCCTGATAAC
TGTTTTTCATTTGTTTTGTTTTGTTTTGTTTTTTTCTTTTTTTGAGATGGAGTCTTGCTCTGTTGC
CCAGGCTGGAGTGCACTGGCATGATCTCAGCTCACAGCAACCTCCGCCTCCCTGGTTCAAGT
GATCCCTCCTGCCTCAGCCTCCTGAGTAGCTGGGATTACAGGCGTCCACCATCACTCCAGGTT
ATTTTTGTGTTTTTAGGAGAGATGGGGTTTCACCATGTTGGCCAGGCTGGTCTCAAACTCCT
GACCTCAGGTGATCCACCCACCTTGGCCTCCCAAATTCCCGTGATTACTGGCATGAGCCACT
GTGCCCGGCCCCTGATGACTCTGCTATTGCCTCTCACCCTCTCCCTCTGGCAGATTCCACTCCA
GCCACACTGGGCTCCTTGCTGTTCTTGGACATGACCGTCATGTTCCCACCTCAGGGCCTTTGC
ACTGGCTGTTCTCGATGCCTGAAACACTCTTCCCCCAGATCTCGATGCATCTCTCCCACTGTTC
CTTCAGATTTTTATGCAAATGTCACCTTCTCAAGAAGCCTTCCCTGACCATGCCTGTACAACTC
CAACATAGCCAGCTTCCCTGTGTGATATTTTTCCCATAGTATTTATTATCTTCTAAAATACTGT
GGATTTTGGATTTTGCTCATTTCTTTCTTTCTTTTCCTATTTTTTTTTATTTTTTGAGACAGAGTC
TCTCTCTGTCATCCTGGCTGGAGTGCAGGGGTATGATCAAGCTCACTCAATCTCCTGGGCTC

AAATGATTCTCCCACTTCAGCCTTTTCGGCAGCTAGGATCACAGGCACGCATGACCATGCCT
GGCTATGTTTTAAAAAATTTTCGTAGAGATGGGGTCTCCCTATGTTGCCCAGGCTGGTCTAG
AACTCCTGACCTCAAGTGATCTTCCCACCTTGGCCTCTCAAATCGTTGGGATTACAGGCCTGA
ACCACCGTGCCCAGCCCCAATATTCCAATGTACTAGGGTTCTGGCATTGTAATATTCTAGAAT
TCCAAGATGCCACTTCTAACAACACTAAGTTCTAGAATTCCAATTTTTTTTTTTTTTTTTGAGA
TGGAGTCTCACTCTGTCTCCCAGGCTGGAGTGCAGTGGTGTGAGCTCAGCTCACTGCCACCT
CCACCTTCTGGGTTCAAGAAATTCTCAGCCTCCCAAGTAGCTGGGATTACAGGTGCCCGCCA
CCACACCCAGCTAATTTTTGTATTTTTAGTAGAGACGGTGTTTCACCATGTTGGCCTGTCTTG
AATTCCTGACCTCAAGTGATCCACCTGTCTTGGCCTCCCAAAGTGTTAAGATTACAGGTGTGA
GCCACCACACCCGGCCT*AGAATTCCAATATTCTAAAGCACTGGAGTCCTTATGACGCAATATT*
CCAGTTTGCAAGGTGCTGGTGGGCCGGGCTGATGGACACCCTAGATCTCCAGGGCCATGGA
GTTTCCTCCTCTGAGTTTTCATCGTCTTTCTCTCCTGCCCAGACACCAGGAGCCTGAATGGGG
*AACG***ATTCTGTCAGCTACGAGTAT***GGGGATTACAGCGACCTCTCGGACCGCCCTGTGGACT*
*GCCTGGATGGCGCCTGCCT***GGCCATCGACCCGCTGCGCG***TGGCCCCGCTCCCACTGTATGCC*
*GCCATCTTCCTGGT***GGGGGTGCCGGGCAATGCCA***TGGTGGCCTGGGTGGCTGGGAAGGTG*
GCCCGCCGGAGGGTGGGTGCCACCTGGTTGCTCCACCTGGCCGTGGCGGATTTGCTGTGCT
GTTTGTCTCTGCCCATCCTGGCAGTGCCCATTGCCCGTGGAGGCCACTGGCCGTATGGTGCA
*GTGGGCTGTCGGGCGCTGCCCTCCATCATCCTGCTGACCATGTA*TGCCAGCGTCCTGCTCCTG
GCAGCTCTCAGTGCCGACCTCTGCTTCCTGGCTCTCGGGCCTGCCTGGTGGTCTACGGTTCA
GCGGGCGTGCGGGGTGCAGGTGGCCTGTGGGGCAGCCTGGACACTGGCCTTGCTGCTCAC
CGTGCCCTCCGCCATCTACCGCCGGCTGCACCAGGAGCACTTCCCAGCCCGGCTGCAGTGTG
TGGTGGACTACGGCGGCTCCTCCAGCACCGAGAATGCGGTGACTGCCATCCGGTTTCTTTTT
GGCTTCCTGGGGCCCCTGGTGGCCGTGGCCAGCTGCCACAGTGCCCTCCTGTGCTGGGCAG
CCCGACGCTGCCGGCCGCTGGGCACAGCCATTGTGGTGGGGTTTTTTGTCTGCTGGGCACCC
TACCACCTGCTGGGGCTGGTGCTCACTGTGGCGGCCCCGAACTCCGCACTCCTGGCCAGGG
CCCTGCGGGCTGAACCCCTCATCGTGGGCCTTGCCCTCGCTCACAGCTGCCTCAATCCCATGC
TCTTCCTGTATTTTGGGAGGGCTCAACTCCGCCGGTCACTGCCAGCTGCCTGTCACTGGGCC
CTGAGGGAGTCCCAGGGCCAGGACGAAAGTGTGGACAGCAAGAAATCCACCAGCCATGAC
CTGGTCTCGGAGATGGAGGTGTAGGCTGGAGAGACATTGTGGGTGTGTATCTTCTTATCTC
ATTTCACAAGACTGGCTTCAGGCATAGCTGGATCCAGGAGCTCAATGATGTCTTCATTTTATT
CCTTCCTTCATTCAACAGATATCCATCATGCACTTGCTATGTGCAAGGCCTTTTTAGGCACTA
GAGATATAGCAGTGACCAAAACAGACACAAATCCTGCCCTCAGGGAGCTGATATTCTTCTAG
TGGAGGAAGACAGACTATAAACAAAGATATATAGGGCCATTTGCGGTGGCTCACGCCTGTA
ATTCCAGGGCTTTGGGAGGCTGAGGCAGGTAGATCACTTGAGGTCAGGACTTCAAGACCAG
CCTAGCCAATATGGTGAAACCCTGTCTCTACTAAAAATACAAAAATTAGCCGGGCATGGTGG
CGCATGCCTGTAGTCCCAGCTACTTGGGAGGCTGAGGCAGAAGAATCGTTTTGAACCCGGG
AGGCAGAGGTGACAGTGAGCCAAGATTGAGCCCCTGCACTCCAGCCTGGGCGACAGAGCG
AGACTCCGTCTCAAAAAATAAATAAATAAAAGATTCTATTTATTTATTTATTTTTTTGAGATGG
AGTCTCGCTCTGTCGCCCAGGCTGGAGTGCAGTGGCACAATCTCGGCTCACTGCAAGCTCCG
CCTCCTGAGTTCACGCCATTCTCCTGCCTCAGCCTCCTGAGTAGCTGGGACTACAGGCGCCC
GCCACCATGCCCAGCTAATTTTTGTATTTTTAGTAGAGAAGGGGTTTCACCTTGTTAGCCAGG
ATGGTCTTGATCTCCTGACCTGGTGATCCACCCGCCTCAGCCTCCCAAAGTGCTGGGATTACA
GGCGTGAGCCACCGCACCCGGCCAAAAGATTTTAATAGGATCCCTCTGGTTGCTGGTGGAG
GTGAGAGTATGGTGTAGGGGCAGTGAAGATCCCAGAGAGGAGGCTACTGTAATGGTCCAA
GCAGGAGGTGATAGCGATTTGGATCAGGGTAACAGAGCTGAGGTGGTGAGAGGCTGACAG
GTCATGCATCTATTTTGAAGGAAAGGCCAAGTCCAGGCTCCTTAGCTCGGCATTCAAGGCTT
CTCTCCACCACTGGACACACTTACTCTCTAGCTTCTCAGACCCTGTAGCAATCAGAATCATGA
CCCCCGGTGATGTCCACATCTTAATCCCCTGAACCTGTGAAGAGGTGACCTTCCATGGCAAA
AGGGACTTTGCAGGTGAGATTAAGTAAAGGATCTTGAGAAGGGGTGGTTATCCTGGATTGT
CTGGGTGGGCTCAATGGAGTCACGAGGGTCCTTTTAAGAGGGAGGCAGGAGGGTCAGGGT
CAGTCACAGGAGGTGACAACGGAAGCAGATGTCATAGTGACGTGAGGAGGTGCCAAGAAA
TGCAGGCAGCTTCCAGAAGCTGAAACAGACAAGGAAACAGATTCTCTCTGAAGCTCCCAGA
AGGAACACAGACCTCCTGACACTTTTAGACCTCTGATCCGCAGACCTTTAAGAAAATACATTT
GTATTGTTTTAAGTCACTATGTTTGGGGTGATTTGTTATAGCAGCCGTGGGAAGCTAATACA

CACCCTTCGGGCTATATTCACGCTTCTGCATCTTTCCTGAAGCTGTGCCACTGGCTGGAATGT
CCTTCTGATCTATGTTGTGCAGTTCAACAATCAAGAGCCATCTGTGGCTATTCAAATTCGAAT
CAATTGGCCAGGCCTGGTGGCTCCTGCCTATAATCTCAGCACTTTGGGAGGCCGAGGTGGG
AGGATTGCATGAGCCCAGGAGTTTGAGACCAGCCTGGGCGACATAGCAAGACCCCATCTCT
ACAAAAAATACAAAAATTAGCCAGACGTGGTGGGGCGTGCCTGTAGTTCCAGCTACTGAGG
AGGGAGTTGCTTGAATCCTTCTGCTTCAATCCTCCTTAAAGCAGGTAGATTGCTTGAGCCCG
GGAAGTGGAGTTTGCAGTGAGCTTAGATCACACCGCTGCACTCCAGCCTGGATGTCAGAAT
GAGACTCCATCTCAAAAAAAAAAAGAAAGAAAGAATAAATTTTCATTTCAAATTTAGTTCCTC
GGGCACACTGGCCATAGTTCAAGTGCTCAGTAGCCACATATGGCTGGTGACTGCCATATTCG
ACAGCACAGCTATAGAACATTGCCATCATAACAGAGATTTCTGTTACAAAATGCTGTTCTAG
AATTTACTTTTGAACTCTACCTGCTCAGATCTTTTAAATTACATGGTAGGCCAGGCATGGTGG
CTCACGCCTGTGATCCCAGCACTTTCGGAGGCCCAGTCGGGAGGATCCCTTGAGCCCAGAA
GCTGGAGACCTGCCTGGGCAACAGAGCAAGACCCCATCTCTACAAAAATAAAAAAAAGAAA
ATTAGCCTGGTTTGGTGGCACATGCCTGTAGTGCCAGCTACTAGGGAGACTGAAGTGGGAG
GATTGCTTCAGCCTGGGAGGTTGAGGCTGCAGTGAGCCGTGATCTCATCACTGCACTCTAGC
CTAGGTGACGGAGCGGGACCCTGCCGCTAAATAAATAAATAAATAAATAACATAGTAGTGA
TACCTGTGTCTGCGGTCATTACTCCAGAACAGCACTTCACATATAGTTTCTCCTTTAAGGTCAT
TCTCACAACAGCCCAGGGAGATAGGGTGGCATGCTTCATTTTATAAGCTGAGGTCCTGGGA
GGGGAGGTCATTTACCCAAGATCACACAGCAAGAACACCAGACAGCTGGAATTTGATCCCA
GTTTTGACTCCAATGCTCTTGCTCTTCATCATCAATAATTTCCTTCAAGGCGTCCCTCAAATGT
CACTTCCTCCAGGAAGCCCTCCCTGATTTATGCTCCTTCCAGAAAGAATGGGCTCTTCCTTTCT
CTGAGTCTCTGGAACACAAGGTCCCAGCTAAACTGTAAATTCCCCAAGGGTAACAACTGGAC
TAATTTTTTTTAATTTAATTTAATTTTATTTTTTTGAGATGAAGTCTTGCTCTGTCACCCAGGCT
GGATTGTAGTGGCACGATCTCGGCTGACCGCAACCTCCACCTCCCGGGTTCAAGCGATTCTT
ATGCCTCAGCCTCCCGAGTAGCTGGGATTACAGGCGCTGCCACCACACTTGGCTAATTTTTG
TATTTTTAGTAGAGACAGGGTTTCACCATGTTGGCCAGGCTGGTCTCGAACTCCTGACCTCA
GGTGATCCACCCACCTTGGCCTCCCAAAGTGCTGGGAATACAGGCATGAGCCACCGTTCCCG
GCCTTATCCTTGACTTAGAATACCTAACCTCCTGGGAATGCAGCCCATAGGTCTCAGCCTTAT
TTCACCCAGCTCCTGTTCAAGATGGAGTCACTCTGGTTCACATGCCTCTGACATTTCCCCGCT
CCCTTTTATAAGAGAACCTTTAATCCTAAGGGTTGTAGAGGGAGGAAGATACAACTTCTGTG
ACTTCTTCAGGCTGGACAGGGGTGACGATATACCTGCCTAACTCTTAGGATCTATTGGATTC
AGGGTAGACAGGAGCTCAGTCAGAAAGCACTGGTATCACTTTTTTTTTTTTTTTTTTTTTGA
GACGGAGTTTCACTCTTGTTGCCCAGGCTGGAGTGCAATGGCACGATCTCAGCTCACCACAG
CCTCCGCCTCCCAGGTTCAAGCGATTCTCCTGCCTCAGCCTCCCCAGTAGCTGGGACTACAG
GCGTGTGCCACCAAACCCAGCTAATGTTTTTTTTTTTTTATTTTTAGTAGAGACGGGGTTTCTC
CATGTTGGCCAGGCTGGTCTCGAACTCCCGACCTCAGGTGATCCACCCGCCTCGGCCTCCCA
AAGTGCTGGGATTACAGACATGAGCCACCACGCCCGGCCTGATATTTTATTACTTAGTATTTT
ACTCTGAATTATCATGCGTGAATTAAGACCAAGGCTGTCTTGTAAAATAAAATTTGTTGTGG
AACAATTTATACAGCTCCTTTGAGGTAGGAGGCAGGACTCAACTCTGGAGATGGGGCTCGG
CTCGAATATTGGACCAAATTGAGGACCAGCTAAAACAGGGAGGAGGCTGAAGCAACTTATT
ATTTTTATTTATTTTTATTTTTTGGAGAAGGAGTCTTGCTCTGTTACCCAGGCTGGAGTGCAG
TGACACGATCTCGGCTCACTGCAACCTCCACCTTCCGGATTCAAGTGATTCTCCTGCCGCAGC
CTCCCGAGTAGCTGGGACTACAGGCGCATGCCACCATGCCCAGCTAATATTTTTGTATTTTTT
AGTAGAGATGGGGTTTCGCCATATTAGCCAGGCTGGTCTTGAACTCCTGACTCAGGTGATCT
GCCCACCTCGGCCTCCCAAAGTGCTGGGATTACAGGTGTGGGCCACCACGCCTGGCCCGAA
GCAACTTTCTATGACACGCCTACCAGTGTGCCATGTCAGTTTGCCATTGCCATGGCAACACAC
CCAGGAGTTACTGCCCCTTCCCATGGCAATGACCCCATGACCCAGAAGTTACTGCCCCTTCCC
TAGATATTTCTGCATAAACTGCCCCTTAATCTACATGTAATTAAAAATAGGTATAGGCTATTT
TTATACCTATATAAATAGGTATAGGCTAAAAATAGGTATAGGCTGGGCGTGGTGGCTCATGT
CTGTAATCCCAGTACTTTGGGAGGCCAATGCAGGTGGATCACCTGAGGTCAGGAGATCAAG
ACCATCCTGGCTAACATAGTGAAACCCTGTCTCTACTAAAAATACAAAAAATTAGCCAGGCG
TGTTGGCGGGAGCCTGTAGACTCAGCTACTCGGGAGGTTGAGGCAGGAGAATGGCGTGAA
CCCAGGAGGCGGAGCTTGCAGTGAGCCGAGATCACACCACTGCACTCCAGCCTGGGTGACA
GAGCAAGACTCCGTCTAAAAAAAAAAAATAGTAAGAAAGAAGGAAAGACACAAAGACAGA

AAGAAGGAAGGAAAGAAAGCAAGCTGTTTTCCCCTGCCTTGCCCCTGCTCACCTTTGAATTC
TTTTCTGGGCAAAGCCAAGAACCCTCGTGGGCTAAAACCCCGCTTTGGGGCTTAAAGTTTGC
AAAATCCTCCCATTAATCTATTGGGACCAGTTGCCACTTAGGAGCATTCTTTGATAACTTTTA
CAAAACATCTTTTGTGGTTTTTGAAATGTTTTCATTTTGTAGATCATTAGCCCTTCTTTTTTGAA
CTGGAATACATTTCACGGGAATTTTCAAATTTAAGTCTGTGCAATGTTACATAAAATACCTTT
GATTATTAAAAGCCATCTGTTTTGCTATAACTTCCCTTTTTTGTTCTAAAGTTTGTCTATTTCTG
CTATTTGTTTTTTTACCATAGAAATATTGATTTCCTTAAGTTTTCAAAGAACCAAGTTATTAAT
AATTTCTCTAAGAACTAGTCTCAAGCTTGCTATACAATCCTATGGTTGATAGACTGTGGCTTT
CTTGTTGATTTCCATTTGTTGTTCATTTCCTCCAATTTTCCTTTTTTAAAAATTATAATTATTGTT
TGGATTATT

C5aR2 Primer Pair 1

Forward Primer: AAGCACTGGAGTCCTTATGACG

Reverse Primer: ACAAACAGCACAGCAAATCCG

C5aR2 Primer Pair 5

Forward Primer: ATATTCCAGTTTGCAAGGTGCTG

Reverse Primer: AACAGCACAGCAAATCCGCC

C5aR2 Primer Pair 6

Forward Primer: CACTGGAGTCCTTATGACGCAAT

Reverse Primer: CAGAGACAAACAGCACAGCAAA

Supplementary Figure 4.2. C5aR2 sgRNA target sequence and primer design. Black: C5aR2 gene sequence, *Green*: Target Amplicon, **Red**: gRNA target sequence.

8.3. C5aR2 Sequence for AJ C5aR2 Primer Design

>NC_000019.10:47331614-47347329 Homo sapiens chromosome 19, GRCh38.p13 Primary Assembly

GCAAGACTCCATCTCTAAAAAAAGTAAAGCATCGCTATGGCCAACAACATCTTCCCATTCTAC
AGATGGAAAATTGAGGCCCAAGAAAGGAGTTGTTTGTGCTTTTTCTACCACTGAGGCGTTG
GGCCCTGCGCTCAGCTGCTGTGGTCTTTTTGTGGAGAATGTGACCCCAGGCTGTCTTCCTCA
GAGCCGAGGAGGAGGGAGGGATGTTTGTCTGTCCTGAGGCTGCAGAAGGGAGGGGTTGA
ACACAGTTAGAGGCCTGGAGGTGGCTGGGGGCAGCTGGCATGTTGTGGGCAAACAGAATC
CAGGCCAAGACCTCTAAGGCGTTAAAGAGCAAACCGCATGCAGGTCTGGCTTCCAGGAAGG
TGGGACTTCGAGACTAGGGTTGGGGACTTGGGATCAGCCCTCCACCCAACCGAGCCCTCTCC
TGCCCTGCCAGCCACCCCGTAATTTTGGGTTCTGTGAGTCACGGGAAGAAGACAGGACAAA
CACACCCTGAGAGCGAGACAAGGCCACTCCTATTTTGTACTGCTTATAAAGATTCACTGGGA
CTGGTGAGGTGGCAGTGCTCAGCAGCATCCGACAGGAGCCCTGGCAAACAGGACGGATTTC
CAGGACTCTACCAGCTGCCAGACACGGCAGGGAGAGACCCCAGACCTCCTGGGTCCTGGCT
GTGGGCCCGGATTGGGCTCCCAAGTGGCGTTTGACTCACGTGGGGACACTCTTGGAAGAGA
CGGTAAGGATGGAGGCTACAAGGGCGGGAAGGAGGGAGAGAGAGATTGCATGATCTTGG
CTTCTCGGAATCATTACTTTCAGAATCTGGGAAGCAGAACTAGAGTTTGAGAAGTGCAGTCT
TATTACAGCCACACTGGAACGCACGTCACAGTCCTGGGCTCTTGAATTAACTTGGGCAGCCC

AGCAGCAAAGCTCTTGTCAAAGGATCTAAGCATTTTTTTTCTTTCTCTTTTTGGAGACAGGTTT
TCATTCTTGTTGCCCAGGCTGGAGTGCAATGGTGCCATCTTGGCTCACCGCAACCTCCACCTC
CCAGGTTCAAGGGATTCTCTTGTCTCAGCTGGGATTACAAGCGCATGCCACCATGCCTGGCT
AATTTTGTATTTTTAGTAGAGATGGGGTTTCTCCATGTTGGTCAGGCTGGTCTCGAACTCCCG
ACCTCAGGTGATCTGTCCGCCTTGGCCTCCCAAAGTGCTGGGATTACAGGCGTGAGCCACTG
TGCCCTGCCCAAATGGTTTTTCACACACAGATGTATGGGAAACAGCCTCTCTCAAACCTGCA
GGAATTCCTGCAGCTTTCGGCAGATCCACCAAACTGTAGCATGTGTAGCAAGCAAGCCCTTT
AACTCAGCGATTCCAATTCTTTTCTCTTTCTTTCCTTTTCTCTCTTTCTTTCTTTTGACAGGGTCT
CACTCTGTCTCCCAGGCTGGAGTGCAGTGGTGCGATCTTGGCTCACTGCAACCTCCGCCTCC
CAGGTTCAAGTGATTCTCCTGCCCCAGCCTGCTGAGTAGCTGGGATTACAGGTGCACGCCAC
CACACCTAGCTAATTTTTGTATTTTTAGTAGAGATGGGGTTTCACCATGTTGGCCAGGCTGGT
CTCCAACTTTTGACCTCAGGTGATCCACCTACCTTGGCCTCCCAAAGTGCTGGGATTACAGGC
GTGAATCACCGTGCCTGGCCCCCTCAATGTTCTATCACAAAATCTGTCCACATTCTTGTGTGG
TGTTTGTTCATTCTCATCGTGTAGAATATTCCACAGGGTGAACACCCCATGATGTGTTTATCC
ATTCTGCTGTGGGTGGCTATTTGGACGGTTTCTCATCTTGGGCTGCTGTGAACATTCTGGCAC
ATGTATTCTGGTGAGCATATGTGTTCTTTTGCGGAAAGGAGGCTGATTGCTGGGTCGTGAG
GGAGGAATCCTAGAAGATGGATGTTCAGGAATAAAGAATGTTCAGACTCCTTTTTTTTTTTTT
TTTTTTTGAGATGGAGTCTTGCTCAGGCTGGAGTGCAGTGGTGCGATCTCGGCTCACTGCAA
CCTCCGCCTCCTGGGTTCACGCCATTCTCCTGCCTCAGCCTCCTGAGTAGCTGGGACTACAGG
CGCCCGCCACCGCGCCCAGCTAATTTTTTGTATTTTTTAGTAGAGATGGGGTTTCACCATGTT
AGCCAGGATGGTCTCGATCTCCTGACCTCGTGATCCACCTGCCTGGGCCTCCCAAAGTGCCG
GGGATTACAGGTGTGAGCCACTGCGCCCGGCCAGCCTTCTTTGATTCTGCTCCAGGGTTTTC
CAGAGCAGAGAACCCAGCAAGACTGGATGCACAGACAGGCGTGCACCAAGAGGCACATGT
GAGGGTGCTTGCAATCACAACAAAAGAAACCTAAGTGACCACTTAGTCTCTCTGTGCCTCAG
TTTACTCTTTTATCCTTTCACTTACCAAATATCGACCATGCCTGTGCTGTGTGCCAGGTTCTGT
CCCAGATGCCAGGGACACAGCGGCACCCGAGGCTGGAAGGAGCTGATGTTGTGGGATATG
AGGATGATAATATTGACCTCAAGGGTTTGTGTTGAGGGTTATATCTTGTAGGTCATAGGTGC
TCAATAAAAGCCATCTATTATTTTAATTATTATGAAATAATAAGAAGGGTACCTATGATTTAA
AAGCTAGATATAAGTACAGACGCTCTTTGACTTACAATGGGGTCCCATCTCTATCAACCCATC
GTAAGGCTGGGCACAGTGGCTCACGCCTGTAATGGCAGCACTTTTGGGAGGCTGAGGTGG
GAGGATTTCTTGAGCCCAGGAGTTTGAGATCAGCCTGGGCAACAGAGTAAGGGCTGTCCAT
ACAGAAAAAAAAAAAAAAATTAGCTGGGCATGATGGCGTGCACCCGTAGTCCCAGCTACTC
CAGAGGCTGAGGCAGGAGGATCAGTTGAGCCTAGGAGGTAGAGGCTGTGGTGAGCCGAG
GTTGAACCACTGAACTCAGCTTGGGTGACTGAACAAGACGAAAACACAAAACAAAAGCCCC
CAACATTTTCAACATAAGTTGAAAATATTGTAAATCAAATTGGATTTAATACACCTAGCTTAC
TGAACATCATAGCCTACTTTTTTTTTTTGAGACAGGGTCTCACTCTGTTGTCCAGGCTGGAGT
GCAGTGGCGCGATCTTGGCTCACTGCAGCCTTGACCTCACGGGCGTAGCCTACCTCAAATGT
GTTCAGAACATTTACATTACCCAACAGCAAGACAAAATCATCTAAGCCAAATCCAATTTTTTT
TTTTTTGAGATGGAGTCTCACTCTGTCACCCATGCTGGAGTGCAGTGGTGTGATCTCAGCTG
ACTGCAACCTCCACCTCCCAGCTTCAAGGGATTCTCCTGCCTCGGCCTTCTGAGTAGCTGAGA
TTACAGGCACTCGCCCCCACGCCCAGCTAATTTTTTTTTTTTTTTTAAATCTTTAGCAGAGATGA
GATTTTATCATGTTGGCCAGGCTGGTCTCAAACTCCTGACCTCAAGTGATCCGTCTGCCTAGG
ACTCCCAAAGCGTTGGGATTACAGGTGTGAGCTTCTGCACCTGGCCCTGTTTCTCATTATTCT
CCTTACCATTGTTATTGAATGGCCTTTAGTTAATAAGCACCACTTGGGCAGACAGTGGACTGT
TTTTGATGCTTTGAGGACGAATGGGGTTGATATCTGTACAGATAGACAGGAAAACAGATAT
CGGGCACGTTAAGTGGAAAAGATGAAGAAATGGAACAACGTATGTTGAAAGCTCCCATTTC
TGGTTAAGACGTTACAAAGGAAATGCCATCTACGATACCATTGCTTTGGGCTTACAGCTGGG
CAAATTATATGCACAGAAAGTTTCCTGGATTGGGCTGGGCATGTTGACTCACGCCTGTAATC
CCAGCACTTTGGGAGGCCGAGGTGGGCGGATCATGAGGTCAGGAGATTGAGACCATCCTG
GCTAACACGGTGAAACCCTGTCTCTACTAAAAATACAAAAAATTAGCCGGAAGTGGTAGCG
GGCGCCTGTAGTCCCAGCTACTCGGGAGACTGAGGCAGGAGAATCATGCGAACCCGGGAG
GTGGAGCTTGCAGTGAGCCGAGATCGCACCACTGCACTCCAGCCTGGGCGACAGAGTGATA
CTCCGTCTCAAAAAAAAAAAAAAAAAAAAAAAAAAAAAAAAGAAAGTTTTCGTTTTCTGGATT
GTAATCAACAAGGGCCAGGAAGGGTGGAGTCTTTGCGGGGTGAGAGGATGCGTGTGGACA

GTGATAACAGCAGCTAGCCTACGTATGACACCCACTGAAAACCAGCGCTATACACTCAGCTC
TACCCTTCTAACTTGTTGAATTCTTACAACACCCCCTAAGGCAGGAATATTATTATTCCCATTT
TACTGAGGCACAGATAGTTTAGGTGACTTGCCCAAGGCCACACAGCTGGTAGGAATTTGAG
GGTTTTTGTTGTTGTTGTTTGTTTGTTTTTTATGATGCAGTCTCGCTGTTGTCGCCCAGG
CTGGAGTGCAGTGGCATGATCTTGGCTCACTGCAACCTCTGCCTCCCGGGTTCCAGCGATTC
TCTTGCCTCAGTCTCCCGAGTAGCTGGAATTACAGGAGCCCACAACCATGCCTGGCTGATTTT
TGTATTTTTAGTAGAGACCAGGTTTCACCATGTTGCTCAGGCTGGTCTTGAACTCCTGGCCTC
AAGTGATCCGCCCACCTCGGCCTCCCAAAGTGCTGGGATTACAGGTGTGAGCCACTGTGCCC
GGCTAGGGGGGGTTCAGTTTTTAAATGCTGTACTCTTTCTTTCTTTCTTTCCTTCCTTCCTTCCT
TCCTTCCTTCCTTCCTTCCTTCCTTCCTTCCTTCCTTCCTTTCTTTCTTTCTTTCTTTTTTCTTT
CTTTCTTGGGACAGGGTCTCACTCTGTTGCTCAGGCTGGAGTGCAGTGGCGCGATCATGGCT
AACTGCAGCCTCAAACTCCTGGGCTCATGTGATCTTCCACCCCAGTCTTAGAAAAGGTTGGG
ATTGCAGGCACGAACCACTATGCCTGGCTAATTTTTAAATTTTTTGTAGAGACAGAGGGTCT
CACTGTGTTGCCTAGGCTGGTCTTGAACTCTTGGCCTCAAGCGATCCTTCCTCCTCAACTCAG
CCTCCCAATGTACTGGGATTACAGGTGTGAGCCACTGCACCTGGCTAAATTCTGCACACCTTT
TACTCTAGGGATAAAAATAATACGAAAGTGGAATGCCAGACTCCGAATACACACACCAAGT
GGCCTGGACTCTTCACTGCTACCTGGCATGGGGGAGGGGAGTGCCCCAACTTCCTCTCTGTC
CTTCCTGTTGCCTCAACACCAGCTGGAGTGCTGAGCAGTGCCAGCCAACCCATAATAGTCAG
CAGAGAGCCTCAGGGCCAGGTCACTCTGACATTGTGGGGGTGGGGGGGTGGGGACTCCTG
CCTGGGTCCTGTGCTACCCACAGCTTTGTCTACCGGAGCCTGTGTGCCACGTGCTGGACAAA
TCTTAACTCCTCAAGGACTCCCAAAACCAGAGGTAGGTTCACCTCAATGACTCTTGTTTCCCC
GATGAGGAAATAGGCACAGCCAGCTGCAACTGACACCCACAGTCATGGAGGCCGGGGCTG
CTCAGGACCACTTGCTGTGCTGCCTGCCAGCTCTCCAGAGCCCAAGATTTGGAGATGGTAAT
ATTCTAGGGCATGGGGTTCTGCAGCGGGGACTAACACACTTTGAAATTTACCTACTTAGGGC
TGGGCGCGGTGGCTCATGCCTGCAATCCCAGCACTTTGGGAGGCTGAGGTGGGCGGATCAC
AAGGTCAGGAGTTCGAGACCAGCCTGGCCAATATGATGAAACCCCGTATCTACTAAAAATAC
ACAAATTAGTTGGGCATGGTGGCGGGTGCCTGTAGTCCCAGCTACTCAGGAGGCTGAGGCG
GGAGAATTGCTTGAACCCTGGAGGCGGAGGTTGCAGTGAGCCGAGATTGCGTCACTGCACT
CCAGCCTGGATGACAGAGCGAGACTCTGTCTCAAAAAAAAAAATTTTACCTACTTAGCTGAG
TGATCTTAGGTAAATTACTTAACTTCTCTGTGCCTTATCTGTAGAATAAATATAACAATAGTG
TCAAATTCAGACAGTTATTATAAGGTTTCAGTGAGGTCAGGCACGGTGGCTCATGCCTGTAA
TCCTAGCACTTTGGGAGGCCGTGGCAGGCAGACCACTTGAGGTCAGGAATTCCAAACCAGC
CTGACCAACATGGTGAAACCCCGTCTCTACTAAAAATACAAAAAATTAGCCCCGGGCATGGT
GGTGCACGCCTGTAATCCCAGCTACTCGGGAGGCTTGTGGCAGGAGTAATGCTTGAACCCA
GGAAGCAGAGGTTGCAGTGAGCCAAAATAGCGCCACTGCACTCCAGCCTGGGTAGCAGAG
TGAGACTCCGTCTCAAAAAAAAAAATAAATAAAATAAAATAAAACAAGGTTTCAGTGATACA
GTGTTTAAAGCTGCGTGGTGGCCACTGCCTGTAGTCCCAGCTACTCAGGGGGCAGAGGTGG
GAGGATCACTTGAGCACAGAGTTTGAGGCTGCAGTGAGCCGTGATTGCACCACTGCACTCC
AGCGTTGGCAAGATGGCGAGACCCTGTCTCTAAAAAAAATATATATATATAAATTTGCCAGG
TGTGGTGGTGCACACCTGTAGTCCCACGTACTCAGGAGGCTGAGGTGGGAGGACCACTTGA
GCCCAGGAGTTCGAGGCTGCAGTGAGCCAAGATAGTGCCATTGCATTCCAGCCTGAGTGAC
AGAGCAATATCTGTCCCTAAAAAAAAAAAAAAAGTTGACACAAAACACAAAATGTTCAAGA
AACAGTGGCTTCCAATAATAATAATTTTATTATTATTATTATTGTCAGGCACAGTGGCAATCA
TGCCTGTAATCCCAGCAGTTTGAGAGGCTGAGACAAGGCAGGTTGCTTAAGCCCCAGAATT
CAAGACCAGCATGGGCAACATGGTGAAACCAGATGACCTCCAAAATAATAATAATAATAAT
AATAATAATAATAATTAATCAGGCATGATGGTGTGCACCTGTAGTCCTAGCTACTTGGGAGG
GTGAGGTGGAGGGTTGCTTGAGCCCAGGAGATGGAGGCTGCAGTGAGCTGGGAAAGTGCC
GCTGCAGTCCAGTCTGGGCTACAGAGCCAGACCCTGTCTCAAAAAATAGTAATAATATAGTA
ATAATATTATTGTGGCCCGACATGGTGGCTCACGCCTGTAATCCCAGCACTTTGGGAGGCTG
AGGCAGGTGGATCACCTGAGGTCAGGAGTTCGACACCAGCCTGGCTAACATGGTGAAACCC
CATCTCTACTAAAAATACAAAAATTAGCCAGGTGTGGTGGCATGTACCTGTAATCTCAGCTA
CTTGGGAGGCTGAGGCAGGAGAATTGCTTGAACCCAGGAGGCGGAGGTTGCAGTGAGCCG
AGATCATGCCACCACACTCCAGCCTGGGCAACAGAGCAAAACTCTGTCTCAAAAAAAATAAA
TTATTGCTATGATAGATTATGTCGCTTCCTTGCTCAGCACCCTCCTATAGCACCTGTCTCATTT

GGAATAAATGATGATGTCCTTGCGTTGCCCACGTGGCCCTACATGCCGTGGCCCCTGATAAC
TGTTTTTCATTTGTTTTGTTTTGTTTTGTTTTTTTCTTTTTTTGAGATGGAGTCTTGCTCTGTTGC
CCAGGCTGGAGTGCACTGGCATGATCTCAGCTCACAGCAACCTCCGCCTCCCTGGTTCAAGT
GATCCCTCCTGCCTCAGCCTCCTGAGTAGCTGGGATTACAGGCGTCCACCATCACTCCAGGTT
ATTTTTGTGTTTTTAGGAGAGATGGGGTTTCACCATGTTGGCCAGGCTGGTCTCAAACTCCT
GACCTCAGGTGATCCACCCACCTTGGCCTCCCAAATTCCCGTGATTACTGGCATGAGCCACT
GTGCCCGGCCCCTGATGACTCTGCTATTGCCTCTCACCCTCTCCCTCTGGCAGATTCCACTCCA
GCCACACTGGGCTCCTTGCTGTTCTTGGACATGACCGTCATGTTCCCACCTCAGGGCCTTTGC
ACTGGCTGTTCTCGATGCCTGAAACACTCTTCCCCCAGATCTCGATGCATCTCTCCCACTGTTC
CTTCAGATTTTTATGCAAATGTCACCTTCTCAAGAAGCCTTCCCTGACCATGCCTGTACAACTC
CAACATAGCCAGCTTCCCTGTGTGATATTTTTCCCATAGTATTTATTATCTTCTAAAATACTGT
GGATTTTGGATTTTGCTCATTTCTTTCTTTCTTTTCCTATTTTTTTTTATTTTTTGAGACAGAGTC
TCTCTCTGTCATCCTGGCTGGAGTGCAGGGGTATGATCAAGCTCACTCAATCTCCTGGGCTC
AAATGATTCTCCCACTTCAGCCTTTTCGGCAGCTAGGATCACAGGCACGCATGACCATGCCT
GGCTATGTTTTAAAAAATTTTCGTAGAGATGGGGTCTCCCTATGTTGCCCAGGCTGGTCTAG
AACTCCTGACCTCAAGTGATCTTCCCACCTTGGCCTCTCAAATCGTTGGGATTACAGGCCTGA
ACCACCGTGCCCAGCCCCAATATTCCAATGTACTAGGGTTCTGGCATTGTAATATTCTAGAAT
TCCAAGATGCCACTTCTAACAACACTAAGTTCTAGAATTCCAATTTTTTTTTTTTTTTTTGAGA
TGGAGTCTCACTCTGTCTCCCAGGCTGGAGTGCAGTGGTGTGAGCTCAGCTCACTGCCACCT
CCACCTTCTGGGTTCAAGAAATTCTCAGCCTCCCAAGTAGCTGGGATTACAGGTGCCCGCCA
CCACACCCAGCTAATTTTTGTATTTTTAGTAGAGACGGTGTTTCACCATGTTGGCCTGTCTTG
AATTCCTGACCTCAAGTGATCCACCTGTCTTGGCCTCCCAAAGTGTTAAGATTACAGGTGTGA
GCCACCACACCCGGCCTAGAATTCCAATATTCTAAAGCACTGGAGTCCTTATGACGCAATATT
CCAGTTTGCAAGGTGCTGGTGGGCCGGGCTGATGGACACCCTAGATCTCCAGGGCCATGGA
GTTTCCTCCTCTGAGTTTTCATCGTCTTTCTCTCCTGCCCAGACACCAGGAGCCTGAATGGGG
AACGATTCTGTCAGCTACGAGTATGGGGATTACAGCGACCTCTCGGACCGCCCTGTGGACTG
CCTGGATGGCGCCTGCCTGGCCATCGACCCGCTGCGCGTGGCCCCGCTCCCACTGTATGCCG
CCATCTTCCTGGTGGGGGTGCCGGGCAATGCCATGGTGGCC*TGGGTGGCTGGGAAGGTGG*
CCCGCCGGAGGGTGGGTGCCACCTGGTTGCTCCACCTGGCCGTGGCGGATTTGCTGTGCTGT
TTGTCTCTGCCCATCCTGGCAGTGCCCATTGCCCGTGGAGGCCACTGGCCGTATGGTGCAGT
GGGCTGTCGGGCGCTGCCCTCCATCATCCTGCTGACCATGTATGCCAGCGTCCTGCTCCTGGC
*AGCTCTCAGTGCCGACCTCTGCTTCCTGGCTCTCGGGCCTGCCT***GGTGGTCTACGGTTCAG***C*
GGGCGTGCGGGGTGCAGGTGGCCTGTGGGGCAGCCTGGACACTGGCCTTGCTGCTCACCGT
GCCCTCCGCCATCTACCGCCGGCTGCACCAGGAGCACTTCCCAGCCCGGCTGCAGTGTGTGG
TGGACTACGGCGGCTCCTCCAGCACCGAGAATGCGGTGACTGCCATCCGGTTTCTTTTTGGCT
TCCTGGGGCCCCTGGTGGCCGTGGCCAGCTGCCACAGTGCCCTCCTGTGCTGGGCAGCCCGA
*C*GCTGCCGGCCGCTGGGCACAGCCATTGTGGTGGGGTTTTTTGTCTGCTGGGCACCCTACCA
CCTGCTGGGGCTGGTGCTCACTGTGGCGGCCCCGAACTCCGCACTCCTGGCCAGGGCCCTG
CGGGCTGAACCCCTCATCGTGGGCCTTGCCCTCGCTCACAGCTGCCTCAATCCCATGCTCTTC
CTGTATTTTGGGAGGGCTCAACTCCGCCGGTCACTGCCAGCTGCCTGTCACTGGGCCCTGAG
GGAGTCCCAGGGCCAGGACGAAAGTGTGGACAGCAAGAAATCCACCAGCCATGACCTGGT
CTCGGAGATGGAGGTGTAGGCTGGAGAGACATTGTGGGTGTGTATCTTCTTATCTCATTTCA
CAAGACTGGCTTCAGGCATAGCTGGATCCAGGAGCTCAATGATGTCTTCATTTTATTCCTTCC
TTCATTCAACAGATATCCATCATGCACTTGCTATGTGCAAGGCCTTTTTAGGCACTAGAGATA
TAGCAGTGACCAAAACAGACACAAATCCTGCCCTCAGGGAGCTGATATTCTTCTAGTGGAG
GAAGACAGACTATAAACAAAGATATATAGGGCCATTTGCGGTGGCTCACGCCTGTAATTCCA
GGGCTTTGGGAGGCTGAGGCAGGTAGATCACTTGAGGTCAGGACTTCAAGACCAGCCTAGC
CAATATGGTGAAACCCTGTCTCTACTAAAAATACAAAAATTAGCCGGGCATGGTGGCGCATG
CCTGTAGTCCCAGCTACTTGGGAGGCTGAGGCAGAAGAATCGTTTTGAACCCGGGAGGCAG
AGGTGACAGTGAGCCAAGATTGAGCCCCTGCACTCCAGCCTGGGCGACAGAGCGAGACTCC
GTCTCAAAAAATAAATAAATAAAAGATTCTATTTATTTATTTATTTTTTTGAGATGGAGTCTCG
CTCTGTCGCCCAGGCTGGAGTGCAGTGGCACAATCTCGGCTCACTGCAAGCTCCGCCTCCTG
AGTTCACGCCATTCTCCTGCCTCAGCCTCCTGAGTAGCTGGGACTACAGGCGCCCGCCACCA
TGCCCAGCTAATTTTTGTATTTTTAGTAGAGAAGGGGTTTCACCTTGTTAGCCAGGATGGTCT

TGATCTCCTGACCTGGTGATCCACCCGCCTCAGCCTCCCAAAGTGCTGGGATTACAGGCGTG
AGCCACCGCACCCGGCCAAAAGATTTTAATAGGATCCCTCTGGTTGCTGGTGGAGGTGAGA
GTATGGTGTAGGGGCAGTGAAGATCCCAGAGAGGAGGCTACTGTAATGGTCCAAGCAGGA
GGTGATAGCGATTTGGATCAGGGTAACAGAGCTGAGGTGGTGAGAGGCTGACAGGTCATG
CATCTATTTTGAAGGAAAGGCCAAGTCCAGGCTCCTTAGCTCGGCATTCAAGGCTTCTCTCCA
CCACTGGACACACTTACTCTCTAGCTTCTCAGACCCTGTAGCAATCAGAATCATGACCCCCGG
TGATGTCCACATCTTAATCCCCTGAACCTGTGAAGAGGTGACCTTCCATGGCAAAAGGGACT
TTGCAGGTGAGATTAAGTAAAGGATCTTGAGAAGGGGTGGTTATCCTGGATTGTCTGGGTG
GGCTCAATGGAGTCACGAGGGTCCTTTTAAGAGGGAGGCAGGAGGGTCAGGGTCAGTCAC
AGGAGGTGACAACGGAAGCAGATGTCATAGTGACGTGAGGAGGTGCCAAGAAATGCAGGC
AGCTTCCAGAAGCTGAAACAGACAAGGAAACAGATTCTCTCTGAAGCTCCCAGAAGGAACA
CAGACCTCCTGACACTTTTAGACCTCTGATCCGCAGACCTTTAAGAAAATACATTTGTATTGT
TTTAAGTCACTATGTTTGGGGTGATTTGTTATAGCAGCCGTGGGAAGCTAATACACACCCTTC
GGGCTATATTCACGCTTCTGCATCTTTCCTGAAGCTGTGCCACTGGCTGGAATGTCCTTCTGA
TCTATGTTGTGCAGTTCAACAATCAAGAGCCATCTGTGGCTATTCAAATTCGAATCAATTGGC
CAGGCCTGGTGGCTCCTGCCTATAATCTCAGCACTTTGGGAGGCCGAGGTGGGAGGATTGC
ATGAGCCCAGGAGTTTGAGACCAGCCTGGGCGACATAGCAAGACCCCATCTCTACAAAAAA
TACAAAAATTAGCCAGACGTGGTGGGGCGTGCCTGTAGTTCCAGCTACTGAGGAGGGAGTT
GCTTGAATCCTTCTGCTTCAATCCTCCTTAAAGCAGGTAGATTGCTTGAGCCCGGGAAGTGG
AGTTTGCAGTGAGCTTAGATCACACCGCTGCACTCCAGCCTGGATGTCAGAATGAGACTCCA
TCTCAAAAAAAAAAAGAAAGAAAGAATAAATTTTCATTTCAAATTTAGTTCCTCGGGCACAC
TGGCCATAGTTCAAGTGCTCAGTAGCCACATATGGCTGGTGACTGCCATATTCGACAGCACA
GCTATAGAACATTGCCATCATAACAGAGATTTCTGTTACAAAATGCTGTTCTAGAATTTACTT
TTGAACTCTACCTGCTCAGATCTTTTAAATTACATGGTAGGCCAGGCATGGTGGCTCACGCCT
GTGATCCCAGCACTTTCGGAGGCCCAGTCGGGAGGATCCCTTGAGCCCAGAAGCTGGAGAC
CTGCCTGGGCAACAGAGCAAGACCCCATCTCTACAAAAATAAAAAAAAGAAAATTAGCCTG
GTTTGGTGGCACATGCCTGTAGTGCCAGCTACTAGGGAGACTGAAGTGGGAGGATTGCTTC
AGCCTGGGAGGTTGAGGCTGCAGTGAGCCGTGATCTCATCACTGCACTCTAGCCTAGGTGA
CGGAGCGGGACCCTGCCGCTAAATAAATAAATAAATAAATAACATAGTAGTGATACCTGTGT
CTGCGGTCATTACTCCAGAACAGCACTTCACATATAGTTTCTCCTTTAAGGTCATTCTCACAAC
AGCCCAGGGAGATAGGGTGGCATGCTTCATTTTATAAGCTGAGGTCCTGGGAGGGGAGGT
CATTTACCCAAGATCACACAGCAAGAACACCAGACAGCTGGAATTTGATCCCAGTTTTGACT
CCAATGCTCTTGCTCTTCATCATCAATAATTTCCTTCAAGGCGTCCCTCAAATGTCACTTCCTC
CAGGAAGCCCTCCCTGATTTATGCTCCTTCCAGAAAGAATGGGCTCTTCCTTTCTCTGAGTCT
CTGGAACACAAGGTCCCAGCTAAACTGTAAATTCCCCAAGGGTAACAACTGGACTAATTTTT
TTTAATTTAATTTAATTTTATTTTTTTGAGATGAAGTCTTGCTCTGTCACCCAGGCTGGATTGT
AGTGGCACGATCTCGGCTGACCGCAACCTCCACCTCCCGGGTTCAAGCGATTCTTATGCCTC
AGCCTCCCGAGTAGCTGGGATTACAGGCGCTGCCACCACACTTGGCTAATTTTTGTATTTTTA
GTAGAGACAGGGTTTCACCATGTTGGCCAGGCTGGTCTCGAACTCCTGACCTCAGGTGATCC
ACCCACCTTGGCCTCCCAAAGTGCTGGGAATACAGGCATGAGCCACCGTTCCCGGCCTTATC
CTTGACTTAGAATACCTAACCTCCTGGGAATGCAGCCCATAGGTCTCAGCCTTATTTCACCCA
GCTCCTGTTCAAGATGGAGTCACTCTGGTTCACATGCCTCTGACATTTCCCCGCTCCCTTTTAT
AAGAGAACCTTTAATCCTAAGGGTTGTAGAGGGAGGAAGATACAACTTCTGTGACTTCTTCA
GGCTGGACAGGGGTGACGATATACCTGCCTAACTCTTAGGATCTATTGGATTCAGGGTAGA
CAGGAGCTCAGTCAGAAAGCACTGGTATCACTTTTTTTTTTTTTTTTTTTTTTGAGACGGAGT
TTCACTCTTGTTGCCCAGGCTGGAGTGCAATGGCACGATCTCAGCTCACCACAGCCTCCGCCT
CCCAGGTTCAAGCGATTCTCCTGCCTCAGCCTCCCCAGTAGCTGGGACTACAGGCGTGTGCC
ACCAAACCCAGCTAATGTTTTTTTTTTTTTATTTTTAGTAGAGACGGGGTTTCTCCATGTTGGC
CAGGCTGGTCTCGAACTCCCGACCTCAGGTGATCCACCCGCCTCGGCCTCCCAAAGTGCTGG
GATTACAGACATGAGCCACCACGCCCGGCCTGATATTTTATTACTTAGTATTTTACTCTGAAT
TATCATGCGTGAATTAAGACCAAGGCTGTCTTGTAAAATAAAATTTGTTGTGGAACAATTTAT
ACAGCTCCTTTGAGGTAGGAGGCAGGACTCAACTCTGGAGATGGGGCTCGGCTCGAATATT
GGACCAAATTGAGGACCAGCTAAAACAGGGAGGAGGCTGAAGCAACTTATTATTTTTATTT
ATTTTTATTTTTTGGAGAAGGAGTCTTGCTCTGTTACCCAGGCTGGAGTGCAGTGACACGAT

CTCGGCTCACTGCAACCTCCACCTTCCGGATTCAAGTGATTCTCCTGCCGCAGCCTCCCGAGT
AGCTGGGACTACAGGCGCATGCCACCATGCCCAGCTAATATTTTTGTATTTTTTAGTAGAGAT
GGGGTTTCGCCATATTAGCCAGGCTGGTCTTGAACTCCTGACTCAGGTGATCTGCCCACCTC
GGCCTCCCAAAGTGCTGGGATTACAGGTGTGGGCCACCACGCCTGGCCCGAAGCAACTTTC
TATGACACGCCTACCAGTGTGCCATGTCAGTTTGCCATTGCCATGGCAACACACCCAGGAGT
TACTGCCCCTTCCCATGGCAATGACCCCATGACCCAGAAGTTACTGCCCCTTCCCTAGATATT
TCTGCATAAACTGCCCCTTAATCTACATGTAATTAAAAATAGGTATAGGCTATTTTTATACCTA
TATAAATAGGTATAGGCTAAAAATAGGTATAGGCTGGGCGTGGTGGCTCATGTCTGTAATC
CCAGTACTTTGGGAGGCCAATGCAGGTGGATCACCTGAGGTCAGGAGATCAAGACCATCCT
GGCTAACATAGTGAAACCCTGTCTCTACTAAAAATACAAAAAATTAGCCAGGCGTGTTGGCG
GGAGCCTGTAGACTCAGCTACTCGGGAGGTTGAGGCAGGAGAATGGCGTGAACCCAGGAG
GCGGAGCTTGCAGTGAGCCGAGATCACACCACTGCACTCCAGCCTGGGTGACAGAGCAAGA
CTCCGTCTAAAAAAAAAAAATAGTAAGAAAGAAGGAAAGACACAAAGACAGAAAGAAGGA
AGGAAAGAAAGCAAGCTGTTTTCCCCTGCCTTGCCCCTGCTCACCTTTGAATTCTTTTCTGGG
CAAAGCCAAGAACCCTCGTGGGCTAAAACCCCGCTTTGGGGCTTAAAGTTTGCAAAATCCTC
CCATTAATCTATTGGGACCAGTTGCCACTTAGGAGCATTCTTTGATAACTTTTACAAAACATC
TTTTGTGGTTTTTGAAATGTTTTCATTTTGTAGATCATTAGCCCTTCTTTTTTGAACTGGAATA
CATTTCACGGGAATTTTCAAATTTAAGTCTGTGCAATGTTACATAAAATACCTTTGATTATTAA
AAGCCATCTGTTTTGCTATAACTTCCCTTTTTTGTTCTAAAGTTTGTCTATTTCTGCTATTTGTT
TTTTTACCATAGAAATATTGATTTCCTTAAGTTTTCAAAGAACCAAGTTATTAATAATTTCTCT
AAGAACTAGTCTCAAGCTTGCTATACAATCCTATGGTTGATAGACTGTGGCTTTCTTGTTGAT
TTCCATTTGTTGTTCATTTCCTCCAATTTTCCTTTTTTAAAAATTATAATTATTGTTTGGATTATT

AJ C5aR2 Original Primer Pair 1

Forward Primer: CACTGTATGCCGCCATCTTC

Reverse Primer: TGTCACGGGAGGACACGA

AJ C5aR2 Original Primer Pair 2

Forward Primer: GATTTGCTGTGCTGTTTGTCTC

Reverse Primer: GTGGGATGGTGGACGACC

AJ C5aR2 Primer Pair 1

Forward Primer: GCTGTGCTGTTTGTCTCTGC

Reverse Primer: CATTCTCGGTGCTGGAGGAG

AJ C5aR2 Primer Pair 2

Forward Primer: CCTGCTGACCATGTATGCCA

Reverse Primer: CCGTAGTCCACCACACACTG

AJ C5aR2 Primer Pair 3

Forward Primer: CCTCCATCATCCTGCTGACC

Reverse Primer: AGAAACCGGATGGCAGTCAC

AJ C5aR2 Primer Pair 4

Forward Primer: GCGGATTTGCTGTGCTGTTT

Reverse Primer: AAGAAACCGGATGGCAGTCA

AJ C5aR2 Primer Pair 5

Forward Primer: CCCTCCATCATCCTGCTGAC

Reverse Primer: ATGGCAGTCACCGCATTCTC

AJ C5aR2 Long Primer Pair 1

Forward Primer: AGCACTGGAGTCCTTATGACG

Reverse Primer: GAAACCGGATGGCAGTCACC

AJ C5aR2 Long Primer Pair 4

Forward Primer: CACCACACCCGGCCTAGAAT

Reverse Primer: GGATGGCAGTCACCGCATT

AJ C5aR2 Long Primer Pair 5

Forward Primer: AAGCACTGGAGTCCTTATGACG

Reverse Primer: AAGAAACCGGATGGCAGTCAC

AJ C5aR2 Long Primer Pair 8

Forward Primer: CATGGAGTTTCCTCCTCTGAGT

Reverse Primer: GCCAAAAAGAAACCGGATGG

AJ C5aR2 Long Primer Pair 10

Forward Primer: ATATTCCAGTTTGCAAGGTGCT

Reverse Primer: GCCCCAGGAAGCCAAAAAGAA

Supplementary Figure 4.3. C5aR2 "AJ C5aR2 KO" sgRNA target sequence and primer design. Black: C5aR2 gene sequence, *Green*: Target Amplicon, **Red**: gRNA target sequence.

8.4. C5aR1 Monoclone Sequencing Data

8.4.1. Forward primer

D6

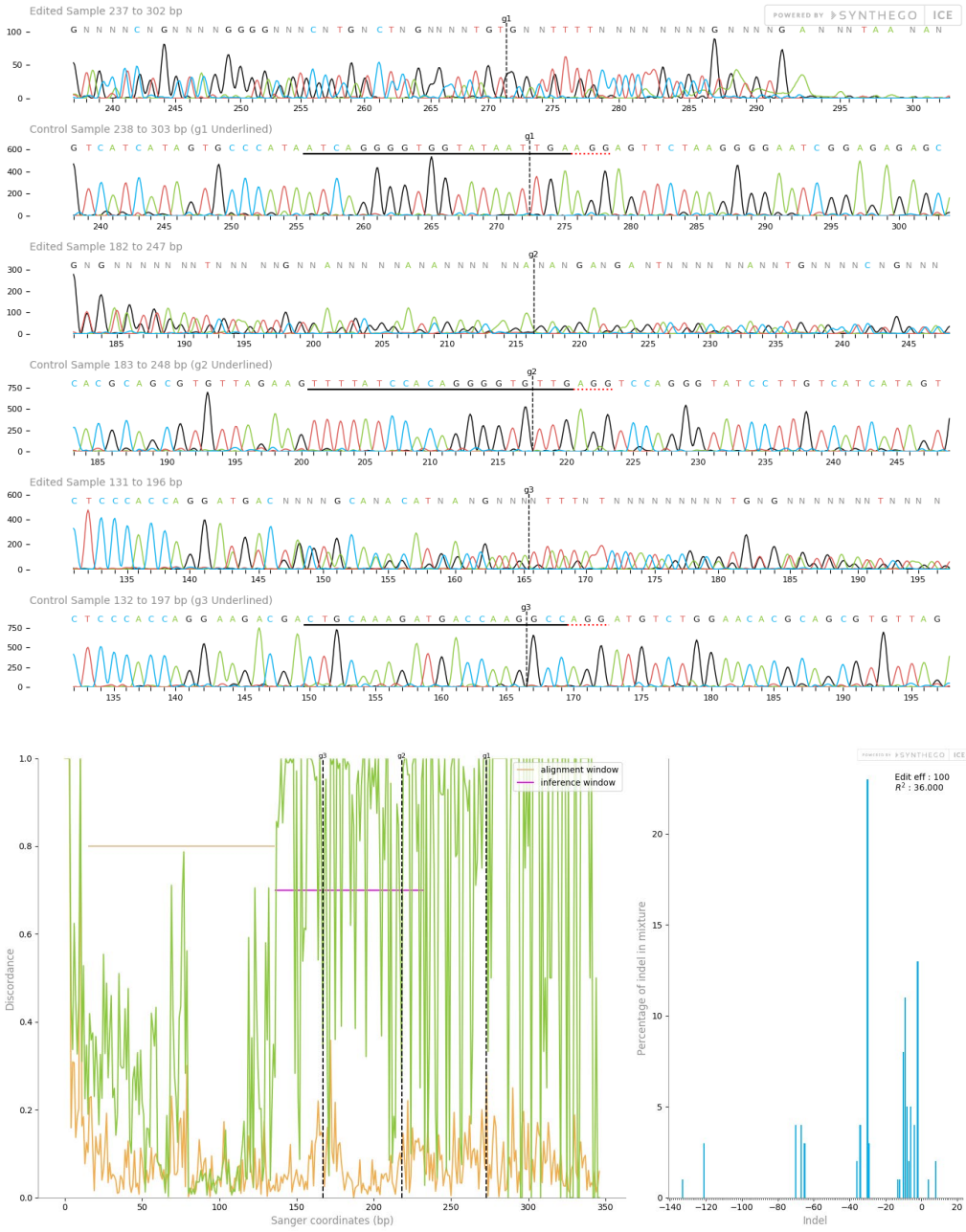

H9


Edited Sample 234 to 299 bp
Control Sample 238 to 303 bp (g1 Underlined)
Edited Sample 179 to 244 bp
Control Sample 183 to 248 bp (g2 Underlined)
Edited Sample 128 to 193 bp
Control Sample 132 to 197 bp (g3 Underlined)
alignment window
inference window
Discordance
Sanger coordinates (bp)
Edit eff : 100
R^2 : 90.000
Percentage of indel in mixture
Indel

8.4.2. Reverse primer

A3

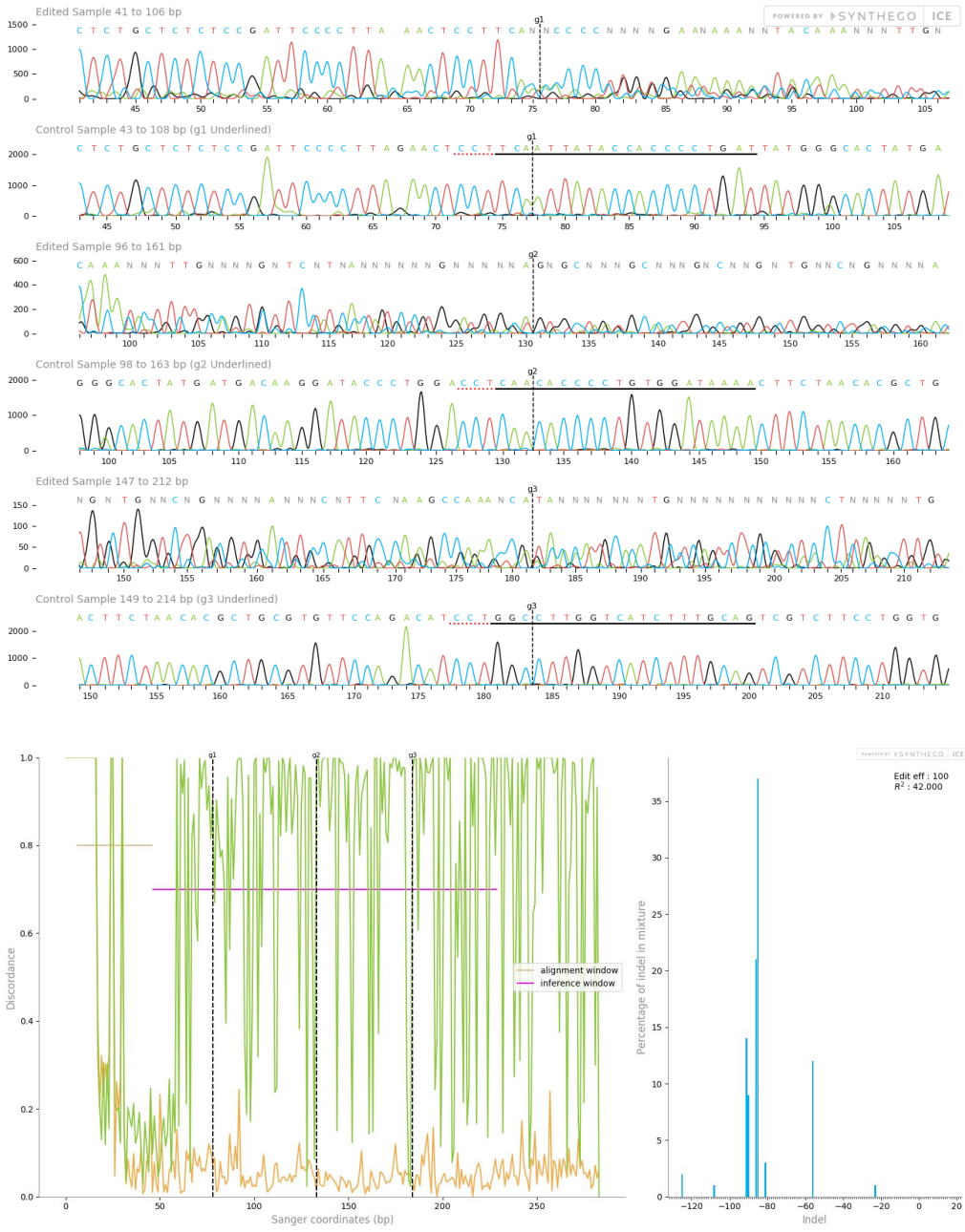

A4

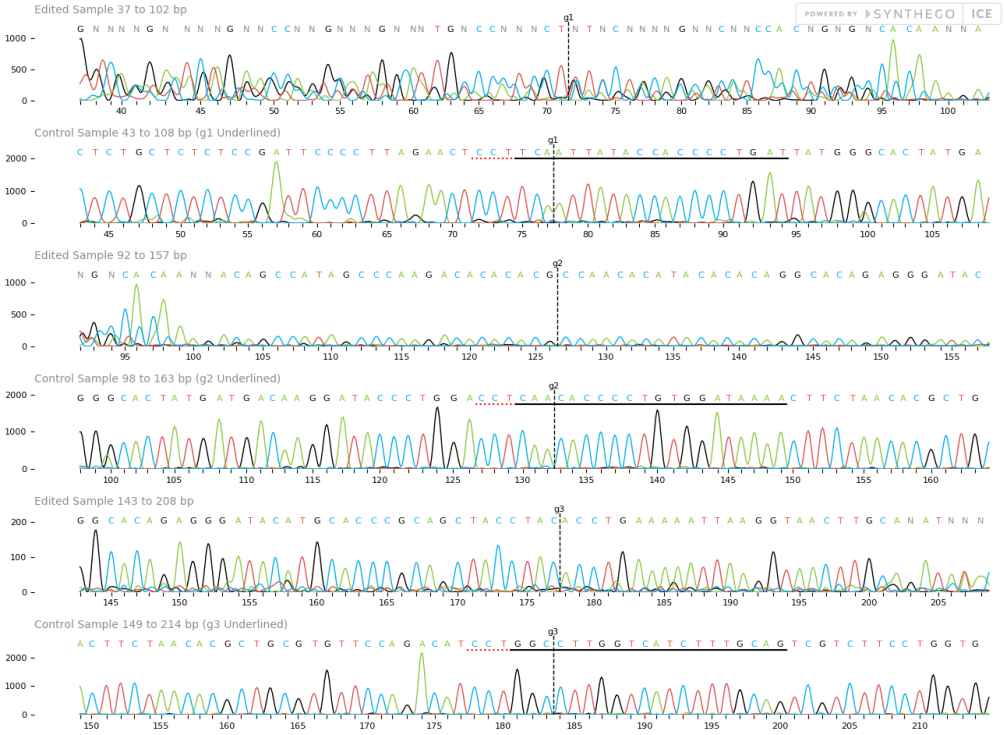
Edited Sample 37 to 102 bp
Control Sample 43 to 108 bp (g1 Underlined)
Edited Sample 92 to 157 bp
Control Sample 98 to 163 bp (g2 Underlined)
Edited Sample 143 to 208 bp
Control Sample 149 to 214 bp (g3 Underlined)

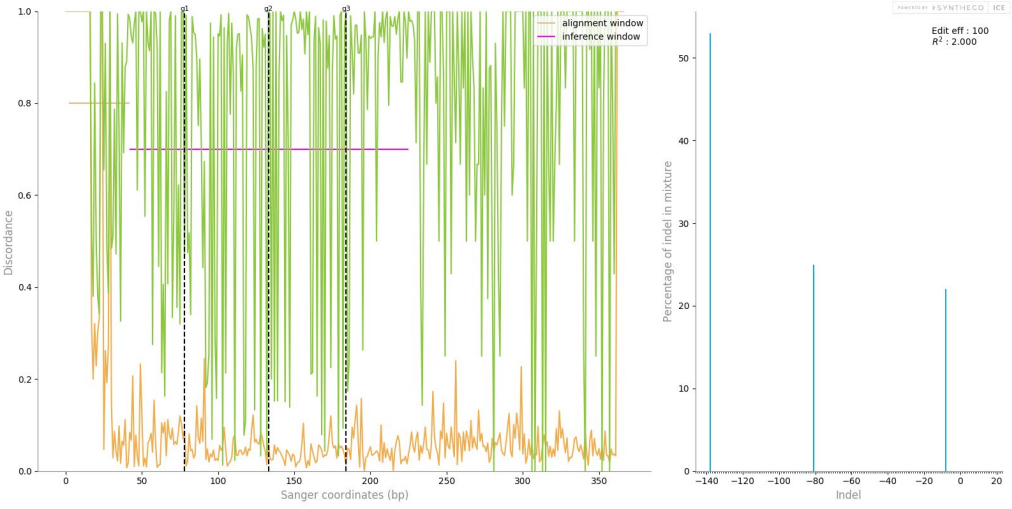
alignment window
inference window
Discordance
Sanger coordinates (bp)
Edit eff : 100
R^2 : 2.000
Percentage of indel in mixture
Indel

A5

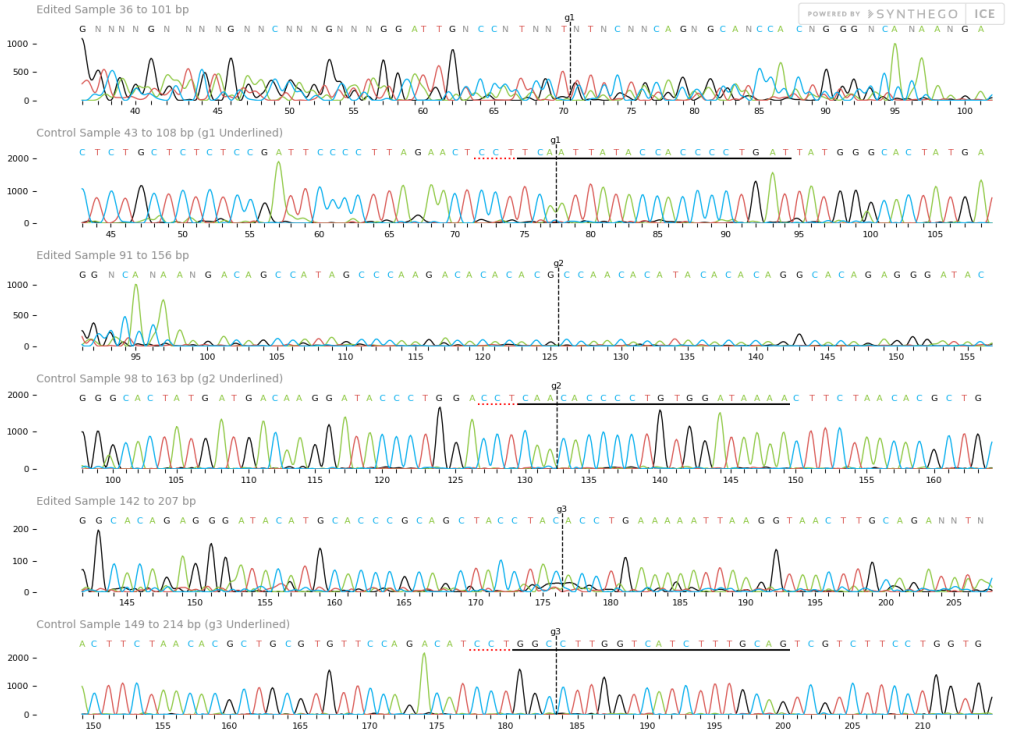
Edited Sample 36 to 101 bp
Control Sample 43 to 108 bp (g1 Underlined)
Edited Sample 91 to 156 bp
Control Sample 98 to 163 bp (g2 Underlined)
Edited Sample 142 to 207 bp
Control Sample 149 to 214 bp (g3 Underlined)

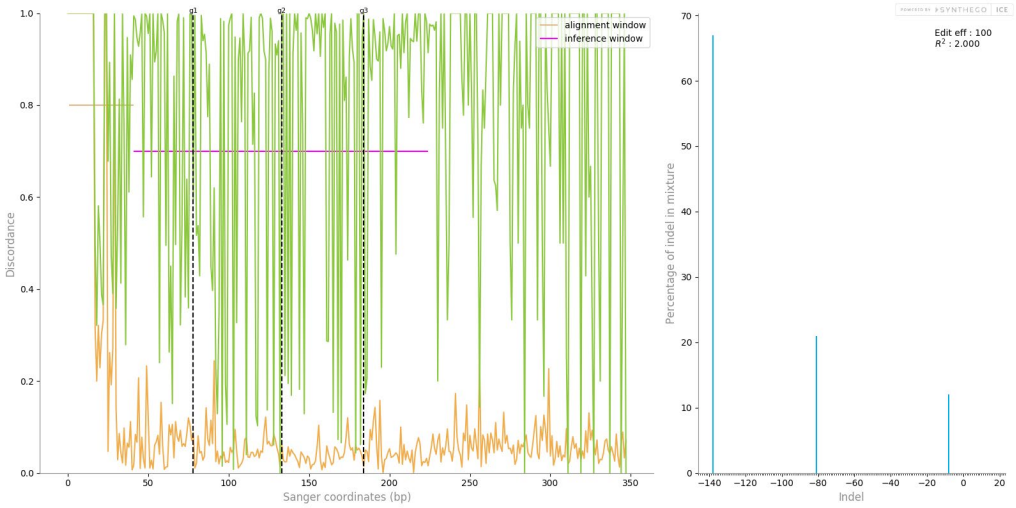
alignment window
inference window
Discordance
Sanger coordinates (bp)
Edit eff : 100
R^2 : 2.000
Percentage of indel in mixture
Indel

B5

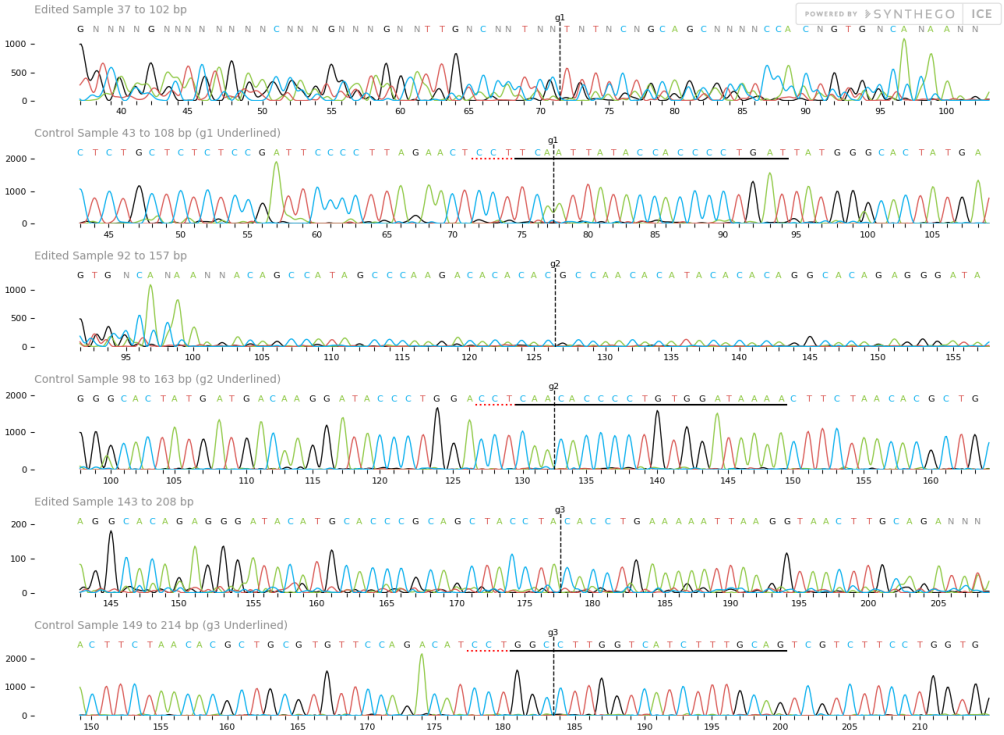
Edited Sample 37 to 102 bp
Control Sample 43 to 108 bp (g1 Underlined)
Edited Sample 92 to 157 bp
Control Sample 98 to 163 bp (g2 Underlined)
Edited Sample 143 to 208 bp
Control Sample 149 to 214 bp (g3 Underlined)

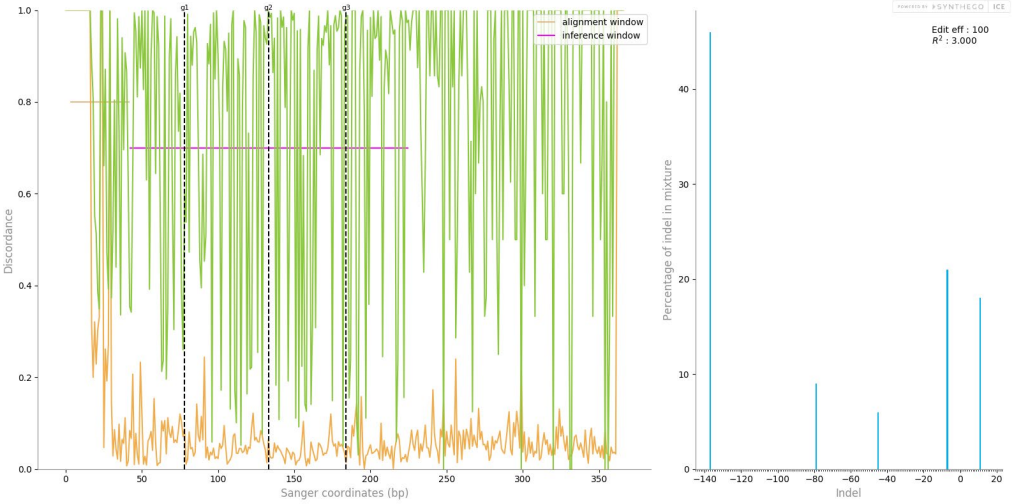
alignment window
inference window
Discordance
Sanger coordinates (bp)
Edit eff : 100
R^2 : 3.000
Percentage of indel in mixture
Indel

B6

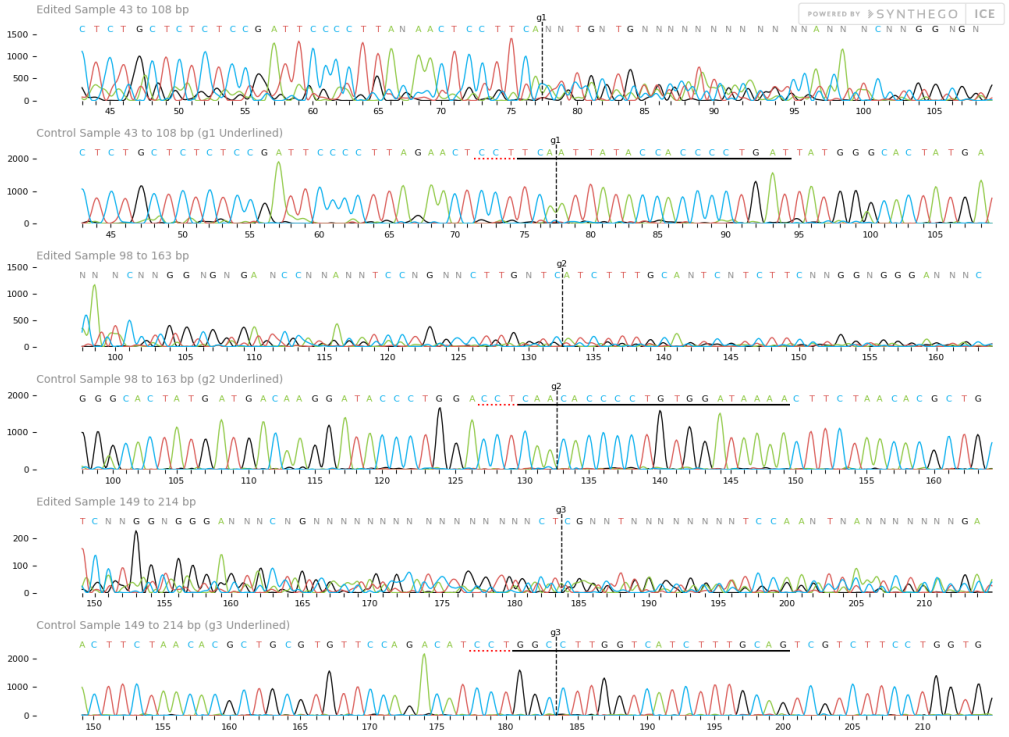
Edited Sample 43 to 108 bp
Control Sample 43 to 108 bp (g1 Underlined)
Edited Sample 98 to 163 bp
Control Sample 98 to 163 bp (g2 Underlined)
Edited Sample 149 to 214 bp
Control Sample 149 to 214 bp (g3 Underlined)

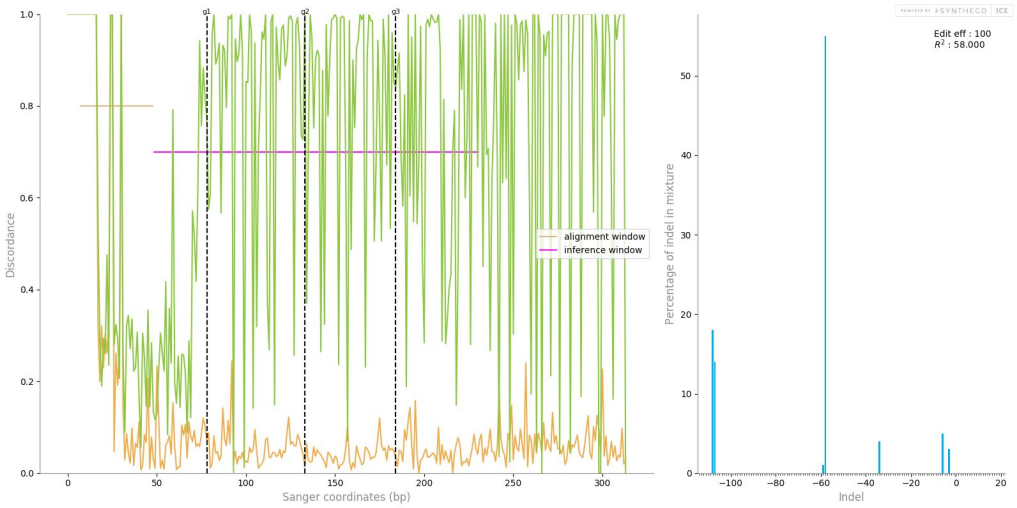
Discordance
Sanger coordinates (bp)
alignment window
inference window
Edit eff : 100
R^2 : 58.000
Percentage of indel in mixture
Indel

C3

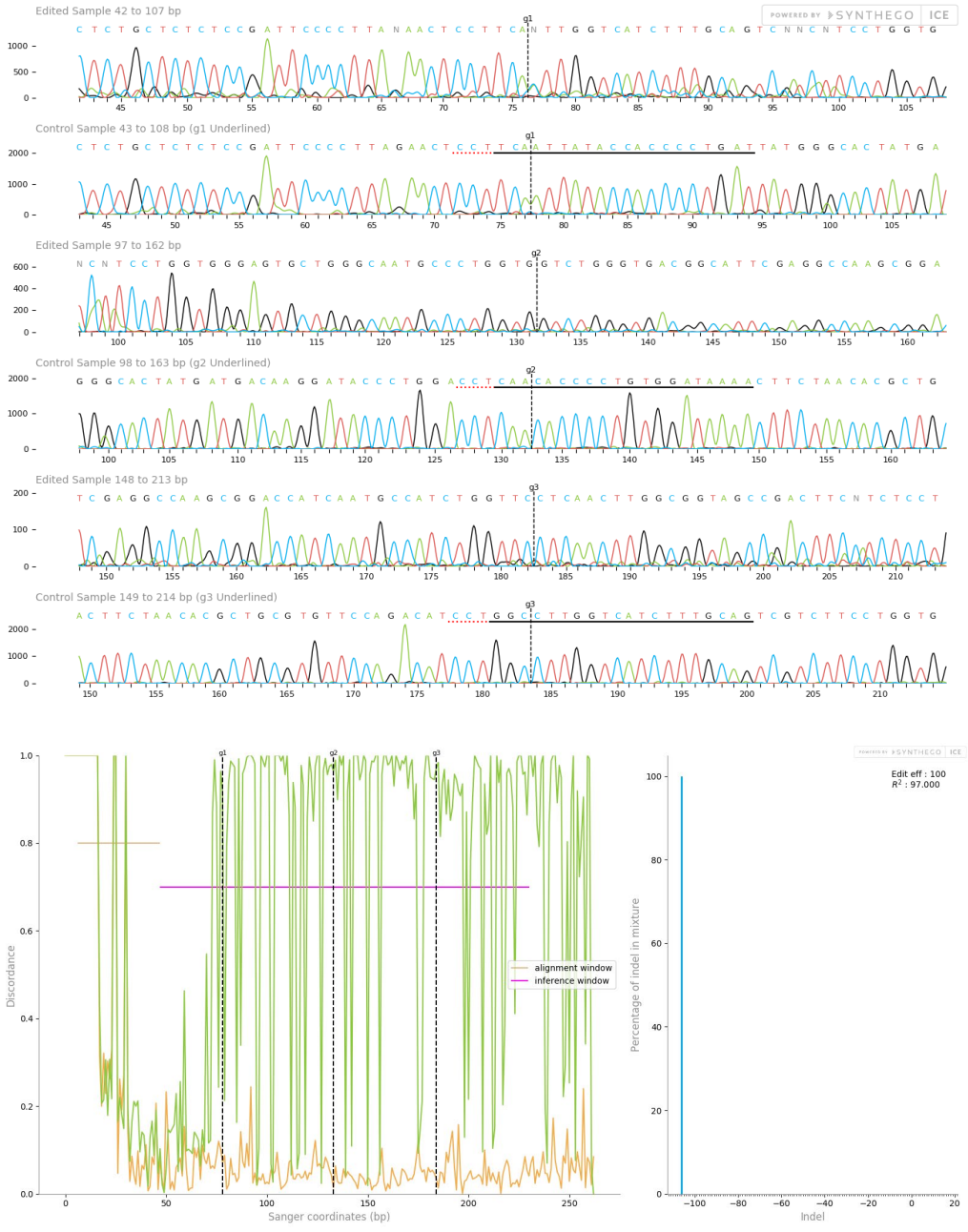
Edited Sample 42 to 107 bp
Control Sample 43 to 108 bp (g1 Underlined)
Edited Sample 97 to 162 bp
Control Sample 98 to 163 bp (g2 Underlined)
Edited Sample 148 to 213 bp
Control Sample 149 to 214 bp (g3 Underlined)
Discordance
Sanger coordinates (bp)
alignment window
inference window
Edit eff : 100
R^2 : 97.000
Percentage of indel in mixture
Indel

C4

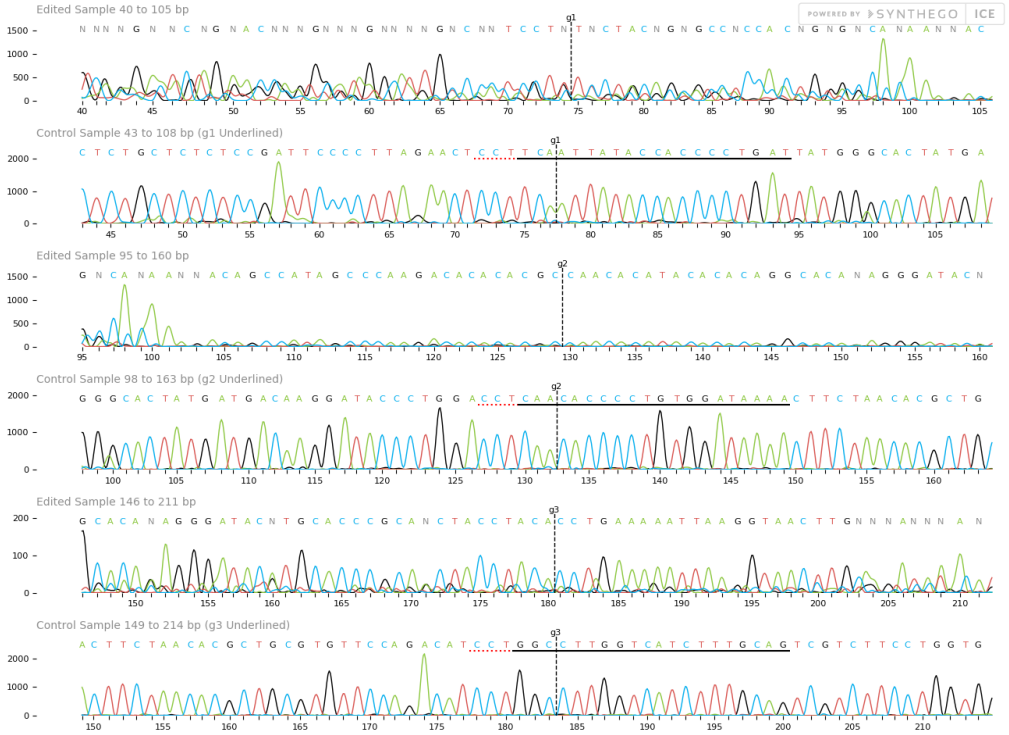
Edited Sample 40 to 105 bp
Control Sample 43 to 108 bp (g1 Underlined)
Edited Sample 95 to 160 bp
Control Sample 98 to 163 bp (g2 Underlined)
Edited Sample 146 to 211 bp
Control Sample 149 to 214 bp (g3 Underlined)

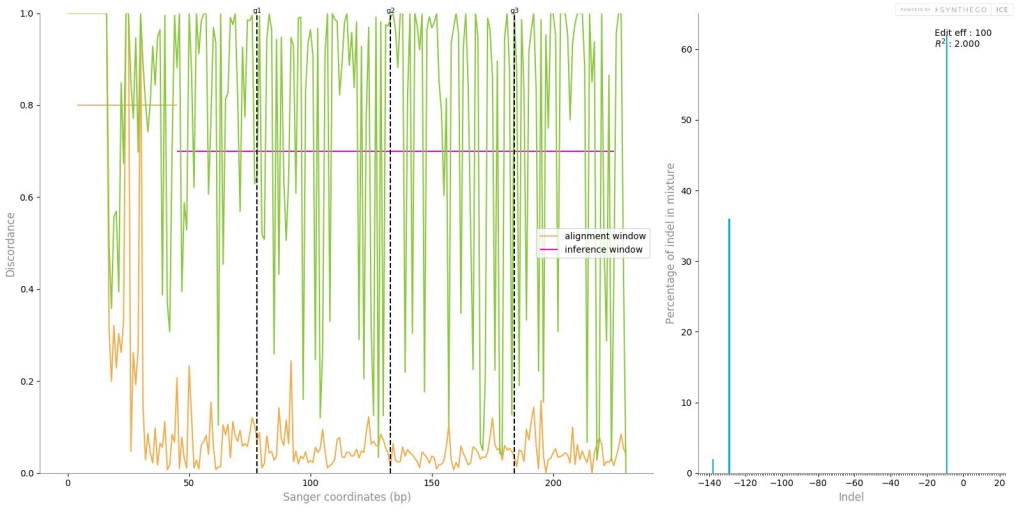
Discordance
Sanger coordinates (bp)
alignment window
inference window
Edit eff : 100
R^2 : 2.000
Percentage of indel in mixture
Indel

E9

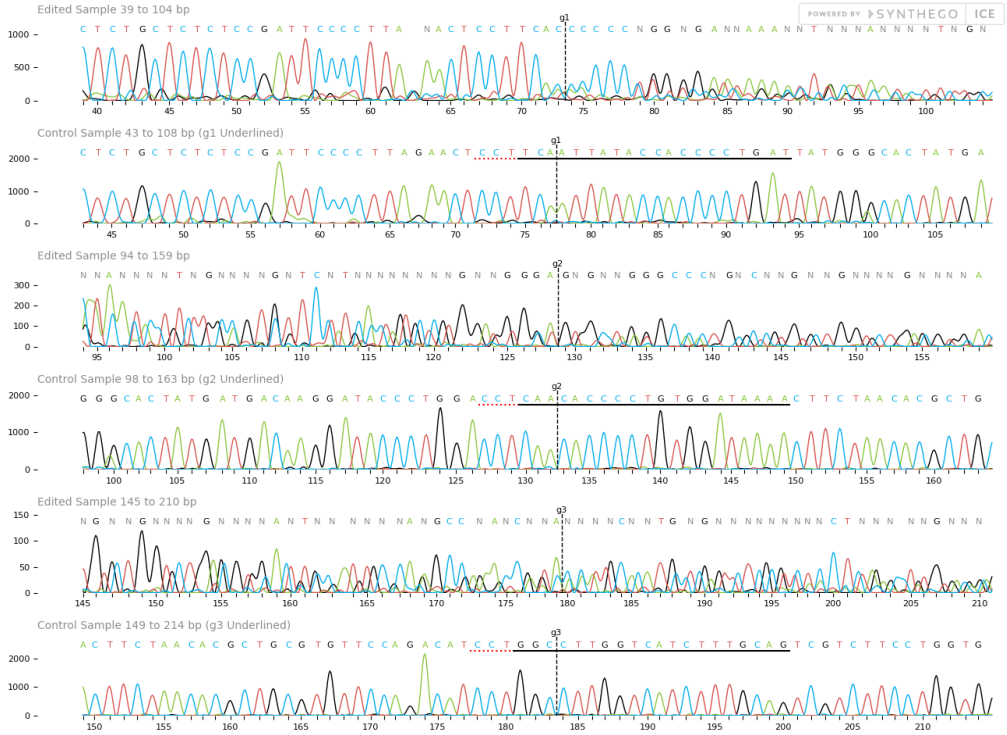
Edited Sample 39 to 104 bp
Control Sample 43 to 108 bp (g1 Underlined)
Edited Sample 94 to 159 bp
Control Sample 98 to 163 bp (g2 Underlined)
Edited Sample 145 to 210 bp
Control Sample 149 to 214 bp (g3 Underlined)

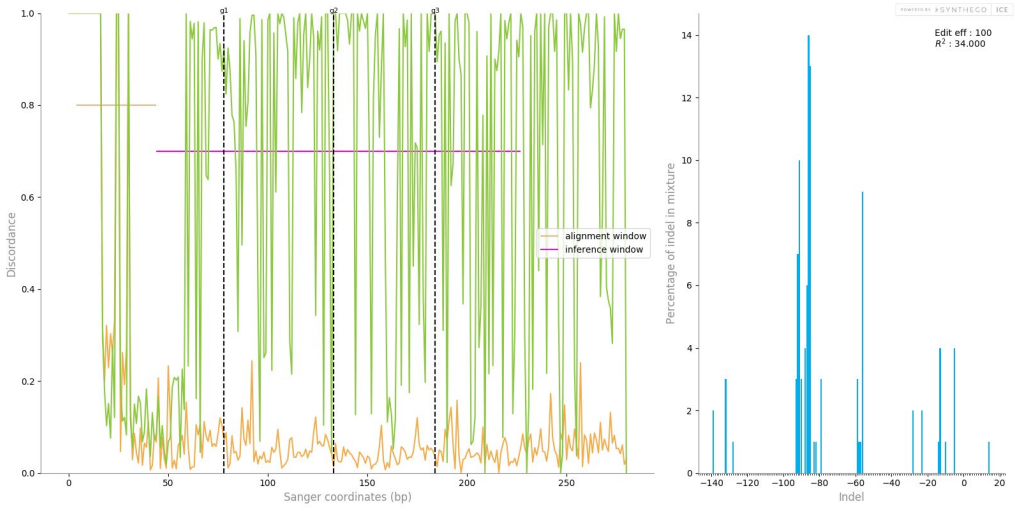
Discordance
Sanger coordinates (bp)
alignment window
inference window
Edit eff : 100
R^2 : 34.000
Percentage of indel in mixture
Indel

F7

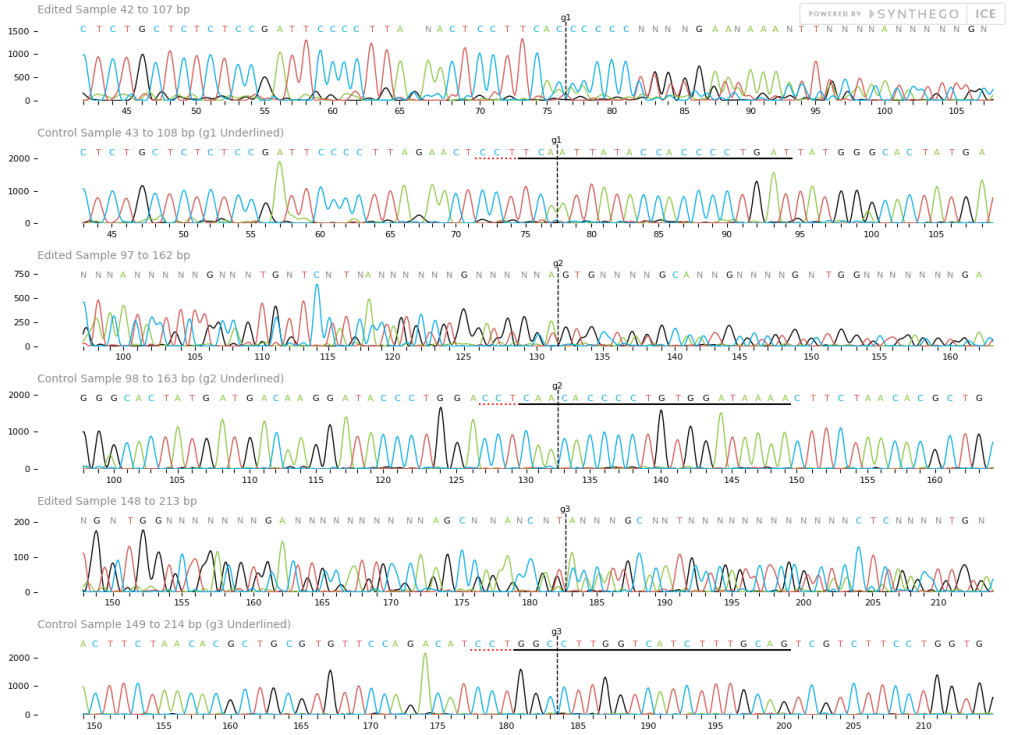
Edited Sample 42 to 107 bp
Control Sample 43 to 108 bp (g1 Underlined)
Edited Sample 97 to 162 bp
Control Sample 98 to 163 bp (g2 Underlined)
Edited Sample 148 to 213 bp
Control Sample 149 to 214 bp (g3 Underlined)

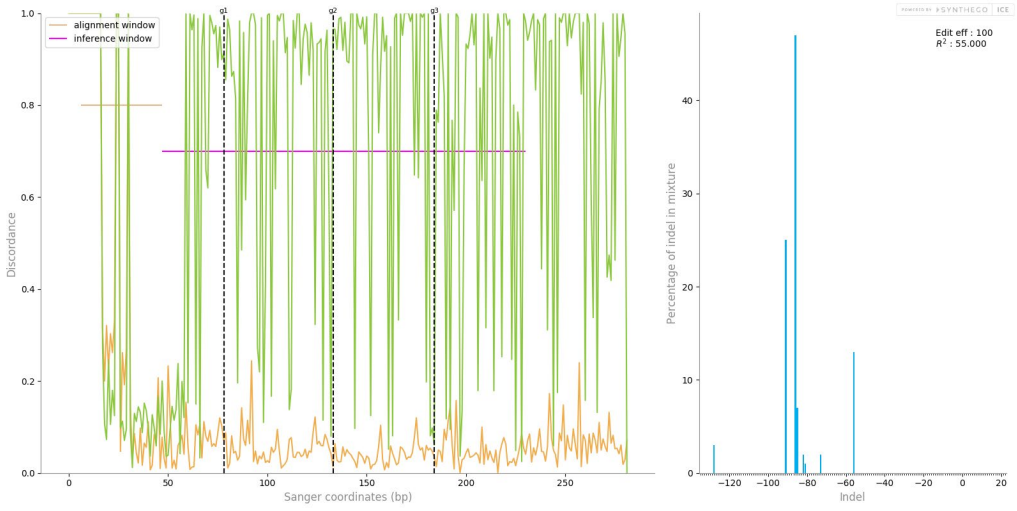
alignment window
inference window
Discordance
Sanger coordinates (bp)
Edit eff : 100
R^2 : 55.000
Percentage of indel in mixture
Indel

F11

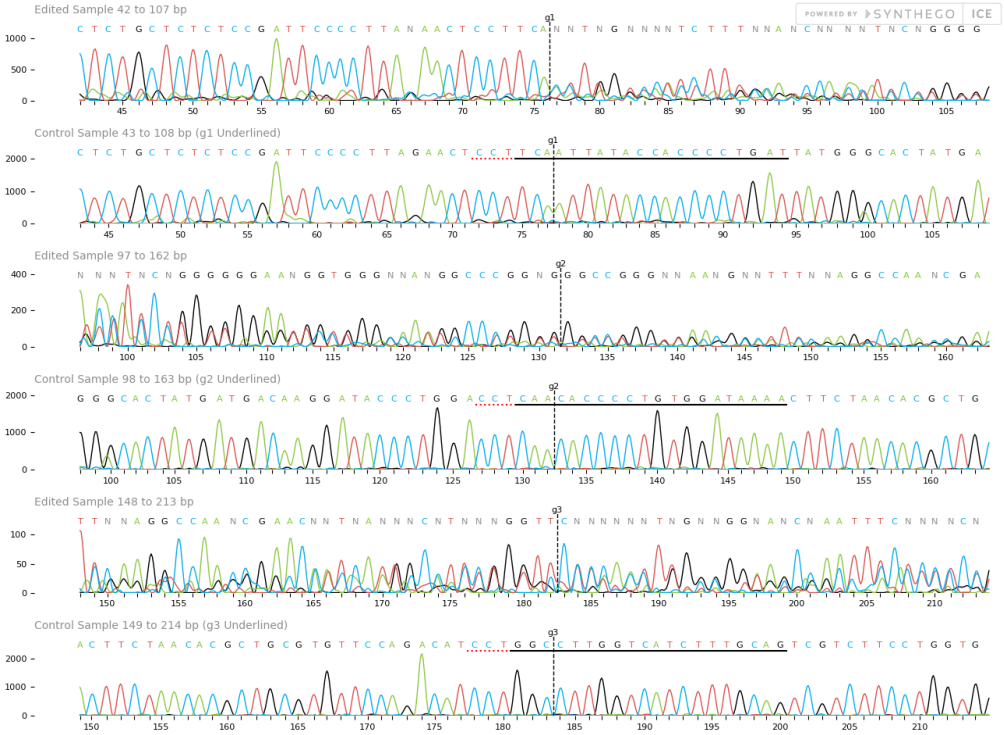
Edited Sample 42 to 107 bp
Control Sample 43 to 108 bp (g1 Underlined)
Edited Sample 97 to 162 bp
Control Sample 98 to 163 bp (g2 Underlined)
Edited Sample 148 to 213 bp
Control Sample 149 to 214 bp (g3 Underlined)

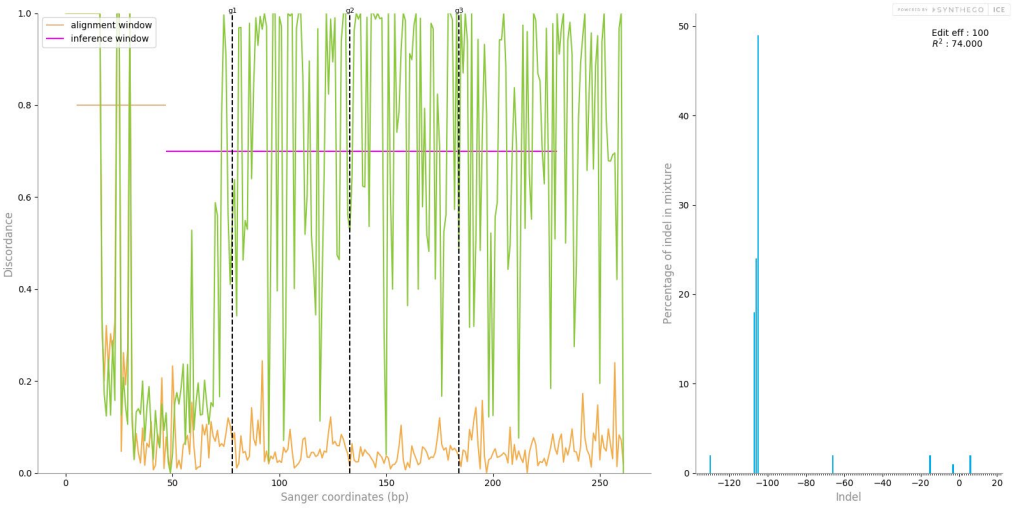
alignment window
inference window
Discordance
Sanger coordinates (bp)
Edit eff : 100
R^2 : 74.000
Percentage of indel in mixture
Indel

F12

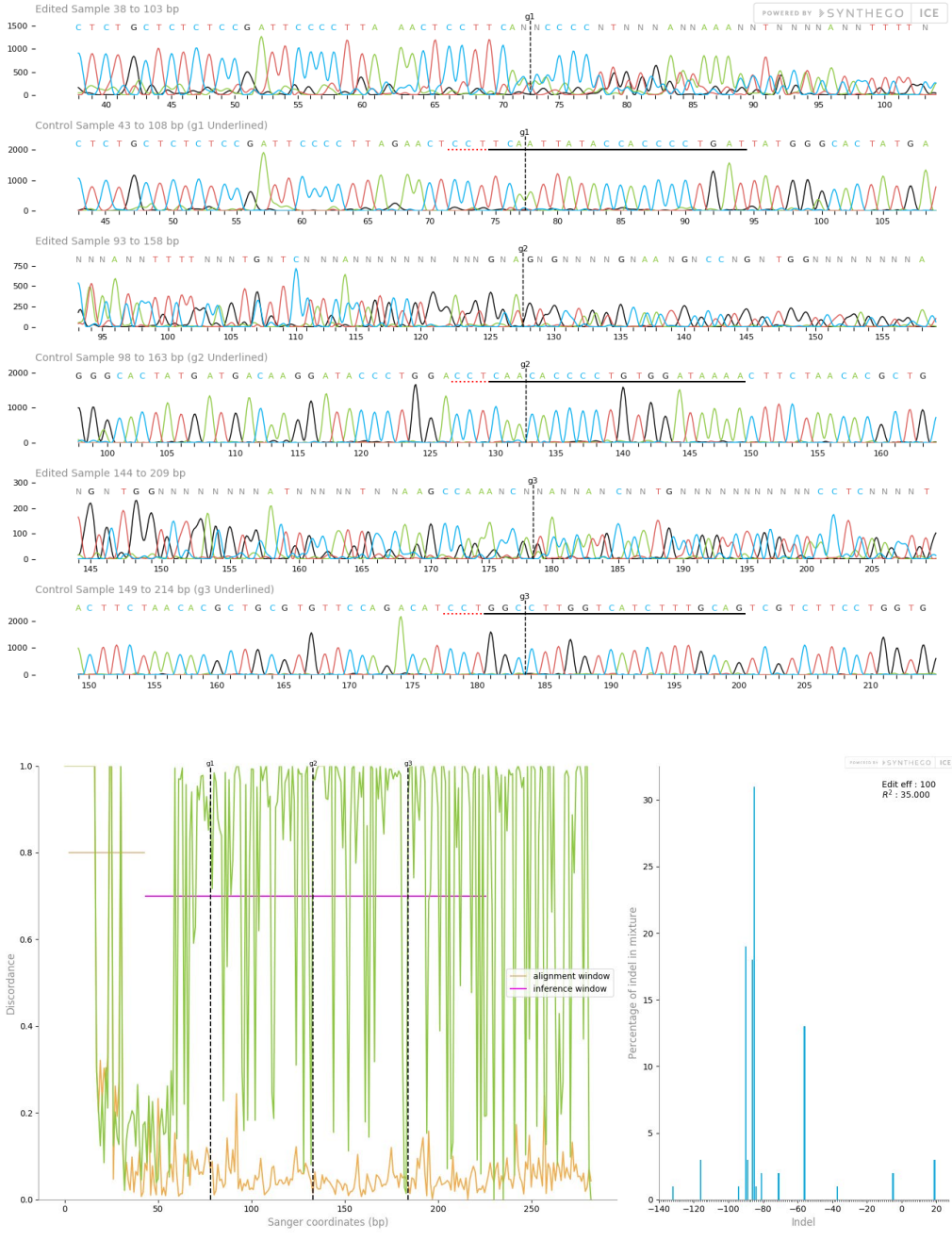
Edited Sample 38 to 103 bp
Control Sample 43 to 108 bp (g1 Underlined)
Edited Sample 93 to 158 bp
Control Sample 98 to 163 bp (g2 Underlined)
Edited Sample 144 to 209 bp
Control Sample 149 to 214 bp (g3 Underlined)
Discordance
Sanger coordinates (bp)
alignment window
inference window
Edit eff : 100
R² : 35.000
Percentage of indel in mixture
Indel

G8

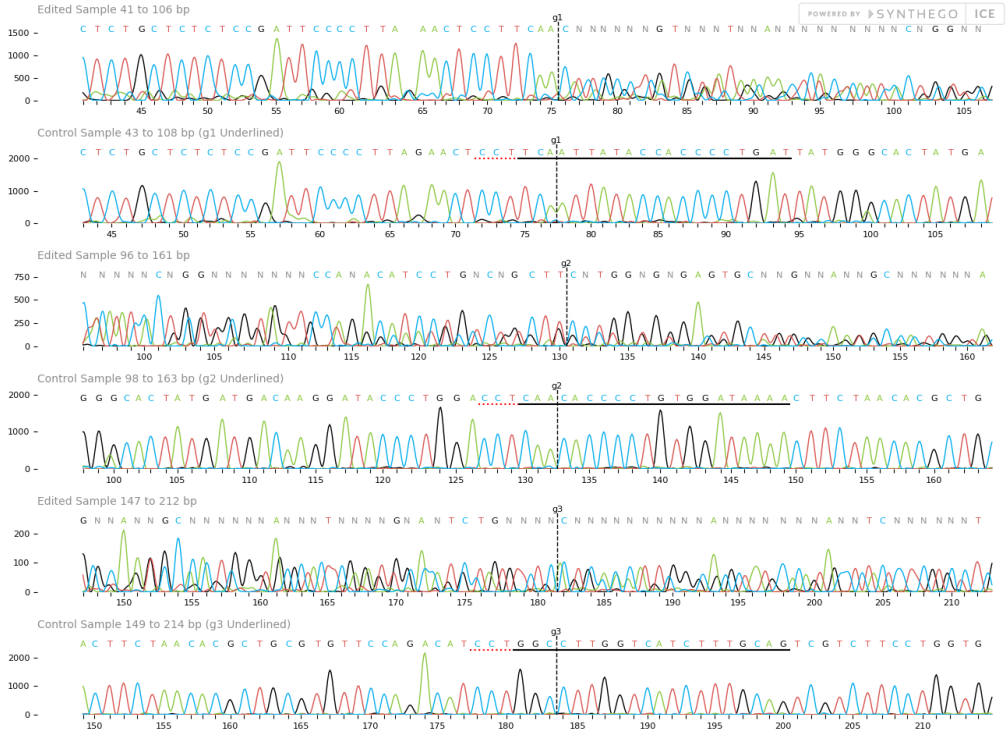
Edited Sample 41 to 106 bp
Control Sample 43 to 108 bp (g1 Underlined)
Edited Sample 96 to 161 bp
Control Sample 98 to 163 bp (g2 Underlined)
Edited Sample 147 to 212 bp
Control Sample 149 to 214 bp (g3 Underlined)

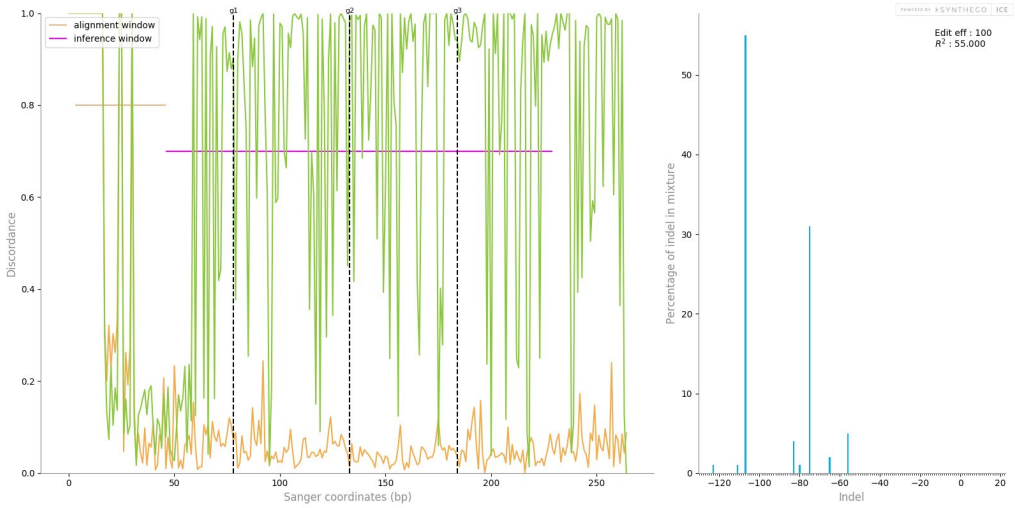
alignment window
inference window
Discordance
Sanger coordinates (bp)
Edit eff : 100
R^2 : 55.000
Percentage of indel in mixture
Indel

G12

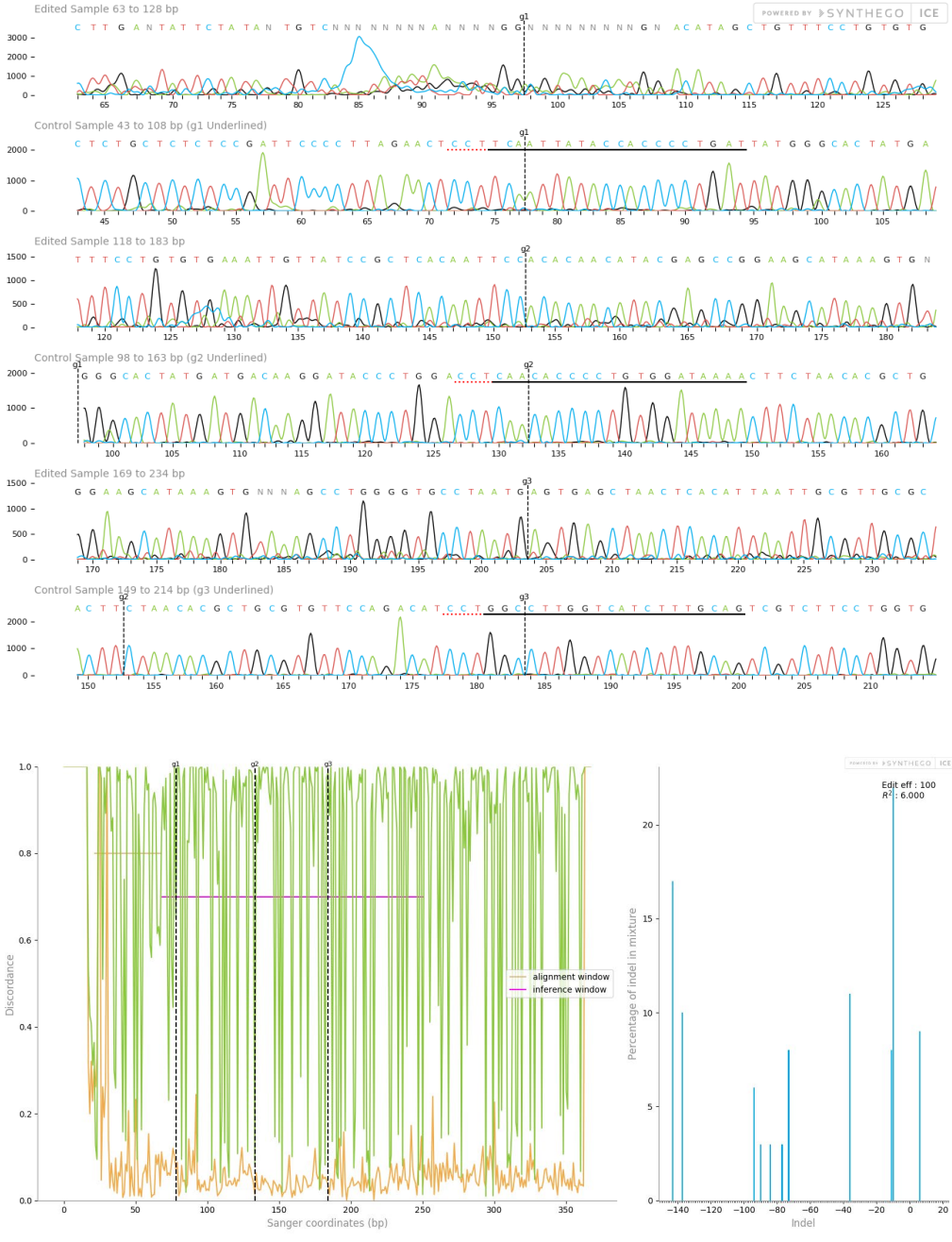
Edited Sample 63 to 128 bp
Control Sample 43 to 108 bp (g1 Underlined)
Edited Sample 118 to 183 bp
Control Sample 98 to 163 bp (g2 Underlined)
Edited Sample 169 to 234 bp
Control Sample 149 to 214 bp (g3 Underlined)
Discordance
Sanger coordinates (bp)
alignment window
inference window
Edit eff : 100
R^2 : 6.000
Percentage of indel in mixture
Indel

H4

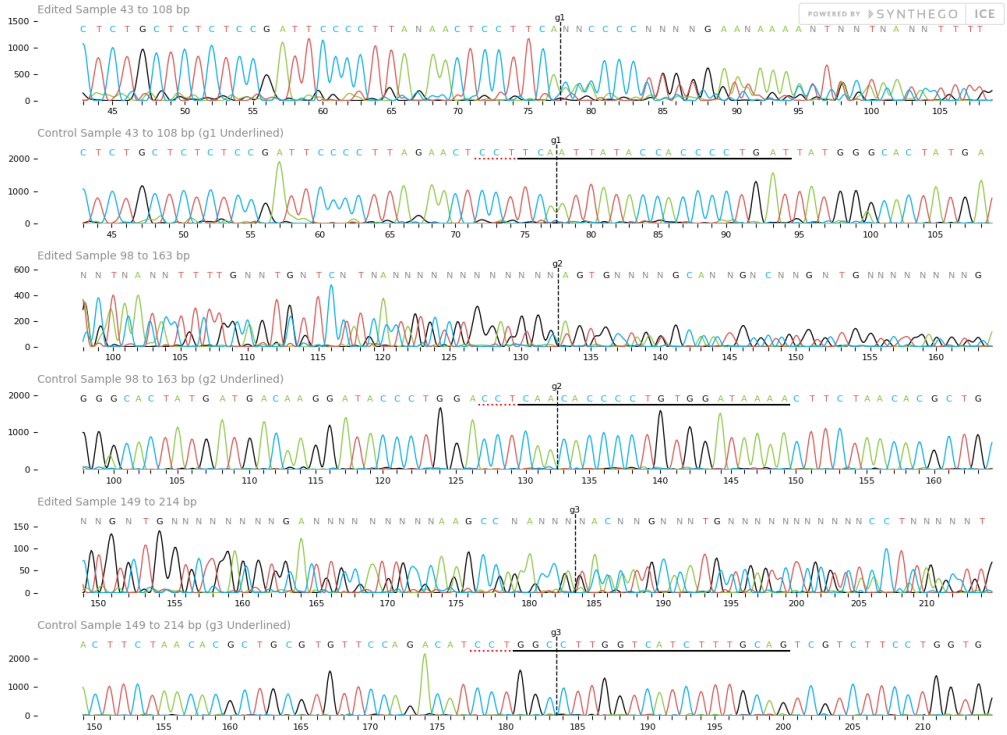
Edited Sample 43 to 108 bp
Control Sample 43 to 108 bp (g1 Underlined)
Edited Sample 98 to 163 bp
Control Sample 98 to 163 bp (g2 Underlined)
Edited Sample 149 to 214 bp
Control Sample 149 to 214 bp (g3 Underlined)

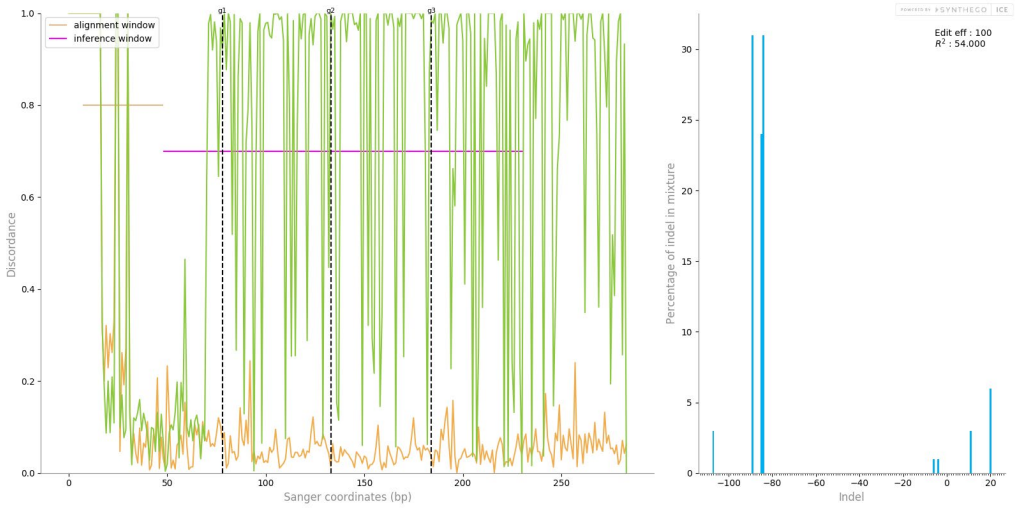
alignment window
inference window
Discordance
Sanger coordinates (bp)
Edit eff : 100
R^2 : 54.000
Percentage of indel in mixture
Indel

H9

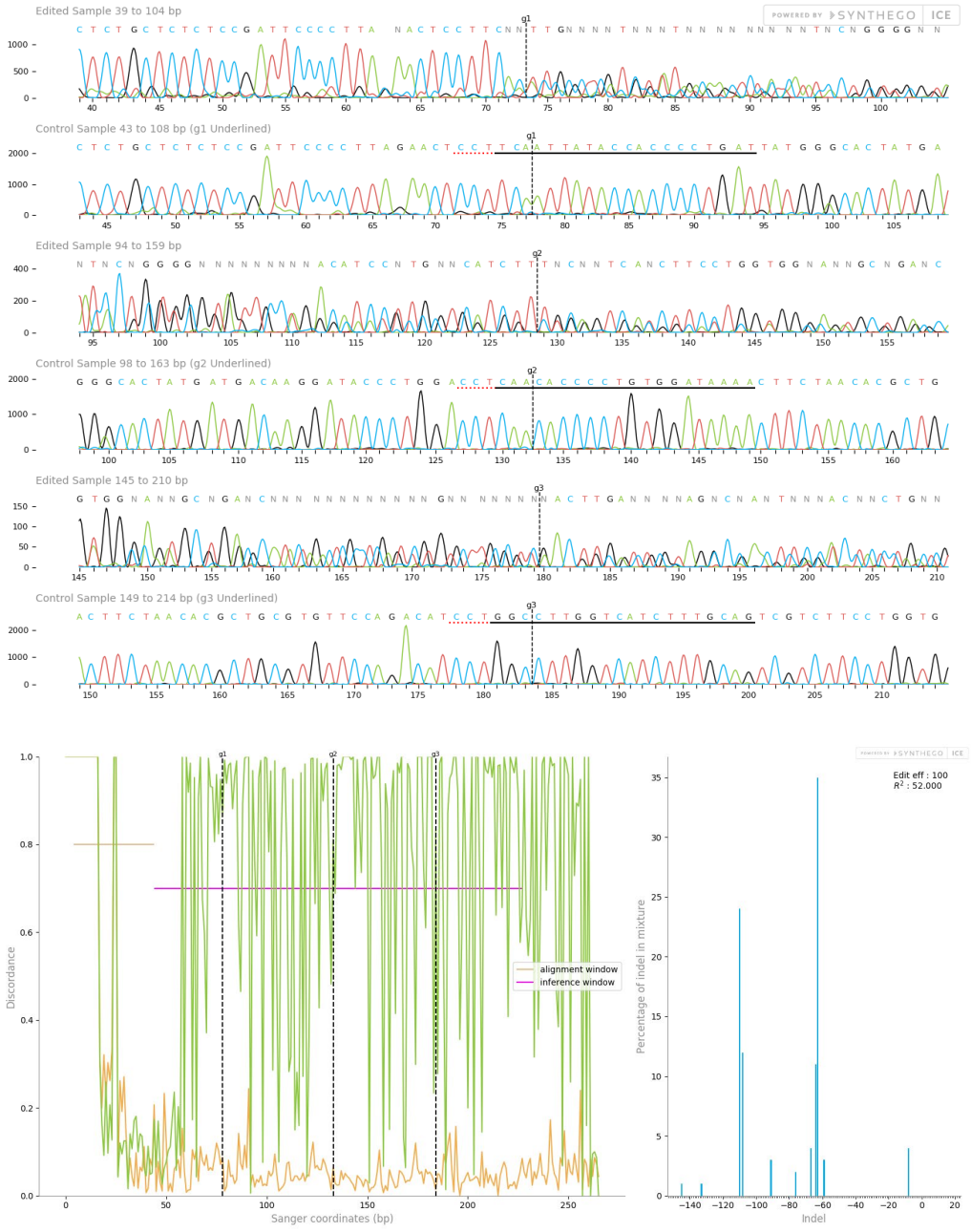

Supplementary Figure 4.4. C5aR1 monoclone sequencing data.

8.5. C5aR2 Monoclone Sequencing Data

8.5.1. Forward primer

A5

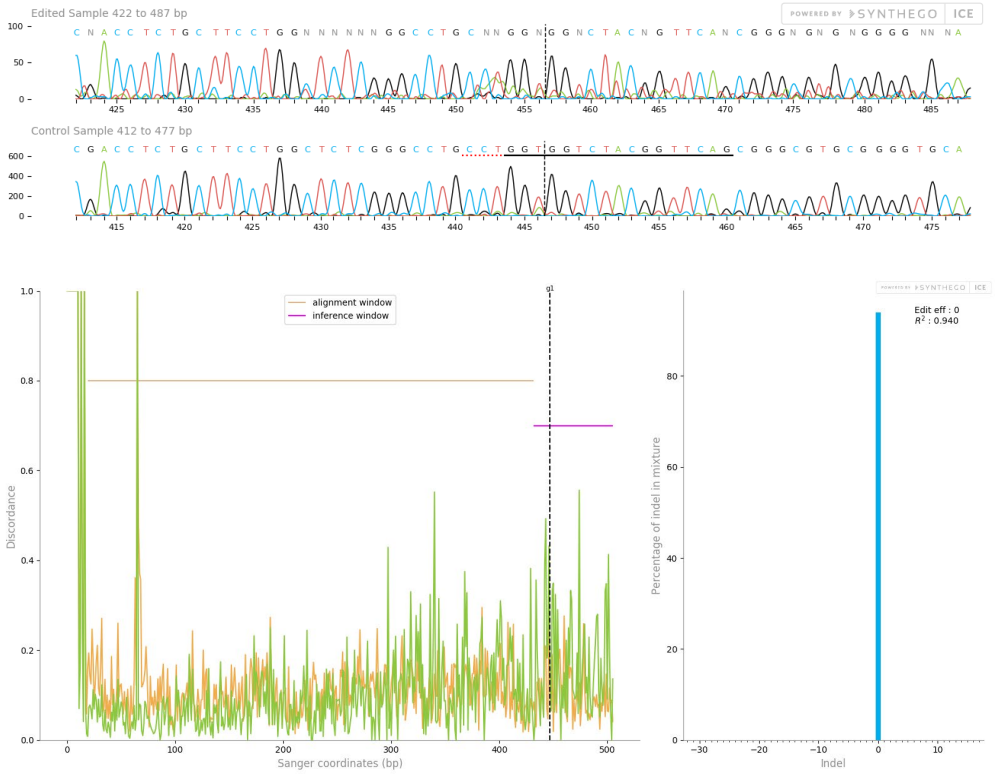

C3

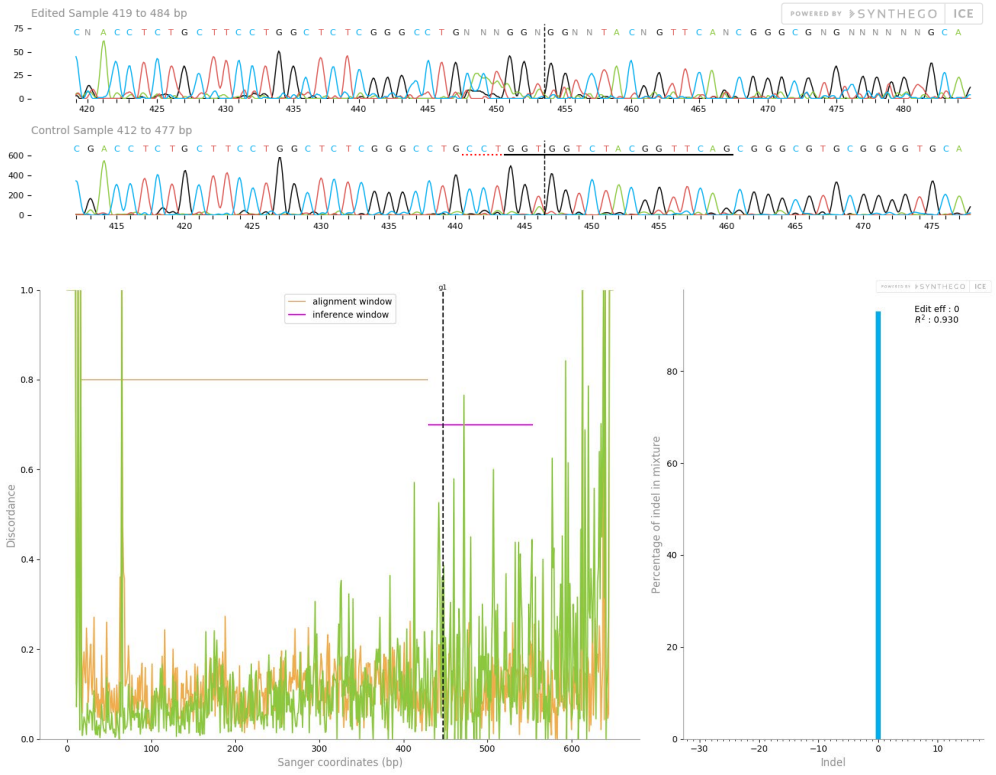

C9

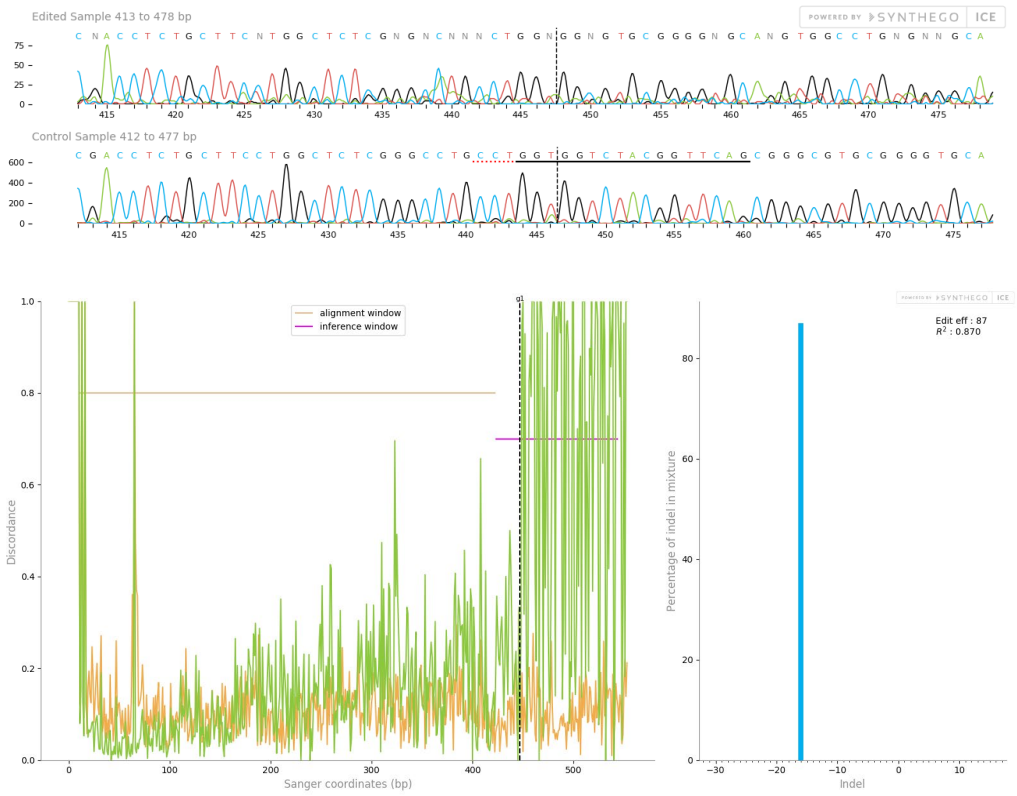
Edited Sample 413 to 478 bp
Control Sample 412 to 477 bp
alignment window
inference window
Discordance
Sanger coordinates (bp)
Edit eff : 87
R^2 : 0.870
Percentage of indel in mixture
Indel

F6

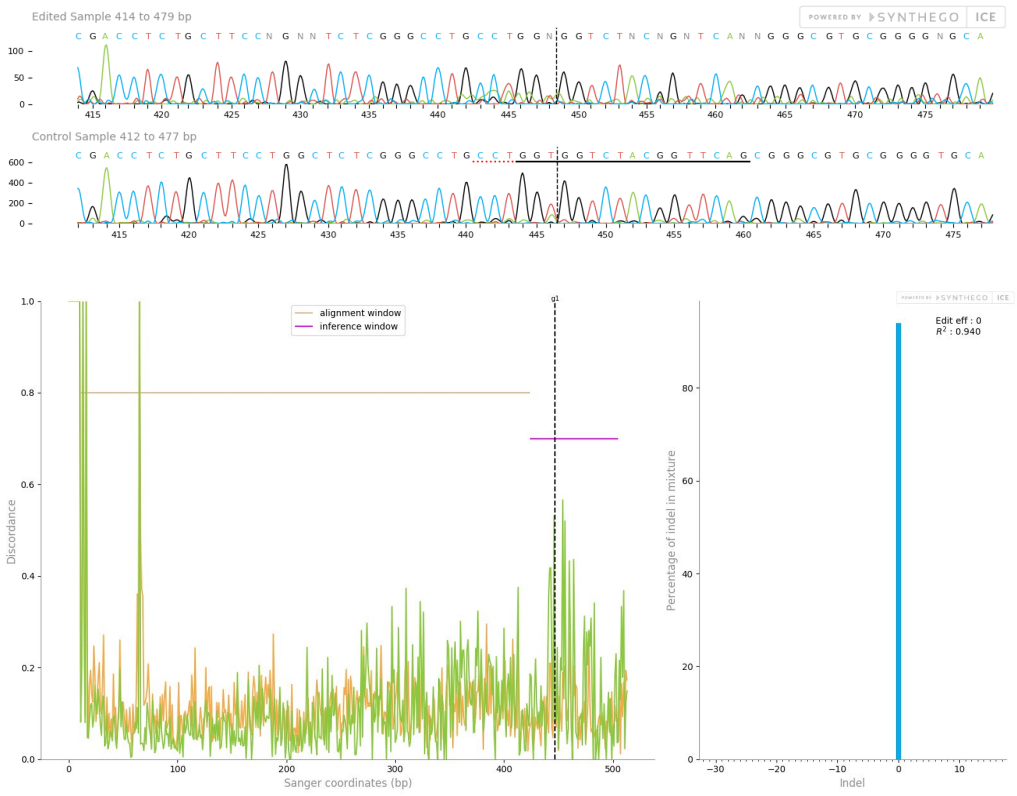
Edited Sample 414 to 479 bp
Control Sample 412 to 477 bp
alignment window
inference window
Discordance
Sanger coordinates (bp)
Edit eff : 0
R^2 : 0.940
Percentage of indel in mixture
Indel

F10

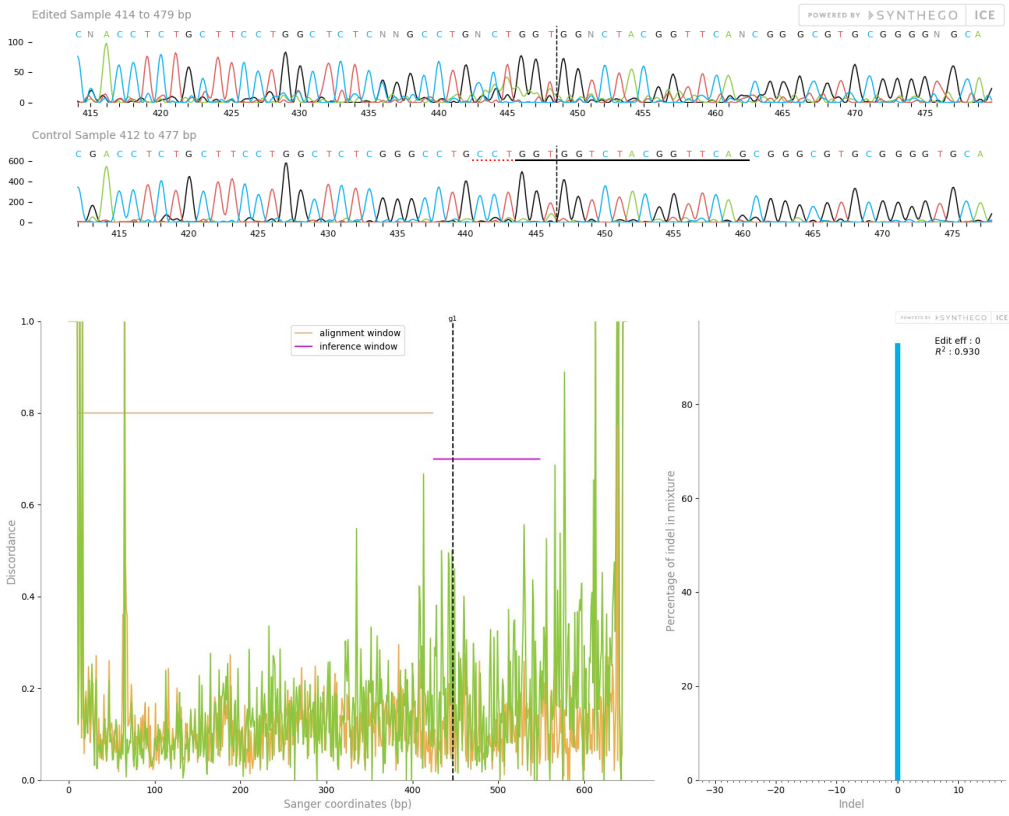
Edited Sample 414 to 479 bp
POWERED BY SYNTHEGO ICE
Control Sample 412 to 477 bp
alignment window
inference window
Discordance
Sanger coordinates (bp)
Edit eff : 0
R^2 : 0.930
Percentage of indel in mixture
Indel

8.5.2. Reverse primer

A1

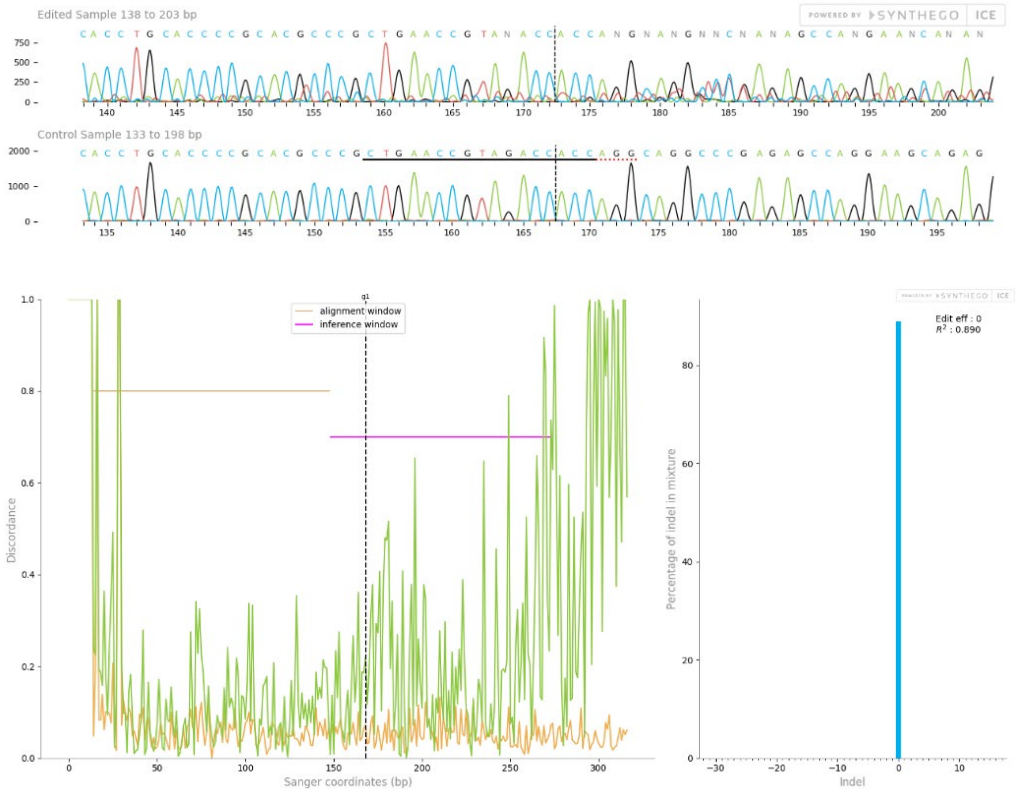

A3

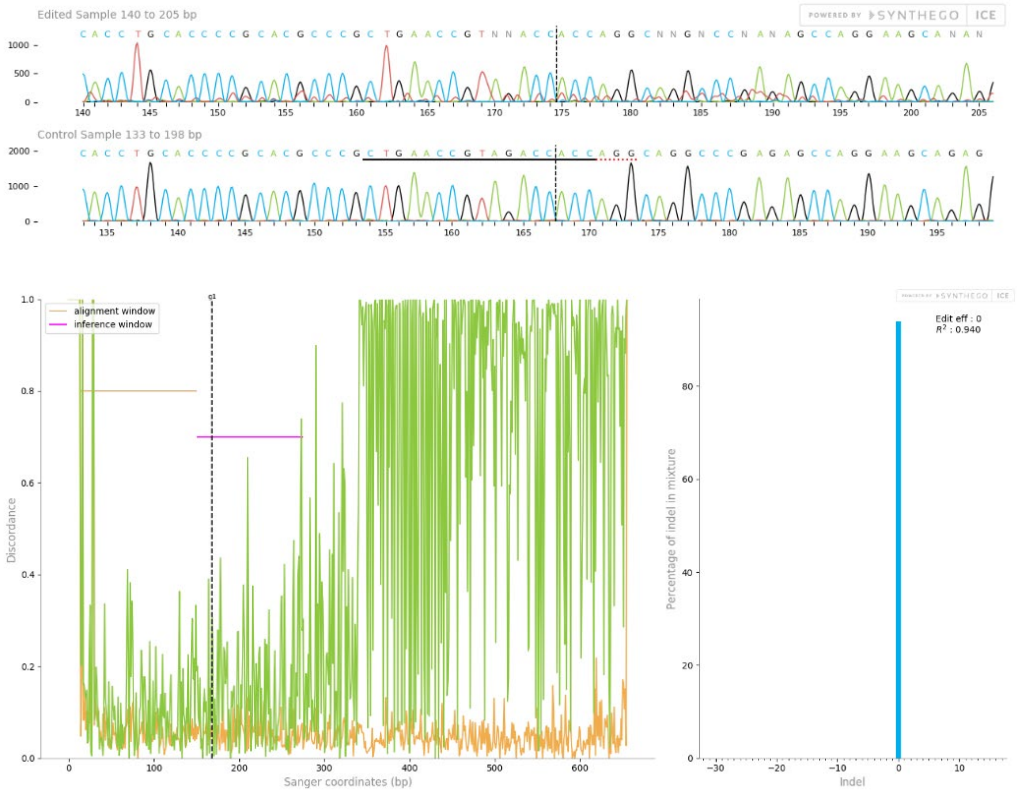

A4

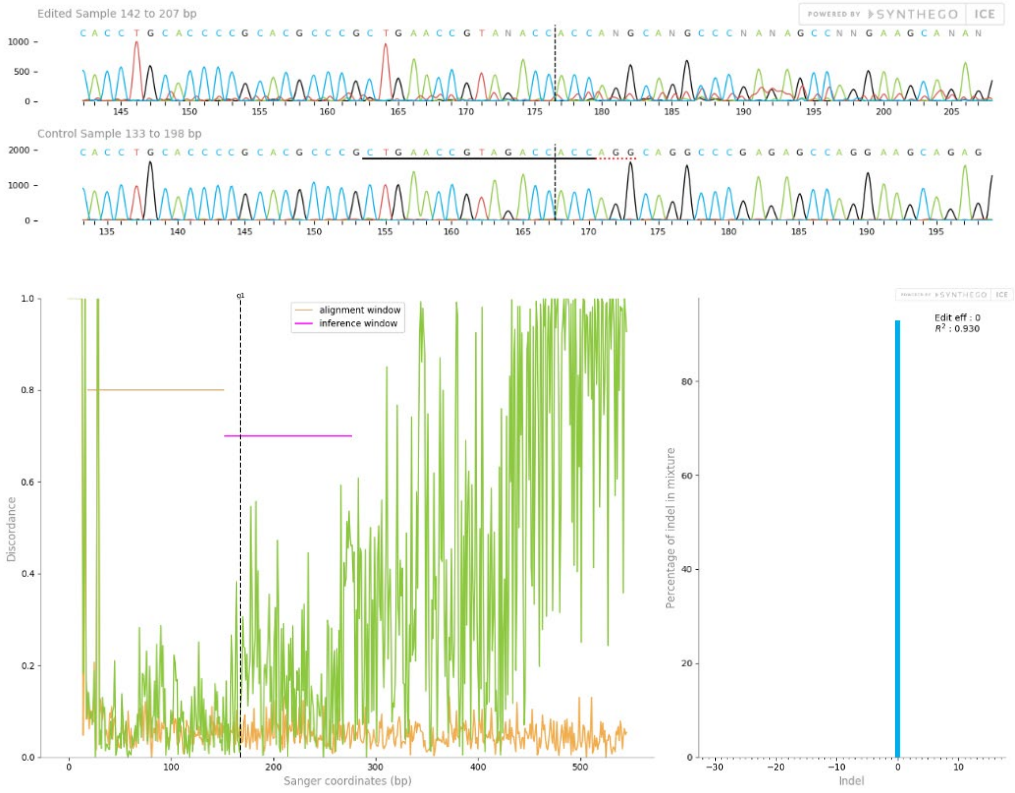
Edited Sample 142 to 207 bp
Control Sample 133 to 198 bp
alignment window
inference window
Discordance
Sanger coordinates (bp)
Percentage of indel in mixture
Indel
Edit eff : 0
R² : 0.930

A5

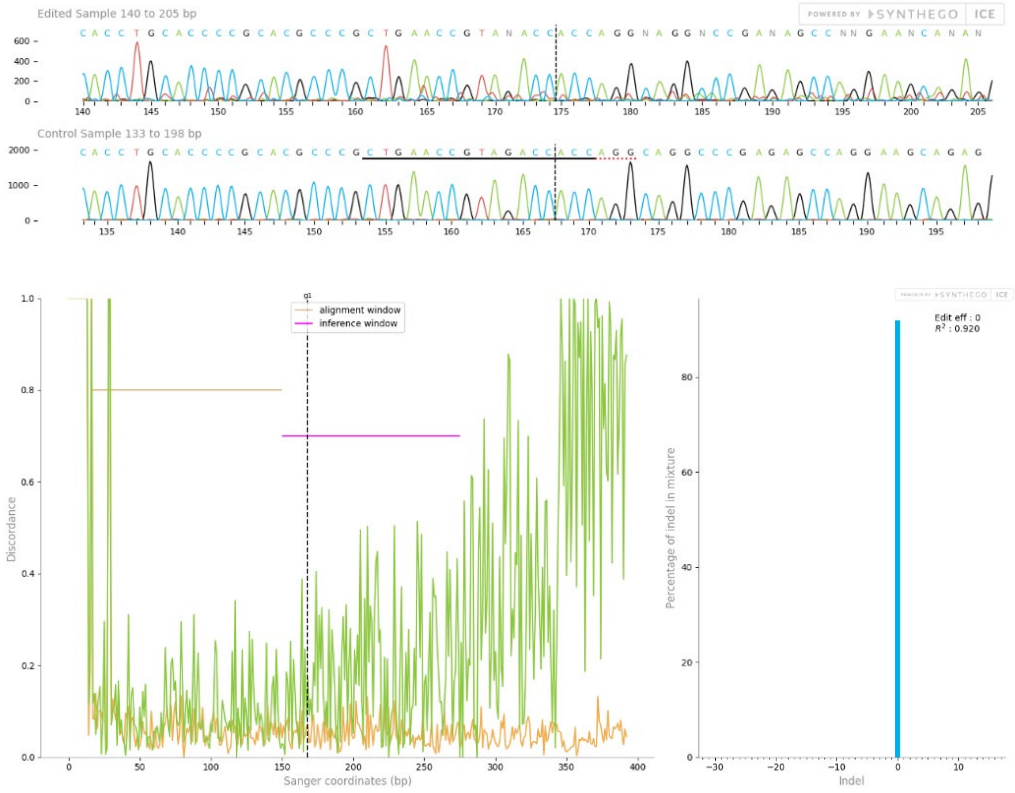
Edited Sample 140 to 205 bp
Control Sample 133 to 198 bp
alignment window
inference window
Discordance
Sanger coordinates (bp)
Percentage of indel in mixture
Indel
Edit eff : 0
R² : 0.920

A6

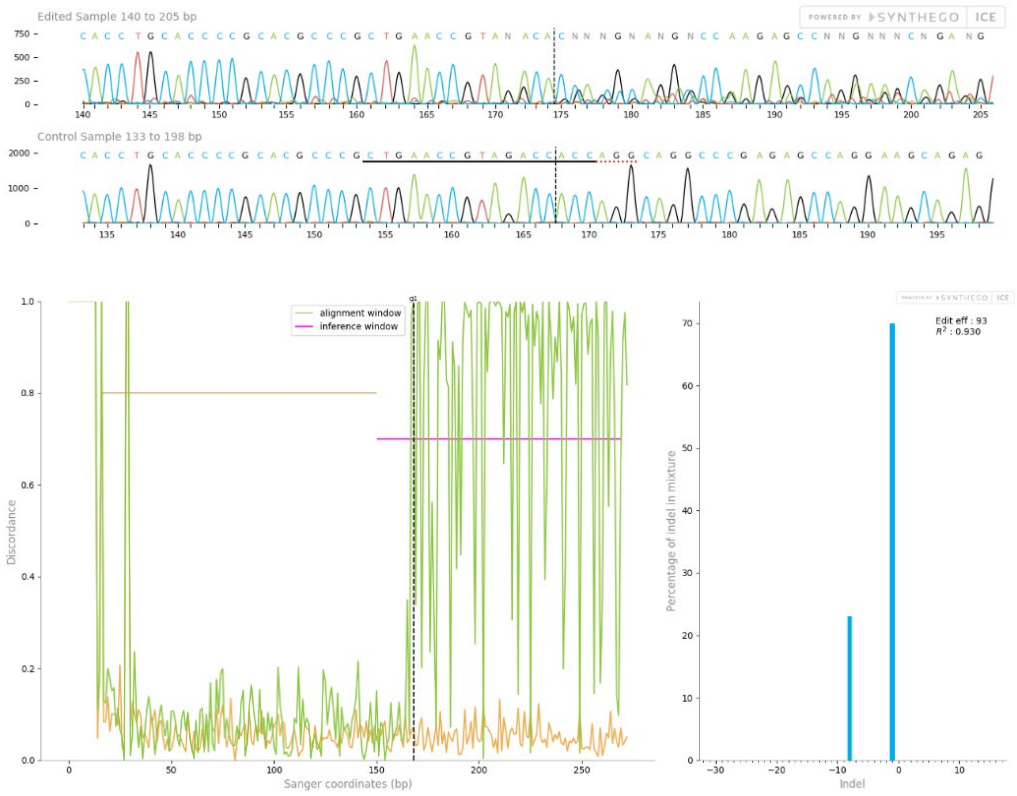
Edited Sample 140 to 205 bp
Control Sample 133 to 198 bp
alignment window
inference window
Discordance
Sanger coordinates (bp)
Edit eff : 93
R^2 : 0.930
Percentage of indel in mixture
Indel

A7

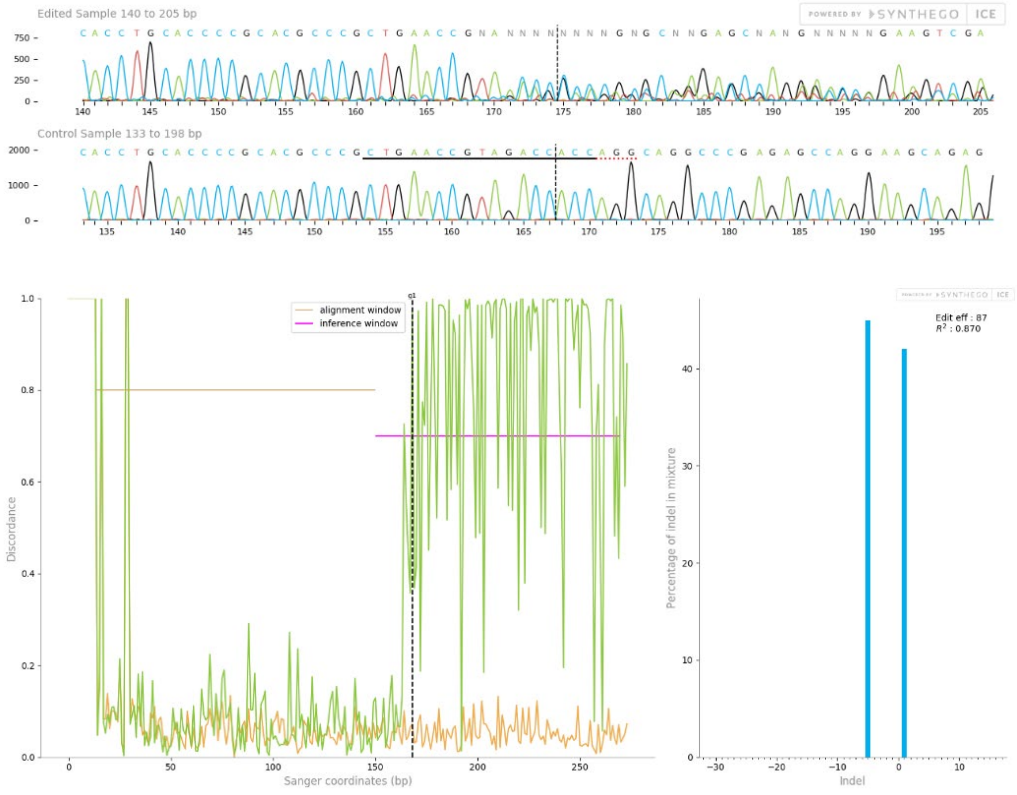
Edited Sample 140 to 205 bp
Control Sample 133 to 198 bp
alignment window
inference window
Discordance
Sanger coordinates (bp)
Edit eff : 87
R^2 : 0.870
Percentage of indel in mixture
Indel

A8

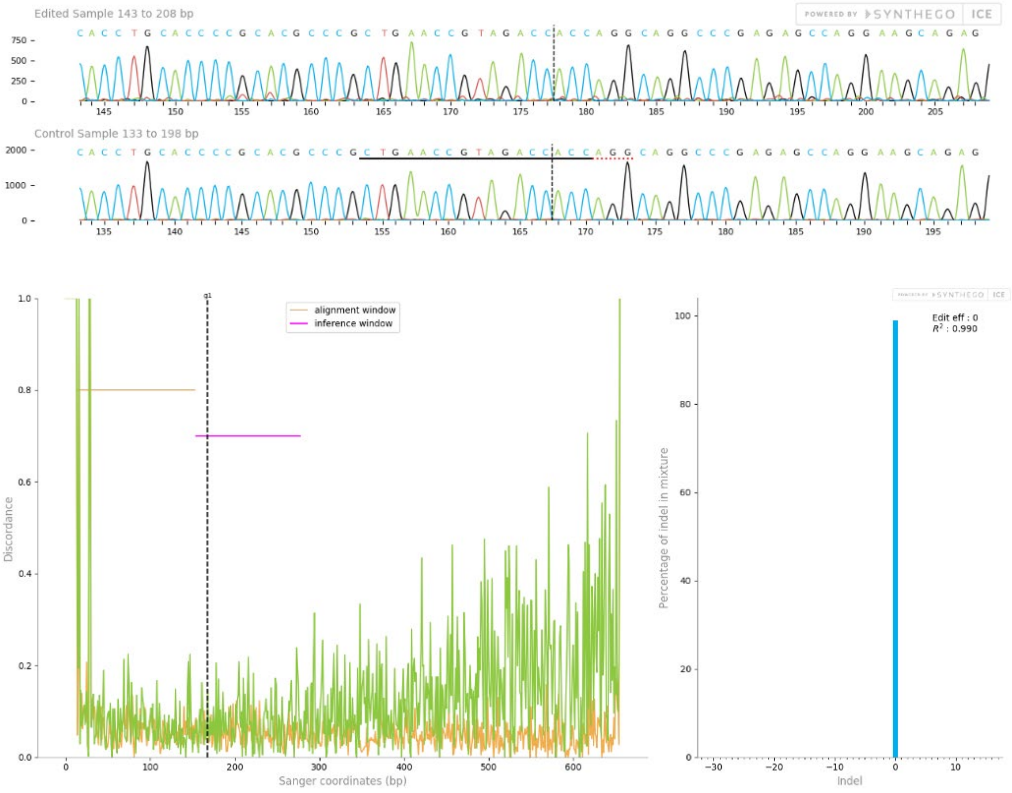
Edited Sample 143 to 208 bp
Control Sample 133 to 198 bp
alignment window
inference window
Discordance
Sanger coordinates (bp)
Edit eff : 0
R^2 : 0.990
Percentage of indel in mixture
Indel

A11

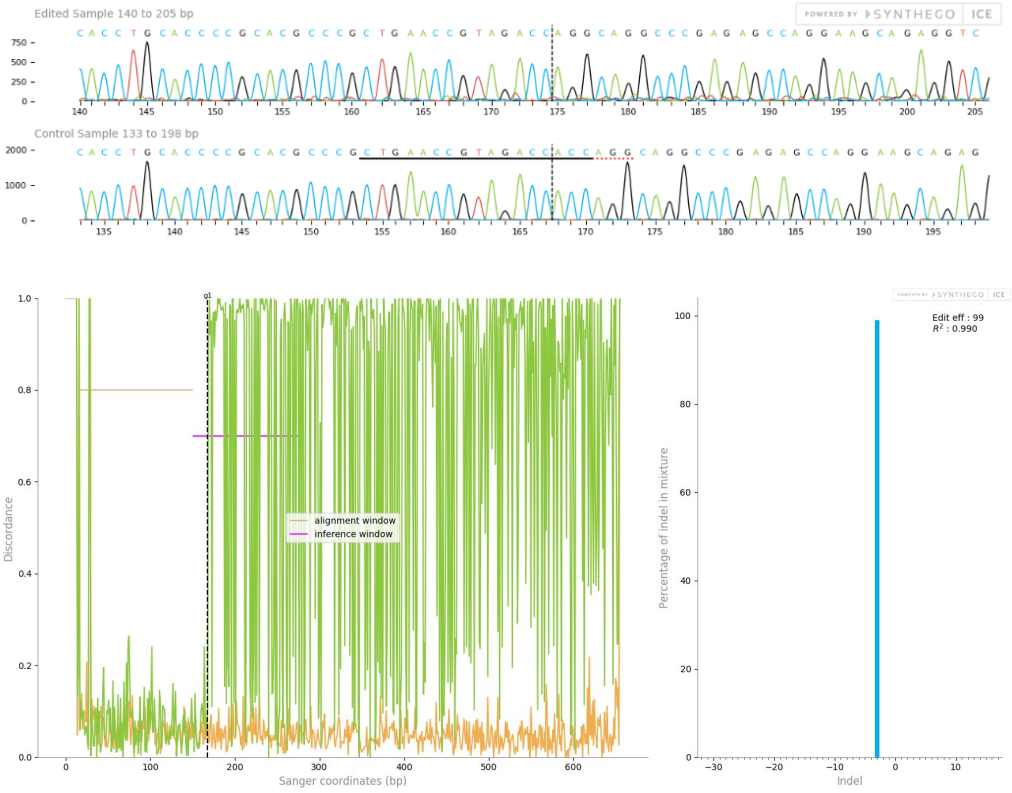
Edited Sample 140 to 205 bp
Control Sample 133 to 198 bp
alignment window
inference window
Discordance
Sanger coordinates (bp)
Edit eff : 99
R^2 : 0.990
Percentage of indel in mixture
Indel

A12

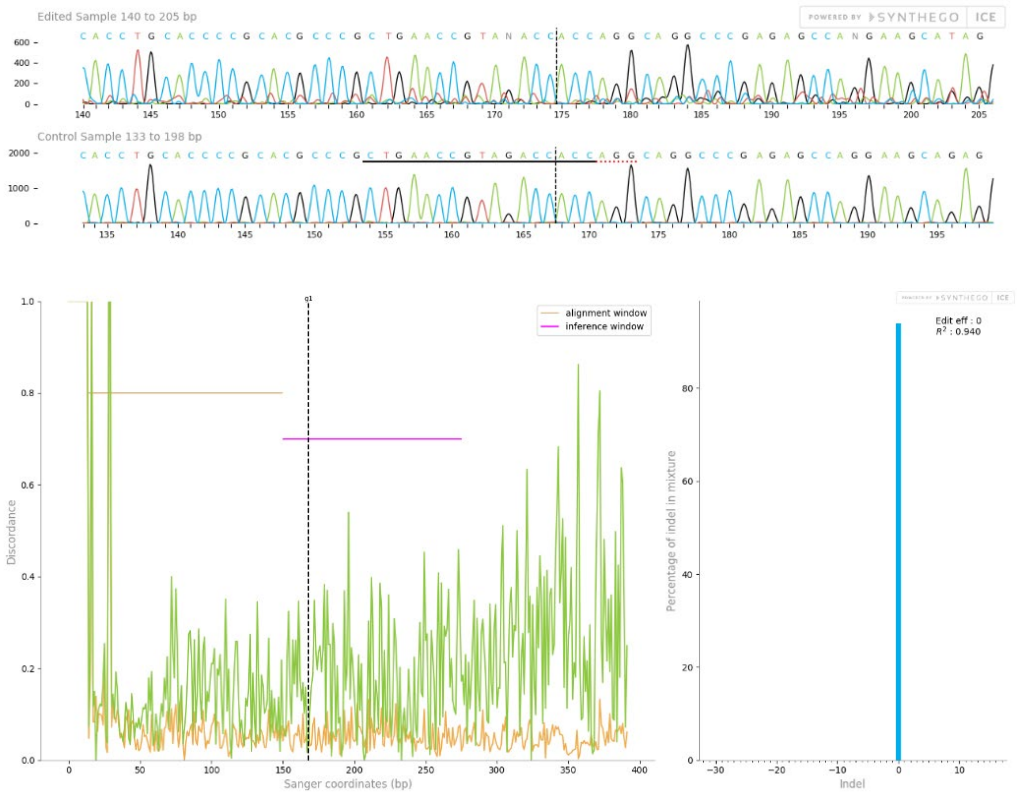
Edited Sample 140 to 205 bp
Control Sample 133 to 198 bp
alignment window
inference window
Edit eff : 0
R^2 : 0.940
Discordance
Sanger coordinates (bp)
Percentage of indel in mixture
Indel

B1

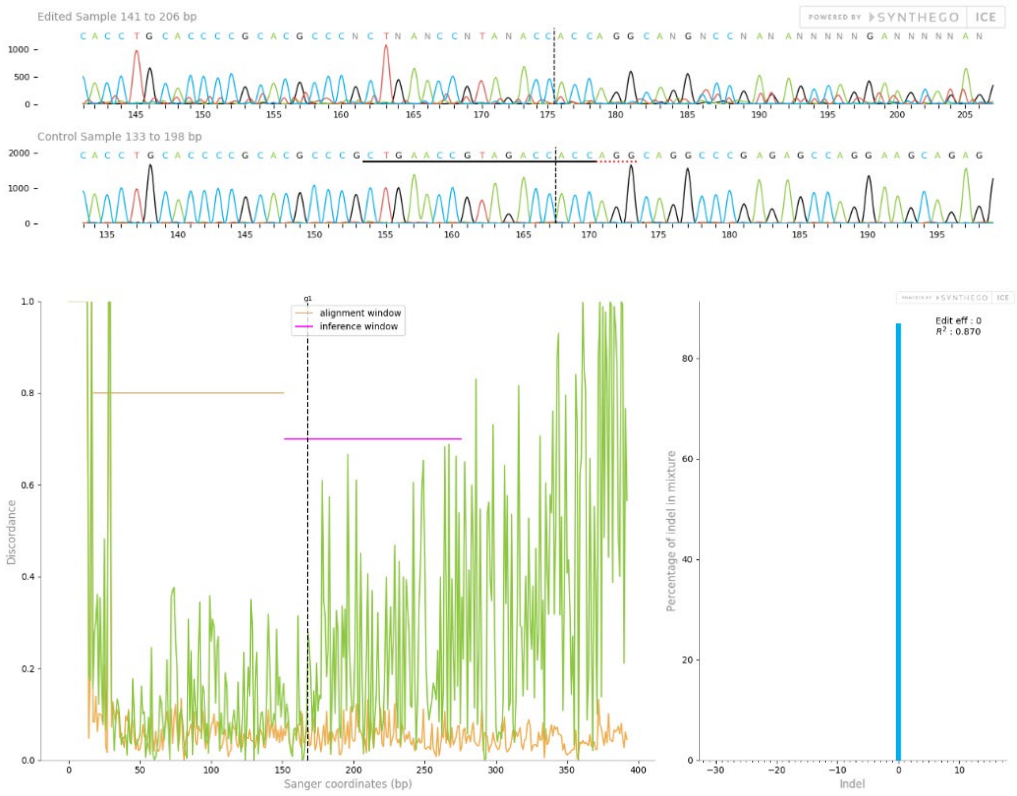
Edited Sample 141 to 206 bp
Control Sample 133 to 198 bp
alignment window
inference window
Edit eff : 0
R^2 : 0.870
Discordance
Sanger coordinates (bp)
Percentage of indel in mixture
Indel

B2

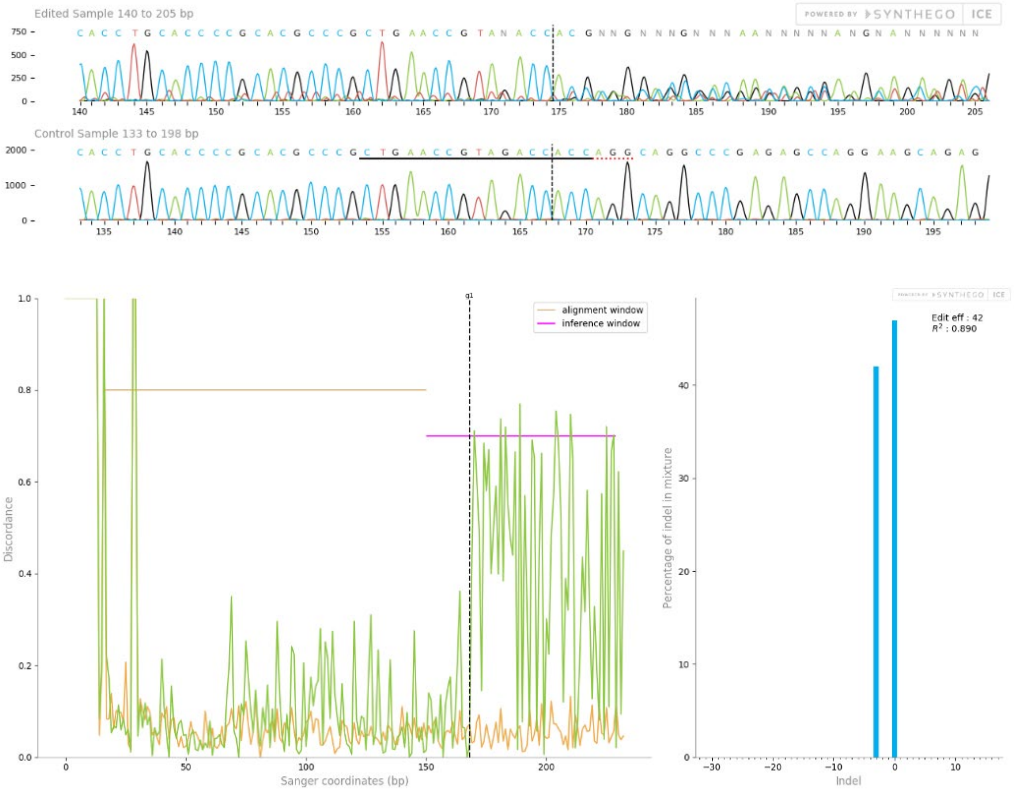
Edited Sample 140 to 205 bp
Control Sample 133 to 198 bp
alignment window
inference window
Discordance
Sanger coordinates (bp)
Edit eff : 42
R^2 : 0.890
Percentage of indel in mixture
Indel

B3

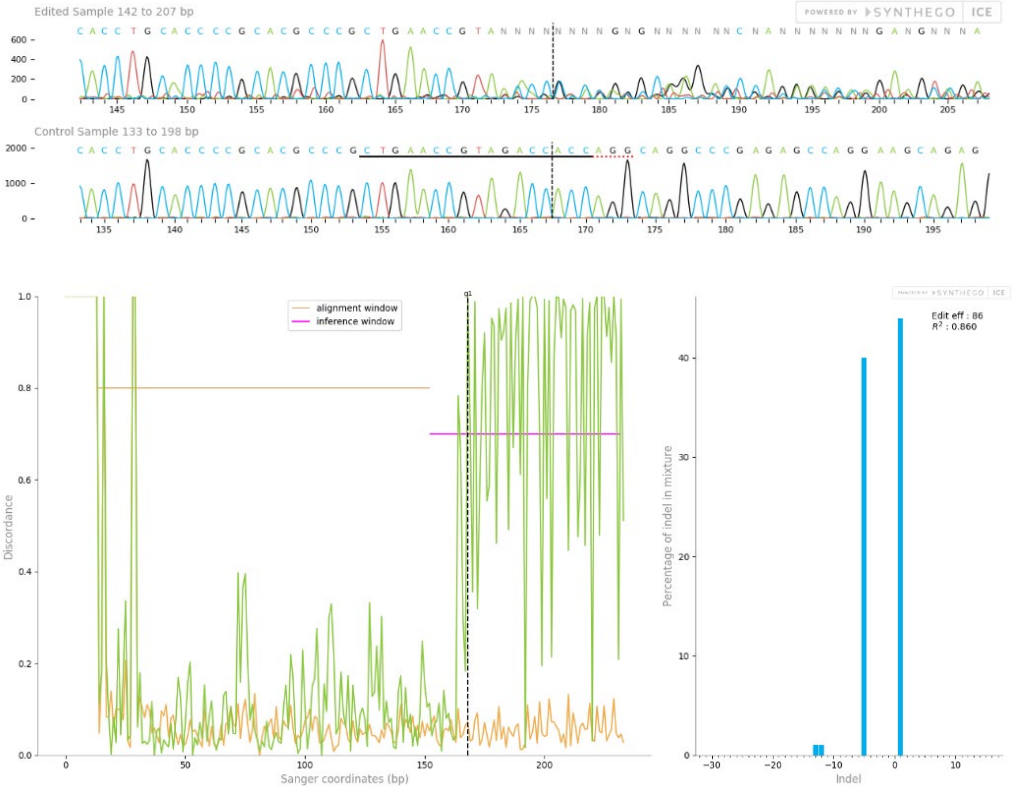
Edited Sample 142 to 207 bp
Control Sample 133 to 198 bp
alignment window
inference window
Discordance
Sanger coordinates (bp)
Edit eff : 86
R^2 : 0.860
Percentage of indel in mixture
Indel

B4

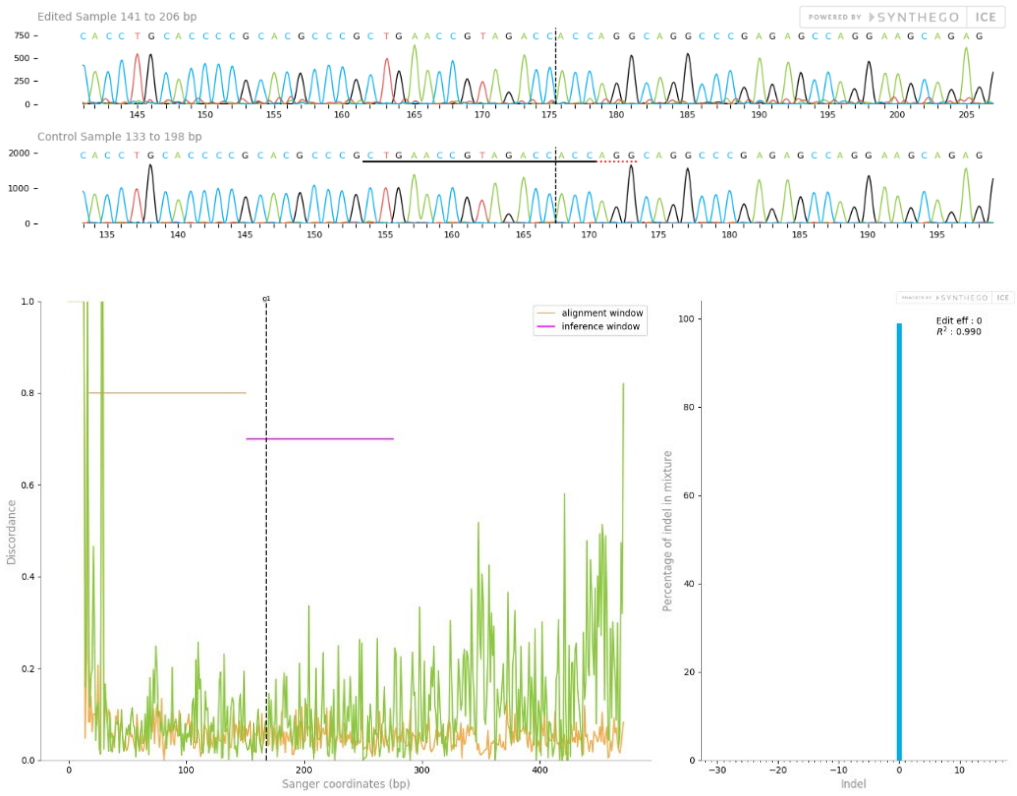
Edited Sample 141 to 206 bp
Control Sample 133 to 198 bp
alignment window
inference window
Discordance
Sanger coordinates (bp)
Edit eff : 0
R^2 : 0.990
Percentage of indel in mixture
Indel

B5

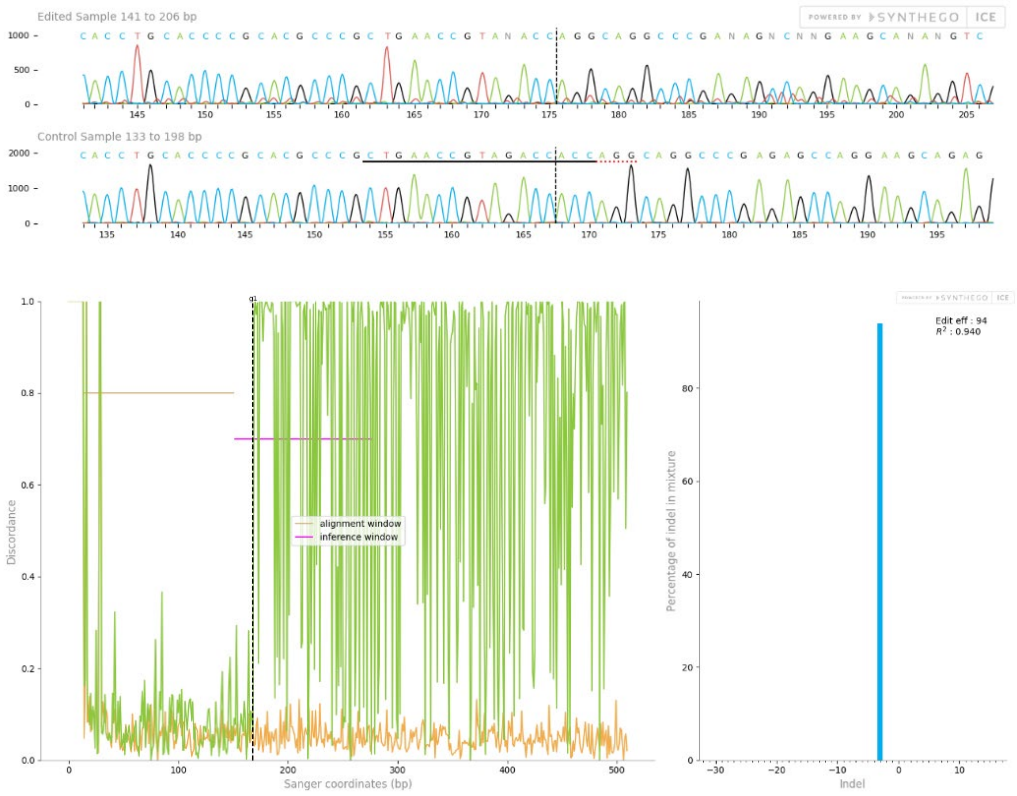
Edited Sample 141 to 206 bp
Control Sample 133 to 198 bp
alignment window
inference window
Discordance
Sanger coordinates (bp)
Edit eff : 94
R^2 : 0.940
Percentage of indel in mixture
Indel

B6

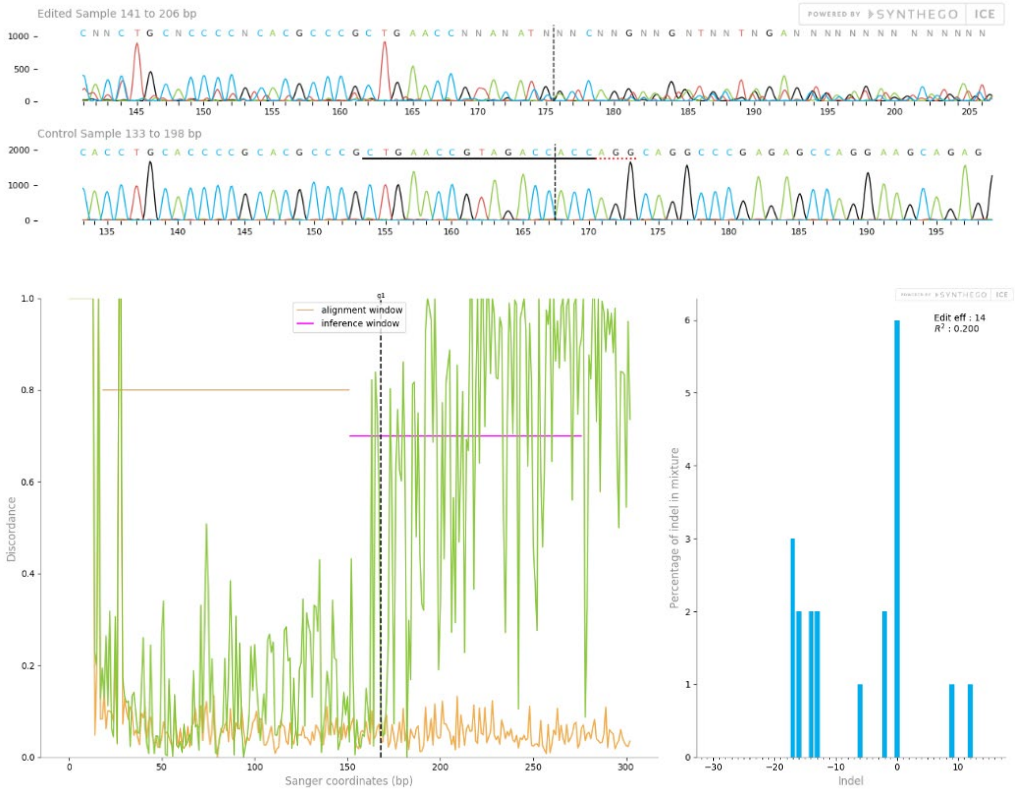
Edited Sample 141 to 206 bp
Control Sample 133 to 198 bp
alignment window
inference window
Discordance
Sanger coordinates (bp)
Edit eff : 14
R^2 : 0.200
Percentage of indel in mixture
Indel

B7

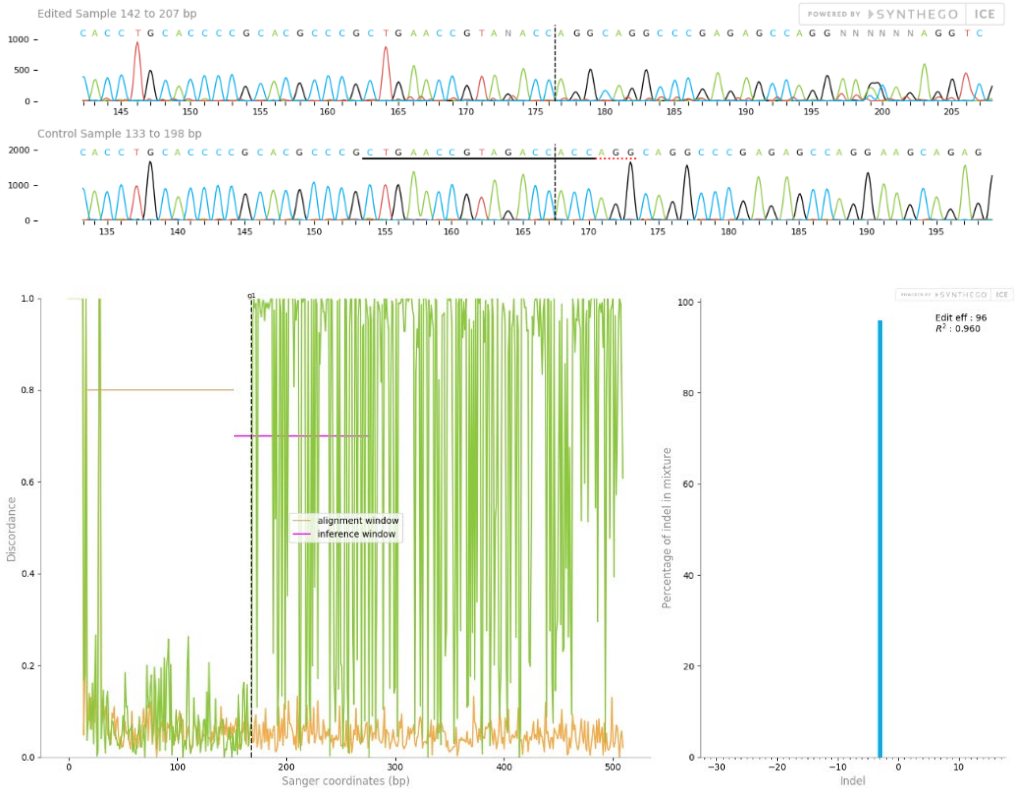
Edited Sample 142 to 207 bp
Control Sample 133 to 198 bp
alignment window
inference window
Discordance
Sanger coordinates (bp)
Edit eff : 96
R^2 : 0.960
Percentage of indel in mixture
Indel

B9

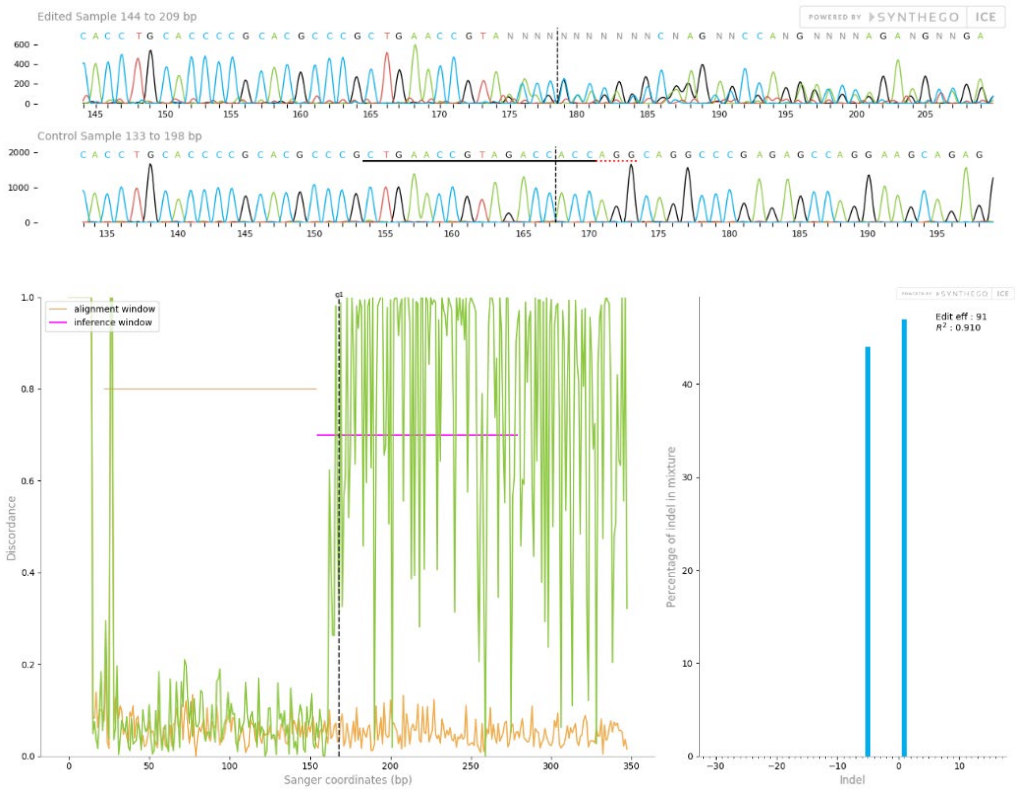
Edited Sample 144 to 209 bp
Control Sample 133 to 198 bp
alignment window
inference window
Discordance
Sanger coordinates (bp)
Edit eff : 91
R^2 : 0.910
Percentage of indel in mixture
Indel

B10

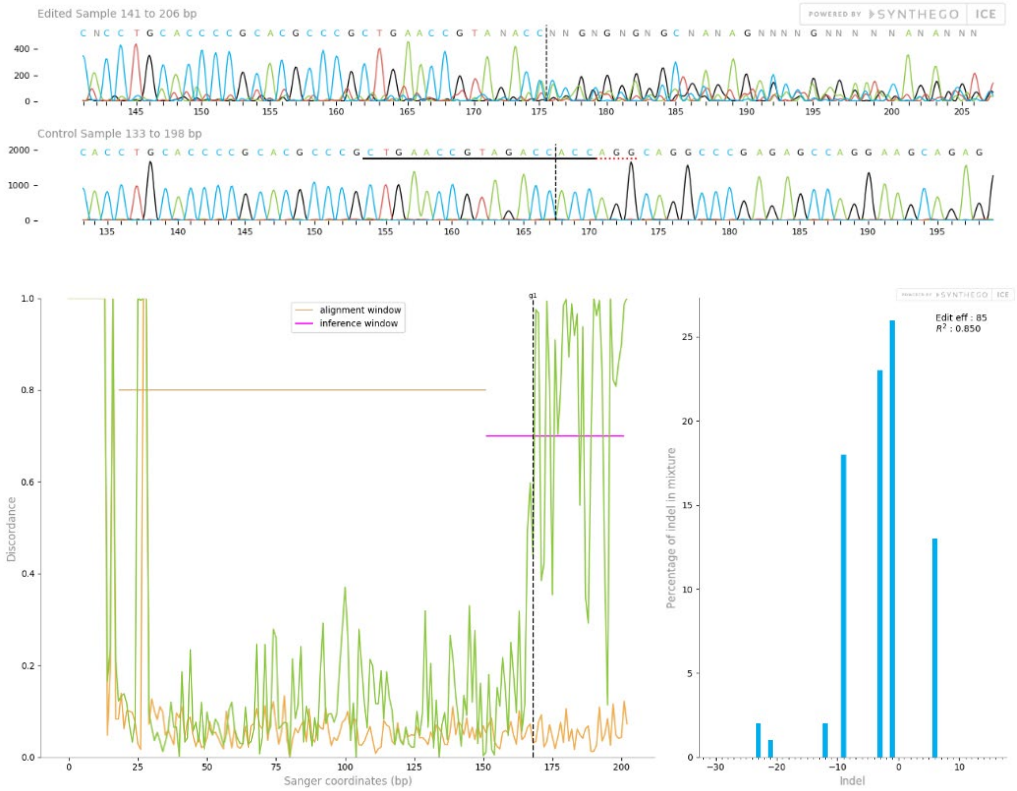
Edited Sample 141 to 206 bp
Control Sample 133 to 198 bp
alignment window
inference window
Discordance
Sanger coordinates (bp)
Edit eff : 85
R^2 : 0.850
Percentage of indel in mixture
Indel

B11

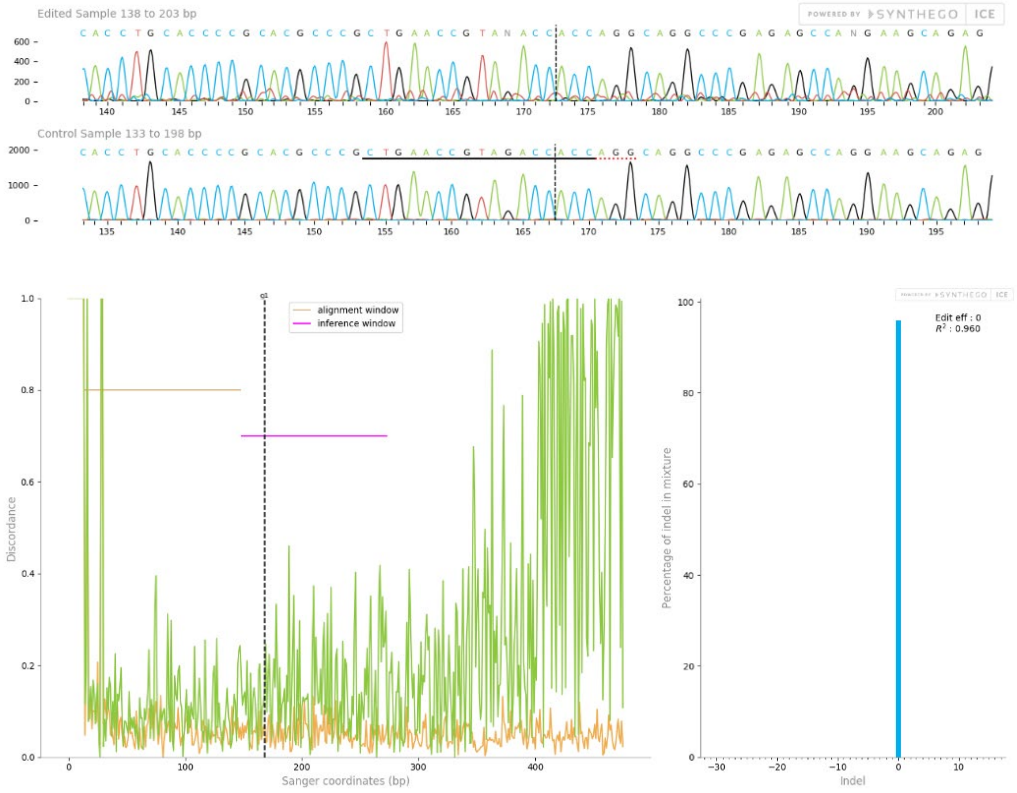
Edited Sample 138 to 203 bp
Control Sample 133 to 198 bp
alignment window
inference window
Discordance
Sanger coordinates (bp)
Edit eff : 0
R^2 : 0.960
Percentage of indel in mixture
Indel

C2

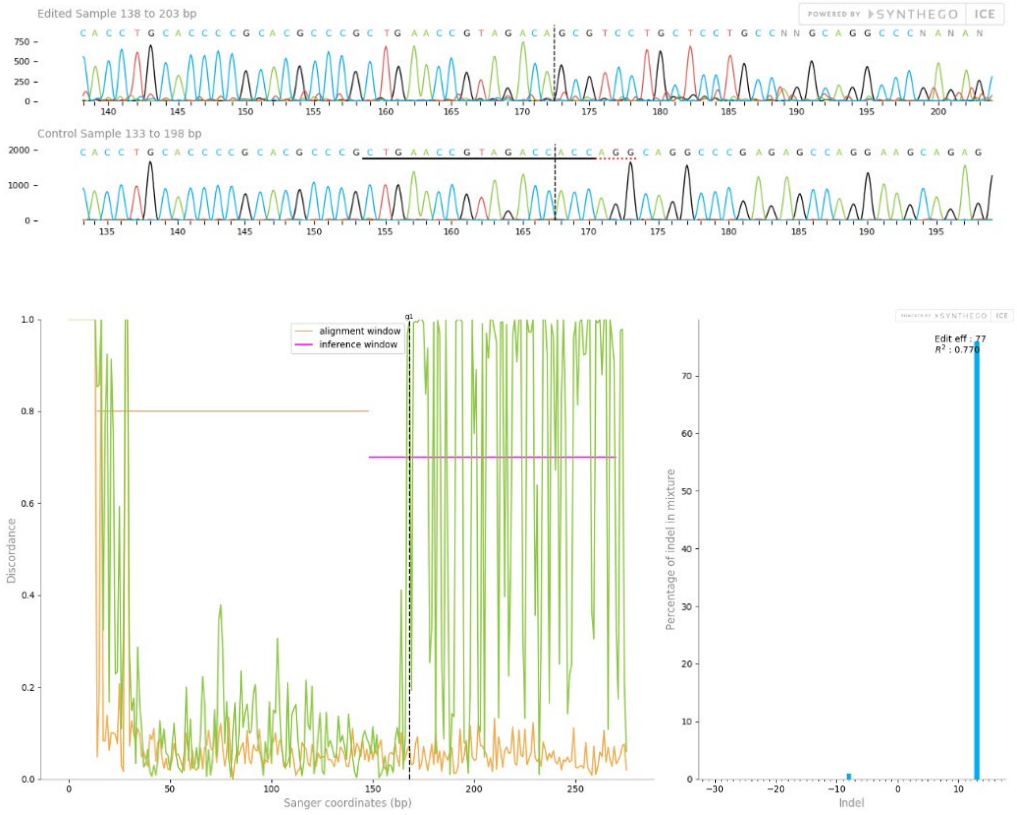
Edited Sample 138 to 203 bp
Control Sample 133 to 198 bp
alignment window
inference window
Discordance
Sanger coordinates (bp)
Edit eff : 77
R^2 : 0.778
Percentage of indel in mixture
Indel

C3

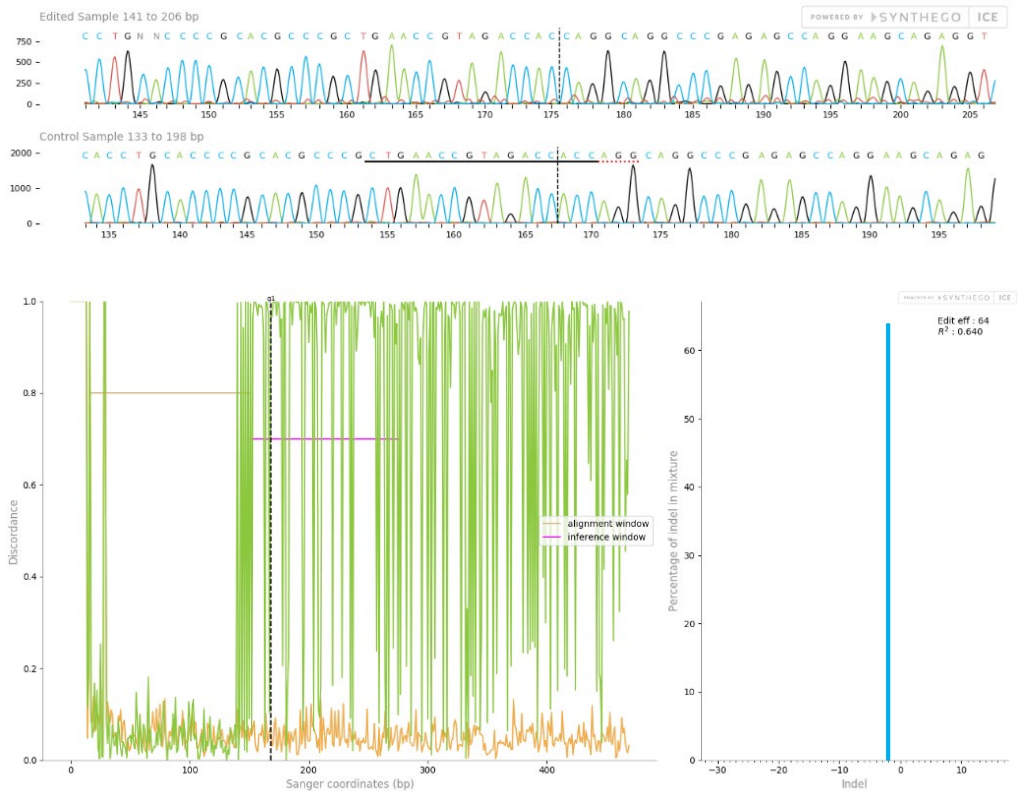
Edited Sample 141 to 206 bp
Control Sample 133 to 198 bp
POWERED BY SYNTHEGO ICE
alignment window
inference window
Discordance
Sanger coordinates (bp)
Percentage of indel in mixture
Indel
Edit eff : 64
R^2 : 0.640

C4

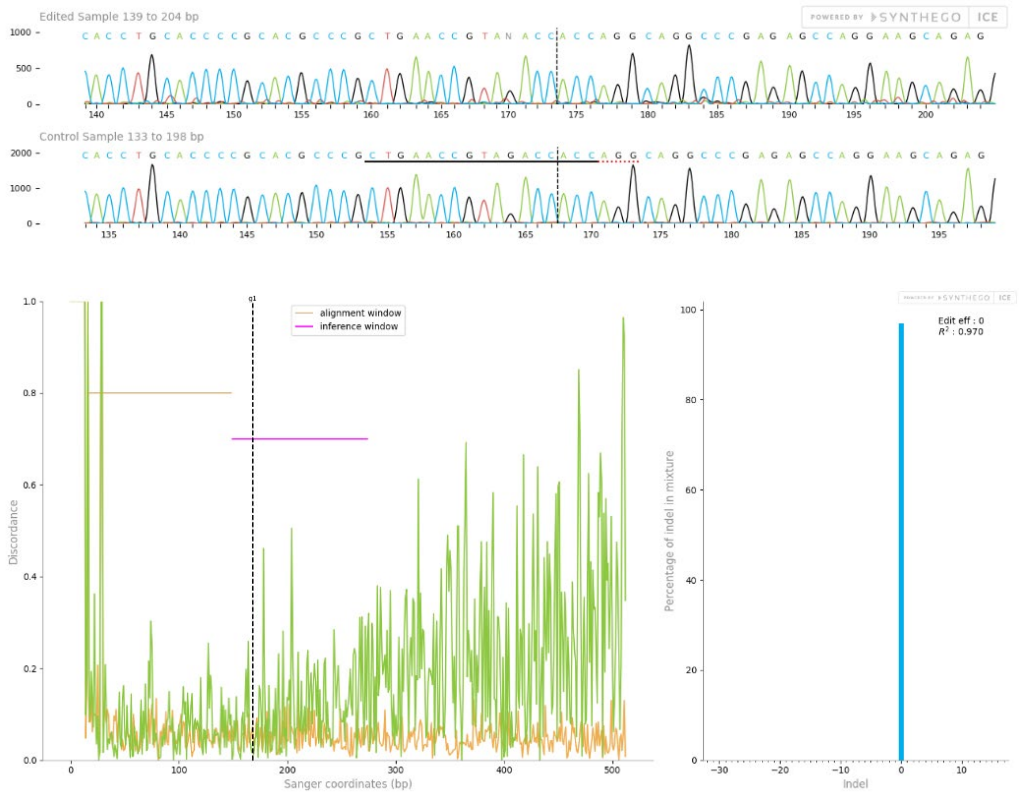
Edited Sample 139 to 204 bp
Control Sample 133 to 198 bp
POWERED BY SYNTHEGO ICE
alignment window
inference window
Discordance
Sanger coordinates (bp)
Percentage of indel in mixture
Indel
Edit eff : 0
R^2 : 0.970

C5

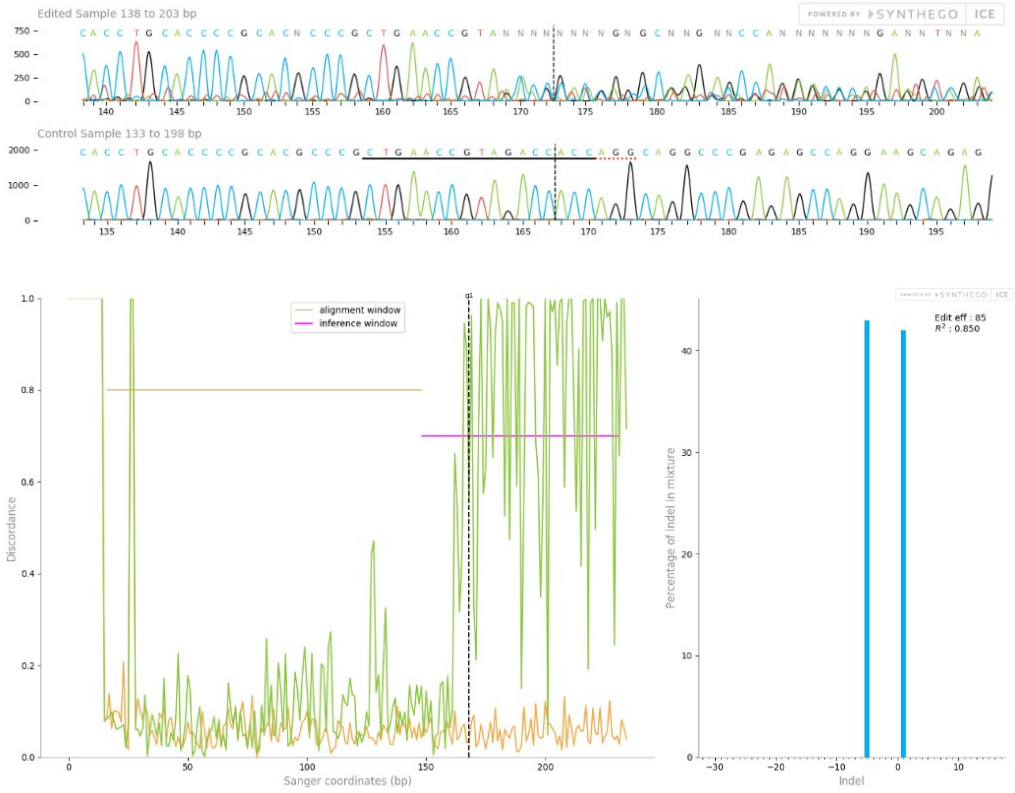
Edited Sample 138 to 203 bp
Control Sample 133 to 198 bp
alignment window
inference window
Discordance
Sanger coordinates (bp)
Edit eff : 85
R^2 : 0.850
Percentage of indel in mixture
Indel

C7

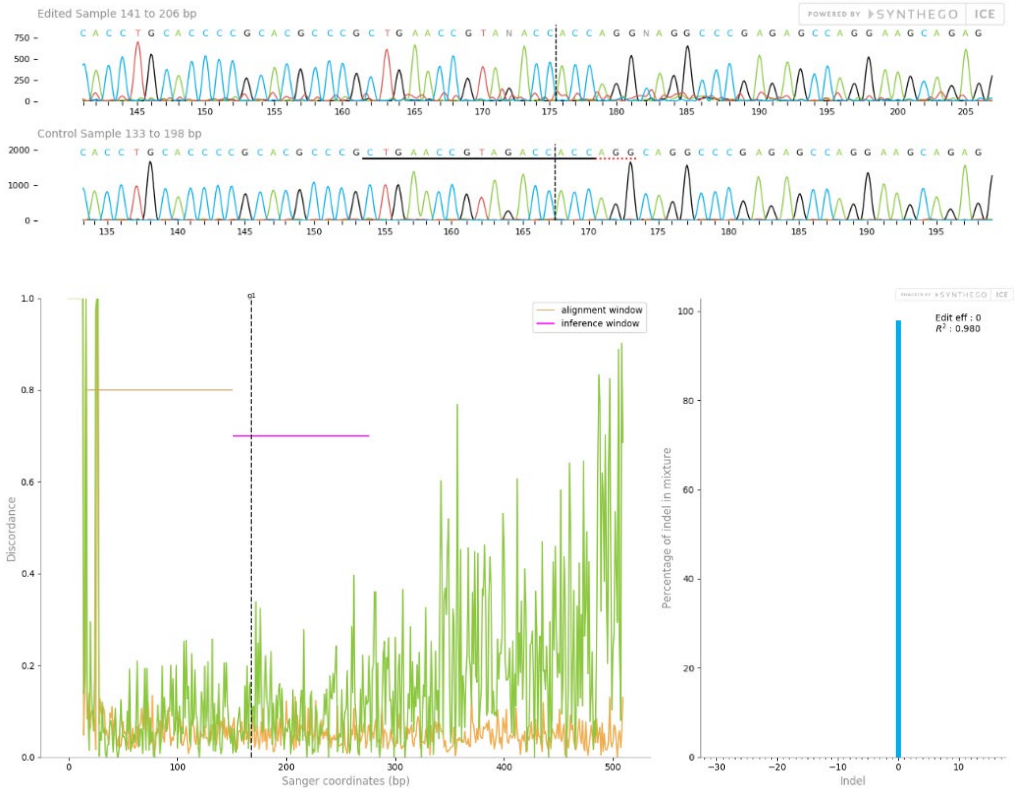
Edited Sample 141 to 206 bp
Control Sample 133 to 198 bp
alignment window
inference window
Discordance
Sanger coordinates (bp)
Edit eff : 0
R^2 : 0.980
Percentage of indel in mixture
Indel

C8

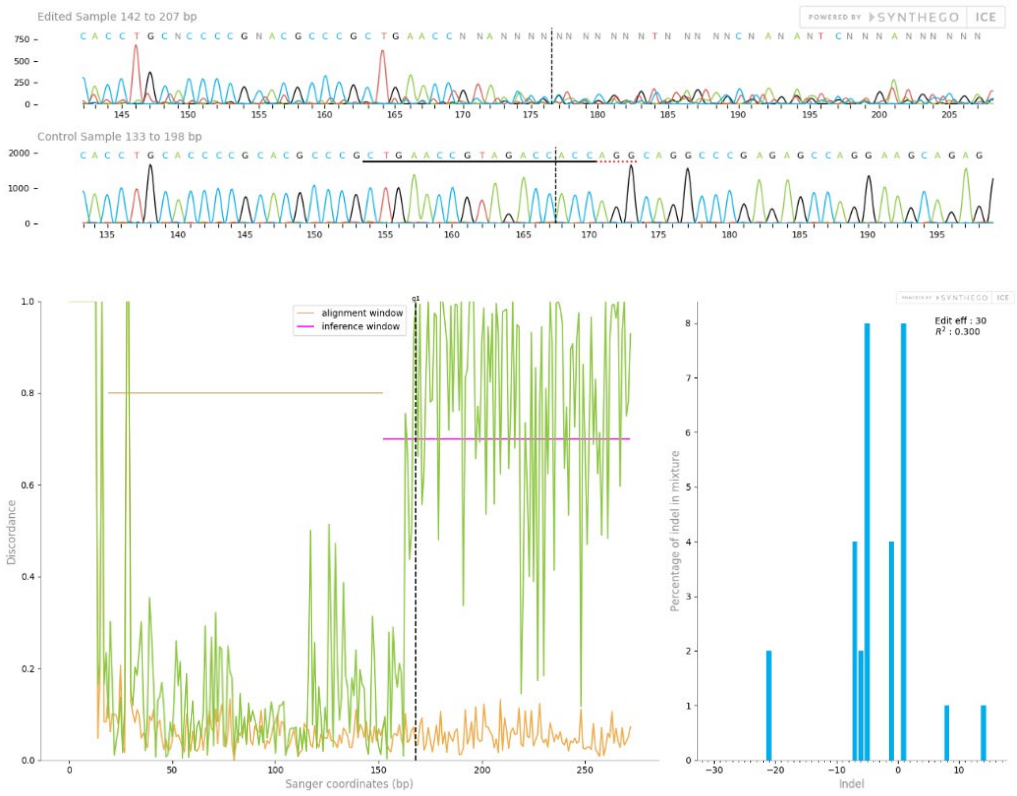
Edited Sample 142 to 207 bp
Control Sample 133 to 198 bp
alignment window
inference window
Discordance
Sanger coordinates (bp)
Edit eff : 30
R^2 : 0.300
Percentage of indel in mixture
Indel

C9

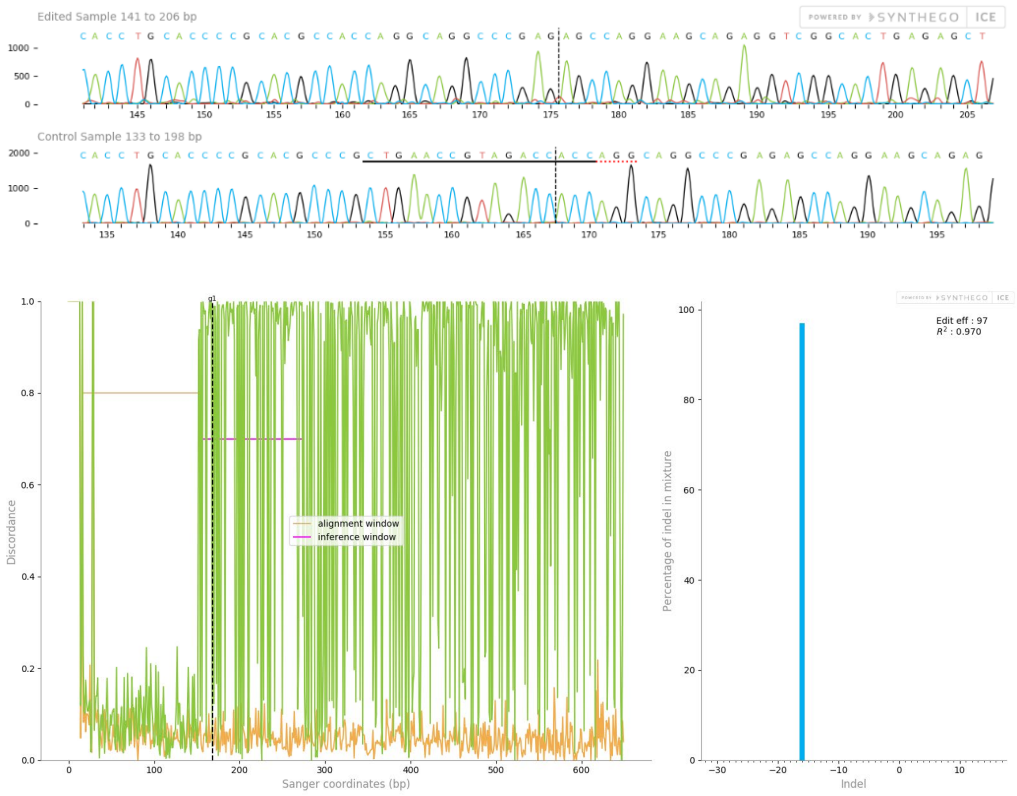
Edited Sample 141 to 206 bp
Control Sample 133 to 198 bp
alignment window
inference window
Discordance
Sanger coordinates (bp)
Edit eff : 97
R^2 : 0.970
Percentage of indel in mixture
Indel

C10

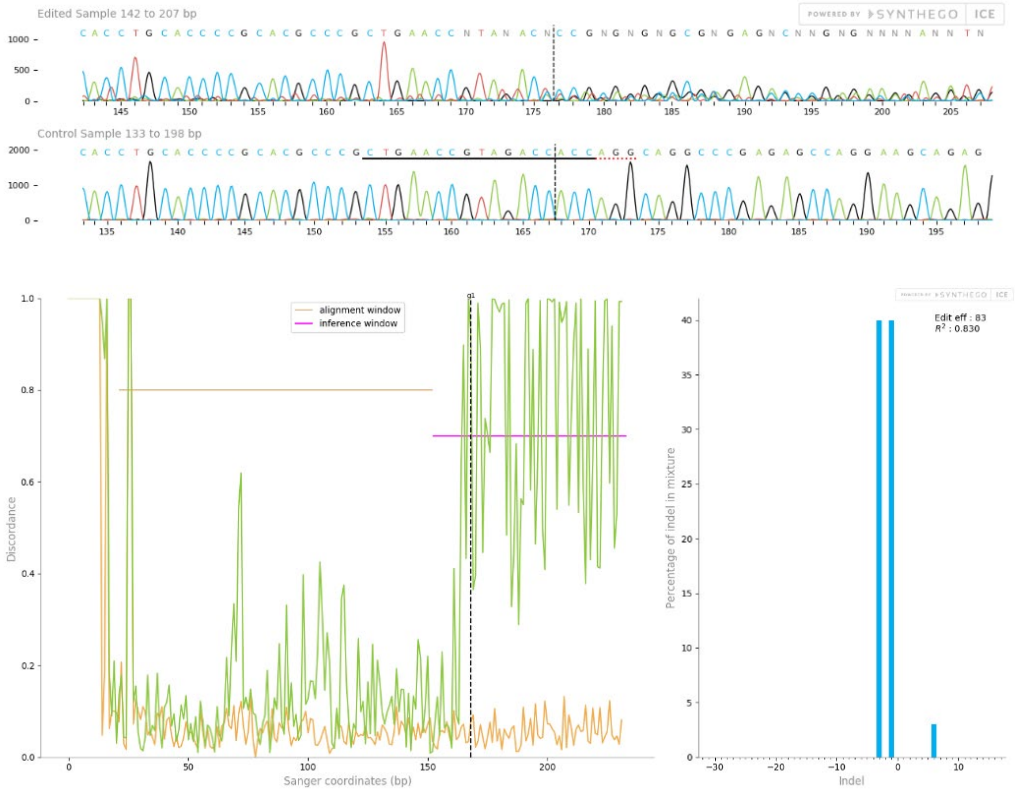
Edited Sample 142 to 207 bp
Control Sample 133 to 198 bp
alignment window
inference window
Discordance
Sanger coordinates (bp)
Edit eff : 83
R^2 : 0.830
Percentage of indel in mixture
Indel

C11

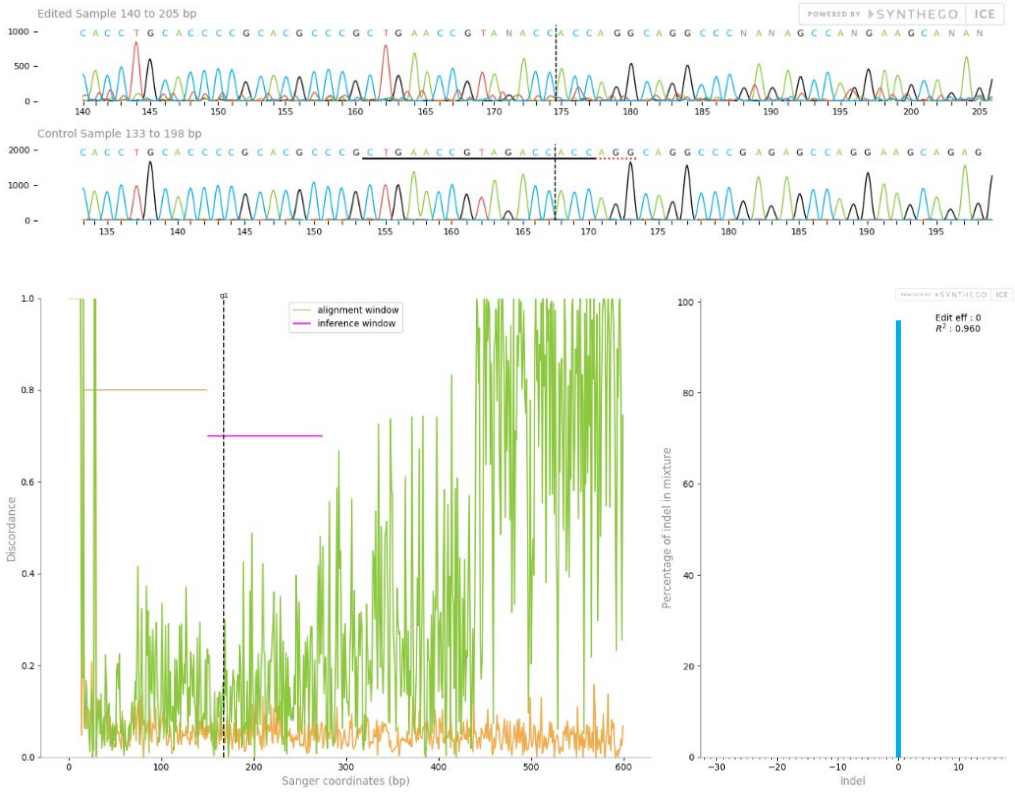
Edited Sample 140 to 205 bp
Control Sample 133 to 198 bp
alignment window
inference window
Discordance
Sanger coordinates (bp)
Edit eff : 0
R^2 : 0.960
Percentage of indel in mixture
Indel

D2

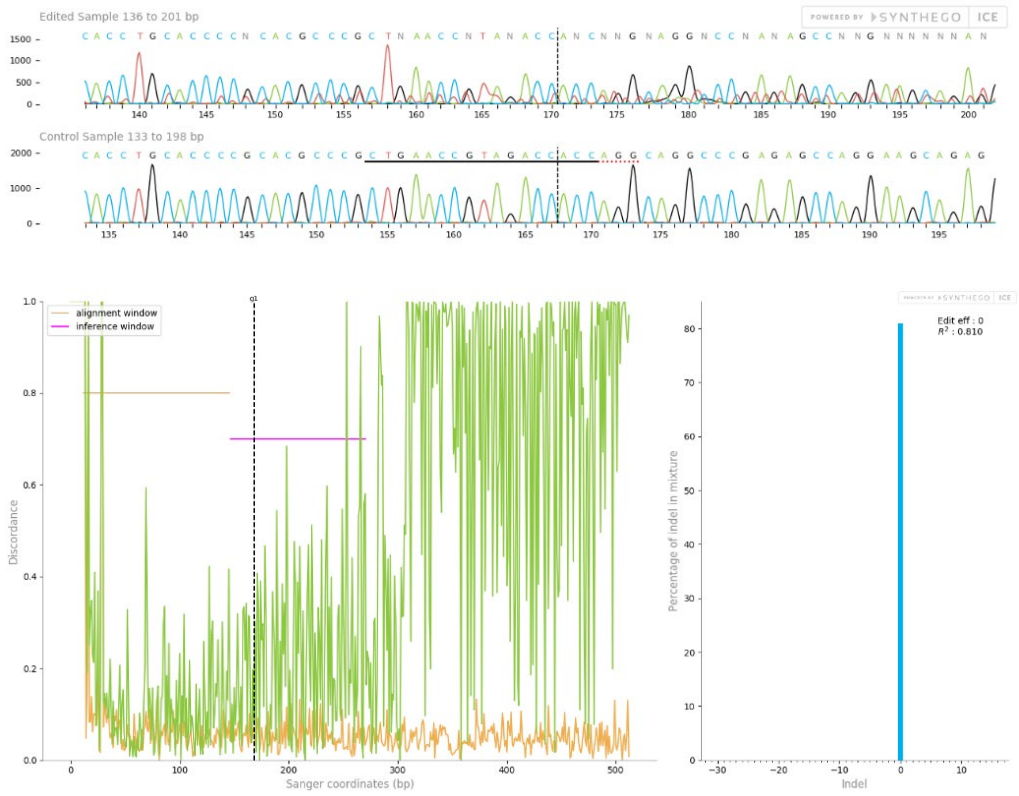
Edited Sample 136 to 201 bp
Control Sample 133 to 198 bp
alignment window
inference window
Discordance
Sanger coordinates (bp)
Edit eff : 0
R^2 : 0.810
Percentage of indel in mixture
Indel

D3

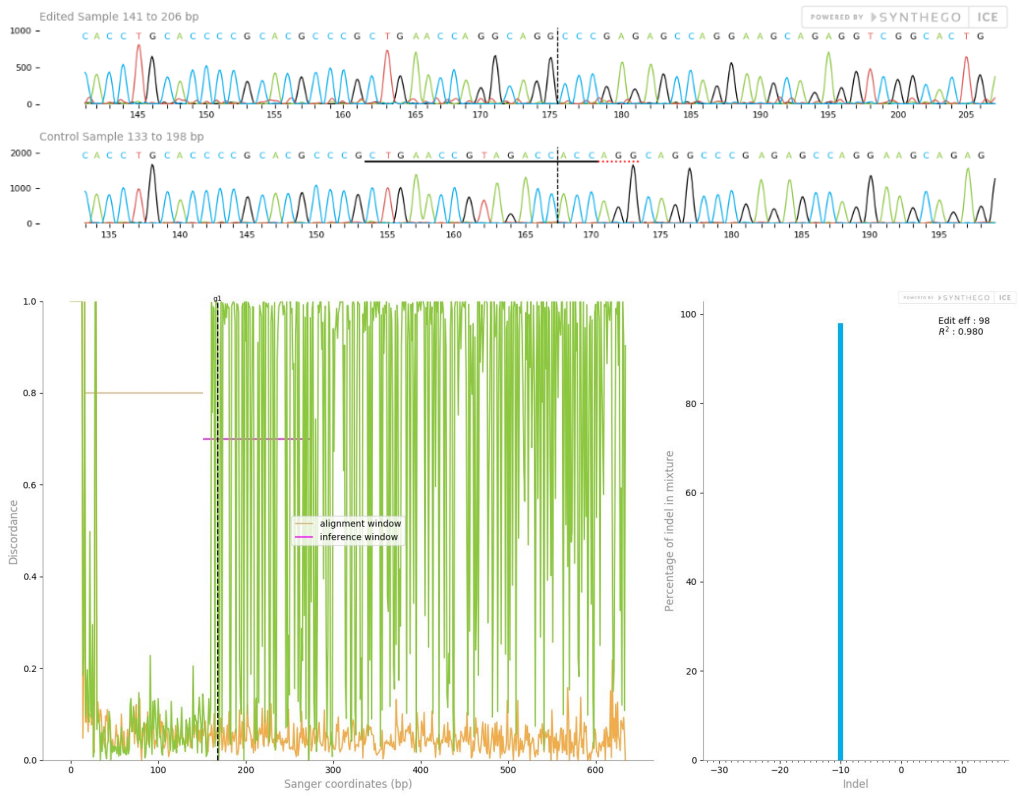
Edited Sample 141 to 206 bp
Control Sample 133 to 198 bp
alignment window
inference window
Discordance
Sanger coordinates (bp)
Edit eff : 98
R^2 : 0.980
Percentage of indel in mixture
Indel

D4

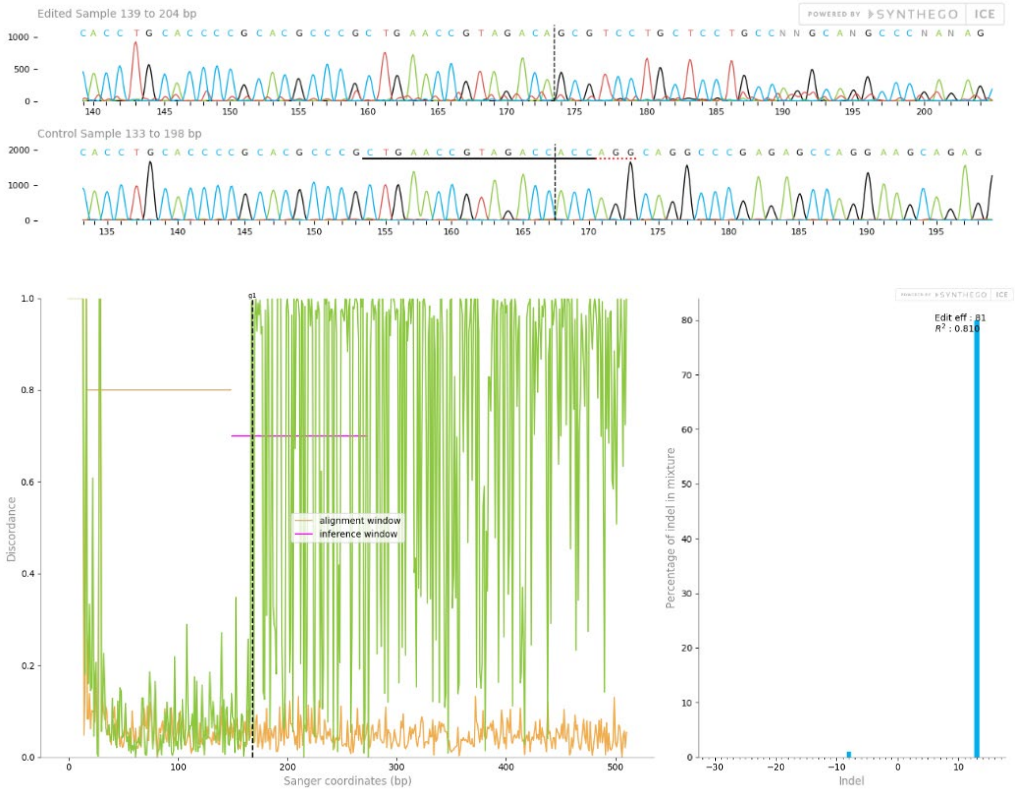
Edited Sample 139 to 204 bp
Control Sample 133 to 198 bp
alignment window
inference window
Discordance
Sanger coordinates (bp)
Edit eff : 81
R^2 : 0.810
Percentage of indel in mixture
Indel

D8

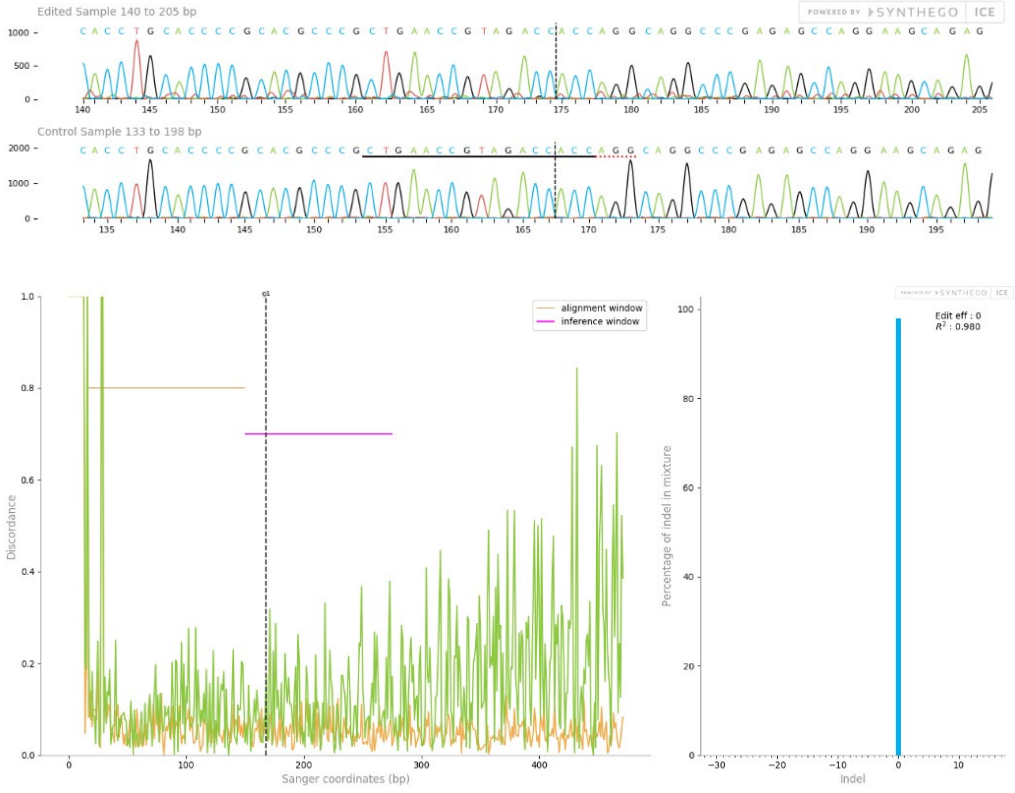
Edited Sample 140 to 205 bp
Control Sample 133 to 198 bp
alignment window
inference window
Discordance
Sanger coordinates (bp)
Edit eff : 0
R^2 : 0.980
Percentage of indel in mixture
Indel

D9

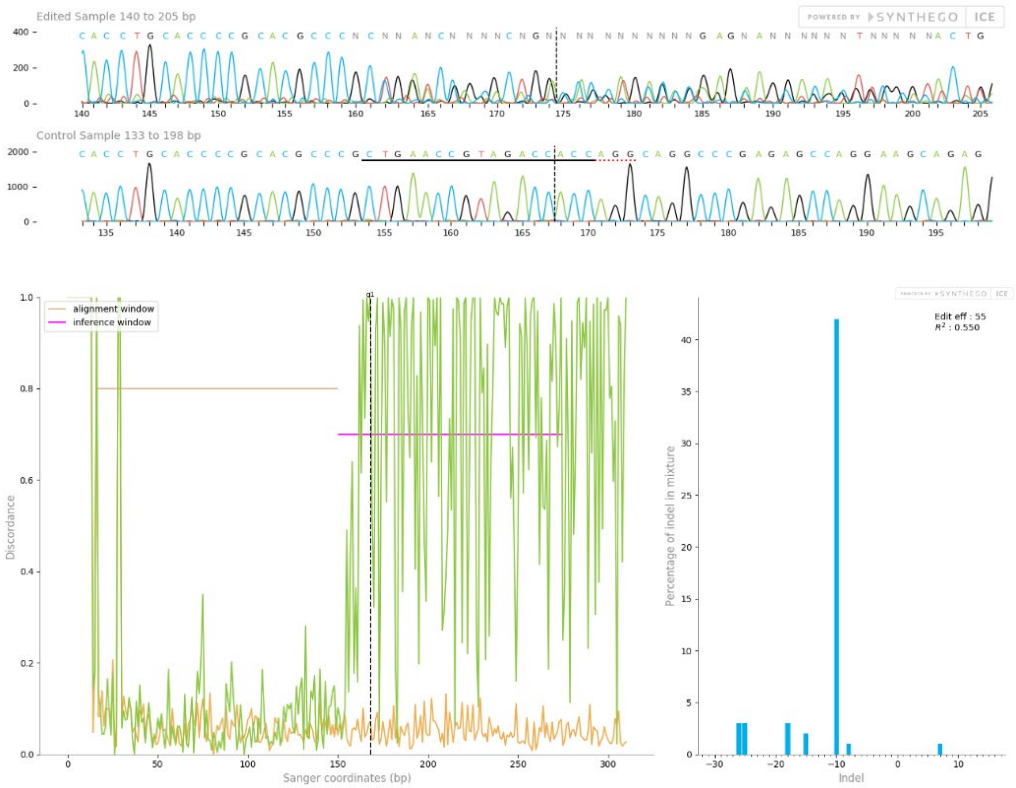
Edited Sample 140 to 205 bp
Control Sample 133 to 198 bp
alignment window
inference window
Discordance
Sanger coordinates (bp)
Edit eff : 55
R^2 : 0.550
Percentage of indel in mixture
Indel

D11

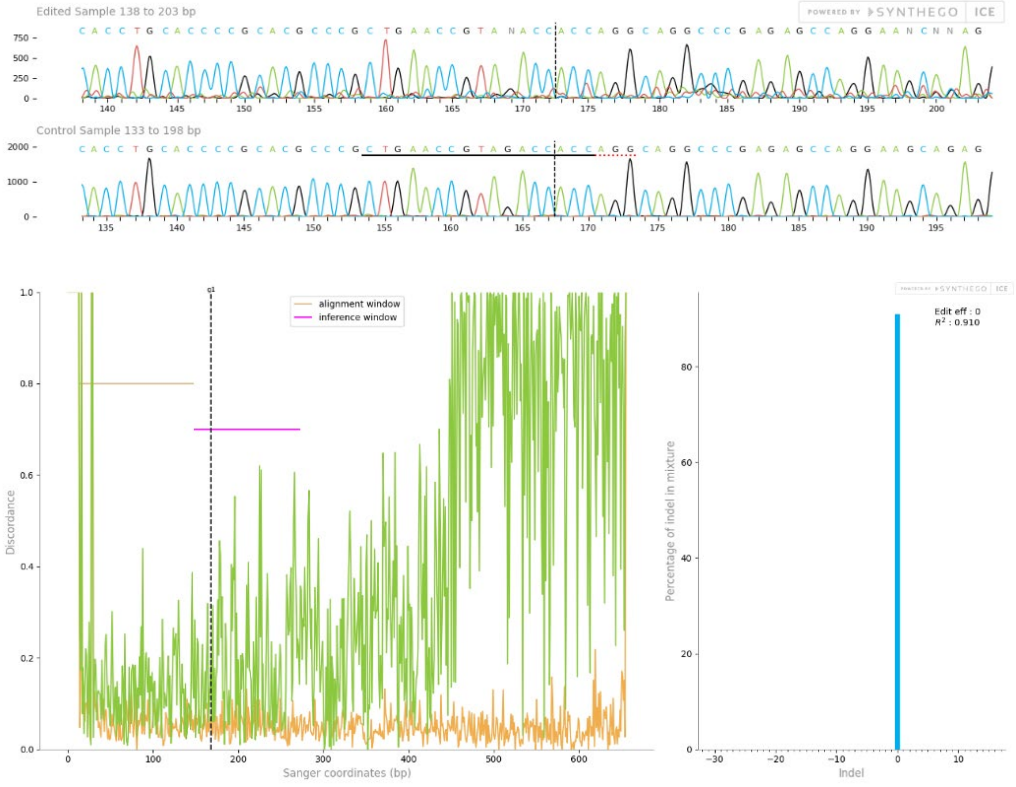
Edited Sample 138 to 203 bp
Control Sample 133 to 198 bp
alignment window
inference window
Discordance
Sanger coordinates (bp)
Edit eff : 0
R^2 : 0.910
Percentage of indel in mixture
Indel

E2

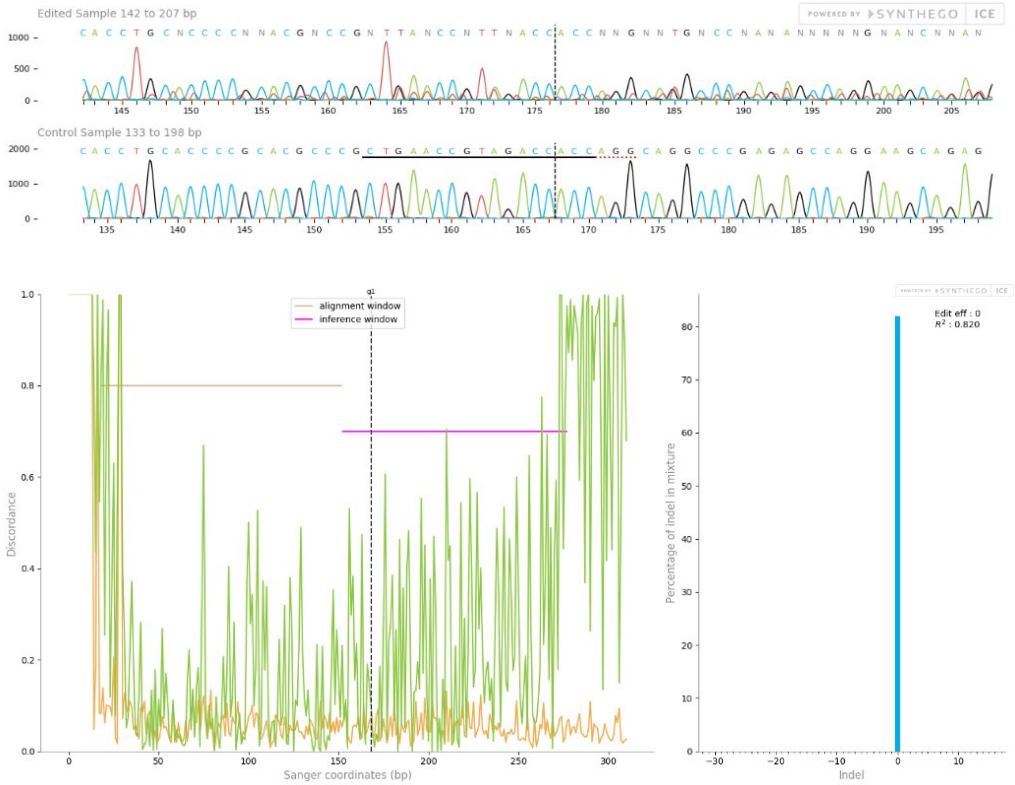
Edited Sample 142 to 207 bp
Control Sample 133 to 198 bp
alignment window
inference window
Discordance
Sanger coordinates (bp)
Edit eff : 0
R² : 0.820
Percentage of indel in mixture
Indel

E3

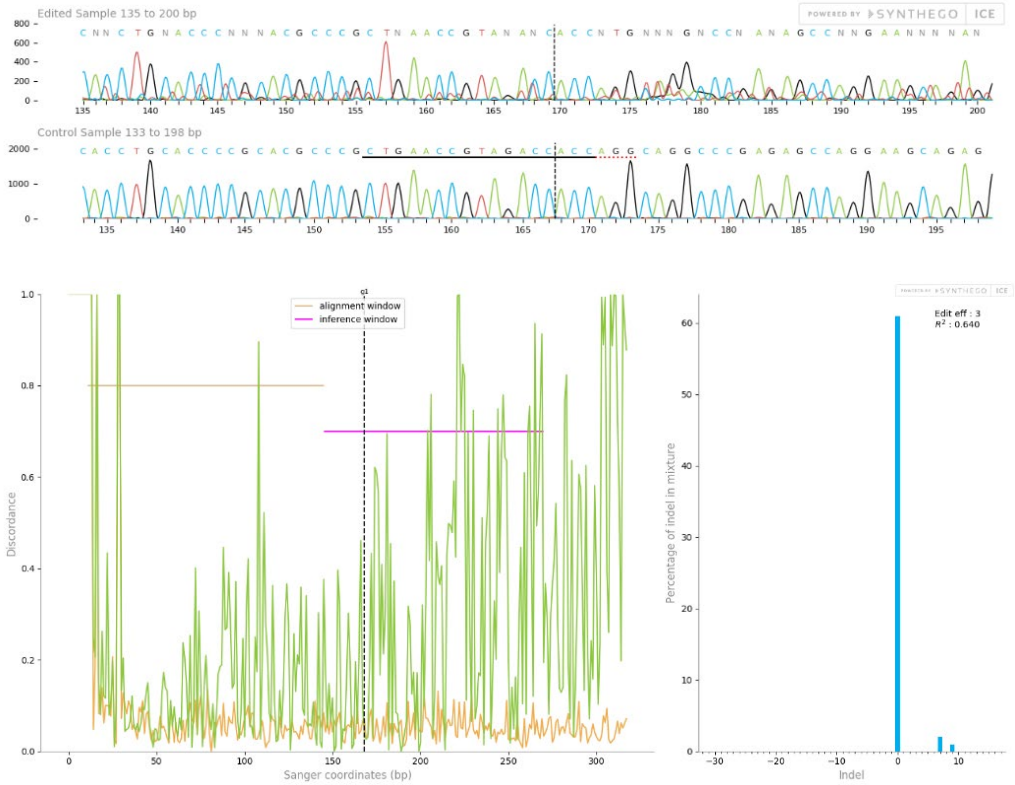
Edited Sample 135 to 200 bp
Control Sample 133 to 198 bp
alignment window
inference window
Discordance
Sanger coordinates (bp)
Edit eff : 3
R² : 0.640
Percentage of indel in mixture
Indel

E4

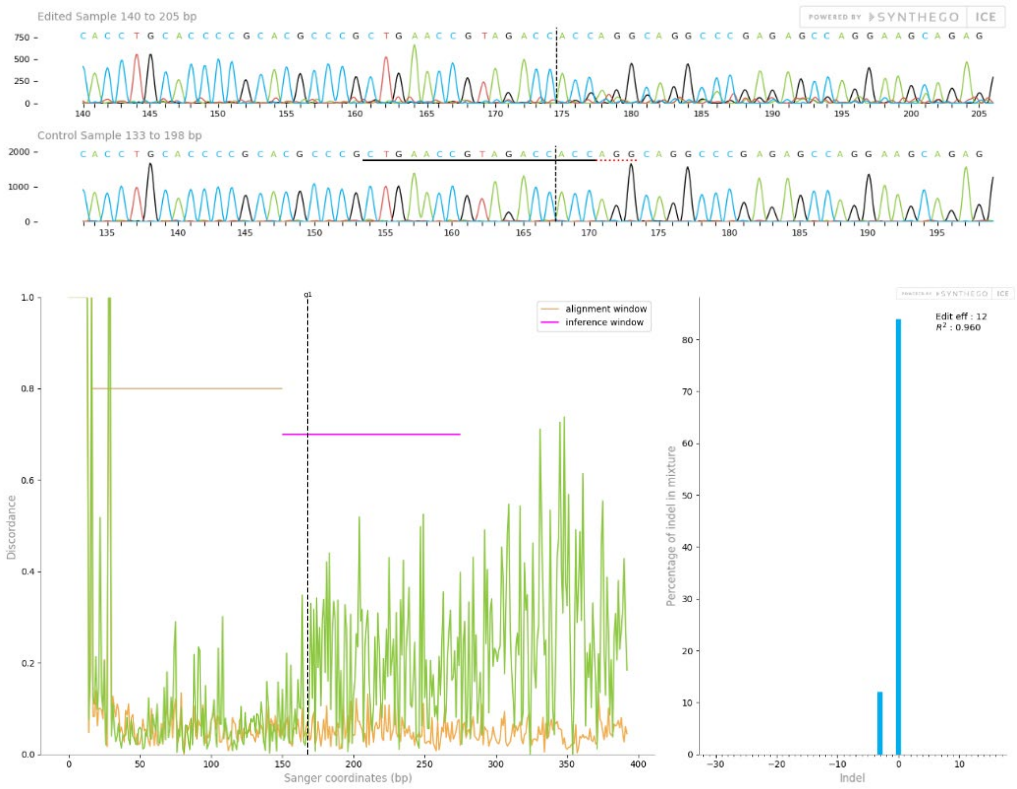
Edited Sample 140 to 205 bp
Control Sample 133 to 198 bp
alignment window
inference window
Discordance
Sanger coordinates (bp)
Percentage of indel in mixture
Indel
Edit eff : 12
R² : 0.960

E5

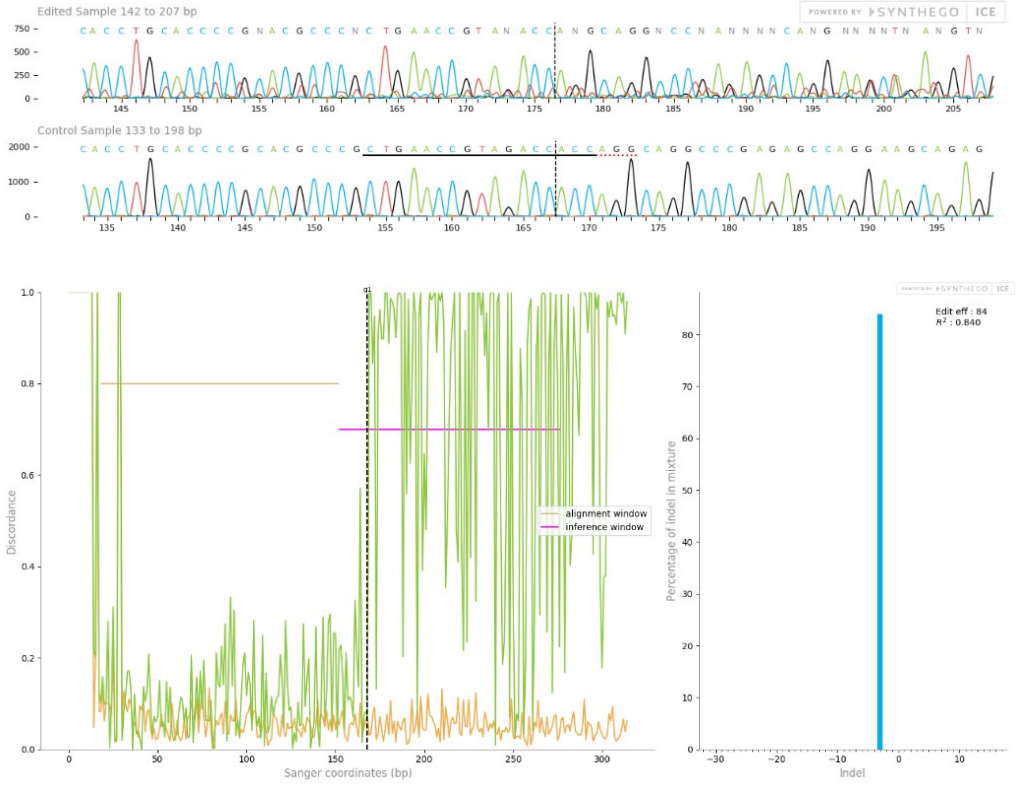
Edited Sample 142 to 207 bp
Control Sample 133 to 198 bp
alignment window
inference window
Discordance
Sanger coordinates (bp)
Percentage of indel in mixture
Indel
Edit eff : 84
R² : 0.840

E6

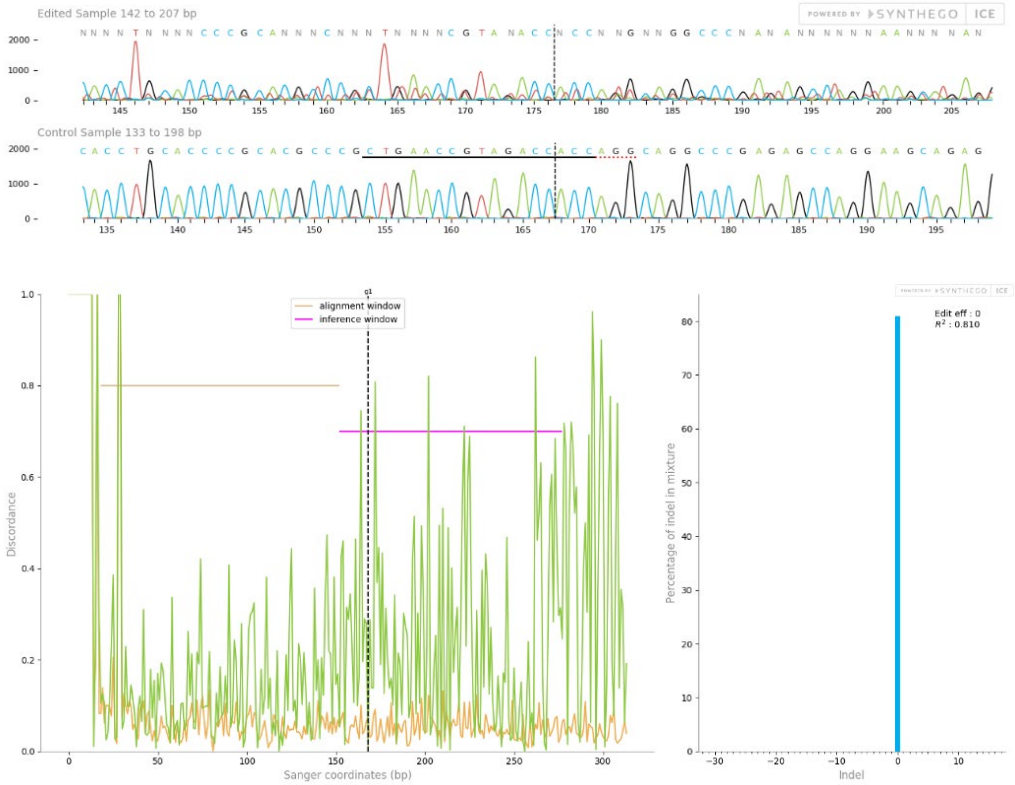
Edited Sample 142 to 207 bp
Control Sample 133 to 198 bp
alignment window
inference window
Discordance
Sanger coordinates (bp)
Edit eff : 0
R^2 : 0.810
Percentage of indel in mixture
Indel

E8

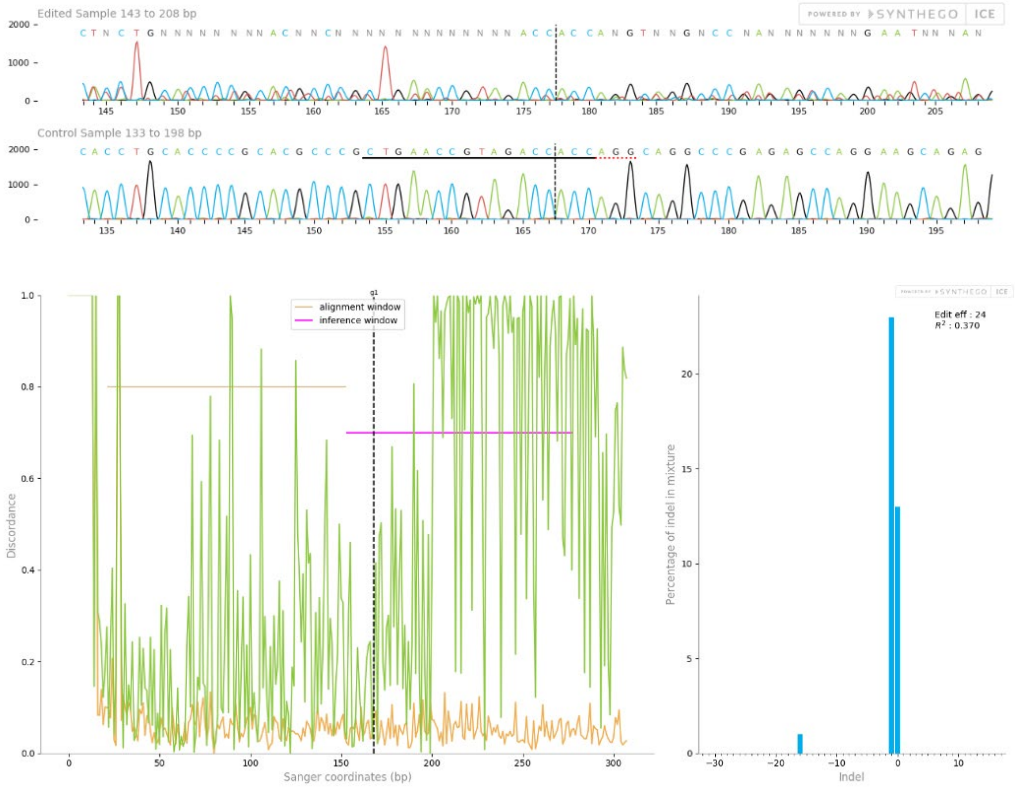
Edited Sample 143 to 208 bp
Control Sample 133 to 198 bp
alignment window
inference window
Discordance
Sanger coordinates (bp)
Edit eff : 24
R^2 : 0.370
Percentage of indel in mixture
Indel

E10

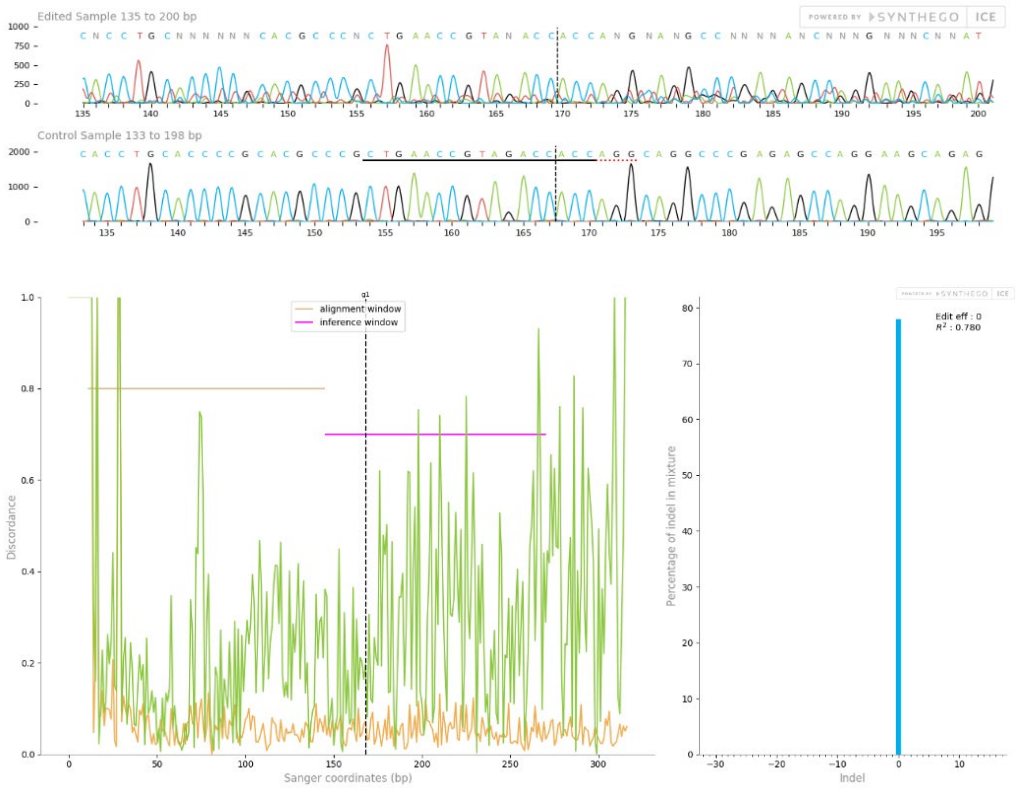
Edited Sample 135 to 200 bp
Control Sample 133 to 198 bp
alignment window
inference window
Discordance
Sanger coordinates (bp)
Percentage of indel in mixture
Indel
Edit eff : 0
R^2 : 0.780

E11

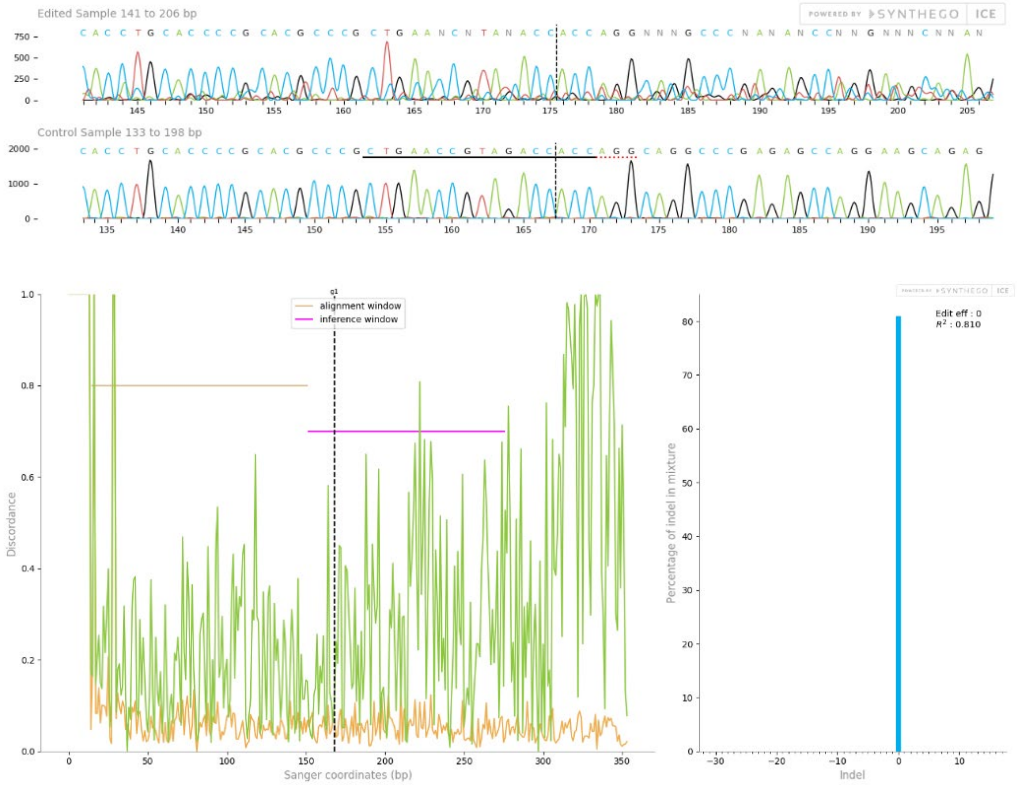
Edited Sample 141 to 206 bp
Control Sample 133 to 198 bp
alignment window
inference window
Discordance
Sanger coordinates (bp)
Percentage of indel in mixture
Indel
Edit eff : 0
R^2 : 0.810

F2

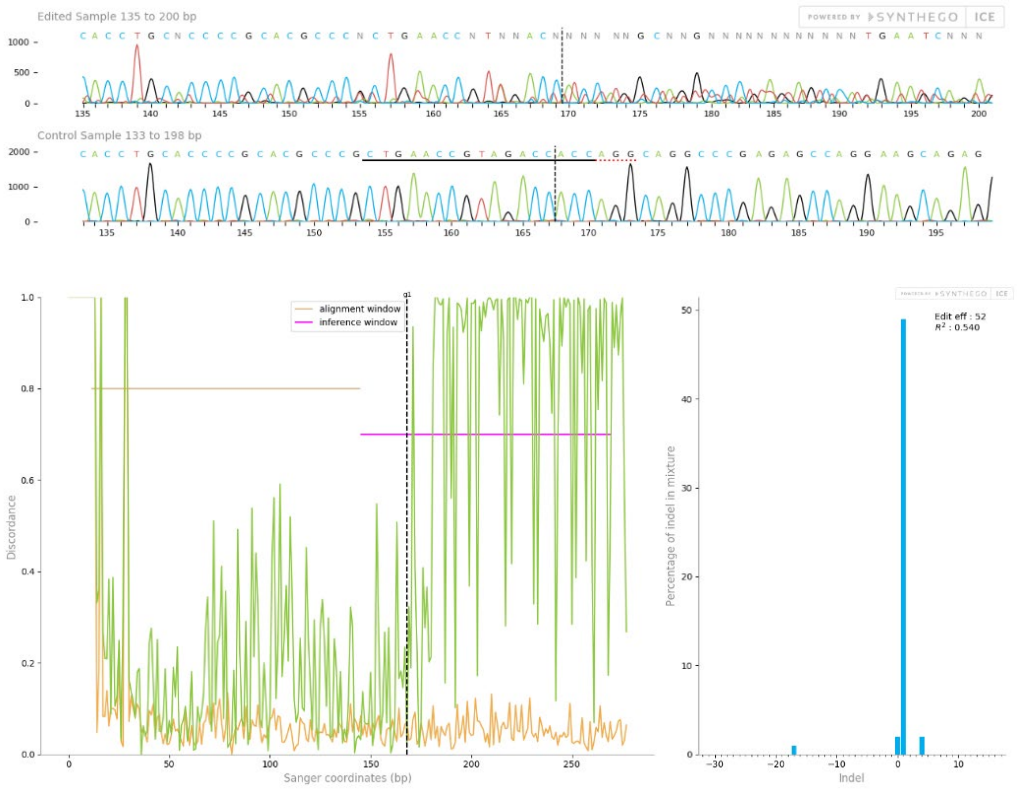
Edited Sample 135 to 200 bp
Control Sample 133 to 198 bp
alignment window
inference window
Discordance
Sanger coordinates (bp)
Edit eff : 52
R^2 : 0.540
Percentage of indel in mixture
Indel

F3

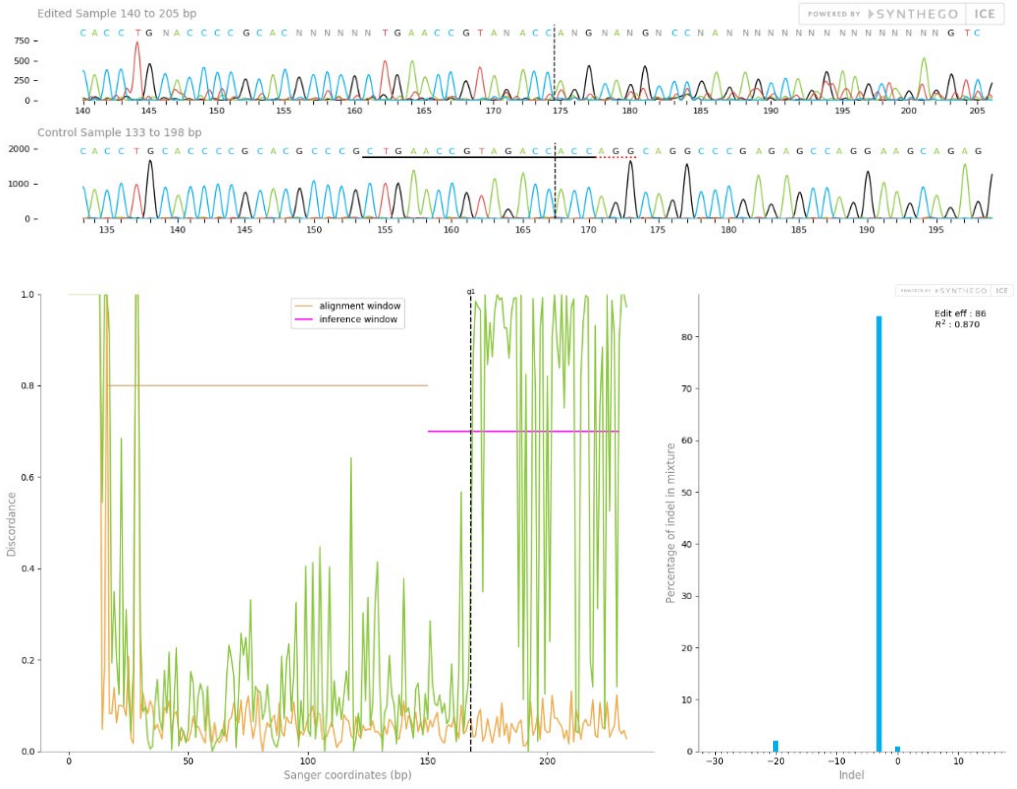
Edited Sample 140 to 205 bp
Control Sample 133 to 198 bp
alignment window
inference window
Discordance
Sanger coordinates (bp)
Edit eff : 86
R^2 : 0.870
Percentage of indel in mixture
Indel

F4

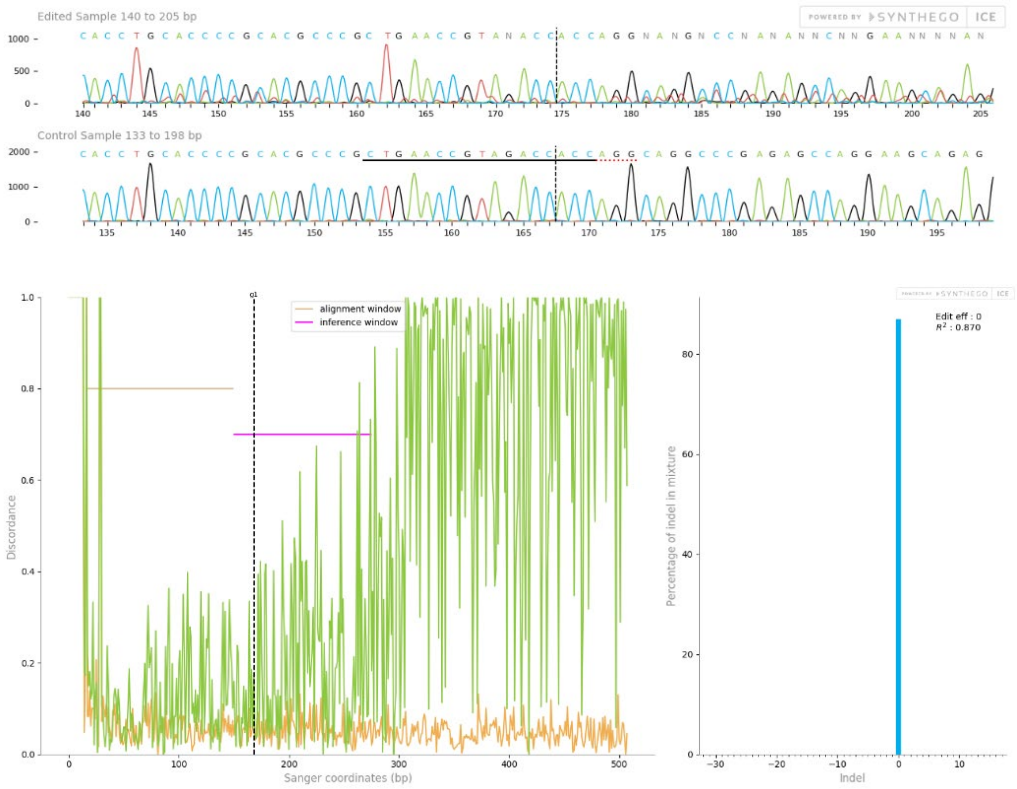
Edited Sample 140 to 205 bp
Control Sample 133 to 198 bp
alignment window
inference window
Discordance
Sanger coordinates (bp)
Percentage of indel in mixture
Indel
Edit eff : 0
R² : 0.870

F5

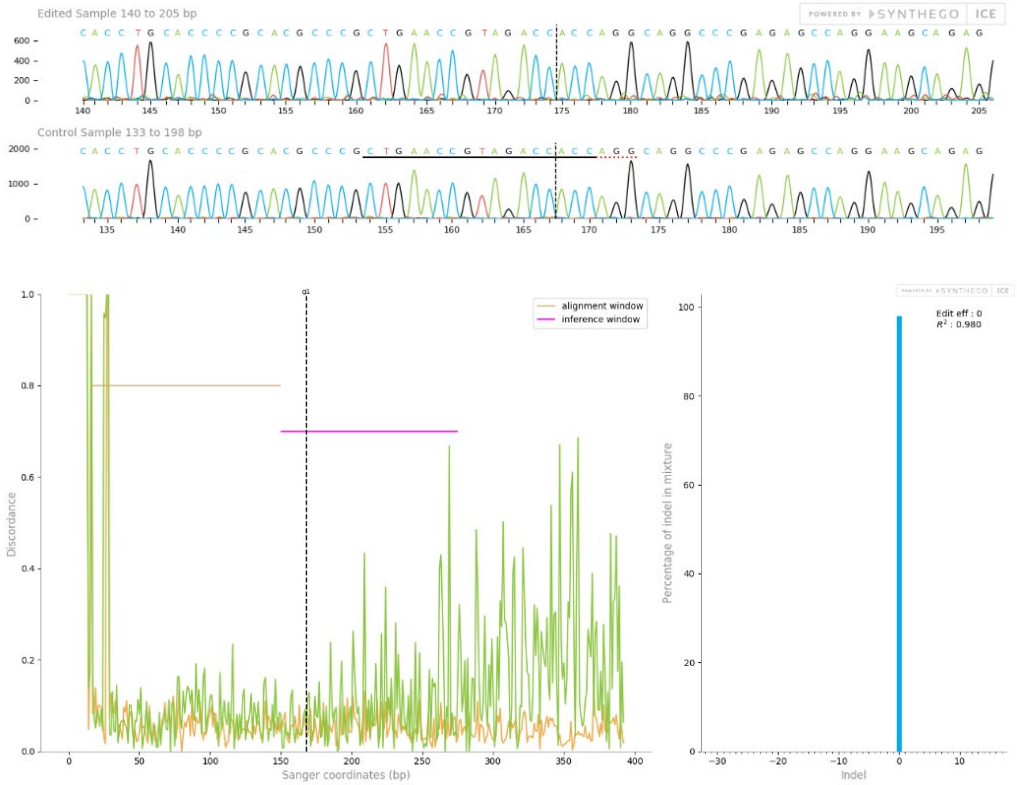
Edited Sample 140 to 205 bp
Control Sample 133 to 198 bp
alignment window
inference window
Discordance
Sanger coordinates (bp)
Percentage of indel in mixture
Indel
Edit eff : 0
R² : 0.980

F6

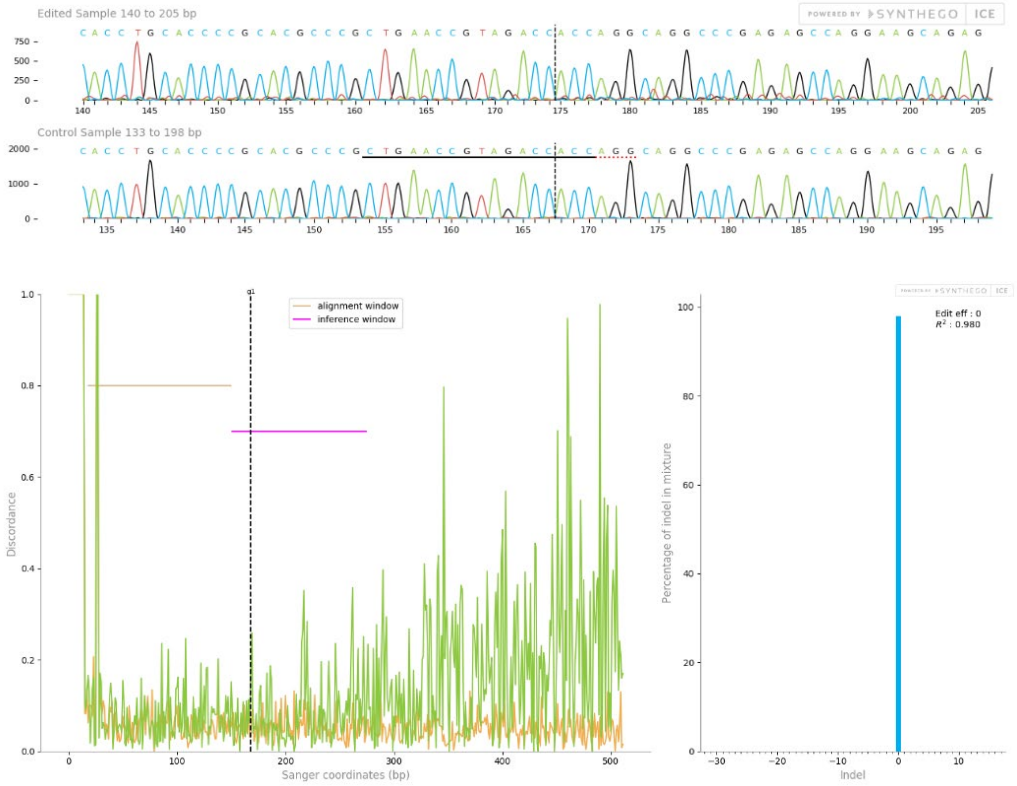
Edited Sample 140 to 205 bp
Control Sample 133 to 198 bp
alignment window
inference window
Discordance
Sanger coordinates (bp)
Percentage of indel in mixture
Indel
Edit eff : 0
R² : 0.980

F7

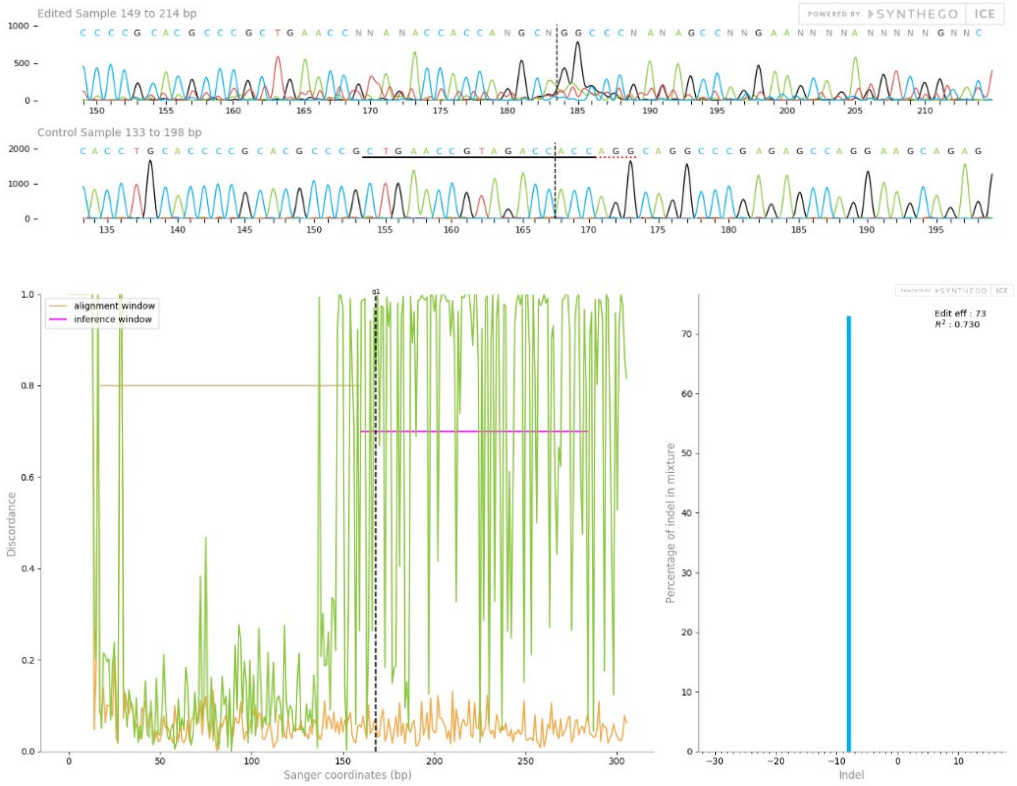
Edited Sample 149 to 214 bp
Control Sample 133 to 198 bp
alignment window
inference window
Discordance
Sanger coordinates (bp)
Percentage of indel in mixture
Indel
Edit eff : 73
R² : 0.730

F9

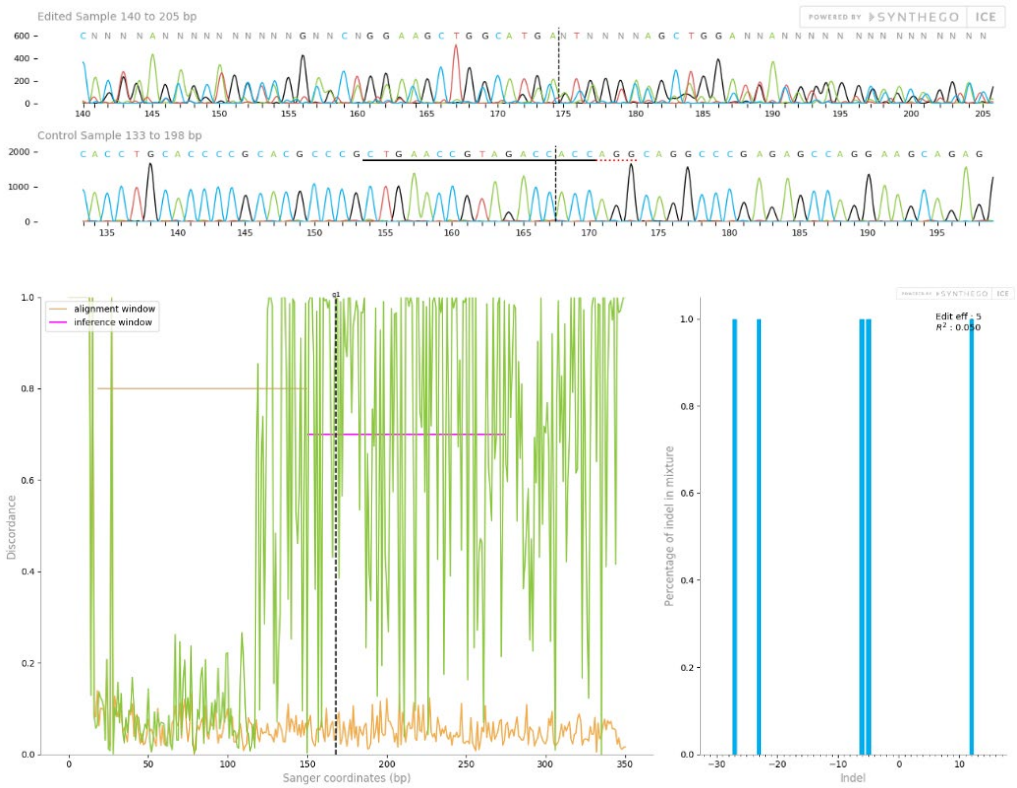
Edited Sample 140 to 205 bp
Control Sample 133 to 198 bp
alignment window
inference window
Discordance
Sanger coordinates (bp)
Percentage of indel in mixture
Indel
Edit eff : 5
R² : 0.050

F10

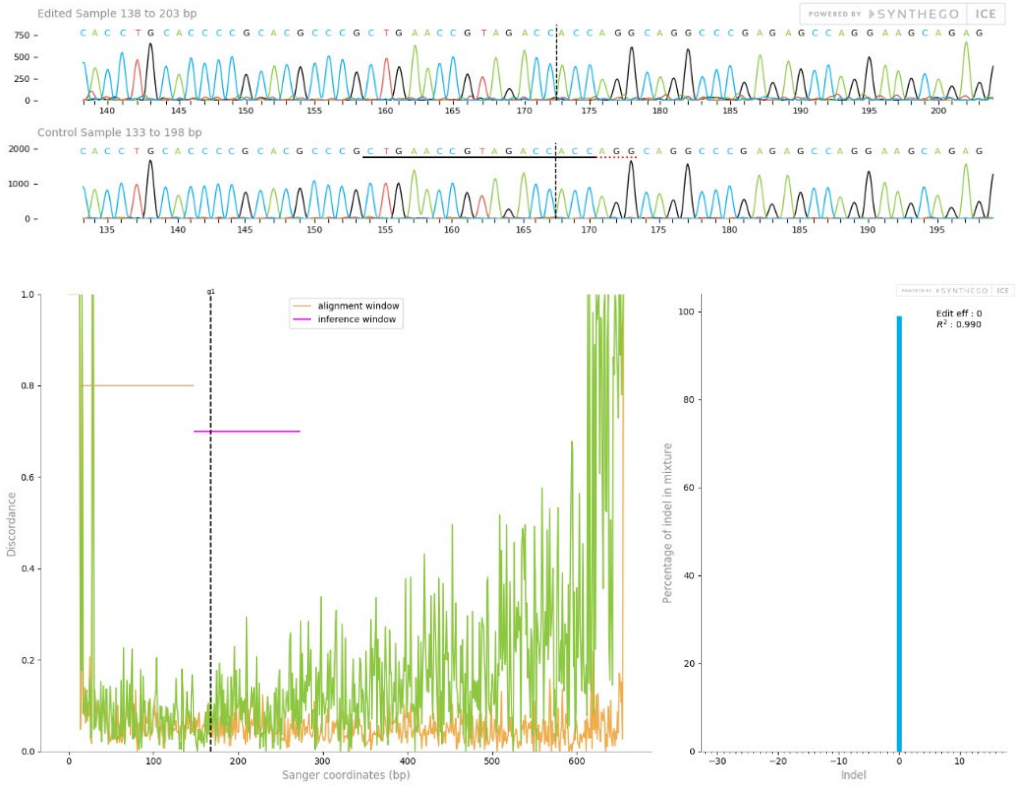
Edited Sample 138 to 203 bp
Control Sample 133 to 198 bp
alignment window
inference window
Discordance
Sanger coordinates (bp)
Percentage of indel in mixture
Indel
Edit eff : 0
R² : 0.990

F11

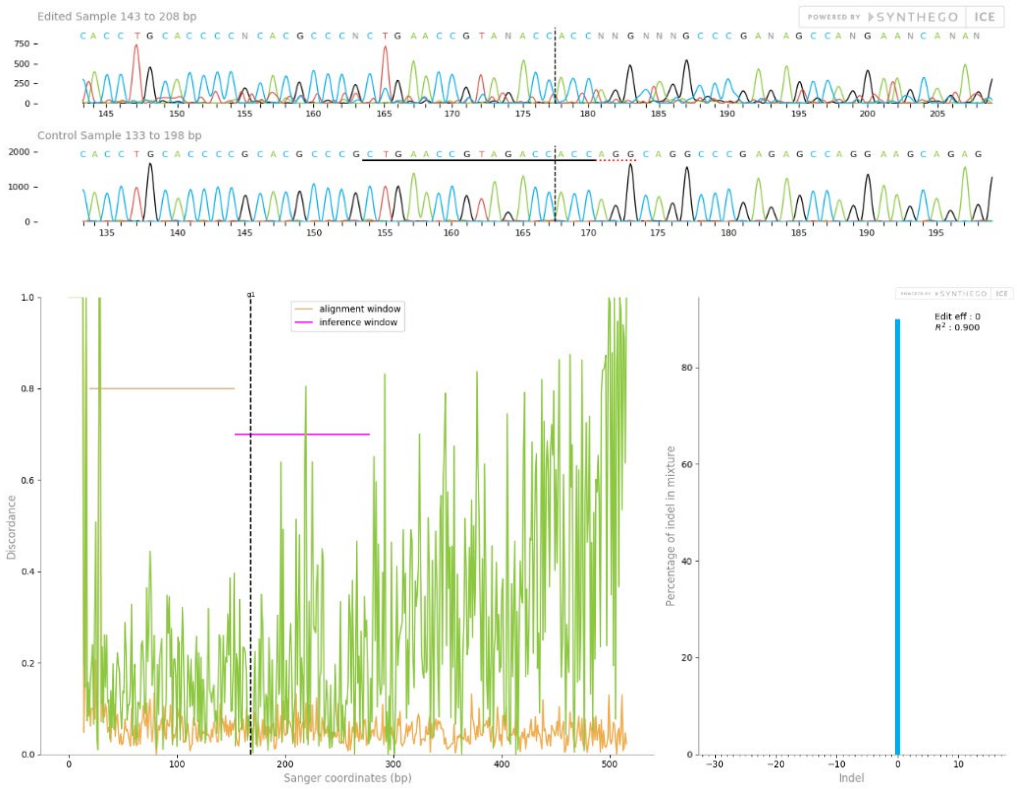
Edited Sample 143 to 208 bp
Control Sample 133 to 198 bp
alignment window
inference window
Discordance
Sanger coordinates (bp)
Edit eff : 0
R^2 : 0.900
Percentage of indel in mixture
Indel

G1

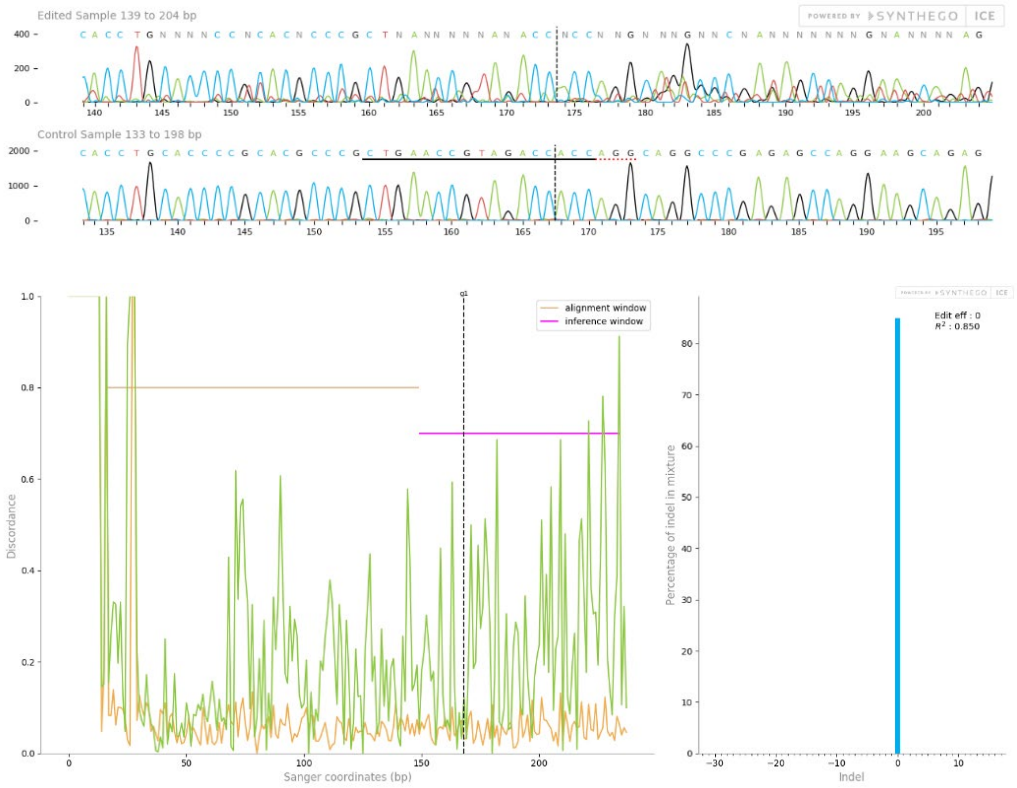
Edited Sample 139 to 204 bp
Control Sample 133 to 198 bp
alignment window
inference window
Discordance
Sanger coordinates (bp)
Edit eff : 0
R^2 : 0.850
Percentage of indel in mixture
Indel

G2

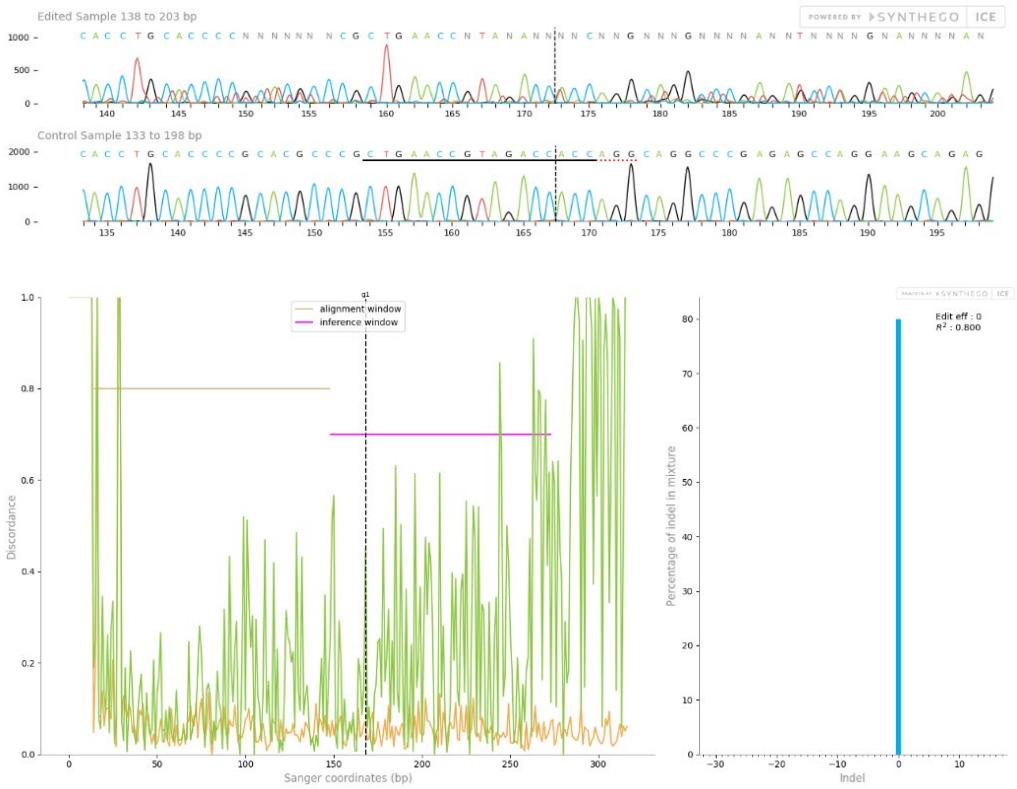
Edited Sample 138 to 203 bp
Control Sample 133 to 198 bp
alignment window
inference window
Discordance
Sanger coordinates (bp)
Edit eff : 0
R^2 : 0.800
Percentage of indel in mixture
Indel

G4

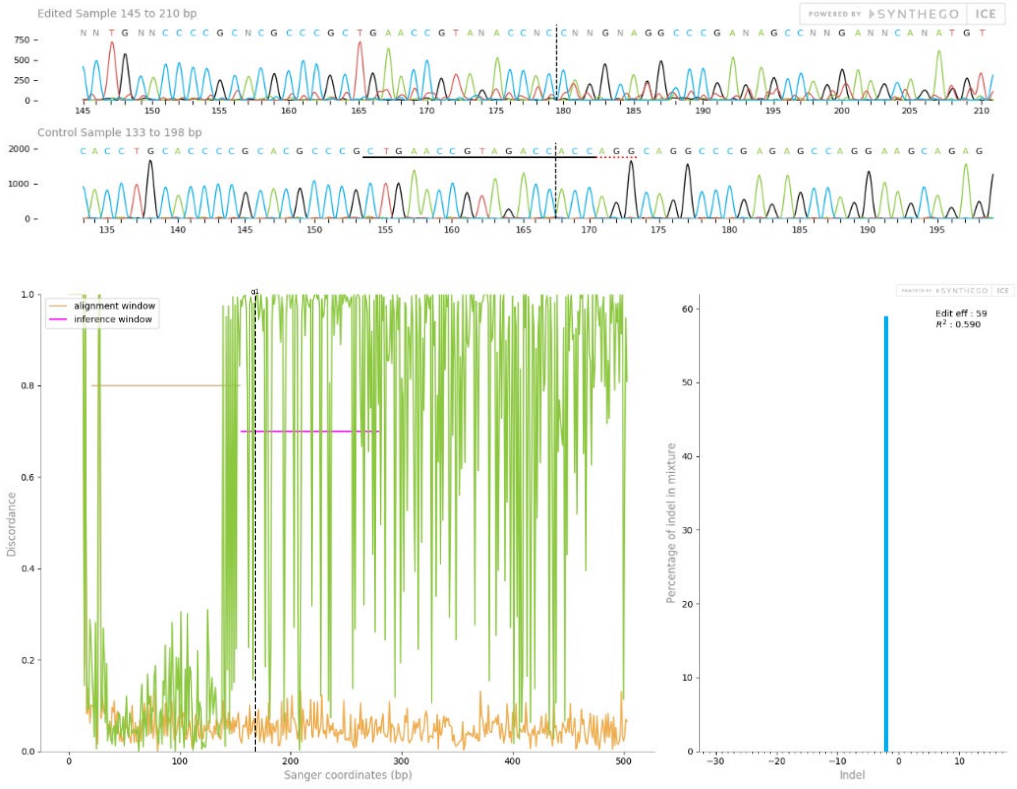
Edited Sample 145 to 210 bp
Control Sample 133 to 198 bp
alignment window
inference window
Discordance
Sanger coordinates (bp)
Edit eff : 59
R^2 : 0.590
Percentage of indel in mixture
Indel

G6

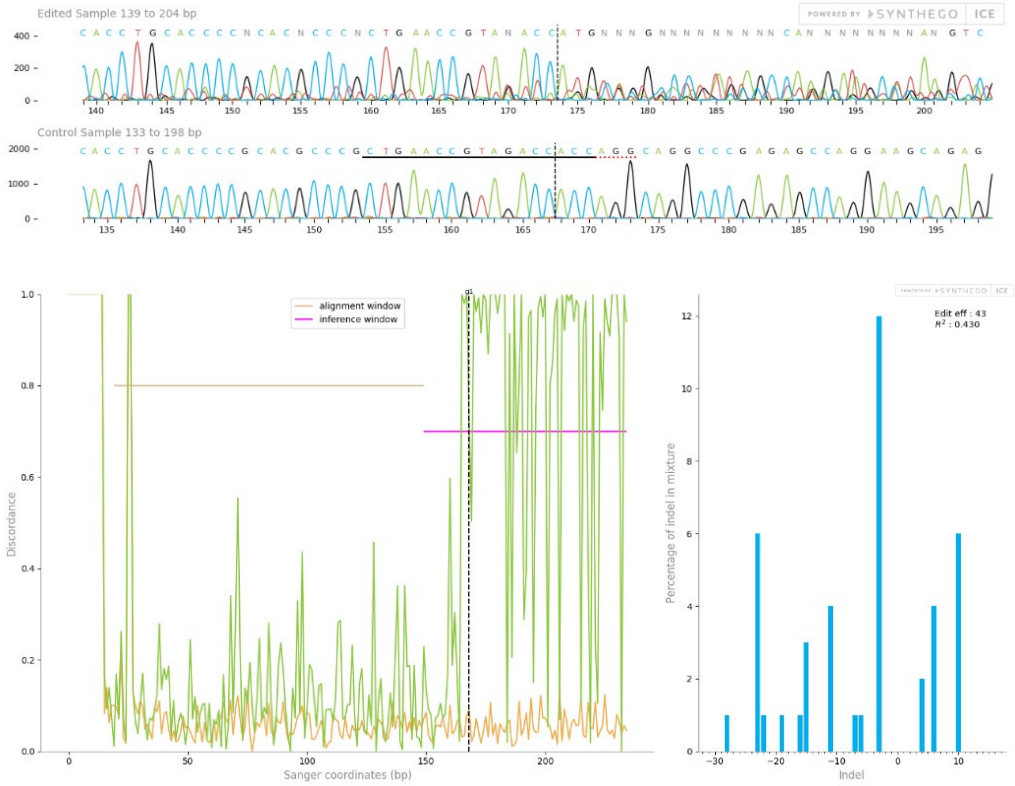

Supplementary Figure 4.5. C5aR2 monoclone sequencing data.

Appendix 2 - Supplementary Data for

Chapter 5

9. Appendix 2 - Supplementary Data for Chapter 5

9.1. Antagonist Vehicle Control Data

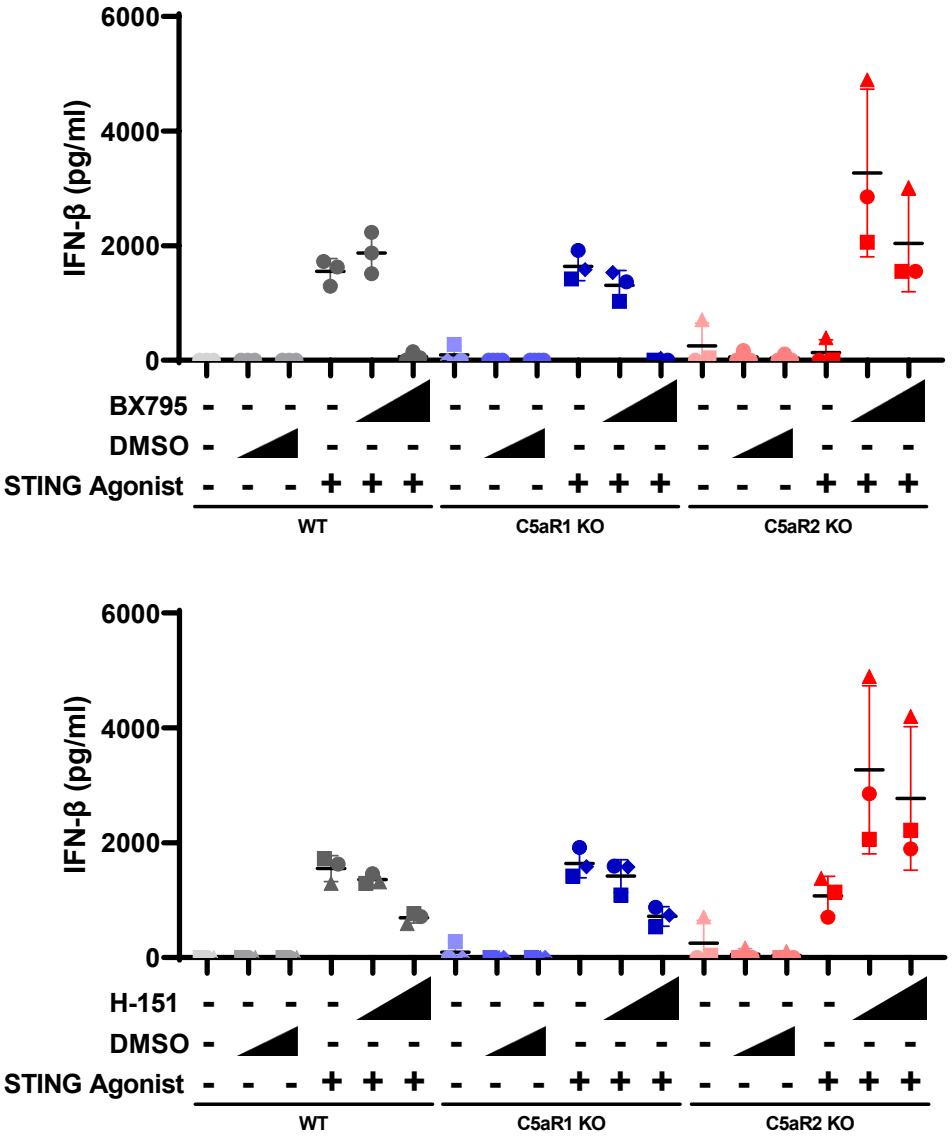

Supplementary Figure 5.1. Figure 5.9 including DMSO figure controls. Cells were incubated with 0.001% or 0.01% DMSO for 6.5 hours, followed by supernatant harvest and assessment for IFN-β by ELISA.

9.2. Peggy Sue Raw Data

WT pSTING

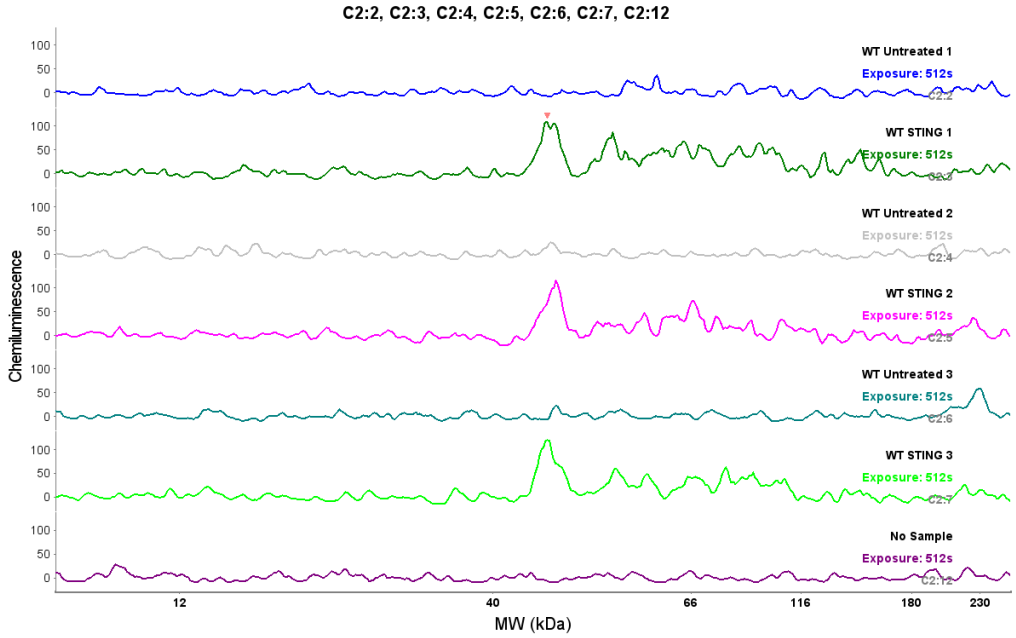

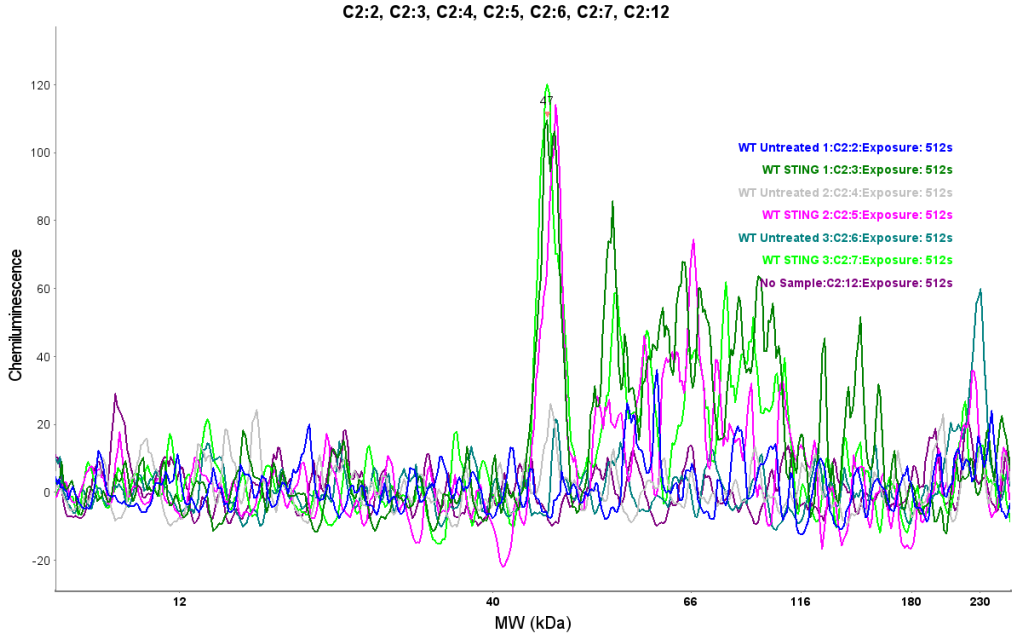

WT STING

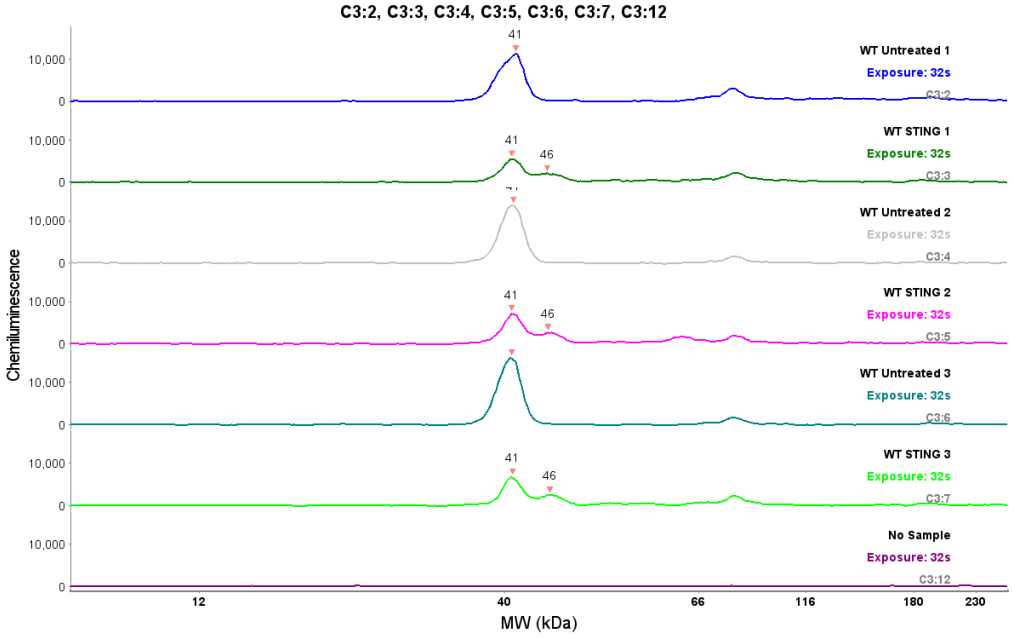
C3:2, C3:3, C3:4, C3:5, C3:6, C3:7, C3:12
Chemiluminescence
MW (kDa)
WT Untreated 1
Exposure: 32s
C3:2
WT STING 1
Exposure: 32s
C3:3
WT Untreated 2
Exposure: 32s
C3:4
WT STING 2
Exposure: 32s
C3:5
WT Untreated 3
Exposure: 32s
C3:6
WT STING 3
Exposure: 32s
C3:7
No Sample
Exposure: 32s
C3:12

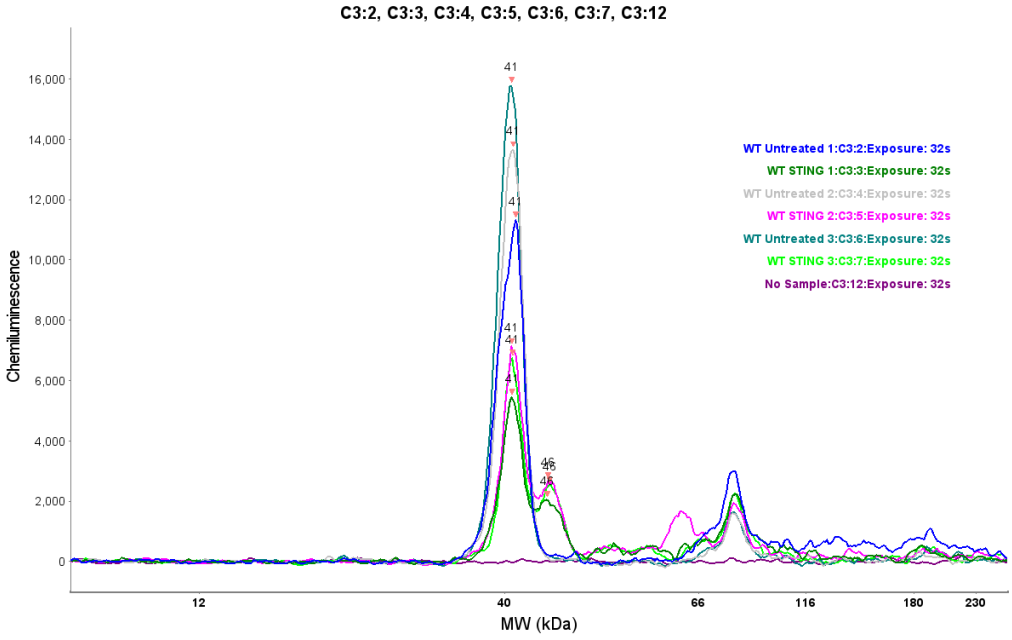
C3:2, C3:3, C3:4, C3:5, C3:6, C3:7, C3:12
Chemiluminescence
MW (kDa)
WT Untreated 1:C3:2:Exposure: 32s
WT STING 1:C3:3:Exposure: 32s
WT Untreated 2:C3:4:Exposure: 32s
WT STING 2:C3:5:Exposure: 32s
WT Untreated 3:C3:6:Exposure: 32s
WT STING 3:C3:7:Exposure: 32s
No Sample:C3:12:Exposure: 32s

WT pIRF3

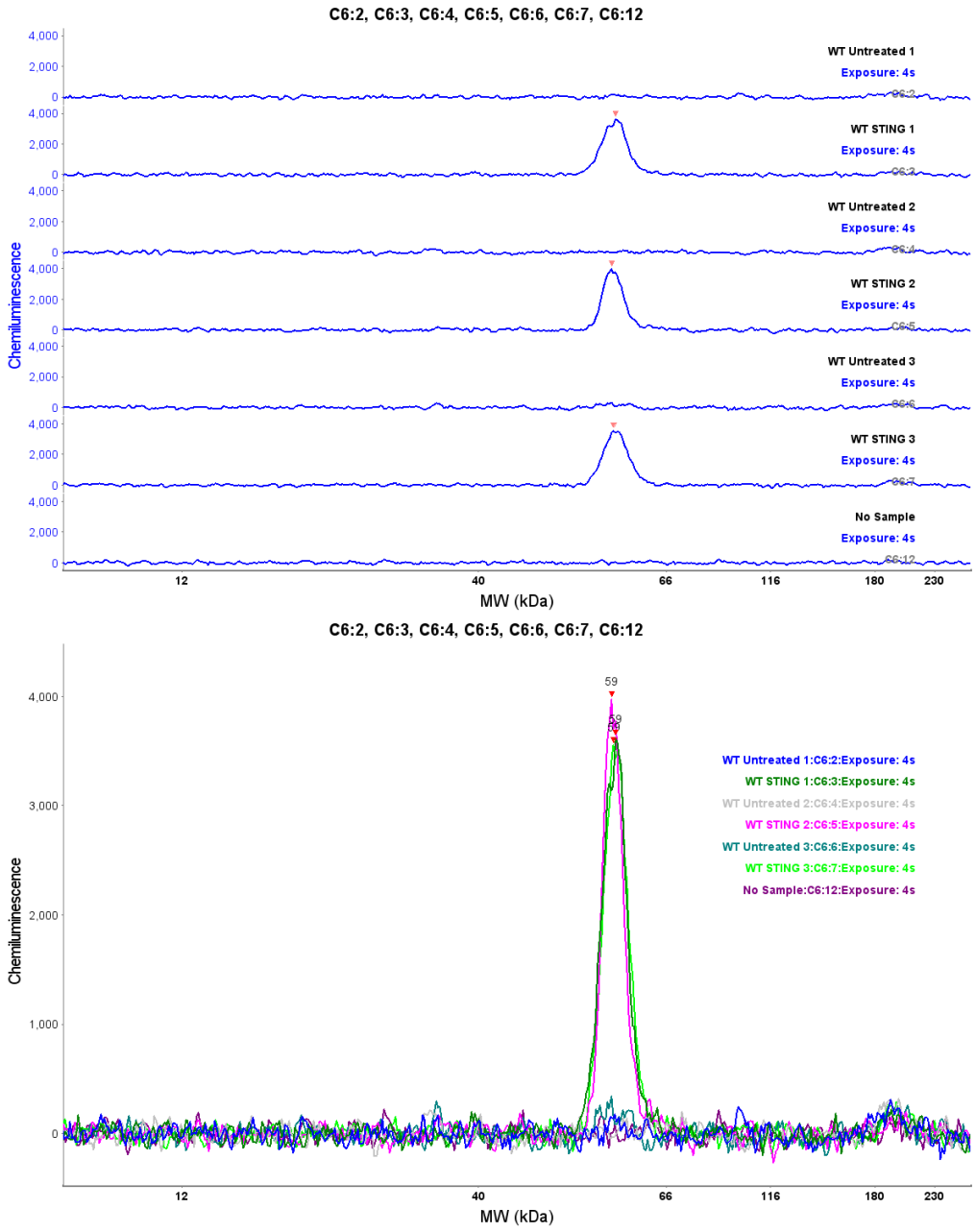
C6:2, C6:3, C6:4, C6:5, C6:6, C6:7, C6:12
Chemiluminescence
WT Untreated 1
Exposure: 4s
WT STING 1
Exposure: 4s
WT Untreated 2
Exposure: 4s
WT STING 2
Exposure: 4s
WT Untreated 3
Exposure: 4s
WT STING 3
Exposure: 4s
No Sample
Exposure: 4s
MW (kDa)
C6:2, C6:3, C6:4, C6:5, C6:6, C6:7, C6:12
59
WT Untreated 1:C6:2:Exposure: 4s
WT STING 1:C6:3:Exposure: 4s
WT Untreated 2:C6:4:Exposure: 4s
WT STING 2:C6:5:Exposure: 4s
WT Untreated 3:C6:6:Exposure: 4s
WT STING 3:C6:7:Exposure: 4s
No Sample:C6:12:Exposure: 4s
Chemiluminescence
MW (kDa)

WT IRF3

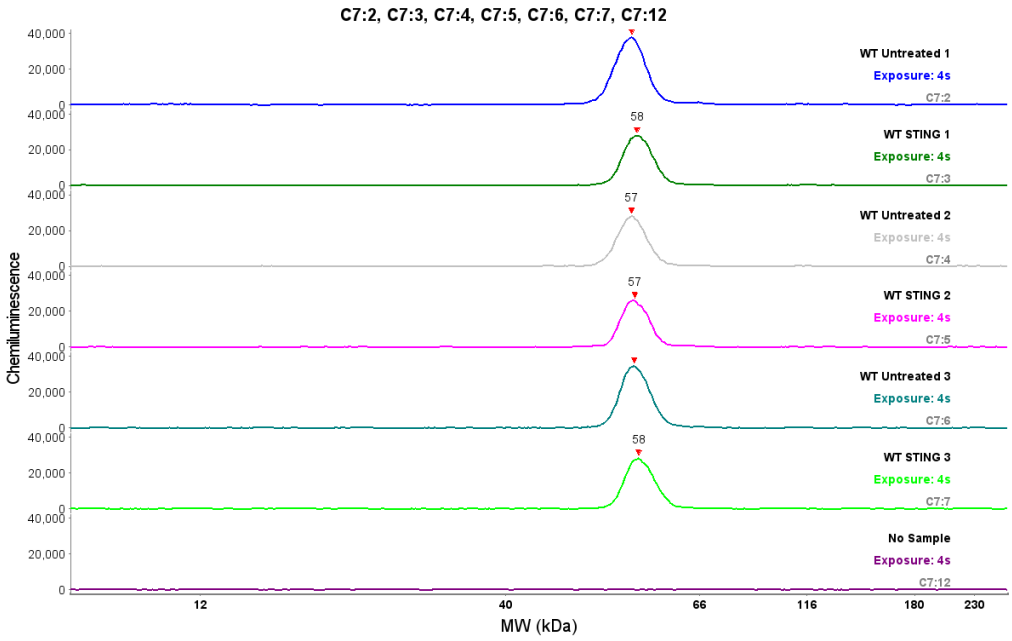
C7:2, C7:3, C7:4, C7:5, C7:6, C7:7, C7:12
Chemiluminescence
MW (kDa)
WT Untreated 1
Exposure: 4s
C7:2
WT STING 1
Exposure: 4s
C7:3
WT Untreated 2
Exposure: 4s
C7:4
WT STING 2
Exposure: 4s
C7:5
WT Untreated 3
Exposure: 4s
C7:6
WT STING 3
Exposure: 4s
C7:7
No Sample
Exposure: 4s
C7:12

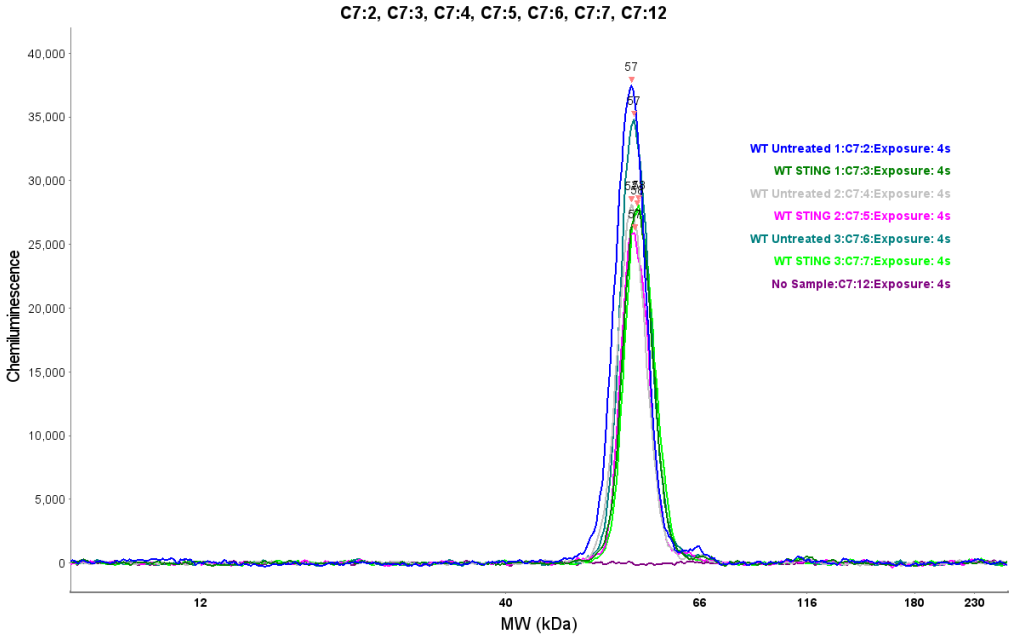
C7:2, C7:3, C7:4, C7:5, C7:6, C7:7, C7:12
Chemiluminescence
MW (kDa)
WT Untreated 1:C7:2:Exposure: 4s
WT STING 1:C7:3:Exposure: 4s
WT Untreated 2:C7:4:Exposure: 4s
WT STING 2:C7:5:Exposure: 4s
WT Untreated 3:C7:6:Exposure: 4s
WT STING 3:C7:7:Exposure: 4s
No Sample:C7:12:Exposure: 4s

WT β-actin

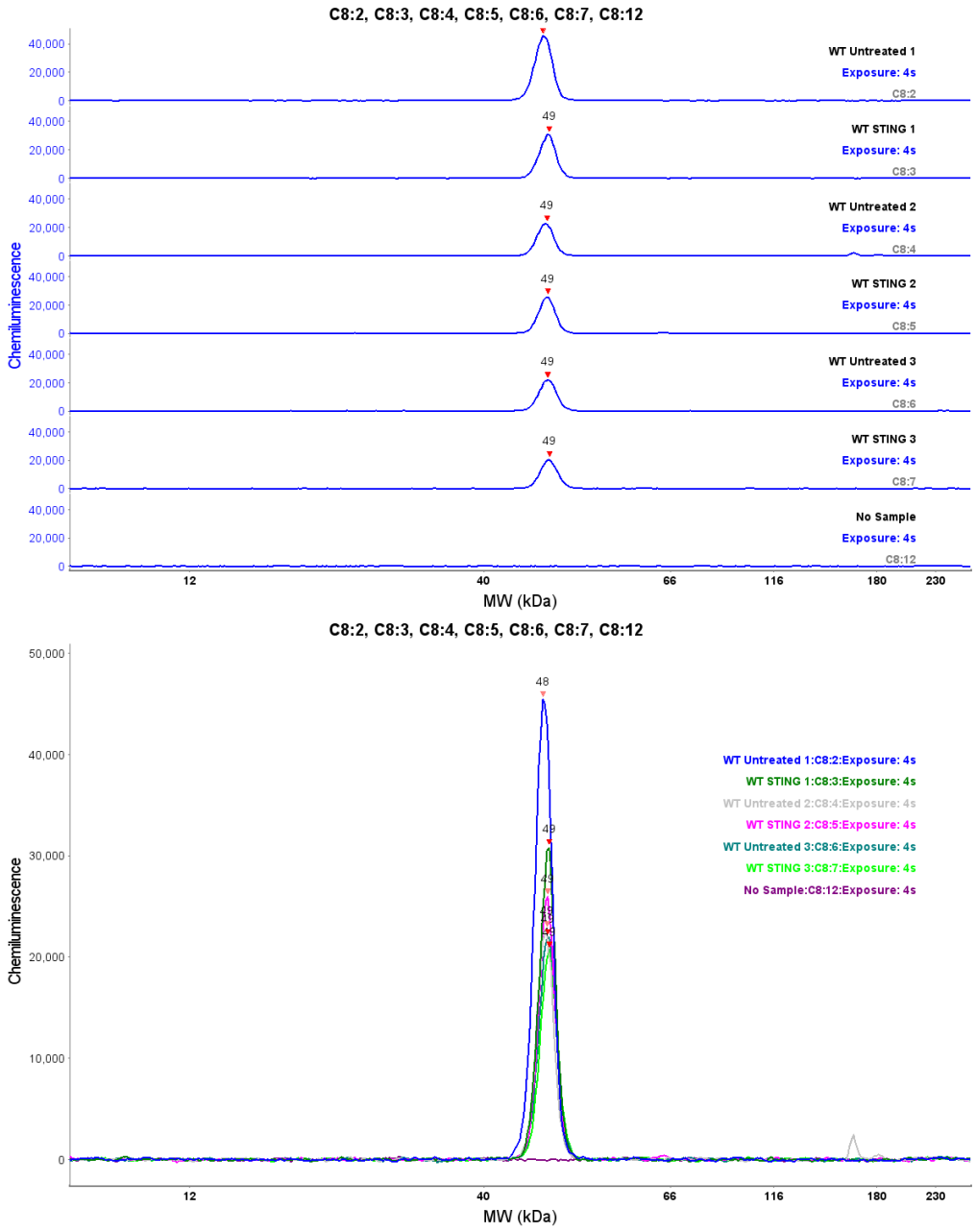
C8:2, C8:3, C8:4, C8:5, C8:6, C8:7, C8:12
Chemiluminescence
WT Untreated 1
Exposure: 4s
C8:2
WT STING 1
Exposure: 4s
C8:3
WT Untreated 2
Exposure: 4s
C8:4
WT STING 2
Exposure: 4s
C8:5
WT Untreated 3
Exposure: 4s
C8:6
WT STING 3
Exposure: 4s
C8:7
No Sample
Exposure: 4s
C8:12
MW (kDa)
C8:2, C8:3, C8:4, C8:5, C8:6, C8:7, C8:12
Chemiluminescence
WT Untreated 1:C8:2:Exposure: 4s
WT STING 1:C8:3:Exposure: 4s
WT Untreated 2:C8:4:Exposure: 4s
WT STING 2:C8:5:Exposure: 4s
WT Untreated 3:C8:6:Exposure: 4s
WT STING 3:C8:7:Exposure: 4s
No Sample:C8:12:Exposure: 4s
MW (kDa)

C5aR2 KO pSTING

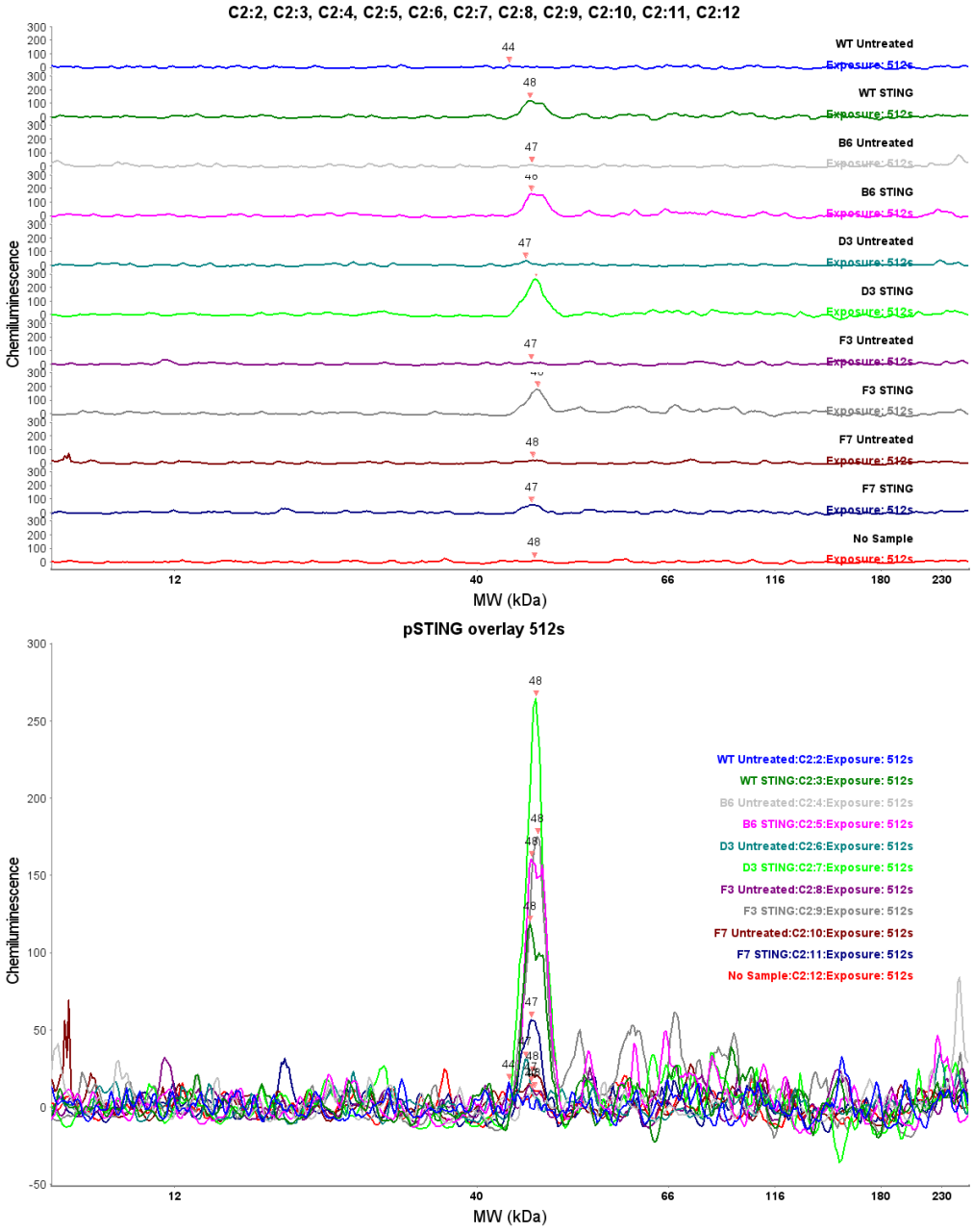

C5aR2 KO STING

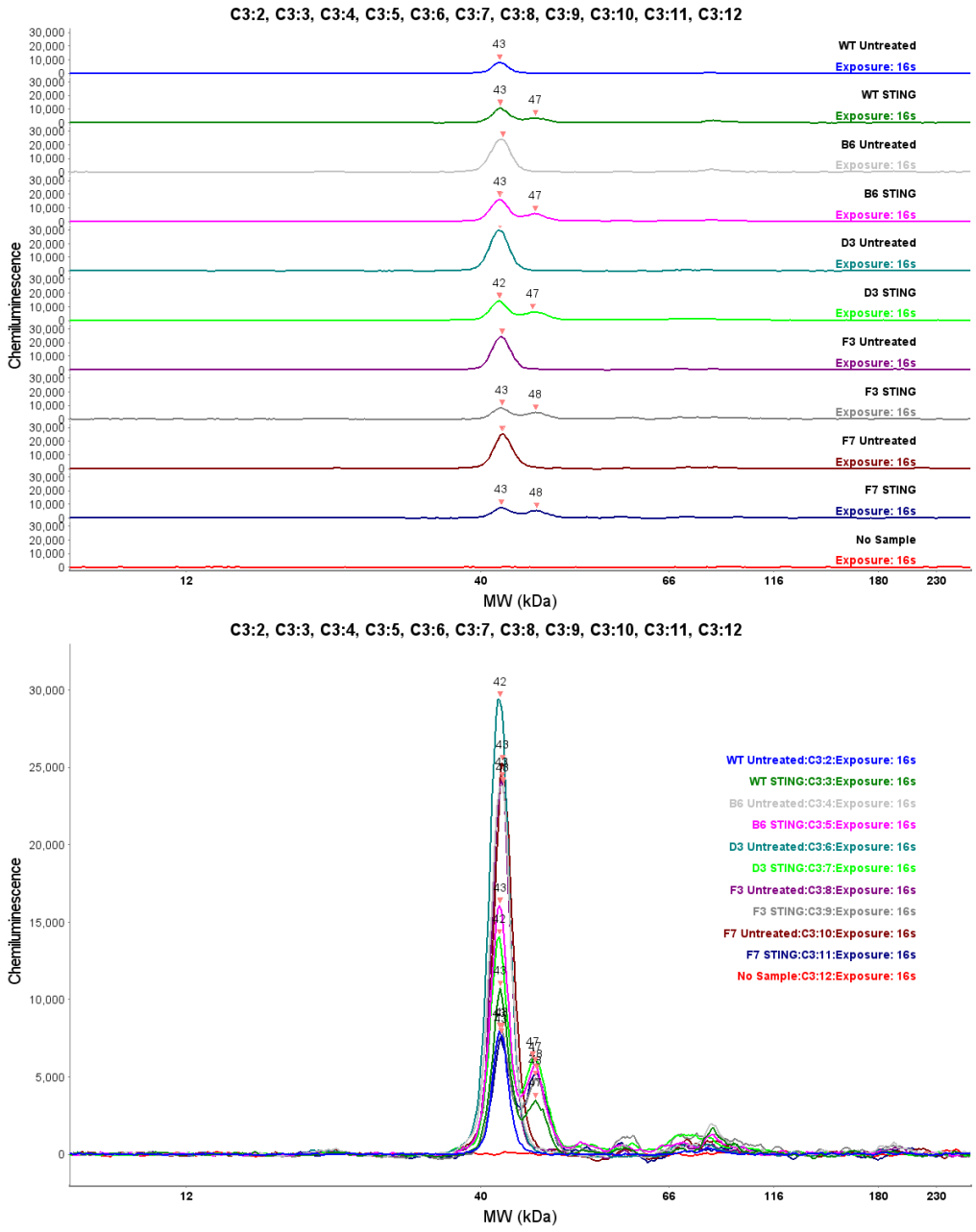

C5aR2 KO pIRF3

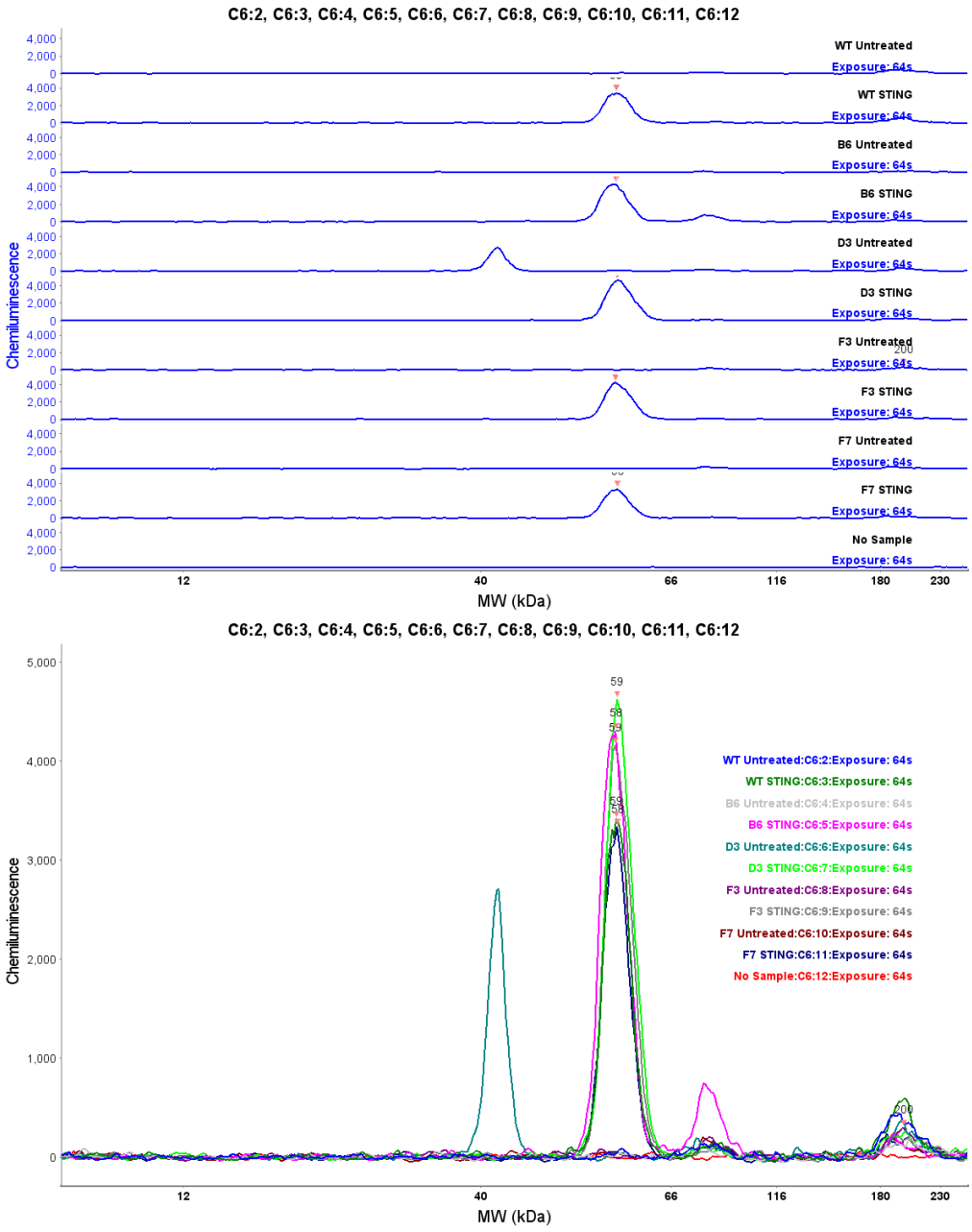

C5aR2 IRF3

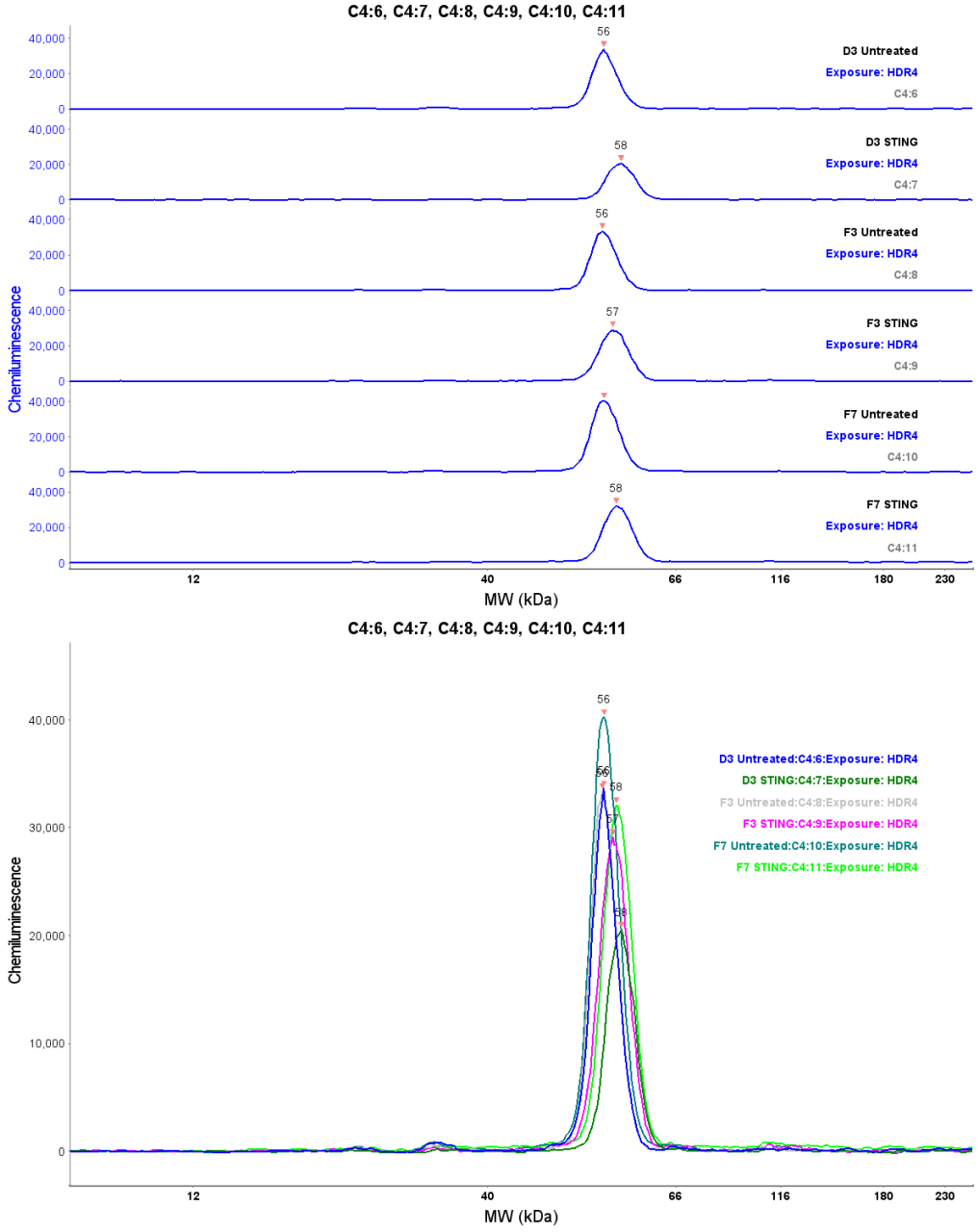
C4:6, C4:7, C4:8, C4:9, C4:10, C4:11
Chemiluminescence
40,000
20,000
0
56
58
56
57
58
D3 Untreated
Exposure: HDR4
C4:6
D3 STING
Exposure: HDR4
C4:7
F3 Untreated
Exposure: HDR4
C4:8
F3 STING
Exposure: HDR4
C4:9
F7 Untreated
Exposure: HDR4
C4:10
F7 STING
Exposure: HDR4
C4:11
12
40
66
116
180
230
MW (kDa)

C4:6, C4:7, C4:8, C4:9, C4:10, C4:11
Chemiluminescence
40,000
30,000
20,000
10,000
0
56
55
58
57
58
D3 Untreated:C4:6:Exposure: HDR4
D3 STING:C4:7:Exposure: HDR4
F3 Untreated:C4:8:Exposure: HDR4
F3 STING:C4:9:Exposure: HDR4
F7 Untreated:C4:10:Exposure: HDR4
F7 STING:C4:11:Exposure: HDR4
12
40
66
116
180
230
MW (kDa)

C5aR2 β-actin (for IRF3 data)

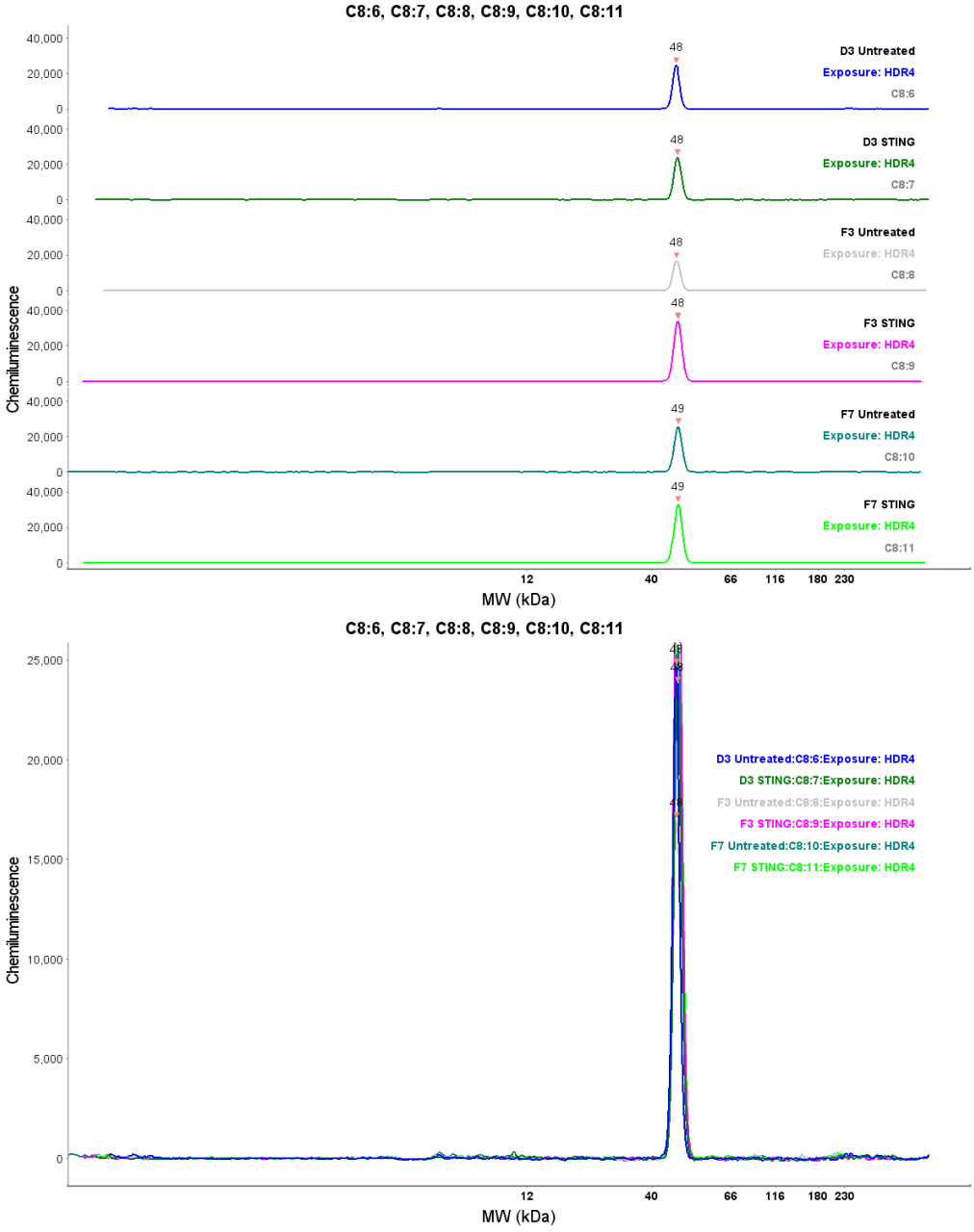

C5aR2 KO β-actin

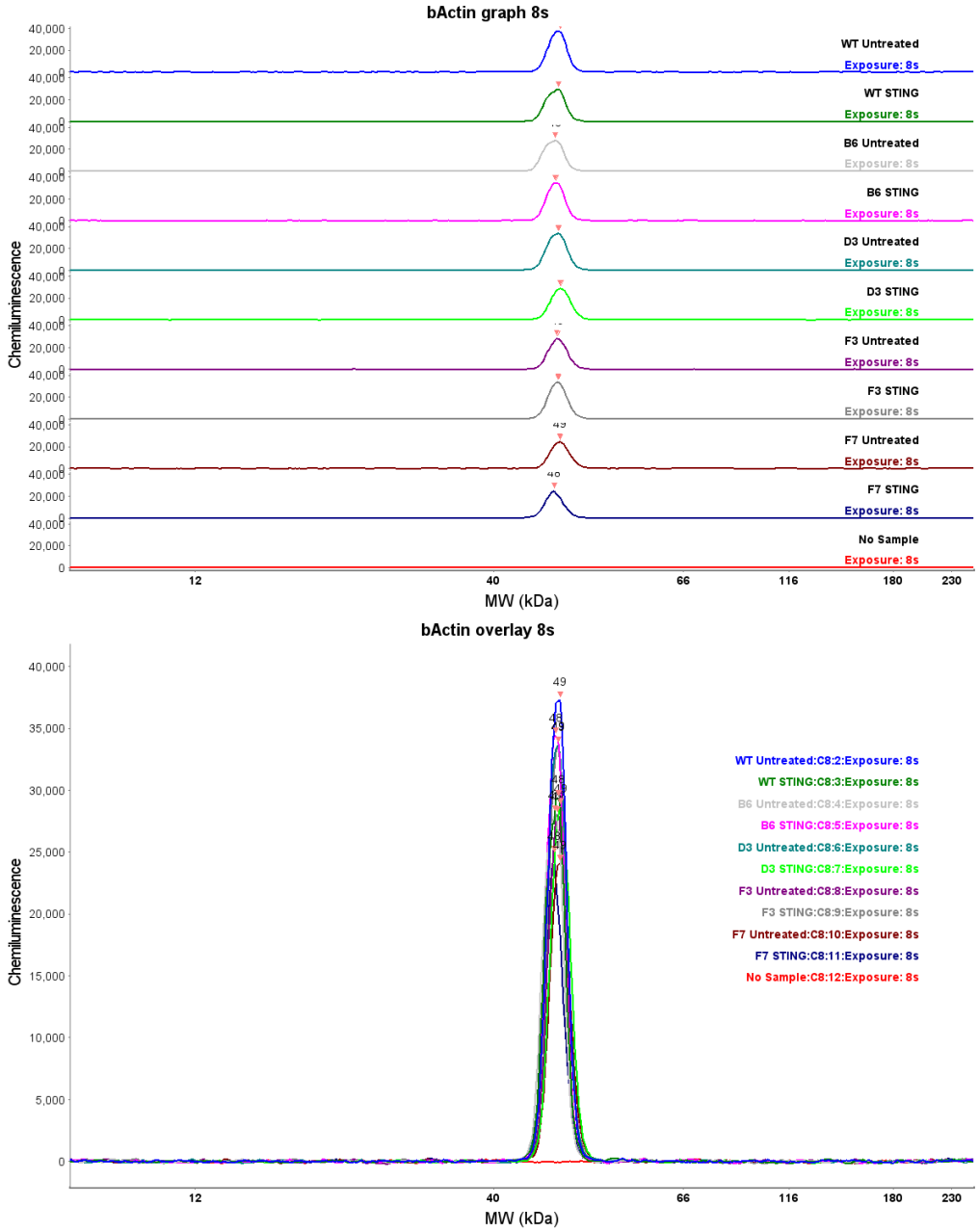

Supplementary Figure 5.2. Peggy Sue area data. Data from Peggy Sue experiment used to generate area under curve plots.

Appendix 3 - Supplementary Data for

Chapter 6

10. Appendix 3 – Supplementary Data for Chapter

10.1. Pathway analysis of Untreated C5aR1/2 KO vs WT cells

Untreated C5aR1 KO vs Untreated WT

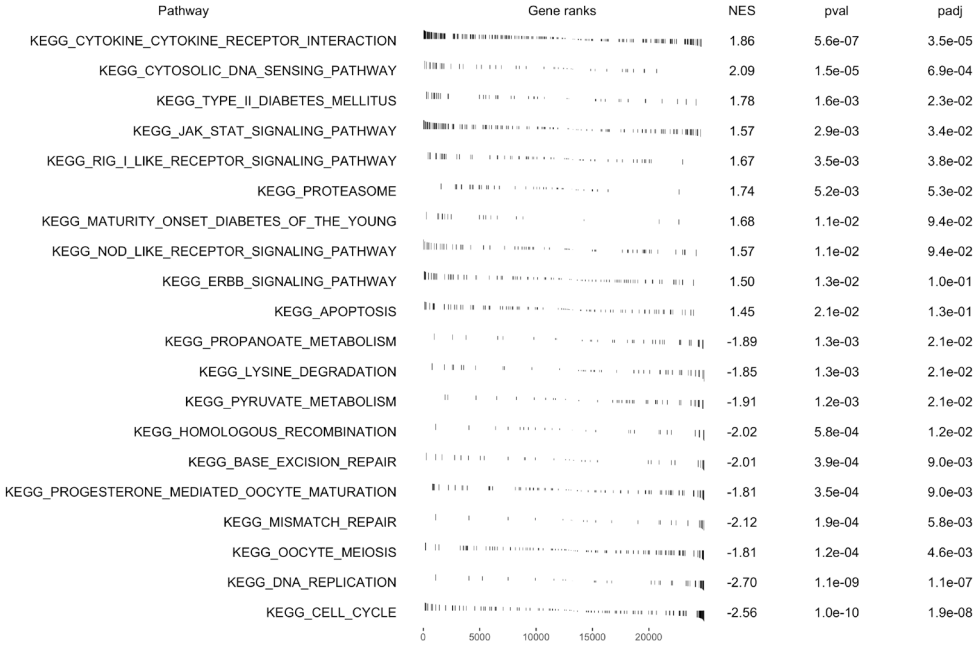

Untreated C5aR2 KO vs Untreated WT

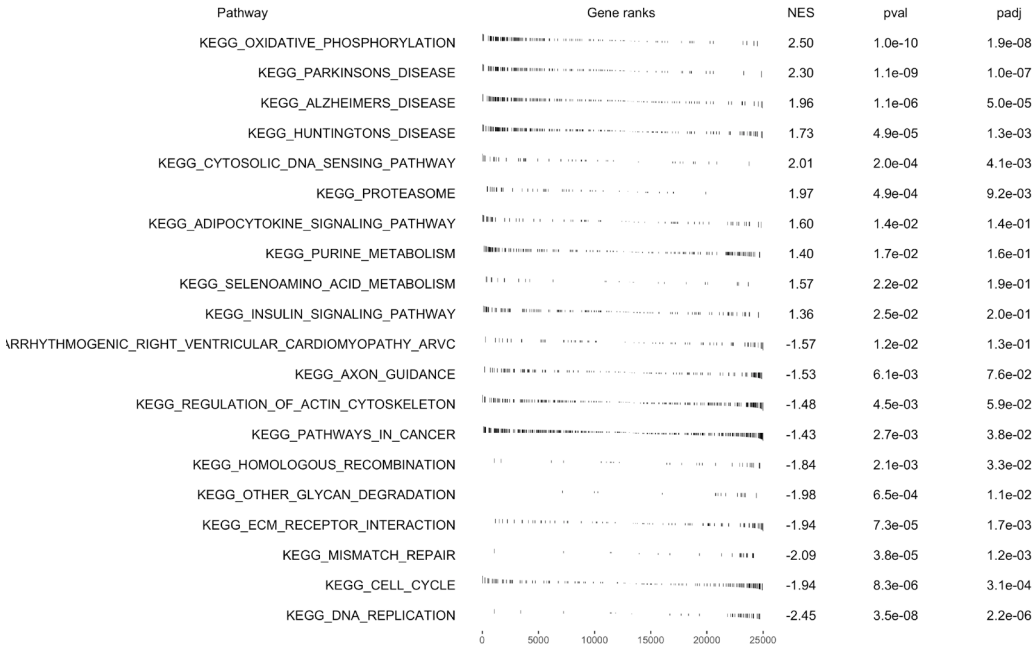

Supplementary Figure 6.1. Additional pathway analysis of untreated C5aR1/2 KO cells vs WT cells using GSEA. Performed by You Zhou (Cardiff University) and Van Dien Nguyen (Cardiff University)**.**

10.2. Gene lists for manually curated KEGG pathways

RLR signaling	adipocytokine signaling	Cytokine cytokine receptor interaction	Cytosolic DNA sensing	JAK STAT signaling	NLR signaling	Complement and coagulation cascades	ECM receptor interaction	Leishmania infection
DDX58	TNF	CCL1	RPC1	IL2	NOD1	F3	COL1A	TLR2
IFIH1	TNFRSF1A	CCL25	RPC2	IL3	RIPK2	F7	COL2A	TLR4
MAVS	TRADD	CCL19	RPC3	IL4	IKBKG	F10	COL4A	MYD88
DHX58	TNFRSF1B	CCL21	RPC4	IL5	IKBKA	F5	COL6A	IRAK1
TRAF3	TRAF2	CCL3	RPC5	IL6	IKBKB	F2	COL9A	IRAK4
TANK	MTOR	CCL4	RPAC1	IL7	NFKBIB	F12	LAMA1_2	TRAF6
AZI2	JNK	CCL17	RPC11	IL9	NFKBIA	F11	LAMA3_5	MAP3K7
TBKBP1	IKBKA	CCL22	RPAC2	IL10	NFKB1	F9	LAMA4	MAP3K7IP1
IKBKG	IKBKB	CCL5	RPC8	IL11	RELA	VWF	LAMB1	MAP3K7IP2
TBK1	IKBKG	CCL8	RPC7	IL12A	IL1B	F8	LAMB2	NFKBIB
IKBKE	NFKBIA	CCL9	RPC6	IL12B	IL18	THBD	LAMB3	NFKBIA
IRF3	NFKBIB	CCL14	RPABC1	IL13	IL6	PROCR	LAMB4	NFKB1
IRF7	NFKBIE	CCL16	RPABC2	IL15	TNF	PROC	LAMC1	RELA
IFNA	NFKB1	CCL15_23	RPABC3	IL17D	IL8	F2R	LAMC2	IL1A
IFNB	RELA	CCL13	RPABC4	IL19	CXCL1_2_3	F2RL2	LAMC3	IL1B
IFNW	SOCS3	CCL6	RPABC5	IL20	CCL2	F2RL3	CHAD	IL12A
IFNE	IRS1	CCL7	DDX58	IL21	CCL5	F13A1	RELN	IL12B
IFNK	IRS2	CCL2	MAVS	IL22	CAMP	F13B	THBS1	TNF
TRADD	IRS3	CCL11	NFKB1	IL23A	NOD2	CPB2	THBS2S	IL4
FADD	IRS4	CCL24	RELA	IL24	MAP3K7	FGA	FN1	NOS2
RIPK1	AKT	CCL26	IL6	IFNA	MAP3K7IP1	FGB	SPP1	IL10
CASP8	CD36	CCL27	MB21D1	IFNB	MAP3K7IP2	FGG	VTN	TGFB1
CASP10	ACSL	CCL28	TMEM173	IFNG	MAP3K7IP3	KLKB1	TN	TGFB2
IKBKA	ACSBG	CCL18	TBK1	IFNE	ERK	KNG	VWF	TGFB3
IKBKB	PRKCQ	CCL20	IKBKE	IFNK	JNK	BDKRB1	IBSP	C3
NFKBIB	LEP	CXCL1_2_3	IRF3	IFNL1	P38	BDKRB2	AGRN	CR1
NFKBIA	LEPR	CXCL5_6	IRF7	IFNL2_3	JUN	PLG	HSPG2	ITGAM
NFKB1	JAK2	IL8	IFNA	IFNW	ATG16L1	TFPI	ITGA1	ITGB2
RELA	STAT3	PPBP	IFNB	OSM	ATG5	SERPINC1	ITGA2	IGH
TRAF2	POMC	PF4	ZBP1	LIF	ATG12	SERPIND1	ITGA2B	FCGR1A
MAP3K7	PRKAA	CXCL9	RIPK1	TSLP	GABARAP	SERPINA5	ITGA3	FCGR2A
TRAF6	PRKAB	CXCL10	RIPK3	CTF1	SUGT1	PROS1	ITGA4	FCGR2C
MAP3K1	PRKAG	CXCL11	IKBKG	CSF2	SHARPIN	SERPINE1	ITGA5	FCGR3
JNK	AGRP	CXCL13	IKBKA	UPD	RBCK1	SERPINB2	ITGA6	GP63
P38	NPY	CXCL12	IKBKB	CNTF	RNF31	PLAT	ITGA7	ITGA4
IL8	PPARGC1A	CXCL16	NFKBIB	CSF3	XIAP	PLAU	ITGA8	ITGB1
TNF	E4.1.1.32	CXCL14	NFKBIA	EPO	CARD6	PLAUR	ITGA9	PTGS2
IL12A	G6PC	CXCL15	CCL4	GH	TRIP6	SERPINA1	ITGA10	PRKCB
IL12B	PTPN11	CXCL17	CCL5	LEP	ERBIN	SERPINF2	ITGA11	NCF1
CXCL10	NR1C1	XCL1	CXCL10	THPO	BIRC2_3	A2M	ITGAV	NCF2

TRIM25	RXRA	XCL2	AIM2	PRL	TRAF2	CFB	ITGB1	NCF4
CYLD	RXRB	CX3CL1	PYCARD	EGF	TRAF5	CFD	ITGB3	NOX2
RNF125	RXRG	IL2	CASP1	PDGFA	TRAF6	C3	ITGB4	CYBA
ISG15	ADIPOQ	IL4	IL1B	PDGFB	CARD9	C5	ITGB5	ERK
ATG5	ADIPOR	IL7	IL18	IL2RA	TNFAIP3	C6	ITGB6	ELK1
ATG12	STK11	IL9	IL33	IL2RB	MAVS	C7	ITGB7	FOS
NLRX1	CAMKK2	IL15	TREX1	IL2RG	TRAF3	C8A	ITGB8	JUN
TMEM173	ACACB	IL21	ADAR	IL3RA	TBK1	C8B	CD44	P38
OTUD5	CPT1A	TSLP	E3L	IL4R	IKBKE	C8G	SDC1	IFNG
SIKE	CPT1B	IL3	M45	IL5RA. CD125	TANK	C9	SDC4	IFNGR1
DDX3X	CPT1C	IL5	IFI202	IL6R	IRF3	C1QA	SV2	IFNGR2
PIN1	SLC2A1	CSF2		IL7R	IRF7	C1QB	CD36	JAK1
DAK	SLC2A4	IL13		IL9R	IFNA	C1QG	GP5	JAK2
		EPO		IL10RA	IFNB	C1R	GP1BA	STAT1
		GH		IL10RB	NLRX1	C1S	GP1BB	MHC2
		PRL		IL11RA	LEF	MBL	GP9	MARCKSL1
		THPO		IL12RB1	PAGA	MASP1	GP6	CPB
		CSF3		IL12RB2	ANTXR	MASP2	DAG1	PTPN6
		LEP		IL13RA1	NLRP1	C2	CD47	
		IL6		IL13RA2	PYCARD	C4	HMMR	
		IL11		IL15RA	CASP1	C3AR1		
		IL12A		IL20RA	BCL2	VSIG4		
		IL12B		IL20RB	BCL2L1	CR1		
		IL23A		IL21R	CTSB	CR2		
		IL27		IL22RA1	NLRP3	ITGAM		
		IL31		IL22RA2	PANX1	ITGB2		
		CLCF1		IL23R	P2RX7	ITGAX		
		CNTF		IL27RA	TRPM2	C5AR1		
		CTF1		IL6ST	TRPM7	CFH		
		LIF		IFNAR1	TRPV2	CFI		
		OSM		IFNAR2	CASR	SERPING1		
		IL10		IFNGR1	GPRC6A	DAF		
		IL19		IFNGR2	PLCB	CD46		
		IL20		IFNLR1	ITPR1	C4BPA		
		IL24		OSMR	ITPR2	C4BPB		
		IL22		LIFR	ITPR3	CD59		
		IL26		TSLPR	VDAC1	CLU		
		IFNL2_3		CNTFR	VDAC2	VTN		
		IFNL1		CSF2RA	VDAC3			
		IFNA		CSF2RB	MCU			
		IFNB		CSF3R	OAS			
		IFNW		EPOR	RNASEL			
		IFNK		GHR	DHX33			
		IFNE		LEPR	MFN1			

		IFNG		TPOR	MFN2			
		IL1A		PRLR	RIPK1			
		IL1B		DOME	RIPK3			
		IL1RN		EGFR	DNM1L			
		IL36RN		PDGFRA	NAMPT			
		IL36A		PDGFRB	NOX2			
		IL36B		JAK1	CYBA			
		IL36G		JAK2	TXNIP			
		IL1F10		JAK3	TRXA			
		IL37		TYK2	NEK7			
		IL18		STAT1	BRCC3			
		IL33		STAT2	HSP90A			
		IL17A		STAT3	CARD8			
		IL17F		STAT4	PYDC1			
		IL17B		STAT5A	PYDC2			
		IL17C		STAT5B	MEFV			

Supplementary Figure 6.2. Gene lists for manually curated KEGG pathways.

10.3. Additional Analysis from STRINGdb

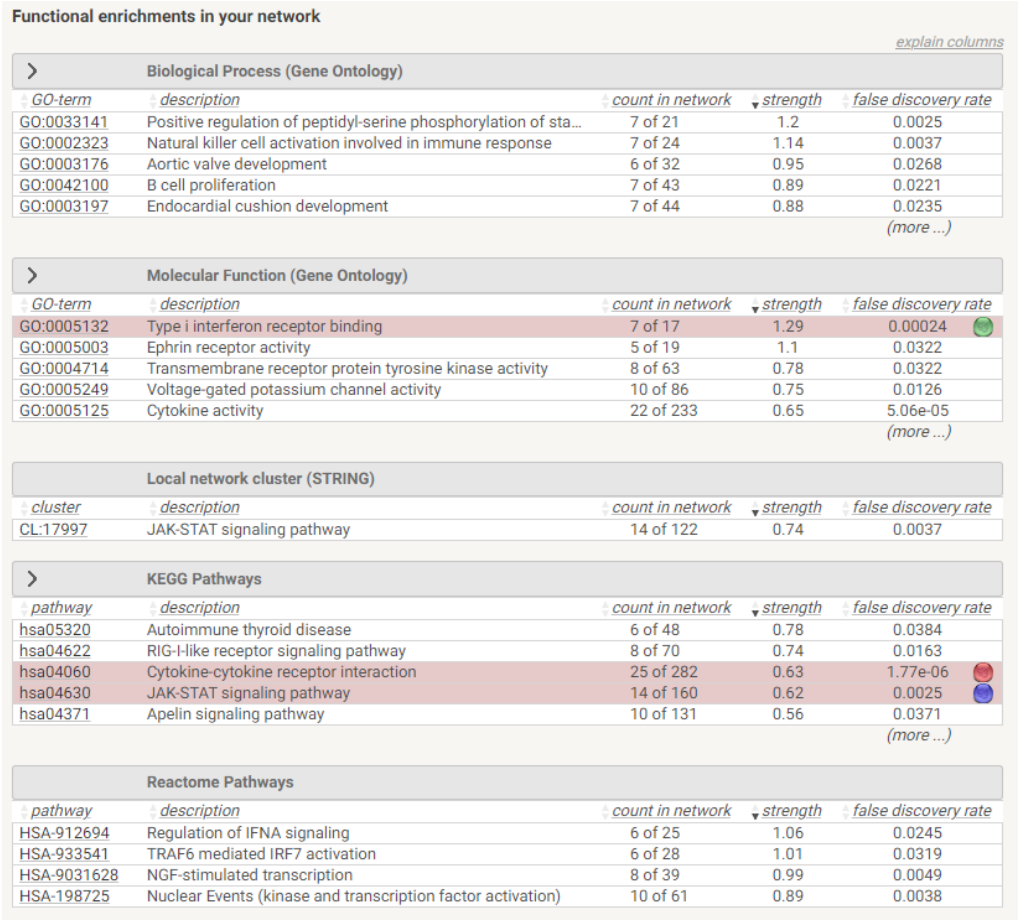

Functional enrichments in your network

explain columns

Biological Process (Gene Ontology)

GO-term	description	count in network	strength	false discovery rate
GO:0033141	Positive regulation of peptidyl-serine phosphorylation of sta...	7 of 21	1.2	0.0025
GO:0002323	Natural killer cell activation involved in immune response	7 of 24	1.14	0.0037
GO:0003176	Aortic valve development	6 of 32	0.95	0.0268
GO:0042100	B cell proliferation	7 of 43	0.89	0.0221
GO:0003197	Endocardial cushion development	7 of 44	0.88	0.0235

(more ...)

Molecular Function (Gene Ontology)

GO-term	description	count in network	strength	false discovery rate
GO:0005132	Type i interferon receptor binding	7 of 17	1.29	0.00024
GO:0005003	Ephrin receptor activity	5 of 19	1.1	0.0322
GO:0004714	Transmembrane receptor protein tyrosine kinase activity	8 of 63	0.78	0.0322
GO:0005249	Voltage-gated potassium channel activity	10 of 86	0.75	0.0126
GO:0005125	Cytokine activity	22 of 233	0.65	5.06e-05

(more ...)

Local network cluster (STRING)

cluster	description	count in network	strength	false discovery rate
CL:17997	JAK-STAT signaling pathway	14 of 122	0.74	0.0037

KEGG Pathways

pathway	description	count in network	strength	false discovery rate
hsa05320	Autoimmune thyroid disease	6 of 48	0.78	0.0384
hsa04622	RIG-I-like receptor signaling pathway	8 of 70	0.74	0.0163
hsa04060	Cytokine-cytokine receptor interaction	25 of 282	0.63	1.77e-06
hsa04630	JAK-STAT signaling pathway	14 of 160	0.62	0.0025
hsa04371	Apelin signaling pathway	10 of 131	0.56	0.0371

(more ...)

Reactome Pathways

pathway	description	count in network	strength	false discovery rate
HSA-912694	Regulation of IFNA signaling	6 of 25	1.06	0.0245
HSA-933541	TRAF6 mediated IRF7 activation	6 of 28	1.01	0.0319
HSA-9031628	NGF-stimulated transcription	8 of 39	0.99	0.0049
HSA-198725	Nuclear Events (kinase and transcription factor activation)	10 of 61	0.89	0.0038

Supplementary Figure 6.3. Functional enrichments in STRINGdb analysis from GO, STRING, KEGG and Reactome pathways.